



Università degli Studi di Ferrara

DOTTORATO DI RICERCA IN  
MATEMATICA E INFORMATICA

CICLO XXV

COORDINATORE Prof. Valeria Ruggiero

MHD stagnation-point flow

Settore Scientifico Disciplinare MAT/07

**Dottoranda**

Dott.ssa Giancesio Giulia

Giulia Giancesio

**Tutore**

Prof.ssa Borrelli Alessandra

Alessandra Borrelli

Anni 2010/2012



# Contents

<b>Introduction</b>	<b>v</b>
<b>1 The stagnation-point flow</b>	<b>1</b>
1.1 Orthogonal stagnation-point flow . . . . .	3
1.1.1 Inviscid fluids . . . . .	3
1.1.2 Newtonian fluids . . . . .	5
1.1.3 Micropolar fluids . . . . .	8
1.2 Oblique stagnation-point flow . . . . .	13
1.2.1 Inviscid fluids . . . . .	15
1.2.2 Newtonian fluids . . . . .	17
1.2.3 Micropolar fluids . . . . .	22
1.3 Three-dimensional stagnation-point flow . . . . .	35
1.3.1 Inviscid fluids . . . . .	35
1.3.2 Newtonian Fluids . . . . .	38
1.3.3 Micropolar Fluids . . . . .	44
<b>2 MHD orthogonal stagnation-point flow</b>	<b>59</b>
2.1 Inviscid fluids . . . . .	59
2.1.1 CASE I . . . . .	61
2.1.2 CASE II . . . . .	63
2.1.3 CASE III . . . . .	66
2.2 Newtonian fluids . . . . .	69
2.2.1 CASE I-N: $\mathbf{E}_0 = E_0\mathbf{e}_3$ . . . . .	70
2.2.2 CASE II-N: $\mathbf{H}_0 = H_0\mathbf{e}_1$ . . . . .	72
2.2.3 CASE III-N: $\mathbf{H}_0 = H_0\mathbf{e}_2$ . . . . .	74
2.3 Micropolar fluids . . . . .	77
2.3.1 CASE I-M: $\mathbf{E}_0 = E_0\mathbf{e}_3$ . . . . .	79
2.3.2 CASE II-M: $\mathbf{H}_0 = H_0\mathbf{e}_1$ . . . . .	82
2.3.3 CASE III-M: $\mathbf{H}_0 = H_0\mathbf{e}_2$ . . . . .	83

<b>3</b>	<b>MHD oblique stagnation-point flow</b>	<b>93</b>
3.1	Inviscid fluids . . . . .	93
3.1.1	CASE I . . . . .	94
3.1.2	CASE II . . . . .	96
3.1.3	CASE III . . . . .	97
3.2	Newtonian fluids . . . . .	100
3.2.1	CASE I-N: $\mathbf{E}_0 = E_0\mathbf{e}_3$ . . . . .	101
3.2.2	CASE II-N: $\mathbf{H}_0 = H_0\mathbf{e}_1$ . . . . .	103
3.2.3	CASE III-N: $\mathbf{H}_0 = \frac{H_0}{\sqrt{4a^2 + b^2}}(-b\mathbf{e}_1 + 2a\mathbf{e}_2)$ . . . . .	104
3.3	Micropolar fluids . . . . .	112
3.3.1	CASE I-M: $\mathbf{E} = E_0\mathbf{e}_3$ . . . . .	114
3.3.2	CASE II-M: $\mathbf{H}_0 = H_0\mathbf{e}_1$ . . . . .	116
3.3.3	CASE III-M: $\mathbf{H}_0 = \frac{H_0}{\sqrt{4a^2 + b^2}}(-b\mathbf{e}_1 + 2a\mathbf{e}_2)$ . . . . .	117
<b>4</b>	<b>MHD three-dimensional stagnation-point flow</b>	<b>135</b>
4.1	Inviscid Fluids . . . . .	135
4.2	Newtonian fluids . . . . .	138
4.2.1	A non existence result for $c < -1$ and $M^2 < 2 c $ . . . . .	145
4.2.2	CASE I-N: $\mathbf{H}_0 = H_0\mathbf{e}_1$ . . . . .	150
4.2.3	CASE II-N: $\mathbf{H}_0 = H_0\mathbf{e}_2$ . . . . .	156
4.2.4	CASE III-N: $\mathbf{H}_0 = H_0\mathbf{e}_3$ . . . . .	160
4.3	Micropolar fluids . . . . .	164
4.3.1	CASE I-M: $\mathbf{H}_0 = H_0\mathbf{e}_1$ . . . . .	175
4.3.2	CASE II-M: $\mathbf{H}_0 = H_0\mathbf{e}_2$ . . . . .	194
4.3.3	CASE III-M: $\mathbf{H}_0 = H_0\mathbf{e}_3$ . . . . .	206
<b>5</b>	<b>MHD orthogonal stagnation-point flow with <math>\mathbf{H}</math> and <math>\mathbf{v}</math> parallel at infinity</b>	<b>223</b>
5.1	Inviscid fluids CASE IV . . . . .	223
5.2	Newtonian fluids CASE IV-N . . . . .	228
5.3	Micropolar fluids CASE IV-M . . . . .	237
<b>6</b>	<b>MHD oblique stagnation-point flow with <math>\mathbf{H}</math> and <math>\mathbf{v}</math> parallel at infinity</b>	<b>249</b>
6.1	Inviscid fluids CASE IV . . . . .	249
6.2	Newtonian fluids CASE IV-N . . . . .	255
6.3	Micropolar fluids CASE IV-M . . . . .	267

---

<b>7</b>	<b>MHD 3D stagnation-point flow with <math>H</math> and <math>v</math> parallel at infinity</b>	<b>299</b>
7.1	Inviscid fluids CASE IV . . . . .	299
7.2	Newtonian fluids CASE IV-N . . . . .	305
7.3	Micropolar fluids CASE IV-M . . . . .	314
<b>8</b>	<b>Conclusions</b>	<b>333</b>
8.1	Newtonian fluids . . . . .	334
8.2	Micropolar fluids . . . . .	336
8.3	Concluding remarks and open problems . . . . .	339
	<b>Bibliography</b>	<b>341</b>



# Introduction

The flow of the classical model of viscous fluids (i.e. Newtonian fluids) is governed by the well known Navier-Stokes equations. The boundary value problems associated to these equations are difficult to solve due to their nonlinearity. Nevertheless if the geometry of the problem is simple or if there are some particular symmetries, then it is possible to find exact solutions (closed form solutions or numerical solutions). Such solutions are a valuable and irreplaceable resource. Actually, as far as the theoretical point of view is concerned, exact solutions of the full equations may be useful as test to check the accuracy of numerical methods and as a basis for stability analysis. Moreover, they have many practical applications because they allow to describe important physical situations: flows in a channel or in a pipe (i.e. Poiseuille and Couette flow), flow induced by a rotating plane (i.e. von Karman and Berker flows), and so on . . . . These solutions hence represent fundamental fluid dynamic flows so that these basic phenomena can be more closely studied.

Exact solutions often arise as similarity solutions in the sense that by means of suitable transformations (similarity transformations) it is possible to reduce the number of independent variables by one or more. In such a way the PDEs that govern the motion are reduced to ordinary non-linear differential equations. An example of motion described by similarity solutions is the stagnation-point flow.

A stagnation point in a fluid flow field is a point where the velocity is zero. These points may occur in the interior or on the boundary of the motion region. The latter possibility appears when the fluid moves past an obstacle. Since this is a common physical situation, stagnation-point flows are ubiquitous in the sense that they inevitably appear as a component of more complicated flow fields.

Hence the research in this area is motivated by its relevance to a wide range of engineering, industrial and technical applications in addition to the possibility of solving exactly the full equations near the stagnation point. Actually, this topic has attracted many studies during the past several decades.

The aim of this Ph.D. Thesis is to study how the steady stagnation-point flow of a Newtonian or a micropolar fluid is influenced by an external electromagnetic field.

As it is well known, an impressed electromagnetic field may modify the motion of an electrically conducting fluid because of the presence of the Lorentz forces.

Example of electrically conducting fluids are liquid metals, biological fluids, electrolyte solutions, ionized gases. The macroscopic interactions between such fluids and electromagnetic fields are studied by Magnetohydrodynamic, which is involved in many natural phenomena and it has relevant engineering, technical and biomedical applications. MHD stagnation-point flow is an area of investigation discussed by several Authors in recent years (see for example [2], [17], [25], [42], [43], [44]). One of the greatest advantages of having exact solutions to these magnetohydrodynamic problems is that the fluid and the electromagnetic field near the obstacle can be described as functions of the parameters and some insight into the nature of magnetohydrodynamic flows can be achieved.

As far as the two models of fluid are concerned, we will focus our attention to the incompressible ones (real liquids). The Newtonian fluid is perhaps one of the best known models and it represents a fluid whose stress at each point is linearly proportional to the strain rate at that point. The constant of proportionality is known as the viscosity. This model well summarizes the behaviour of many real gases and liquids. Indeed the micropolar fluids physically represent fluids consisting of rigid randomly oriented particles suspended in a viscous medium which have an intrinsic rotational micromotion. Extensive reviews of the theory and its applications can be found in [20], [21] and [41]. The main advantage of using the micropolar fluid model in comparison to other classes of non-Newtonian fluids is that it takes into account the rotation of fluid particles by means of an independent kinematic vector called the microrotation vector. This model is considered to describe, for example, biological fluids in thin vessels and in capillaries, polymeric suspensions, slurries, liquid crystals, colloidal fluids. We point out that in most of the studies found in literature a restrictive approach has been followed on the material parameters which makes the equations to contain only one parameter ([1], [31], [32], [37]). In our research we have not required restrictive conditions so that three material parameters appear in the dimensionless ODEs (see for example [27]).

As far as the boundary conditions are concerned, we associate to the two models the no-slip condition for the velocity and the strict adherence condition for the microrotation.

Further we require a condition deduced from the physical experience: we suppose that the pressure and the flow of a viscous fluid approach the pressure and the flow of an inviscid fluid far from the obstacle. So the region where the viscosity appears is only a small region near the obstacle and far from it there is no trace of the viscous nature of the fluid. However it is important to underline that the stagnation-point of the inviscid fluid, whose behaviour is approached by the viscous fluids far from the obstacle, does not coincide with the stagnation-point of the viscous fluid (see for example [47] for the Newtonian case). Hence in order to study the stagnation-point flow for a Newtonian or a micropolar fluid, it is convenient to start with the same flow for an inviscid fluid.

In this Thesis, we will consider three different types of steady stagnation-point flow for incompressible fluids: plane orthogonal, plane oblique and three-dimensional.

Orthogonal stagnation-point flow appears when a fluid impinges orthogonally on an obstacle. Hiemenz ([33]) was the first to study the two-dimensional stagnation-point flow for a Newtonian fluid using a similarity transformation to reduce the Navier-Stokes equations to a non-linear ordinary differential equation.

The orthogonal plane and axially symmetric stagnation-point flow of a micropolar fluid were treated by Guram and Smith ([27]), who reduced the equations to dimensionless form, including three dimensionless parameters, and integrated them numerically. Previously Ahmadi ([1]) obtained self-similar solutions of the boundary layer equations for micropolar flow asking restrictive conditions on the material parameters which make the equations to contain only one parameter.

Oblique stagnation-point flow appears when a jet of fluid impinges obliquely on a rigid wall at an arbitrary angle of incidence. From a mathematical point of view, such a flow is obtained by combining the traditional orthogonal stagnation-point flow with a shear flow directed parallel to the wall. The steady two-dimensional oblique stagnation-point flow of a Newtonian fluid has been the object of many investigations starting from the paper of Stuart in 1959 ([50]). One interesting feature of this problem is that the angle of incidence of the impinging stream does not appear in the equations governing the motion. The oblique solution was later studied by Tamada ([52]), Dorrepaal ([16], [18]), Wang ([54], [55]); recently Drazin and Raley ([19]) and Tooke and Blyth ([53]) reviewed the problem and included a free parameter associated with the shear flow component. This free parameter alters the structure of the shear flow component by varying the magnitude of the pressure gradient.

An important example of flow past a body, where the three velocity components appear, is the three-dimensional stagnation-point flow.

The steady three-dimensional stagnation-point flow of a Newtonian fluid has been studied by Homman ([35]), Howarth ([36]), Davey and Schofield ([13], [48]). Similarity transformations reduce the Navier-Stokes equations to a system of nonlinear ODEs, to which suitable boundary conditions have to be appended. The ODEs system obtained depends on a parameter which is a measure of three-dimensionality. Guram and Anwar Kamal ([26]) studied the analogous problem for a micropolar fluid, but they didn't consider the occurrence of the reverse flow, the thickness of the boundary layer and the influence of some parameters on the solution.

As we have already pointed out, the aim of this Ph.D. Thesis is to understand how an external electromagnetic field modifies the steady stagnation-point flow of a Newtonian or a micropolar fluid. The motions we find depend on the orientation of the applied electromagnetic field relative to the object boundary, which is supposed to be a rigid plane wall. In every case through similarity transformations we reduce the PDEs, which govern the motion, to a system of nonlinear ODEs.

Due to the nonlinearity of the ODEs problems, the solutions cannot be expressed in closed form, but we can use a numerical technique to find them. Some numerical examples and pictures are given in order to illustrate the effects due to the magnetic field in all the cases. These numerical solutions are obtained by using the `bvp4c` MATLAB routine. Such a routine is a finite difference code that implements the three-stage Lobatto IIIa formula. This is a collocation formula and here the collocation polynomial provides a  $C^1$ -continuous solution that is fourth-order accurate uniformly in  $[0, 5]$ . Mesh selection and error control are based on the residual of the continuous solution. We set the relative and the absolute tolerance equal to  $10^{-7}$ . The method was used and described in [49].

Moreover, in all the physical situations here analyzed, we will always compute both the velocity profiles and the pressure field. In the chapters, we will underline the importance of the pressure field, which usually is not computed in the literature (see for example [37], [39]). Actually, the approach followed by several Authors uses the equations of the boundary layer and the stream function to derive the ODEs boundary problem which governs the motion. In this way the ODEs problems are the same as ours, but this approach is not mathematically justified. Further, it can't be applied to the three-dimensional stagnation-point flow and it doesn't compute the pressure field, which is very important to understand the behaviour of the motion.

The geometry of the problems is always the same: the coordinate axes are fixed in such a way that the stagnation-point is the origin and that the motion occurs in the region  $x_2 > 0$ . The obstacle is represented by the plane  $x_2 = 0$ , which is supposed to be rigid and fixed. In the first four chapters the vacuum occupies the region  $x_2 < 0$  under the obstacle, while in Chapters 5, 6, 7 the rigid wall  $x_2 = 0$  is the boundary of a solid which is a rigid uncharged dielectric at rest occupying  $x_2 < 0$ .

The Thesis has been organized as follows:

- Chapter 1 is devoted to define the three different types of stagnation-point flow for Newtonian and micropolar fluids. Actually, we will recall and extend the results found in literature in the absence of an external electromagnetic field (see for example [19], [33], [35], [47], [50], [55]).
- In the second chapter we analyze the MHD orthogonal stagnation-point flow of a Newtonian or a micropolar fluid when an external uniform electromagnetic field  $(\mathbf{E}_0, \mathbf{H}_0)$  is applied.

First of all, we introduce the MHD PDEs which govern the motion and the suitable boundary conditions for the electromagnetic field. We then consider the inviscid fluid analyzing three cases which are significant from a physical point of view. In the first two cases an external constant electric or magnetic field is impressed parallel to the rigid wall. In both cases we find that an orthogonal stagnation-point flow exists and we get the exact induced magnetic

field. The presence of the electromagnetic field modifies the pressure  $p$ , which is smaller than the pressure in the purely hydrodynamical flow. In the third case, we suppose that  $\mathbf{E}_0$  vanishes and  $\mathbf{H}_0$  lies in the plane of the flow with a direction not parallel to the boundary. Under the hypothesis that the magnetic Reynolds number is small, we neglect the induced magnetic field, as it is usual in the literature. We prove that the orthogonal stagnation-point flow exists if, and only if,  $\mathbf{H}_0$  is orthogonal to the wall  $x_2 = 0$ . The presence of  $\mathbf{H}_0$  modifies  $p$ , which becomes smaller than the pressure in the purely hydrodynamical flow.

In the second part we consider the same problems for a Newtonian fluid. As it is usual when one studies the plane stagnation-point flow for a Newtonian fluid, we assume that at infinity the flow approaches the flow of an inviscid fluid for which the stagnation-point is shifted from the origin ([19], [47]). The coordinates of this new stagnation-point contain a constant  $A$ , which is determined as part of the solution for the flow. The existence of this constant can be obtained from the numerical integration and it has been proved theoretically by Hartmann in [28].

As far as the flow is concerned, in the first two cases we find the same equations of the orthogonal stagnation-point flow in absence of electromagnetic field and the induced magnetic field is obtained by direct integration. Hence, the external uniform electromagnetic field doesn't influence the flow and modifies only the pressure.

When  $\mathbf{H}_0$  is orthogonal to  $x_2 = 0$ , we find that the flow has to satisfy an ordinary differential problem whose solution depends on  $\mathbf{H}_0$  through the Hartmann number  $M^2$ . In this case,  $A$  (and so the stagnation-point) depends on  $M^2$  and decreases as  $M^2$  is increased. The influence of the viscosity appears only in a layer near the wall depending on  $M^2$  whose thickness decreases as  $M^2$  increases from zero, as it is usual in magnetohydrodynamics.

For this class of fluids also, the external uniform electromagnetic field doesn't influence the flow, and modifies only the pressure  $p$ . The induced magnetic field is obtained by direct integration.

Finally, in the case in which  $\mathbf{H}_0$  is orthogonal to  $x_2 = 0$ , we find that the flow has to satisfy an ordinary differential problem whose solution depends on  $\mathbf{H}_0$  through the Hartmann number  $M^2$ , as for the Newtonian model. When the material parameters are fixed, the effect of the viscosity appears only in a layer near the wall depending on  $M^2$  whose thickness decreases as  $M^2$  increases from zero and is smaller than in the Newtonian case.

We have also considered the influence of the three material parameters involved in the micropolar fluids on the motion.

- In Chapter 3 we study how the steady oblique stagnation-point flow of a Newtonian or a micropolar fluid is influenced by an external uniform electromagnetic field  $(\mathbf{E}_0, \mathbf{H}_0)$ . The results obtained in this chapter have been published in [5] and [6].

First of all, as in the previous chapter, we consider an inviscid fluid and analyze three cases which are relevant from a physical point of view. As in the orthogonal stagnation-point flow, in the first two cases an external constant electric or magnetic field is applied parallel to the rigid wall. In both cases we find that an oblique stagnation-point flow exists and we get the exact induced magnetic field. The presence of the electromagnetic field modifies the pressure  $p$ , which is smaller than the pressure in the purely hydrodynamical flow. In the third case, we suppose that  $\mathbf{E}_0$  vanishes and  $\mathbf{H}_0$  lies in the plane of the flow with a direction not parallel to the boundary. Under the hypothesis that the magnetic Reynolds number is small, we neglect the induced magnetic field and we prove that the oblique stagnation-point flow exists if, and only if,  $\mathbf{H}_0$  is parallel to the dividing streamline. In regard to this result we point out that the analysis contained in [25] appears incorrect because the Authors carry out their analysis by supposing the external magnetic field orthogonal to the boundary, but we prove in Theorem 3.1.5 that in that case the oblique stagnation-point flow does not exist for an inviscid fluid. The presence of  $\mathbf{H}_0$  parallel to the dividing streamline modifies  $p$ , which is smaller than the pressure in the purely hydrodynamical flow.

In the second and third part we consider the same problems for a Newtonian or a micropolar fluid, respectively. As usual, we assume that at infinity the flow approaches the flow of an inviscid fluid for which the stagnation-point is shifted from the origin ([19], [47], [53]). The coordinates of this new stagnation-point contain two constants  $A, B$ , where  $A$  is determined as part of the solution for the orthogonal flow and  $B$  is free.

In the first two cases the external uniform electromagnetic field influences only the pressure and the induced magnetic field is obtained by direct integration. Moreover,  $\nabla p$  has a constant component parallel to the wall proportional to  $B - A$ , which does not appear in the orthogonal stagnation-point flow. This component determines the displacement of the uniform shear flow parallel to the boundary. The flow is obtained for different values of  $B$  by numerical integration. We remark that the thickness of the layer affected by the viscosity is larger than that in the orthogonal stagnation-point flow.

In the case in which  $\mathbf{H}_0$  is parallel to the dividing streamline of the inviscid flow, we find that the flow has to satisfy an ordinary differential problem whose solution depend on  $\mathbf{H}_0$  through the Hartmann number  $M^2$ . In this case,  $A$  and the thickness of the boundary layer decrease as  $M^2$  increases.

We then analyze the behaviour of the flow near the wall; it depends on the

Hartmann number in the third case.

We calculate along the wall, three important coordinates: the origin, which is the stagnation-point, the point of maximum pressure and the point of zero tangential stress (zero skin friction) where the dividing streamline meets the boundary. These points depend on  $M^2$  in the third case. The ratio of the slope of the dividing streamline at the wall to its slope at the infinity is independent of the angle of incidence; in the last case it depends on  $M^2$ .

The presence of the microrotation influences all the descriptive quantities of the motion, which are smaller than in the Newtonian case.

- Chapter 4 presents the study of the influence of a uniform external electromagnetic field ( $\mathbf{E}_0, \mathbf{H}_0$ ) on the steady three-dimensional stagnation-point flow of an electrically conducting Newtonian and micropolar fluid. The results are contained in [4], [7], and [8].

First of all, we study the steady three-dimensional stagnation-point flow of an inviscid fluid in the presence of a uniform external magnetic field  $\mathbf{H}_0$  and when the induced magnetic field is neglected. Under this assumption we prove that  $\mathbf{H}_0$  has to be parallel to one of the axes.

Then we consider the same problems for a Newtonian and a micropolar fluid. Taking into account the results obtained for an inviscid fluid, we find that the flow has to satisfy an ordinary differential problem depending on two parameters:  $c$  and  $M^2$ . As usual,  $c$  is a measure of three-dimensionality and  $M^2$  is the Hartmann number.

As far as the micropolar fluids are concerned, in all three case, in addition to the well known phenomenon of the reverse flow, we have found a new interesting result: there is a zone of reverse microrotation for some negative values of  $c$ . The range of  $c$  for which the reverse microrotation appears is included in the range of  $c$  for which the reverse flow occurs.

By means of our numerical results, we find that  $\mathbf{H}_0$  tends to prevent the occurrence of the reverse flow, which occurs in the absence of the magnetic field for suitable negative values of  $c$  ([13]). The influence of the magnetic field on the reverse flow was also found in [3] in other physical situations.

In the micropolar case, we find that  $\mathbf{H}_0$  tends to prevent also the occurrence of the reverse microrotation.

The presence of  $\mathbf{H}_0$  modifies the thickness of the boundary layer of the velocity and of the microrotation, which decreases as  $M^2$  increases. This effect occurs in all cases studied.

We have also classified the stagnation-point as nodal or saddle point and as attachment or separation point. The classification depends on  $c$  and  $M^2$ . In CASE II-N-M and CASE III-N-M, as for  $M^2 = 0$ , the origin is a point of attachment. In CASE I-N-M, we find a new result: when  $M^2$  is sufficiently large

and  $c$  assumes suitable negative values, then the stagnation-point becomes a separation point. In all the three cases, if  $c > 0$  or where there is the reverse flow, the origin is a nodal point, while when  $c < 0$  and the reverse flow does not appear, it is a saddle point.

We also stress that the three dimensional displacement thickness  $h_d$  can be negative and we find that  $h_d$  is always negative when the reverse flow appears. Finally, the solution does not exist for  $c < -1$  in CASE III-N ([13]), while the non existence in CASEs I-II-N is proved for  $c < -1$  and  $M^2 < -2c$ .

- In Chapter 5 we analyze the MHD orthogonal stagnation-point flow of a Newtonian or a micropolar fluid when the magnetic field  $\mathbf{H}$  is parallel to the flow at infinity. We underline that  $\mathbf{H}$  is not uniform and it depends on a sufficiently regular unknown function  $h = h(x_2)$  to be determined under a hypothesis assuring that far from the obstacle  $\mathbf{H} \times \mathbf{v} = \mathbf{0}$ .

We assume that an external magnetic field  $\mathbf{H}_e$  permeates the whole space and the external electric field is absent.

The region where the motion appears is bordered by the boundary of a solid which is a rigid uncharged dielectric at rest.

We point out that this problem has been studied in [17] for a Newtonian fluid, but the Authors didn't explain properly the physics of the problem and didn't take into consideration the thickness of the boundary layer, the behaviour of the solution and the influence of the parameters on the solution. We remark that the results presented for the micropolar fluids are new ([9]).

First of all, we consider an inviscid fluid and the situation of the solid.

As far as the electromagnetic field in the solid ( $\mathbf{H}_s, \mathbf{E}_s$ ) is concerned, of course  $\mathbf{E}_s$  is zero and we determine  $\mathbf{H}_s$  by asking that the non-degenerate field lines of  $\mathbf{H}_s$  tend to  $x_2 = 0$  as  $x_1$  goes to infinity.

For the inviscid fluid we have that  $(\mathbf{H}, \mathbf{E}) = (\mathbf{H}_e, \mathbf{0})$  and the pressure field is not modified by the presence of  $\mathbf{H}$ .

In the second and third part of the chapter we consider the same problem for a Newtonian and a micropolar fluid assuming that at infinity the flow approaches the flow of an inviscid fluid for which the stagnation-point is shifted from the origin.

We find that the pressure field and the flow depend on  $h(x_2)$ .  $\mathbf{H}$  and  $\mathbf{v}$  satisfy an ordinary differential boundary value problem which depends on two parameters  $R_m$  and  $\beta_m$ .  $R_m$  is the Reynolds number, while  $\beta_m$  is a measure of the strength of the applied magnetic field. The parameter  $\beta_m$  has to be less than 1 in order to preserve the parallelism of  $\mathbf{H}$  and  $\mathbf{v}$  at infinity, as it is underlined in [17].

For both fluids we find that the thickness of the boundary layer depends on

$R_m$  and  $\beta_m$ . More precisely, it increases when  $\beta_m$  increases, while it decreases when  $R_m$  increases. This behaviour is not surprising because as it is underlined in [17] when the magnetic field is strong the disturbances are no longer contained within a boundary layer along the wall. This means that boundary conditions can no longer be prescribed at infinity. In particular, in [17] it is proved that in a perfectly conducting fluid the displacement thickness becomes infinite as  $\beta_m$  goes to  $1^-$ .

As far as the dependence of the thickness of the boundary layer on  $R_m$  is concerned, this fact is in agreement with the results obtained for the orthogonal stagnation-point flow in Chapter 2, where we have shown that the thickness of the boundary layer decreases when the Hartmann number  $M^2$  increases. Actually,  $R_m$  and  $M^2$  are both proportional to the electrical conductivity.

Finally, we display the streamlines and the magnetic field lines in order to underline that the flow and the magnetic field are completely overlapped far from the obstacle and the more  $R_m$  increases the more the two lines coincide.

- The purpose of Chapter 6 is to study the MHD oblique stagnation-point flow of a Newtonian or a micropolar fluid when the magnetic field  $\mathbf{H}$  is parallel to the flow at infinity.  $\mathbf{H}$  is not uniform and it depends on two sufficiently regular unknown functions  $h = h(x_2)$ ,  $k = k(x_2)$ .

We suppose that an external magnetic field  $\mathbf{H}_e$  and an external uniform electric field  $\mathbf{E}_e$  (perpendicular to the plane of the flow) permeate the whole space.

As in Chapter 5, the region where the motion appears is bordered by the boundary of a solid which is a rigid uncharged dielectric at rest.

This problem has been studied in [17] for a Newtonian fluid and that the results presented for the micropolar fluids are new ([10]).

First of all, we consider an inviscid fluid and the situation of the solid.

As far as the electromagnetic field in the solid ( $\mathbf{H}_s, \mathbf{E}_s$ ) is concerned, of course  $\mathbf{E}_s = \mathbf{E}_e$  and we determine  $\mathbf{H}_s$  by asking that the non-degenerate field lines of  $\mathbf{H}_s$ , which are hyperbolas, have centre in the origin and they tend to  $x_2 = 0$  as  $x_1$  goes to infinity.

For the inviscid fluid we get  $\mathbf{E} = \mathbf{E}_e$  and it is univocally determined by  $\mathbf{H}_e$ . Moreover, we find that  $\mathbf{H} = \mathbf{H}_e$  and that the pressure field is modified by the presence of  $\mathbf{H}$ .

In the second and third part of the chapter we consider the same problem for a Newtonian and a micropolar fluid. As usual, we assume that at infinity the flow approaches the flow of an inviscid fluid for which the stagnation-point is shifted from the origin. The coordinates of this new stagnation-point contain the constants  $A, B$ .

As far as the flow is concerned, we find that the pressure field and the flow depend on  $h(x_2)$  and  $k(x_2)$ .  $\mathbf{H}$  and  $\mathbf{v}$  satisfy an ordinary differential boundary

value problem which depends on  $R_m$ ,  $\beta_m$  and  $B - A$ . The gradient of the pressure has a constant component parallel to the wall proportional to  $B - A$ , which does not appear in the orthogonal stagnation-point flow and which now depends on  $\mathbf{H}$ . This component determines the displacement of the uniform shear flow parallel to the boundary.

For both the models of the fluid we find that the thickness of the boundary layer depends on  $R_m$  and  $\beta_m$ . More precisely, it increases when  $\beta_m$  increases, while it decreases when  $R_m$  increases (as it happens in the orthogonal stagnation-point flow). The thickness of the layer affected by the viscosity is larger than that in the orthogonal case.

We underline that the more  $R_m$  is small and the more  $\beta_m$  is close to 1 the more the thickness of the boundary layer is larger than in the other cases of oblique stagnation-point flow treated in this Thesis (see Chapters 1.2 and 3). We calculate along the wall the point of maximum pressure and the point of zero tangential stress. These points depend both directly and indirectly on  $\beta_m$  and  $R_m$ . In this situation also the ratio of the slope of the dividing streamline at the wall to its slope at the infinity is independent of the angle of incidence. Finally, we see that the flow and the magnetic field are completely parallel far from the obstacle.

- Chapter 7 is dedicated to the analysis of the MHD three-dimensional stagnation-point flow of a Newtonian or a micropolar fluid when the magnetic field  $\mathbf{H}$  is parallel to the flow at infinity.  $\mathbf{H}$  is not uniform and it depends on two sufficiently regular unknown functions  $h = h(x_2)$ ,  $k = k(x_2)$  to be determined under a hypothesis assuring that far from the obstacle  $\mathbf{H} \times \mathbf{v} = \mathbf{0}$ . Further  $\mathbf{H}$  depends on  $c$  (the measure of the three dimensionality of the flow).

We assume that an external magnetic field  $\mathbf{H}_e$  permeates the whole space and the external electric field is absent.

All the results of this chapter are original ([11]).

First of all, we consider an inviscid fluid and the situation of the solid.

As far as the electromagnetic field in the solid ( $\mathbf{H}_s, \mathbf{E}_s$ ) is concerned, of course  $\mathbf{E}_s = \mathbf{E}_e$  and we compute  $\mathbf{H}_s$  by asking that the non-degenerate field lines of  $\mathbf{H}_s$  belong to a surface which tends to  $x_2 = 0$  as  $|x_1|, |x_3|$  goes to infinity.

For the inviscid fluid we have that  $(\mathbf{H}, \mathbf{E}) = (\mathbf{H}_e, \mathbf{0})$  and the pressure field is not modified by the presence of  $\mathbf{H}$ .

In the second and third part of the chapter we consider the same problem for a Newtonian and a micropolar fluid.

We prove that the three dimensional stagnation-point flow is possible if, and only if, the motion is axial symmetric with respect to  $x_2$  axis.

The pressure field and the flow depend on  $h(x_2)$ .  $\mathbf{H}$  and  $\mathbf{v}$  satisfy an ordinary differential boundary value problem which depends on  $R_m$  and  $\beta_m$ .

For both the models of the fluid we find that the thickness of the boundary layer depends on  $R_m$  and  $\beta_m$ . More precisely, it increases when  $\beta_m$  increases, while it decreases when  $R_m$  increases (as it happens in the orthogonal and the oblique stagnation-point flow).

We underline that the more  $R_m$  is small and the more  $\beta_m$  is close to 1 the more the thickness of the boundary layer is larger than in the other cases of three-dimensional stagnation-point flow treated in this Thesis (see Chapters 1.3 and 4).

Finally, we classify the origin: the stagnation-point is now always a nodal point of attachment.

- In Chapter 8 the results obtained are summarized and compared and some open problems are proposed.

To facilitate access to the individual topics, the chapters are rendered as self-contained as possible.

All the MHD results here obtained reduce to that found in literature when  $M^2 = 0$  or  $R_m = 0$  and  $\beta_m = 0$ .

It can be interesting to compare the results of the micropolar fluid with the corresponding results for the Newtonian fluid: the micropolar fluids reduce the thickness of the boundary layer, and in general all the descriptive quantities of the motion.

In all cases here considered the results continue to hold even if there are external conservative body forces by modifying the pressure field appropriately. Moreover, our analysis can be applied when the obstacle is the surface of a body with any shape, because near the stagnation-point the body may be represented by its tangent plane.

Finally, it should be pointed out that a number of aspects of these problems should be further investigated, for example the consideration of temperature or time dependence and the proof of the existence or the non-existence of solutions of the problems here considered (especially in the micropolar case).



# Chapter 1

## The stagnation-point flow

This chapter is devoted to define three different types of stagnation-point flow for Newtonian and micropolar fluids. Actually, even if the aim of this Thesis is to study the Magnetohydrodynamic aspects of such motions, it is appropriate to start by recalling the results found in the literature in the absence of an external electromagnetic field. As we will see, part of the results presented in this chapter extend the existing ones.

First of all we note that a stagnation point in a flow is a point where fluid velocity components are zero. These points occur very often physically: for example when a fluid hits an obstacle (see Figure 1.1<sub>1</sub>) or when an object moves in a fluid. Hence stagnation-point flows appear generally as a part of more complicated flow fields. In our analysis, we will consider fluids which move towards to a rigid material wall. From a mathematical point of view, these flows belong to a specific class of exact solutions of the PDEs which usually govern the motion of such fluids: similarity solutions. The main feature of similarity solutions is that they reduce the PDEs through similarity transformations to a system of nonlinear ODEs to which appropriate boundary conditions should be appended.

For these reasons, the stagnation-point flow is a fundamental topic in fluid dynamics and it has attracted many investigations during the past several decades.

Since we want to find exact solutions of the PDEs which usually govern the motion, we search classical solutions.

Due to the nonlinearity of the ODEs problem, we will use a numerical technique to find the approximate solution. These numerical solutions are here obtained by using the `bvp4c` MATLAB routine, as described in [49].

As far as the models of fluid are concerned, the Newtonian one is perhaps the best known model and it represents a fluid whose viscosity does not change with rate of flow. This model well summarizes the behaviour of many real gases and liquids. As it is well known, the motion of Newtonian fluid is governed by the Navier-Stokes equations. This important system of PDEs has, however, a limitation: it cannot

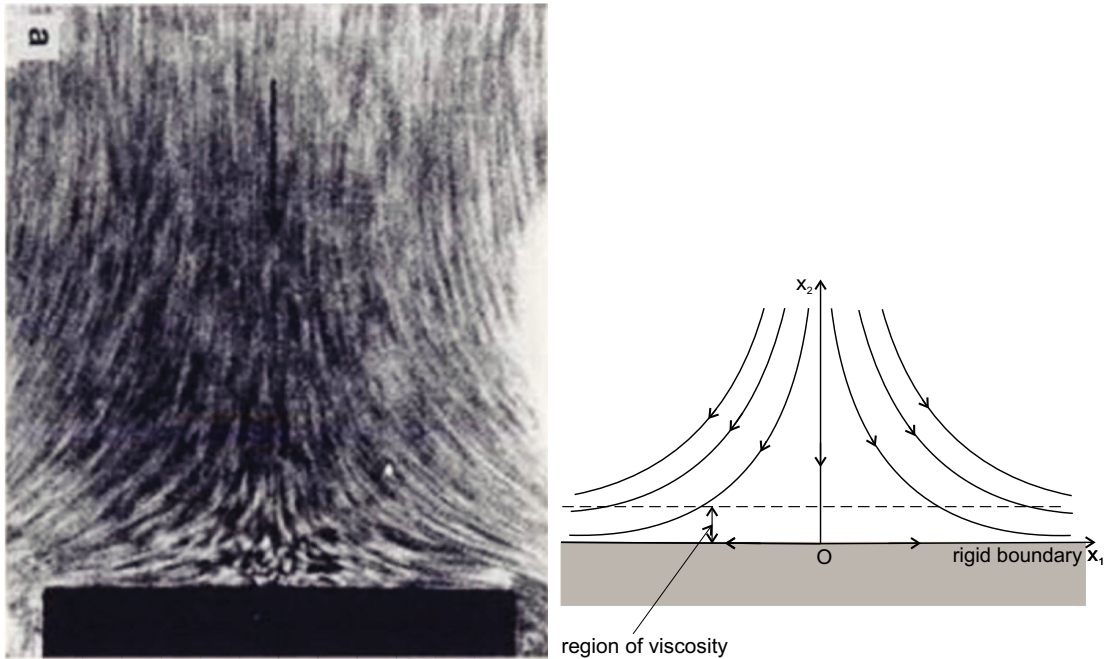


Figure 1.1: In Figure 1.1<sub>1</sub> it is shown a picture of the orthogonal stagnation-point flow ([47]), while Figure 1.1<sub>2</sub> elucidate the region where the viscosity appears.

describe fluids with microstructures which are very important in practical applications ([41]). The theory of micropolar fluids introduced by Eringen is one of the best theory of Non-Newtonian models which takes into account the microstructures ([20], [21]). Briefly, the micropolar fluids physically represent fluids consisting of rigid randomly oriented particles suspended in a viscous medium which have an intrinsic rotational micromotion. The rotation of the fluid particles is described by the microrotation field.

We associate to these two models the no-slip condition for the velocity and the strict adherence condition for the microrotation. Moreover, we add another condition deduced from the physical experience: we suppose that the pressure and the flow of a viscous fluid approach the pressure and the flow of an inviscid fluid far from the obstacle. So the region where the viscosity appears is only a small region near the obstacle and far from it there is no trace of the viscous nature of the fluid (see Figure 1.1<sub>2</sub>).

This is why the starting point of our analysis will always be to study the stagnation-point flow of an inviscid fluid.

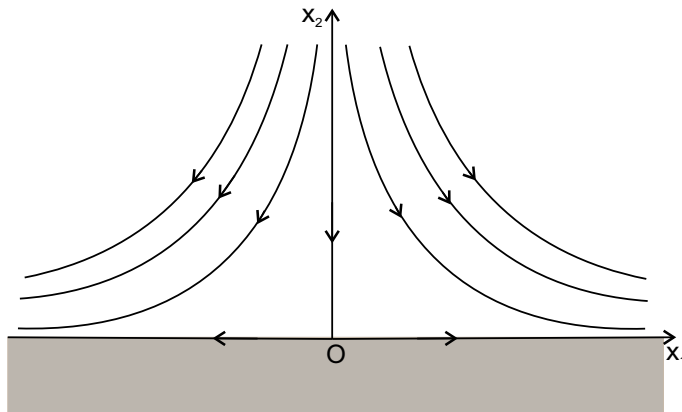


Figure 1.2: Orthogonal stagnation-point flow description.

## 1.1 Orthogonal stagnation-point flow

Orthogonal stagnation-point flow appears for example when a jet of fluid impinges orthogonally on a rigid wall.

Hiemenz ([33]) was the first to study the two-dimensional stagnation-point flow for a Newtonian fluid and to obtain a similarity solution of the governing Navier-Stokes equations.

The same flow of a micropolar fluid was treated by Guram and Smith ([27]), who reduced the equations to dimensionless form, including three dimensionless parameters. It is noteworthy that previously Ahmadi ([1]) obtained exact solutions of the boundary layer equations for micropolar flow asking restrictive conditions on the material parameters. Under these conditions the dimensionless ODEs that describe the motion contain only one parameter.

In our analysis we will always follow the Guram and Smith's approach ([27]) and we won't impose any restrictive condition on the parameters.

### 1.1.1 Inviscid fluids

Consider the steady plane flow of a homogeneous, incompressible inviscid fluid near a stagnation point occupying the region  $\mathcal{S}$  (see Figure 1.2) given by

$$\mathcal{S} = \{\mathbf{x} \in \mathbb{R}^3 : (x_1, x_3) \in \mathbb{R}^2, x_2 > 0\}. \quad (1.1)$$

The boundary of  $\mathcal{S}$  having the equation  $x_2 = 0$  is a rigid, fixed wall.

The coordinate axes are fixed so that the stagnation-point is the origin. As usual, we denote by  $(\mathbf{e}_1, \mathbf{e}_2, \mathbf{e}_3)$  the canonical base of  $\mathbb{R}^3$ .

The equations governing such a flow in the absence of external mechanical body forces are:

$$\begin{aligned}\rho \mathbf{v} \cdot \nabla \mathbf{v} &= -\nabla p, \\ \nabla \cdot \mathbf{v} &= 0, \end{aligned} \quad \text{in } \mathcal{S} \quad (1.2)$$

where  $\mathbf{v}$  is the velocity field,  $p$  is the pressure,  $\rho$  is the mass density (constant  $> 0$ ).

REMARK 1.1.1. *Equations (1.2) continue to hold even if there are external conservative body forces. Indeed in this case it is sufficient to modify the pressure field appropriately.*

To equations (1.2) we append the usual no-penetration boundary condition for  $\mathbf{v}$ :

$$v_2 = 0 \quad \text{at } x_2 = 0. \quad (1.3)$$

We are interested in the orthogonal plane stagnation-point flow so that

$$v_1 = ax_1, \quad v_2 = -ax_2, \quad v_3 = 0, \quad x_1 \in \mathbb{R}, \quad x_2 \in \mathbb{R}^+, \quad (1.4)$$

with  $a$  constant. The constant  $a$  has to be positive because the fluid moves towards the wall  $x_2 = 0$ .

As it is easy to verify, the following theorem holds:

THEOREM 1.1.2. *Let a homogeneous, incompressible, inviscid fluid occupy the region  $\mathcal{S}$ . The steady orthogonal plane stagnation-point flow of such a fluid has the form:*

$$\mathbf{v} = ax_1 \mathbf{e}_1 - ax_2 \mathbf{e}_2, \quad p = -\frac{1}{2} \rho a^2 (x_1^2 + x_2^2) + p_0, \quad p_0 \in \mathbb{R}, \quad x_1 \in \mathbb{R}, \quad x_2 \in \mathbb{R}^+.$$

REMARK 1.1.3. *Here and subsequently, the constant  $p_0$  represents the pressure at the stagnation-point.*

*Moreover, in the following  $p_0^*$  will indicate a suitable constant.*

REMARK 1.1.4. *As we will explain in the details in the next section, in order to study the orthogonal stagnation-point flow for Newtonian and micropolar fluids, it is convenient to consider a more general flow. More precisely, we suppose the inviscid fluid orthogonally impinging on the flat plane  $x_2 = A$ , so that*

$$v_1 = ax_1, \quad v_2 = -a(x_2 - A), \quad v_3 = 0 \quad x_1 \in \mathbb{R}, \quad x_2 \geq A, \quad (1.5)$$

*with  $A = \text{constant}$ .*

*In such a way the stagnation point is not  $(0, 0)$  but the point  $(0, A)$  and the pressure field is given by:*

$$p = -\frac{1}{2} \rho a^2 [x_1^2 + (x_2 - A)^2] + p_0.$$

### 1.1.2 Newtonian fluids

Consider now the steady two-dimensional orthogonal flow of a homogeneous, incompressible Newtonian fluid near a stagnation point occupying the region  $\mathcal{S}$  given by (1.1).

The equations governing such a flow in the absence of external mechanical body forces are the equations (1.2) where  $(1.2)_1$  is replaced by:

$$\mathbf{v} \cdot \nabla \mathbf{v} = -\frac{1}{\rho} \nabla p + \nu \Delta \mathbf{v}, \quad (1.6)$$

where  $\nu$  is the kinematic viscosity. Of course, Remark 1.1.1 holds.

As far as the boundary conditions are concerned, we modify the condition for  $\mathbf{v}$ , assuming the no-slip boundary condition :

$$\mathbf{v}|_{x_2=0} = \mathbf{0}. \quad (1.7)$$

Since the velocity field given by (1.4) does not satisfy the no-slip condition, it is not an acceptable solution of the equations of viscous flow. This is why we shall search a velocity field of the form ([33])

$$v_1 = ax_1 f'(x_2), \quad v_2 = -af(x_2), \quad v_3 = 0, \quad x_1 \in \mathbb{R}, \quad x_2 \in \mathbb{R}^+, \quad (1.8)$$

together with  $f$  sufficiently regular unknown function ( $f \in C^3(\mathbb{R}^+)$ ). This function represents the similarity transformation which reduces the Navier-Stokes equation to a nonlinear ordinary differential equation. The form of the velocity assures that the fluid is incompressible.

Condition (1.7) supplies

$$f(0) = 0, \quad f'(0) = 0. \quad (1.9)$$

As it is reasonable from the physical point of view, we assume also that at infinity the flow of a viscous fluid approaches the flow of an inviscid fluid whose velocity is given by (1.5) ([19]).

Therefore to (1.6) and (1.2)<sub>2</sub> we must also append the following boundary condition

$$\lim_{x_2 \rightarrow +\infty} f'(x_2) = 1. \quad (1.10)$$

The previous condition implies

$$\lim_{x_2 \rightarrow +\infty} v_1 = ax_1,$$

while for the second component of the velocity we can only conclude that

$$v_2 \sim -ax_2 \text{ for } x_2 \rightarrow +\infty,$$

because, as can be easily obtained from the L'Hôpital's rule, if  $f'(x_2) = 1$  for  $x_2 \rightarrow +\infty$ , then

$$\lim_{x_2 \rightarrow +\infty} \frac{f(x_2)}{x_2} = 1,$$

that is  $f \sim x_2$  for  $x_2 \rightarrow +\infty$ .

Actually, as we will see from the numerical integration, there exists a constant  $A$  different from zero such that the asymptotic behaviour of  $f$  at infinity is related to  $A$  in the following way:

$$\lim_{x_2 \rightarrow +\infty} [f(x_2) - x_2] = -A. \quad (1.11)$$

Further  $A$  is not an arbitrary constant but is determined as part of the solution of the flow ([47]). The existence of this constant has been proved by Hartmann in [28].

As it is well known, it is easy to prove the following ([33]):

**THEOREM 1.1.5.** *Let a homogeneous, incompressible Newtonian fluid occupy the region  $\mathcal{S}$ . The steady orthogonal plane stagnation-point flow of such a fluid has the following form:*

$$\begin{aligned} \mathbf{v} &= ax_1 f'(x_2) \mathbf{e}_1 - af(x_2) \mathbf{e}_2, \\ p &= -\rho \frac{a^2}{2} [x_1^2 + f^2(x_2)] - \rho a \nu f'(x_2) + p_0, \quad x_1 \in \mathbb{R}, \quad x_2 \in \mathbb{R}^+, \end{aligned}$$

where  $f$  satisfies equation

$$\frac{\nu}{a} f''' + f f'' - f'^2 + 1 = 0, \quad (1.12)$$

with the boundary conditions (1.9) and (1.10).

If we put

$$\eta = \sqrt{\frac{a}{\nu}} x_2, \quad \varphi(\eta) = \sqrt{\frac{a}{\nu}} f \left( \sqrt{\frac{\nu}{a}} \eta \right), \quad (1.13)$$

then we can write problem (1.12), (1.9), (1.10) in dimensionless form

$$\begin{aligned} \varphi''' + \varphi \varphi'' - \varphi'^2 + 1 &= 0, \\ \varphi(0) = 0, \quad \varphi'(0) &= 0, \\ \lim_{\eta \rightarrow +\infty} \varphi'(\eta) &= 1. \end{aligned} \quad (1.14)$$

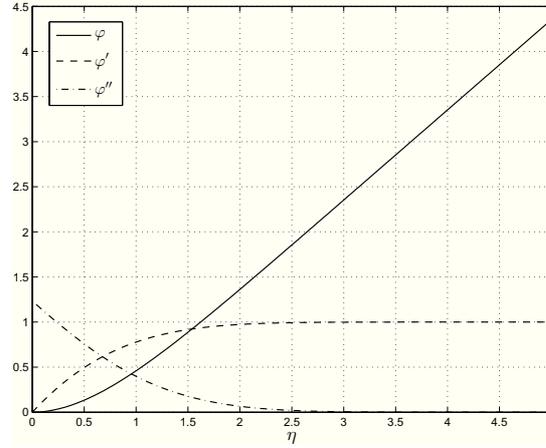


Figure 1.3: Plot showing the behaviour of  $\varphi$  (Hiemenz function),  $\varphi'$ ,  $\varphi''$ .

With this transformation, we also denote by

$$\alpha = \sqrt{\frac{a}{\nu}} A. \quad (1.15)$$

The function  $\varphi$  satisfies the well known Hiemenz equation ([47], [19], [33]). Due to the non-linearity of (1.14), the solution of the Hiemenz stagnation-point flow cannot be expressed in closed form, however we can compute it by a numerical integration.

Existence and uniqueness of the solution to Hiemenz stagnation-point flow were shown by Hartmann ([28]), Tam ([51]), Craven and Peletier ([12]).

We have solved numerically problem (1.14) using the `bvp4c` MATLAB routine. Figure 1.3 shows the graphics of Hiemenz function and its derivatives.

**REMARK 1.1.6.** *As one can see from Figure 1.3, the solution  $\varphi$  of problem (1.14) satisfies the conditions*

$$\lim_{\eta \rightarrow +\infty} \varphi''(\eta) = 0, \quad \lim_{\eta \rightarrow +\infty} \varphi'(\eta) = 1;$$

therefore we define:

- $\bar{\eta}_\varphi$  the value of  $\eta$  such that  $\varphi'(\bar{\eta}_\varphi) = 0.99$ .

Hence if  $\eta > \bar{\eta}_\varphi$ , then  $\varphi \cong \eta - \alpha$  and in this region the Newtonian fluid behaves like an inviscid one.

The thickness of the layer affected by the viscosity is  $\delta_v := \bar{\eta}_\varphi \sqrt{\frac{\nu}{a}}$ .

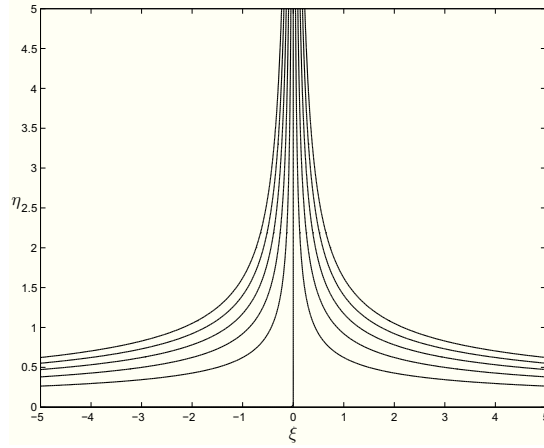


Figure 1.4: Plots showing the streamlines in the orthogonal stagnation-point flow of a Newtonian fluid.

From the numerical integration, we get

- $\varphi''(0) = 1.2326$ ;
- at  $\eta = 2.3796$  one has  $\varphi' = 0.99$  and if  $\eta > 2.3795$  then  $\varphi \cong \eta - 0.6479$ .

Hence  $\alpha = 0.6479$  and the viscosity appears only in a small region near the boundary whose thickness is

$$\delta_v = 2.3796 \sqrt{\frac{\nu}{a}}.$$

Figure 1.4 shows the streamlines of the flow ( $\xi = \sqrt{\frac{a}{2}}x_1$ ). Our results are consistent with the previous studies ([33], [19], [55]).

### 1.1.3 Micropolar fluids

Let us consider the steady two-dimensional orthogonal stagnation-point flow of a homogeneous, incompressible micropolar fluid towards a flat surface coinciding with the plane  $x_2 = 0$ , the flow being confined to the region  $\mathcal{S}$  having the equation (1.1).

In the absence of external mechanical body forces and body couples, the equations for such a fluid are ([41])

$$\begin{aligned} \mathbf{v} \cdot \nabla \mathbf{v} &= -\frac{1}{\rho} \nabla p + (\nu + \nu_r) \Delta \mathbf{v} + 2\nu_r (\nabla \times \mathbf{w}), \\ \nabla \cdot \mathbf{v} &= 0, \\ I\mathbf{v} \cdot \nabla \mathbf{w} &= \lambda \Delta \mathbf{w} + \lambda_0 \nabla (\nabla \cdot \mathbf{w}) - 4\nu_r \mathbf{w} + 2\nu_r (\nabla \times \mathbf{v}), \end{aligned} \quad (1.16)$$

where  $\mathbf{w}$  is the microrotation field,  $\nu$  is the kinematic newtonian viscosity coefficient,  $\nu_r$  is the microrotation viscosity coefficient,  $\lambda, \lambda_0$  (positive constants) are material parameters related to the coefficient of angular viscosity and  $I$  is the microinertia coefficient. Of course, Remark 1.1.1 holds.

We notice that in [20], [21], eqs. (1.16) are slightly different, as they are deduced as a special case of much more general model of microfluids. For the details, we refer to [41], p.23.

As far as the boundary conditions are concerned, of course, we modify condition (1.3) and we prescribe the strict adherence condition for the microrotation  $\mathbf{w}$ , i.e.

$$\mathbf{v}|_{x_2=0} = \mathbf{0}, \quad \mathbf{w}|_{x_2=0} = \mathbf{0}. \quad (1.17)$$

Other boundary conditions for the microrotation are possible. We refer to Eringen ([20], p.17-18) for a complete discussion. In our studies we will always assume the strict adherence condition for the microrotation field.

Following Guram and Smith ([27]) we use the following similarity transformation to the describe the velocity and the microrotation

$$\begin{aligned} v_1 &= ax_1 f'(x_2), \quad v_2 = -af(x_2), \quad v_3 = 0, \\ w_1 &= 0, \quad w_2 = 0, \quad w_3 = x_1 F(x_2), \quad x_1 \in \mathbb{R}, \quad x_2 \in \mathbb{R}^+, \end{aligned} \quad (1.18)$$

where  $f, F$  are sufficiently regular unknown functions ( $f \in C^3(\mathbb{R}^+)$ ,  $F \in C^2(\mathbb{R}^+)$ ).

From conditions (1.17) we get

$$f(0) = 0, \quad f'(0) = 0, \quad F(0) = 0. \quad (1.19)$$

As explained previously, we assume that at infinity, the flow approaches the flow of an inviscid fluid given by (1.5).

Therefore to (1.18) we also append the following conditions

$$\lim_{x_2 \rightarrow +\infty} f'(x_2) = 1, \quad \lim_{x_2 \rightarrow +\infty} F(x_2) = 0. \quad (1.20)$$

Condition (1.20)<sub>2</sub> means that at infinity,  $\mathbf{w} = \frac{1}{2} \nabla \times \mathbf{v}$ , i.e. the micropolar fluid behaves like an inviscid fluid whose velocity  $\mathbf{v}$  is given by (1.5).

As for the Newtonian fluid, the asymptotic behaviour of  $f$  at infinity is related to the constant  $A$ , which is determined as part of the solution of the problem, in the following way:

$$\lim_{x_2 \rightarrow +\infty} [f(x_2) - x_2] = -A. \quad (1.21)$$

THEOREM 1.1.7. *Let a homogeneous, incompressible micropolar fluid occupy the region  $\mathcal{S}$ . The steady orthogonal plane stagnation-point flow of such a fluid has the following form:*

$$\begin{aligned} \mathbf{v} &= ax_1 f'(x_2) \mathbf{e}_1 - af(x_2) \mathbf{e}_2, \quad \mathbf{w} = x_1 F(x_2) \mathbf{e}_3, \\ p &= -\rho \frac{a^2}{2} [x_1^2 + f^2(x_2)] - \rho a(\nu + \nu_r) f'(x_2) - 2\nu_r \rho \int_0^{x_2} F(s) ds + p_0, \\ x_1 &\in \mathbb{R}, \quad x_2 \in \mathbb{R}^+, \end{aligned}$$

where  $(f, F)$  satisfies the problem

$$\begin{aligned} \frac{\nu + \nu_r}{a} f''' + f f'' - f'^2 + 1 + \frac{2\nu_r}{a^2} F' &= 0, \\ \lambda F'' + aI(fF' - f'F) - 2\nu_r(2F + af'') &= 0, \end{aligned} \quad (1.22)$$

and (1.19), (1.20), provided  $F \in L^1([0, +\infty))$ .

REMARK 1.1.8. *If  $\nu_r = 0$ , then (1.22)<sub>1</sub> is the equation governing the orthogonal stagnation-point flow of a Newtonian fluid (Hiemenz equation, see previous section).*

We now write the system (1.22), together with the conditions (1.19) and (1.20), in dimensionless form. To this end we put

$$\begin{aligned} \eta &= \sqrt{\frac{a}{\nu + \nu_r}} x_2, \quad \varphi(\eta) = \sqrt{\frac{a}{\nu + \nu_r}} f \left( \sqrt{\frac{\nu + \nu_r}{a}} \eta \right), \\ \Phi(\eta) &= \frac{2\nu_r}{a^2} \sqrt{\frac{a}{\nu + \nu_r}} F \left( \sqrt{\frac{\nu + \nu_r}{a}} \eta \right). \end{aligned} \quad (1.23)$$

So system (1.22), (1.19) and (1.20) can be written as

$$\begin{aligned} \varphi''' + \varphi \varphi'' - \varphi'^2 + 1 + \Phi' &= 0, \\ \Phi'' + c_3(\varphi \Phi' - \varphi' \Phi) - c_2 \Phi - c_1 \varphi'' &= 0, \\ \varphi(0) = 0, \quad \varphi'(0) = 0, \quad \Phi(0) = 0, \\ \lim_{\eta \rightarrow +\infty} \varphi'(\eta) = 1, \quad \lim_{\eta \rightarrow +\infty} \Phi(\eta) = 0, \end{aligned} \quad (1.24)$$

where

$$c_1 = \frac{4\nu_r^2}{\lambda a}, \quad c_2 = \frac{4\nu_r(\nu + \nu_r)}{\lambda a}, \quad c_3 = \frac{I}{\lambda}(\nu + \nu_r) \quad (1.25)$$

are the material parameters which describe the micropolar nature of the fluid.

We put

$$\alpha = \sqrt{\frac{a}{\nu + \nu_r}} A. \quad (1.26)$$

Problem (1.24) is a nonlinear ordinary differential boundary value problem so it is possible to compute numerically its solution.

REMARK 1.1.9. *The numerical integration reveals that*

$$\lim_{\eta \rightarrow +\infty} \varphi''(\eta) = 0, \quad \lim_{\eta \rightarrow +\infty} \varphi'(\eta) = 1, \quad \lim_{\eta \rightarrow +\infty} \Phi(\eta) = 0.$$

Therefore we denote by:

- $\bar{\eta}_\varphi$  the value of  $\eta$  such that  $\varphi'(\bar{\eta}_\varphi) = 0.99$ ;
- $\bar{\eta}_\Phi$  the value of  $\eta$  such that  $\Phi(\bar{\eta}_\Phi) = -0.01$ .

Hence if  $\eta > \bar{\eta}_\varphi$  then  $\varphi \cong \eta - \alpha$ , and if  $\eta > \bar{\eta}_\Phi$ , then  $\Phi \cong 0$ . This means that the influence of the viscosity on the velocity and on the microrotation appears only in a layer lining the boundary whose thickness is  $\bar{\eta}_\varphi$  for the velocity and  $\bar{\eta}_\Phi$  for the microrotation.

The thickness  $\delta$  of the boundary layer for the flow is defined as

$$\delta := \max(\bar{\eta}_\varphi, \bar{\eta}_\Phi).$$

Further, the thickness of the layer affected by the viscosity is proportional to  $\sqrt{\frac{\nu + \nu_r}{a}}$ .

We have solved numerically problem (1.24) for different values of  $c_1, c_2, c_3$ , chosen according to Guram and Smith ([27]).

Figure 1.5<sub>1</sub> shows the graphics of  $\varphi$  function and its derivatives for  $c_1 = 0.5, c_2 = 3.0, c_3 = 0.5$ , while the behaviour of  $\Phi$  and  $\Phi'$  for  $c_1 = 0.5, c_2 = 3.0, c_3 = 0.5$  is displayed in Figure 1.5<sub>2</sub>.

We have provided these two representative graphs to elucidate the trends of the functions describing the velocity and the microrotation. The other choices of  $c_1, c_2, c_3$  modify the trends of these functions very slightly.

The values selected of  $c_1, c_2, c_3$  are given in Table 1.1, where we reported also the consequent values of  $\alpha, \varphi''(0), \Phi'(0), \bar{\eta}_\varphi, \bar{\eta}_\Phi$ .

From Table 1.1 it appears that if we fix two parameters among  $c_1, c_2, c_3$ , then the values of  $\alpha, \varphi''(0), \Phi'(0)$ , have the following behaviour :

- they increase as  $c_2$  or  $c_3$  increases;

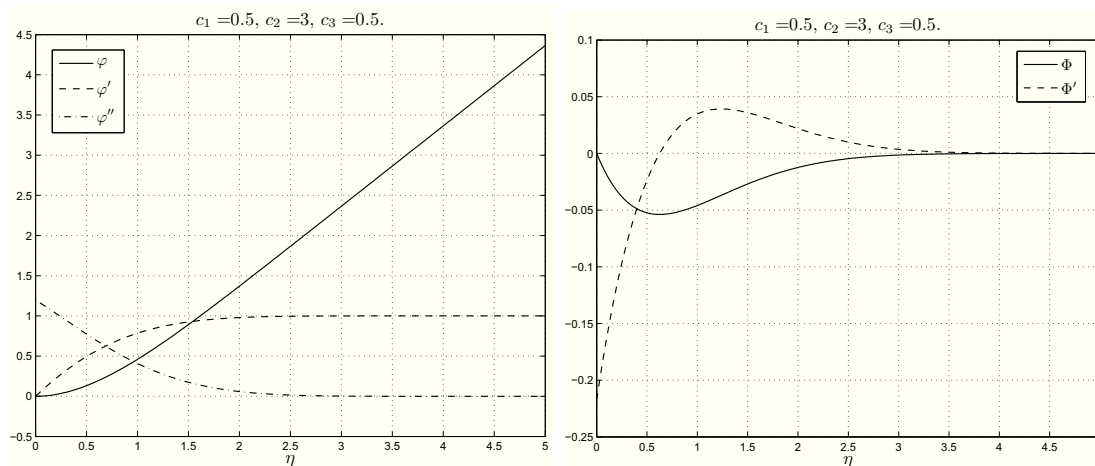


Figure 1.5: Plots showing the behaviour of  $\varphi$ ,  $\varphi'$ ,  $\varphi''$  and  $\Phi$ ,  $\Phi'$ , respectively, for  $c_1 = 0.5$ ,  $c_2 = 3.0$ ,  $c_3 = 0.5$ .

Table 1.1: Descriptive quantities of the motion for some values of  $c_1$ ,  $c_2$ ,  $c_3$ .

$c_1$	$c_2$	$c_3$	$\varphi''(0)$	$\Phi'(0)$	$\alpha$	$\bar{\eta}_\varphi$	$\bar{\eta}_\Phi$	$\delta$
0.1	1.5	0.1	1.2218	-0.0532	0.6446	2.3257	1.6004	2.3257
		0.5	1.2231	-0.0510	0.6448	2.3369	1.3324	2.3369
	3.0	0.1	1.2250	-0.0444	0.6453	2.3466	1.0012	2.3466
		0.5	1.2256	-0.0434	0.6454	2.3517	0.8459	2.3517
0.5	1.5	0.1	1.1780	-0.2659	0.6310	2.1269	2.9083	2.9083
		0.5	1.1848	-0.2553	0.6321	2.1676	2.4321	2.4321
	3.0	0.1	1.1943	-0.2220	0.6350	2.2154	2.3427	2.3427
		0.5	1.1972	-0.2173	0.6356	2.2389	2.1179	2.2389

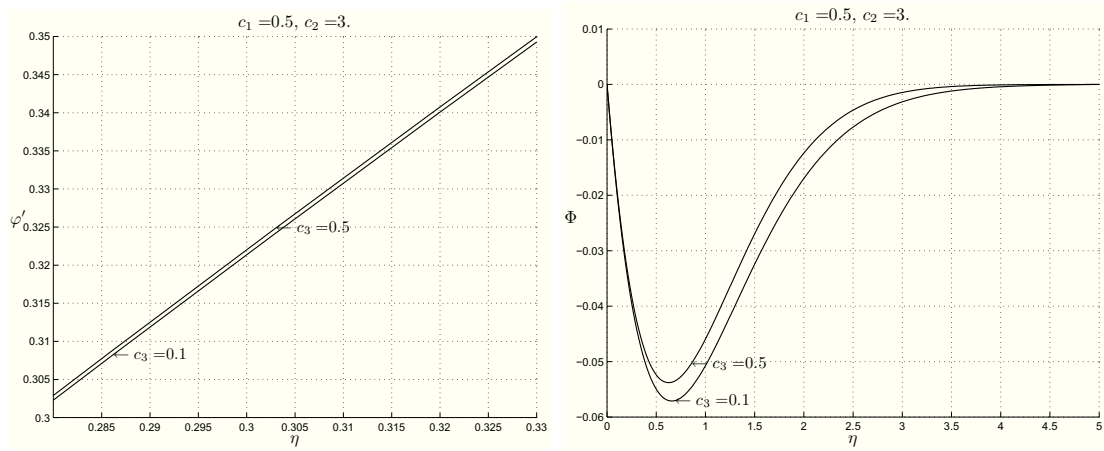


Figure 1.6: Plots showing the behaviour of  $\varphi'$  and  $\Phi$  for  $c_1 = 0.5$ ,  $c_2 = 3.0$  fixed, and for different values of  $c_3$ .

- they decrease as  $c_1$  increases.

The influence of  $c_1$  appears more considerable also on the other quantities quoted in the Table.

Figures 1.6, 1.7, and 1.8 elucidate the dependence of the functions  $\varphi'$ ,  $\Phi$  on the parameters  $c_1$ ,  $c_2$ ,  $c_3$ . We can see that the function which appears most influenced by  $c_1$ ,  $c_2$ ,  $c_3$  is  $\Phi$ , in other words the microrotation. More precisely, the profile of  $\Phi$  rises as  $c_3$  or  $c_2$  increases and  $c_1$  decreases. As it happened for the descriptive quantities of the motion,  $c_1$  is the parameter that most affects the microrotation. The function  $\varphi'$  does not show considerable variations as  $c_1$ ,  $c_2$ ,  $c_3$  assume different values.

From Table 1.1, it appears also that the presence of the microrotation modifies the values of  $\alpha$ ,  $\varphi''(0)$ ,  $\bar{\eta}_\varphi$ , which are smaller than in the case of a Newtonian fluid (see Chapter 1.1.2). Hence the thickness of the boundary layer for the velocity is smaller than that of the Newtonian fluid.

Our results are consistent with the studies available in the literature and extend them.

Finally, Figure 1.9 shows the streamlines of the flow for  $c_1 = 0.5$ ,  $c_2 = 3.0$ ,  $c_3 = 0.5$ .

## 1.2 Oblique stagnation-point flow

From a mathematical point of view, it is possible to combine the orthogonal stagnation-point flow with a shear flow parallel to the wall. In this way we get the oblique

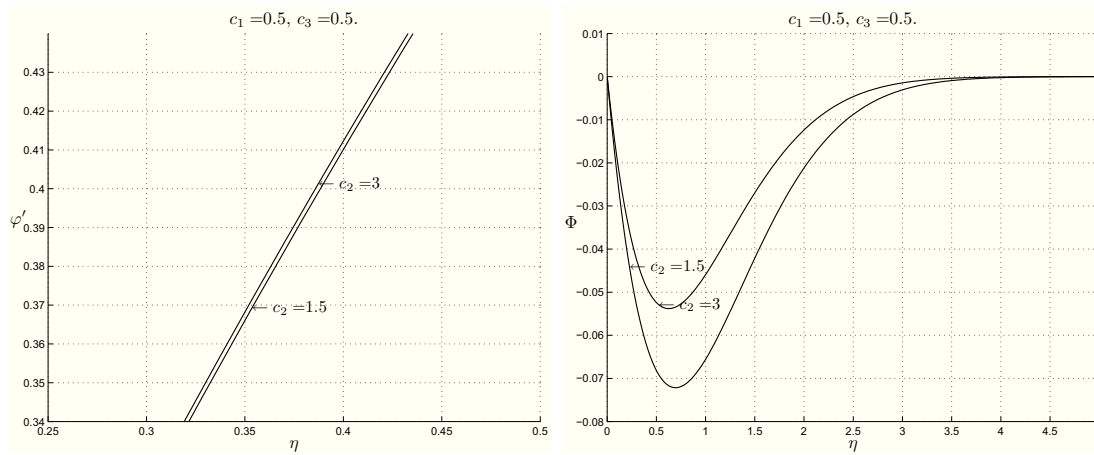


Figure 1.7: Plots showing the behaviour of  $\varphi'$  and  $\Phi$  for  $c_1 = 0.5$ ,  $c_3 = 0.5$  fixed, and for different values of  $c_2$ .

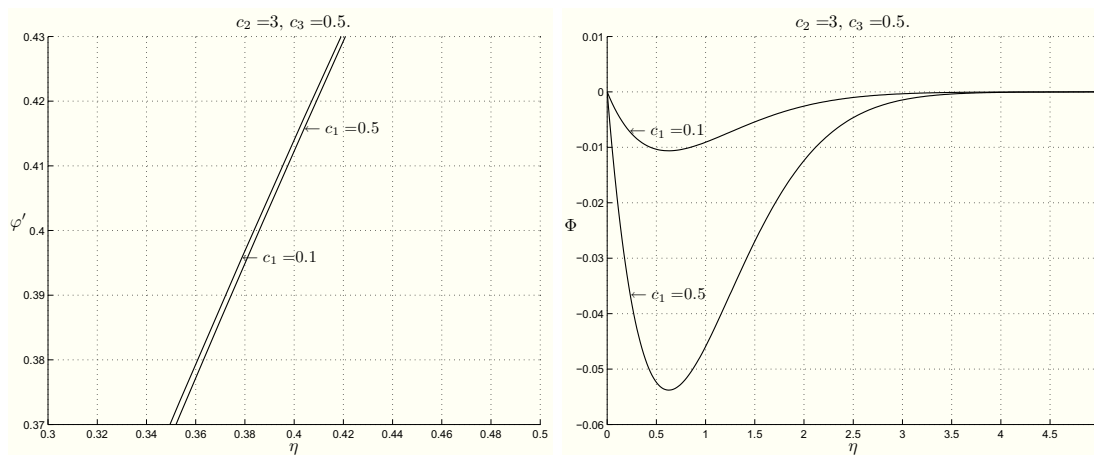


Figure 1.8: Plots showing the behaviour of  $\varphi'$  and  $\Phi$  for  $c_2 = 3.0$ ,  $c_3 = 0.5$  fixed, and for different values of  $c_1$ .

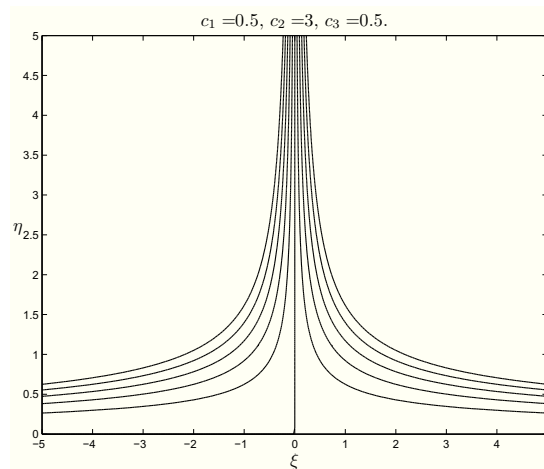


Figure 1.9: Plots showing the streamlines in the orthogonal stagnation-point flow of a micropolar fluid for  $c_1 = 0.5$ ,  $c_2 = 3.0$ ,  $c_3 = 0.5$ .

stagnation-point flow, which appears physically for example when a jet of fluid impinges obliquely on a rigid wall at an arbitrary angle of incidence.

The steady two-dimensional oblique stagnation-point flow of a Newtonian fluid has been studied for the first time by Stuart in 1959 ([50]). The oblique solution has attracted many investigations during the past several decades (i.e. [52], [16], [18], [54], [55]). It should be mentioned among the recent papers that Drazin and Raley ([19]) and Tooke and Blyth ([53]) reviewed the problem and included a free parameter associated with the shear flow component. As we will see, this free parameter alters the structure of the shear flow component by varying the magnitude of the pressure gradient.

The oblique stagnation-point flow of a micropolar fluid has been studied in [39], and [40] under restrictive assumptions on the material parameters and following a different approach from ours. Hence the results presented here for this model of fluids are new.

In order to study such a flow for a Newtonian and a micropolar fluid, it is appropriate to start with the analysis of the same flow for an inviscid fluid.

### 1.2.1 Inviscid fluids

Consider the steady plane flow of a homogeneous, incompressible inviscid fluid near a stagnation point occupying the region  $\mathcal{S}$  given by (1.1).

The equations governing such a flow in the absence of external mechanical body forces are (1.2) to which we append the no-penetration condition (1.3) for the velocity  $\mathbf{v}$ .

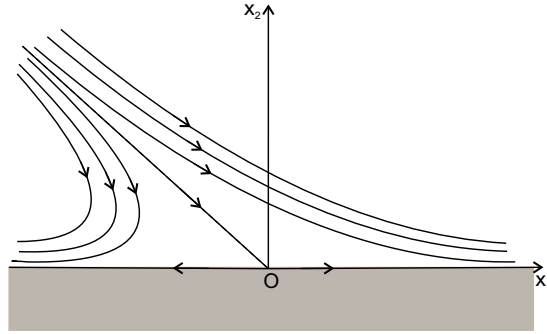


Figure 1.10: Oblique stagnation-point flow description.

The oblique plane stagnation-point flow of such a fluid is described by a velocity field of the form

$$v_1 = ax_1 + bx_2, \quad v_2 = -ax_2, \quad v_3 = 0, \quad x_1 \in \mathbb{R}, \quad x_2 \in \mathbb{R}^+, \quad (1.27)$$

with  $a, b$  constants ( $a > 0$ ).

As known, the streamlines of such a flow are hyperbolas whose asymptotes have the equations:

$$x_2 = 0 \quad \text{and} \quad x_2 = -\frac{2a}{b}x_1.$$

These two straight-lines are degenerate streamlines too (see Figure 1.10).

It is easy to check that it holds:

**THEOREM 1.2.1.** *Let a homogeneous, incompressible inviscid fluid occupy the region  $\mathcal{S}$ . The steady oblique plane stagnation-point flow of such a fluid has the following form:*

$$\begin{aligned} \mathbf{v} &= (ax_1 + bx_2)\mathbf{e}_1 - ax_2\mathbf{e}_2, \\ p &= -\frac{1}{2}\rho a^2(x_1^2 + x_2^2) + p_0, \quad x_1 \in \mathbb{R}, \quad x_2 \in \mathbb{R}^+. \end{aligned}$$

**REMARK 1.2.2.** *As in the orthogonal case, in order to study the oblique stagnation-point flow of Newtonian or micropolar fluids, it is convenient to consider a more general flow. Actually, we suppose the fluid obliquely impinging on the flat plane  $x_2 = A$  and*

$$v_1 = ax_1 + b(x_2 - B), \quad v_2 = -a(x_2 - A), \quad v_3 = 0, \quad x_1 \in \mathbb{R}, \quad x_2 \geq A, \quad (1.28)$$

with  $A, B = \text{constants}$ .

*In this way, the stagnation point is  $\left(\frac{b}{a}(B - A), A\right)$  and the streamlines are hyperbolas whose asymptotes are  $x_2 = -\frac{2a}{b}x_1 + 2B - A$  and  $x_2 = A$ .*

It is easy to compute the pressure field:

$$p = -\frac{1}{2}\rho a^2 \left[ \left( x_1 - \frac{b}{a}(B-A) \right)^2 + (x_2 - A)^2 \right] + p_0.$$

Hence under these new assumptions, the result contained in Theorem 1.2.1 continues to hold by replacing  $x_1, x_2$  with  $x_1 - \frac{b}{a}(B-A), x_2 - A$ , respectively.

### 1.2.2 Newtonian fluids

We now consider the same flow of a homogeneous, incompressible Newtonian fluid.

The equations governing the oblique stagnation-point flow of such a fluid in the absence of external mechanical body forces are the equations (1.2) where  $(1.2)_1$  is replaced by (1.6).

We prescribe the no-slip boundary condition (1.7) for the velocity.

We are interested in the oblique plane stagnation-point flow so that

$$v_1 = ax_1 f'(x_2) + bg(x_2), \quad v_2 = -af(x_2), \quad v_3 = 0, \quad x_1 \in \mathbb{R}, \quad x_2 \in \mathbb{R}^+, \quad (1.29)$$

with  $f, g$  sufficiently regular unknown functions ( $f \in C^3(\mathbb{R}^+)$ ,  $g \in C^2(\mathbb{R}^+)$ ). The condition (1.7) supplies

$$f(0) = 0, \quad f'(0) = 0, \quad g(0) = 0. \quad (1.30)$$

Likewise to the orthogonal stagnation-point flow, we assume that at infinity the flow approaches the motion of an inviscid fluid given by (1.27) ([19], [53]).

Therefore  $f, g$  have also to satisfy the following boundary conditions

$$\lim_{x_2 \rightarrow +\infty} f'(x_2) = 1, \quad \lim_{x_2 \rightarrow +\infty} g'(x_2) = 1. \quad (1.31)$$

In particular, the asymptotic behaviour of  $f$  and  $g$  at infinity is related to the constants  $A, B$  in Remark 1.2.2 in the following way:

$$\lim_{x_2 \rightarrow +\infty} [f(x_2) - x_2] = -A, \quad \lim_{x_2 \rightarrow +\infty} [g(x_2) - x_2] = -B. \quad (1.32)$$

As we will see,  $A$  is determined as part of the solution of the orthogonal flow ([47]), instead  $B$  is a free parameter ([19]).

The results found in literature can be summarize in

**THEOREM 1.2.3.** *Let a homogeneous, incompressible Newtonian fluid occupy the region  $\mathcal{S}$ . The steady oblique plane stagnation-point flow of such a fluid has the*

following form:

$$\begin{aligned} \mathbf{v} &= [ax_1f'(x_2) + bg(x_2)]\mathbf{e}_1 - af(x_2)\mathbf{e}_2, \\ p &= -\rho\frac{a^2}{2}\left[x_1^2 - 2\frac{b}{a}(B - A)x_1 + f^2(x_2)\right] - \rho a\nu f'(x_2) + p_0, \quad x_1 \in \mathbb{R}, \quad x_2 \in \mathbb{R}^+, \end{aligned} \quad (1.33)$$

where  $(f, g)$  satisfies the problem

$$\begin{aligned} \frac{\nu}{a}f''' + ff'' - f'^2 + 1 &= 0, \\ \frac{\nu}{a}g'' + fg' - f'g &= B - A, \end{aligned} \quad (1.34)$$

together with the boundary conditions (1.30) and (1.31).

We remark that the function  $f$  satisfies the same differential problem that governs the orthogonal stagnation-point flow (Chapter 1.1.2).

As we can see from (1.33)<sub>2</sub>,  $\nabla p$  has a constant component in the  $x_1$  direction proportional to  $B - A$ , which does not appear in the orthogonal stagnation-point flow. This component determines the displacement of the uniform shear flow parallel to the wall  $x_2 = 0$ .

If we put

$$\eta = \sqrt{\frac{a}{\nu}}x_2, \quad \varphi(\eta) = \sqrt{\frac{a}{\nu}}f\left(\sqrt{\frac{\nu}{a}}\eta\right), \quad \gamma(\eta) = \sqrt{\frac{a}{\nu}}g\left(\sqrt{\frac{\nu}{a}}\eta\right), \quad (1.35)$$

we can write problem (1.34), (1.30), (1.31) in dimensionless form

$$\begin{aligned} \varphi''' + \varphi\varphi'' - \varphi'^2 + 1 &= 0, \\ \gamma'' + \varphi\gamma' - \varphi'\gamma &= \beta - \alpha, \\ \varphi(0) = 0, \quad \varphi'(0) = 0, \quad \gamma(0) = 0, \\ \lim_{\eta \rightarrow +\infty} \varphi'(\eta) = 1, \quad \lim_{\eta \rightarrow +\infty} \gamma'(\eta) = 1, \end{aligned} \quad (1.36)$$

where

$$\alpha = \sqrt{\frac{a}{\nu}}A, \quad \beta = \sqrt{\frac{a}{\nu}}B. \quad (1.37)$$

Notice the one-way coupling, that the function  $\varphi$  influences the functions  $\gamma$ , but not viceversa.

The function  $\varphi$  satisfies the Hiemenz equation ([47], [19]). As we said in Chapter

1.1.2, the solution of the Hiemenz stagnation flow cannot be expressed in closed form but we can compute it numerically. From the numerical integration we also get the value of  $\alpha$  and so we just have to fix the value of  $\beta$  in order to solve problem (1.36)<sub>2,5,7</sub>.

Nevertheless, if we regard  $f$  as a known function, then the solution of problem (1.36)<sub>2,5,7</sub> is formally obtained as ([19])

$$\gamma(\eta) = (\alpha - \beta)\varphi'(\eta) + C\varphi''(\eta)\Xi(\eta), \quad (1.38)$$

with

$$C = \varphi''(0)[\gamma'(0) - \varphi''(0)(\alpha - \beta)], \quad \Xi(\eta) = \int_0^\eta [(\varphi''(s))^{-2} e^{-\int_0^s \varphi(t) dt}] ds. \quad (1.39)$$

We note that the constant  $C$  contains  $\alpha$ ,  $\varphi''(0)$ ,  $\gamma'(0)$ , which are not a priori assigned but their values are determined by part of the solutions of problem (1.36).

We have computed the functions  $\gamma$ ,  $\gamma'$  (as well as  $\varphi$ ,  $\varphi'$ ,  $\varphi''$ ) numerically for various values of the parameter  $\beta$ . Precisely we have chosen  $\beta - \alpha = -5 - \alpha$ ,  $-\alpha$ ,  $0$ ,  $\alpha$ ,  $5 - \alpha$  (as in [53]). Other Authors (e.g. Stuart ([50]) and Tamada ([52])) take  $\beta = \alpha$ , while Dorrepaal takes  $\beta = 0$  ([16], [18]). Equations (1.36)<sub>1,2</sub> have been solved simultaneously.

**REMARK 1.2.4.** *As pointed out by Dorrepaal ([16], [18]), along the wall  $x_2 = 0$  there are three important coordinates: the origin  $x_1 = 0$ , which is the stagnation point, the point  $x_1 = x_p$  of maximum pressure and the point  $x_1 = x_s$  of zero tangential stress (zero skin friction) where the dividing streamline of equation*

$$\xi\varphi(\eta) + \frac{b}{a} \int_0^\eta \gamma(s) ds = 0, \quad \xi = \sqrt{\frac{\nu}{a}} x_1 \quad (1.40)$$

*meets the boundary.*

*In consideration of (1.33) and (1.29), one shows that*

$$x_p = b\sqrt{\frac{\nu}{a^3}}(\beta - \alpha), \quad x_s = -b\sqrt{\frac{\nu}{a^3}} \frac{\gamma'(0)}{\varphi''(0)}. \quad (1.41)$$

*We note that the ratio*

$$\frac{x_p}{x_s} = (\alpha - \beta) \frac{\varphi''(0)}{\gamma'(0)}$$

*is the same for all angles of incidence.*

*Finally, studying the small- $\eta$  behaviour of*

$$\frac{\int_0^\eta \gamma(s) ds}{\varphi(\eta)},$$

the slope of the dividing streamline at the wall is given by ([19]):

$$m_s = -\frac{3a[\varphi''(0)]^2}{b[(\beta - \alpha)\varphi''(0) + \gamma'(0)]}$$

and it does not depend on the kinematic viscosity. Thus, the ratio of this slope to that of the dividing streamline at infinity

$$m_i = -\frac{2a}{b}$$

is the same for all oblique stagnation-point flows and it is given by

$$\frac{m_s}{m_i} = \frac{3}{2} \frac{[\varphi''(0)]^2}{[(\beta - \alpha)\varphi''(0) + \gamma'(0)]}. \quad (1.42)$$

This ratio is independent of  $a$  and  $b$ , depending on the constant pressure gradient parallel to the boundary through  $B - A$  ([18]).

REMARK 1.2.5. As we will see,  $\varphi$  and  $\gamma$  satisfy conditions (1.36)<sub>6,7</sub>. Further we find that

$$\lim_{\eta \rightarrow +\infty} [\varphi(\eta) - \eta] = -\alpha, \quad \lim_{\eta \rightarrow +\infty} [\gamma(\eta) - \eta] = -\beta.$$

Similarly to the orthogonal stagnation-point flow of a Newtonian fluid, we define:

- $\bar{\eta}_\varphi$  the value of  $\eta$  such that  $\varphi'(\bar{\eta}_\varphi) = 0.99$ ;
- $\bar{\eta}_\gamma$  the value of  $\eta$  such that  $\gamma'(\bar{\eta}_\gamma) = 0.99$ , if  $\beta - \alpha \geq 0$ , or  $\gamma' = 1.01$ , if  $\beta - \alpha < 0$ .

From the previous definitions follows that if  $\eta > \bar{\eta}_\varphi$  ( $\eta > \bar{\eta}_\gamma$ ), then  $\varphi \cong \eta - \alpha$  ( $\gamma \cong \eta - \beta$ ).

We define by  $\delta := \max(\bar{\eta}_\varphi, \bar{\eta}_\gamma)$  the thickness of the layer lining the boundary where the effect of the viscosity appears. This layer is proportional to  $\sqrt{\frac{\nu}{a}}$ .

Figure 1.11 shows the behaviour of Hiemenz function and its derivatives. As one can see,

$$\lim_{\eta \rightarrow +\infty} \varphi''(\eta) = 0, \quad \lim_{\eta \rightarrow +\infty} \varphi'(\eta) = 1.$$

At  $\eta = 2.4 =: \bar{\eta}_\varphi$  one has  $\varphi' = 0.99$  and if  $\eta > \bar{\eta}_\varphi$  then  $\varphi \sim \eta - 0.6479$ , so  $\alpha = 0.6479$ . From the numerical integration, we get  $\varphi''(0) = 1.2326$ . Our results are the same as in the previous studies and of course as in Chapter 1.1.2 since  $\varphi$  doesn't depend on  $\beta$ .

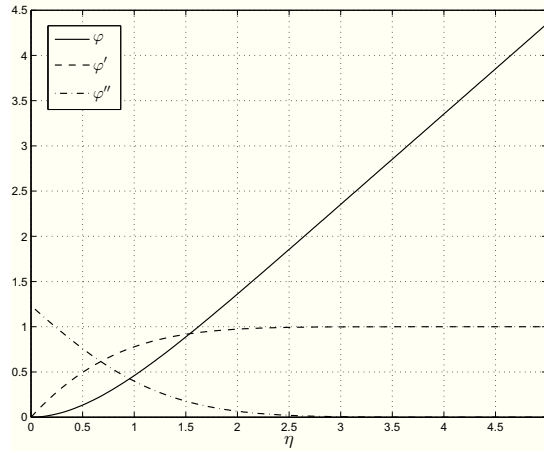


Figure 1.11: Plot showing the behaviour of  $\varphi$  (Hiemenz function),  $\varphi'$ ,  $\varphi''$ .

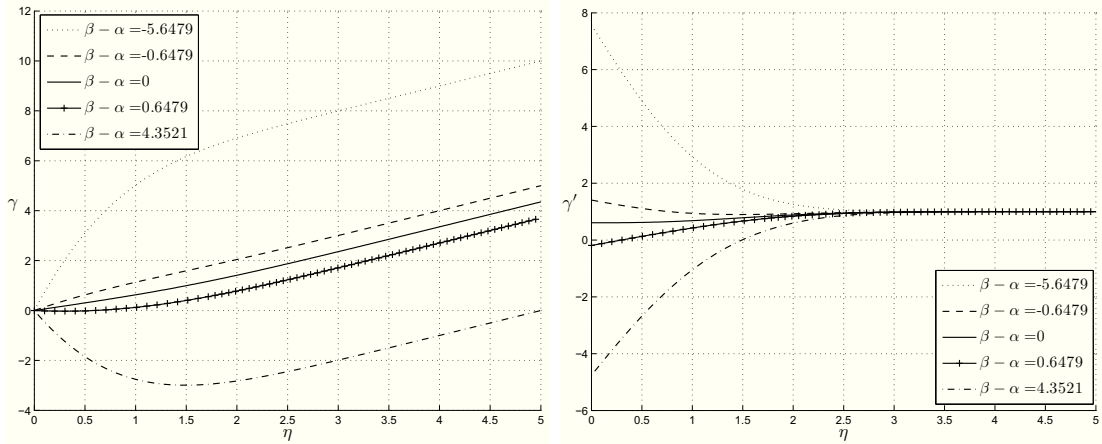


Figure 1.12: Figures 1.12<sub>1</sub> and 1.12<sub>2</sub> show  $\gamma$  and  $\gamma'$  with, from above,  $\beta - \alpha = -5 - \alpha, -\alpha, 0, \alpha, 5 - \alpha$ , respectively.

Table 1.2: Descriptive quantities of the motion for different values of  $\beta - \alpha$ .

$\beta - \alpha$	$\alpha$	$\beta$	$\varphi''(0)$	$\gamma'(0)$	$C$	$\frac{x_p}{x_s}$	$\frac{m_s}{m_i}$	$\bar{\eta}_\varphi$	$\bar{\eta}_\gamma$	$\delta$
-5.6479	0.6479	-5	1.2326	7.5695	0.7494	0.9197	3.7485	2.3795	3.0577	3.0577
-0.6479	0.6479	0	1.2326	1.4066	0.7494	0.5678	3.7485	2.3795	3.1099	3.1099
0	0.6479	0.6479	1.2326	0.6080	0.7494	0	3.7485	2.3795	3.1911	3.1911
0.6479	0.6479	1.2957	1.2326	-0.1906	0.7494	4.1892	3.7484	2.3795	3.2523	3.2523
4.3521	0.6479	5	1.2326	-4.7564	0.7494	1.1278	3.7484	2.3795	3.4556	3.4556

Figures 1.12<sub>1</sub>, 1.12<sub>2</sub> show the profiles of  $\gamma(\eta)$ ,  $\gamma'(\eta)$ , for  $\beta - \alpha = -5 - \alpha$ ,  $-\alpha$ ,  $0$ ,  $\alpha$ ,  $5 - \alpha$ .

As far as  $\gamma'(0)$  is concerned, we report in Table 1.2 its values for different  $\beta$  ( $\beta = -5, 0, \alpha, 2\alpha, 5$ ) together with the other characteristic quantities of the motion.

Table 1.2 points out that the constant  $C$  given by (1.39)<sub>1</sub> has always the same value,  $\simeq 0.749$ . This is in agreement to the value determined by Stuart and Glauert ([50], [22]) by means of asymptotic estimate of the integral  $\Xi(\eta)$  at infinity.

In Table 1.2 we list also the numerically computed values of  $\bar{\eta}_\varphi$  and of  $\bar{\eta}_\gamma$ . We have that  $\bar{\eta}_\gamma$  is always greater than  $\bar{\eta}_\varphi$ . Hence the influence of the viscosity appears only in a layer lining the boundary whose thickness is  $\bar{\eta}_\gamma$ . This thickness is larger than that in the orthogonal stagnation-point flow which is  $2.3795\sqrt{\frac{\nu}{a}}$ .

Observing again Table 1.2 we notice that  $x_s$  (given by (1.41)<sub>2</sub>) has the sign of  $b$  if  $\beta - \alpha > 0$  and the sign of  $-b$  if  $\beta - \alpha \leq 0$ . If  $b$  is positive (negative)  $x_s$  increases (decreases) as  $\beta - \alpha$  increases. As far as  $|x_s|$  is concerned, if  $\beta - \alpha$  increases from a negative value to zero,  $|x_s|$  decreases and so  $x_s$  approaches the origin, otherwise, as  $\beta - \alpha$  increases from zero to a positive value,  $|x_s|$  increases and so  $x_s$  departs from the origin.

Figures 1.13<sub>1</sub>, 1.13<sub>2</sub>, 1.13<sub>3</sub> show the streamlines and the points

$$\xi_p = \sqrt{\frac{a}{\nu}}x_p, \quad \xi_s = \sqrt{\frac{a}{\nu}}x_s$$

for  $\frac{b}{a} = 1$  and  $\beta - \alpha = -\alpha, 0, \alpha$ , respectively.

### 1.2.3 Micropolar fluids

Let us now discuss the steady two-dimensional oblique stagnation-point flow of a homogeneous, incompressible micropolar fluid towards a flat surface coinciding with the plane  $x_2 = 0$ . The region where the motion occurs is  $\mathcal{S}$  (given by (1.1)) and the origin is the stagnation-point.

In the absence of external mechanical body forces and body couples, the equations for such a fluid are (1.16) and the boundary conditions are (1.17).

Examination of equations (1.16) shows that these equations admit a similarity solution of the form

$$\begin{aligned} v_1 &= ax_1f'(x_2) + bg(x_2), & v_2 &= -af(x_2), & v_3 &= 0, \\ w_1 &= 0, & w_2 &= 0, & w_3 &= x_1F(x_2) + G(x_2), & x_1 &\in \mathbb{R}, & x_2 &\in \mathbb{R}^+, \end{aligned} \quad (1.43)$$

where  $f, g, F, G$  are sufficiently regular unknown functions ( $f \in C^3(\mathbb{R}^+)$ ,  $g, F, G \in C^2(\mathbb{R}^+)$ ).

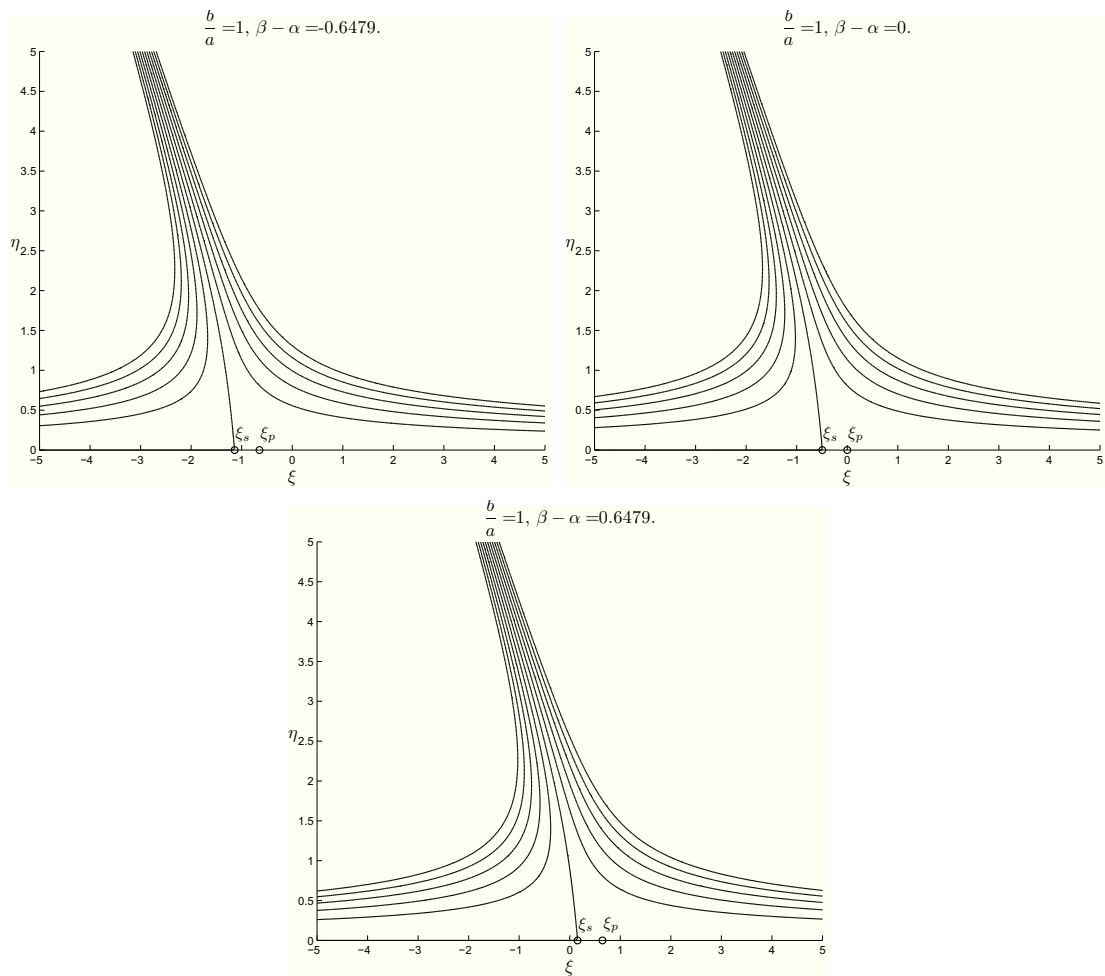


Figure 1.13: Plots showing the streamlines and the points  $\xi_p, \xi_s$  for  $\frac{b}{a} = 1$  and  $\beta - \alpha = -\alpha, 0, \alpha$ , respectively.

The conditions (1.17) supply

$$\begin{aligned} f(0) = 0, \quad f'(0) = 0, \quad g(0) = 0, \\ F(0) = 0, \quad G(0) = 0. \end{aligned} \quad (1.44)$$

Moreover, as it is reasonable from the physical point of view, we assume that at infinity, the flow of the micropolar fluid approaches the flow of an inviscid fluid given by (1.28).

Therefore to (1.44) we must also append the following conditions

$$\begin{aligned} \lim_{x_2 \rightarrow +\infty} f'(x_2) = 1, \quad \lim_{x_2 \rightarrow +\infty} g'(x_2) = 1, \\ \lim_{x_2 \rightarrow +\infty} F(x_2) = 0, \quad \lim_{x_2 \rightarrow +\infty} G(x_2) = -\frac{b}{2}. \end{aligned} \quad (1.45)$$

We stress that conditions (1.45)<sub>3,4</sub> assure that at infinity  $\mathbf{w} = \frac{1}{2}\nabla \times \mathbf{v}$ , i.e. the micropolar fluid behaves like an inviscid fluid whose velocity  $\mathbf{v}$  is given by (1.28).

The asymptotic behaviour of  $f$  and  $g$  at infinity is related to the constants  $A, B$ , in the following way:

$$\lim_{x_2 \rightarrow +\infty} [f(x_2) - x_2] = -A, \quad \lim_{x_2 \rightarrow +\infty} [g(x_2) - x_2] = -B. \quad (1.46)$$

As we will see and as it happened in the Newtonian case,  $B$  is the only free parameter because the value of  $A$  is computed as part of the solution of the orthogonal flow.

It is easy to prove the following:

**THEOREM 1.2.6.** *Let a homogeneous, incompressible micropolar fluid occupy the region  $\mathcal{S}$ . The steady oblique plane stagnation-point flow of such a fluid has the following form:*

$$\begin{aligned} \mathbf{v} = [ax_1 f'(x_2) + bg(x_2)]\mathbf{e}_1 - af(x_2)\mathbf{e}_2, \quad \mathbf{w} = [x_1 F(x_2) + G(x_2)]\mathbf{e}_3, \\ p = -\rho \frac{a^2}{2} [x_1^2 - 2\frac{b}{a}(B - A)x_1 + f^2(x_2)] - \rho a(\nu + \nu_r) f'(x_2) \\ - 2\nu_r \rho \int_0^{x_2} F(s) ds + p_0, \quad x_1 \in \mathbb{R}, \quad x_2 \in \mathbb{R}^+, \end{aligned} \quad (1.47)$$

where  $(f, g, F, G)$  satisfies the problem

$$\begin{aligned} \frac{\nu + \nu_r}{a} f''' + f f'' - f'^2 + 1 + \frac{2\nu_r}{a^2} F' &= 0, \\ \frac{\nu + \nu_r}{a} g'' + f g' - g f' + \frac{2\nu_r}{ab} G' &= B - A, \\ \lambda F'' + aI(fF' - f'F) - 2\nu_r(2F + af'') &= 0, \\ \lambda G'' + I(afG' - bgF) - 2\nu_r(2G + bg') &= 0, \end{aligned} \quad (1.48)$$

with boundary conditions (1.44), and (1.45), provided  $F \in L^1([0, +\infty))$ .

It is worth noting that in the literature, the oblique stagnation-point flow of a micropolar fluid has been studied in [39], and [40] under restrictive assumptions on the material parameters, and following a different approach. Hence Theorem 1.2.6 extends the results known.

REMARK 1.2.7. *If  $\nu_r = 0$ , then (1.48)<sub>1</sub> and (1.48)<sub>2</sub> are the equations governing the oblique stagnation-point flow of a Newtonian fluid (Chapter 1.2.2).*

*We observe that (1.48)<sub>1</sub> and (1.48)<sub>3</sub> have the same form as the equations found by Guram and Smith ([27]) for the orthogonal stagnation-point flow of a micropolar fluid (Chapter 1.1.3).*

Now we write the system (1.48), together with the conditions (1.44) and (1.45), in dimensionless form in order to facilitate the numerical integration. To this end we use the following dimensionless change of variables

$$\begin{aligned} \eta &= \sqrt{\frac{a}{\nu + \nu_r}} x_2, \quad \varphi(\eta) = \sqrt{\frac{a}{\nu + \nu_r}} f \left( \sqrt{\frac{\nu + \nu_r}{a}} \eta \right), \\ \gamma(\eta) &= \sqrt{\frac{a}{\nu + \nu_r}} g \left( \sqrt{\frac{\nu + \nu_r}{a}} \eta \right), \quad \Phi(\eta) = \frac{2\nu_r}{a^2} \sqrt{\frac{a}{\nu + \nu_r}} F \left( \sqrt{\frac{\nu + \nu_r}{a}} \eta \right), \\ \Gamma(\eta) &= \frac{2\nu_r}{b(\nu + \nu_r)} G \left( \sqrt{\frac{\nu + \nu_r}{a}} \eta \right). \end{aligned} \quad (1.49)$$

So system (1.48) can be written as

$$\begin{aligned} \varphi''' + \varphi\varphi'' - \varphi'^2 + 1 + \Phi' &= 0, \\ \gamma'' + \varphi\gamma' - \varphi'\gamma + \Gamma' &= \beta - \alpha, \\ \Phi'' + c_3(\varphi\Phi' - \varphi'\Phi) - c_2\Phi - c_1\varphi'' &= 0, \\ \Gamma'' + c_3(\varphi\Gamma' - \Phi\gamma) - c_2\Gamma - c_1\gamma' &= 0, \end{aligned} \quad (1.50)$$

where

$$\begin{aligned} c_1 &= \frac{4\nu_r^2}{\lambda a}, \quad c_2 = \frac{4\nu_r(\nu + \nu_r)}{\lambda a}, \quad c_3 = \frac{I}{\lambda}(\nu + \nu_r), \\ \alpha &= \sqrt{\frac{a}{\nu + \nu_r}}A, \quad \beta = \sqrt{\frac{a}{\nu + \nu_r}}B. \end{aligned} \quad (1.51)$$

The boundary conditions in dimensionless form become:

$$\begin{aligned} \varphi(0) &= 0, \quad \varphi'(0) = 0, \quad \gamma(0) = 0, \\ \Phi(0) &= 0, \quad \Gamma(0) = 0, \\ \lim_{\eta \rightarrow +\infty} \varphi'(\eta) &= 1, \quad \lim_{\eta \rightarrow +\infty} \gamma'(\eta) = 1 \\ \lim_{\eta \rightarrow +\infty} \Phi(\eta) &= 0, \quad \lim_{\eta \rightarrow +\infty} \Gamma(\eta) = -\frac{c_1}{c_2}. \end{aligned} \quad (1.52)$$

Problem (1.50), (1.52) can be integrated numerically in order to find the behaviour of the solution.

REMARK 1.2.8. *As in the Newtonian case, along the wall  $x_2 = 0$ , there are three important coordinates: the origin  $x_1 = 0$ , which is the stagnation point, the point  $x_1 = x_p$  of maximum pressure, and the point  $x_1 = x_s$  of zero tangential stress (zero skin friction) where the dividing streamline of equation*

$$\xi\varphi(\eta) + \frac{b}{a} \int_0^\eta \gamma(s)ds = 0, \quad \xi = \sqrt{\frac{\nu + \nu_r}{a}}x_1 \quad (1.53)$$

meets the boundary.

In consideration of (1.47), we see that

$$x_p = b\sqrt{\frac{\nu + \nu_r}{a^3}}(\beta - \alpha). \quad (1.54)$$

The wall shear stress is given by

$$\tau = \rho(\nu + \nu_r) \left. \frac{\partial v_1}{\partial x_2} \right|_{x_2=0}$$

and the position  $x_s$  is obtained by putting  $\tau = 0$ . Hence

$$x_s = -b\sqrt{\frac{\nu + \nu_r}{a^3}} \frac{\gamma'(0)}{\varphi''(0)}. \quad (1.55)$$

We point out that the ratio

$$\frac{x_p}{x_s} = (\alpha - \beta) \frac{\varphi''(0)}{\gamma'(0)}$$

is the same for all angles of incidence.

We then compute the slope of the dividing streamline at the wall:

$$m_s = -\frac{3a[\varphi''(0)]^2}{b[(\beta - \alpha - \Gamma'(0))\varphi''(0) + (1 + \Phi'(0))\gamma'(0)]}.$$

This slope does not depend on the kinematic viscosities so that the ratio of  $m_s$  to the slope of the dividing streamline at infinity

$$m_i = -\frac{2a}{b}$$

is the same for all oblique stagnation-point flows and it is given by

$$\frac{m_s}{m_i} = \frac{3}{2} \frac{[\varphi''(0)]^2}{[\beta - \alpha - \Gamma'(0)]\varphi''(0) + [1 + \Phi'(0)]\gamma'(0)}. \quad (1.56)$$

This ratio is independent of  $a$  and  $b$ , depending on the constant pressure gradient parallel to the boundary through  $B - A$ , as with Newtonian fluids ([18]).

REMARK 1.2.9. Our numerical results show that  $\varphi$ ,  $\gamma$ ,  $\Phi$  and  $\Gamma$  satisfy condition (1.52)<sub>6,7,8,9</sub>, therefore let us denote by:

- $\bar{\eta}_\varphi$  ( $\bar{\eta}_\gamma$ ) the value of  $\eta$  such that  $\varphi'(\bar{\eta}_\varphi) = 0.99$  ( $\gamma'(\bar{\eta}_\gamma) = 0.99$ , if  $\beta - \alpha \geq 0$ , or  $\gamma' = 1.01$ , if  $\beta - \alpha < 0$ );
- $\bar{\eta}_\Phi$  ( $\bar{\eta}_\Gamma$ ) the value of  $\eta$  such that  $\Phi(\bar{\eta}_\Phi) = -0.01$  ( $\Gamma(\bar{\eta}_\Gamma) = -\frac{c_1}{c_2} + 0.01$ ).

Hence if  $\eta > \bar{\eta}_\varphi$  ( $\eta > \bar{\eta}_\gamma$ ), then  $\varphi \cong \eta - \alpha$  ( $\gamma \cong \eta - \beta$ ), and if  $\eta > \bar{\eta}_\Phi$  ( $\eta > \bar{\eta}_\Gamma$ ), then  $\Phi \cong 0$  ( $\Gamma \cong -\frac{c_1}{c_2}$ ).

The effect of the viscosity on the velocity and on the microrotation appears only in a layer lining the boundary whose thickness is  $\delta_v = \max(\bar{\eta}_\varphi, \bar{\eta}_\gamma)$  for the velocity and  $\delta_w = \max(\bar{\eta}_\Phi, \bar{\eta}_\Gamma)$  for the microrotation. The thickness  $\delta$  of the boundary layer for the flow is defined as

$$\delta := \max(\delta_v, \delta_w)$$

and it is proportional to  $\sqrt{\frac{\nu + \nu_r}{a}}$ .

Table 1.3: Descriptive quantities of motion for some values of  $c_1$ ,  $c_2$ ,  $c_3$  and  $\beta - \alpha$ .

$c_1$	$c_2$	$c_3$	$\beta - \alpha$	$\alpha$	$\beta$	$\varphi''(0)$	$\gamma'(0)$	$\Phi'(0)$	$\Gamma'(0)$	$\frac{x_p}{x_s}$	$\frac{m_s}{m_i}$	
0.1	1.5	0.1	-0.6446	0.6446	0	1.2218	1.3648	-0.0532	-0.0892	0.5770	3.6488	
			0	0.6446	0.6454	1.2218	0.5772	-0.0532	-0.0550	0	3.6490	
			0.6446	0.6446	1.2901	1.2218	-0.2104	-0.0532	-0.0207	3.7439	3.6492	
	3.0	0.5	0.1	-0.6448	0.6448	0	1.2231	1.3652	-0.0510	-0.0889	0.5777	3.6454
				0	0.6448	0.6449	1.2231	0.5765	-0.0510	-0.0560	0	3.6454
				0.6448	0.6448	1.2897	1.2231	-0.2121	-0.0510	-0.0231	3.7180	3.6455
		0.5	0.1	-0.6453	0.6453	0	1.2250	1.3818	-0.0444	-0.0658	0.5721	3.6872
				0	0.6453	0.6455	1.2250	0.5912	-0.0444	-0.0372	0	3.6872
				0.6453	0.6453	1.2908	1.2250	-0.1993	-0.0444	-0.0085	3.9657	3.6872
0.5	1.5	0.1	-0.6454	0.6454	0	1.2256	1.3822	-0.0434	-0.0652	0.5723	3.6872	
			0	0.6454	0.6454	1.2256	0.5911	-0.0434	-0.0372	0	3.6872	
			0.6454	0.6454	1.2909	1.2256	-0.1999	-0.0434	-0.0092	3.9572	3.6872	
	0.5	0.1	-0.6310	0.6310	0	1.1780	1.1972	-0.2659	-0.4282	0.6209	3.2527	
			0	0.6310	0.6342	1.1780	0.4538	-0.2659	-0.2604	0	3.2534	
			0.6310	0.6310	1.2661	1.1780	-0.2897	-0.2659	-0.0925	2.5661	3.2540	
0.5	1.5	0.5	-0.6321	0.6321	0	1.1848	1.1988	-0.2553	-0.4275	0.6247	3.2374	
			0	0.6321	0.6326	1.1848	0.4499	-0.2553	-0.2661	0	3.2375	
			0.6321	0.6321	1.2648	1.1848	-0.2990	-0.2553	-0.1047	2.5048	3.2375	
	3.0	0.1	-0.6350	0.6350	0	1.1943	1.2826	-0.2220	-0.3200	0.5913	3.4421	
			0	0.6350	0.6357	1.1943	0.5241	-0.2220	-0.1790	0	3.4423	
			0.6350	0.6350	1.2709	1.1943	-0.2343	-0.2220	-0.0380	3.2365	3.4424	
3.0	0.5	0.1	-0.6356	0.6356	0	1.1972	1.2846	-0.2173	-0.3174	0.5923	3.4424	
			0	0.6356	0.6357	1.1972	0.5237	-0.2173	-0.1793	0	3.4424	
			0.6356	0.6356	1.2713	1.1972	-0.2372	-0.2173	-0.0412	3.2081	3.4424	

The boundary value problem (1.52), (1.50) was solved numerically using the MATLAB program `bvp4c`.

The values of the parameters  $c_1$ ,  $c_2$ ,  $c_3$  were chosen according to Guram and Smith ([27]) and are given in Table 1.3, where we also assign some values to  $\beta$  (i.e.  $\beta - \alpha = -\alpha, 0, \alpha$ ). The consequent values of  $\alpha$ ,  $\varphi''(0)$ ,  $\gamma'(0)$ ,  $\Phi'(0)$ ,  $\Gamma'(0)$ ,  $\frac{x_p}{x_s}$ ,  $\frac{m_s}{m_i}$  are reported in this table.

From Table 1.3 it appears that if we fix two parameters among  $c_1, c_2, c_3$ , when  $\beta - \alpha$  is positive, then  $\gamma'(0)$  and  $\Gamma'(0)$  decrease as  $c_3$  increases, otherwise the values of  $\alpha$ ,  $\varphi''(0)$ ,  $\gamma'(0)$ ,  $\Phi'(0)$ ,  $\Gamma'(0)$  have the following behaviour :

- they increase as  $c_2$  or  $c_3$  increases;
- they decrease as  $c_1$  increases.

As it happened in the orthogonal stagnation-point flow, the influence of  $c_1$  appears more considerable.

We have displayed some representative graphs to elucidate the trend of the functions describing the velocities.

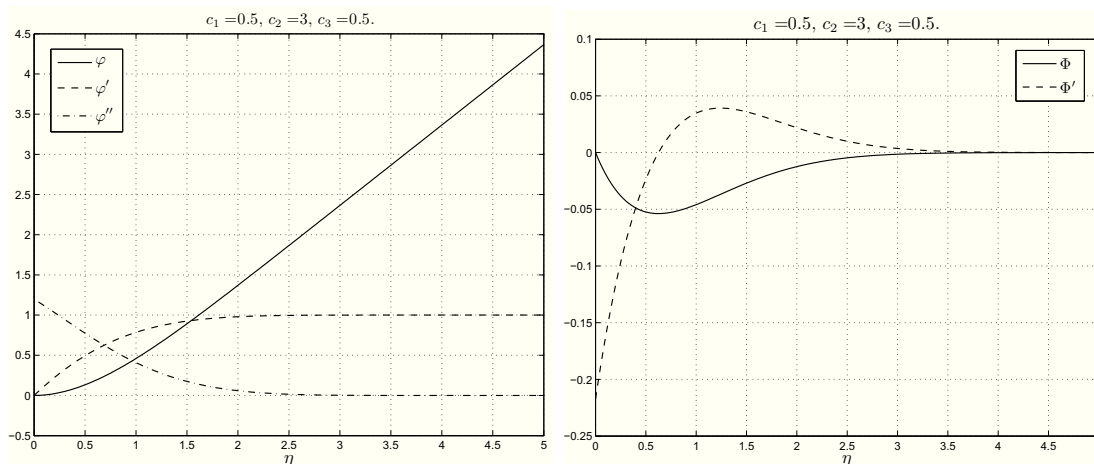


Figure 1.14: Plots showing the behaviour of  $\varphi$ ,  $\varphi'$ ,  $\varphi''$  and  $\Phi$ ,  $\Phi'$ , respectively, for  $c_1 = 0.5$ ,  $c_2 = 3.0$ ,  $c_3 = 0.5$ .

In particular, Figures 1.14, 1.15, and 1.16 show  $\varphi$ ,  $\varphi'$ ,  $\varphi''$ ,  $\Phi$ ,  $\Phi'$ ,  $\gamma$ ,  $\gamma'$ ,  $\Gamma$ ,  $\Gamma'$  for  $c_1 = 0.5$ ,  $c_2 = 3.0$ ,  $c_3 = 0.5$ . If we change the values of these parameters, then the trend of the velocities doesn't change much.

Of course, the behaviour of  $\varphi$ ,  $\Phi$  doesn't depend on  $\beta - \alpha$ , unlike  $\gamma, \Gamma$ .

If we compare the velocity profile with the solution for Newtonian flow, then we see that the behaviour is very similar, as was found in [27] and in Chapter 1.1.3 for orthogonal stagnation-point flow.

Figures 1.17, 1.18, and 1.19 elucidate the dependence of the functions  $\varphi'$ ,  $\gamma$ ,  $\Phi$ ,  $\Gamma$  on the parameters  $c_1$ ,  $c_2$ ,  $c_3$ . As it was easy to figure out, the influence of these parameters appears more on the functions  $\Phi$ , and  $\Gamma$  (i.e. the microrotation). The other two functions,  $\varphi'$  and  $\gamma$ , do not show considerable variations as  $c_1$ ,  $c_2$ ,  $c_3$  assume different values. From the pictures we have that the profile of  $\Phi$  rises as  $c_3$  or  $c_2$  increases and  $c_1$  decreases, while the profile of  $\Gamma$  rises as  $c_2$  increases and  $c_1$  or  $c_3$  decreases. Further  $c_1$  is the parameter that most influences the microrotation.

In Table 1.4 we list the values of  $\bar{\eta}_\varphi$ ,  $\bar{\eta}_\gamma$ ,  $\bar{\eta}_\Phi$ ,  $\bar{\eta}_\Gamma$  when  $c_1$ ,  $c_2$ ,  $c_3$  and  $\beta - \alpha$  change. We see that  $\bar{\eta}_\gamma$  is always greater than  $\bar{\eta}_\varphi$ , as in the Newtonian case (see previous section). Thus the effect of the viscosity on the velocity appears only in a layer lining the boundary of thickness  $\bar{\eta}_\gamma$  which is larger than that of the orthogonal stagnation-point flow.

The presence of the microrotation modifies  $\bar{\eta}_\varphi$  and  $\bar{\eta}_\gamma$ , which are smaller than those of the Newtonian fluids (see Table 1.2).

As far as the microrotation is concerned,  $\bar{\eta}_\Gamma$  is almost always bigger than  $\bar{\eta}_\Phi$ . So the region where the influence of the viscosity on the microrotation appears is a layer lining the boundary of thickness  $\bar{\eta}_\Gamma$ . This region is larger than that in the orthogonal stagnation-point flow.

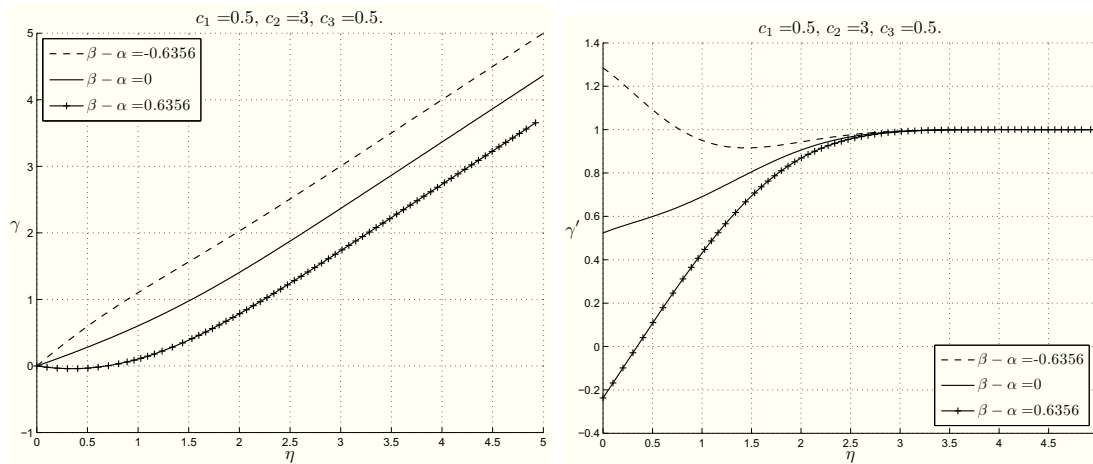


Figure 1.15: Figures 1.15<sub>1</sub> and 1.15<sub>2</sub> show  $\gamma$  and  $\gamma'$  for  $c_1 = 0.5$ ,  $c_2 = 3.0$ ,  $c_3 = 0.5$  and with, from above,  $\beta - \alpha = -\alpha$ ,  $0$ ,  $\alpha$ , respectively.

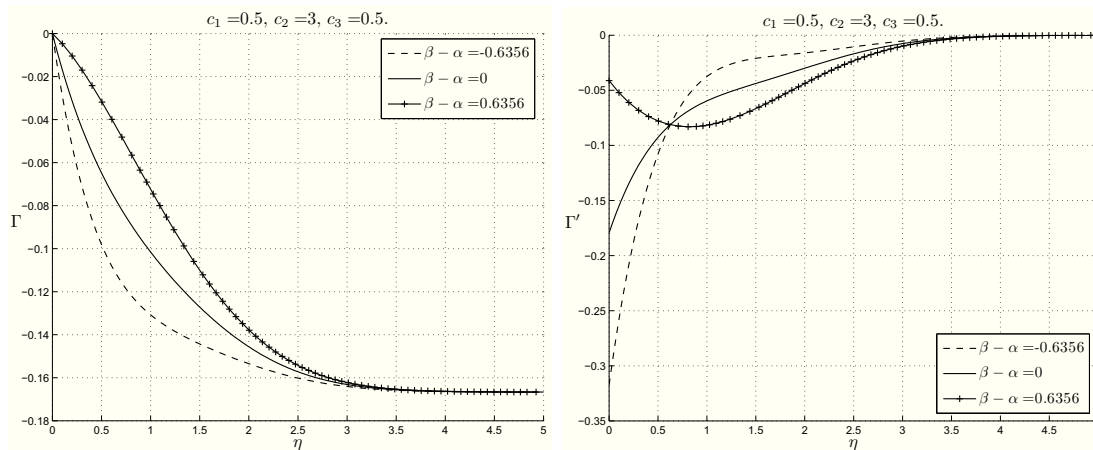


Figure 1.16: Figures 1.16<sub>1</sub> and 1.16<sub>2</sub> show  $\Gamma$  and  $\Gamma'$  for  $c_1 = 0.5$ ,  $c_2 = 3.0$ ,  $c_3 = 0.5$  and with, from above,  $\beta - \alpha = -\alpha$ ,  $0$ ,  $\alpha$ , respectively.

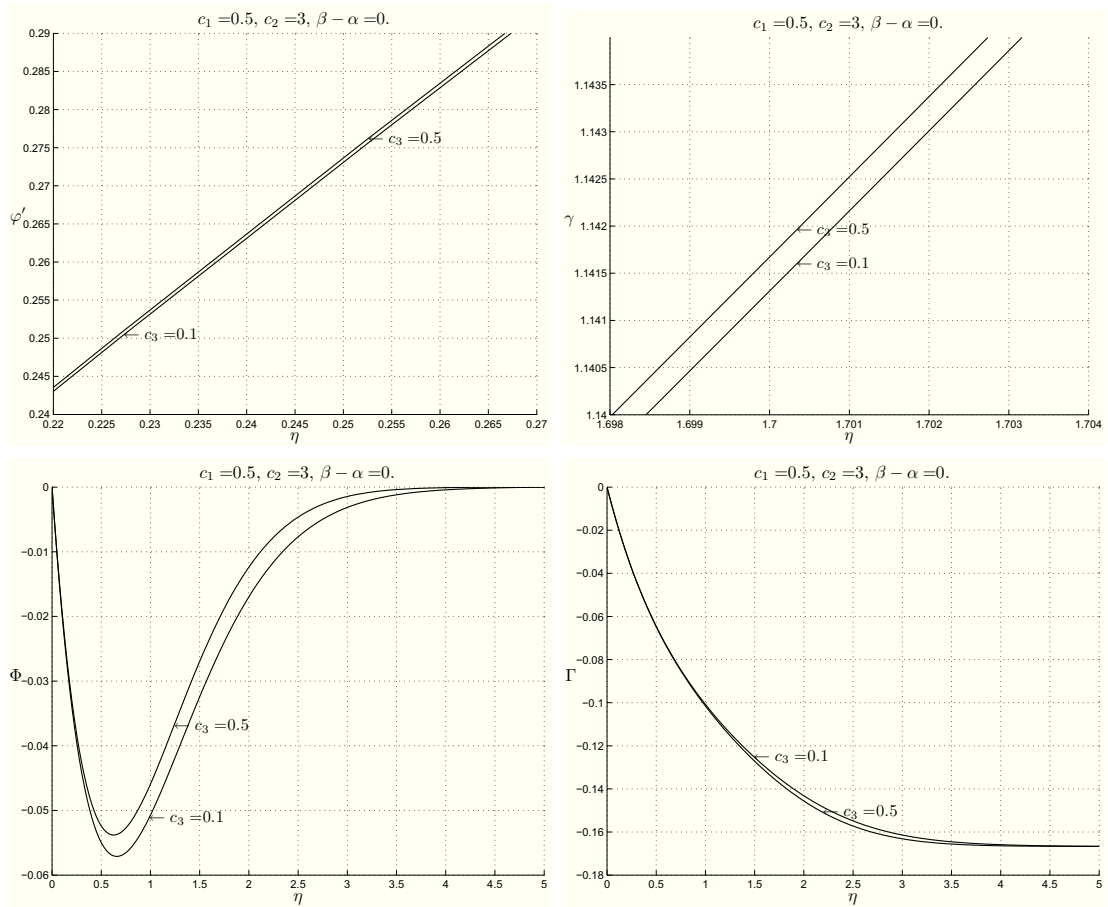


Figure 1.17: Plots showing the behaviour of  $\varphi'$ ,  $\gamma$ ,  $\Phi$  and  $\Gamma$  for  $c_1 = 0.5$ ,  $c_2 = 3.0$  fixed, and for different values of  $c_3$ .

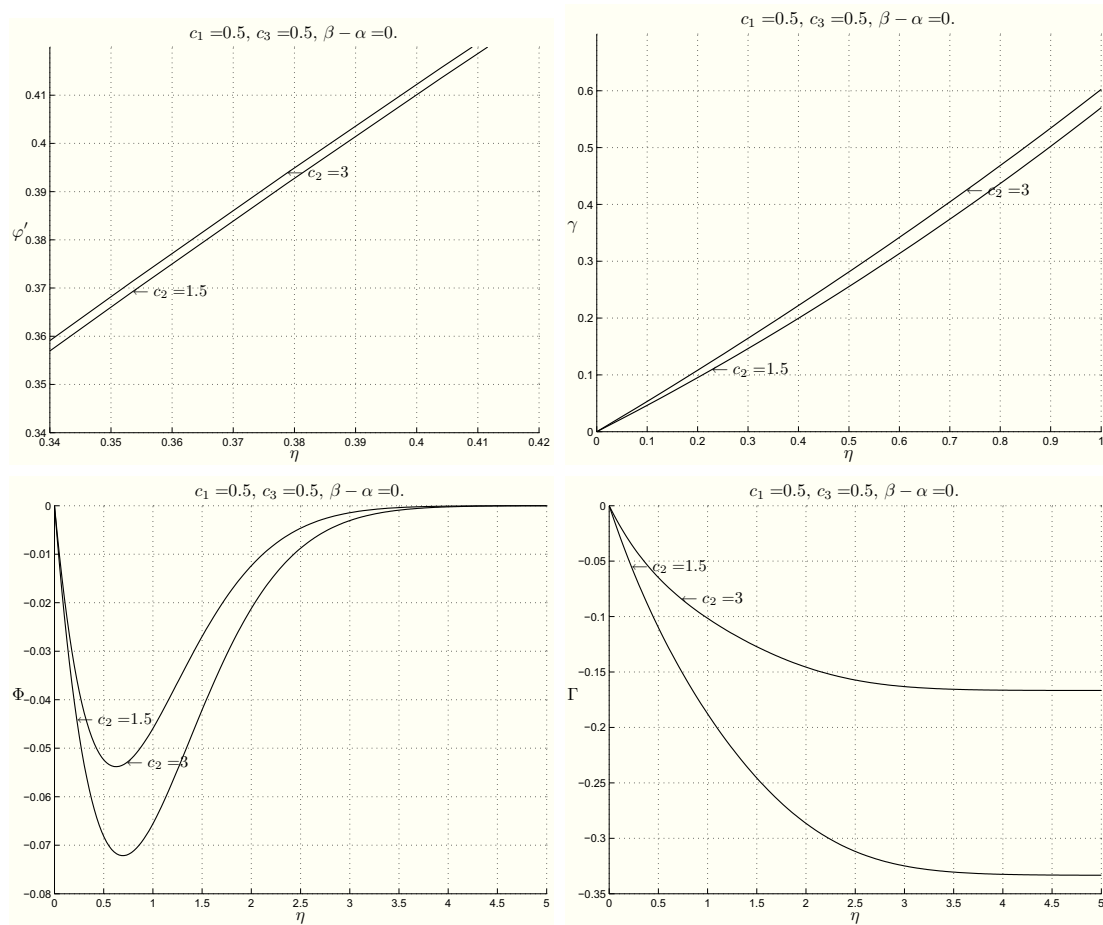


Figure 1.18: Plots showing the behaviour of  $\varphi'$ ,  $\gamma$ ,  $\Phi$  and  $\Gamma$  for  $c_1 = 0.5$ ,  $c_3 = 0.5$  fixed, and for different values of  $c_2$ .

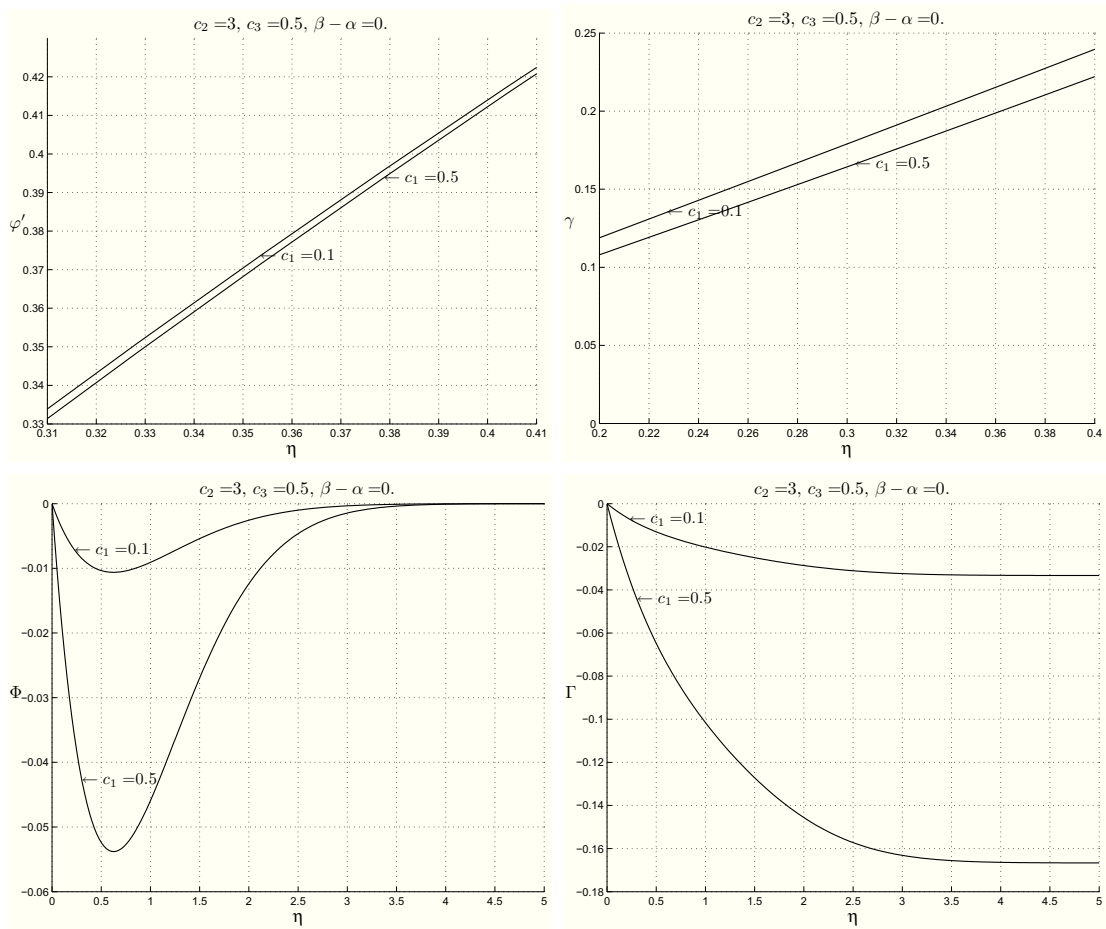


Figure 1.19: Plots showing the behaviour of  $\varphi'$ ,  $\gamma$ ,  $\Phi$  and  $\Gamma$  for  $c_2 = 3.0$ ,  $c_3 = 0.5$  fixed, and for different values of  $c_1$ .

Table 1.4: Thickness of the boundary layer for some values of  $c_1$ ,  $c_2$ ,  $c_3$  and  $\beta - \alpha$ .

$c_1$	$c_2$	$c_3$	$\beta - \alpha$	$\bar{\eta}_\varphi$	$\bar{\eta}_\gamma$	$\bar{\eta}_\Phi$	$\bar{\eta}_\Gamma$	$\delta_v$	$\delta_w$	$\delta$	
0.1	1.5	0.1	-0.6446	2.3257	0.7367	1.6004	1.8319	2.3257	1.8319	2.3257	
			0	2.3257	3.0819	1.6004	2.2421	3.0819	2.2421	3.0819	
			0.6446	2.3257	3.1413	1.6004	2.4912	3.1413	2.4912	3.1413	
	3.0	0.5	0.1	-0.6448	2.3369	0.7370	1.3324	1.7757	2.3369	1.7757	2.3369
				0	2.3369	3.0881	1.3324	2.0469	3.0881	2.0469	3.0881
				0.6448	2.3369	3.1506	1.3324	2.2164	3.1506	2.2164	3.1506
		0.5	0.1	-0.6453	2.3466	0.7435	1.0012	0.6870	2.3466	1.0012	2.3466
				0	2.3466	3.1376	1.0012	1.3339	3.1376	1.3339	3.1376
				0.6453	2.3466	3.1963	1.0012	1.7337	3.1963	1.7337	3.1963
0.5	1.5	0.1	-0.6310	2.1269	0.6904	2.9083	3.0511	2.1269	3.0511	3.0511	
			0	2.1269	2.6399	2.9083	3.3393	2.6399	3.3393	3.3393	
			0.6310	2.1269	2.7091	2.9083	3.5321	2.7091	3.5321	3.5321	
	3.0	0.5	0.1	-0.6321	2.1676	0.6939	2.4321	2.7711	2.1676	2.7711	2.7711
				0	2.1676	2.6436	2.4321	2.9153	2.6436	2.9153	2.9153
				0.6321	2.1676	2.7228	2.4321	3.0181	2.7228	3.0181	3.0181
		0.5	0.1	-0.6350	2.2154	0.7424	2.3427	2.2116	2.2154	2.3427	2.3427
				0	2.2154	2.9128	2.3427	2.6096	2.9128	2.6096	2.9128
				0.6350	2.2154	2.9621	2.3427	2.8159	2.9621	2.8159	2.9621
0.5	0.1	-0.6356	2.2389	0.7422	2.1179	2.2124	2.2389	2.2124	2.2389		
		0	2.2389	2.9279	2.1179	2.4676	2.9279	2.4676	2.9279		
		0.6356	2.2389	2.9854	2.1179	2.6121	2.9854	2.6121	2.9854		

Observing  $\varphi''(0)$ ,  $\gamma'(0)$  in Table 1.3 we notice that they are smaller than in the Newtonian case and that  $x_s$  (given by (1.55)) has the sign of  $b$  if  $\beta - \alpha > 0$  and the sign of  $-b$  if  $\beta - \alpha \leq 0$ . If  $b$  is positive (negative)  $x_s$  increases (decreases) as  $\beta - \alpha$  increases. As far as  $|x_s|$  is concerned, if  $\beta - \alpha$  increases from a negative value to zero,  $|x_s|$  decreases and so  $x_s$  approaches the origin, otherwise, as  $\beta - \alpha$  increases from zero to a positive value,  $|x_s|$  increases and so  $x_s$  departs from the origin. The same results were also found for Newtonian fluids.

From Table 1.3 we see that  $x_p$  and  $x_s$  lie on the same side of the origin, and  $\frac{m_s}{m_i}$  is constant once  $c_1$ ,  $c_2$ ,  $c_3$  are fixed. The values of these points do not change significantly due to the presence of microrotation, while the ratio of the slopes is smaller than in the Newtonian case.

Figure 1.20 shows the streamlines and the points

$$\xi_p = \sqrt{\frac{a}{\nu}} x_p, \quad \xi_s = \sqrt{\frac{a}{\nu}} x_s$$

for  $\frac{b}{a} = 1$  and  $\beta - \alpha = -\alpha$ ,  $0$ ,  $\alpha$ , respectively.

## 1.3 Three-dimensional stagnation-point flow

The steady three-dimensional stagnation-point flow of a Newtonian fluid has been studied by Homman ([35]), Howarth ([36]), Davey and Schoffield ([13], [48]). The governing partial differential equations are transformed into a system of nonlinear ODEs, which depends on a parameter that is a measure of three-dimensionality.

Guram and Anwar Kamal ([26]) studied the steady three-dimensional stagnation-point flow of a micropolar fluid, where, however, the Authors didn't take into consideration the occurrence of the reverse flow, the reverse microrotation, the thickness of the boundary layer and the influence of some parameters on the motion. Hence the results presented here for the micropolar fluid extend the literature.

In order to study the three-dimensional stagnation-point flow for a Newtonian or a micropolar fluid, it is convenient to start with the same flow for an inviscid one.

### 1.3.1 Inviscid fluids

Consider the steady three-dimensional flow of a homogeneous incompressible inviscid fluid near a stagnation point filling the half-space  $\mathcal{S}$ , given by (1.1) (see Figure 1.21).

As it is well known in the three-dimensional stagnation-point flow the velocity field is given by

$$v_1 = ax_1, \quad v_2 = -a(1+c)x_2, \quad v_3 = acx_3, \quad (x_1, x_3) \in \mathbb{R}^2, \quad x_2 \in \mathbb{R}^+, \quad (1.57)$$

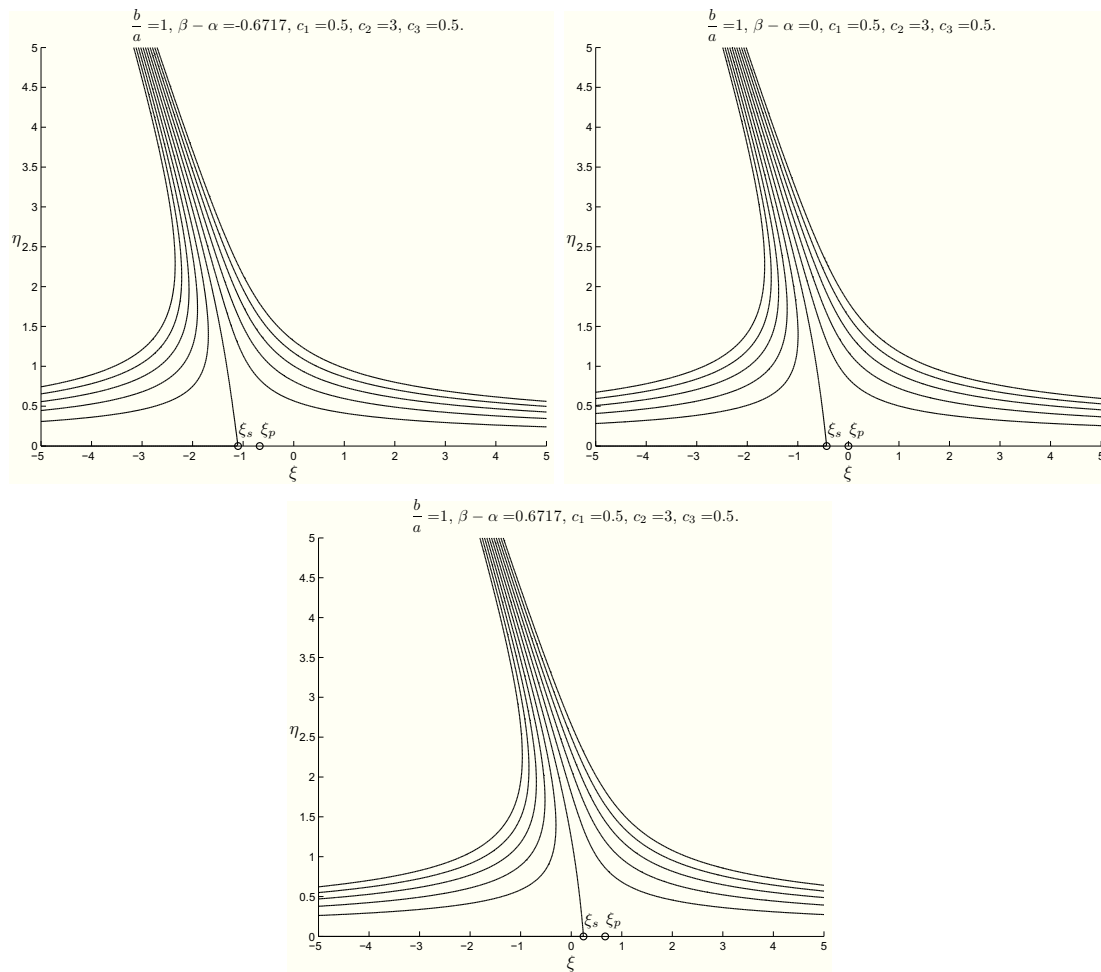


Figure 1.20: Plots showing the streamlines and the points  $\xi_p, \xi_s$  for  $\frac{b}{a} = 1, c_1 = 0.5, c_2 = 3.0, c_3 = 0.5$  and  $\beta - \alpha = -\alpha, 0, \alpha$ , respectively.

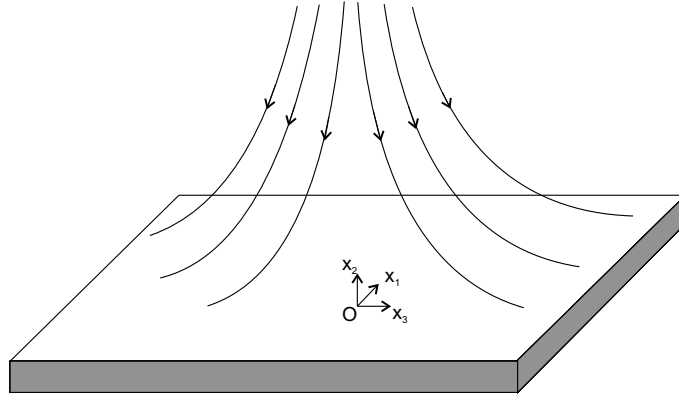


Figure 1.21: Three-dimensional stagnation-point flow description.

where  $a, c$  are constants. As in the previous types of stagnation-point flow, the constant  $a$  is positive. The parameter  $c$  is a measure of the three-dimensionality of the motion because when  $c = 0$  we obtain the plane stagnation-point flow.

We suppose  $c > -1$ , because we impose the condition  $v_2 < 0$ , so that the fluid moves towards the wall  $x_2 = 0$ .

REMARK 1.3.1. *If  $c = 1$ , the velocity is axial symmetric with respect to  $x_2$  axis:*

$$v_1 = ax_1, \quad v_2 = -2ax_2, \quad v_3 = ax_3.$$

The equations governing such a flow in the absence of external mechanical body forces are (1.2) together with the no-penetration condition (1.3).

Under the previous assumptions, it holds:

THEOREM 1.3.2. *Let a homogeneous, incompressible inviscid fluid occupy the half-space  $\mathcal{S}$ . The steady three-dimensional stagnation-point flow of such a fluid is given by*

$$\begin{aligned} \mathbf{v} &= ax_1\mathbf{e}_1 - a(1+c)x_2\mathbf{e}_2 + acx_3\mathbf{e}_3, \\ p &= -\frac{1}{2}\rho a^2[x_1^2 + (1+c)^2x_2^2 + c^2x_3^2] + p_0, \quad (x_1, x_3) \in \mathbb{R}^2, \quad x_2 \in \mathbb{R}^+. \end{aligned} \quad (1.58)$$

REMARK 1.3.3. *In order to study the three-dimensional stagnation-point flow for other models of fluid, we suppose the fluid impinging on the flat plane  $x_2 = C$  and*

$$v_1 = ax_1, \quad v_2 = -a(1+c)(x_2 - C), \quad v_3 = acx_3, \quad (x_1, x_3) \in \mathbb{R}^2, \quad x_2 \geq C, \quad (1.59)$$

*with  $C$  some constant.*

*In this way, the stagnation point is not the origin but the point  $(0, C, 0)$  and the pressure in Theorem 1.3.2 must be modified by replacing  $x_2$  with  $x_2 - C$ .*

### 1.3.2 Newtonian Fluids

Let us now consider the steady three-dimensional stagnation-point flow of a homogeneous, incompressible Newtonian fluid towards a flat surface coinciding with the plane  $x_2 = 0$ .

Howarth ([36]) expressed the velocity components of the flow in the form

$$v_1 = ax_1 f'(x_2), \quad v_2 = -a[f(x_2) + cg(x_2)], \quad v_3 = acx_3 g'(x_2), \quad (x_1, x_3) \in \mathbb{R}^2, \quad x_2 \in \mathbb{R}^+, \quad (1.60)$$

where  $f, g$  are sufficiently regular unknown functions ( $f, g \in C^3(\mathbb{R}^+)$ ).

In the absence of external mechanical body forces, the equations for such a fluid are (1.6) and (1.2)<sub>2</sub>.

As far as the boundary condition for  $\mathbf{v}$  is concerned, we prescribe the no-slip condition (1.7), which is certainly satisfied if

$$f(0) = 0, \quad f'(0) = 0, \quad g(0) = 0, \quad g'(0) = 0. \quad (1.61)$$

We assume that far from the wall, the flow approaches the flow of an inviscid fluid, whose velocity is given by (1.59), so that we ask

$$\lim_{x_2 \rightarrow +\infty} f'(x_2) = 1, \quad \lim_{x_2 \rightarrow +\infty} g'(x_2) = 1. \quad (1.62)$$

The constant  $C$  in (1.59) is related to the behaviour of  $f$  and  $g$  at infinity. Actually, if

$$\lim_{x_2 \rightarrow +\infty} [f(x_2) - x_2] = -A, \quad \lim_{x_2 \rightarrow +\infty} [g(x_2) - x_2] = -B, \quad (1.63)$$

with  $A, B$  some constants, then

$$\lim_{x_2 \rightarrow +\infty} [f(x_2) + cg(x_2) - (1+c)x_2] = -(1+c)C, \quad (1.64)$$

where

$$C = \frac{A + cB}{1 + c}.$$

As we will see, the constants  $A, B, C$  are not assigned a priori, but their values can be found as part of the solution of the problem.

**THEOREM 1.3.4.** *Let a homogeneous, incompressible Newtonian fluid occupy the half-space  $\mathcal{S}$ . The steady three-dimensional stagnation-point flow of such a fluid has the form*

$$\begin{aligned} \mathbf{v} &= ax_1 f'(x_2) \mathbf{e}_1 - [af(x_2) + bg(x_2)] \mathbf{e}_2 + bx_3 g'(x_2) \mathbf{e}_3, \\ p &= -\rho \frac{a^2}{2} [x_1^2 + (f(x_2) + cg(x_2))^2 + c^2 x_3^2] - \rho a \nu [f'(x_2) + cg'(x_2)] + p_0, \\ &(x_1, x_3) \in \mathbb{R}^2, \quad x_2 \in \mathbb{R}^+, \end{aligned} \quad (1.65)$$

where  $(f, g)$  satisfies

$$\begin{aligned}\frac{\nu}{a}f''' + (f + cg)f'' - f'^2 + 1 &= 0, \\ \frac{\nu}{a}g''' + (f + cg)g'' - cg'^2 + c &= 0,\end{aligned}\tag{1.66}$$

with the boundary conditions (1.61) and (1.62).

If we use transformation (1.35), then we can rewrite problems (1.66), (1.61), (1.62) in dimensionless form

$$\begin{aligned}\varphi''' + (\varphi + c\gamma)\varphi'' - \varphi'^2 + 1 &= 0, \\ \gamma''' + (\varphi + c\gamma)\gamma'' - c\gamma'^2 + c &= 0, \\ \varphi(0) = 0, \quad \varphi'(0) &= 0, \\ \gamma(0) = 0, \quad \gamma'(0) &= 0, \\ \lim_{\eta \rightarrow +\infty} \varphi'(\eta) = 1, \quad \lim_{\eta \rightarrow +\infty} \gamma'(\eta) &= 1.\end{aligned}\tag{1.67}$$

We also put

$$\alpha = \sqrt{\frac{a}{\nu}}A, \quad \beta = \sqrt{\frac{a}{\nu}}B, \quad h_d = \frac{\alpha + c\beta}{1 + c}.\tag{1.68}$$

The constant  $h_d$  is the three-dimensional displacement thickness ([13]) and it represents the height of the plane towards which the inviscid fluid moves.

REMARK 1.3.5. In [13] under the hypothesis that  $\gamma$  is analytical, it is proved that the problem (1.67) does not admit solution for  $c < -1$ , as it is reasonable from the physical point of view. As far as existence of solution is concerned, we refer to [29], [30].

REMARK 1.3.6. In [36] it was underlined that regular solution to problem (1.67) are invariant under the following transformation

$$\varphi\left(\eta, \frac{1}{c}\right) = \sqrt{c}\gamma\left(\frac{\eta}{\sqrt{c}}, c\right), \quad \gamma\left(\eta, \frac{1}{c}\right) = \sqrt{c}\varphi\left(\frac{\eta}{\sqrt{c}}, c\right), \quad c > 0$$

so that we could confine our analysis to  $c \in (-1, 1)$ ,  $c \neq 0$ .

Finally,  $c = 1$  furnishes the axisymmetric flow.

REMARK 1.3.7. It is important to give the explicit form of the pressure field because, as it is well known, when a fluid moves past a body, if one of the components of

the pressure gradient along a body surface has the same sign as the corresponding component of the velocity, then the reverse flow appears.

The numerical results ([13], [14], [7]) reveal that there exists a negative value  $c_r$  of  $c$  such that if  $c \geq c_r$ , then  $\gamma', \gamma'' > 0 \forall \eta > 0$ , and if  $c < c_r$  then near the wall  $\gamma', \gamma'' < 0$ , so that the reverse flow appears (i.e.  $v_3$  has the same sign as  $\frac{\partial p}{\partial x_3}$ ).

The reverse flow is also related to a sign change of the scalar component of the skin friction ( $\tau_0$ ) in the direction of  $\mathbf{e}_3$  (see (1.70)).

REMARK 1.3.8. As it is underlined in [38], at a very small distance  $\eta$  from the surface of an obstacle, the velocity of a Newtonian fluid is approximately

$$\mathbf{v} \cong \sqrt{\frac{\nu}{a} \frac{\tau_0}{\mu}} \eta, \quad (1.69)$$

where  $\tau_0$  is the skin friction vector, which in our situation is given by

$$\tau_0 = \rho a \sqrt{\nu a} [x_1 \varphi''(0) \mathbf{e}_1 + c x_3 \gamma''(0) \mathbf{e}_3]. \quad (1.70)$$

The normal component of the velocity at a higher order of approximation is

$$v_2 \cong -\frac{1}{2} \frac{\nu}{a} \nabla \cdot \left( \frac{\tau_0}{\mu} \right) \eta^2 := -\frac{1}{2} \Delta_s \eta^2. \quad (1.71)$$

We see from (1.69) that close to the obstacle the direction of streamlines becomes parallel to its surface, except where  $\tau_0 = \mathbf{0}$ . This condition that both tangential components of skin friction vanish simultaneously, is satisfied in general only at isolated points of the surface, which are called ‘points of separation’ if  $\Delta_s < 0$  (so that the normal velocity (1.71) is positive) and ‘points of attachment’ if  $\Delta_s > 0$ .

In our analysis, the only isolated point such that  $\tau_0 = \mathbf{0}$  is the origin, i.e. the stagnation-point, and

$$\Delta_s = \sqrt{\nu a} [\varphi''(0) + c \gamma''(0)].$$

Streamlines very near the surface lie closely along the skin friction line, as (1.69) indicates.

There is just one skin friction line and one vortex line through each point of the surface, except a point of attachment or separation. These last are ‘singular points’ of the differential equations of both systems of curves. Such singular points are classified into two main types, depending on the sign of:

$$J_s = \frac{\partial \tau_{01}}{\partial x_1} \frac{\partial \tau_{03}}{\partial x_3} - \frac{\partial \tau_{01}}{\partial x_3} \frac{\partial \tau_{03}}{\partial x_1}. \quad (1.72)$$

A singular point where  $J_s < 0$  is a ‘saddle point’, and where  $J_s > 0$  there is a ‘nodal point’.

In our case, we have

$$J_s = \rho^2 \nu a^3 [c\varphi''(0)\gamma''(0)].$$

From these considerations it is clear that we need to know the signs of  $c$ ,  $\varphi''(0)$ ,  $\gamma''(0)$  in order to classify the stagnation-point.

As it is underlined in [14] and as we will see, from the numerical results one has that the stagnation-point is a nodal point of attachment if  $c > 0$  or  $c < c_r = -0.4294$ , while it is a saddle point of attachment if  $c_r \leq c < 0$ .

We point out that in [14] the Author corrected the classification of the stagnation-point contained in [13]. However in the literature, most of the papers refer to the uncorrected classification in [13].

Finally, there is a limiting direction of our flow at the boundary, which is also the direction of the resultant skin friction, and this direction is inclined to the main stream at an angle  $\epsilon$ :

$$\epsilon = \arctan\left(c \frac{x_3 \gamma''(0)}{x_1 \varphi''(0)}\right) - \arctan\left(c \frac{x_3}{x_1}\right). \quad (1.73)$$

REMARK 1.3.9. In the sequel, we will see that the solution  $(\varphi, \gamma)$  of the problem considered in Theorem 1.3.4 satisfies the conditions (1.67)<sub>7,8</sub>; therefore we define:

- $\bar{\eta}_\varphi$  ( $\bar{\eta}_\gamma$ ) the value of  $\eta$  such that  $\varphi'(\bar{\eta}_\varphi) = 0.99$  ( $\gamma'(\bar{\eta}_\gamma) = 0.99$ ).

Hence if  $\eta > \bar{\eta}_\varphi$  ( $\eta > \bar{\eta}_\gamma$ ), then  $\varphi \cong \eta - \alpha$  ( $\gamma \cong \eta - \beta$ ), so that the influence of the viscosity appears only in a layer lining the boundary whose thickness is

$$\delta = \max(\bar{\eta}_\varphi, \bar{\eta}_\gamma).$$

This thickness is proportional to  $\sqrt{\frac{\nu}{a}}$ .

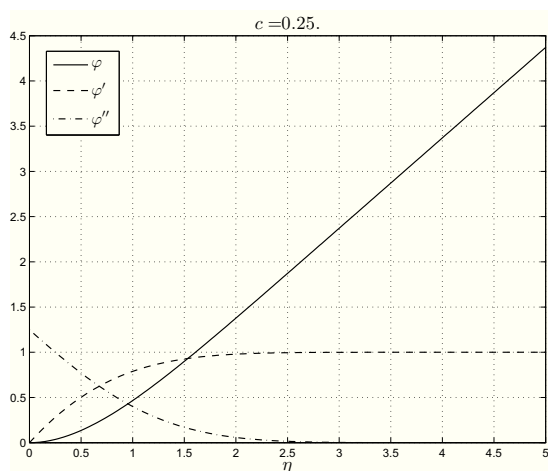
We have solved problem (1.67) numerically for different values of  $c$  taken according to [36] and [13].

Figure 1.22 shows the graphics of  $\varphi$ ,  $\varphi'$ ,  $\varphi''$  for  $c = 0.25$ .

The numerical integration furnishes the value of  $\alpha$ ,  $\varphi''(0)$ ,  $\gamma''(0)$ ,  $h_d$ ,  $\beta$ ,  $\bar{\eta}_\varphi$ ,  $\bar{\eta}_\gamma$ ,  $\delta$  when  $c$  changes, as it is shown in Table 1.5.

Our results are consistent with the previous studies ([13], [36]). In particular, when  $c = 1$  we obtain the axisymmetric flow:  $\alpha = \beta = h_d$  and  $\varphi''(0) = \gamma''(0)$ .

As far as the behaviour of  $\gamma$ ,  $\gamma'$ ,  $\gamma''$  is concerned, if  $c \geq c_r$  then the behaviour of  $\gamma$ ,  $\gamma'$ ,  $\gamma''$  is shown in Figure 1.23<sub>2</sub>, otherwise it is given in Figure 1.23<sub>1</sub> (reverse flow appears near the boundary).

Figure 1.22: Profiles of  $\varphi, \varphi', \varphi''$  for  $c = 0.25$ .Table 1.5: Descriptive quantities of motion for some values of  $c$ .

$c$	$\varphi''(0)$	$\gamma''(0)$	$h_d$	$\alpha$	$\beta$	$\bar{\eta}_\varphi$	$\bar{\eta}_\gamma$	$\delta$
-0.75	1.2465	-0.4690	-5.0704	0.6378	2.5405	2.3772	4.5298	4.5298
-0.25	1.2251	0.2681	0.4211	0.6593	1.3741	2.4684	3.6223	3.6223
0.25	1.2476	0.8051	0.6699	0.6294	0.8317	2.2624	2.6363	2.6363
1.00	1.3119	1.3119	0.5689	0.5689	0.5689	1.9444	1.9444	1.9444

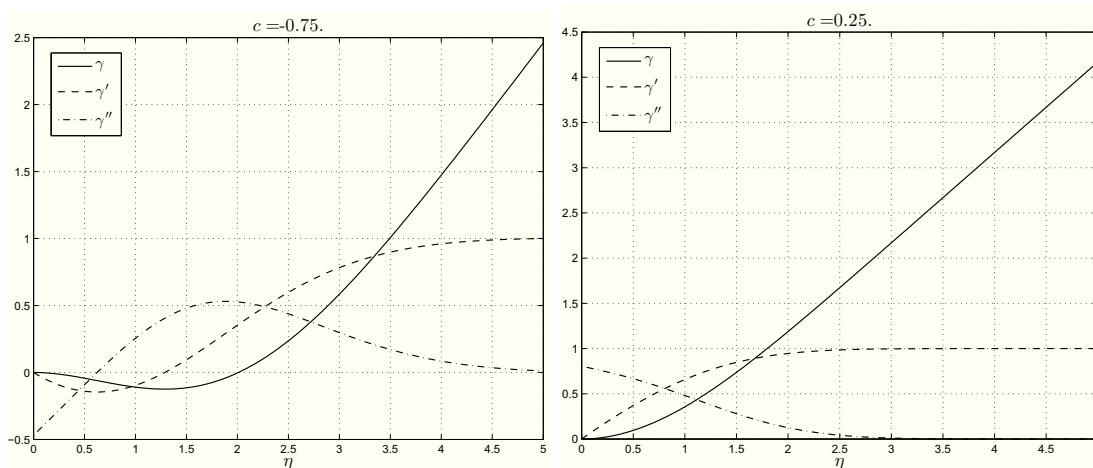
Figure 1.23: The first picture shows the profiles of  $\gamma, \gamma', \gamma''$  in the reverse flow ( $c = -0.75$ ). The second picture shows the profile of  $\gamma, \gamma', \gamma''$  in the absence of the reverse flow ( $c = 0.25$ ).

Table 1.6: Values of  $h_d$ ,  $\varphi''(0) + c\gamma''(0)$  and  $c\varphi''(0)\gamma''(0)$  in dependence on the values of  $c$ .

$c$	$h_d$	$\varphi''(0)$	$\gamma''(0)$	$\varphi''(0) + c\gamma''(0)$	$c\varphi''(0)\gamma''(0)$
-0.90	-20.9401	1.2612	-0.6761	1.8697	0.7674
-0.85	-12.1568	1.2563	-0.6133	1.7777	0.6550
-0.80	-7.8544	1.2517	-0.5489	1.6908	0.5496
-0.75	-5.3300	1.2473	-0.4822	1.6090	0.4511
-0.60	-1.7254	1.2359	-0.2666	1.3959	0.1977
-0.50	-0.6513	1.2302	-0.1115	1.2859	0.0686
-0.45	-0.3012	1.2281	-0.0325	1.2427	0.0180
$c_r = -0.4294$	-0.1829	1.2273	0	1.2273	0
-0.40	-0.0363	1.2265	0.0460	1.2081	-0.0226
$c_h = -0.3919$	0	1.2263	0.0586	1.2033	-0.0281
-0.30	0.3113	1.2250	0.1970	1.1659	-0.0724
-0.25	0.4207	1.2251	0.2680	1.1581	-0.0821
-0.10	0.5997	1.2284	0.4594	1.1825	-0.0564
0.10	0.6678	1.2379	0.6707	1.3050	0.0830
0.25	0.6699	1.2476	0.8051	1.4489	0.2511
0.50	0.6430	1.2669	0.9981	1.7659	0.6322
0.75	0.6058	1.2886	1.1643	2.1619	1.1253
1.00	0.5689	1.3119	1.3119	2.6239	1.7212

We are also able to compute  $c_r = -0.4294$  (see Table 1.6).

Table 1.5 shows that when  $c$  increases, the value of  $\gamma''(0)$  increases, while the values of  $\beta$ ,  $\bar{\eta}_\gamma$  decrease. As far as  $\varphi''(0)$ ,  $\bar{\eta}_\varphi$  and  $\alpha$  are concerned, we have that  $\varphi''(0)$  and  $\bar{\eta}_\varphi$  increase if  $c > 0$ , otherwise decrease, and  $\alpha$  decreases if  $c > 0$ , otherwise increases.

Hence the thickness of the boundary layer decreases when  $c$  increases. Further since  $\bar{\eta}_\varphi < \bar{\eta}_\gamma$ ,  $\delta = \bar{\eta}_\gamma$  so that the boundary layer is thicker than that in the orthogonal stagnation-point flow. If  $c > 0$ , then  $\delta$  is smaller than in the oblique flow.

Table 1.5 elucidates the behaviour of  $h_d$  and of the origin in dependence on  $c$ . Actually, from this Table it appears that  $h_d$  can be negative (in particular, if  $c < -0.3919 =: c_h$ , then  $h_d < 0$ ) and, since  $c_h > c_r$ , it is always negative when the reverse flow appears ([13]).

As far as the classification of the stagnation-point is concerned, then it is always a point of attachment. If  $c > 0$  or where there is the reverse flow, the origin is a nodal point, while when  $c < 0$  and the reverse flow does not appear, it is a saddle point (see Figure 1.24).

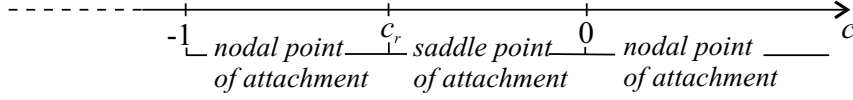


Figure 1.24: Classification of the stagnation-point in dependence on  $c$ .

### 1.3.3 Micropolar Fluids

We now consider the steady three-dimensional stagnation-point flow of a homogeneous, incompressible micropolar fluid towards a flat surface coinciding with the plane  $x_2 = 0$ , the flow being confined to the half-space  $\mathcal{S}$ .

In the absence of external mechanical body forces and body couples, the equations for such a fluid are (1.16) and we prescribe boundary conditions (1.17).

From [26], we have that  $\mathbf{v}$ ,  $\mathbf{w}$  are given by

$$\begin{aligned} v_1 &= ax_1 f'(x_2), & v_2 &= -a[f(x_2) + cg(x_2)], & v_3 &= acx_3 g'(x_2), \\ w_1 &= -cx_3 F(x_2), & w_2 &= 0, & w_3 &= x_1 G(x_2), \end{aligned} \quad (x_1, x_3) \in \mathbb{R}^2, \quad x_2 \in \mathbb{R}^+, \quad (1.74)$$

where  $f, g, F, G$  are sufficiently regular unknown functions ( $f, g \in C^3(\mathbb{R}^+)$ ,  $F, G \in C^2(\mathbb{R}^+)$ ).

To satisfy conditions (1.17), we ask

$$\begin{aligned} f(0) &= 0, & f'(0) &= 0, & g(0) &= 0, & g'(0) &= 0, \\ F(0) &= 0, & G(0) &= 0. \end{aligned} \quad (1.75)$$

Since we assume that at infinity the flow approaches the flow of an inviscid fluid, whose velocity is given by (1.60), we require also the following conditions

$$\begin{aligned} \lim_{x_2 \rightarrow +\infty} f'(x_2) &= 1, & \lim_{x_2 \rightarrow +\infty} g'(x_2) &= 1, \\ \lim_{x_2 \rightarrow +\infty} F(x_2) &= 0, & \lim_{x_2 \rightarrow +\infty} G(x_2) &= 0. \end{aligned} \quad (1.76)$$

Conditions (1.76)<sub>3,4</sub> mean that at infinity,  $\mathbf{w} = \frac{1}{2}\nabla \times \mathbf{v} = \mathbf{0}$ , i.e. the micropolar fluid behaves like an inviscid fluid whose velocity  $\mathbf{v}$  is given by (1.59).

The constant  $C$  is related to the asymptotic behaviour of  $f$  and  $g$  at infinity as for the Newtonian case. So relations (1.63) and (1.64) continue to hold.

The results found in the literature ([26]) can be summarized in the following:

**THEOREM 1.3.10.** *Let a homogeneous, incompressible micropolar fluid occupy the half-space  $\mathcal{S}$ . The steady three-dimensional stagnation-point flow of such a fluid has*

the form

$$\begin{aligned}
\mathbf{v} &= ax_1 f'(x_2) \mathbf{e}_1 - a[f(x_2) + cg(x_2)] \mathbf{e}_2 + acx_3 g'(x_2) \mathbf{e}_3, \\
\mathbf{w} &= -cx_3 F(x_2) \mathbf{e}_1 + x_1 G(x_2) \mathbf{e}_2, \\
p &= -\rho \frac{a^2}{2} [x_1^2 + (f(x_2) + cg(x_2))^2 + c^2 x_3^2] - \rho a(\nu + \nu_r)[f'(x_2) + cg'(x_2)] \\
&\quad - 2\nu_r \rho \int_0^{x_2} [cF(s) + G(s)] ds + p_0, \quad (x_1, x_3) \in \mathbb{R}^2, \quad x_2 \in \mathbb{R}^+, \quad (1.77)
\end{aligned}$$

where  $(f, g, F, G)$  satisfies system

$$\begin{aligned}
\frac{\nu + \nu_r}{a} f''' + (f + cg) f'' - f'^2 + 1 + \frac{2\nu_r}{a^2} G' &= 0, \\
\frac{\nu + \nu_r}{a} g''' + (f + cg) g'' - cg'^2 + c + \frac{2\nu_r}{a^2} F' &= 0, \\
\lambda F'' + Ia[F'(f + cg) - cFg'] - 2\nu_r(2F + ag'') &= 0, \\
\lambda G'' + Ia[G'(f + cg) - Gf'] - 2\nu_r(2G + af'') &= 0, \quad (1.78)
\end{aligned}$$

provided  $F, G \in L^1([0, +\infty))$  and boundary conditions (1.75) and (1.76).

REMARK 1.3.11. From (1.77) we see that the pressure takes again its maximum along the wall  $x_2 = 0$  in the stagnation-point.

REMARK 1.3.12. If  $c = 1$ ,  $f = g$ ,  $F = G$ , the axial symmetric case is obtained.

In order to reduce the number of the material parameters, it is convenient to rewrite the boundary value problem of Theorem 1.3.10 in dimensionless form. To this end we use transformation (1.49), so that system (1.78) can be written as

$$\begin{aligned}
\varphi''' + (\varphi + c\gamma)\varphi'' - \varphi'^2 + 1 + \Gamma' &= 0, \\
\gamma''' + (\varphi + c\gamma)\gamma'' - c\gamma'^2 + c + \Phi' &= 0, \\
\Phi'' + c_3\Phi'(\varphi + c\gamma) - \Phi(c_3c\gamma' + c_2) - c_1\gamma'' &= 0, \\
\Gamma'' + c_3\Gamma'(\varphi + c\gamma) - \Gamma(c_3\varphi' + c_2) - c_1\varphi'' &= 0, \quad (1.79)
\end{aligned}$$

where  $c_1, c_2, c_3$  are the material parameters given by (1.25).

In this way, we have

$$\alpha = \sqrt{\frac{a}{\nu + \nu_r}} A, \quad \beta = \sqrt{\frac{a}{\nu + \nu_r}} B, \quad h_d = \frac{\alpha + c\beta}{1 + c}. \quad (1.80)$$

The boundary conditions (1.75) and (1.76) in dimensionless form become:

$$\begin{aligned}
\varphi(0) &= 0, & \varphi'(0) &= 0, \\
\gamma(0) &= 0, & \gamma'(0) &= 0, \\
\Phi(0) &= 0, & \Gamma(0) &= 0, \\
\lim_{\eta \rightarrow +\infty} \varphi'(\eta) &= 1, & \lim_{\eta \rightarrow +\infty} \gamma'(\eta) &= 1, \\
\lim_{\eta \rightarrow +\infty} \Phi(\eta) &= 0, & \lim_{\eta \rightarrow +\infty} \Gamma(\eta) &= 0.
\end{aligned} \tag{1.81}$$

REMARK 1.3.13. *Equations (1.79) are of course the same found by Guram and Anwar Kamal in [26].*

REMARK 1.3.14. *It is easy to verify that regular solutions of problem (1.79), (1.81) are invariant under the following transformation*

$$\begin{aligned}
\varphi\left(\eta, \frac{1}{c}, \frac{c_1}{c}, \frac{c_2}{c}, c_3\right) &= \sqrt{c} \gamma\left(\frac{\eta}{\sqrt{c}}, c, c_1, c_2, c_3\right), \\
\gamma\left(\eta, \frac{1}{c}, \frac{c_1}{c}, \frac{c_2}{c}, c_3\right) &= \sqrt{c} \varphi\left(\frac{\eta}{\sqrt{c}}, c, c_1, c_2, c_3\right), \\
\Phi\left(\eta, \frac{1}{c}, \frac{c_1}{c}, \frac{c_2}{c}, c_3\right) &= \frac{1}{\sqrt{c}} \Gamma\left(\frac{\eta}{\sqrt{c}}, c, c_1, c_2, c_3\right), \\
\Gamma\left(\eta, \frac{1}{c}, \frac{c_1}{c}, \frac{c_2}{c}, c_3\right) &= \frac{1}{\sqrt{c}} \Phi\left(\frac{\eta}{\sqrt{c}}, c, c_1, c_2, c_3\right), \quad c > 0
\end{aligned}$$

so that we could confine the attention to  $c \in (-1, 1)$ ,  $c \neq 0$ .

REMARK 1.3.15. *As for the Newtonian model, it is important to give the explicit form of the pressure field because, if one of the components of the pressure gradient parallel to the wall has the same sign as the corresponding component of the velocity or of the microrotation curl field, then the reverse flow or the reverse microrotation appears.*

*This effect is well known for the velocity field of a Newtonian fluid ([13], [14], [7]), while the reverse microrotation has never been observed in the literature ([8]).*

*The numerical results show that there exists a negative value  $c_r$  of  $c$  such that if  $c \geq c_r$ , then  $\gamma', \gamma'' > 0 \forall \eta > 0$ , and if  $c < c_r$  then near the wall  $\gamma', \gamma'' < 0$ , so that the flow reverses (i.e.  $v_3$  has the same sign as  $\frac{\partial p}{\partial x_3}$ ).*

*We have found numerically that there exists a negative value  $c_{rw}$  of  $c$  such that if  $c \geq c_{rw}$ , then  $\Phi'(0) < 0$ ,  $\Phi(\eta) < 0 \forall \eta > 0$ , and if  $c < c_{rw}$  then near the wall*

$\Phi, \Phi' > 0$  so that the reverse microrotation appears (i.e.  $(\nabla \times \mathbf{w})_3 = \frac{a^2}{2\nu_r} cx_3 \Phi'(\eta)$ ) has the same sign as  $\frac{\partial p}{\partial x_3}$  and  $\mathbf{w}_1$  has opposite sign that of  $x_3$ .

The reverse flow and the reverse microrotation are also related to a sign change of the scalar component of the skin friction ( $\tau_0$ ) in the direction of  $\mathbf{e}_3$  and of the scalar component of the skin couple friction ( $\sigma_0$ ) in the direction of  $\mathbf{e}_1$ :

$$\begin{aligned}\tau_0 &= \rho a^{3/2} (\nu + \nu_r)^{1/2} [x_1 (\varphi''(0) + \Gamma(0)) \mathbf{e}_1 + cx_3 (\gamma''(0) + \Phi(0)) \mathbf{e}_3] \\ &= \rho a^{3/2} (\nu + \nu_r)^{1/2} [x_1 \varphi''(0) \mathbf{e}_1 + cx_3 \gamma''(0) \mathbf{e}_3],\end{aligned}\quad (1.82)$$

$$\sigma_0 = \rho \lambda \frac{a^2}{2\nu_r} [-cx_3 \Phi'(0) \mathbf{e}_1 + x_1 \Gamma'(0) \mathbf{e}_3]. \quad (1.83)$$

REMARK 1.3.16. As for the Newtonian model, following Remark 1.3.8, we see from (1.82) that the stagnation-point is the only isolated point such that  $\tau_0 = \mathbf{0}$ . The classification of the origin can be done modifying slightly Remark 1.3.8. Actually, in this case we have:

$$\mathbf{v} \cong \sqrt{\frac{\nu + \nu_r}{a} \frac{\tau_0}{\mu}} \eta, \quad (1.84)$$

$$v_2 \cong -\frac{1}{2} \frac{\nu + \nu_r}{a} \nabla \cdot \left( \frac{\tau_0}{\mu} \right) \eta^2 := -\frac{1}{2} \Delta_s \eta^2, \quad (1.85)$$

$$\Delta_s = \sqrt{(\nu + \nu_r) a} [\varphi''(0) + c\gamma''(0)], \quad (1.86)$$

$$J_s = \rho^2 (\nu + \nu_r) a^3 [c\varphi''(0)\gamma''(0)]. \quad (1.87)$$

We recall that if  $\Delta_s < 0$ , then the origin is called ‘point of separation’, otherwise it is a ‘point of attachment’.

Where  $J_s < 0$ , there is a ‘saddle point’, and where  $J_s > 0$  there is a ‘nodal point’.

Hence if we know the signs of  $c, \varphi''(0), \gamma''(0)$ , then we are able to classify the stagnation-point.

For the micropolar fluid as well, the velocity vanishes at the boundary, but there is a limiting direction of flow there, which is inclined to the main flow direction at an angle  $\epsilon$  given formally by (1.73).

REMARK 1.3.17. In the sequel, we will show numerically that the solution  $(\varphi, \gamma, \Phi, \Gamma)$  of the problem considered in Theorem 1.3.10 satisfies the conditions (1.84)<sub>7,8,9,10</sub>; therefore we define:

- $\bar{\eta}_\varphi$  ( $\bar{\eta}_\gamma$ ) the value of  $\eta$  such that  $\varphi'(\bar{\eta}_\varphi) = 0.99$  ( $\gamma'(\bar{\eta}_\gamma) = 0.99$ );
- $\bar{\eta}_\Phi$  ( $\bar{\eta}_\Gamma$ ) the value of  $\eta$  such that  $\Phi(\bar{\eta}_\Phi) = -0.01$  ( $\Gamma(\bar{\eta}_\Gamma) = -0.01$ ).

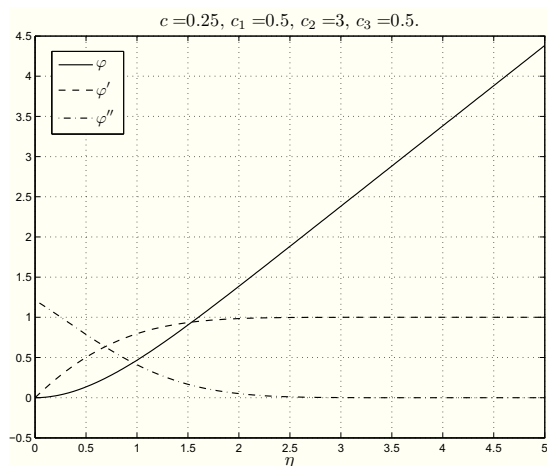


Figure 1.25:  $\varphi, \varphi', \varphi''$  profiles.

Hence if  $\eta > \bar{\eta}_\varphi$  ( $\eta > \bar{\eta}_\gamma$ ), then  $\varphi \cong \eta - \alpha$  ( $\gamma \cong \eta - \beta$ ), and if  $\eta > \bar{\eta}_\Phi$  ( $\eta > \bar{\eta}_\Gamma$ ), then  $\Phi \cong 0$  ( $\Gamma \cong 0$ ).

From the numerical integration we will also see that the influence of the viscosity on the velocity and on the microrotation appears only in a layer lining the boundary whose thickness is  $\delta_v = \max(\bar{\eta}_\varphi, \bar{\eta}_\gamma)$  for the velocity and  $\delta_w = \max(\bar{\eta}_\Phi, \bar{\eta}_\Gamma)$  for the microrotation.

The thickness  $\delta$  of the boundary layer for the flow is defined as

$$\delta := \max(\delta_v, \delta_w)$$

and it is proportional to  $\sqrt{\frac{\nu + \nu_r}{a}}$ .

We now deal with the numerical solution of problem (1.79), (1.81).

The values of the parameters  $c, c_1, c_2, c_3$  are chosen according to [13], [36], [26]: actually, we take the same values of  $c$  of Chapter 1.3.2 and of  $c_1, c_2, c_3$  of Chapter 1.1.3 and 1.2.3.

Figure 1.25 shows the behaviour of  $\varphi, \varphi', \varphi''$  when the parameters are fixed.

As one can see,

$$\lim_{\eta \rightarrow +\infty} \varphi''(\eta) = 0, \quad \lim_{\eta \rightarrow +\infty} \varphi'(\eta) = 1, \quad \lim_{\eta \rightarrow +\infty} [\varphi(\eta) - \eta] = -\alpha.$$

As far as the behaviour of  $\gamma, \gamma', \gamma''$  is concerned, if  $c < c_r$  then it is shown in Figure 1.26<sub>1</sub>, otherwise it is given in Figure 1.26<sub>2</sub>.

As we have already said, we have found a new interesting result: the function  $\Phi$  also presents a zone of reverse microrotation for some negative values of  $c$ . If

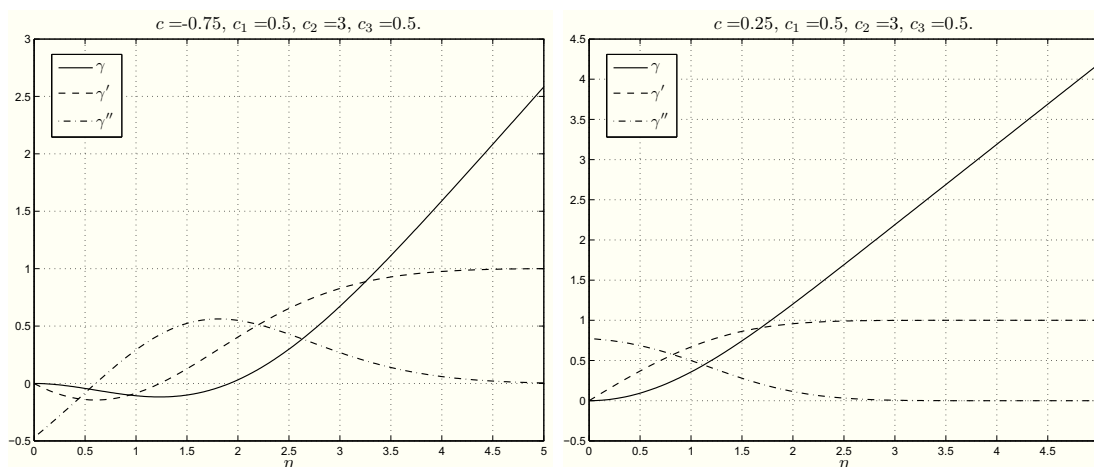


Figure 1.26: The first picture shows the profiles of  $\gamma, \gamma', \gamma''$  in the reverse flow ( $c = -0.75$ ). The second picture shows the profiles of  $\gamma, \gamma', \gamma''$  in the absence of the reverse flow ( $c = 0.25$ ).

$c < c_{rw}$  ( $\Phi'(0) > 0$ ) then the behaviour of  $\Phi, \Phi'$  is shown in Figure 1.27<sub>1</sub>, otherwise it is given in Figure 1.27<sub>2</sub>.

We underline that the thickness of the reverse microrotation zone is very small.

Figure 1.28 shows the profiles of  $\Gamma, \Gamma'$ .

The numerical integration furnishes the value of  $\varphi''(0), \gamma''(0), \Phi'(0), \Gamma'(0), h_d, \alpha, \beta, \bar{\eta}_\varphi, \bar{\eta}_\gamma, \bar{\eta}_\Phi, \bar{\eta}_\Gamma, \delta_v, \delta_w$  and  $\delta$  when  $c, c_1, c_2, c_3$  change: we provide them in Table 1.7 and in Table 1.8.

Our results extend and complete the previous studies ([26]), because the Authors didn't take into consideration the occurrence of the reverse flow and of the reverse microrotation, the thickness of the boundary layer, the parameters  $\alpha, \beta, h_d$  and the influence of  $c_1, c_2, c_3$  on the solution.

In particular, when  $c = 1$  we obtain the axisymmetric flow:  $\alpha = \beta = h_d, \varphi''(0) = \gamma''(0)$  and  $\Phi'(0) = \Gamma'(0)$ .

From Table 1.7 it appears that if we fix two parameters among  $c_1, c_2, c_3$ , then the influence of  $c_1$  on the descriptive quantities of motion is more evident.

Figures from 1.29 to 1.31 elucidate the dependence of the functions  $\varphi', \gamma', \Phi, \Gamma$ , on the parameters  $c_1, c_2, c_3$ . We can see that the functions which appear most influenced by  $c_1, c_2, c_3$  are  $\Phi$  and  $\Gamma$ , in other words the microrotation. More precisely, the profiles of  $\Phi$  and  $\Gamma$  rise as  $c_2$  or  $c_3$  increases and  $c_1$  decreases;  $c_1$  is the parameter that most influences the microrotation. The other two functions,  $\varphi'$  and  $\gamma'$ , do not show considerable variations as  $c_1, c_2, c_3$  assume different values.

From Table 1.8 it appears that when we set  $c$  and the reverse flow and the reverse microrotation don't occur, if we fix two parameters among  $c_1, c_2, c_3$ , then the values

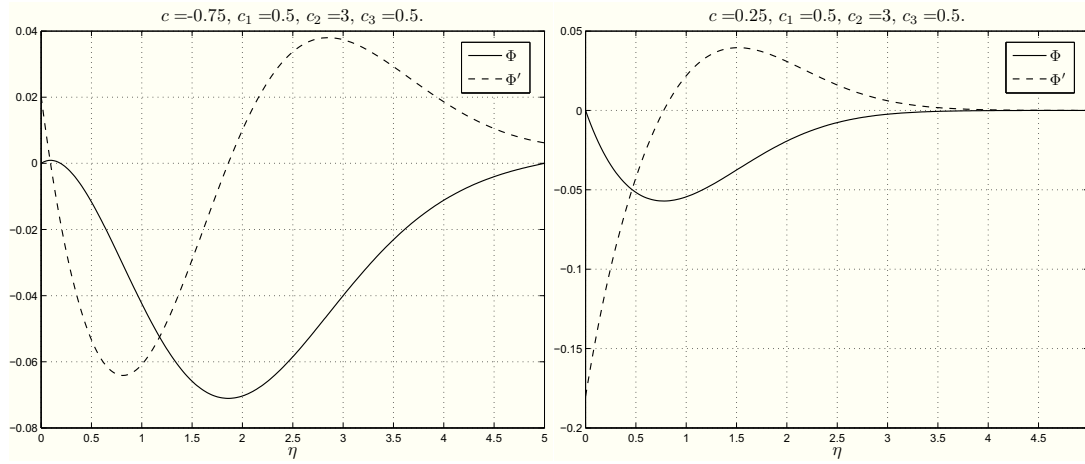


Figure 1.27: The first picture shows the profiles of  $\Phi, \Phi'$  in the reverse microrotation ( $c = -0.75$ ). The second picture shows the profiles of  $\Phi, \Phi'$  in the absence of the reverse microrotation ( $c = 0.25$ ).

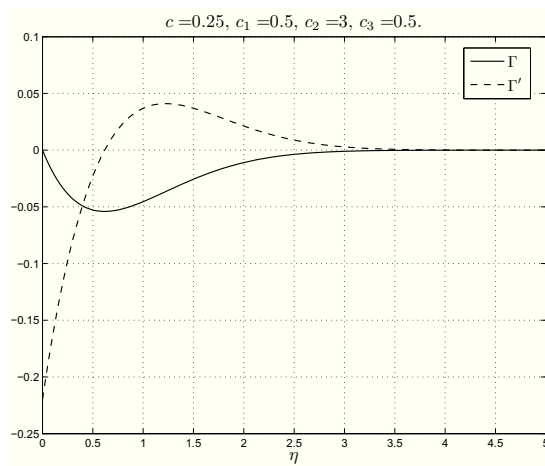


Figure 1.28:  $\Gamma, \Gamma'$  profiles.

Table 1.7: Descriptive quantities of motion for some values of  $c$ ,  $c_1$ ,  $c_2$ ,  $c_3$ .

$c$	$c_1$	$c_2$	$c_3$	$\varphi''(0)$	$\gamma''(0)$	$\Phi'(0)$	$\Gamma'(0)$	$h_d$	$\alpha$	$\beta$	
-0.75	0.1	1.5	0.1	1.2357	-0.4704	-0.0005	-0.0536	-4.9584	0.6343	2.4986	
			0.5	1.2371	-0.4709	-0.0015	-0.0514	-4.9640	0.6347	2.5009	
		3.0	0.1	1.2389	-0.4692	0.0050	-0.0448	-5.0094	0.6352	2.5167	
			0.5	1.2395	-0.4695	0.0046	-0.0438	-5.0111	0.6353	2.5175	
		0.5	1.5	0.1	1.1916	-0.4715	-0.0123	-0.2680	-4.3976	0.6209	2.2937
				0.5	1.1984	-0.4753	-0.0163	-0.2573	-4.4520	0.6225	2.3140
	3.0		0.1	1.2082	-0.4694	0.0222	-0.2242	-4.7357	0.6248	2.4116	
			0.5	1.2112	-0.4708	0.0202	-0.2194	-4.7497	0.6256	2.4173	
	-0.25	0.1	1.5	0.1	1.2144	0.2605	-0.0289	-0.0529	0.4224	0.6558	1.3558
				0.5	1.2156	0.2611	-0.0290	-0.0508	0.4226	0.6560	1.3563
			3.0	0.1	1.2176	0.2636	-0.0205	-0.0441	0.4214	0.6566	1.3625
				0.5	1.2181	0.2638	-0.0207	-0.0432	0.4215	0.6568	1.3627
0.5			1.5	0.1	1.1705	0.2296	-0.1479	-0.2643	0.4289	0.6414	1.2788
				0.5	1.1770	0.2323	-0.1490	-0.2541	0.4294	0.6427	1.2825
		3.0	0.1	1.1870	0.2454	-0.1042	-0.2205	0.4228	0.6458	1.3148	
			0.5	1.1897	0.2462	-0.1051	-0.2160	0.4232	0.6464	1.3160	
0.25		0.1	1.5	0.1	1.2369	0.7946	-0.0454	-0.0537	0.6662	0.6263	0.8257
				0.5	1.2383	0.7958	-0.0443	-0.0514	0.6664	0.6265	0.8260
			3.0	0.1	1.2400	0.7982	-0.0362	-0.0449	0.6671	0.6270	0.8274
				0.5	1.2406	0.7986	-0.0359	-0.0439	0.6672	0.6271	0.8275
	0.5		1.5	0.1	1.1931	0.7515	-0.2276	-0.2687	0.6514	0.6139	0.8013
				0.5	1.2003	0.7576	-0.2227	-0.2575	0.6524	0.6149	0.8027
		3.0	0.1	1.2092	0.7698	-0.1817	-0.2247	0.6559	0.6174	0.8099	
			0.5	1.2124	0.7722	-0.1801	-0.2198	0.6564	0.6179	0.8104	
	1.00	0.1	1.5	0.1	1.3013	1.3013	-0.0558	-0.0558	0.5665	0.5665	0.5665
				0.5	1.3030	1.3030	-0.0531	-0.0531	0.5667	0.5667	0.5667
			3.0	0.1	1.3043	1.3043	-0.0470	-0.0470	0.5670	0.5670	0.5670
				0.5	1.3051	1.3051	-0.0458	-0.0458	0.5671	0.5671	0.5671
0.5			1.5	0.1	1.2583	1.2583	-0.2793	-0.2793	0.5568	0.5568	0.5568
				0.5	1.2669	1.2669	-0.2657	-0.2657	0.5576	0.5576	0.5576
		3.0	0.1	1.2734	1.2734	-0.2354	-0.2354	0.5594	0.5594	0.5594	
			0.5	1.2774	1.2774	-0.2292	-0.2292	0.5598	0.5598	0.5598	

Table 1.8: Descriptive quantities of the boundary layer for some values of  $c$ ,  $c_1$ ,  $c_2$ ,  $c_3$ .

$c$	$c_1$	$c_2$	$c_3$	$\bar{\eta}_\varphi$	$\bar{\eta}_\gamma$	$\bar{\eta}_\Phi$	$\bar{\eta}_\Gamma$	$\delta_v$	$\delta_w$	$\delta$
-0.75	0.1	1.5	0.1	2.3204	4.4516	3.6586	1.5789	4.4516	3.6586	4.4516
			0.5	2.3332	4.4701	3.4224	1.3102	4.4701	3.4224	4.4701
		3.0	0.1	2.3424	4.4915	2.8943	0.9930	4.4915	2.8943	4.4915
			0.5	2.3486	4.4976	2.7868	0.8370	4.4976	2.7868	4.4976
	0.5	1.5	0.1	2.1157	3.9136	4.5392	2.9134	3.9136	4.5392	4.5392
			0.5	2.1616	4.0678	4.3181	2.4464	4.0678	4.3181	4.3181
		3.0	0.1	2.2046	4.2871	4.2340	2.3241	4.2871	4.2340	4.2871
			0.5	2.2319	4.3326	4.0645	2.1007	4.3326	4.0645	4.3326
-0.25	0.1	1.5	0.1	2.4106	3.5133	2.6648	1.6156	3.5133	2.6648	3.5133
			0.5	2.4222	3.5366	2.4337	1.3547	3.5366	2.4337	3.5366
		3.0	0.1	2.4334	3.5658	1.7784	0.9979	3.5658	1.7784	3.5658
			0.5	2.4387	3.5745	1.6902	0.8452	3.5745	1.6902	3.5745
	0.5	1.5	0.1	2.1959	3.0656	3.8678	2.9608	3.0656	3.8678	3.8678
			0.5	2.2389	3.1574	3.4688	2.5088	3.1574	3.4688	3.4688
		3.0	0.1	2.2932	3.3251	3.3429	2.3762	3.3251	3.3429	3.3429
			0.5	2.3177	3.3681	3.1414	2.1642	3.3681	3.1414	3.3681
0.25	0.1	1.5	0.1	2.2136	2.5693	1.9307	1.5711	2.5693	1.9307	2.5693
			0.5	2.2241	2.5848	1.6679	1.2934	2.5848	1.6679	2.5848
		3.0	0.1	2.2319	2.5978	1.2652	1.0015	2.5978	1.2652	2.5978
			0.5	2.2371	2.6044	1.1405	0.8419	2.6044	1.1405	2.6044
	0.5	1.5	0.1	2.0329	2.3194	3.1593	2.8349	2.3194	3.1593	3.1593
			0.5	2.0717	2.3749	2.6586	2.3296	2.3749	2.6586	2.6586
		3.0	0.1	2.1111	2.4429	2.6063	2.2902	2.4429	2.6063	2.6063
			0.5	2.1339	2.4727	2.3687	2.0482	2.4727	2.3687	2.4727
1.00	0.1	1.5	0.1	1.9071	1.9071	1.4569	1.4569	1.9071	1.4569	1.9071
			0.5	1.9166	1.9166	1.1527	1.1527	1.9166	1.1527	1.9166
		3.0	0.1	1.9201	1.9201	0.9782	0.9782	1.9201	0.9782	1.9201
			0.5	1.9251	1.9251	0.8015	0.8015	1.9251	0.8015	1.9251
	0.5	1.5	0.1	1.7701	1.7701	2.6108	2.6108	1.7701	2.6108	2.6108
			0.5	1.8056	1.8056	2.0339	2.0339	1.8056	2.0339	2.0339
		3.0	0.1	1.8246	1.8246	2.1206	2.1206	1.8246	2.1206	2.1206
			0.5	1.8464	1.8464	1.8292	1.8292	1.8464	1.8292	1.8464

Table 1.9: Values of  $c_r$ ,  $c_{rw}$  and  $c_h$  for  $c_1, c_2, c_3$ .

$c_1$	$c_2$	$c_3$	$c_r$	$c_{rw}$	$c_h$
0.10	1.50	0.10	-0.4268	-0.7606	-0.3953
		0.50	-0.4267	-0.7813	-0.3953
	3.00	0.10	-0.4279	-0.6428	-0.3941
		0.50	-0.4278	-0.6500	-0.3941
0.50	1.50	0.10	-0.4158	-0.8034	-0.4082
		0.50	-0.4152	-0.8226	-0.4077
	3.00	0.10	-0.4217	-0.6542	-0.4002
		0.50	-0.4214	-0.6614	-0.4002

of  $\alpha$ ,  $\beta$ ,  $|h_d|$ ,  $\varphi''(0)$ ,  $\gamma''(0)$ ,  $\Phi'(0)$ ,  $\Gamma'(0)$

- increase as  $c_2$  or  $c_3$  increases;
- decrease as  $c_1$  increases.

When the reverse flow and the reverse microrotation appear, the only difference is that  $\gamma''(0)$  and  $\Phi'(0)$  decrease if  $c_3$  increases.

As far as the comparison of the two models of fluids is concerned, we see from Tables 1.5 and 1.7-1.8 that the micropolar fluid reduces the values of  $\varphi''(0)$ ,  $|\gamma''(0)|$ ,  $\Phi'(0)$ ,  $\Gamma'(0)$ ,  $\alpha$ ,  $\beta$ ,  $\bar{\eta}_\varphi$ ,  $\bar{\eta}_\gamma$ . Therefore the thickness of the boundary layer of the velocity is smaller than that of the Newtonian fluid.

Table 1.9 shows the values of  $c_r$  and of  $c_{rw}$  for the reverse flow and the reverse microrotation, respectively, when  $c_1, c_2, c_3$  change. We can easily see that the range of  $c$  for which the reverse microrotation appears is included in the range of  $c$  for which the reverse flow occurs.

In this Table we also list the values of  $c_h$ , which is the value of  $c$  starting from which  $h_d$  is positive (i.e. if  $c < c_h$ , then  $h_d < 0$  and if  $c \geq c_h$ , then  $h_d \geq 0$ ). Since  $c_h$  is always bigger than  $c_r$  and  $c_{rw}$ , we have that  $h_d$  is always negative when the reverse flow and the reverse microrotation appear, similar to the Newtonian case.

Finally, as far as the classification of the stagnation-point is concerned, from Tables 1.10, 1.11 and 1.7 it appears that it is always a point of attachment. If  $c > 0$  or where there is the reverse flow, the origin is a nodal point, while when  $c < 0$  and the reverse flow does not appear, it is a saddle point (as it happened in the Newtonian case, see Figure 1.24).

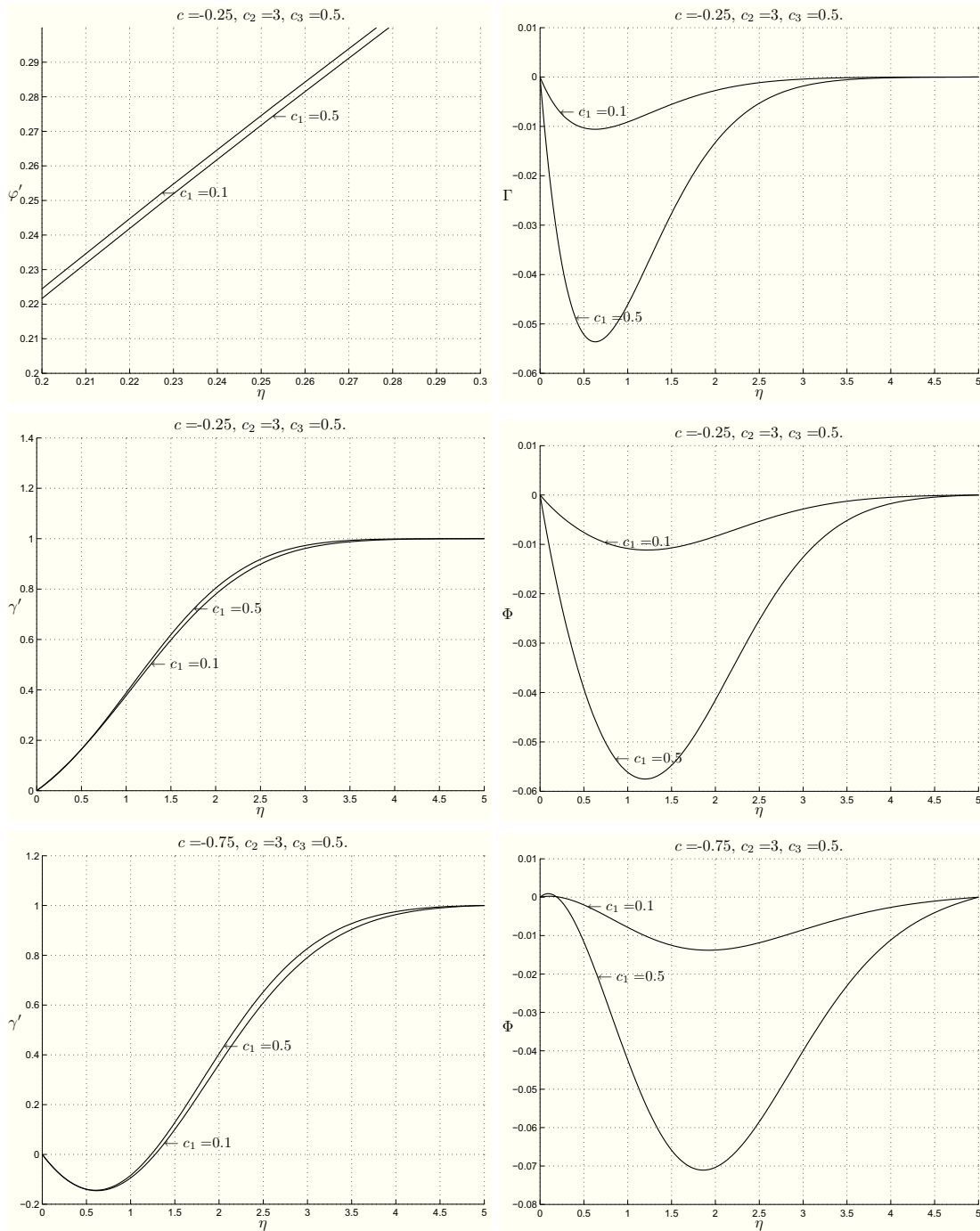


Figure 1.29:  $\varphi'$ ,  $\gamma'$ ,  $\Phi$ ,  $\Gamma$  profiles for  $c_2 = 3$ ,  $c_3 = 0.5$  when  $c_1 = 0.1$  and  $c_1 = 0.5$ . In the first four pictures  $c = -0.25$  and there are not reverse flow and reverse microrotation. The last two pictures show the behaviour of  $\gamma'$  and  $\Phi$  with respect to  $c_1$  when the reverse flow and the reverse microrotation occur ( $c = -0.75$ ).

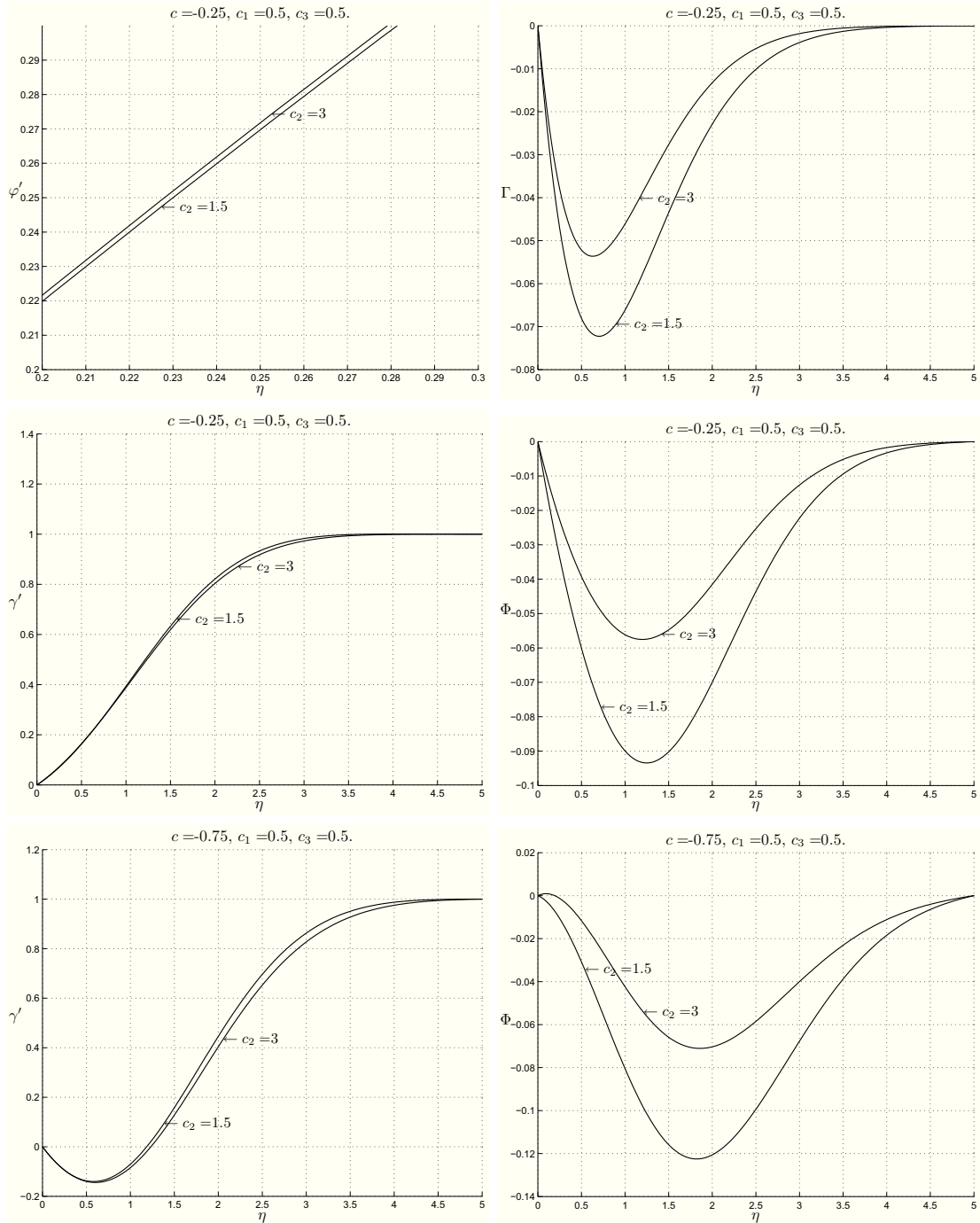


Figure 1.30:  $\varphi', \gamma', \Phi, \Gamma$  profiles for  $c_1 = 0.5, c_3 = 0.5$  when  $c_2 = 1.5$  and  $c_2 = 3$ . In the first four pictures  $c = -0.25$  and there are not reverse flow and reverse microrotation. The last two pictures show the behaviour of  $\gamma'$  and  $\Phi$  with respect to  $c_2$  when the reverse flow and the reverse microrotation occur ( $c = -0.75$ ).

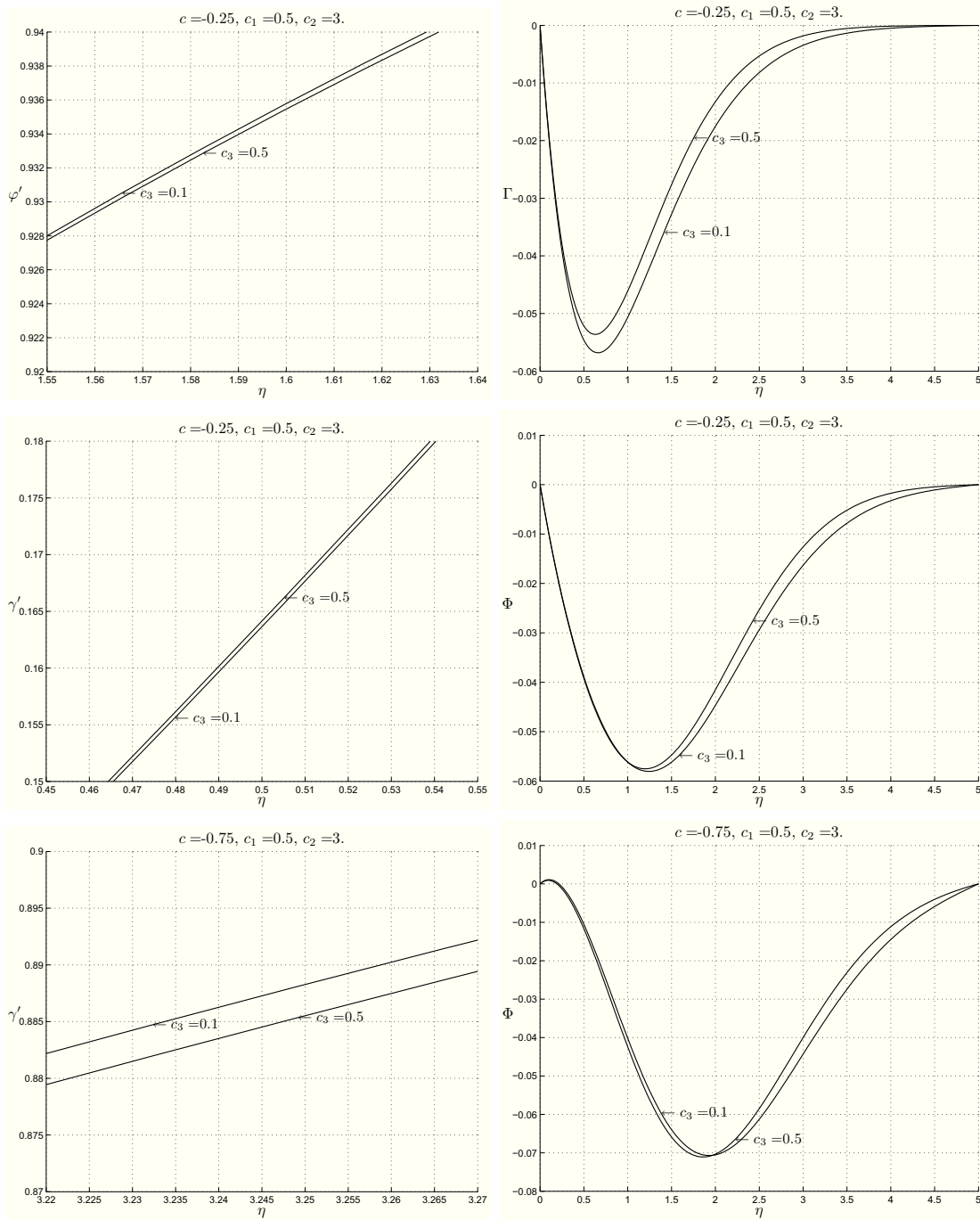


Figure 1.31:  $\varphi', \gamma', \Phi, \Gamma$  profiles for  $c_1 = 0.5, c_2 = 3$  when  $c_3 = 0.1$  and  $c_3 = 0.5$ . In the first four pictures  $c = -0.25$  and there are not reverse flow and reverse microrotation. The last two pictures show the behaviour of  $\gamma'$  and  $\Phi$  with respect to  $c_3$  when the reverse flow and the reverse microrotation occur ( $c = -0.75$ ).

Table 1.10: Values of  $\varphi''(0) + c\gamma''(0)$  and  $c\varphi''(0)\gamma''(0)$  in dependence on the values of  $c$ ,  $c_1$ ,  $c_2$ , and  $c_3$ .

$c$	$c_1$	$c_2$	$c_3$	$\varphi''(0)$	$\gamma''(0)$	$\varphi''(0) + c\gamma''(0)$	$c\varphi''(0)\gamma''(0)$	
-0.6428	0.10	1.50	0.10	1.2279	-0.3291	1.4394	0.2597	
			0.50	1.2293	-0.3309	1.4420	0.2615	
		3.00	0.10	1.2312	-0.3299	1.4433	0.2611	
			0.50	1.2318	-0.3305	1.4443	0.2617	
		0.50	1.50	0.10	1.1827	-0.3174	1.3867	0.2413
				0.50	1.1899	-0.3295	1.4018	0.2521
	3.00		0.10	1.2002	-0.3269	1.4103	0.2522	
			0.50	1.2032	-0.3300	1.4153	0.2553	
	-0.45	0.10	1.50	0.10	1.2172	-0.0360	1.2334	0.0197
				0.50	1.2185	-0.0363	1.2348	0.0199
			3.00	0.10	1.2205	-0.0345	1.2360	0.0190
				0.50	1.2210	-0.0346	1.2366	0.0190
0.50			1.50	0.10	1.1731	-0.0495	1.1954	0.0261
				0.50	1.1796	-0.0514	1.2027	0.0273
		3.00	0.10	1.1897	-0.0427	1.2089	0.0228	
			0.50	1.1925	-0.0433	1.2120	0.0233	
-0.4279		0.10	1.50	0.10	1.2165	-0.0017	1.2172	0.0009
				0.50	1.2177	-0.0019	1.2185	0.0010
			3.00	0.10	1.2197	0	1.2197	0
				0.50	1.2202	-0.0001	1.2203	0.0000
	0.50		1.50	0.10	1.1724	-0.0175	1.1799	0.0088
				0.50	1.1788	-0.0187	1.1868	0.0094
		3.00	0.10	1.1890	-0.0094	1.1930	0.0048	
			0.50	1.1918	-0.0098	1.1960	0.0050	
	-0.40	0.10	1.50	0.10	1.2157	0.0414	1.1991	-0.0201
				0.50	1.2169	0.0413	1.2004	-0.0201
			3.00	0.10	1.2189	0.0433	1.2016	-0.0211
				0.50	1.2194	0.0432	1.2021	-0.0211
0.50			1.50	0.10	1.1716	0.0228	1.1625	-0.0107
				0.50	1.1781	0.0223	1.1691	-0.0105
		3.00	0.10	1.1882	0.0324	1.1752	-0.0154	
			0.50	1.1910	0.0321	1.1781	-0.0153	

Table 1.11: Continuum of Table 1.10.

$c$	$c_1$	$c_2$	$c_3$	$\varphi''(0)$	$\gamma''(0)$	$\varphi''(0) + c\gamma''(0)$	$c\varphi''(0)\gamma''(0)$	
-0.3941	0.10	1.50	0.10	1.2155	0.0504	1.1956	-0.0242	
			0.50	1.2168	0.0503	1.1969	-0.0241	
		3.00	0.10	1.2187	0.0524	1.1981	-0.0252	
	0.50		1.2193	0.0524	1.1986	-0.0252		
	0.50	1.50	0.10	1.1715	0.0312	1.1592	-0.0144	
			0.50	1.1779	0.0309	1.1657	-0.0144	
		3.00	0.10	1.1881	0.0412	1.1718	-0.0193	
			0.50	1.1908	0.0410	1.1747	-0.0192	
	-0.10	0.10	1.50	0.10	1.2177	0.4503	1.1726	-0.0548
				0.50	1.2189	0.4510	1.1738	-0.0550
3.00			0.10	1.2209	0.4538	1.1755	-0.0554	
			0.50	1.2214	0.4540	1.1760	-0.0555	
0.50		1.50	0.10	1.1738	0.4129	1.1326	-0.0485	
			0.50	1.1805	0.4168	1.1388	-0.0492	
		3.00	0.10	1.1902	0.4309	1.1471	-0.0513	
			0.50	1.1930	0.4321	1.1498	-0.0516	

# Chapter 2

## MHD orthogonal stagnation-point flow

In this chapter we wish to investigate the influence of an external uniform electromagnetic field  $(\mathbf{E}_0, \mathbf{H}_0)$  on the steady plane orthogonal stagnation-point flow of a Newtonian or a micropolar fluid. Part of the results here presented are original.

Even if in Chapter 1.1 we have already defined the orthogonal stagnation-point flow for these two classes of fluids, it is now suitable to recall this motion and to introduce the equations which govern the motion of electrically conducting fluids and the usual boundary conditions for the electromagnetic field. To these equations and to these boundary conditions we will refer in the next chapters. Our purpose is to find exact solutions of these PDEs through similarity transformations.

As in the absence of the external electromagnetic field, the equations which govern the motion will be reduced to nonlinear ordinary differential boundary value problems which will be solved by the `bvp4c` MATLAB routine.

In order to reach our goal, the convenient starting-point of our analysis is the study of the steady plane MHD orthogonal stagnation-point flow of an inviscid fluid in three situations which are significant from a physical point of view.

### 2.1 Inviscid fluids

Consider the steady plane MHD flow of a homogeneous, incompressible, electrically conducting inviscid fluid near a stagnation point occupying the region  $\mathcal{S}$  given by

$$\mathcal{S} = \{\mathbf{x} \in \mathbb{R}^3 : (x_1, x_3) \in \mathbb{R}^2, x_2 > 0\}. \quad (2.1)$$

The boundary of  $\mathcal{S}$  having the equation  $x_2 = 0$  is a rigid fixed non-electrically conducting wall.

The equations governing such a flow in the absence of external mechanical body

forces and free electric charges are:

$$\begin{aligned}
\rho \mathbf{v} \cdot \nabla \mathbf{v} &= -\nabla p + \mu_e (\nabla \times \mathbf{H}) \times \mathbf{H}, \\
\nabla \cdot \mathbf{v} &= 0, \\
\nabla \times \mathbf{H} &= \sigma_e (\mathbf{E} + \mu_e \mathbf{v} \times \mathbf{H}), \\
\nabla \times \mathbf{E} &= \mathbf{0}, \quad \nabla \cdot \mathbf{E} = 0, \quad \nabla \cdot \mathbf{H} = 0,
\end{aligned}
\tag{2.2}$$

where  $\mathbf{v}$  is the velocity field,  $p$  is the pressure,  $\mathbf{E}$  and  $\mathbf{H}$  are the electric and magnetic fields, respectively,  $\rho$  is the mass density (constant  $> 0$ ),  $\mu_e$  is the magnetic permeability,  $\sigma_e$  is the electrical conductivity ( $\mu_e, \sigma_e = \text{constants} > 0$ ). We note that equation (2.2)<sub>1</sub> differs from (1.2)<sub>1</sub> for the term due to the Lorentz forces.

We assume that the region

$$\mathcal{S}^- = \{\mathbf{x} \in \mathbb{R}^3 : (x_1, x_3) \in \mathbb{R}^2, x_2 < 0\}
\tag{2.3}$$

is vacuum (free space) and that  $\mu_e$  is equal to the magnetic permeability of free space. The condition on  $\mu_e$  is not particularly restrictive, because it is satisfied by many liquid metals.

To equations (2.2) we append the no-penetration condition:

$$v_2 = 0 \quad \text{at} \quad x_2 = 0.
\tag{2.4}$$

As it is usual in electromagnetism, we will make the following transmission conditions:

- the tangential components of  $\mathbf{H}$  and  $\mathbf{E}$  are continuous across the plane  $x_2 = 0$ ; (2.5)

- the normal components of  $\mathbf{B} = \mu_e \mathbf{H}$  and  $\mathbf{D} = \varepsilon_e \mathbf{E}$  are continuous across the plane  $x_2 = 0$ ; (2.6)

where  $\mathbf{B}$  is the magnetic induction vector,  $\mathbf{D}$  the electric displacement field,  $\varepsilon_e$  the dielectric permittivity.

We recall that the orthogonal plane stagnation-point flow of such a fluid is described by a velocity field of the form

$$v_1 = ax_1, \quad v_2 = -ax_2, \quad v_3 = 0, \quad x_1 \in \mathbb{R}, \quad x_2 \in \mathbb{R}^+,
\tag{2.7}$$

with  $a$  positive constant.

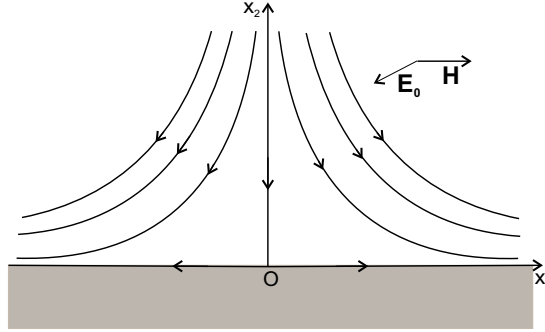


Figure 2.1: Description flow in CASE I.

As known, the streamlines of such a flow are hyperbolas whose asymptotes have the equations:

$$x_1 = 0 \quad \text{and} \quad x_2 = 0.$$

These two straight-lines are degenerate streamlines too.

Our aim is to study how such a flow is influenced by an external uniform electromagnetic field  $(\mathbf{E}_0, \mathbf{H}_0)$ . To this purpose, we consider three cases which are relevant from a physical point of view.

### 2.1.1 CASE I

$$\mathbf{E}_0 = E_0 \mathbf{e}_3, \quad \mathbf{H}_0 = \mathbf{0}, \quad E_0 = \text{constant}.$$

Let the induced electromagnetic field  $(\mathbf{E}^i, \mathbf{H}^i \equiv \mathbf{H})$  be in the form

$$\mathbf{E}^i = E_1^i \mathbf{e}_1 + E_2^i \mathbf{e}_2 + E_3^i \mathbf{e}_3,$$

$$\mathbf{H} = h(x_2) \mathbf{e}_1,$$

where  $h = h(x_2) \in C^1(\mathbb{R}^+)$ ,  $E_j^i = E_j^i(x_1, x_2, x_3) \in C^2(\mathbb{R}^3)$  for  $j = 1, 2, 3$  are unknown functions.

REMARK 2.1.1. *The solution of the problem relative to the electromagnetic field in  $\mathcal{S}^-$  is  $\mathbf{E} = \mathbf{E}_0 = E_0 \mathbf{e}_3$  and  $\mathbf{H} = \mathbf{H}_0 = \mathbf{0}$ .*

By the previous Remark, the boundary conditions (2.5) require that

$$E_1^i = 0, E_3^i = 0 \quad \text{at} \quad x_2 = 0,$$

$$h(0) = 0. \tag{2.8}$$

From (2.2)<sub>4</sub> follows that

$$\mathbf{E} \equiv \mathbf{E}^i + \mathbf{E}_0 = -\nabla\psi,$$

where  $\psi$  is the electrostatic scalar potential.

Moreover, (2.2)<sub>3</sub> provides  $\psi = \psi(x_3)$  and

$$\frac{d\psi}{dx_3}(x_3) = a\mu_e h(x_2)x_2 + \frac{h'(x_2)}{\sigma_e}.$$

From the previous equation we deduce that both members are equal to the same constant. Boundary condition (2.8)<sub>2</sub> furnishes

$$\begin{aligned} h' + a\sigma_e\mu_e hx_2 &= -\sigma_e E_0, & x_2 > 0, \\ \psi &= -E_0x_3 + \psi_0, & x_3 \in \mathbb{R}. \end{aligned} \quad (2.9)$$

The integration of differential problem (2.9)<sub>1</sub>, (2.8)<sub>3</sub> gives

$$h(x_2) = -\sigma_e E_0 e^{-\frac{ax_2^2}{2\eta_e}} \int_0^{x_2} e^{\frac{at^2}{2\eta_e}} dt, \quad x_2 \in \mathbb{R}^+, \quad (2.10)$$

with  $\eta_e = \frac{1}{\sigma_e\mu_e}$  = electrical resistivity.

As far as the pressure field is concerned, from (2.2)<sub>1</sub> we get

$$p = -\frac{1}{2}\rho a^2(x_1^2 + x_2^2) - \frac{\mu_e}{2}h^2(x_2) + p_0, \quad x_1 \in \mathbb{R}, \quad x_2 \in \mathbb{R}^+,$$

where  $h$  is given by (2.10) and  $p_0$  is the pressure at the stagnation point (see Remark 1.1.3).

We observe that the presence of  $\mathbf{E}_0$  modifies the pressure field, which is smaller than the pressure in the purely hydrodynamical flow.

Our results can be summarized in the following:

**THEOREM 2.1.2.** *Let a homogeneous, incompressible, electrically conducting inviscid fluid occupy the region  $\mathcal{S}$ . The steady plane MHD orthogonal stagnation-point flow of such a fluid has the following form when an external uniform electric field  $\mathbf{E}_0 = E_0\mathbf{e}_3$  is impressed :*

$$\begin{aligned} \mathbf{v} &= ax_1\mathbf{e}_1 - ax_2\mathbf{e}_2, & \mathbf{H} &= h(x_2)\mathbf{e}_1, & \mathbf{E} &= E_0\mathbf{e}_3, \\ p &= -\frac{1}{2}\rho a^2(x_1^2 + x_2^2) - \frac{\mu_e}{2}h^2(x_2) + p_0, & x_1 &\in \mathbb{R}, & x_2 &\in \mathbb{R}^+, \end{aligned}$$

where

$$h(x_2) = -\sigma_e E_0 e^{-\frac{ax_2^2}{2\eta_e}} \int_0^{x_2} e^{\frac{at^2}{2\eta_e}} dt.$$

REMARK 2.1.3. We note that the function in (2.10)

$$e^{-x^2} \int_0^x e^{t^2} dt =: daw(x), \quad x \in \mathbb{R}^+$$

is known as Dawson's integral and has the properties:

- $x \ll 1 \Rightarrow daw(x) \sim x$ ,
- $x \gg 1 \Rightarrow daw(x) \sim \frac{1}{2x}$ .

In order to plot the function  $h$ , it is suitable to introduce dimensionless parameters and variables.

To this end, we denote by  $V$  a characteristic velocity and put

$$L = \frac{V}{a}, \quad \eta = \frac{x_2}{L}, \quad \Psi(\eta) = \frac{h(L\eta)}{\sigma_e L E_0}.$$

So (2.9)<sub>1</sub> can be written as

$$\Psi'(\eta) + R_m \eta \Psi(\eta) = -1$$

where

$$R_m = \frac{LV}{\eta_e}$$

is the magnetic Reynolds number.

Therefore

$$\Psi(\eta) = -e^{-\frac{R_m}{2}\eta^2} \int_0^\eta e^{\frac{R_m}{2}t^2} dt.$$

Figures 2.2 show the graphs of the function  $\Psi$  for some values of  $R_m$ . We see that there is a layer lining the boundary beyond which  $\Psi$  vanishes. Its thickness increases if  $R_m$  decreases. At  $\eta = \frac{1}{\sqrt{R_m}}$  the function  $\Psi$  assumes a minimum whose value decreases as  $R_m$  decreases.

### 2.1.2 CASE II

$$\mathbf{E}_0 = \mathbf{0}, \quad \mathbf{H}_0 = H_0 \mathbf{e}_1, \quad H_0 = \text{constant}.$$

REMARK 2.1.4. Obviously,  $\mathbf{E} = \mathbf{E}_0 = \mathbf{0}$  and  $\mathbf{H} = \mathbf{H}_0 = H_0 \mathbf{e}_1$  in  $\mathcal{S}^-$ .

We take the induced electromagnetic field ( $\mathbf{E}^i \equiv \mathbf{E}, \mathbf{H}^i$ ) in the following form

$$\begin{aligned} \mathbf{E} &= E_1 \mathbf{e}_1 + E_2 \mathbf{e}_2 + E_3 \mathbf{e}_3, \\ \mathbf{H} &= [h(x_2) + H_0] \mathbf{e}_1, \end{aligned}$$

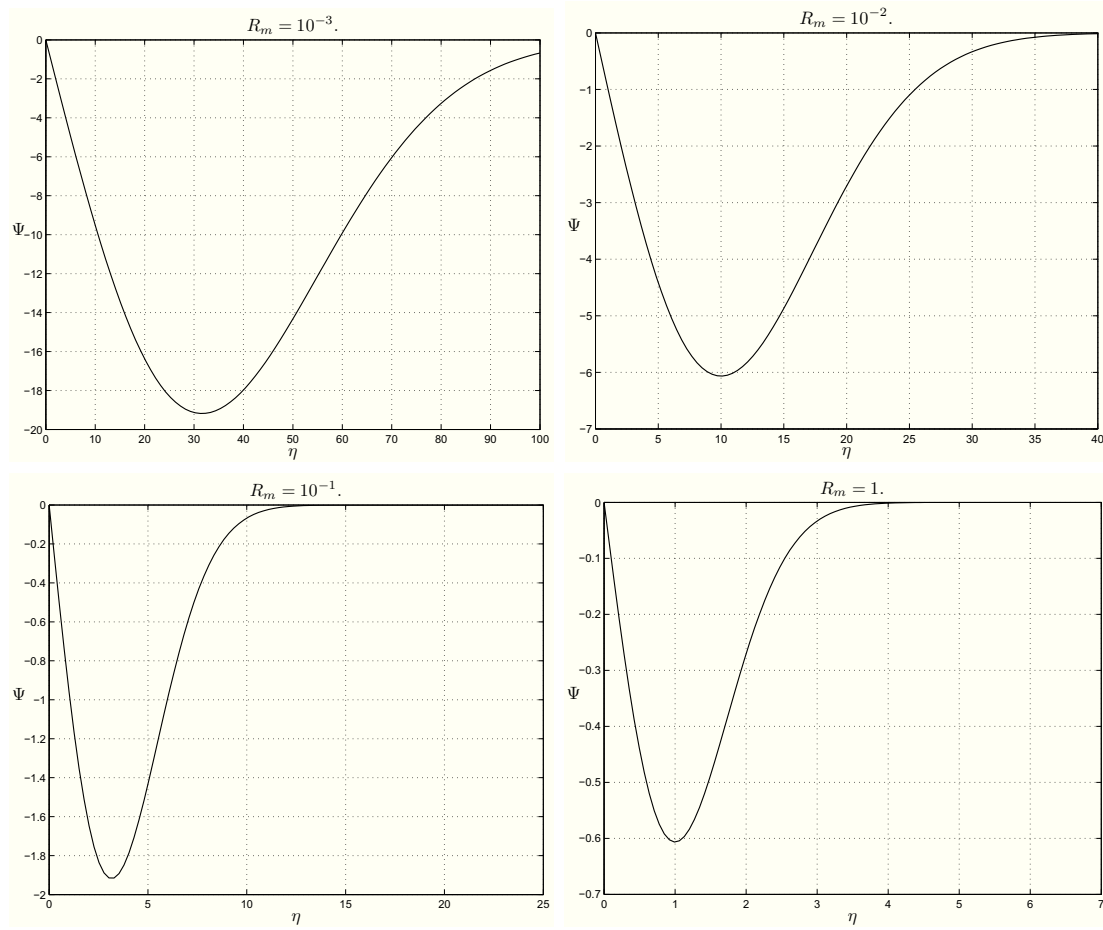


Figure 2.2: CASE I: plots showing the graphic of  $\Psi$  for  $R_m = 10^{-3}, 10^{-2}, 10^{-1}, 1$ .

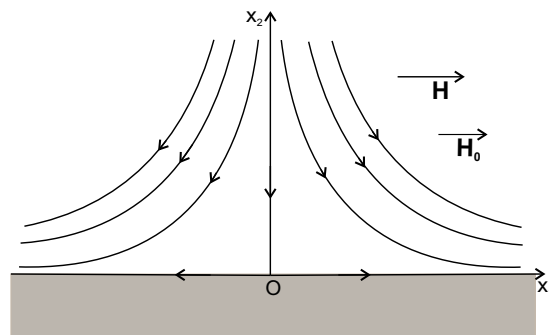


Figure 2.3: Description flow in CASE II.

where  $E_j = E_j(x_1, x_2, x_3) \in C^2(\mathbb{R}^3)$  for  $j = 1, 2, 3$ ,  $h \in C^1(\mathbb{R}^+)$  unknown functions. We append the boundary conditions (2.8).

By proceeding as in CASE I, we deduce  $\psi = \psi(x_3)$  and

$$\frac{d\psi}{dx_3}(x_3) = a\mu_e[h(x_2) + H_0]x_2 + \frac{h'(x_2)}{\sigma_e}.$$

From this relation, we get

$$\begin{aligned} h' + \frac{a}{\eta_e}hx_2 &= -\frac{a}{\eta_e}x_2H_0, \quad x_2 > 0, \\ h(0) &= 0 \end{aligned} \tag{2.11}$$

and  $\psi = \psi_0$  from which  $\mathbf{E} = \mathbf{0}$ .

The solution of (2.11) is

$$h(x_2) = H_0 \left( e^{-\frac{ax_2^2}{2\eta_e}} - 1 \right), \quad x_2 \in \mathbb{R}^+, \tag{2.12}$$

so that

$$\mathbf{H} = H_0 e^{-\frac{ax_2^2}{2\eta_e}} \mathbf{e}_1.$$

By virtue of (2.2)<sub>1</sub> we deduce that the pressure field is given by

$$p(x_1, x_2) = -\frac{1}{2}\rho a^2(x_1^2 + x_2^2) - \frac{\mu_e}{2}H_0^2 e^{-\frac{ax_2^2}{\eta_e}} + p_0^*, \quad x_1 \in \mathbb{R}, \quad x_2 \in \mathbb{R}^+.$$

We observe that the value of the pressure at the stagnation point is  $p_0^* - \mu_e \frac{H_0^2}{2}$ .

Finally, also in this case the presence of  $\mathbf{H}_0$  modifies the pressure, which is smaller than the pressure in the purely hydrodynamical flow.

Therefore we have obtained the following:

**THEOREM 2.1.5.** *Let a homogeneous, incompressible, electrically conducting inviscid fluid occupy the region  $\mathcal{S}$ . The steady plane MHD orthogonal stagnation-point flow of such a fluid has the following form when an external uniform magnetic field  $\mathbf{H}_0 = H_0\mathbf{e}_1$  is impressed:*

$$\mathbf{v} = ax_1\mathbf{e}_1 - ax_2\mathbf{e}_2, \quad \mathbf{H} = H_0 e^{-\frac{ax_2^2}{2\eta_e}} \mathbf{e}_1, \quad \mathbf{E} = \mathbf{0},$$

$$p = -\frac{1}{2}\rho a^2(x_1^2 + x_2^2) - \frac{\mu_e}{2}H_0^2 e^{-\frac{ax_2^2}{\eta_e}} + p_0^*, \quad x_1 \in \mathbb{R}, \quad x_2 \in \mathbb{R}^+.$$

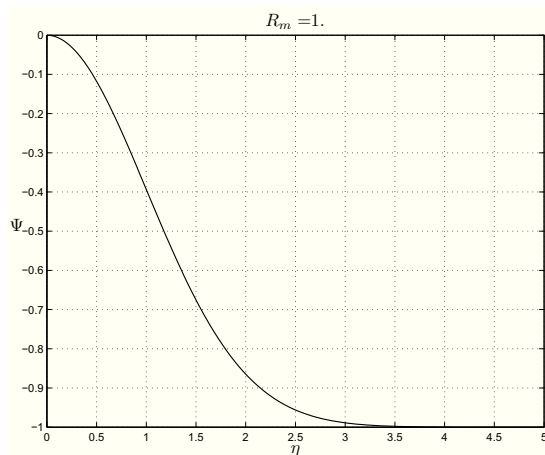
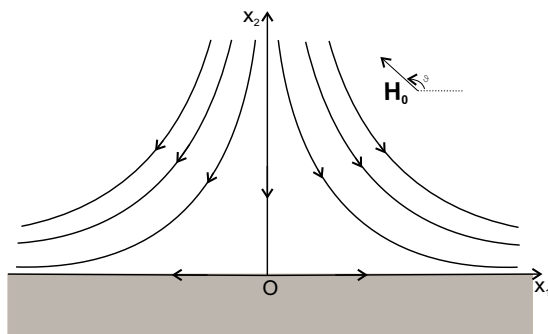
Figure 2.4: CASE II: plot showing  $\Psi$  for  $R_m = 1$ .

Figure 2.5: Description flow in CASE III.

In dimensionless form  $h$  becomes

$$\Psi(\eta) = e^{-\frac{R_m}{2}\eta^2} - 1, \quad \eta \in \mathbb{R}^+,$$

where

$$\Psi(\eta) = \frac{h(L\eta)}{H_0}.$$

Figure 2.4 shows that  $\Psi$  has an inflection point at  $\eta = \frac{1}{\sqrt{R_m}}$ .

### 2.1.3 CASE III

$$\mathbf{E}_0 = \mathbf{0}, \quad \mathbf{H}_0 = H_0(\cos \vartheta \mathbf{e}_1 + \sin \vartheta \mathbf{e}_2),$$

with  $\vartheta$  fixed in  $(0, \pi)$  and  $H_0$  constant.

Suppose the induced electromagnetic field ( $\mathbf{E}^i \equiv \mathbf{E}, \mathbf{H}^i$ ) to be in the form

$$\begin{aligned}\mathbf{E} &= E_1 \mathbf{e}_1 + E_2 \mathbf{e}_2 + E_3 \mathbf{e}_3, \\ \mathbf{H}^i &= h_1(x_1, x_2) \mathbf{e}_1 + h_2(x_1, x_2) \mathbf{e}_2,\end{aligned}$$

with  $h_1, h_2 \in C^1(\mathbb{R} \times \mathbb{R}^+)$ ,  $E_j = E_j(x_1, x_2, x_3) \in C^2(\mathbb{R}^3)$  for  $j = 1, 2, 3$  unknown functions.

Taking into account (2.2)<sub>3</sub>, (2.7) we obtain:

$$\sigma_e \mathbf{E} = \left[ \frac{\partial h_2}{\partial x_1} - \frac{\partial h_1}{\partial x_2} - \sigma_e \mu_e (v_1 h_2 - v_2 h_1 + H_0 v_1 \sin \vartheta - H_0 v_2 \cos \vartheta) \right] \mathbf{e}_3. \quad (2.13)$$

Hence  $\psi = \psi(x_3)$  and we conclude that  $\mathbf{E} = \mathbf{0}$ , as we have in CASE II.

Therefore from (2.2)<sub>3</sub>

$$\nabla \times \mathbf{H} = \sigma_e \mu_e \mathbf{v} \times \mathbf{H}$$

and

$$(\nabla \times \mathbf{H}) \times \mathbf{H} = \sigma_e \mu_e (\mathbf{v} \times \mathbf{H}) \times \mathbf{H},$$

from which it follows

$$\begin{aligned}\frac{\partial h_2}{\partial x_1}(x_1, x_2) - \frac{\partial h_1}{\partial x_2}(x_1, x_2) &= \\ \sigma_e \mu_e [a x_1 (h_2(x_1, x_2) + H_0 \sin \vartheta) + a x_2 (h_1(x_1, x_2) + H_0 \cos \vartheta)].\end{aligned} \quad (2.14)$$

To this equation we must add (2.2)<sub>6</sub> :

$$\frac{\partial h_1}{\partial x_1} + \frac{\partial h_2}{\partial x_2} = 0. \quad (2.15)$$

So  $(h_1, h_2)$  satisfies the PDEs system (2.14), (2.12) with suitable boundary conditions.

It is very difficult to find an explicit solution to this differential problem; so we proceed as it is usual in the literature by neglecting the induced magnetic field  $(h_1, h_2)$ . This approximation is motivated by physical arguments for MHD flow at small magnetic Reynolds number, e.g. in the flow of liquid metals. Then

$$\begin{aligned}(\nabla \times \mathbf{H}) \times \mathbf{H} &\simeq \sigma_e \mu_e (\mathbf{v} \times \mathbf{H}_0) \times \mathbf{H}_0 = \\ \sigma_e \mu_e H_0^2 [a \sin \vartheta x_1 + (b \sin \vartheta + a \cos \vartheta) x_2] (-\sin \vartheta \mathbf{e}_1 + \cos \vartheta \mathbf{e}_2).\end{aligned}$$

On substituting this approximation into (2.2)<sub>1</sub> we get:

$$\begin{aligned}\frac{\partial p}{\partial x_1} &= -\rho a^2 x_1 - aB_0^2 \sigma_e \sin \vartheta (\sin \vartheta x_1 + \cos \vartheta x_2), \\ \frac{\partial p}{\partial x_2} &= -\rho a^2 x_2 + aB_0^2 \sigma_e \cos \vartheta (\sin \vartheta x_1 + \cos \vartheta x_2), \\ \frac{\partial p}{\partial x_3} &= 0 \Rightarrow p = p(x_1, x_2),\end{aligned}\tag{2.16}$$

with  $B_0 = \mu_e H_0$ .

It is possible to find a function  $p = p(x_1, x_2)$  satisfying equations (2.16) if, and only if,

$$\frac{\partial^2 p}{\partial x_1 \partial x_2} = \frac{\partial^2 p}{\partial x_2 \partial x_1}.\tag{2.17}$$

Taking into account (2.16), the previous condition furnishes

$$\sin \vartheta \cos \vartheta = 0.\tag{2.18}$$

From (2.18), we get

$$\cos \vartheta = 0 \Rightarrow \vartheta = \frac{\pi}{2}.\tag{2.19}$$

So in this case the MHD orthogonal stagnation-point flow is possible if, and only if,  $\mathbf{H}_0$  is parallel to the streamline  $x_1 = 0$ .

Under the condition (2.19), the pressure field has the form

$$p = -\frac{1}{2}\rho a^2(x_1^2 + x_2^2) - \sigma_e B_0^2 \frac{a}{2} x_1^2 + p_0, \quad x_1 \in \mathbb{R}, \quad x_2 \in \mathbb{R}^+.\tag{2.20}$$

We have thus proved the following:

**THEOREM 2.1.6.** *Let a homogeneous, incompressible, electrically conducting inviscid fluid occupy the region  $\mathcal{S}$ . If we impress an external magnetic field*

$$\mathbf{H}_0 = H_0(\cos \vartheta \mathbf{e}_1 + \sin \vartheta \mathbf{e}_2), \quad 0 < \vartheta < \pi,$$

*and we neglect the induced magnetic field, then the steady MHD orthogonal plane stagnation-point flow of such a fluid is possible if, and only if,*

$$\vartheta = \frac{\pi}{2}, \quad \text{i.e.} \quad \mathbf{H}_0 = H_0 \mathbf{e}_2.$$

Moreover,

$$\mathbf{v} = ax_1 \mathbf{e}_1 - ax_2 \mathbf{e}_2,$$

$$p = -\frac{1}{2}\rho a^2(x_1^2 + x_2^2) - \sigma_e B_0^2 \frac{a}{2} x_1^2 + p_0, \quad x_1 \in \mathbb{R}, \quad x_2 \in \mathbb{R}^+.$$

REMARK 2.1.7. *In order to study the orthogonal stagnation-point flow for viscous fluids, it is convenient to recall Remark 1.1.4. More precisely, we suppose the inviscid fluid orthogonally impinging on the flat plane  $x_2 = A$  and*

$$v_1 = ax_1, \quad v_2 = -a(x_2 - A), \quad v_3 = 0 \quad x_1 \in \mathbb{R}, \quad x_2 \geq A, \quad (2.21)$$

with  $A = \text{constant}$ .

*In such a way the stagnation point is  $(0, A)$  and the streamlines are hyperbolas whose asymptotes are  $x_1 = 0$  and  $x_2 = A$ .*

*Under these assumptions Theorems 2.1.2, 2.1.5, 2.1.6 continue to hold by replacing  $x_2$  with  $x_2 - A$ .*

## 2.2 Newtonian fluids

We now study the steady plane MHD flow of a homogeneous, incompressible, electrically conducting Newtonian fluid near a stagnation point occupying the region  $\mathcal{S}$  given by (2.1).

The MHD equations governing such a flow in the absence of external mechanical body forces and free electric charges are the equations

$$\begin{aligned} \mathbf{v} \cdot \nabla \mathbf{v} &= -\frac{1}{\rho} \nabla p + \nu \Delta \mathbf{v} + \frac{\mu_e}{\rho} (\nabla \times \mathbf{H}) \times \mathbf{H}, \\ \nabla \cdot \mathbf{v} &= 0, \\ \nabla \times \mathbf{H} &= \sigma_e (\mathbf{E} + \mu_e \mathbf{v} \times \mathbf{H}), \\ \nabla \times \mathbf{E} &= \mathbf{0}, \quad \nabla \cdot \mathbf{E} = 0, \quad \nabla \cdot \mathbf{H} = 0, \end{aligned} \quad \text{in } \mathcal{S}, \quad (2.22)$$

where  $\nu$  is the kinematic viscosity.

As far as boundary conditions are concerned, we only modify the condition for  $\mathbf{v}$ , assuming the no-slip boundary condition

$$\mathbf{v}|_{x_2=0} = \mathbf{0}. \quad (2.23)$$

We assume the velocity components to be of the same form as in the non-magnetic case (see Chapter 1.1.2)

$$v_1 = ax_1 f'(x_2), \quad v_2 = -af(x_2), \quad v_3 = 0, \quad x_1 \in \mathbb{R}, \quad x_2 \in \mathbb{R}^+, \quad (2.24)$$

with  $f$  sufficiently regular unknown function ( $f \in C^3(\mathbb{R}^+)$ ) to be determined so that

$$f(0) = 0, \quad f'(0) = 0. \quad (2.25)$$

$$\lim_{x_2 \rightarrow +\infty} f'(x_2) = 1. \quad (2.26)$$

Condition (2.25) is the no-slip boundary condition, while (2.26) means that we require that at infinity the flow of a Newtonian fluid approaches the flow of an inviscid fluid given by (2.21) ([19]).

Hence in the sequel, when we will refer to an inviscid fluid, all results obtained in Chapter 2.1 have to be modified replacing  $x_2$  with  $x_2 - A$ , respectively. In particular, the asymptotic behaviour of  $f$  at infinity is related to the constant  $A$  in the following way:

$$\lim_{x_2 \rightarrow +\infty} [f(x_2) - x_2] = -A. \quad (2.27)$$

As for the case of an inert fluid (Chapter 1.1.2),  $A$  is determined as part of the solution of the problem ([47]).

In order to study the influence of an external uniform electromagnetic field, we consider the three cases analyzed for the inviscid fluid.

### 2.2.1 CASE I-N: $\mathbf{E}_0 = E_0 \mathbf{e}_3$ .

By proceeding as for an inviscid fluid, from (2.22)<sub>3</sub>, (2.22)<sub>4</sub> and boundary conditions for electromagnetic field (2.5), we obtain

$$\begin{aligned} h' + \frac{a}{\eta_e} f h &= -\eta_e E_0, \quad x_2 > 0, \quad h(0) = 0, \\ \psi(x_3) &= -E_0 x_3 + \psi_0, \quad x_3 \in \mathbb{R}. \end{aligned} \quad (2.28)$$

If we regard  $f$  as a known function, then the integration of the differential problem (2.28) gives

$$h(x_2) = -\sigma_e E_0 e^{-\frac{a}{\eta_e} \int_0^{x_2} f(t) dt} \int_0^{x_2} e^{\frac{a}{\eta_e} \int_0^s f(t) dt} ds, \quad x_2 \in \mathbb{R}^+. \quad (2.29)$$

As it is easy to verify, the induced magnetic fields given by (2.29) and (2.10) have the same asymptotic behaviour at infinity  $\left( \sim -\frac{\eta_e E_0 \sigma_e}{a(x_2 - A)} \right)$ .

We now proceed in order to determine  $p, f$ . Substituting (2.24) into (2.22) we obtain:

$$\begin{aligned} p &= p(x_1, x_2), \\ ax_1(\nu f''' + af f'' - af'^2) &= \frac{1}{\rho} \frac{\partial p}{\partial x_1}, \\ \nu af'' + a^2 f' f + \frac{\mu_e}{\rho} h' h &= -\frac{1}{\rho} \frac{\partial p}{\partial x_2}. \end{aligned} \quad (2.30)$$

The integration of (2.30)<sub>3</sub> furnishes

$$p(x_1, x_2) = -\frac{1}{2}\rho a^2 f^2(x_2) - \rho a \nu f'(x_2) - \frac{\mu_e}{2} h^2(x_2) + P(x_1),$$

where  $P(x_1)$  is determined supposing that, far from the wall, the pressure  $p$  has the same behaviour as for an inviscid electroconducting fluid whose velocity is given by (2.21).

Therefore, since the induced magnetic fields given by (2.29) and (2.10) have the same asymptotic behaviour, we get, by virtue of (2.26), (2.27)

$$P(x_1) = -\rho \frac{a^2}{2} x_1^2 + \rho a \nu + p_0^*.$$

Finally,

$$p(x_1, x_2) = -\rho \frac{a^2}{2} [x_1^2 + f^2(x_2)] - \rho a \nu f'(x_2) - \frac{\mu_e}{2} h^2(x_2) + p_0, \quad (2.31)$$

with  $p_0 = p_0^* + \rho a \nu$ .

Equation (2.30)<sub>2</sub> together with (2.31) furnishes

$$\frac{\nu}{a} f''' + f f'' - f'^2 + 1 = 0, \quad (2.32)$$

with

$$f(0) = 0, \quad f'(0) = 0, \quad \lim_{x_2 \rightarrow +\infty} f'(x_2) = 1. \quad (2.33)$$

The function  $f$  satisfies the same differential problem that governs the orthogonal stagnation-point flow in the absence of an electromagnetic field (see Chapter 1.1.2). Hence, the external uniform electromagnetic field doesn't influence the flow.

Summarizing, we have:

**THEOREM 2.2.1.** *Let a homogeneous, incompressible, electrically conducting Newtonian fluid occupy the region  $\mathcal{S}$ . The steady MHD orthogonal plane stagnation-point flow of such a fluid has the following form when an external uniform electric field  $\mathbf{E}_0 = E_0 \mathbf{e}_3$  is impressed:*

$$\mathbf{v} = a x_1 f'(x_2) \mathbf{e}_1 - a f(x_2) \mathbf{e}_2, \quad \mathbf{H} = h(x_2) \mathbf{e}_1, \quad \mathbf{E} = E_0 \mathbf{e}_3,$$

$$p = -\rho \frac{a^2}{2} [x_1^2 + f^2(x_2)] - \rho a \nu f'(x_2) - \frac{\mu_e}{2} h^2(x_2) + p_0, \quad x_1 \in \mathbb{R}, \quad x_2 \in \mathbb{R}^+,$$

where  $f$  satisfies the problem (2.32), (2.33) and  $h(x_2)$  is given by (2.29).

If we use the dimensionless variables given by (1.13) and if we put

$$\Psi(\eta) = \sqrt{\frac{a}{\nu}} \frac{h(\sqrt{\frac{\nu}{a}}\eta)}{\eta_e E_0},$$

then we can write problem (2.32), (2.33), (2.28) in dimensionless form

$$\begin{aligned} \varphi''' + \varphi\varphi'' - \varphi'^2 + 1 &= 0, \\ \Psi' + R_m\varphi\Psi &= -1, \\ \varphi(0) = 0, \quad \varphi'(0) = 0, \quad \Psi(0) &= 0, \\ \lim_{\eta \rightarrow +\infty} \varphi'(\eta) &= 1, \end{aligned} \tag{2.34}$$

where we have

$$\alpha = \sqrt{\frac{a}{\nu}} A, \quad R_m = \frac{\nu}{\eta_e} = \text{magnetic Reynolds number.}$$

We have chosen  $V = \sqrt{\nu a}$  as the characteristic velocity of the magnetic Reynolds number. This particular magnetic Reynolds number is also known in the literature as the magnetic Prandtl number.

Notice the one-way coupling, that the function  $\varphi$  influences the function  $\Psi$  but not viceversa.

The function  $\varphi$  satisfies the Hiemenz equation ([47], [19]), which has already been solved numerically in Chapter 1.1.2 (its behaviour is displayed in Figure 1.3).

In dimensionless form the induced magnetic field is given by:

$$\Psi(\eta) = -e^{-R_m \int_0^\eta \varphi(s) ds} \int_0^\eta e^{R_m \int_0^t \varphi(s) ds} dt, \quad \eta \in \mathbb{R}^+.$$

Figure 2.6<sub>1</sub> shows the trend of the induced magnetic field  $\Psi$  with  $R_m = 1$ , that is similar to the behaviour of  $\Psi$  in CASE I (inviscid fluid). Figure 2.6<sub>2</sub> provides the profile of the induced magnetic field when  $R_m = 10^{-6}$ : for  $\eta \in [0, 5]$  the graphic is approximately linear because in this interval, for very small values of  $R_m$ , the equation (2.34)<sub>2</sub> reduces to  $\Psi' \cong -1$ .

### 2.2.2 CASE II-N: $\mathbf{H}_0 = H_0 \mathbf{e}_1$ .

As for an inviscid fluid and as in CASE I-N, from (2.22)<sub>3</sub>, (2.22)<sub>4</sub> and (2.5), we get

$$h' + \frac{a}{\eta_e} fh = -\frac{a}{\eta_e} f H_0, \quad x_2 > 0, \quad h(0) = 0, \tag{2.35}$$

$$\psi(x_3) = \psi_0 \Rightarrow \mathbf{E} = \mathbf{0}.$$

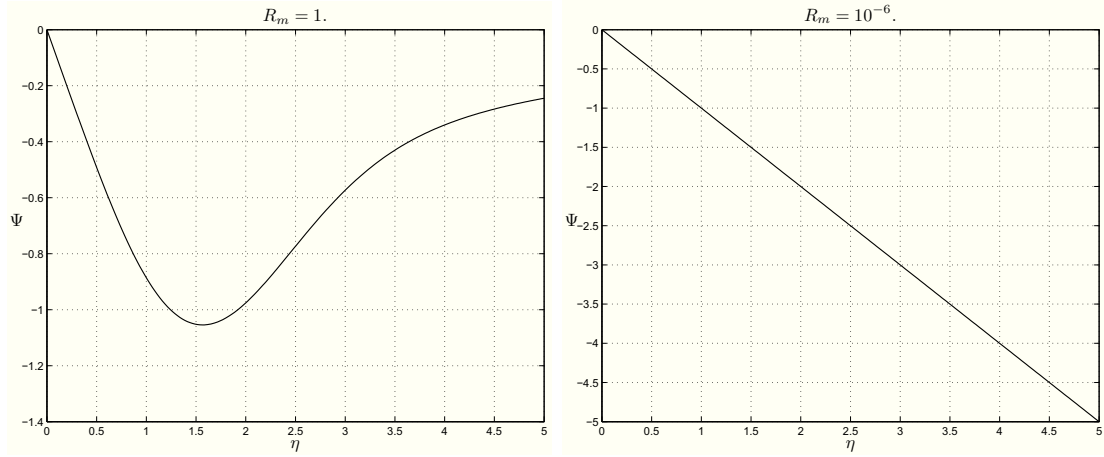


Figure 2.6: CASE I-N: plots showing  $\Psi$  with  $R_m = 1, 10^{-6}$ .

The integration of (2.35) leads to

$$h(x_2) = H_0 \left[ e^{-\frac{a}{\eta_e} \int_0^{x_2} f(t) dt} - 1 \right], \quad x_2 \in \mathbb{R}^+, \quad (2.36)$$

so that

$$\mathbf{H} = H_0 e^{-\frac{a}{\eta_e} \int_0^{x_2} f(s) ds} \mathbf{e}_1.$$

The pressure field then becomes

$$p(x_1, x_2) = -\rho \frac{a^2}{2} [x_1^2 + f^2(x_2)] - \rho a \nu f'(x_2) - \frac{\mu_e}{2} [h(x_2) + H_0]^2 + p_0^*, \quad (2.37)$$

$$p_0^* = p_0 + \rho a \nu,$$

and  $f$  satisfies problem (2.32), (2.33).

Hence in this case also the external uniform electromagnetic field does not influence the flow.

So we have got the following:

**THEOREM 2.2.2.** *Let a homogeneous, incompressible, electrically conducting Newtonian fluid occupy the region  $\mathcal{S}$ . The steady MHD orthogonal plane stagnation-point flow of such a fluid has the following form when an external uniform magnetic field  $\mathbf{H}_0 = H_0 \mathbf{e}_1$  is impressed:*

$$\mathbf{v} = ax_1 f'(x_2) \mathbf{e}_1 - af(x_2) \mathbf{e}_2, \quad \mathbf{H} = [h(x_2) + H_0] \mathbf{e}_1, \quad \mathbf{E} = \mathbf{0},$$

$$p = -\rho \frac{a^2}{2} [x_1^2 + f^2(x_2)] - \rho a \nu f'(x_2) - \frac{\mu_e}{2} [h(x_2) + H_0]^2 + p_0^*,$$

$$x_1 \in \mathbb{R}, \quad x_2 \in \mathbb{R}^+,$$

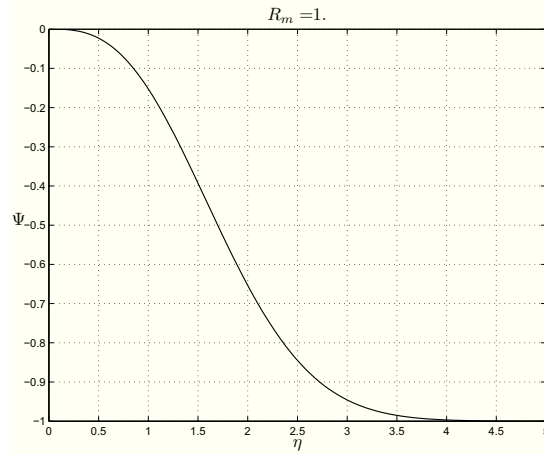


Figure 2.7: CASE II-N: plot showing  $\Psi$  for  $R_m = 1$

where  $h(x_2)$  is given by (2.36) and  $f$  satisfies the problem (2.32), (2.33).

In dimensionless form,  $h(x_2)$  is transformed into

$$\Psi(\eta) = e^{-R_m \int_0^\eta \varphi(t) dt} - 1, \quad \eta \in \mathbb{R}^+, \quad (2.38)$$

where

$$\Psi(\eta) = \frac{h(\sqrt{\frac{z}{a}}\eta)}{H_0}.$$

Of course the ordinary differential problem governing  $\varphi$  is the same as in (2.34); we have only to compute  $\Psi(\eta)$  given by (2.38).

Figure 2.7 shows that  $\Psi$  has a similar behaviour to the induced magnetic field in CASE II.

### 2.2.3 CASE III-N: $\mathbf{H}_0 = H_0 \mathbf{e}_2$ .

Taking into account the results obtained for an inviscid fluid, we assume

$$\mathbf{H}_0 = H_0 \mathbf{e}_2, \quad \mathbf{E}_0 = \mathbf{0}.$$

By means of the same arguments of CASE III, we deduce

$$\mathbf{E} = \mathbf{0} \Rightarrow \nabla \times \mathbf{H} = \sigma_e \mu_e (\mathbf{v} \times \mathbf{H})$$

and we neglect the induced magnetic field, replacing (2.22)<sub>1</sub> with the equation:

$$\mathbf{v} \cdot \nabla \mathbf{v} = -\frac{1}{\rho} \nabla p + \nu \Delta \mathbf{v} + \frac{\mu_e}{\rho} (\mathbf{v} \times \mathbf{H}_0) \times \mathbf{H}_0. \quad (2.39)$$

In order to determine  $p, f$  we substitute (2.24) into (2.39) to arrive at

$$\begin{aligned} p &= p(x_1, x_2), \\ ax_1 \left( \nu f''' + af f'' - af'^2 - \frac{\sigma_e B_0^2}{\rho} f' \right) &= \frac{1}{\rho} \frac{\partial p}{\partial x_1}, \\ \nu a f'' + a^2 f' f &= -\frac{1}{\rho} \frac{\partial p}{\partial x_2}. \end{aligned} \quad (2.40)$$

The integration of (2.40)<sub>3</sub> gives

$$p(x_1, x_2) = -\frac{1}{2} \rho a^2 f^2(x_2) - \rho a \nu f'(x_2) + P(x_1),$$

where  $P(x_1)$  has to be found as in CASE I-N, II-N.

Precisely, after some calculations, we obtain

$$P(x_1) = -\rho \frac{a^2}{2} \left( 1 + \frac{\sigma_e B_0^2}{\rho a} \right) x_1^2 + p_0^*.$$

So the pressure field is:

$$\begin{aligned} p(x_1, x_2) &= -\rho \frac{a^2}{2} [x_1^2 + f^2(x_2)] - \rho a \nu f'(x_2) - \frac{a}{2} \sigma_e B_0^2 x_1^2 + p_0, \\ x_1 &\in \mathbb{R}, \quad x_2 \in \mathbb{R}^+. \end{aligned} \quad (2.41)$$

Then (2.40)<sub>2</sub> furnishes

$$\frac{\nu}{a} f''' + f f'' - f'^2 + 1 + M^2(1 - f') = 0 \quad (2.42)$$

where

$$M^2 = \frac{\sigma_e B_0^2}{\rho a} = \text{Hartmann number.}$$

To equation (2.42) we append boundary conditions (2.33).

We remark that, unlike the previous cases, the external electromagnetic field modifies the flow and if  $M^2 = 0$ , then equation (2.42) reduces to (2.32).

**THEOREM 2.2.3.** *Let a homogeneous, incompressible, electrically conducting Newtonian fluid occupy the region  $\mathcal{S}$ . If we impress an external magnetic field  $\mathbf{H}_0 = H_0 \mathbf{e}_2$  and we neglect the induced magnetic field, then the steady MHD orthogonal plane stagnation-point flow of such a fluid has the form*

$$\mathbf{v} = ax_1 f'(x_2) \mathbf{e}_1 - af(x_2) \mathbf{e}_2, \quad \mathbf{E} = \mathbf{0},$$

$$p = -\rho \frac{a^2}{2} [x_1^2 + f^2(x_2)] - \rho a \nu f'(x_2) - \frac{a}{2} \sigma_e B_0^2 x_1^2 + p_0, \quad x_1 \in \mathbb{R}, \quad x_2 \in \mathbb{R}^+,$$

where  $f$  satisfies problem (2.42), (2.33).

Table 2.1: CASE III-N: descriptive quantities of the motion for several values of  $M^2$ .

$M^2$	$\varphi''(0)$	$\alpha$	$\bar{\eta}_\varphi$
1	1.5853	0.5410	2.1059
2	1.8735	0.4748	1.9127
4	2.3467	0.3936	1.6482
5	2.5507	0.3661	1.5517
10	3.3917	0.2831	1.2394

System (2.42), (2.33) in dimensionless form becomes

$$\begin{aligned}
 \varphi''' + \varphi\varphi'' - \varphi'^2 + 1 + M^2(1 - \varphi') &= 0, \\
 \varphi(0) = 0, \quad \varphi'(0) &= 0, \\
 \lim_{\eta \rightarrow +\infty} \varphi'(\eta) &= 1.
 \end{aligned} \tag{2.43}$$

REMARK 2.2.4. *The solution of the differential boundary value problem (2.43) exists and it is unique as proved by Hoernel in [34].*

REMARK 2.2.5. *As in the absence of the external magnetic field (Remark 1.1.6), we will see that*

$$\lim_{\eta \rightarrow +\infty} \varphi''(\eta) = 0, \quad \lim_{\eta \rightarrow +\infty} \varphi'(\eta) = 1.$$

Therefore we define:

- $\bar{\eta}_\varphi$  the value of  $\eta$  such that  $\varphi'(\bar{\eta}_\varphi) = 0.99$ .

Hence if  $\eta > \bar{\eta}_\varphi$ , then  $\varphi \cong \eta - \alpha$ , with  $\alpha = \sqrt{\frac{a}{\nu}}A$ .

We have solved numerically problem (2.43) using the `bvp4c` MATLAB routine.

The values of  $\alpha$  and  $\varphi''(0)$  depend on  $M^2$ , as we can see from Table 2.1. More precisely,  $\alpha$  decreases and  $\varphi''(0)$  increases as  $M^2$  is increased from 0, as well as we can aspect physically.

In Figure 2.8 we can see the profiles  $\varphi, \varphi', \varphi''$  for  $M^2 = 1$ , while Figure 2.9 shows the behaviour of  $\varphi'$  for different  $M^2$ .

We have plotted the profiles of  $\varphi, \varphi', \varphi''$  only for  $M^2 = 1$  because they have an analogous behaviour for  $M^2 \neq 1$  (similar to the trend in the absence of the external magnetic field).

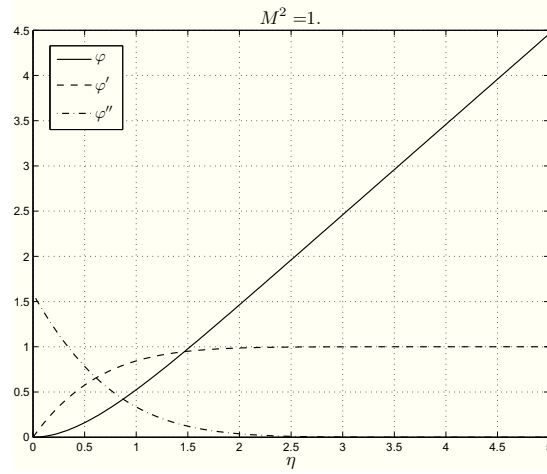


Figure 2.8: CASE III-N: plots showing  $\varphi$ ,  $\varphi'$ ,  $\varphi''$  for  $M^2 = 1$ .

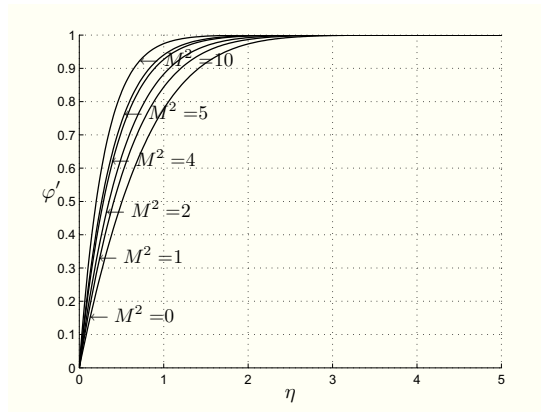


Figure 2.9: CASE III-N: plots showing  $\varphi'$  for different  $M^2$ .

Table 2.1 underlines that the thickness of the boundary layer depends on  $M^2$  and it decreases when  $M^2$  increases (as is easy to see in Figure 2.9). This effect is standard in magnetohydrodynamics and it means that more  $\mathbf{H}$  is strong more the region where the viscosity appears is small.

Finally, we display the streamlines of the flow in Figure 2.10.

## 2.3 Micropolar fluids

Let us consider the steady two-dimensional MHD orthogonal stagnation-point flow of a homogeneous, incompressible, electrically conducting micropolar fluid towards a flat surface coinciding with the plane  $x_2 = 0$ ; the flow being confined to the region

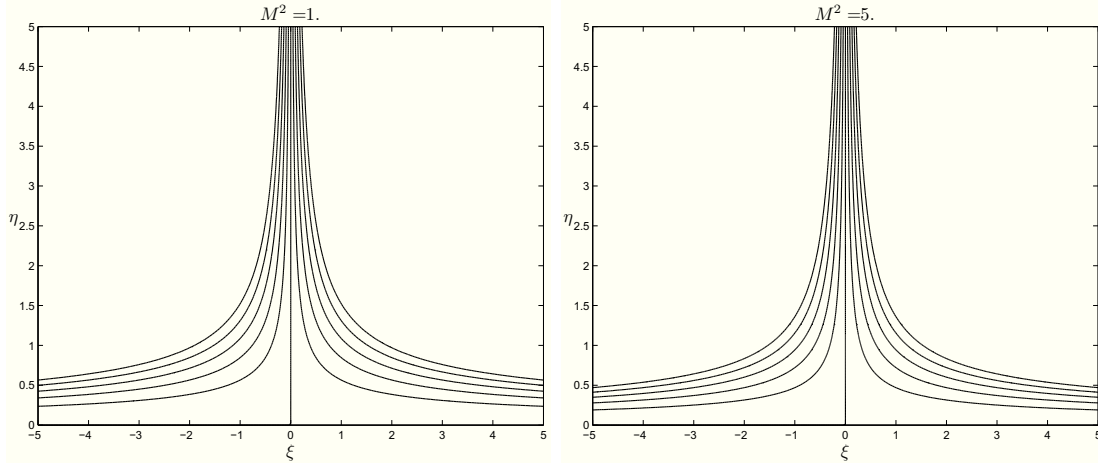


Figure 2.10: CASE III-N: figures show the streamlines for  $M^2 = 1$  and  $M^2 = 5$ , respectively.

$\mathcal{S}$ .

In the absence of free electric charges and external mechanical body forces and body couples, the MHD equations governing such a fluid are

$$\begin{aligned}
 \mathbf{v} \cdot \nabla \mathbf{v} &= -\frac{1}{\rho} \nabla p + (\nu + \nu_r) \Delta \mathbf{v} + 2\nu_r (\nabla \times \mathbf{w}) + \frac{\mu_e}{\rho} (\nabla \times \mathbf{H}) \times \mathbf{H}, \\
 \nabla \cdot \mathbf{v} &= 0, \\
 I \mathbf{v} \cdot \nabla \mathbf{w} &= \lambda \Delta \mathbf{w} + \lambda_0 \nabla (\nabla \cdot \mathbf{w}) - 4\nu_r \mathbf{w} + 2\nu_r (\nabla \times \mathbf{v}), \\
 \nabla \times \mathbf{H} &= \sigma_e (\mathbf{E} + \mu_e \mathbf{v} \times \mathbf{H}), \\
 \nabla \times \mathbf{E} &= \mathbf{0}, \quad \nabla \cdot \mathbf{E} = 0, \quad \nabla \cdot \mathbf{H} = 0, \quad \text{in } \mathcal{S}. \quad (2.44)
 \end{aligned}$$

We underline that the microrotation is influenced by the external electromagnetic field through the first previous equation.

We prescribe to the velocity and to the microrotation

$$\mathbf{v}|_{x_2=0} = \mathbf{0}, \quad \mathbf{w}|_{x_2=0} = \mathbf{0} \quad (\text{strict adherence condition}), \quad (2.45)$$

and we ask that the electromagnetic field satisfies conditions (2.5) and (2.6).

As in Chapter 1.1.3, we search  $\mathbf{v}$ ,  $\mathbf{w}$  in the following form

$$\begin{aligned}
 v_1 &= ax_1 f'(x_2), \quad v_2 = -af(x_2), \quad v_3 = 0, \\
 w_1 &= 0, \quad w_2 = 0, \quad w_3 = x_1 F(x_2), \quad x_1 \in \mathbb{R}, \quad x_2 \in \mathbb{R}^+, \quad (2.46)
 \end{aligned}$$

where  $f, F$  are sufficiently regular unknown functions ( $f \in C^3(\mathbb{R}^+)$ ,  $F \in C^2(\mathbb{R}^+)$ ). The conditions (2.45) supply

$$f(0) = 0, \quad f'(0) = 0, \quad F(0) = 0. \quad (2.47)$$

If we assume that at infinity, the flow of a micropolar fluid approaches the flow of an inviscid fluid given by (2.21), then to (2.46) we must also append the following conditions

$$\lim_{x_2 \rightarrow +\infty} f'(x_2) = 1, \quad \lim_{x_2 \rightarrow +\infty} F(x_2) = 0. \quad (2.48)$$

Further, the asymptotic behaviour of  $f$  at infinity is related to the constant  $A$ , in the same way as in the Newtonian case:

$$\lim_{x_2 \rightarrow +\infty} [f(x_2) - x_2] = -A. \quad (2.49)$$

We now take into consideration the three previous physical situations in order to understand the behaviour of the motion when a uniform external electromagnetic field is impressed.

### 2.3.1 CASE I-M: $\mathbf{E}_0 = E_0 \mathbf{e}_3$ .

In a similar manner to CASEs I and I-N, from (2.44)<sub>3</sub>, (2.44)<sub>4</sub> and boundary conditions for electromagnetic field, we obtain  $\mathbf{E} = E_0 \mathbf{e}_3$  and the induced magnetic field  $h(x_2)$  satisfies

$$h' + \frac{a}{\eta_e} f h = -\eta_e E_0, \quad x_2 > 0, \quad h(0) = 0. \quad (2.50)$$

If we regard  $f$  as a known function, then we have

$$h(x_2) = -\sigma_e E_0 e^{-\frac{a}{\eta_e} \int_0^{x_2} f(t) dt} \int_0^{x_2} e^{\frac{a}{\eta_e} \int_0^s f(t) dt} ds, \quad x_2 \in \mathbb{R}^+. \quad (2.51)$$

As is easy to verify, the induced magnetic fields given by (2.51) and (2.10) have the same asymptotic behaviour at infinity  $\left( \sim -\frac{\eta_e E_0 \sigma_e}{a(x_2 - A)} \right)$ .

To determine  $p, f, F$  we substitute (2.51) into (2.44)<sub>1,3</sub>. After some calculations, we arrive at

$$\begin{aligned} p &= p(x_1, x_2), \\ ax_1 \left[ (\nu + \nu_r) f''' + a f f'' - a f'^2 + \frac{2\nu_r}{a} F' \right] &= -\frac{1}{\rho} \frac{\partial p}{\partial x_1} \\ (\nu + \nu_r) a f'' + a^2 f' f + 2\nu_r F + \frac{\mu_e}{\rho} h' h &= -\frac{1}{\rho} \frac{\partial p}{\partial x_2}, \\ x_1 [\alpha F'' + I a (F' f - F f') - 2\nu_r (2F + a f'')] &= 0. \end{aligned} \quad (2.52)$$

Then, by integrating (2.52)<sub>3</sub>, we find

$$p(x_1, x_2) = -\frac{1}{2}\rho a^2 f^2(x_2) - \rho a(\nu + \nu_r)f'(x_2) - 2\nu_r\rho \int_0^{x_2} F(s)ds \\ - \frac{\mu_e}{2}h^2(x_2) + P(x_1),$$

where the function  $P(x_1)$  is determined supposing that, far from the wall, the pressure  $p$  has the same behaviour as for an inviscid electroconducting fluid, whose velocity is given by (2.21).

Therefore, under the assumption  $F \in L^1([0, +\infty))$ , by virtue of (2.48), (2.49), (2.51) and (2.10), we get

$$P(x_1) = -\rho \frac{a^2}{2}x_1^2 + p_0^* + \rho a(\nu + \nu_r).$$

After all, the pressure field is

$$p(x_1, x_2) = -\rho \frac{a^2}{2}[x_1^2 + f^2(x_2)] - \rho a(\nu + \nu_r)f'(x_2) \\ - 2\nu_r\rho \int_0^{x_2} F(s)ds - \frac{\mu_e}{2}h^2(x_2) + p_0, \quad (2.53)$$

with  $p_0 = p_0^* + \rho a(\nu + \nu_r) - \rho \frac{b^2}{2}(B - A)^2$ .

In consideration of (2.52)<sub>2,4</sub> and (2.53), we obtain the ordinary differential equations

$$\frac{\nu + \nu_r}{a}f''' + ff'' - f'^2 + 1 + \frac{2\nu_r}{a^2}F' = 0, \\ \lambda F'' + aI(ff' - f'F) - 2\nu_r(2F + af'') = 0, \quad (2.54)$$

subject to the boundary conditions (2.47), (2.48).

We stress that the system (2.54) governs the orthogonal stagnation-point flow of an inert electromagnetic micropolar fluid (see Chapter 1.1.3). In the literature, such a flow has been studied in [27].

**THEOREM 2.3.1.** *Let a homogeneous, incompressible, electrically conducting micropolar fluid occupy the region  $\mathcal{S}$ . The steady MHD orthogonal plane stagnation-point flow of such a fluid has the following form when an external uniform electric field*

$\mathbf{E}_0 = E_0 \mathbf{e}_3$  is impressed:

$$\mathbf{v} = ax_1 f'(x_2) \mathbf{e}_1 - af(x_2) \mathbf{e}_2, \quad \mathbf{w} = x_1 F(x_2) \mathbf{e}_3,$$

$$\mathbf{H} = h(x_2) \mathbf{e}_1, \quad \mathbf{E} = E_0 \mathbf{e}_3,$$

$$p = -\rho \frac{a^2}{2} [x_1^2 + f^2(x_2)] - \rho a(\nu + \nu_r) f'(x_2) - 2\nu_r \rho \int_0^{x_2} F(s) ds - \frac{\mu_e}{2} h^2(x_2) + p_0,$$

$$x_1 \in \mathbb{R}, \quad x_2 \in \mathbb{R}^+,$$

where  $(f, F)$  satisfies the problem (2.54), (2.47), and (2.48), provided  $F \in L^1([0, +\infty))$ , and  $h(x_2)$  is given by (2.51).

We now write (2.54) and (2.50), together with the boundary conditions (2.47), (2.48), in dimensionless form. To this end we use the dimensionless variables (1.23) and we put

$$\Psi(\eta) = \frac{1}{\sigma_e E_0} \sqrt{\frac{a}{\nu + \nu_r}} h \left( \sqrt{\frac{\nu + \nu_r}{a}} \eta \right).$$

System (2.54) and equation (2.50) can be written as

$$\begin{aligned} \varphi''' + \varphi\varphi'' - \varphi'^2 + 1 + \Phi' &= 0, \\ \Phi'' + c_3(\varphi\Phi' - \varphi'\Phi) - c_2\Phi - c_1\varphi'' &= 0, \\ \Psi' + R_m\varphi\Psi &= -1, \end{aligned} \tag{2.55}$$

where  $c_1, c_2, c_3$  are given by (1.25) and

$$\alpha = \sqrt{\frac{a}{\nu + \nu_r}} A, \quad R_m = \frac{\nu + \nu_r}{\eta_e} = \text{magnetic Reynolds number.}$$

The boundary conditions in dimensionless form become:

$$\begin{aligned} \varphi(0) = 0, \quad \varphi'(0) = 0, \quad \Phi(0) = 0, \quad \Psi(0) = 0, \\ \lim_{\eta \rightarrow +\infty} \varphi'(\eta) = 1, \quad \lim_{\eta \rightarrow +\infty} \Phi(\eta) = 0. \end{aligned} \tag{2.56}$$

The last equation in (2.55), if we regard  $\varphi$  as a known function, can be formally integrated to give

$$\Psi(\eta) = -e^{-R_m \int_0^\eta \varphi(s) ds} \int_0^\eta e^{R_m \int_0^t \varphi(s) ds} dt, \quad \eta \in \mathbb{R}^+.$$

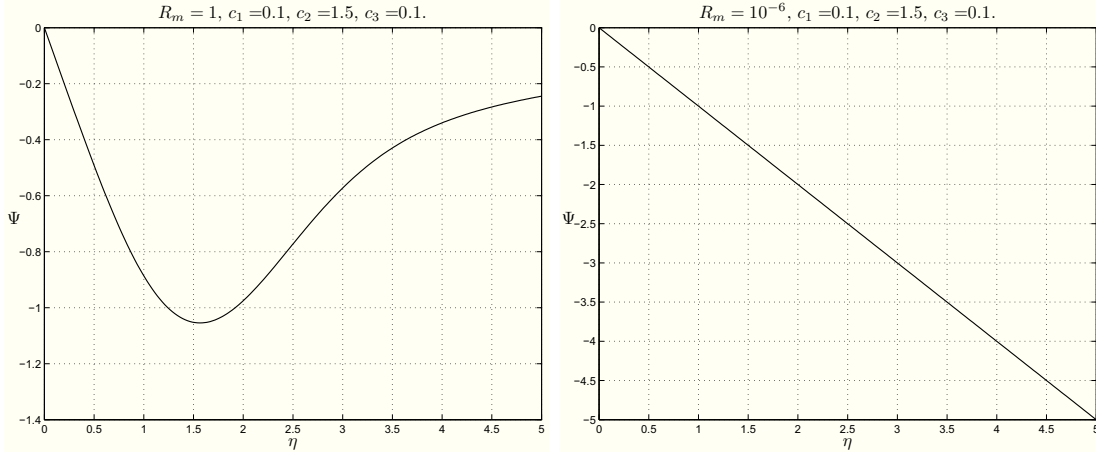


Figure 2.11: CASE I-M: plots showing  $\Psi$  with  $R_m = 1, 10^{-6}$ .

The remaining equations have to be integrated numerically. More precisely, we have already determined and plotted  $\varphi, \varphi', \varphi'', \Phi, \Phi'$  in Chapter 1.1.3.

Figure 2.11<sub>1</sub> provides the behaviour of the induced magnetic field  $\Psi$  with  $R_m = 1$ . It is similar to the behaviour of  $\Psi$  in CASE I (inviscid fluid) and in CASE I-N (Newtonian fluid). The graph displayed in Figure 2.11<sub>2</sub> shows that when  $R_m = 10^{-6}$  the trend of  $\Psi$  is approximately linear. This happens because in  $\eta \in [0, 5]$ , for very small values of  $R_m$ , equation (2.55)<sub>3</sub> reduces to  $\Psi' \cong -1$  (as in CASE I-N).

### 2.3.2 CASE II-M: $\mathbf{H}_0 = H_0 \mathbf{e}_1$ .

By proceeding as one would with an inviscid or a Newtonian fluid, we get

$$h' + \frac{a}{\eta_e} f h = -\frac{a}{\eta_e} f H_0, \quad x_2 > 0, \quad h(0) = 0. \quad (2.57)$$

We can formally integrate (2.57) to find

$$h(x_2) = H_0 \left[ e^{-\frac{a}{\eta_e} \int_0^{x_2} f(t) dt} - 1 \right], \quad x_2 \in \mathbb{R}^+, \quad (2.58)$$

which implies

$$\mathbf{H} = H_0 e^{-\frac{a}{\eta_e} \int_0^{x_2} f(s) ds} \mathbf{e}_1.$$

Under the previous assumptions, it is easy to compute the pressure field and get

$$\begin{aligned} p(x_1, x_2) = & -\rho \frac{a^2}{2} [x_1^2 + f^2(x_2)] - \rho a (\nu + \nu_r) f'(x_2) \\ & - 2\nu_r \rho \int_0^{x_2} F(s) ds - \frac{\mu_e}{2} [h(x_2) + H_0]^2 + p_0^*, \end{aligned} \quad (2.59)$$

where  $(f, F)$  satisfies system (2.54), together with boundary conditions (2.47) and (2.48).

In this case as well, the uniform external electromagnetic field only influences the pressure.

Thus, we obtain the following:

**THEOREM 2.3.2.** *Let a homogeneous, incompressible, electrically conducting micropolar fluid occupy the region  $\mathcal{S}$ . The steady MHD orthogonal plane stagnation-point flow of such a fluid has the following form when a uniform external magnetic field  $\mathbf{H}_0 = H_0 \mathbf{e}_1$  is impressed:*

$$\begin{aligned} \mathbf{v} &= ax_1 f'(x_2) \mathbf{e}_1 - af(x_2) \mathbf{e}_2, \quad \mathbf{w} = x_1 F(x_2) \mathbf{e}_3, \\ \mathbf{H} &= [h(x_2) + H_0] \mathbf{e}_1, \quad \mathbf{E} = E_0 \mathbf{e}_3, \\ p &= -\rho \frac{a^2}{2} [x_1^2 + f^2(x_2)] - \rho a (\nu + \nu_r) f'(x_2) - 2\nu_r \rho \int_0^{x_2} F(s) ds \\ &\quad - \frac{\mu_e}{2} [h(x_2) + H_0]^2 + p_0^*, \quad x_1 \in \mathbb{R}, \quad x_2 \in \mathbb{R}^+, \end{aligned}$$

where  $(f, F)$  satisfies the problem (2.54), (2.47), and (2.48), provided  $F \in L^1([0, +\infty))$ , and  $h(x_2)$  is given by (2.58).

The function  $h(x_2)$  can be written in dimensionless form as

$$\Psi(\eta) = e^{-R_m \int_0^\eta \varphi(t) dt} - 1, \quad \eta \in \mathbb{R}^+, \quad (2.60)$$

where

$$\Psi(\eta) = \frac{1}{H_0} h \left( \sqrt{\frac{\nu + \nu_r}{a}} \eta \right).$$

In this case the ordinary differential problem governing  $\varphi$ ,  $\Phi$  is the same as in (1.24), so that the behaviour of the flow is displayed in Figure 1.5.

Figure 2.12 shows that  $\Psi$  has a similar behaviour to  $\Psi$  in CASE II and CASE II-N, as we can see.

### 2.3.3 CASE III-M: $\mathbf{H}_0 = H_0 \mathbf{e}_2$ .

In this case, we impress

$$\mathbf{H}_0 = H_0 \mathbf{e}_2, \quad \mathbf{E}_0 = \mathbf{0}.$$

Similar to CASEs III and III-N, we deduce

$$\mathbf{E} = \mathbf{0} \Rightarrow \nabla \times \mathbf{H} = \sigma_e \mu_e (\mathbf{v} \times \mathbf{H})$$

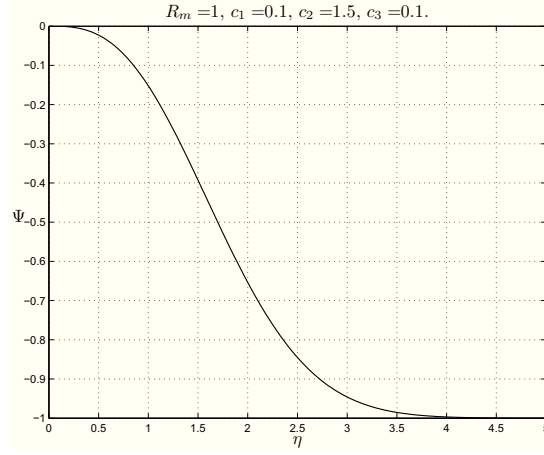


Figure 2.12: CASE II-M: plot showing  $\Psi$  for  $R_m = 1$

and we neglect the induced magnetic field, replacing (2.44)<sub>1</sub> with

$$\mathbf{v} \cdot \nabla \mathbf{v} = -\frac{1}{\rho} \nabla p + (\nu + \nu_r) \Delta \mathbf{v} + 2\nu_r (\nabla \times \mathbf{w}) + \frac{\mu_e}{\rho} (\mathbf{v} \times \mathbf{H}_0) \times \mathbf{H}_0. \quad (2.61)$$

This approximation is motivated by physical arguments for MHD flow at small magnetic Reynolds numbers.

We substitute (2.46) into (2.61) to determine  $p, f, F$ . This yields

$$\begin{aligned} p &= p(x_1, x_2), \\ ax_1 \left[ (\nu + \nu_r) f''' + af'' - af'^2 + \frac{2\nu_r}{a} F' - \frac{\sigma_e B_0^2}{\rho} f' \right] &= \frac{1}{\rho} \frac{\partial p}{\partial x_1}, \\ (\nu + \nu_r) af'' + a^2 f' f + 2\nu_r F &= -\frac{1}{\rho} \frac{\partial p}{\partial x_2}. \end{aligned} \quad (2.62)$$

The integration of (2.62)<sub>3</sub> gives

$$p(x_1, x_2) = -\frac{1}{2} \rho a^2 f^2(x_2) - \rho a (\nu + \nu_r) f'(x_2) - 2\nu_r \rho \int_0^{x_2} F(s) ds + P(x_1),$$

where  $P(x_1)$  has to be found as in CASEs I-M, II-M.

After some calculations, we find

$$P(x_1) = -\rho \frac{a^2}{2} \left( 1 + \frac{\sigma_e B_0^2}{\rho a} \right) x_1^2 + p_0^*,$$

so that the pressure field is:

$$p(x_1, x_2) = -\rho \frac{a^2}{2} [x_1^2 + f^2(x_2)] - \rho a(\nu + \nu_r) f'(x_2) - 2\nu_r \rho \int_0^{x_2} F(s) ds - \frac{\sigma_e B_0^2}{2} a x_1^2 + p_0, \quad x_1 \in \mathbb{R}, \quad x_2 \in \mathbb{R}^+. \quad (2.63)$$

Then, (2.62)<sub>2</sub> supplies

$$\frac{\nu + \nu_r}{a} f''' + f f'' - f'^2 + 1 + \frac{2\nu_r}{a^2} F' + M^2(1 - f') = 0, \quad (2.64)$$

where  $M^2 = \frac{\sigma_e B_0^2}{\rho a}$  is the Hartmann number.

Of course  $(f, F)$  also satisfies equation (2.54)<sub>2</sub>. We append boundary conditions (2.47) and (2.48) to the system in (2.64) and (2.54)<sub>2</sub>.

Unlike the previous cases, the external electromagnetic field modifies the flow. If  $M^2 = 0$ , then the system (2.64), (2.54)<sub>2</sub> reduces to the system (2.54).

**REMARK 2.3.3.** *If  $\nu_r = 0$ , then (2.64) reduces to the equation governing the MHD orthogonal stagnation-point flow of a Newtonian fluid (CASE III-N (2.42)).*

We can now state:

**THEOREM 2.3.4.** *Let a homogeneous, incompressible, electrically conducting micropolar fluid occupy the region  $\mathcal{S}$ . If we impress the external magnetic field  $\mathbf{H}_0 = H_0 \mathbf{e}_2$  and if we neglect the induced magnetic field, then the steady MHD orthogonal plane stagnation-point flow of such a fluid has the form*

$$\begin{aligned} \mathbf{v} &= a x_1 f'(x_2) \mathbf{e}_1 - a f(x_2) \mathbf{e}_2, \quad \mathbf{w} = x_1 F(x_2) \mathbf{e}_3, \quad \mathbf{E} = \mathbf{0}, \\ p &= -\rho \frac{a^2}{2} [x_1^2 + f^2(x_2)] - \rho a(\nu + \nu_r) f'(x_2) - 2\nu_r \rho \int_0^{x_2} F(s) ds \\ &\quad - \frac{\sigma_e B_0^2}{2} a x_1^2 + p_0, \quad x_1 \in \mathbb{R}, \quad x_2 \in \mathbb{R}^+, \end{aligned}$$

where  $(f, F)$  satisfies problem (2.64), (2.54)<sub>2</sub>, (2.47), and (2.48), provided  $F \in L^1([0, +\infty))$ .

In dimensionless form, we arrive at the following ordinary differential boundary value problem:

$$\begin{aligned} \varphi''' + \varphi \varphi'' - \varphi'^2 + 1 + \Phi' + M^2(1 - \varphi') &= 0, \\ \Phi'' + c_3(\varphi \Phi' - \varphi' \Phi) - c_2 \Phi - c_1 \varphi'' &= 0, \\ \varphi(0) = 0, \quad \varphi'(0) = 0, \quad \Phi(0) = 0, \\ \lim_{\eta \rightarrow +\infty} \varphi'(\eta) = 1, \quad \lim_{\eta \rightarrow +\infty} \Phi(\eta) = 0. \end{aligned} \quad (2.65)$$

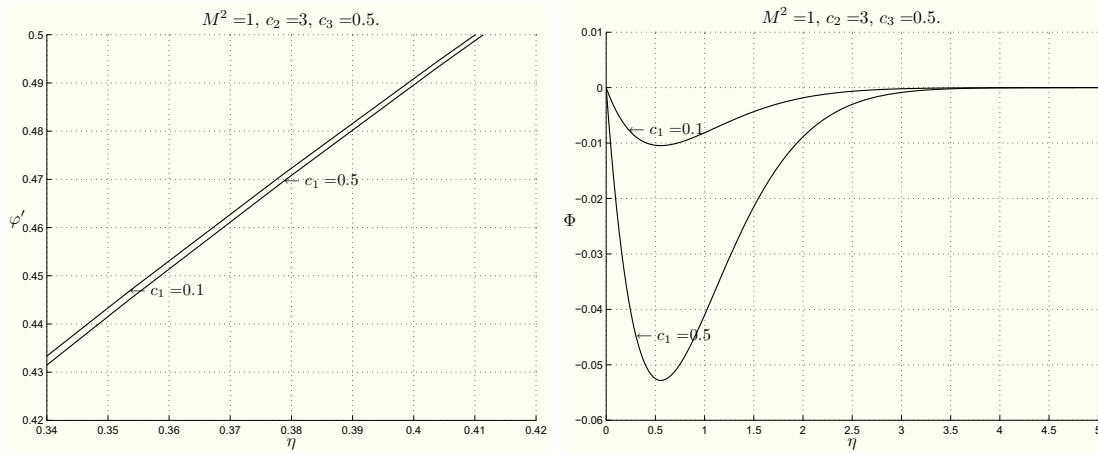


Figure 2.13: CASE III-M:  $\varphi'$ ,  $\Phi$  profiles for  $M^2 = 1$ ,  $c_2 = 3$ ,  $c_3 = 0.5$  when  $c_1 = 0.1$  and  $c_1 = 0.5$ .

REMARK 2.3.5. *In the sequel, we will see that the solution  $(\varphi, \Phi)$  of problem (2.65) satisfies the conditions (2.65)<sub>6,7</sub>. For this reason, as in Remark 1.1.9, we denote by:*

- $\bar{\eta}_\varphi$  the value of  $\eta$  such that  $\varphi'(\bar{\eta}_\varphi) = 0.99$ ;
- $\bar{\eta}_\Phi$  the value of  $\eta$  such that  $\Phi(\bar{\eta}_\Phi) = -0.01$ ;

so that if  $\eta > \bar{\eta}_\varphi$  then  $\varphi \cong \eta - \alpha$ , and if  $\eta > \bar{\eta}_\Phi$ , then  $\Phi \cong 0$ .

From the numerical integration we will find that the influence of the viscosity on the velocity and on the microrotation only appears in a layer lining the boundary whose thickness is  $\bar{\eta}_\varphi$  for the velocity and  $\bar{\eta}_\Phi$  for the microrotation. The thickness  $\delta$  of the boundary layer for the flow is defined as

$$\delta = \max(\bar{\eta}_\varphi, \bar{\eta}_\Phi).$$

We now show the numerical solution of problem (2.65).

In Tables 2.2 and 2.3 we list the numerical results of the descriptive quantities of the motion for the same values of  $c_1, c_2, c_3$  of the case of an inert micropolar fluid, choosing  $M^2 = 1, 2, 4, 5, 10$ , as for the Newtonian case.

If we fix  $M^2$ , then the considerations of the case in the absence of the external magnetic field (Chapter 1.1.3) continue to hold (as easily seen in Figures from 2.13 to 2.15).

As far as the dependence on  $M^2$  is concerned, we can see that  $\alpha$  and  $\Phi'(0)$  decrease and  $\varphi''(0)$  increases as  $M^2$  is increased from 0, as we would expect physically.

In Figure 2.16<sub>1</sub>, we have plotted the profiles  $\varphi, \varphi', \varphi''$  for  $M^2 = 1$  and  $c_1 = 0.5, c_2 = 3.0, c_3 = 0.5$ , while Figure 2.17<sub>1</sub> shows the behaviour of  $\varphi'$  for different  $M^2$  and the same values of  $c_1, c_2, c_3$ .

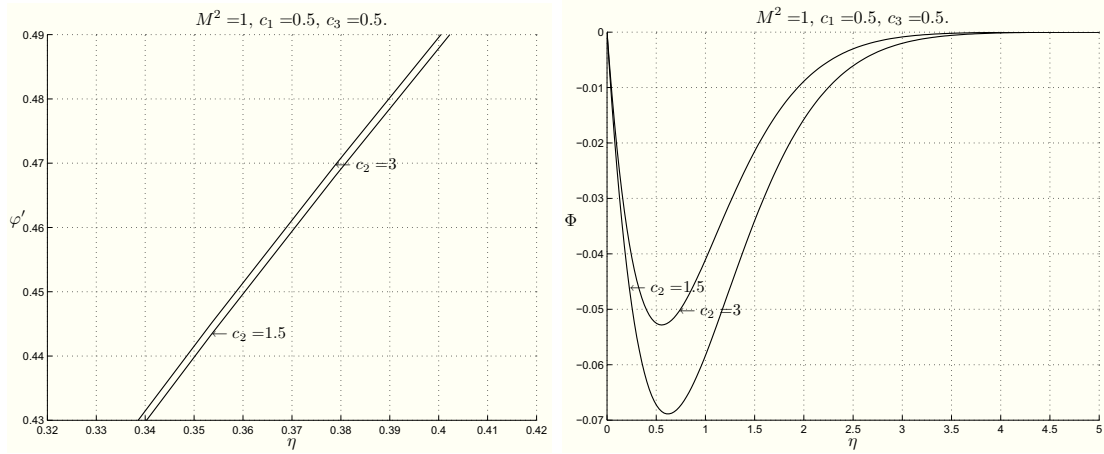


Figure 2.14: CASE III-M:  $\varphi'$ ,  $\Phi$  profiles for  $M^2 = 1$ ,  $c_1 = 0.5$ ,  $c_3 = 0.5$  when  $c_2 = 1.5$  and  $c_2 = 3$ .

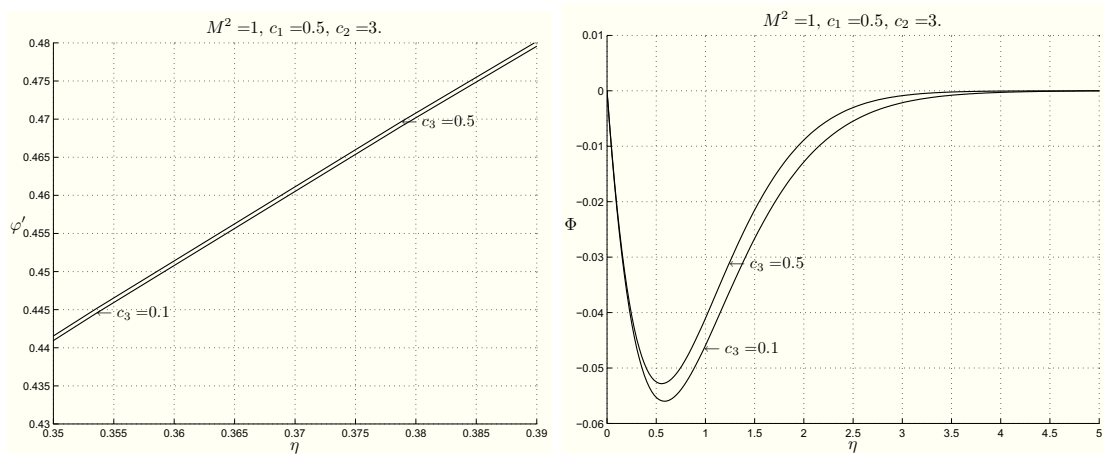


Figure 2.15: CASE III-M:  $\varphi'$ ,  $\Phi$  profiles for  $M^2 = 1$ ,  $c_1 = 0.5$ ,  $c_2 = 3$  when  $c_3 = 0.1$  and  $c_3 = 0.5$ .

Table 2.2: CASE III-M: descriptive quantities of the motion for several values of  $M^2$ .

$M^2$	$c_1$	$c_2$	$c_3$	$\alpha$	$\varphi''(0)$	$\Phi'(0)$	$\bar{\eta}_\varphi$	$\bar{\eta}_\Phi$	$\delta$		
1	0.1	1.5	0.1	1.5751	-0.0583	0.5386	2.0626	1.4064	2.0626		
			0.5	1.5762	-0.0560	0.5388	2.0699	1.1642	2.0699		
		3.0	0.1	1.5778	-0.0497	0.5392	2.0779	0.8690	2.0779		
			0.5	1.5783	-0.0487	0.5392	2.0817	0.7245	2.0817		
		0.5	1.5	0.1	1.5335	-0.2913	0.5290	1.9039	2.7106	2.7106	
				0.5	1.5392	-0.2802	0.5298	1.9301	2.2492	2.2492	
	3.0		0.1	1.5475	-0.2487	0.5317	1.9677	2.1526	2.1526		
			0.5	1.5501	-0.2434	0.5321	1.9846	1.9384	1.9846		
			2	0.1	1.5	1.8637	-0.0617	0.4730	1.8771	1.2744	1.8771
					0.5	1.8647	-0.0594	0.4731	1.8821	1.0505	1.8821
	0.5	3.0	0.1	1.8661	-0.0534	0.4734	1.8886	0.7769	1.8886		
			0.5	1.8666	-0.0523	0.4735	1.8916	0.6340	1.8916		
1.5		0.1	1.8239	-0.3085	0.4656	1.7464	2.5743	2.5743			
		0.5	1.8290	-0.2971	0.4663	1.7639	2.1257	2.1257			
		3.0	0.1	1.8363	-0.2670	0.4676	1.7942	2.0249	2.0249		
			0.5	1.8387	-0.2614	0.4679	1.8066	1.8192	1.8192		
4	0.1	1.5	0.1	2.3375	-0.0663	0.3924	1.6226	1.0935	1.6226		
			0.5	2.3383	-0.0640	0.3924	1.6249	0.8950	1.6249		
		3.0	0.1	2.3395	-0.0584	0.3926	1.6296	0.6417	1.6296		
			0.5	2.3400	-0.0572	0.3927	1.6312	0.4573	1.6312		
		0.5	1.5	0.1	2.3005	-0.3315	0.3874	1.5286	2.3876	2.3876	
				0.5	2.3048	-0.3199	0.3878	1.5367	1.9599	1.9599	
	3.0		0.1	2.3108	-0.2922	0.3886	1.5574	1.8549	1.8549		
			0.5	2.3129	-0.2862	0.3889	1.5644	1.6617	1.6617		

Table 2.3: CASE III-M: continuum of Table 2.2.

$M^2$	$c_1$	$c_2$	$c_3$	$\alpha$	$\varphi''(0)$	$\Phi'(0)$	$\bar{\eta}_\varphi$	$\bar{\eta}_\Phi$	$\delta$
5	0.1	1.5	0.1	2.5418	-0.0680	0.3650	1.5294	1.0259	1.5294
			0.5	2.5426	-0.0656	0.3651	1.5311	0.8364	1.5311
			3.0	2.5437	-0.0603	0.3652	1.5351	0.5849	1.5351
	0.5	1.5	0.1	2.5441	-0.0591	0.3653	1.5364	0.4383	1.5364
			0.5	2.5059	-0.3398	0.3608	1.4479	2.3184	2.3184
			3.0	2.5099	-0.3283	0.3612	1.4534	1.8992	1.8992
		3.0	0.1	2.5155	-0.3014	0.3618	1.4709	1.7934	1.7934
			0.5	2.5175	-0.2954	0.3620	1.4764	1.6051	1.6051
			0.5	2.5175	-0.2954	0.3620	1.4764	1.6051	1.6051
10	0.1	1.5	0.1	3.3838	-0.0734	0.2825	1.2269	0.7892	1.2269
			0.5	3.3844	-0.0712	0.2826	1.2270	0.6262	1.2270
			3.0	3.3852	-0.0665	0.2826	1.2289	0.3948	1.2289
	0.5	1.5	0.1	3.3855	-0.0652	0.2826	1.2294	0.3775	1.2294
			0.5	3.3522	-0.3671	0.2802	1.1807	2.0837	2.0837
			3.0	3.3552	-0.3559	0.2804	1.1809	1.6979	1.6979
		3.0	0.1	3.3593	-0.3324	0.2807	1.1894	1.5897	1.5897
			0.5	3.3609	-0.3262	0.2808	1.1910	1.4189	1.4189
			0.5	3.3609	-0.3262	0.2808	1.1910	1.4189	1.4189

In Figure 2.16<sub>2</sub>, we can see the profiles  $\Phi, \Phi'$  for  $M^2 = 1$  and  $c_1 = 0.5, c_2 = 3.0, c_3 = 0.5$ , while Figure 2.17<sub>2</sub> shows the behaviour of  $\Phi$  for different  $M^2$  and the same values of  $c_1, c_2, c_3$ .

We have only plotted the profiles of  $\varphi, \varphi', \varphi'', \Phi, \Phi'$  for  $M^2 = 1$  and  $c_1 = 0.5, c_2 = 3.0, c_3 = 0.5$ , because they have an analogous behaviour for  $M^2 \neq 1$  and different  $c_1, c_2, c_3$ .

From Tables 2.2-2.3, it appears also that the thickness of the boundary layer depends on  $M^2$  and it decreases as  $M^2$  increases (as easily seen in Figures 2.17). This effect is standard in magnetohydrodynamics. Moreover, the thickness of the boundary layer of the velocity is smaller than that of the corresponding case of the Newtonian fluid (CASE III-N).

Finally, we display the streamlines for  $c_1 = 0.5, c_2 = 3.0, c_3 = 0.5$  and  $M^2 = 1, 5$  in Figure 2.18.

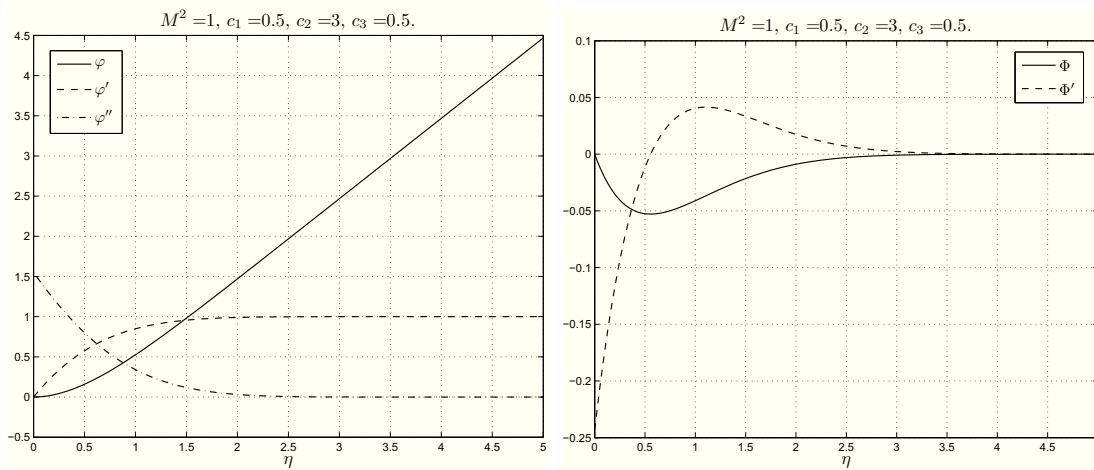


Figure 2.16: CASE III-M: plots showing  $\varphi, \varphi', \varphi''$  and  $\Phi, \Phi'$  (respectively) for  $c_1 = 0.5, c_2 = 3.0, c_3 = 0.5$  and  $M^2 = 1$ .

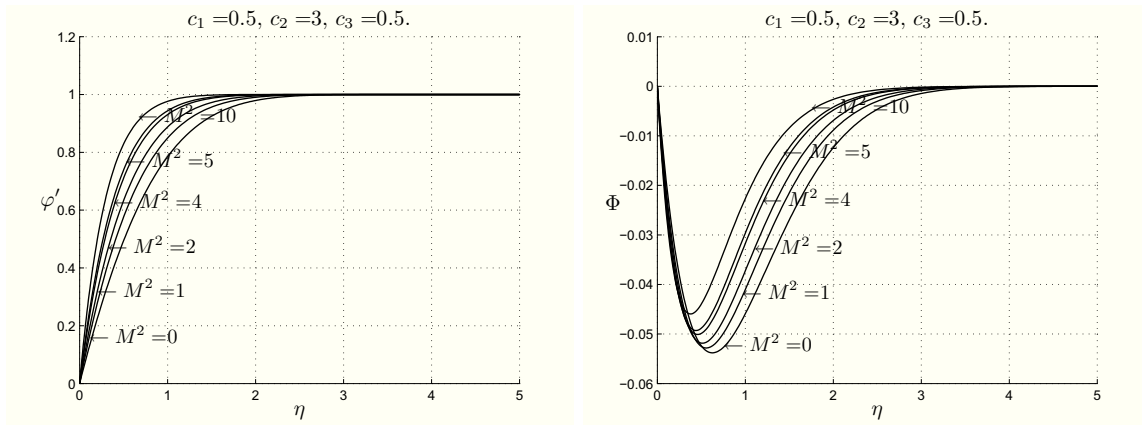


Figure 2.17: CASE III-M: plots showing  $\varphi'$  and  $\Phi$  with  $c_1 = 0.5, c_2 = 3.0, c_3 = 0.5$  and for different  $M^2$ .

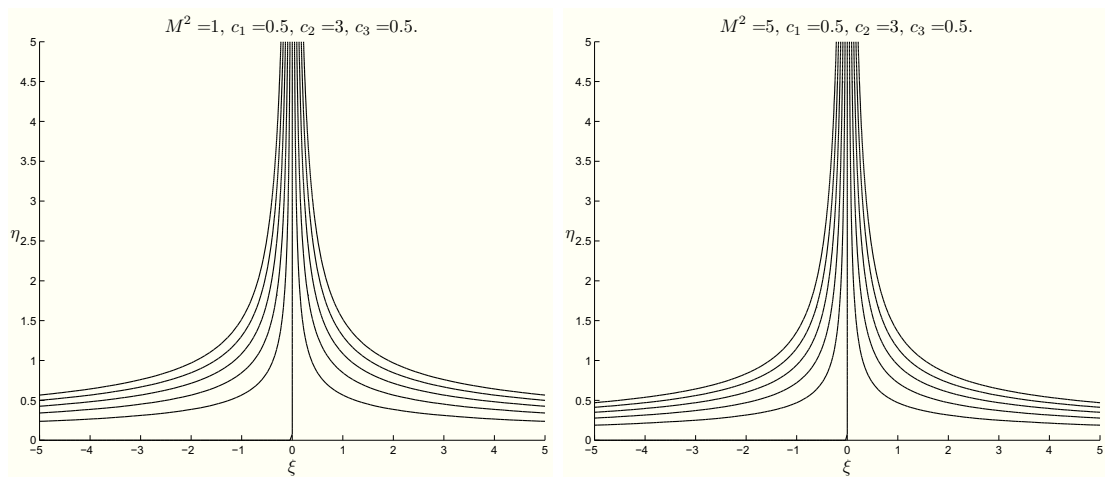


Figure 2.18: CASE III-M: streamlines for  $c_1 = 0.5$ ,  $c_2 = 3.0$ ,  $c_3 = 0.5$  and  $M^2 = 1$ ,  $M^2 = 5$ , respectively.



# Chapter 3

## MHD oblique stagnation-point flow

This chapter is devoted to understand how the steady oblique stagnation-point flow of a Newtonian or a micropolar fluid is influenced by an external uniform electromagnetic field  $(\mathbf{E}_0, \mathbf{H}_0)$ .

To this end we will recall the definition of oblique stagnation-point flow given in Chapter 1.2 and we will consider three situations which are relevant from a physical point of view.

The results obtained have been published in [5] and [6].

### 3.1 Inviscid fluids

We shall first consider the steady plane MHD flow of a homogeneous, incompressible, electrically conducting inviscid fluid near a stagnation point occupying the region  $\mathcal{S}$  given by (2.1).

The boundary of  $\mathcal{S}$  having the equation  $x_2 = 0$  is a rigid fixed non-electrically conducting wall and we assume that the region  $\mathcal{S}^-$  given by (2.3) is vacuum. We take  $\mu_e$  equal to the magnetic permeability of free space.

The MHD equations governing such a flow in the absence of external mechanical body forces and free electric charges are (2.2).

We require the no-penetration condition (2.4) and the transmission relations (2.6), (2.5) to the velocity and to the electromagnetic field, respectively.

The oblique flow in the immediate neighbourhood of the stagnation point  $(0, 0)$  is characterized by a velocity field of the form

$$v_1 = ax_1 + bx_2, \quad v_2 = -ax_2, \quad v_3 = 0, \quad x_1 \in \mathbb{R}, \quad x_2 \in \mathbb{R}^+, \quad (3.1)$$

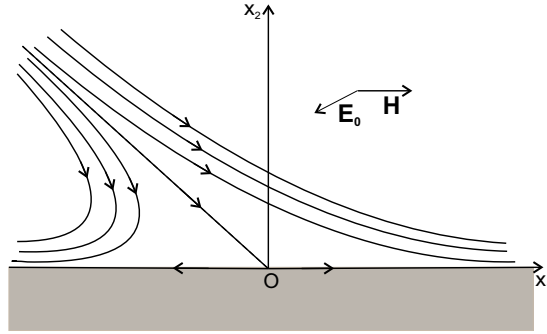


Figure 3.1: Description flow in CASE I.

with  $a, b$  constants ( $a > 0$ ), see Chapter 1.2.1.

As underlined in Chapter 1, the streamlines of such a flow are hyperbolas whose asymptotes are degenerate streamlines of equations:

$$x_2 = 0 \quad \text{and} \quad x_2 = -\frac{2a}{b}x_1. \quad (3.2)$$

We are interested in finding the behaviour of such a flow when an external uniform electromagnetic field  $(\mathbf{E}_0, \mathbf{H}_0)$  is applied. We now analyze three physically relevant cases to achieve our purpose.

### 3.1.1 CASE I

First of all, we impress

$$\mathbf{E}_0 = E_0 \mathbf{e}_3, \quad \mathbf{H}_0 = \mathbf{0}, \quad E_0 = \text{constant}.$$

REMARK 3.1.1. *The solution of the problem relative to the electromagnetic field in  $\mathcal{S}^-$  is  $\mathbf{E} = \mathbf{E}_0 = \mathbf{0}$  and  $\mathbf{H} = \mathbf{H}_0 = H_0 \mathbf{e}_1$ .*

We take the induced electromagnetic field  $(\mathbf{E}^i, \mathbf{H}^i \equiv \mathbf{H})$  as follows

$$\mathbf{E}^i = E_1^i \mathbf{e}_1 + E_2^i \mathbf{e}_2 + E_3^i \mathbf{e}_3,$$

$$\mathbf{H} = h(x_2) \mathbf{e}_1,$$

where  $h \in C^1(\mathbb{R}^+)$ ,  $E_j^i \in C^2(\mathbb{R}^3)$  for  $j = 1, 2, 3$  unknown functions.

From the boundary conditions (2.5) and the Remark (3.1.1) we get

$$\begin{aligned} E_1^i &= 0, \quad E_3^i = 0 \quad \text{at} \quad x_2 = 0, \\ h(0) &= 0. \end{aligned} \quad (3.3)$$

Equation (2.2)<sub>4</sub> implies

$$\mathbf{E} \equiv \mathbf{E}^i + \mathbf{E}_0 = -\nabla\psi.$$

Thanks to (2.2)<sub>3</sub> we find that the electrostatic scalar potential  $\psi$  depends only on  $x_3$  and satisfies

$$\frac{d\psi}{dx_3}(x_3) = a\mu_e h(x_2)x_2 + \frac{h'(x_2)}{\sigma_e}.$$

The previous equation is possible if both its members are equal to the same constant.

This constant is determined by the boundary condition (3.3)<sub>2</sub>:

$$\begin{aligned} h' + a\sigma_e\mu_e h x_2 &= -\sigma_e E_0, & x_2 > 0, \\ \psi &= -E_0 x_3 + \psi_0, & x_3 \in \mathbb{R}. \end{aligned} \quad (3.4)$$

The differential problem (3.4)<sub>1</sub>, (3.3)<sub>3</sub> can be integrated to get

$$h(x_2) = -\sigma_e E_0 e^{-\frac{ax_2^2}{2\eta_e}} \int_0^{x_2} e^{\frac{at^2}{2\eta_e}} dt, \quad x_2 \in \mathbb{R}^+, \quad (3.5)$$

with  $\eta_e = \frac{1}{\sigma_e\mu_e}$  = electrical resistivity.

From (2.2)<sub>1</sub> we get the form of the pressure field:

$$p = -\frac{1}{2}\rho a^2(x_1^2 + x_2^2) - \frac{\mu_e}{2}h^2(x_2) + p_0, \quad x_1 \in \mathbb{R}, \quad x_2 \in \mathbb{R}^+,$$

where  $h$  is given by (3.5).

The presence of  $\mathbf{E}_0$  modifies the pressure field, which is smaller than the pressure in Theorem 1.2.1, but it doesn't influence the velocity.

We are now able to formulate:

**THEOREM 3.1.2.** *Let a homogeneous, incompressible, electrically conducting inviscid fluid occupy the region  $\mathcal{S}$ . The steady plane MHD oblique stagnation-point flow of such a fluid has the following form when an external uniform electric field  $\mathbf{E}_0 = E_0\mathbf{e}_3$  is impressed:*

$$\begin{aligned} \mathbf{v} &= (ax_1 + bx_2)\mathbf{e}_1 - ax_2\mathbf{e}_2, & \mathbf{H} &= h(x_2)\mathbf{e}_1, & \mathbf{E} &= E_0\mathbf{e}_3, \\ p &= -\frac{1}{2}\rho a^2(x_1^2 + x_2^2) - \frac{\mu_e}{2}h^2(x_2) + p_0, & x_1 &\in \mathbb{R}, & x_2 &\in \mathbb{R}^+, \end{aligned}$$

where

$$h(x_2) = -\sigma_e E_0 e^{-\frac{ax_2^2}{2\eta_e}} \int_0^{x_2} e^{\frac{at^2}{2\eta_e}} dt.$$

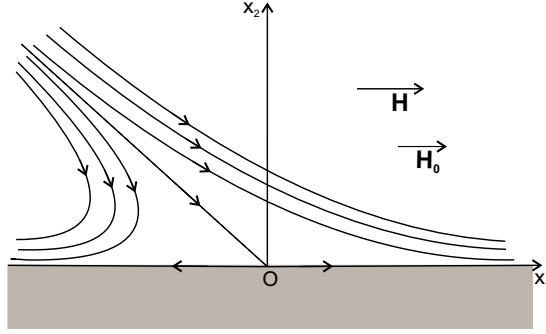


Figure 3.2: Description flow in CASE II.

We underline that  $h$  is the same as in the MHD orthogonal stagnation-point flow CASE I, so its behaviour is shown in Figures 2.2 in dimensionless form. Evidently, Remark 2.1.3 holds.

### 3.1.2 CASE II

Let the external uniform magnetic field be

$$\mathbf{E}_0 = \mathbf{0}, \quad \mathbf{H}_0 = H_0 \mathbf{e}_1, \quad H_0 = \text{constant}.$$

REMARK 3.1.3.  $(\mathbf{E}, \mathbf{H}) = (\mathbf{0}, H_0 \mathbf{e}_1)$  is the solution of the problem in  $\mathcal{S}^-$ .

The induced electromagnetic field  $(\mathbf{E}^i \equiv \mathbf{E}, \mathbf{H}^i)$  can be searched in the following form

$$\begin{aligned} \mathbf{E} &= E_1 \mathbf{e}_1 + E_2 \mathbf{e}_2 + E_3 \mathbf{e}_3, \\ \mathbf{H} &= [h(x_2) + H_0] \mathbf{e}_1, \end{aligned}$$

where  $h \in C^1(\mathbb{R}^+)$  and  $E_1, E_2, E_3 \in C^2(\mathbb{R}^3)$  unknown functions.

Repeating the arguments of CASE I, we have  $\psi = \psi(x_3)$  and

$$\frac{d\psi}{dx_3}(x_3) = a\mu_e[h(x_2) + H_0]x_2 + \frac{h'(x_2)}{\sigma_e}.$$

The previous equality and the boundary conditions furnish

$$\begin{aligned} h' + \frac{a}{\eta_e} h x_2 &= -\frac{a}{\eta_e} x_2 H_0, \quad x_2 > 0, \\ h(0) &= 0, \end{aligned} \tag{3.6}$$

and  $\psi = \psi_0$ , from which

$$\mathbf{E} = \mathbf{0}.$$

The solution of problem (3.6) is

$$h(x_2) = H_0 \left( e^{-\frac{ax_2^2}{2\eta_e}} - 1 \right), \quad x_2 \in \mathbb{R}^+, \quad (3.7)$$

which implies

$$\mathbf{H} = H_0 e^{-\frac{ax_2^2}{2\eta_e}} \mathbf{e}_1.$$

From (2.2) we can now compute the pressure field

$$p(x_1, x_2) = -\frac{1}{2}\rho a^2(x_1^2 + x_2^2) - \frac{\mu_e}{2}H_0^2 e^{-\frac{ax_2^2}{\eta_e}} + p_0^*, \quad x_1 \in \mathbb{R}, \quad x_2 \in \mathbb{R}^+.$$

The pressure at the stagnation point is  $p_0^* - \mu_e \frac{H_0^2}{2}$ , so that the presence of  $\mathbf{H}_0$  modifies the pressure, which is smaller than the pressure in the purely hydrodynamical flow.

Theorem 3.1.4 summarizes our results.

**THEOREM 3.1.4.** *Let a homogeneous, incompressible, electrically conducting inviscid fluid occupy the region  $\mathcal{S}$ . The steady plane MHD oblique stagnation-point flow of such a fluid has the following form when an external uniform magnetic field  $\mathbf{H}_0 = H_0 \mathbf{e}_1$  is impressed:*

$$\begin{aligned} \mathbf{v} &= (ax_1 + bx_2)\mathbf{e}_1 - ax_2\mathbf{e}_2, \quad \mathbf{H} = H_0 e^{-\frac{ax_2^2}{2\eta_e}} \mathbf{e}_1, \quad \mathbf{E} = \mathbf{0}, \\ p &= -\frac{1}{2}\rho a^2(x_1^2 + x_2^2) - \frac{\mu_e}{2}H_0^2 e^{-\frac{ax_2^2}{\eta_e}} + p_0^*, \quad x_1 \in \mathbb{R}, \quad x_2 \in \mathbb{R}^+. \end{aligned}$$

We have that  $h$  depends only on  $f$  and so it is the same as in CASE II of the MHD orthogonal stagnation-point flow (Chapter 2.1.2). Its trend in dimensionless form is shown in Figure 2.4.

### 3.1.3 CASE III

$$\mathbf{E}_0 = \mathbf{0}, \quad \mathbf{H}_0 = H_0(\cos \vartheta \mathbf{e}_1 + \sin \vartheta \mathbf{e}_2),$$

where  $\vartheta$  is fixed in  $(0, \pi)$  and  $H_0$  is constant. We want to understand which orientation of the external electromagnetic field allows the oblique plane stagnation-point flow.

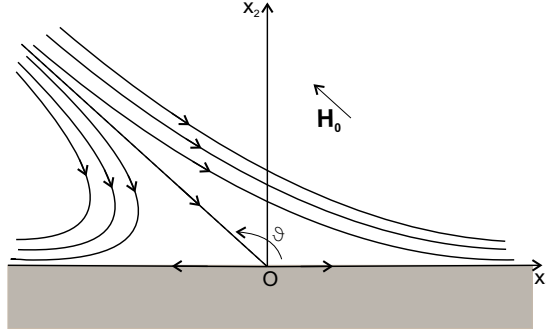


Figure 3.3: Description flow in CASE III.

Let the induced electromagnetic field ( $\mathbf{E}^i \equiv \mathbf{E}, \mathbf{H}^i$ ) to be in the form

$$\mathbf{E} = E_1 \mathbf{e}_1 + E_2 \mathbf{e}_2 + E_3 \mathbf{e}_3,$$

$$\mathbf{H}^i = h_1(x_1, x_2) \mathbf{e}_1 + h_2(x_1, x_2) \mathbf{e}_2,$$

where  $h_1, h_2, E_1, E_2, E_3$  are sufficiently regular unknown functions ( $h_1, h_2 \in C^1(\mathbb{R} \times \mathbb{R}^+)$ ,  $E_1, E_2, E_3 \in C^2(\mathbb{R}^3)$ ).

Combining (2.2)<sub>3</sub>, (3.1) we have

$$\sigma_e \mathbf{E} = \left[ \frac{\partial h_2}{\partial x_1} - \frac{\partial h_1}{\partial x_2} - \sigma_e \mu_e (v_1 h_2 - v_2 h_1 + H_0 v_1 \sin \vartheta - H_0 v_2 \cos \vartheta) \right] \mathbf{e}_3, \quad (3.8)$$

from which follows  $\psi = \psi(x_3)$  and we conclude that  $\mathbf{E} = \mathbf{0}$ , as we have in CASE II.

Therefore from (2.2)<sub>3</sub> we find

$$\begin{aligned} \frac{\partial h_2}{\partial x_1}(x_1, x_2) - \frac{\partial h_1}{\partial x_2}(x_1, x_2) = \\ \sigma_e \mu_e [(ax_1 + bx_2)(h_2(x_1, x_2) + H_0 \sin \vartheta) + ax_2(h_1(x_1, x_2) + H_0 \cos \vartheta)]. \end{aligned} \quad (3.9)$$

The functions  $h_1$  and  $h_2$  have also to satisfy (2.2)<sub>6</sub>:

$$\frac{\partial h_1}{\partial x_1} + \frac{\partial h_2}{\partial x_2} = 0. \quad (3.10)$$

Without loss of generality, we now assume that the magnetic Reynolds number is small (e.g. in the flow of liquid metals) so that we can neglect the induced magnetic field ( $h_1, h_2$ ).

Hence

$$\begin{aligned} (\nabla \times \mathbf{H}) \times \mathbf{H} \simeq \sigma_e \mu_e (\mathbf{v} \times \mathbf{H}_0) \times \mathbf{H}_0 = \\ \sigma_e \mu_e H_0^2 [a \sin \vartheta x_1 + (b \sin \vartheta + a \cos \vartheta) x_2] (-\sin \vartheta \mathbf{e}_1 + \cos \vartheta \mathbf{e}_2). \end{aligned}$$

If we substitute this approximation into (2.2)<sub>1</sub>, then we find that the pressure field satisfies

$$\begin{aligned}\frac{\partial p}{\partial x_1} &= -\rho a^2 x_1 - B_0^2 \sigma_e \sin \vartheta [a \sin \vartheta x_1 + (b \sin \vartheta + a \cos \vartheta) x_2], \\ \frac{\partial p}{\partial x_2} &= -\rho a^2 x_2 + B_0^2 \sigma_e \cos \vartheta [a \sin \vartheta x_1 + (b \sin \vartheta + a \cos \vartheta) x_2], \\ \frac{\partial p}{\partial x_3} &= 0 \Rightarrow p = p(x_1, x_2),\end{aligned}\tag{3.11}$$

with  $B_0 = \mu_e H_0$ .

Equations (3.11) are compatible if, and only if,

$$\frac{\partial^2 p}{\partial x_1 \partial x_2} = \frac{\partial^2 p}{\partial x_2 \partial x_1}.$$

The previous condition and (3.11) give

$$\sin \vartheta (2a \cos \vartheta + b \sin \vartheta) = 0,\tag{3.12}$$

from which we get

$$\tan \vartheta = -\frac{2a}{b}.\tag{3.13}$$

Hence the MHD oblique stagnation-point flow is possible if, and only if,  $\mathbf{H}_0$  is parallel to the dividing streamline  $x_2 = -\frac{2a}{b}x_1$ .

In particular, we note that if  $\mathbf{H}_0$  is normal to the plane  $x_2 = 0$  (i.e.  $\vartheta = \pi/2$ ), then there is no pressure that satisfies equations (3.11) and therefore the oblique stagnation-point flow given by (3.1) does not exist.

When (3.13) holds, the pressure field is

$$p = -\frac{1}{2}\rho a^2(x_1^2 + x_2^2) - \frac{\sigma_e B_0^2}{4a^2 + b^2} \frac{a}{2}(2ax_1 + bx_2)^2 + p_0, \quad x_1 \in \mathbb{R}, \quad x_2 \in \mathbb{R}^+.\tag{3.14}$$

Our results can be summarized in the following:

**THEOREM 3.1.5.** *Let a homogeneous, incompressible, electrically conducting inviscid fluid occupy the region  $\mathcal{S}$ . If we impress an external magnetic field  $\mathbf{H}_0 = H_0(\cos \vartheta \mathbf{e}_1 + \sin \vartheta \mathbf{e}_2)$ ,  $0 < \vartheta < \pi$ , and we neglect the induced magnetic field, then the steady MHD oblique plane stagnation-point flow of such a fluid is possible if, and only if,*

$$\vartheta = \arctan\left(-\frac{2a}{b}\right), \quad i.e. \quad \mathbf{H}_0 = \frac{H_0}{\sqrt{4a^2 + b^2}}(-b\mathbf{e}_1 + 2a\mathbf{e}_2).$$

Moreover,

$$\mathbf{v} = (ax_1 + bx_2)\mathbf{e}_1 - ax_2\mathbf{e}_2, \quad \mathbf{E} = \mathbf{0},$$

$$p = -\frac{1}{2}\rho a^2(x_1^2 + x_2^2) - \frac{\sigma_e B_0^2}{4a^2 + b^2} \frac{a}{2}(2ax_1 + bx_2)^2 + p_0, \quad x_1 \in \mathbb{R}, \quad x_2 \in \mathbb{R}^+.$$

REMARK 3.1.6. To take into account the motion of a Newtonian or a micropolar fluid, it is convenient to suppose that the inviscid fluid obliquely impinges on the flat plane  $x_2 = A$  and

$$v_1 = ax_1 + b(x_2 - B), \quad v_2 = -a(x_2 - A), \quad v_3 = 0, \quad x_1 \in \mathbb{R}, \quad x_2 \geq A, \quad (3.15)$$

with  $A, B = \text{constants}$ .

In this situation, the stagnation point is not  $(0, 0)$  but the point

$$\left( \frac{b}{a}(B - A), A \right),$$

while the streamlines are hyperbolas whose asymptotes are

$$x_2 = -\frac{2a}{b}x_1 + 2B - A \quad \text{and} \quad x_2 = A.$$

The results contained in Theorems 3.1.2, 3.1.4, 3.1.5 can be easily extended by replace  $x_1, x_2$  with  $x_1 - \frac{b}{a}(B - A), x_2 - A$ , respectively.

## 3.2 Newtonian fluids

We now consider the steady oblique plane MHD flow of a homogeneous, incompressible, electrically conducting Newtonian fluid near a stagnation point occupying the region  $\mathcal{S}$  given by (2.1).

The MHD equations governing such a flow in the absence of external mechanical body forces and free electric charges are the equations (2.22) and the usual boundary conditions are (2.23), (2.5), (2.6).

The velocity in the oblique plane stagnation-point flow depends on the similarity transformation  $(f, g)$  as follows

$$v_1 = ax_1 f'(x_2) + bg(x_2), \quad v_2 = -af(x_2), \quad v_3 = 0, \quad x_1 \in \mathbb{R}, \quad x_2 \in \mathbb{R}^+. \quad (3.16)$$

As we said in Chapter 1.2.3,  $f, g$  are sufficiently regular unknown functions ( $f \in C^3(\mathbb{R}^+)$ ,  $g \in C^2(\mathbb{R}^+)$ ).

The condition (2.23) supplies

$$f(0) = 0, \quad f'(0) = 0, \quad g(0) = 0. \quad (3.17)$$

At infinity we require that the flow approaches the flow of an inviscid fluid given by (3.15), so that

$$\lim_{x_2 \rightarrow +\infty} f'(x_2) = 1, \quad \lim_{x_2 \rightarrow +\infty} g'(x_2) = 1. \quad (3.18)$$

In the sequel, when we will refer to an inviscid fluid, all results obtained in Chapter 3.1 have to be modified replacing  $x_1, x_2$  with  $x_1 - \frac{b}{a}(B - A), x_2 - A$ , respectively.

It is worth recalling that the asymptotic behaviour of  $f, g$  at infinity is related to  $A, B$ :

$$\lim_{x_2 \rightarrow +\infty} [f(x_2) - x_2] = -A, \quad \lim_{x_2 \rightarrow +\infty} [g(x_2) - x_2] = -B. \quad (3.19)$$

As we have in Chapter 1,  $A$  is determined as part of the solution of the orthogonal flow, while  $B$  is a free parameter.

After these preliminaries, we can now analyze the three physical situations studied in the previous section.

### 3.2.1 CASE I-N: $\mathbf{E}_0 = E_0 \mathbf{e}_3$ .

Similarly to CASE I, from (2.22)<sub>3</sub>, (2.22)<sub>4</sub> and boundary conditions for the electromagnetic field, we get

$$h' + \frac{a}{\eta_e} f h = -\eta_e E_0, \quad x_2 > 0, \quad h(0) = 0, \quad (3.20)$$

$$\psi(x_3) = -E_0 x_3 + \psi_0, \quad x_3 \in \mathbb{R}.$$

The solution of the previous differential problem can be formally expressed by

$$h(x_2) = -\sigma_e E_0 e^{-\frac{a}{\eta_e} \int_0^{x_2} f(t) dt} \int_0^{x_2} e^{\frac{a}{\eta_e} \int_0^s f(t) dt} ds, \quad x_2 \in \mathbb{R}^+, \quad (3.21)$$

if we regard  $f$  as a known function.

We note that the induced magnetic fields given by (3.21) and (3.5) have the same asymptotic behaviour at infinity  $\left( \sim -\frac{\eta_e E_0 \sigma_e}{a(x_2 - A)} \right)$ .

In order to determine  $p, f, g$ , we substitute (3.16) into (2.22)<sub>1</sub> so that

$$\begin{aligned} p &= p(x_1, x_2), \\ ax_1(\nu f''' + af f'' - af'^2) + b[\nu g'' + a(fg' - f'g)] &= \frac{1}{\rho} \frac{\partial p}{\partial x_1}, \\ \nu a f'' + a^2 f' f + \frac{\mu_e}{\rho} h' h &= -\frac{1}{\rho} \frac{\partial p}{\partial x_2}. \end{aligned} \quad (3.22)$$

Then, by integrating (3.22)<sub>3</sub>, we find

$$p(x_1, x_2) = -\frac{1}{2} \rho a^2 f^2(x_2) - \rho a \nu f'(x_2) - \frac{\mu_e}{2} h^2(x_2) + P(x_1),$$

where  $P(x_1)$  is determined supposing that, far from the wall, the flow approaches the flow of an inviscid electroconducting fluid, whose velocity is given by (3.15).

By virtue of (3.18), (3.19), (3.21), (3.5), we obtain

$$P(x_1) = -\rho \frac{a^2}{2} \left[ x_1 - \frac{b}{a} (B - A) \right]^2 + \rho a \nu + p_0^*,$$

from which we find

$$\begin{aligned} p(x_1, x_2) &= -\rho \frac{a^2}{2} \left[ x_1^2 - 2 \frac{b}{a} (B - A) x_1 + f^2(x_2) \right] - \rho a \nu f'(x_2) \\ &\quad - \frac{\mu_e}{2} h^2(x_2) + p_0, \end{aligned} \quad (3.23)$$

where  $p_0 = p_0^* + \rho a \nu - \rho \frac{b^2}{2} (B - A)^2$ .

On substituting the pressure given by (3.23) into (3.22)<sub>2</sub>, we find that  $(f, g)$  satisfies the same differential problem which governs the oblique stagnation-point flow in the absence of an electromagnetic field (see Chapter 1.2.2):

$$\begin{aligned} \frac{\nu}{a} f''' + f f'' - f'^2 + 1 &= 0, \\ \frac{\nu}{a} g'' + f g' - f' g &= B - A, \end{aligned} \quad (3.24)$$

with

$$\begin{aligned} f(0) = 0, \quad f'(0) = 0, \quad g(0) = 0, \\ \lim_{x_2 \rightarrow +\infty} f'(x_2) = 1, \quad \lim_{x_2 \rightarrow +\infty} g'(x_2) = 1. \end{aligned} \quad (3.25)$$

It is clear, therefore, that the external uniform electromagnetic field influences the flow only through the pressure.

We recall that, as we can see from (3.23),  $\nabla p$  has a constant component in the  $x_1$  direction proportional to  $B - A$ , which does not appear in the orthogonal stagnation-point flow. This component determines the displacement of the uniform shear flow parallel to the wall  $x_2 = 0$ , as it happened in the absence of the external magnetic field.

We have thus proved:

**THEOREM 3.2.1.** *Let a homogeneous, incompressible, electrically conducting Newtonian fluid occupy the region  $\mathcal{S}$ . The steady MHD oblique plane stagnation-point flow of such a fluid has the following form when an external uniform electric field  $\mathbf{E}_0 = E_0 \mathbf{e}_3$  is impressed:*

$$\begin{aligned} \mathbf{v} &= [ax_1 f'(x_2) + bg(x_2)]\mathbf{e}_1 - af(x_2)\mathbf{e}_2, \quad \mathbf{H} = h(x_2)\mathbf{e}_1, \quad \mathbf{E} = E_0\mathbf{e}_3, \\ p &= -\rho \frac{a^2}{2}[x_1^2 - 2\frac{b}{a}(B - A)x_1 + f^2(x_2)] - \rho a \nu f'(x_2) - \frac{\mu_e}{2}h^2(x_2) + p_0, \\ x_1 &\in \mathbb{R}, \quad x_2 \in \mathbb{R}^+, \end{aligned}$$

where  $(f, g)$  satisfies the problem (3.24), (3.25) and  $h(x_2)$  is given by (3.21).

Since the presence of the external electric field doesn't influence  $f$  and  $g$ , (3.24)-(3.25) is system (1.36), which governs the oblique stagnation-point flow of a homogeneous, incompressible, inert Newtonian fluid. Its solution has already been computed numerically in Chapter 1.2.2. Of course Remark 1.2.4 still holds.

As far as the induced magnetic field is concerned, we note that  $h$  depends only on the function  $f$  and this function verifies equation (3.24)<sub>1</sub>, which governs the orthogonal stagnation-point flow of a homogeneous, incompressible, inert Newtonian fluid. So the behaviour of  $h$  in dimensionless form is shown in Figure 2.6.

### 3.2.2 CASE II-N: $\mathbf{H}_0 = H_0 \mathbf{e}_1$ .

The same arguments of CASE II, equations (2.22)<sub>3</sub> and (2.22)<sub>4</sub>, relations (2.5) allow us to conclude

$$\begin{aligned} h' + \frac{a}{\eta_e} f h &= -\frac{a}{\eta_e} f H_0, \quad x_2 > 0, \quad h(0) = 0, \\ \psi(x_3) = \psi_0 &\Rightarrow \mathbf{E} = \mathbf{0}. \end{aligned} \tag{3.26}$$

If we regard  $f$  as a known function, then from (3.26) we can formally compute

$$h(x_2) = H_0 \left[ e^{-\frac{a}{\eta_e} \int_0^{x_2} f(t) dt} - 1 \right], \quad x_2 \in \mathbb{R}^+, \tag{3.27}$$

so that

$$\mathbf{H} = H_0 e^{-\frac{a}{\eta_e} \int_0^{x_2} f(s) ds} \mathbf{e}_1.$$

In this case, the pressure field becomes

$$p(x_1, x_2) = -\rho \frac{a^2}{2} [x_1^2 - 2\frac{b}{a}(B-A)x_1 + f^2(x_2)] - \rho a \nu f'(x_2) - \frac{\mu_e}{2} [h(x_2) + H_0]^2 + p_0^*, \quad (3.28)$$

$$p_0^* = p_0 + \rho a \nu - \rho \frac{b^2}{2} (B-A)^2,$$

and  $(f, g)$  satisfies problem (3.24), (3.25).

Therefore, in this case also, the external uniform electromagnetic field modifies only the pressure.

**THEOREM 3.2.2.** *Let a homogeneous, incompressible, electrically conducting Newtonian fluid occupy the region  $\mathcal{S}$ . The steady MHD oblique plane stagnation-point flow of such a fluid has the following form when an external uniform magnetic field  $\mathbf{H}_0 = H_0 \mathbf{e}_1$  is impressed:*

$$v_1 = [ax_1 f'(x_2) + bg(x_2)] \mathbf{e}_1 - af(x_2) \mathbf{e}_2, \quad \mathbf{H} = [h(x_2) + H_0] \mathbf{e}_1, \quad \mathbf{E} = \mathbf{0},$$

$$p = -\rho \frac{a^2}{2} [x_1^2 - 2\frac{b}{a}(B-A)x_1 + f^2(x_2)] - \rho a \nu f'(x_2) - \frac{\mu_e}{2} [h(x_2) + H_0]^2 + p_0^*,$$

$$x_1 \in \mathbb{R}, \quad x_2 \in \mathbb{R}^+,$$

where  $h(x_2)$  is given by (3.27) and  $(f, g)$  satisfies problem (3.24), (3.25).

As in the previous case, the ordinary differential problem governing  $f, g$  is the same as in Chapter 1.2.2 and  $h$  is the same as in Chapter 3.2.2. In Figure 2.7 we can see the profile of  $h$  in dimensionless form.

### 3.2.3 CASE III-N: $\mathbf{H}_0 = \frac{H_0}{\sqrt{4a^2 + b^2}} (-b\mathbf{e}_1 + 2a\mathbf{e}_2)$ .

As a result of Theorem 3.1.5, we impress

$$\mathbf{H}_0 = \frac{H_0}{\sqrt{4a^2 + b^2}} (-b\mathbf{e}_1 + 2a\mathbf{e}_2), \quad \mathbf{E}_0 = \mathbf{0},$$

and we neglect the induced magnetic field, replacing (1.16) with

$$\mathbf{v} \cdot \nabla \mathbf{v} = -\frac{1}{\rho} \nabla p + \nu \Delta \mathbf{v} + \frac{\mu_e}{\rho} (\mathbf{v} \times \mathbf{H}_0) \times \mathbf{H}_0. \quad (3.29)$$

By proceeding as in CASE III, we deduce

$$\mathbf{E} = \mathbf{0}.$$

We now substitute (3.16) into (3.29), so that we get  $p = p(x_1, x_2)$  and

$$\begin{aligned} & ax_1 \left( \nu f''' + a f f'' - a f'^2 - 4a^2 \frac{\sigma_e}{\rho} \frac{B_0^2}{4a^2 + b^2} f' \right) \\ & + b \left[ \nu g'' + a(fg' - f'g) - 2a^2 \frac{\sigma_e}{\rho} \frac{B_0^2}{4a^2 + b^2} (2g - f) \right] = \frac{1}{\rho} \frac{\partial p}{\partial x_1}, \\ & \nu a f'' + a^2 f' f + \frac{\sigma_e}{\rho} \frac{B_0^2}{4a^2 + b^2} [2a^2 b x_1 f' + ab^2 (2g - f)] = -\frac{1}{\rho} \frac{\partial p}{\partial x_2}. \end{aligned} \quad (3.30)$$

From equation (3.30)<sub>3</sub>, we find

$$\begin{aligned} p(x_1, x_2) &= -\frac{1}{2} \rho a^2 f^2(x_2) - \rho a \nu f'(x_2) \\ &\quad - \sigma_e \frac{B_0^2}{4a^2 + b^2} \left[ 2a^2 b x_1 f(x_2) + ab^2 \int_0^{x_2} (2g(s) - f(s)) ds \right] + P(x_1), \end{aligned}$$

where  $P(x_1)$  has to be found as in CASE I-N, II-N.

After some calculations, we get

$$P(x_1) = -\rho \frac{a^2}{2} \left( 1 + \frac{4a}{\rho} \frac{\sigma_e B_0^2}{4a^2 + b^2} \right) \left[ x_1 - \frac{b}{a} (B - A) \right]^2 + p_0^*.$$

Hence the pressure field is:

$$\begin{aligned} p(x_1, x_2) &= -\rho \frac{a^2}{2} [x_1^2 - 2\frac{b}{a} (B - A)x_1 + f^2(x_2)] - \rho a \nu f'(x_2) \\ &\quad - \frac{\sigma_e B_0^2}{4a^2 + b^2} \left[ 2a^2 b x_1 f(x_2) + ab^2 \int_0^{x_2} (2g(s) - f(s)) ds \right. \\ &\quad \left. - 2a^3 \left( \frac{2b}{a} (B - A)x_1 - x_1^2 \right) \right] + p_0, \quad x_1 \in \mathbb{R}, \quad x_2 \in \mathbb{R}^+, \end{aligned} \quad (3.31)$$

which together with (3.30)<sub>2</sub> supplies

$$\begin{aligned} \frac{\nu}{a} f''' + f f'' - f'^2 + 1 + M^2(1 - f') &= 0, \\ \frac{\nu}{a} g'' + f g' - g f' + M^2(f - g) &= (1 + M^2)(B - A), \end{aligned} \quad (3.32)$$

where

$$M^2 = 4a \frac{\sigma_e B_0^2}{\rho(4a^2 + b^2)} = \text{Hartmann number.}$$

We append boundary conditions (3.18), (3.19) to the system (3.32).

Unlike the previous cases, the external electromagnetic field now modifies both the velocity and the pressure. Nevertheless, if  $M^2 = 0$ , then the system (3.32) reduces to the system (3.24).

Summarizing, we have:

**THEOREM 3.2.3.** *Let a homogeneous, incompressible, electrically conducting Newtonian fluid occupy the region  $\mathcal{S}$ . If we impress an external magnetic field*

$$\mathbf{H}_0 = \frac{H_0}{\sqrt{4a^2 + b^2}}(-b\mathbf{e}_1 + 2a\mathbf{e}_2)$$

and if we neglect the induced magnetic field, then the steady MHD oblique plane stagnation-point flow of such a fluid has the form

$$\begin{aligned} \mathbf{v} &= [ax_1 f'(x_2) + bg(x_2)]\mathbf{e}_1 - af(x_2)\mathbf{e}_2, \quad \mathbf{E} = \mathbf{0}, \\ p &= -\rho \frac{a^2}{2} [x_1^2 - 2\frac{b}{a}(B-A)x_1 + f^2(x_2)] - \rho a \nu f'(x_2) \\ &\quad - \frac{\sigma_e B_0^2}{4a^2 + b^2} \left[ 2a^2 b x_1 f(x_2) + ab^2 \int_0^{x_2} (2g(s) - f(s)) ds \right. \\ &\quad \left. - 2a^3 \left( \frac{2b}{a}(B-A)x_1 - x_1^2 \right) \right] + p_0, \quad x_1 \in \mathbb{R}, \quad x_2 \in \mathbb{R}^+, \end{aligned}$$

where  $(f, g)$  satisfies problem (3.32), (3.18), (3.19).

In dimensionless form system (3.32), (3.18), (3.19) can be written as

$$\begin{aligned} \varphi''' + \varphi\varphi'' - \varphi'^2 + 1 + M^2(1 - \varphi') &= 0, \\ \gamma'' + \varphi\gamma' - \varphi'\gamma + M^2(\varphi - \gamma) &= (1 + M^2)(\beta - \alpha), \\ \varphi(0) = 0, \quad \varphi'(0) = 0, \quad \gamma(0) = 0, \\ \lim_{x_2 \rightarrow +\infty} \varphi'(x_2) = 1, \quad \lim_{x_2 \rightarrow +\infty} \gamma'(x_2) = 1, \end{aligned} \tag{3.33}$$

where we recall that

$$\alpha = \sqrt{\frac{a}{\nu}}A, \quad \beta = \sqrt{\frac{a}{\nu}}B.$$

We see that the function  $\varphi$  influences the function  $\gamma$ , but not viceversa.

REMARK 3.2.4. *The solution of the differential problem (3.33)<sub>1,3,4,6</sub> exists and it is unique as proved by Hoernel in [34].*

*As far as  $\gamma$  is concerned, if we regard  $\varphi$  as a known function, then it satisfies a linear second order non-homogeneous differential equation.*

*After some calculations, we obtain that  $\gamma$  is formally expressed by*

$$\begin{aligned} \gamma(\eta) = & (\alpha - \beta)\varphi'(\eta) + C\varphi''(\eta)\Xi(\eta) \\ & + M^2\varphi''(\eta) \left[ \int_0^\eta \Xi(s)\varphi(s)\varphi''(s)e^{\int_0^s \varphi(t)dt} ds - \Xi(\eta) \int_0^\eta \varphi(s)\varphi''(s)e^{\int_0^s \varphi(t)dt} ds \right], \end{aligned} \quad (3.34)$$

where  $C$ ,  $\Xi(\eta)$  are given again by (1.39). We note that if  $M^2 = 0$ , then (3.34) reduces to (1.38).

REMARK 3.2.5. *The points  $x_1 = x_p$  of maximum pressure and  $x_1 = x_s$  of zero tangential stress on  $x_2 = 0$  are formally the same as in the absence of external electromagnetic field (see (1.41), Chapter 1.2.2, Remark 1.2.4). However, these points depend on  $M^2$ .*

*The slope of the dividing streamline at the wall is now given by:*

$$- \frac{3a[\varphi''(0)]^2}{(1 + M^2)b[(\beta - \alpha)\varphi''(0) + \gamma'(0)]}. \quad (3.35)$$

REMARK 3.2.6. *The numerical integration will reveal that the solution  $(\varphi, \gamma)$  of the problem here considered satisfies the conditions (3.33)<sub>6,7</sub>; therefore following Remark 1.2.5 we denote by:*

- $\bar{\eta}_\varphi$  ( $\bar{\eta}_\gamma$ ) the value of  $\eta$  such that  $\varphi'(\bar{\eta}_\varphi) = 0.99$  ( $\gamma'(\bar{\eta}_\gamma) = 0.99$ ),

so that if  $\eta > \bar{\eta}_\varphi$  ( $\eta > \bar{\eta}_\gamma$ ), then  $\varphi \cong \eta - \alpha$  ( $\gamma \cong \eta - \beta$ ).

*Hence the influence of the viscosity on the velocity appears only in a layer lining the boundary whose thickness is  $\delta = \max(\bar{\eta}_\varphi, \bar{\eta}_\gamma)$ .*

The ordinary differential equations (3.32) subject to the boundary conditions (3.18) and (3.19) was solved numerically together for different values of  $M^2$  and  $\beta - \alpha$  chosen according to the previous chapters.

The values of  $\alpha$  and  $\varphi''(0)$  depend on  $M^2$ , as we can see from Table 3.1, which is of course the same of Table 2.1 in Chapter 3.2.3.

More precisely,  $\alpha$  decreases and  $\varphi''(0)$  increases as  $M^2$  increases.

Table 3.2 shows numerical results of some parameters significant from a physical point of view for  $M^2 = 1, 2, 4, 5, 10$  and  $\beta - \alpha = -5 - \alpha, -\alpha, 0, \alpha, 5 - \alpha$ .

As far as the dependence of  $\gamma'(0)$  on  $M^2$  is concerned, from Table 3.2 we can see that its value increases when  $M^2$  increases if  $\beta - \alpha < 0$ , otherwise it decreases.

Table 3.1: CASE III-N: dependence of  $\alpha$  and  $\varphi''(0)$  on  $M^2$ .

$M^2$	$\alpha$	$\varphi''(0)$
1	0.5410	1.5853
2	0.4748	1.8735
4	0.3936	2.3467
5	0.3661	2.5507
10	0.2831	3.3917

Table 3.2: CASE III-N: descriptive quantities of the motion for some values of  $M^2$  and  $\beta - \alpha$ .

$M^2$	$\beta - \alpha$	$\beta$	$\gamma'(0)$	$C$	$\frac{\gamma'(0)}{\varphi''(0)}$	$\frac{x_p}{x_s}$	$\frac{m_s}{m_i}$	$\bar{\eta}_\varphi$	$\bar{\eta}_\gamma$	$\delta$
1	-5.5410	-5	9.3506	0.8978	5.8982	0.9394	3.3285	2.1059	2.8353	2.8353
	-0.5410	0	1.4240	0.8978	0.8982	0.6023	3.3285	2.1059	0.5912	2.1059
	0	0.5410	0.5663	0.8978	0.3572	0	3.3285	2.1059	2.8059	2.8059
	0.5410	1.0820	-0.2914	0.8978	-0.1838	2.9437	3.3285	2.1059	2.8741	2.8741
	4.4590	5	-6.5027	0.8978	-4.1018	1.0871	3.3285	2.1059	3.1276	3.1276
2	-5.4748	-5	10.8049	1.0261	5.7672	0.9493	3.2045	1.9127	2.6559	2.6559
	-0.4748	0	1.4373	1.0261	0.7672	0.6189	3.2045	1.9127	0.5024	1.9127
	0	0.4748	0.5477	1.0261	0.2923	0	3.2045	1.9127	2.5331	2.5331
	0.4748	0.9497	-0.3419	1.0261	-0.1825	2.6018	3.2045	1.9127	2.6046	2.6046
	4.5252	5	-7.9303	1.0261	-4.2328	1.0691	3.2045	1.9127	2.8904	2.8904
4	-5.3936	-5	13.1874	1.2448	5.6196	0.9598	3.1145	1.6482	2.3854	2.3854
	-0.3936	0	1.4541	1.2448	0.6196	0.6352	3.1145	1.6482	0.4017	1.6482
	0	0.3936	0.5304	1.2448	0.2260	0	3.1145	1.6482	2.1622	2.1622
	0.3936	0.7872	-0.3932	1.2448	-0.1675	2.3491	3.1145	1.6482	2.2347	2.2347
	4.6064	5	-10.2792	1.2448	-4.3804	1.0516	3.1145	1.6482	2.5561	2.5561
5	-5.3661	-5	14.2129	1.3410	5.5722	0.9630	3.0935	1.5517	2.2801	2.2801
	-0.3661	0	1.4596	1.3410	0.5722	0.6398	3.0935	1.5517	0.3697	1.5517
	0	0.3661	0.5258	1.3410	0.2061	0	3.0935	1.5517	2.0284	2.0284
	0.3661	0.7322	-0.4080	1.3410	-0.1600	2.2886	3.0935	1.5517	2.1001	2.1001
	4.6339	5	-11.2938	1.3410	-4.4278	1.0466	3.0935	1.5517	2.4311	2.4311
10	-5.2831	-5	18.4331	1.7452	5.4348	0.9721	3.0486	1.2394	1.9159	1.9159
	-0.2831	0	1.4748	1.7452	0.4348	0.6511	3.0486	1.2394	0.2783	1.2394
	0	0.2831	0.5146	1.7452	0.1517	0	3.0486	1.2394	1.6024	1.6024
	0.2831	0.5662	-0.4457	1.7452	-0.1314	2.1546	3.0486	1.2394	1.6676	1.6676
	4.7169	5	-15.4836	1.7452	-4.5652	1.0332	3.0486	1.2394	2.0127	2.0127

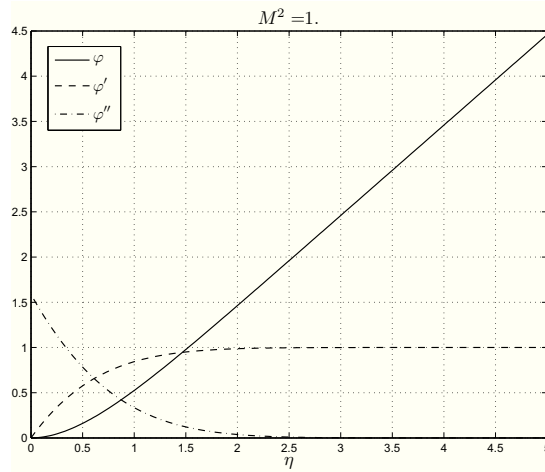


Figure 3.4: CASE III-N: plots showing  $\varphi, \varphi', \varphi''$  for  $M^2 = 1$ .

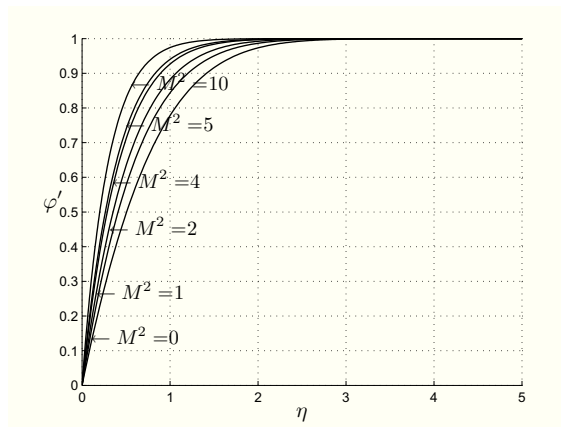


Figure 3.5: CASE III-N: plots showing  $\varphi'$  for different  $M^2$ .

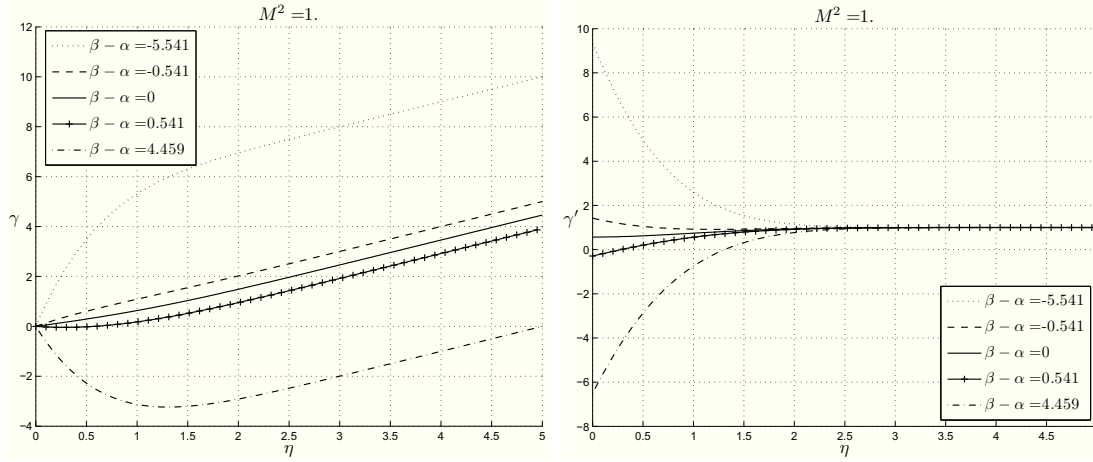


Figure 3.6: CASE III-N: plots showing  $\gamma, \gamma'$  with  $M^2 = 1$  and, from above,  $\beta - \alpha = -5 - \alpha, -\alpha, 0, \alpha, 5 - \alpha$ , respectively.

In Figure 3.4 we display  $\varphi, \varphi', \varphi''$  for  $M^2 = 1$ , while  $\varphi'$  is plotted against  $\eta$  for various values of  $M^2$  in Figure 3.5.

Figures 3.6<sub>1</sub>, 3.6<sub>2</sub> show the profiles of  $\gamma(\eta), \gamma'(\eta)$ , for  $M^2 = 1$  and for some values of  $\beta - \alpha$ , i.e.  $\beta - \alpha = -5 - \alpha, -\alpha, 0, \alpha, 5 - \alpha$ .

Figures 3.4 and 3.6 provide the behaviour of the velocity when  $M^2 = 1$ . Other values of  $M^2$  slightly modify the trend of  $\mathbf{v}$ .

In Figures 3.7, 3.8, 3.9 we show the trend of  $\gamma'$  for different  $M^2$  when  $\beta - \alpha$  is fixed.

Table 3.2 reveals that the constant  $C$  in (1.39) has approximately always the same value if we fix  $M^2$  and it increases as  $M^2$  increases.

In Table 3.2 we note that  $\bar{\eta}_\gamma$  is greater than the corresponding value of  $\bar{\eta}_\varphi$ ; so the influence of the viscosity appears only in the region  $\eta < \bar{\eta}_\gamma$ , i.e.  $x_2 < \sqrt{\frac{\nu}{a}} \bar{\eta}_\gamma$ , as it happened for an inert Newtonian fluid (see Chapter 1.2.2).

Further we underline that the thickness of this layer depends on  $M^2$  and decreases when  $M^2$  increases (as is easy to see in Figures 3.5, 3.7, 3.8, 3.9). Hence, as in the orthogonal case, the magnetic field tends to accelerate the fluid motion due to the Lorentz forces, which reduce the growth of the boundary layer.

Finally, we notice that the points  $x_p, x_s$ , given by (1.41), lie on the same side of the origin. Their location depends on  $M^2$  and  $\beta - \alpha$ , as one can see in Table 3.2. The Figure 3.10 shows the streamlines and the points  $\xi_p, \xi_s$  for  $\frac{b}{a} = 1, \beta - \alpha = -\alpha, 0, \alpha$ , and  $M^2 = 1, 5$ . We see that  $\frac{x_p}{x_s}$  tends to 1 as  $M^2$  increases.

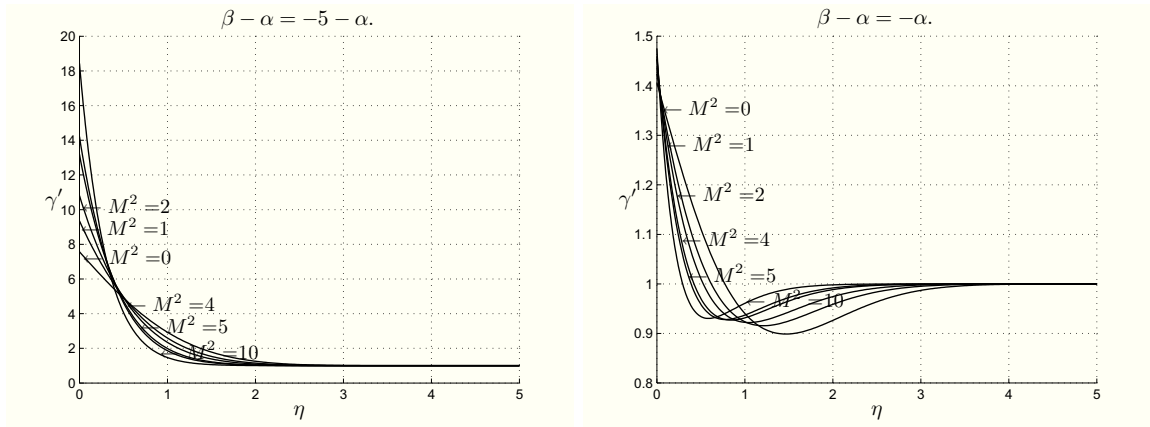


Figure 3.7: CASE III-N: plots showing  $\gamma'$  for different  $M^2$ . In the first picture  $\beta - \alpha = -5 - \alpha$ , in the second  $\beta - \alpha = -\alpha$ .

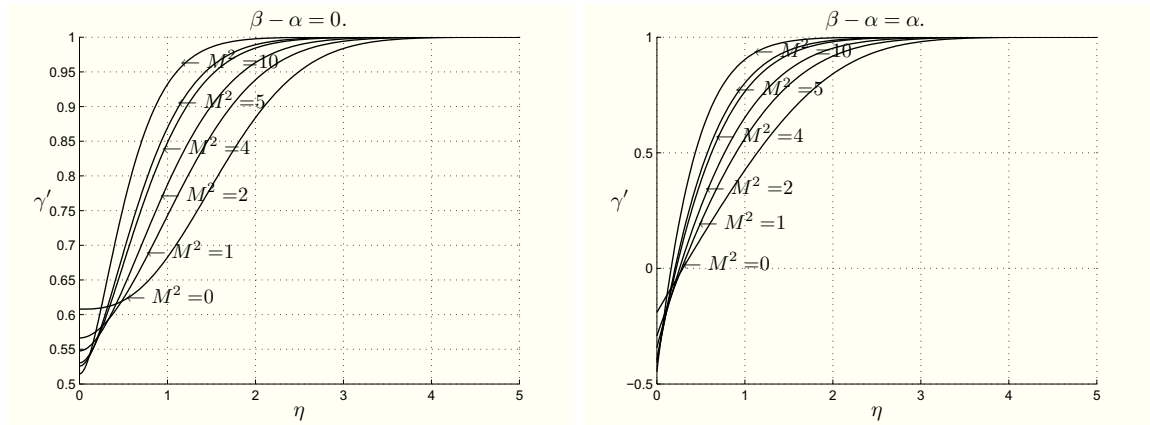


Figure 3.8: CASE III-N: plots showing  $\gamma'$  for different  $M^2$ . In the first picture  $\beta - \alpha = 0$ , in the second  $\beta - \alpha = \alpha$ .

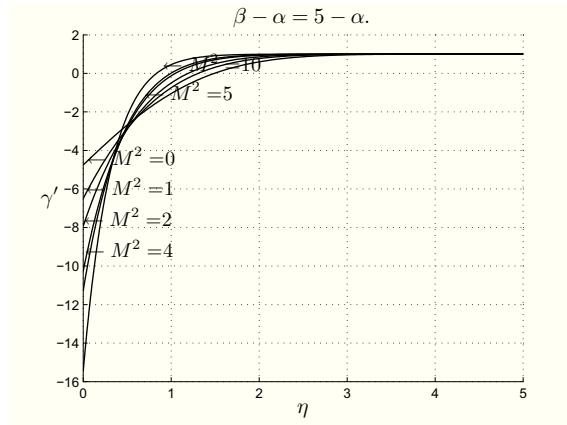


Figure 3.9: CASE III-N: plots showing  $\gamma'$  for different  $M^2$  with  $\beta - \alpha = 5 - \alpha$ .

### 3.3 Micropolar fluids

Consider the steady two-dimensional MHD oblique stagnation-point flow of a homogeneous, incompressible, electrically conducting micropolar fluid towards a flat surface coinciding with the plane  $x_2 = 0$ .

In the absence of external mechanical body forces and body couples and free electric charges, the MHD equations which govern the motion in  $\mathcal{S}$  for such a fluid are (2.44), subject to the boundary conditions (2.45), (2.5), (2.6).

We seek  $\mathbf{v}$ ,  $\mathbf{w}$  as

$$\begin{aligned} v_1 &= ax_1 f'(x_2) + bg(x_2), & v_2 &= -af(x_2), & v_3 &= 0, \\ w_1 &= 0, & w_2 &= 0, & w_3 &= x_1 F(x_2) + G(x_2), & x_1 \in \mathbb{R}, & x_2 \in \mathbb{R}^+, \end{aligned} \quad (3.36)$$

where  $f \in C^3(\mathbb{R}^+)$ ,  $g, F, G \in C^2(\mathbb{R}^+)$  are unknown functions to be determined so that

$$\begin{aligned} f(0) &= 0, & f'(0) &= 0, & g(0) &= 0, \\ F(0) &= 0, & G(0) &= 0. \end{aligned} \quad (3.37)$$

The previous conditions arise from (2.45).

The similarity transformation  $(f, g, F, G)$  also has to satisfy

$$\begin{aligned} \lim_{x_2 \rightarrow +\infty} f'(x_2) &= 1, & \lim_{x_2 \rightarrow +\infty} g'(x_2) &= 1, \\ \lim_{x_2 \rightarrow +\infty} F(x_2) &= 0, & \lim_{x_2 \rightarrow +\infty} G(x_2) &= -\frac{b}{2}. \end{aligned} \quad (3.38)$$

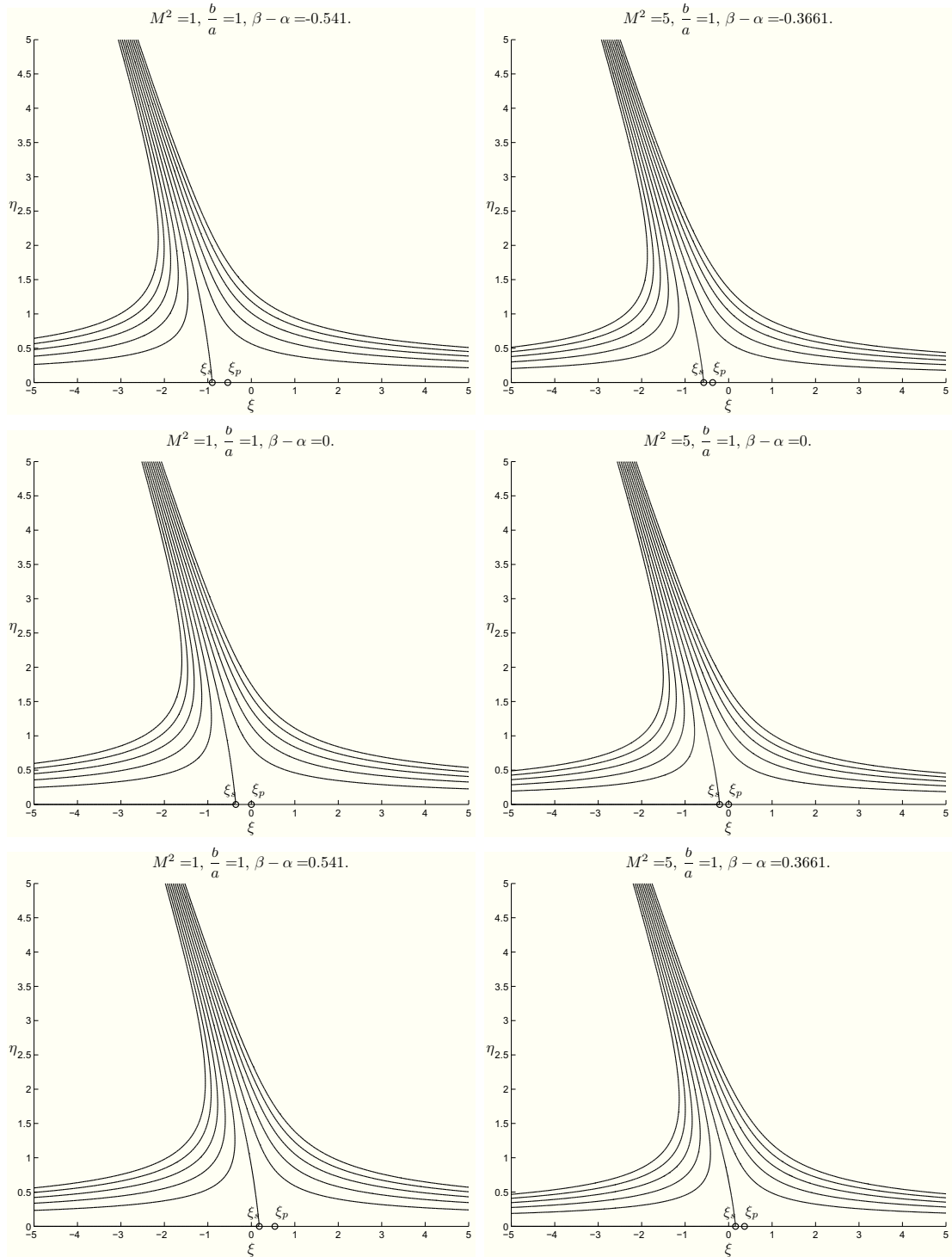


Figure 3.10: CASE III-N: figures 3.10<sub>1,3,5</sub> show the streamlines and the points  $\xi_p, \xi_s$  for  $\frac{b}{a} = 1, M^2 = 1$  and  $\beta - \alpha = -\alpha, 0, \alpha$ , respectively. Figures 3.10<sub>2,4,6</sub> for  $M^2 = 5$ .

We recall that in all the following cases, when we will refer to inviscid fluid, all results have to be modified by replacing  $x_1, x_2$  with  $x_1 - \frac{b}{a}(B - A), x_2 - A$ , respectively. In particular, the asymptotic behaviour of  $f$  and  $g$  at infinity is related to the constants  $A, B$ , in the same way of the Newtonian fluids:

$$\lim_{x_2 \rightarrow +\infty} [f(x_2) - x_2] = -A, \quad \lim_{x_2 \rightarrow +\infty} [g(x_2) - x_2] = -B. \quad (3.39)$$

In order to study the influence of a uniform external electromagnetic field, we consider the three cases analyzed in the previous section.

### 3.3.1 CASE I-M: $\mathbf{E} = E_0 \mathbf{e}_3$ .

By proceeding as in CASE I and I-N, from (2.44)<sub>3</sub>, (2.45)<sub>4</sub> and boundary conditions for electromagnetic field, we obtain  $\mathbf{E} = E_0 \mathbf{e}_3$ . Further, the induced magnetic field  $h(x_2)$  satisfies

$$h' + \frac{a}{\eta_e} f h = -\eta_e E_0, \quad x_2 > 0, \quad h(0) = 0, \quad (3.40)$$

which can be integrate if we regard  $f$  as a known function to get

$$h(x_2) = -\sigma_e E_0 e^{-\frac{a}{\eta_e} \int_0^{x_2} f(t) dt} \int_0^{x_2} e^{\frac{a}{\eta_e} \int_0^s f(t) dt} ds, \quad x_2 \in \mathbb{R}^+. \quad (3.41)$$

The induced magnetic fields given by (3.41) and (3.5) have the same asymptotic behaviour at infinity

$$-\frac{\eta_e E_0 \sigma_e}{a(x_2 - A)}.$$

In order to determine  $p, f, g, F, G$  we substitute (3.36) into (2.44)<sub>1,3</sub> and, after some calculations, we arrive at  $p = p(x_1, x_2)$  and

$$\begin{aligned} & ax_1 \left[ (\nu + \nu_r) f''' + a f f'' - a f'^2 + \frac{2\nu_r}{a} F' \right] \\ & + b \left[ (\nu + \nu_r) g'' + a(fg' - f'g) + \frac{2\nu_r}{b} G' \right] = \frac{1}{\rho} \frac{\partial p}{\partial x_1}, \\ & (\nu + \nu_r) a f'' + a^2 f' f + 2\nu_r F + \frac{\mu_e}{\rho} h' h = -\frac{1}{\rho} \frac{\partial p}{\partial x_2}, \\ & x_1 [\alpha F''' + I a (F' f - F f') - 2\nu_r (2F + a f'')] \\ & + \lambda G''' + I (a G' f - b F g) - 2\nu_r (2G + b g') = 0. \end{aligned} \quad (3.42)$$

Then, by integrating (3.42)<sub>3</sub>, we find

$$p = -\frac{1}{2}\rho a^2 f^2(x_2) - \rho a(\nu + \nu_r)f'(x_2) - 2\nu_r\rho \int_0^{x_2} F(s)ds \\ - \frac{\mu_e}{2}h^2(x_2) + P(x_1),$$

where the function  $P(x_1)$  is determined supposing that, far from the wall, the pressure  $p$  has the same behaviour as for an inviscid electroconducting fluid, whose velocity is given by (3.15). Since the induced electromagnetic fields given by (3.41) and (3.5) have the same asymptotic behaviour, under the assumption  $F \in L^1([0, +\infty))$ , by virtue of (3.38), (3.39), we get

$$P(x_1) = -\rho \frac{a^2}{2} \left[ x_1 - \frac{b}{a}(B - A) \right]^2 + p_0^* + \rho a(\nu + \nu_r).$$

Thus the pressure field assumes the form

$$p(x_1, x_2) = -\rho \frac{a^2}{2} [x_1^2 - 2\frac{b}{a}(B - A)x_1 + f^2(x_2)] - \rho a(\nu + \nu_r)f'(x_2) \\ - 2\nu_r\rho \int_0^{x_2} F(s)ds - \frac{\mu_e}{2}h^2(x_2) + p_0, \quad (3.43)$$

with  $p_0 = p_0^* + \rho a(\nu + \nu_r) - \rho \frac{b^2}{2}(B - A)^2$ .

Taking into account (3.43), we have the nonlinear ordinary differential equations

$$\frac{\nu + \nu_r}{a} f''' + f f'' - f'^2 + 1 + \frac{2\nu_r}{a^2} F' = 0, \\ \frac{\nu + \nu_r}{a} g'' + f g' - g f' + \frac{2\nu_r}{ab} G' = B - A, \\ \lambda F'' + aI(fF' - f'F) - 2\nu_r(2F + af'') = 0, \\ \lambda G'' + I(afG' - bgF) - 2\nu_r(2G + bg') = 0, \quad (3.44)$$

subject to the boundary conditions (3.37), (3.38).

We remark that system (3.44), (3.37), (3.38) governs the oblique stagnation-point flow of an inert electromagnetic micropolar fluid, see Chapter 1.2.3.

**REMARK 3.3.1.** *If  $\nu_r = 0$ , then (3.44)<sub>1</sub> and (3.44)<sub>2</sub> are the equations governing the oblique stagnation-point flow of a Newtonian fluid (Chapter 1.2.2).*

*We observe that (3.44)<sub>1</sub> and (3.44)<sub>3</sub> have the same form as the equations found by Guram and Smith ([27]) for the orthogonal stagnation-point flow of a micropolar fluid (Chapter 1.2.3).*

**THEOREM 3.3.2.** *Let a homogeneous, incompressible, electrically conducting micropolar fluid occupy the region  $\mathcal{S}$ . The steady MHD oblique plane stagnation-point flow of such a fluid has the following form when an external uniform electric field  $\mathbf{E}_0 = E_0 \mathbf{e}_3$  is impressed:*

$$\begin{aligned} \mathbf{v} &= [ax_1 f'(x_2) + bg(x_2)] \mathbf{e}_1 - af(x_2) \mathbf{e}_2, \quad \mathbf{H} = h(x_2) \mathbf{e}_1, \quad \mathbf{E} = E_0 \mathbf{e}_3, \\ \mathbf{w} &= [x_1 F(x_2) + G(x_2)] \mathbf{e}_3, \\ p &= -\rho \frac{a^2}{2} [x_1^2 - 2 \frac{b}{a} (B - A)x_1 + f^2(x_2)] - \rho a(\nu + \nu_r) f'(x_2) \\ &\quad - 2\nu_r \rho \int_0^{x_2} F(s) ds - \frac{\mu_e}{2} h^2(x_2) + p_0, \\ x_1 &\in \mathbb{R}, \quad x_2 \in \mathbb{R}^+, \end{aligned}$$

where  $(f, g, F, G)$  satisfies the problem (3.44), (3.37), and (3.38), provided  $F \in L^1([0, +\infty))$ , and  $h(x_2)$  is given by (3.41).

By Remark 3.3.1 and by the fact that  $h$  is the same as in CASE I-M orthogonal (see Chapter 2.3.1), we have already solved the problem. In particular, the behaviour of  $h$  is given in Figure 2.11. Of course, Remark 1.2.8 continues to hold.

### 3.3.2 CASE II-M: $\mathbf{H}_0 = H_0 \mathbf{e}_1$ .

As in CASE II and II-N, from (2.44)<sub>3</sub>, (2.44)<sub>4</sub> and (2.5), we get

$$h' + \frac{a}{\eta_e} f h = -\frac{a}{\eta_e} f H_0, \quad x_2 > 0, \quad h(0) = 0. \quad (3.45)$$

The integration of (3.45) leads to

$$h(x_2) = H_0 \left[ e^{-\frac{a}{\eta_e} \int_0^{x_2} f(t) dt} - 1 \right], \quad x_2 \in \mathbb{R}^+, \quad (3.46)$$

so that

$$\mathbf{H} = H_0 e^{-\frac{a}{\eta_e} \int_0^{x_2} f(s) ds} \mathbf{e}_1.$$

The pressure field can be now easily computed

$$\begin{aligned} p(x_1, x_2) &= -\rho \frac{a^2}{2} [x_1^2 - 2 \frac{b}{a} (B - A)x_1 + f^2(x_2)] - \rho a(\nu + \nu_r) f'(x_2) \\ &\quad - 2\nu_r \rho \int_0^{x_2} F(s) ds - \frac{\mu_e}{2} [h(x_2) + H_0]^2 + p_0^*, \end{aligned} \quad (3.47)$$

where  $(f, g, F, G)$  satisfies system (3.44), together with boundary conditions (3.37) and (3.38).

Therefore, in this case as well, the uniform external electromagnetic field does not influence the velocities.

We can summarize our results in the following:

**THEOREM 3.3.3.** *Let a homogeneous, incompressible, electrically conducting micropolar fluid occupy the region  $\mathcal{S}$ . The steady MHD oblique plane stagnation-point flow of such a fluid has the following form when a uniform external magnetic field  $\mathbf{H}_0 = H_0\mathbf{e}_1$  is impressed:*

$$\begin{aligned}\mathbf{v} &= [ax_1f'(x_2) + bg(x_2)]\mathbf{e}_1 - af(x_2)\mathbf{e}_2, & \mathbf{H} &= [h(x_2) + H_0]\mathbf{e}_1, & \mathbf{E} &= E_0\mathbf{e}_3, \\ \mathbf{w} &= [x_1F(x_2) + G(x_2)]\mathbf{e}_3, \\ p &= -\rho\frac{a^2}{2}[x_1^2 - 2\frac{b}{a}(B-A)x_1 + f^2(x_2)] - \rho a(\nu + \nu_r)f'(x_2) - 2\nu_r\rho \int_0^{x_2} F(s)ds \\ &\quad - \frac{\mu_e}{2}[h(x_2) + H_0]^2 + p_0^*, & x_1 &\in \mathbb{R}, & x_2 &\in \mathbb{R}^+, \end{aligned}$$

where  $(f, g, F, G)$  satisfies the problem (3.44), (3.37), and (3.38), provided  $F \in L^1([0, +\infty))$ , and  $h(x_2)$  is given by (3.46).

In dimensionless form,  $h(x_2)$  becomes

$$\Psi(\eta) = e^{-R_m \int_0^\eta \varphi(t)dt} - 1, \quad \eta \in \mathbb{R}^+, \quad (3.48)$$

and it is the same as in CASE II-M orthogonal (see Chapter 2.3.2, Figure 2.12).

Of course, Remark 1.2.8 holds even in this case.

### 3.3.3 CASE III-M: $\mathbf{H}_0 = \frac{H_0}{\sqrt{4a^2 + b^2}}(-b\mathbf{e}_1 + 2a\mathbf{e}_2)$ .

Taking into account Theorem 3.1.5, we impress

$$\mathbf{H}_0 = \frac{H_0}{\sqrt{4a^2 + b^2}}(-b\mathbf{e}_1 + 2a\mathbf{e}_2), \quad \mathbf{E}_0 = \mathbf{0},$$

and we deduce

$$\mathbf{E} = \mathbf{0} \Rightarrow \nabla \times \mathbf{H} = \sigma_e \mu_e (\mathbf{v} \times \mathbf{H}).$$

We proceed by neglecting the induced magnetic field so that we can replace (2.44)<sub>1</sub> with

$$\mathbf{v} \cdot \nabla \mathbf{v} = -\frac{1}{\rho} \nabla p + (\nu + \nu_r) \Delta \mathbf{v} + 2\nu_r (\nabla \times \mathbf{w}) + \frac{\mu_e}{\rho} (\mathbf{v} \times \mathbf{H}_0) \times \mathbf{H}_0. \quad (3.49)$$

On substituting (3.36) into (3.49), we have  $p = p(x_1, x_2)$  and

$$\begin{aligned} & ax_1 \left[ (\nu + \nu_r) f''' + a f f'' - a f'^2 + \frac{2\nu_r}{a} F' - 4a^2 \frac{\sigma_e}{\rho} \frac{B_0^2}{4a^2 + b^2} f' \right] \\ & + b \left[ (\nu + \nu_r) g'' + a(fg' - f'g) + \frac{2\nu_r}{b} G' - 2a^2 \frac{\sigma_e}{\rho} \frac{B_0^2}{4a^2 + b^2} (2g - f) \right] = \frac{1}{\rho} \frac{\partial p}{\partial x_1}, \\ & (\nu + \nu_r) a f'' + a^2 f' f + 2\nu_r F + \frac{\sigma_e}{\rho} \frac{B_0^2}{4a^2 + b^2} [2a^2 b x_1 f' + ab^2 (2g - f)] = -\frac{1}{\rho} \frac{\partial p}{\partial x_2}. \end{aligned} \quad (3.50)$$

The integration of (3.50)<sub>3</sub> yields

$$\begin{aligned} p(x_1, x_2) = & -\frac{1}{2} \rho a^2 f^2(x_2) - \rho a (\nu + \nu_r) f'(x_2) - 2\nu_r \rho \int_0^{x_2} F(s) ds \\ & - \sigma_e \frac{B_0^2}{4a^2 + b^2} \left[ 2a^2 b x_1 f(x_2) + ab^2 \int_0^{x_2} (2g(s) - f(s)) ds \right] + P(x_1), \end{aligned}$$

where  $P(x_1)$  has to be found as in the previous cases, so that we get

$$P(x_1) = -\rho \frac{a^2}{2} \left( 1 + \frac{4a}{\rho} \frac{\sigma_e B_0^2}{4a^2 + b^2} \right) \left[ x_1 - \frac{b}{a} (B - A) \right]^2 + p_0^*.$$

The pressure field is then given by

$$\begin{aligned} p(x_1, x_2) = & -\rho \frac{a^2}{2} [x_1^2 - 2\frac{b}{a} (B - A)x_1 + f^2(x_2)] - \rho a (\nu + \nu_r) f'(x_2) \\ & - 2\nu_r \rho \int_0^{x_2} F(s) ds - \frac{\sigma_e B_0^2}{4a^2 + b^2} \left[ 2a^2 b x_1 f(x_2) + \int_0^{x_2} (2g(s) - f(s)) ds \right. \\ & \left. - 2a^3 \left( \frac{2b}{a} (B - A)x_1 - x_1^2 \right) \right] + p_0, \quad x_1 \in \mathbb{R}, \quad x_2 \in \mathbb{R}^+. \end{aligned} \quad (3.51)$$

From (3.50)<sub>2</sub> we get

$$\begin{aligned} & \frac{\nu + \nu_r}{a} f''' + f f'' - f'^2 + 1 + \frac{2\nu_r}{a^2} F' + M^2(1 - f') = 0, \\ & \frac{\nu + \nu_r}{a} g'' + f g' - g f' + \frac{2\nu_r}{ab} G' + M^2(f - g) = (1 + M^2)(B - A), \end{aligned} \quad (3.52)$$

where  $M^2$  is the Hartmann number.

The solution  $(f, g, F, G)$  also satisfies the equations (3.44)<sub>3,4</sub>. We append boundary conditions (3.37) and (3.38) to the system in (3.52) and (3.44)<sub>3,4</sub>.

We remark that the external electromagnetic field now modifies the velocities and that if  $M^2 = 0$ , then the system (3.52) and (3.44)<sub>3,4</sub> reduces to the system (3.44).

REMARK 3.3.4. If  $\nu_r = 0$ , then (3.52)<sub>1</sub> are the equations governing oblique stagnation-point flow CASE III-N of a Newtonian fluid (Chapter 3.2.3).

THEOREM 3.3.5. Let a homogeneous, incompressible, electrically conducting micropolar fluid occupy the region  $\mathcal{S}$ . If we impress the external magnetic field

$$\mathbf{H}_0 = \frac{H_0}{\sqrt{4a^2 + b^2}}(-b\mathbf{e}_1 + 2a\mathbf{e}_2)$$

and if we neglect the induced magnetic field, then the steady MHD oblique plane stagnation-point flow of such a fluid has the form

$$\begin{aligned} \mathbf{v} &= [ax_1f'(x_2) + bg(x_2)]\mathbf{e}_1 - af(x_2)\mathbf{e}_2, \\ \mathbf{w} &= [x_1F(x_2) + G(x_2)]\mathbf{e}_3, \quad \mathbf{E} = \mathbf{0}, \\ p &= -\rho\frac{a^2}{2}[x_1^2 - 2\frac{b}{a}(B-A)x_1 + f^2(x_2)] - \rho a(\nu + \nu_r)f'(x_2) \\ &\quad - 2\nu_r\rho \int_0^{x_2} F(s)ds - \frac{\sigma_e B_0^2}{4a^2 + b^2} \left[ 2a^2bx_1f(x_2) + \int_0^{x_2} (2g(s) - f(s))ds \right. \\ &\quad \left. - 2a^3\left(\frac{2b}{a}(B-A)x_1 - x_1^2\right) \right] + p_0, \quad x_1 \in \mathbb{R}, \quad x_2 \in \mathbb{R}^+, \end{aligned}$$

where  $(f, g, F, G)$  satisfies problem (3.52), (3.44)<sub>3,4</sub>, (3.37), and (3.38), provided  $F \in L^1([0, +\infty))$ .

In dimensionless form, we can rewrite the previous ordinary differential boundary value problem as

$$\begin{aligned} \varphi''' + \varphi\varphi'' - \varphi'^2 + 1 + \Phi' + M^2(1 - \varphi') &= 0, \\ \gamma'' + \varphi\gamma' - \varphi'\gamma + \Gamma' + M^2(\varphi - \gamma) &= (1 + M^2)(\beta - \alpha), \\ \Phi'' + c_3(\varphi\Phi' - \varphi'\Phi) - c_2\Phi - c_1\varphi'' &= 0, \\ \Gamma'' + c_3(\varphi\Gamma' - \Phi\gamma) - c_2\Gamma - c_1\gamma' &= 0, \\ \varphi(0) = 0, \quad \varphi'(0) = 0, \quad \gamma(0) = 0, \\ \Phi(0) = 0, \quad \Gamma(0) = 0, \\ \lim_{\eta \rightarrow +\infty} \varphi'(\eta) = 1, \quad \lim_{\eta \rightarrow +\infty} \gamma'(\eta) = 1 \\ \lim_{\eta \rightarrow +\infty} \Phi(\eta) = 0, \quad \lim_{\eta \rightarrow +\infty} \Gamma(\eta) = -\frac{c_1}{c_2}, \end{aligned} \tag{3.53}$$

where  $\alpha, \beta, c_1, c_2, c_3$  are given by (1.51).

REMARK 3.3.6. The points  $x_1 = x_p$  of maximum pressure and  $x_1 = x_s$  of zero tangential stress on  $x_2 = 0$  are formally the same as in CASE I-M and II-M (Remark 1.2.8), but these points now depend on  $M^2$ .

The slope of the dividing streamline at the wall is now given by:

$$m_s = -\frac{3a[\varphi''(0)]^2}{b[(\beta - \alpha)(1 + M^2) - \Gamma'(0)]\varphi''(0) + [1 + M^2 + \Phi'(0)]\gamma'(0)}.$$

REMARK 3.3.7. As in the case in the absence of the external electromagnetic field (Remark 1.2.9), we will show that the solution  $(\varphi, \gamma, \Phi, \Gamma)$  of the problem here considered satisfies the conditions at infinity. From this reason, we define:

- $\bar{\eta}_\varphi$  ( $\bar{\eta}_\gamma$ ) the value of  $\eta$  such that  $\varphi'(\bar{\eta}_\varphi) = 0.99$  ( $\gamma'(\bar{\eta}_\gamma) = 0.99$ );
- $\bar{\eta}_\Phi$  ( $\bar{\eta}_\Gamma$ ) the value of  $\eta$  such that  $\Phi(\bar{\eta}_\Phi) = -0.01$  ( $\Gamma(\bar{\eta}_\Gamma) = +0.01 - \frac{c_1}{c_2}$ ),

so that if  $\eta > \bar{\eta}_\varphi$  ( $\eta > \bar{\eta}_\gamma$ ), then  $\varphi \cong \eta - \alpha$  ( $\gamma \cong \eta - \beta$ ), and if  $\eta > \bar{\eta}_\Phi$  ( $\eta > \bar{\eta}_\Gamma$ ), then  $\Phi \cong 0$  ( $\Gamma \cong -\frac{c_1}{c_2}$ ).

We define as

$$\delta_v = \max(\bar{\eta}_\varphi, \bar{\eta}_\gamma), \quad (3.54)$$

$$\delta_w = \max(\bar{\eta}_\Phi, \bar{\eta}_\Gamma) \quad (3.55)$$

the thickness of the layer lining the boundary where the effect of the viscosity occurs on the velocity and on the microrotation, respectively.

The thickness  $\delta$  of the boundary layer for the flow is defined as

$$\delta := \max(\delta_v, \delta_w).$$

We have integrated numerically problem (3.53) for some values of  $\beta - \alpha$ ,  $c_1$ ,  $c_2$ ,  $c_3$ ,  $M^2$ , chosen according to the previous chapters (see Tables 3.3 and 3.4). These Tables elucidate the dependence of the relevant quantities of the flow on the material parameters and on the magnetic field.

From Tables 3.3 and 3.4 it appears that if we fix two parameters among  $c_1, c_2, c_3$ , then the values of  $\alpha$ ,  $\varphi''(0)$ ,  $\gamma'(0)$ ,  $\Phi'(0)$ ,  $\Gamma'(0)$  have the same behaviour as in the case in the absence of external magnetic field (Chapter 1.2.3).

We have displayed some representative graphs to elucidate the trends of the functions describing the velocity and the microrotation.

In particular, Figures 3.11, 3.12, and 3.13 show  $\varphi$ ,  $\varphi'$ ,  $\varphi''$ ,  $\Phi$ ,  $\Phi'$ ,  $\gamma$ ,  $\gamma'$ ,  $\Gamma$ ,  $\Gamma'$  for  $c_1 = 0.5$ ,  $c_2 = 3.0$ ,  $c_3 = 0.5$  and  $M^2 = 1$ .

Table 3.3: CASE III-M: descriptive quantities of motion for some values of  $c_1, c_2, c_3, M^2$ , and  $\beta - \alpha$ .

$M^2$	$c_1$	$c_2$	$c_3$	$\beta - \alpha$	$\alpha$	$\beta$	$\varphi''(0)$	$\gamma'(0)$	$\Phi'(0)$	$\Gamma'(0)$	$\frac{x_p}{x_s}$	$\frac{m_s}{m_i}$		
1	0.1	1.5	0.1	-0.5386	0.5386	0	1.5751	1.3886	-0.0583	-0.0876	0.6110	3.2715		
				0	0.5386	0.5389	1.5751	0.5402	-0.0583	-0.0562	0	3.2715		
						0.5386	0.5386	1.0776	1.5751	-0.3082	-0.0583	-0.0249	2.7529	3.2715
				0.5	-0.5388	0.5388	0	1.5762	1.3887	-0.0560	-0.0879	0.6116	3.2702	
					0	0.5388	0.5388	1.5762	0.5394	-0.0560	-0.0577	0	3.2702	
					0.5388	0.5388	1.0776	1.5762	-0.3098	-0.0560	-0.0275	2.7411	3.2702	
			3.0	0.1	-0.5392	0.5392	0	1.5778	1.4024	-0.0497	-0.0642	0.6066	3.2902	
	0	0.5392			0.5392	1.5778	0.5517	-0.0497	-0.0374	0	3.2902			
					0.5392	0.5392	1.0784	1.5778	-0.2990	-0.0497	-0.0106	2.8452	3.2902	
					0.5	-0.5392	0.5392	0	1.5783	1.4027	-0.0487	-0.0638	0.6068	3.2902
					0	0.5392	0.5392	1.5783	0.5516	-0.0487	-0.0376	0	3.2902	
					0.5392	0.5392	1.0785	1.5783	-0.2995	-0.0487	-0.0114	2.8417	3.2902	
		0.5	1.5	0.1	-0.5290	0.5290	0.0009	1.5335	1.2465	-0.2913	-0.4247	0.6508	3.0438	
	0				0.5290	0.5301	1.5335	0.4353	-0.2913	-0.2706	0	3.0439		
					0.5290	0.5290	1.0594	1.5335	-0.3758	-0.2913	-0.1165	2.1583	3.0439	
					0.5	-0.5298	0.5298	0	1.5392	1.2469	-0.2802	-0.4267	0.6541	3.0372
					0	0.5298	0.5300	1.5392	0.4313	-0.2802	-0.2783	0	3.0372	
					0.5298	0.5298	1.0599	1.5392	-0.3843	-0.2802	-0.1299	2.1223	3.0372	
			3.0	0.1	-0.5317	0.5317	0	1.5475	1.3160	-0.2487	-0.3140	0.6252	3.1370	
	0	0.5317			0.5319	1.5475	0.4932	-0.2487	-0.1818	0	3.1370			
					0.5317	0.5317	1.0636	1.5475	-0.3296	-0.2487	-0.0496	2.4960	3.1370	
					0.5	-0.5321	0.5321	0	1.5501	1.3175	-0.2434	-0.3124	0.6261	3.1373
					0	0.5321	0.5322	1.5501	0.4926	-0.2434	-0.1829	0	3.1373	
					0.5321	0.5321	1.0643	1.5501	-0.3322	-0.2434	-0.0534	2.4827	3.1373	
2	0.1	1.5	0.1	-0.4730	0.4730	0	1.8637	1.4057	-0.0617	-0.0867	0.6271	3.1626		
				0	0.4730	0.4732	1.8637	0.5242	-0.0617	-0.0576	0	3.1626		
					0.4730	0.4730	0.9462	1.8637	-0.3574	-0.0617	-0.0284	2.4667	3.1626	
					0.5	-0.4731	0.4731	0	1.8647	1.4056	-0.0594	-0.0874	0.6277	3.1617
					0	0.4731	0.4732	1.8647	0.5234	-0.0594	-0.0593	0	3.1617	
					0.4731	0.4731	0.9463	1.8647	-0.3589	-0.0594	-0.0312	2.4585	3.1617	
			3.0	0.1	-0.4734	0.4734	0	1.8661	1.4177	-0.0534	-0.0633	0.6231	3.1749	
	0	0.4734			0.4734	1.8661	0.5343	-0.0534	-0.0380	0	3.1749			
					0.4734	0.4734	0.9468	1.8661	-0.3491	-0.0534	-0.0127	2.5304	3.1749	
					0.5	-0.4735	0.4735	0	1.8666	1.4179	-0.0523	-0.0631	0.6233	3.1750
					0	0.4735	0.4735	1.8666	0.5342	-0.0523	-0.0383	0	3.1750	
					0.4735	0.4735	0.9469	1.8666	-0.3496	-0.0523	-0.0136	2.5280	3.1750	
		0.5	1.5	0.1	-0.4656	0.4656	0	1.8239	1.2789	-0.3085	-0.4229	0.6640	2.9950	
	0				0.4656	0.4662	1.8239	0.4298	-0.3085	-0.2793	0	2.9950		
					0.4656	0.4656	0.9319	1.8239	-0.4194	-0.3085	-0.1356	2.0248	2.9950	
					0.5	-0.4663	0.4663	0	1.8290	1.2786	-0.2971	-0.4268	0.6670	2.9904
					0	0.4663	0.4663	1.8290	0.4258	-0.2971	-0.2882	0	2.9904	
					0.4663	0.4663	0.9326	1.8290	-0.4271	-0.2971	-0.1497	1.9970	2.9904	
			3.0	0.1	-0.4676	0.4676	0	1.8363	1.3393	-0.2670	-0.3106	0.6411	3.0568	
	0	0.4676			0.4677	1.8363	0.4806	-0.2670	-0.1858	0	3.0568			
					0.4676	0.4676	0.9353	1.8363	-0.3780	-0.2670	-0.0609	2.2715	3.0568	
					0.5	-0.4679	0.4679	0	1.8387	1.3404	-0.2614	-0.3097	0.6419	3.0568
					0	0.4679	0.4680	1.8387	0.4800	-0.2614	-0.1874	0	3.0568	
					0.4679	0.4679	0.9359	1.8387	-0.3804	-0.2614	-0.0650	2.2619	3.0568	

Table 3.4: CASE III-M: continuum of Table 3.3.

$M^2$	$c_1$	$c_2$	$c_3$	$\beta - \alpha$	$\alpha$	$\beta$	$\varphi''(0)$	$\gamma'(0)$	$\Phi'(0)$	$\Gamma'(0)$	$\frac{x_p}{x_s}$	$\frac{m_s}{m_i}$	
5	0.1	1.5	0.1	-0.3650	0.3650	0	2.5418	1.4343	-0.0680	-0.0854	0.6469	3.0686	
				0	0.3650	0.3651	2.5418	0.5064	-0.0680	-0.0606	0	3.0686	
				0.3650	0.3650	0.7302	2.5418	-0.4215	-0.0680	-0.0358	2.2015	3.0686	
	0.5	0.1	0.1	-0.3651	0.3651	0	2.5426	1.4340	-0.0656	-0.0868	0.6474	3.0681	
				0	0.3651	0.3651	2.5426	0.5056	-0.0656	-0.0629	0	3.0681	
				0.3651	0.3651	0.7302	2.5426	-0.4227	-0.0656	-0.0389	2.1962	3.0681	
		3.0	0.1	0.1	-0.3652	0.3652	0	2.5437	1.4434	-0.0603	-0.0619	0.6436	3.0747
					0	0.3652	0.3653	2.5437	0.5144	-0.0603	-0.0398	0	3.0747
					0.3652	0.3652	0.7305	2.5437	-0.4147	-0.0603	-0.0178	2.2404	3.0747
	0.5	0.1	0.1	-0.3653	0.3653	0	2.5441	1.4435	-0.0591	-0.0619	0.6438	3.0746	
				0	0.3653	0.3653	2.5441	0.5142	-0.0591	-0.0403	0	3.0746	
				0.3653	0.3653	0.7306	2.5441	-0.4151	-0.0591	-0.0188	2.2388	3.0746	
0.5	1.5	0.1	-0.3608	0.3608	0	2.5059	1.3330	-0.3398	-0.4201	0.6783	2.9691		
			0	0.3608	0.3611	2.5059	0.4288	-0.3398	-0.2975	0	2.9691		
			0.3608	0.3608	0.7219	2.5059	-0.4753	-0.3398	-0.1748	1.9021	2.9691		
	0.5	0.1	0.1	-0.3612	0.3612	0	2.5099	1.3315	-0.3283	-0.4274	0.6808	2.9664	
				0	0.3612	0.3612	2.5099	0.4250	-0.3283	-0.3089	0	2.9664	
				0.3612	0.3612	0.7224	2.5099	-0.4816	-0.3283	-0.1903	1.8824	2.9664	
3.0	0.1	0.1	-0.3618	0.3618	0	2.5155	1.3790	-0.3014	-0.3052	0.6601	2.9991		
			0	0.3618	0.3619	2.5155	0.4688	-0.3014	-0.1961	0	2.9991		
			0.3618	0.3618	0.7237	2.5155	-0.4414	-0.3014	-0.0871	2.0619	2.9991		
	0.5	0.1	0.1	-0.3620	0.3620	0	2.5175	1.3795	-0.2954	-0.3056	0.6607	2.9988	
				0	0.3620	0.3620	2.5175	0.4680	-0.2954	-0.1987	0	2.9988	
				0.3620	0.3620	0.7241	2.5175	-0.4434	-0.2954	-0.0918	2.0555	2.9988	
10	0.1	1.5	0.1	-0.2825	0.2825	0	3.3838	1.4545	-0.0734	-0.0845	0.6573	3.0330	
				0	0.2825	0.2826	3.3838	0.4985	-0.0734	-0.0638	0	3.0330	
				0.2825	0.2825	0.5651	3.3838	-0.4575	-0.0734	-0.0430	2.0896	3.0330	
		0.5	0.1	0.1	-0.2826	0.2826	0	3.3844	1.4541	-0.0712	-0.0866	0.6577	3.0327
					0	0.2826	0.2826	3.3844	0.4978	-0.0712	-0.0665	0	3.0327
					0.2826	0.2826	0.5651	3.3844	-0.4585	-0.0712	-0.0464	2.0857	3.0327
	3.0	0.1	0.1	-0.2826	0.2826	0	3.3852	1.4616	-0.0665	-0.0608	0.6546	3.0361	
				0	0.2826	0.2826	3.3852	0.5048	-0.0665	-0.0420	0	3.0361	
				0.2826	0.2826	0.5653	3.3852	-0.4519	-0.0665	-0.0232	2.1171	3.0361	
	0.5	1.5	0.1	-0.2826	0.2826	0	3.3855	1.4616	-0.0652	-0.0611	0.6547	3.0360	
				0	0.2826	0.2826	3.3855	0.5047	-0.0652	-0.0426	0	3.0360	
				0.2826	0.2826	0.5653	3.3855	-0.4522	-0.0652	-0.0242	2.1160	3.0360	
3.0		0.1	0.1	-0.2802	0.2802	0	3.3522	1.3735	-0.3671	-0.4180	0.6838	2.9706	
				0	0.2802	0.2803	3.3522	0.4343	-0.3671	-0.3151	0	2.9706	
				0.2802	0.2802	0.5605	3.3522	-0.5050	-0.3671	-0.2123	1.8600	2.9706	
0.5	1.5	0.1	-0.2804	0.2804	0	3.3552	1.3714	-0.3559	-0.4285	0.6860	2.9690		
			0	0.2804	0.2804	3.3552	0.4307	-0.3559	-0.3287	0	2.9690		
			0.2804	0.2804	0.5608	3.3552	-0.5100	-0.3559	-0.2290	1.8444	2.9690		
3.0	0.1	0.1	-0.2807	0.2807	0	3.3593	1.4089	-0.3324	-0.3010	0.6693	2.9861		
			0	0.2807	0.2807	3.3593	0.4660	-0.3324	-0.2077	0	2.9861		
			0.2807	0.2807	0.5614	3.3593	-0.4769	-0.3324	-0.1144	1.9770	2.9861		
	0.5	1.5	0.1	-0.2808	0.2808	0	3.3609	1.4089	-0.3262	-0.3027	0.6698	2.9857	
				0	0.2808	0.2808	3.3609	0.4652	-0.3262	-0.2112	0	2.9857	
				0.2808	0.2808	0.5616	3.3609	-0.4786	-0.3262	-0.1196	1.9720	2.9857	

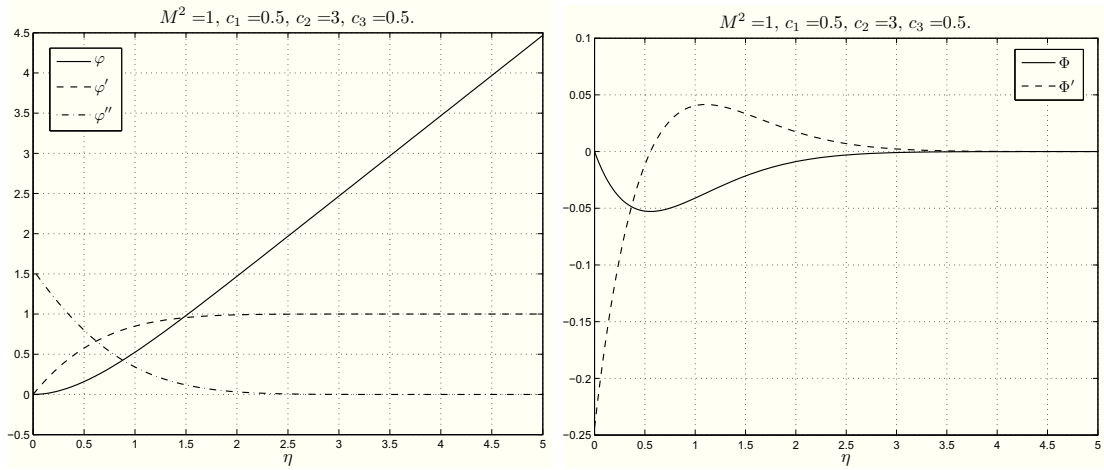


Figure 3.11: CASE III-M: plots showing  $\varphi, \varphi', \varphi''$  and  $\Phi, \Phi'$  (respectively) for  $c_1 = 0.5$ ,  $c_2 = 3.0$ ,  $c_3 = 0.5$  and  $M^2 = 1$ .

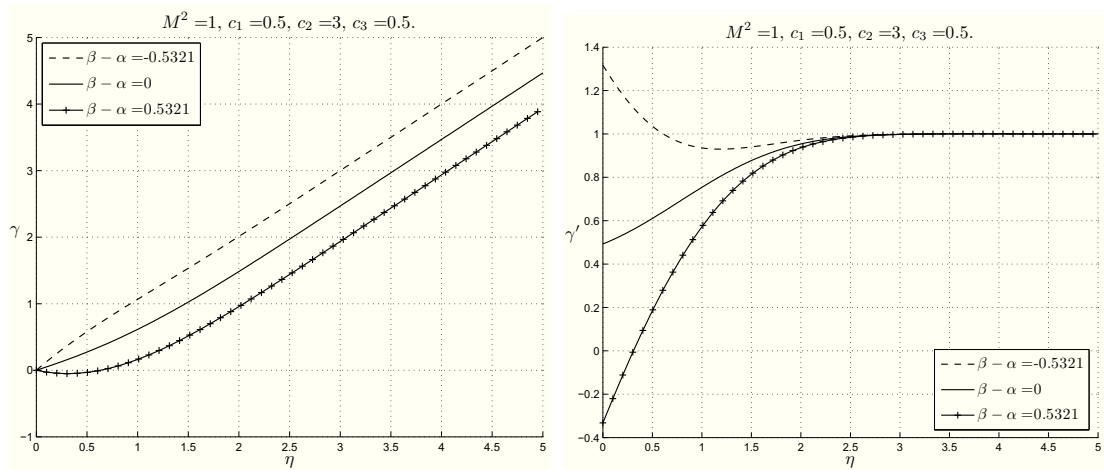


Figure 3.12: CASE III-M: plots showing  $\gamma, \gamma'$  with  $M^2 = 1$ ,  $c_1 = 0.5$ ,  $c_2 = 3.0$ ,  $c_3 = 0.5$  and, from above,  $\beta - \alpha = -\alpha, 0, \alpha$ , respectively.

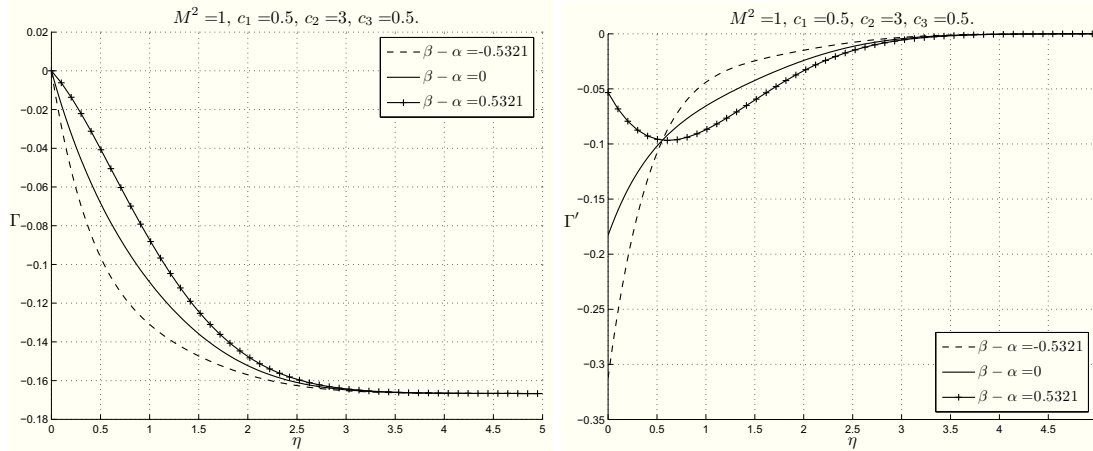


Figure 3.13: CASE III-M: plots showing  $\Gamma, \Gamma'$  with  $M^2 = 1, c_1 = 0.5, c_2 = 3.0, c_3 = 0.5$  and, from above,  $\beta - \alpha = -\alpha, 0, \alpha$ , respectively.

The other choices of these parameters modify the trends of these functions very slightly.

Of course, the behaviour of  $\varphi, \Phi$  doesn't depend on  $\beta - \alpha$ , unlike  $\gamma, \Gamma$ .

If we compare the velocity profile with the solution for Newtonian fluid (previous sections), we note that the trend is very similar, as was found in [27] and in Chapter 2 for the MHD orthogonal stagnation-point flow.

Figures 3.14, 3.15, and 3.16 show the effects of the parameters  $c_1, c_2, c_3$  varying one at a time on the functions  $\varphi', \gamma, \Phi, \Gamma$ . The functions which appear most influenced by these parameters are  $\Phi$ , and  $\Gamma$ . Further if  $M^2$  is fixed, then the considerations in Chapter 1.2.3 still hold.

As far as the dependence on  $M^2$  is concerned, we can see that  $\alpha$  and  $\Phi'(0)$  decrease and  $\varphi''(0)$  increases as  $M^2$  increases, as it is customary in magnetohydrodynamics.

As far as the dependence of  $\gamma'(0)$  and  $\Gamma'(0)$  on  $M^2$  are concerned, from Tables 3.3 and 3.4 we can see that their values increase as  $M^2$  increases if  $\beta - \alpha < 0$ , otherwise they decrease.

Figure 3.17 shows the behaviour of  $\varphi'$  for different  $M^2$  and  $c_1 = 0.5, c_2 = 3.0, c_3 = 0.5$ .

In Figures 3.18 we provide the trend of  $\gamma'$  for different  $M^2$  when  $c_1 = 0.5, c_2 = 3.0, c_3 = 0.5$  and  $\beta - \alpha$  is fixed.

Figure 3.19 shows the profile of  $\Phi$  for  $c_1 = 0.5, c_2 = 3.0, c_3 = 0.5$  and different  $M^2$ .

In Figures 3.20 we provide the behaviour of  $\Gamma$  for different  $M^2$  when  $c_1 = 0.5, c_2 = 3.0, c_3 = 0.5$  and  $\beta - \alpha$  is fixed.

We have only plotted the profiles of  $\varphi, \varphi', \varphi'', \gamma, \gamma', \Phi, \Phi', \Gamma, \Gamma'$  for  $M^2 = 1$

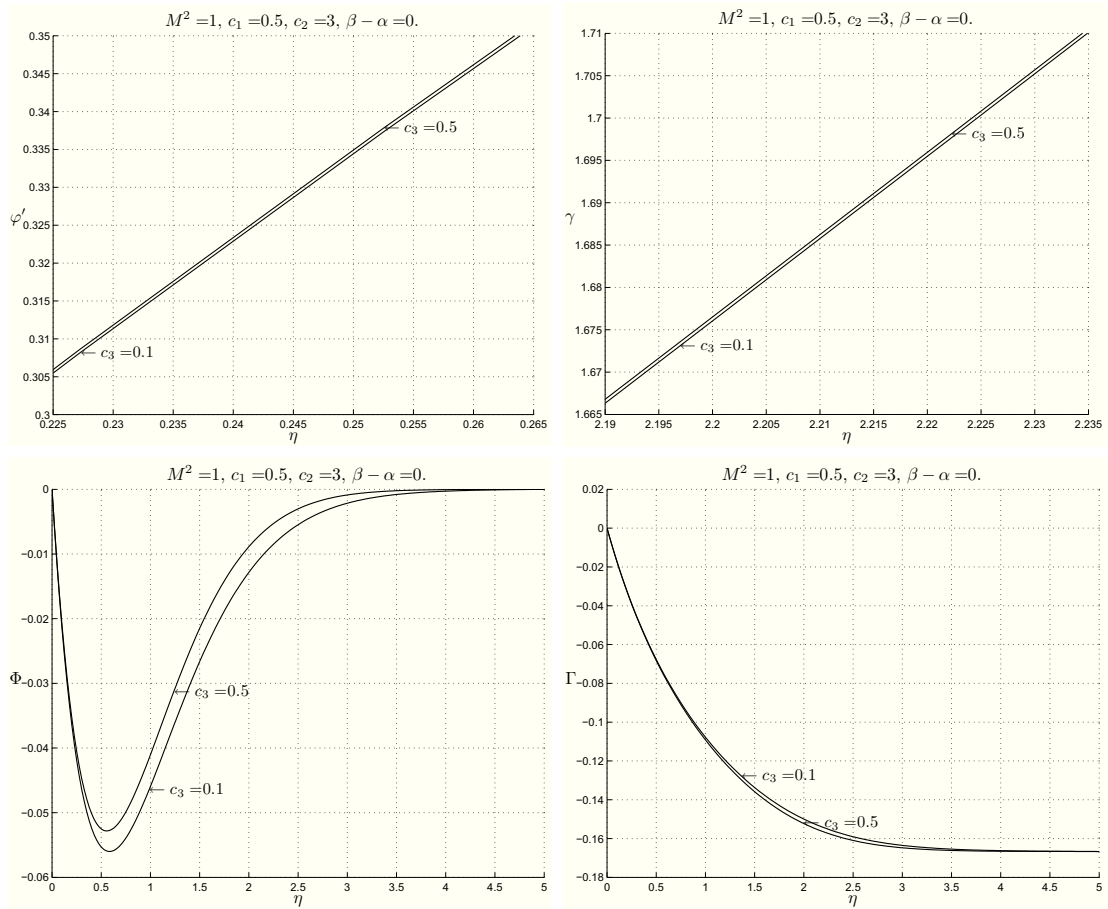


Figure 3.14: CASE III-M: plots showing the behaviour of  $\varphi'$ ,  $\gamma$ ,  $\Phi$  and  $\Gamma$  for  $c_1 = 0.5$ ,  $c_2 = 3.0$  fixed, and for different values of  $c_3$ .

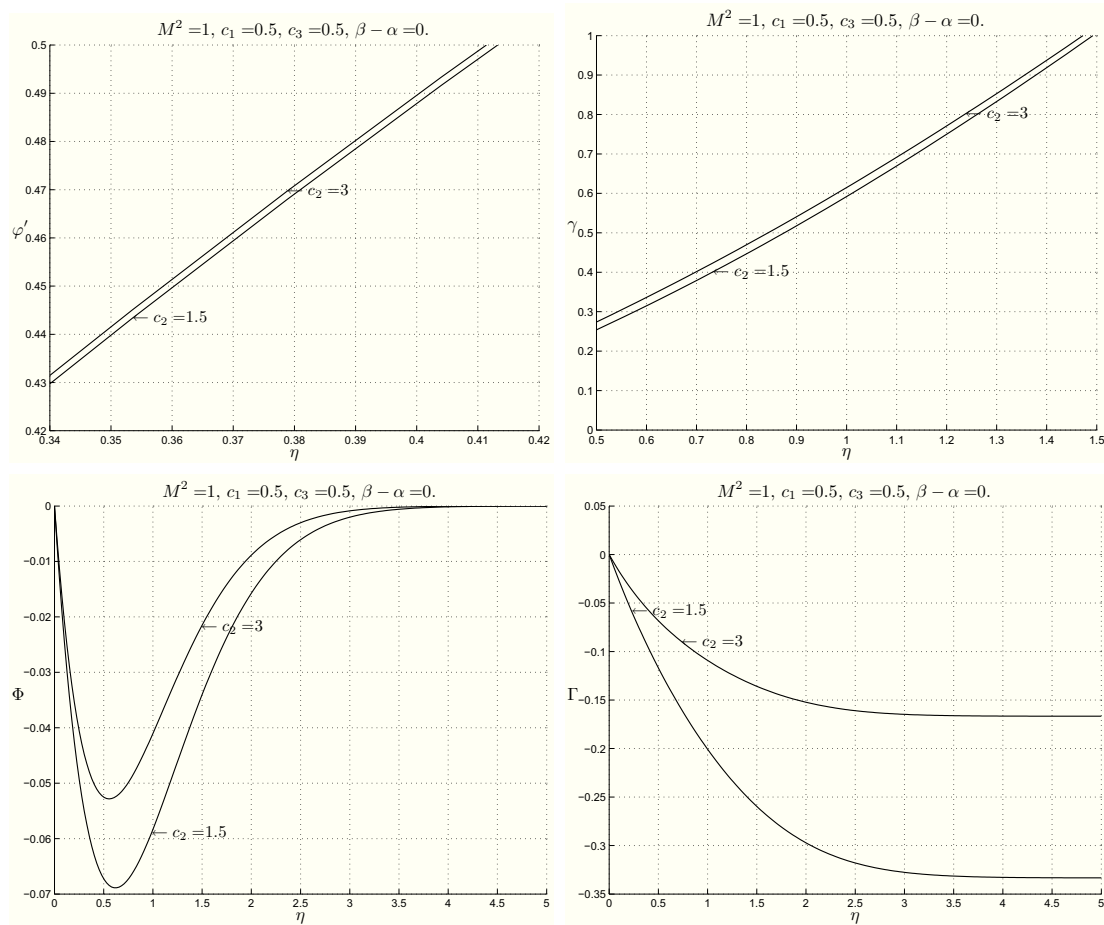


Figure 3.15: CASE III-M: plots showing the behaviour of  $\varphi'$ ,  $\gamma$ ,  $\Phi$  and  $\Gamma$  for  $c_1 = 0.5$ ,  $c_3 = 0.5$  fixed, and for different values of  $c_2$ .

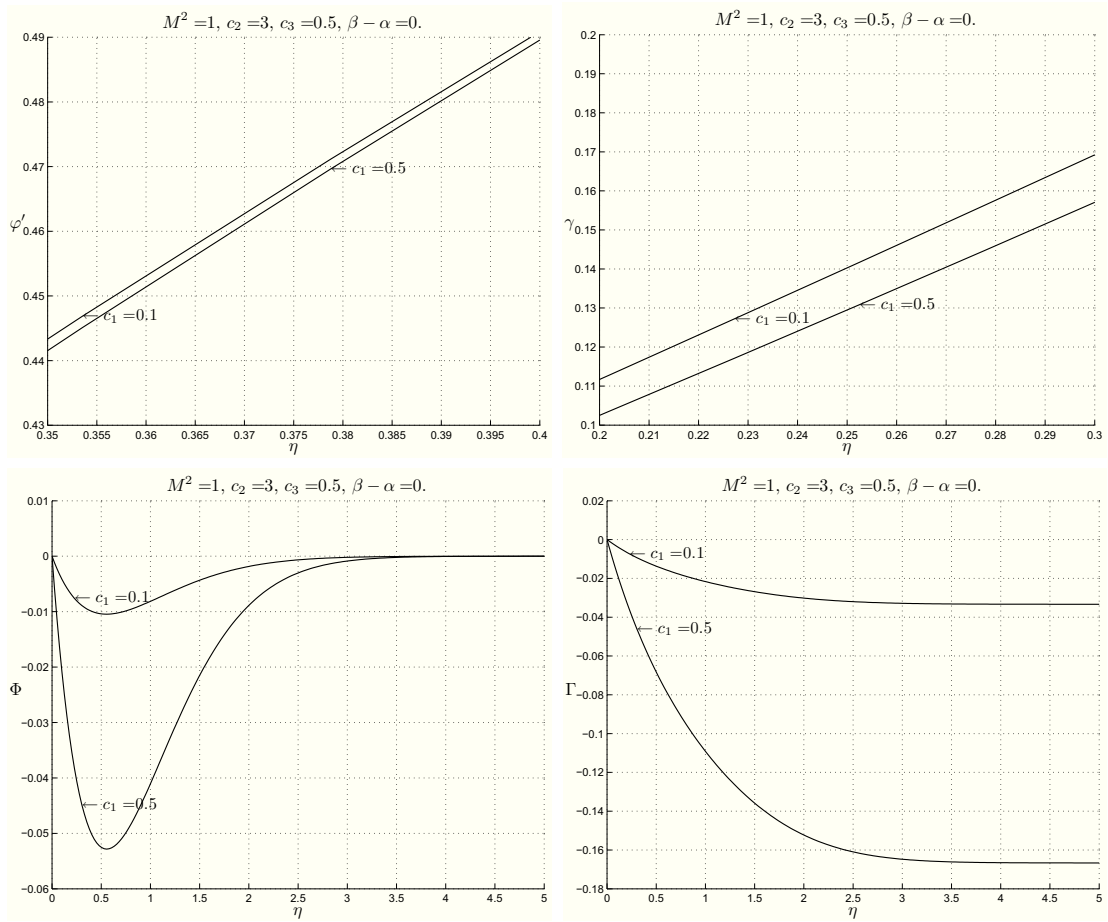


Figure 3.16: CASE III-M: plots showing the behaviour of  $\varphi'$ ,  $\gamma$ ,  $\Phi$  and  $\Gamma$  for  $c_2 = 3.0$ ,  $c_3 = 0.5$  fixed, and for different values of  $c_1$ .

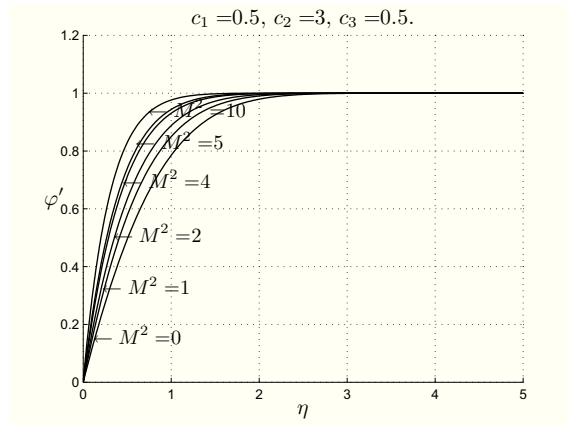


Figure 3.17: CASE III-M: plots showing  $\varphi'$  with  $c_1 = 0.5$ ,  $c_2 = 3.0$ ,  $c_3 = 0.5$  and for different  $M^2$ .

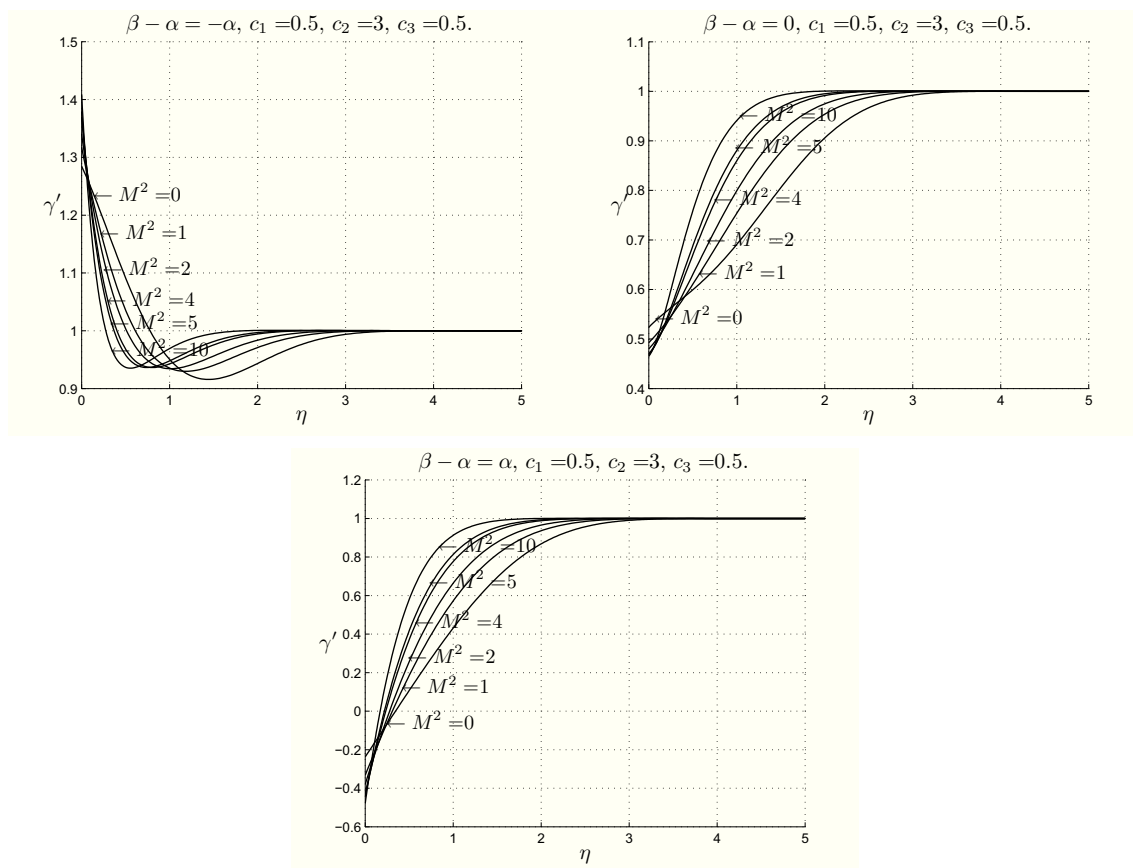


Figure 3.18: CASE III-M: plots showing  $\gamma'$  with  $c_1 = 0.5$ ,  $c_2 = 3.0$ ,  $c_3 = 0.5$  and for different  $M^2$ .

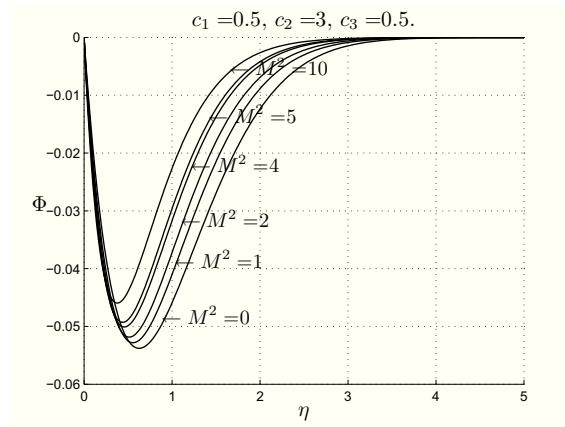


Figure 3.19: CASE III-M: plots showing  $\Phi$  with  $c_1 = 0.5, c_2 = 3.0, c_3 = 0.5$  and for different  $M^2$ .

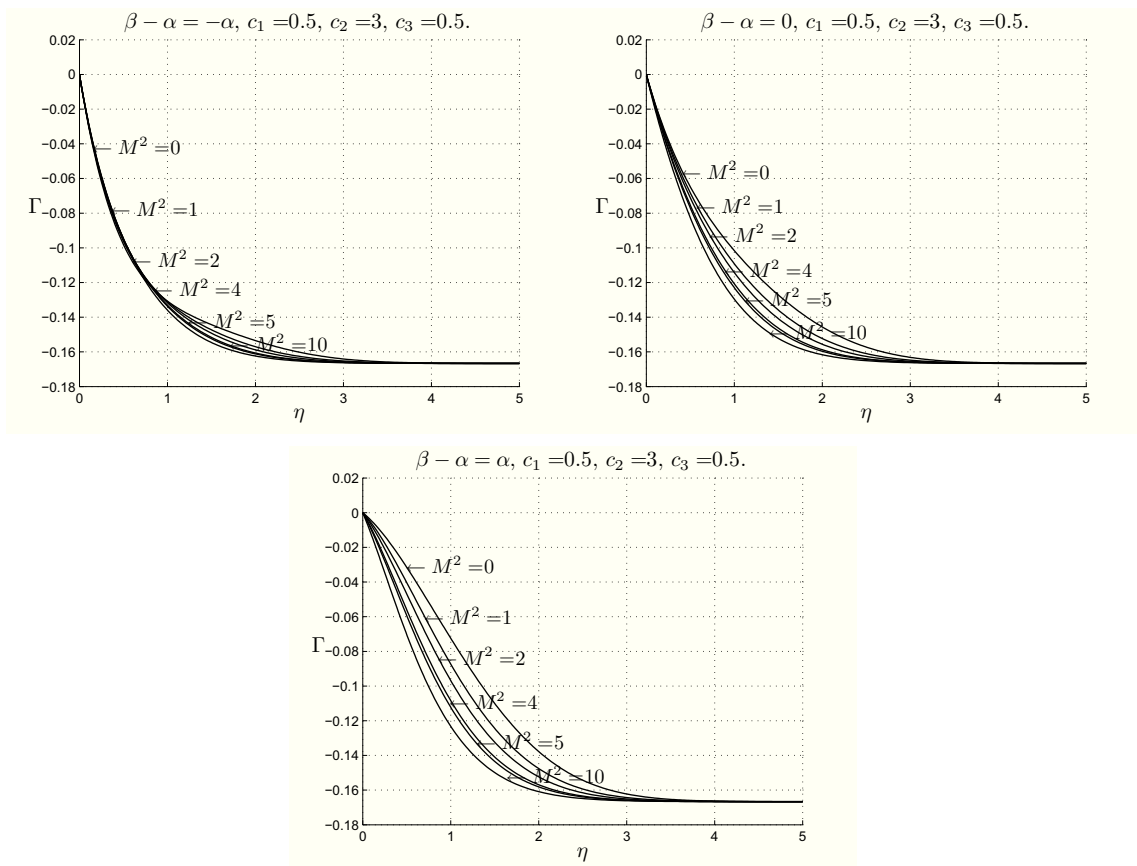


Figure 3.20: CASE III-M: plots showing  $\Gamma$  with  $c_1 = 0.5, c_2 = 3.0, c_3 = 0.5$  and for different  $M^2$ .

and  $c_1 = 0.5$ ,  $c_2 = 3.0$ ,  $c_3 = 0.5$ , because they have an analogous behaviour for  $M^2 \neq 1$  and different  $c_1$ ,  $c_2$ ,  $c_3$ .

As far as the boundary layer is concerned, in Tables 3.5 and 3.6, we list the values of  $\bar{\eta}_\varphi$ ,  $\bar{\eta}_\gamma$ ,  $\bar{\eta}_\Phi$ ,  $\bar{\eta}_\Gamma$ ,  $\delta_v$ ,  $\delta_w$  and  $\delta$  in dependence of  $M^2$ ,  $c_1$ ,  $c_2$ ,  $c_3$  and  $\beta - \alpha$ .

We see that  $\bar{\eta}_\gamma$  is always greater than  $\bar{\eta}_\varphi$ , so that the influence of the viscosity on the velocity appears only in a layer of thickness  $\bar{\eta}_\gamma$  lining the boundary, as in the Newtonian case, see Chapter 3.2.3.

Moreover,  $\bar{\eta}_\Gamma$  is almost greater than the corresponding value of  $\bar{\eta}_\Phi$ ; so the influence of the viscosity on the microrotation appears usually only in the region  $\eta < \bar{\eta}_\Gamma$ , as in Chapter 1.2.3. The influence of the viscosity on the microrotation appears only in a layer of thickness larger than in the orthogonal case.

The thickness  $\delta$  of the boundary layer depends on  $M^2$  and it decreases as  $M^2$  increases (as easily seen in Figures 3.17, 3.18, 3.19 and 3.20). This effect is normal in magnetohydrodynamics.

Finally, we notice that the points  $x_p, x_s$ , given by (1.54) and by (1.55), lie on the same side of the origin. Their location depends on  $M^2$ ,  $c_1$ ,  $c_2$ ,  $c_3$  and  $\beta - \alpha$ , as seen in Table 3.3. The Figure 3.21 shows these points in dimensionless form (i.e.  $\xi_p, \xi_s$ ) and the streamlines of the flow for  $\frac{b}{a} = 1$ ,  $c_1 = 0.5$ ,  $c_2 = 3.0$ ,  $c_3 = 0.5$ ,  $\beta - \alpha = -\alpha$ ,  $0$ ,  $\alpha$ , and  $M^2 = 1, 5$ .

Table 3.5: CASE III-M: descriptive quantities of the boundary layer for some values of  $c_1, c_2, c_3, M^2$ , and  $\beta - \alpha$ .

$M^2$	$c_1$	$c_2$	$c_3$	$\beta - \alpha$	$\bar{\eta}_\varphi$	$\bar{\eta}_\gamma$	$\bar{\eta}_\Phi$	$\bar{\eta}_\Gamma$	$\delta_v$	$\delta_w$	$\delta$		
1	0.1	1.5	0.1	-0.5386	2.0627	0.5810	1.4064	1.7360	2.0627	1.7360	2.0627		
				0	2.0627	2.7028	1.4064	2.0321	2.7028	2.0321	2.7028		
				0.5386	2.0627	2.7711	1.4064	2.2384	2.7711	2.2384	2.7711		
		0.5	3.0	0.1	-0.5388	2.0700	0.5814	1.1642	1.6481	2.0700	1.6481	2.0700	
					0	2.0700	2.7064	1.1642	1.8489	2.7064	1.8489	2.7064	
					0.5388	2.0700	2.7771	1.1642	1.9900	2.7771	1.9900	2.7771	
			3.0	0.1	-0.5392	2.0779	0.5889	0.8692	0.7235	2.0779	0.8692	2.0779	
					0	2.0779	2.7556	0.8692	1.1686	2.7556	1.1686	2.7556	
					0.5392	2.0779	2.8222	0.8692	1.4800	2.8222	1.4800	2.8222	
	0.5			1.5	0.1	-0.5392	2.0818	0.5889	0.7244	0.7421	2.0818	0.7421	2.0818
						0	2.0818	2.7585	0.7244	1.1410	2.7585	1.1410	2.7585
						0.5392	2.0818	2.8265	0.7244	1.4044	2.8265	1.4044	2.8265
		0.5		1.5	0.1	-0.5290	1.9039	0.5181	2.7106	2.9182	1.9039	2.9182	2.9182
						0	1.9039	2.3103	2.7106	3.1489	2.3103	3.1489	3.1489
						0.5290	1.9039	2.3947	2.7106	3.3157	2.3947	3.3157	3.3157
			0.5	3.0	0.1	-0.5298	1.9300	0.5203	2.2492	2.6084	1.9300	2.6084	2.6084
						0	1.9300	2.3044	2.2492	2.7263	2.3044	2.7263	2.7263
						0.5298	1.9300	2.3959	2.2492	2.8157	2.3959	2.8157	2.8157
	3.0			0.1	-0.5317	1.9678	0.5760	2.1525	1.9923	1.9678	2.1525	2.1525	
					0	1.9678	2.5481	2.1525	2.3343	2.5481	2.3343	2.5481	
					0.5317	1.9678	2.6102	2.1525	2.5300	2.6102	2.5300	2.6102	
		0.5		3.0	0.1	-0.5321	1.9846	0.5769	1.9384	1.9777	1.9846	1.9777	1.9846
						0	1.9846	2.5587	1.9384	2.2074	2.5587	2.2074	2.5587
						0.5321	1.9846	2.6264	1.9384	2.3459	2.6264	2.3459	2.6264
2			0.1	1.5	0.1	-0.4730	1.8770	0.4915	1.2744	1.6862	1.8770	1.6862	1.8770
						0	1.8770	2.4382	1.2744	1.9178	2.4382	1.9178	2.4382
						0.4730	1.8770	2.5110	1.2744	2.0918	2.5110	2.0918	2.5110
	0.5			3.0	0.1	-0.4731	1.8820	0.4918	1.0505	1.5808	1.8820	1.5808	1.8820
						0	1.8820	2.4393	1.0505	1.7391	2.4393	1.7391	2.4393
						0.4731	1.8820	2.5140	1.0505	1.8582	2.5140	1.8582	2.5140
		3.0		0.1	-0.4734	1.8886	0.4989	0.7769	0.7377	1.8886	0.7769	1.8886	
					0	1.8886	2.4861	0.7769	1.0808	2.4861	1.0808	2.4861	
					0.4734	1.8886	2.5566	0.7769	1.3360	2.5566	1.3360	2.5566	
			0.5	3.0	0.1	-0.4735	1.8915	0.4990	0.6341	0.7475	1.8915	0.7475	1.8915
						0	1.8915	2.4882	0.6341	1.0521	2.4882	1.0521	2.4882
						0.4735	1.8915	2.5597	0.6341	1.2693	2.5597	1.2693	2.5597
	0.5			1.5	0.1	-0.4656	1.7465	0.4299	2.5743	2.8562	1.7465	2.8562	2.8562
						0	1.7465	2.0911	2.5743	3.0453	2.0911	3.0453	3.0453
						0.4656	1.7465	2.1813	2.5743	3.1900	2.1813	3.1900	3.1900
		0.5		3.0	0.1	-0.4663	1.7638	0.4313	2.1257	2.5205	1.7638	2.5205	2.5205
						0	1.7638	2.0793	2.1257	2.6184	2.0793	2.6184	2.6184
						0.4663	1.7638	2.1746	2.1257	2.6958	2.1746	2.6958	2.6958
			3.0	0.1	-0.4676	1.7941	0.4809	2.0249	1.8890	1.7941	2.0249	2.0249	
					0	1.7941	2.2948	2.0249	2.1762	2.2948	2.1762	2.2948	
					0.4676	1.7941	2.3642	2.0249	2.3554	2.3642	2.3554	2.3642	
	0.5			3.0	0.1	-0.4679	1.8066	0.4820	1.8191	1.8574	1.8066	1.8574	1.8574
						0	1.8066	2.3020	1.8191	2.0550	2.3020	2.0550	2.3020
						0.4679	1.8066	2.3750	1.8191	2.1826	2.3750	2.1826	2.3750

Table 3.6: CASE III-M: continuum of 3.5.

$M^2$	$c_1$	$c_2$	$c_3$	$\beta - \alpha$	$\bar{\eta}_\varphi$	$\bar{\eta}_\gamma$	$\bar{\eta}_\Phi$	$\bar{\eta}_\Gamma$	$\delta_v$	$\delta_w$	$\delta$			
5	0.1	1.5	0.1	-0.3650	1.5294	0.3604	1.0258	1.6142	1.5294	1.6142	1.6142			
				0	1.5294	1.9550	1.0258	1.7548	1.9550	1.7548	1.9550			
					0.3650	1.5294	2.0297	1.0258	1.8721	2.0297	1.8721	2.0297		
				0.5	-0.3651	1.5312	0.3604	0.8363	1.4823	1.5312	1.4823	1.5312		
					0	1.5312	1.9524	0.8363	1.5789	1.9524	1.5789	1.9524		
					0.3651	1.5312	2.0277	0.8363	1.6591	2.0277	1.6591	2.0277		
			3.0	0.1	-0.3652	1.5351	0.3656	0.5850	0.7450	1.5351	0.7450	1.5351		
				0	1.5351	1.9895	0.5850	0.9525	1.9895	0.9525	1.9895			
				0.3652	1.5351	2.0615	0.5850	1.1202	2.0615	1.1202	2.0615			
				0.5	-0.3653	1.5364	0.3658	0.4383	0.7403	1.5364	0.7403	1.5364		
				0	1.5364	1.9902	0.4383	0.9222	1.9902	0.9222	1.9902			
				0.3653	1.5364	2.0625	0.4383	1.0660	2.0625	1.0660	2.0625			
		0.5	1.5	0.1	-0.3608	1.4479	0.3140	2.3183	2.7823	1.4479	2.7823	2.7823		
					0	1.4479	1.7025	2.3183	2.9032	1.7025	2.9032	2.9032		
					0.3608	1.4479	1.7920	2.3183	3.0045	1.7920	3.0045	3.0045		
					0.5	-0.3612	1.4534	0.3136	1.8993	2.3980	1.4534	2.3980	2.3980	
					0	1.4534	1.6857	1.8993	2.4611	1.6857	2.4611	2.4611		
					0.3612	1.4534	1.7772	1.8993	2.5151	1.7772	2.5151	2.5151		
				3.0	0.1	-0.3618	1.4709	0.3465	1.7933	1.7566	1.4709	1.7933	1.7933	
				0	1.4709	1.8368	1.7933	1.9451	1.8368	1.9451	1.9451			
				0.3618	1.4709	1.9122	1.7933	2.0820	1.9122	2.0820	2.0820			
				0.5	-0.3620	1.4765	0.3471	1.6050	1.6942	1.4765	1.6942	1.6942		
				0	1.4765	1.8379	1.6050	1.8276	1.8379	1.8276	1.8379			
				0.3620	1.4765	1.9147	1.6050	1.9256	1.9147	1.9256	1.9256			
10	0.1	1.5	0.1	-0.2825	1.2269	0.2715	0.7891	1.5668	1.2269	1.5668	1.5668			
				0	1.2269	1.5513	0.7891	1.6520	1.5513	1.6520	1.6520			
						0.2825	1.2269	1.6191	0.7891	1.7280	1.6191	1.7280	1.7280	
						0.5	-0.2826	1.2270	0.2713	0.6263	1.4155	1.2270	1.4155	1.4155
						0	1.2270	1.5477	0.6263	1.4738	1.5477	1.4738	1.5477	
						0.2826	1.2270	1.6156	0.6263	1.5255	1.6156	1.5255	1.6156	
					3.0	0.1	-0.2826	1.2290	0.2749	0.3948	0.7377	1.2290	0.7377	1.2290
					0	1.2290	1.5727	0.3948	0.8644	1.5727	0.8644	1.5727		
					0.2826	1.2290	1.6387	0.3948	0.9732	1.6387	0.9732	1.6387		
					0.5	-0.2826	1.2293	0.2749	0.3775	0.7226	1.2293	0.7226	1.2293	
					0	1.2293	1.5723	0.3775	0.8332	1.5723	0.8332	1.5723		
					0.2826	1.2293	1.6385	0.3775	0.9268	1.6385	0.9268	1.6385		
			0.5	1.5	0.1	-0.2802	1.1806	0.2400	2.0836	2.7449	1.1806	2.7449	2.7449	
				0	1.1806	1.3796	2.0836	2.8196	1.3796	2.8196	2.8196			
				0.2802	1.1806	1.4578	2.0836	2.8862	1.4578	2.8862	2.8862			
				0.5	-0.2804	1.1810	0.2392	1.6979	2.3221	1.1810	2.3221	2.3221		
				0	1.1810	1.3642	1.6979	2.3611	1.3642	2.3611	2.3611			
				0.2804	1.1810	1.4430	1.6979	2.3965	1.4430	2.3965	2.3965			
				3.0	0.1	-0.2807	1.1895	0.2594	1.5896	1.6805	1.1895	1.6805	1.6805	
				0	1.1895	1.4596	1.5896	1.7994	1.4596	1.7994	1.7994			
				0.2807	1.1895	1.5305	1.5896	1.8959	1.5305	1.8959	1.8959			
				0.5	-0.2808	1.1911	0.2597	1.4190	1.5945	1.1911	1.5945	1.5945		
				0	1.1911	1.4577	1.4190	1.6795	1.4577	1.6795	1.6795			
				0.2808	1.1911	1.5287	1.4190	1.7486	1.5287	1.7486	1.7486			

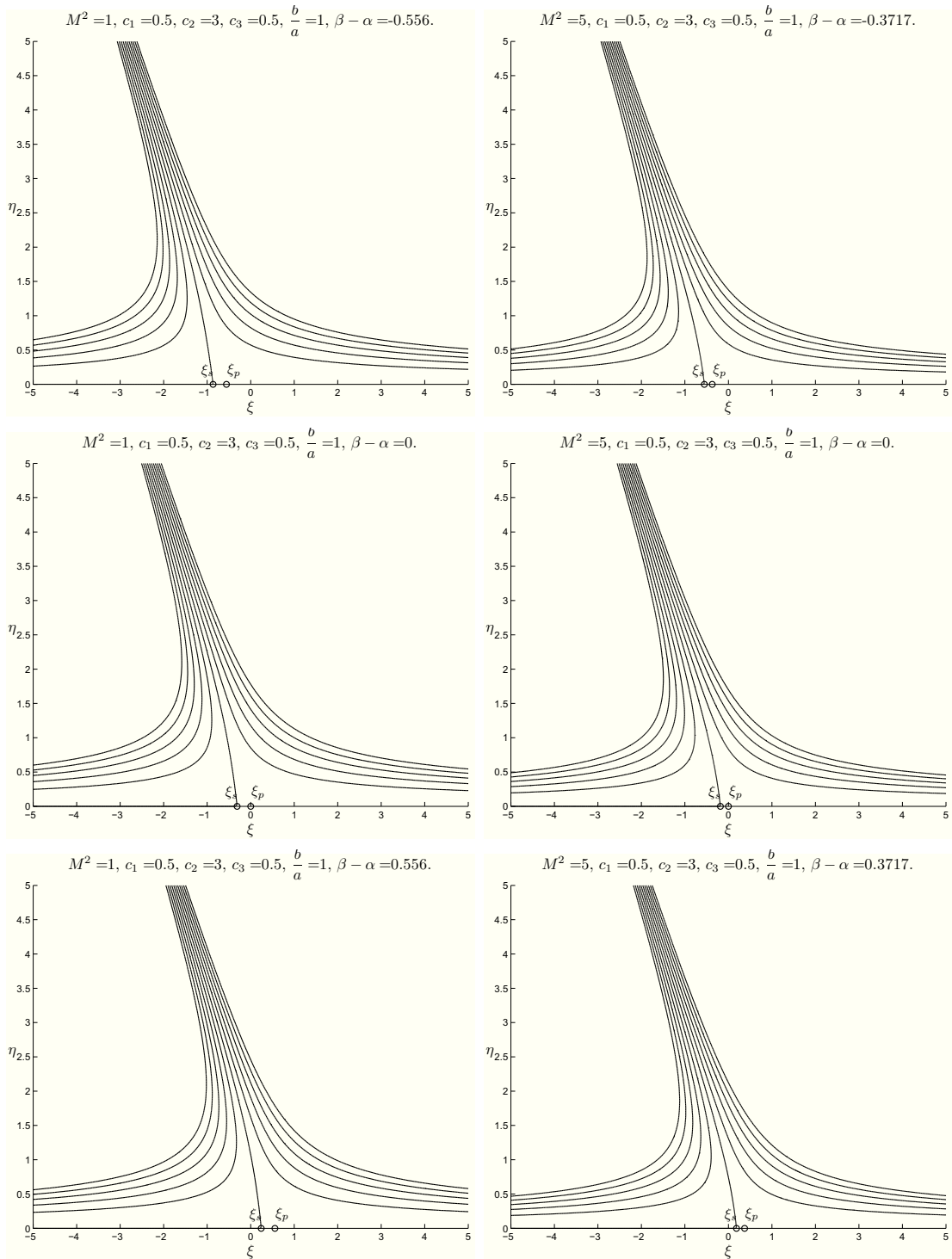


Figure 3.21: CASE III-M: figures 3.21<sub>1,3,5</sub> show the streamlines and the points  $\xi_p, \xi_s$  for  $\frac{b}{a} = 1, c_1 = 0.5, c_2 = 3.0, c_3 = 0.5$  and  $\beta - \alpha = -\alpha, 0, \alpha$ , respectively and  $M^2 = 1$ . Figures 3.21<sub>2,4,6</sub> for  $M^2 = 5$ .



# Chapter 4

## MHD three-dimensional stagnation-point flow

The aim of this chapter is to understand how the steady three-dimensional stagnation-point flow of a Newtonian or a micropolar fluid is influenced by an external uniform magnetic field  $\mathbf{H}_0$  when we neglect the induced magnetic field. The hypothesis of neglecting the induced magnetic field is customary in the literature and it is motivated by physical arguments when the magnetic Reynolds number is very small.

To this purpose we will recall how the three-dimensional stagnation-point flow is defined and we will start with the analysis of the same problem for an inviscid fluid.

The results obtained have been published or submitted for publication in [4], [7] and [8].

### 4.1 Inviscid Fluids

We begin with the study of the steady three-dimensional MHD stagnation-point flow of a homogeneous, incompressible, electrically conducting inviscid fluid near a stagnation point filling the half-space  $\mathcal{S}$ , given by (2.1).

In the three-dimensional stagnation-point flow we seek the velocity field as

$$v_1 = ax_1, \quad v_2 = -a(1+c)x_2, \quad v_3 = acx_3, \quad (x_1, x_3) \in \mathbb{R}^2, \quad x_2 \in \mathbb{R}^+, \quad (4.1)$$

where  $a, c$  are constants (Chapter 1.3.1). We suppose  $a > 0$ ,  $c \neq 0$  and  $c > -1$ .

Equations (2.2) govern such a flow in the absence of external mechanical body forces and free electric charges. To these equations we add boundary conditions (2.4), (2.5), (2.6).

We assume that a uniform external magnetic field  $\mathbf{H}_0$  is impressed and that the electric field is absent.

As it is customary in the literature, we assume that the magnetic Reynolds number is very small, so that the induced magnetic field is negligible in comparison to the imposed field. Then

$$(\nabla \times \mathbf{H}) \times \mathbf{H} \simeq \sigma_e \mu_e (\mathbf{v} \times \mathbf{H}_0) \times \mathbf{H}_0. \quad (4.2)$$

We proceed to prove the following:

**THEOREM 4.1.1.** *Let a homogeneous, incompressible, electrically conducting inviscid fluid occupy the half-space  $\mathcal{S}$ . If we impress an external magnetic field  $\mathbf{H}_0$ , and we neglect the induced magnetic field, then the steady three-dimensional MHD stagnation-point flow of such a fluid is possible for all  $c > -1$  if, and only if,  $\mathbf{H}_0$  is parallel to one of the axes.*

*Proof.* For the sake of brevity, we will denote by  $\mathbf{H}$  the external magnetic field:

$$\mathbf{H} = H_1 \mathbf{e}_1 + H_2 \mathbf{e}_2 + H_3 \mathbf{e}_3. \quad (4.3)$$

On substituting the approximation (4.2) into (2.2)<sub>1</sub>, taking into account that the velocity field  $\mathbf{v}$  is given by (4.1), we get:

$$\begin{aligned} \frac{\partial p}{\partial x_1} &= -\rho a^2 x_1 + \sigma_e a [c B_1 B_3 x_3 - (B_2^2 + B_3^2) x_1 - (1+c) B_1 B_2 x_2], \\ \frac{\partial p}{\partial x_2} &= -\rho a^2 (1+c)^2 x_2 + \sigma_e a [B_1 B_2 x_1 + (1+c)(B_1^2 + B_3^2) x_2 + c B_2 B_3 x_3], \\ \frac{\partial p}{\partial x_3} &= -\rho a^2 c^2 x_3 + \sigma_e a [-(1+c) B_2 B_3 x_2 - c(B_1^2 + B_2^2) x_3 + B_1 B_3 x_1], \end{aligned} \quad (4.4)$$

where  $\mathbf{B} = \mu_e \mathbf{H}$ .

It is possible to find a function  $p = p(x_1, x_2, x_3)$  satisfying (4.4) if, and only if,

$$\frac{\partial^2 p}{\partial x_i \partial x_j} = \frac{\partial^2 p}{\partial x_j \partial x_i}, \quad i, j = 1, 2, 3, \quad i \neq j. \quad (4.5)$$

On the other hand we have

$$\frac{\partial^2 p}{\partial x_1 \partial x_2} = -\sigma_e a (1+c) B_1 B_2, \quad \frac{\partial^2 p}{\partial x_2 \partial x_1} = \sigma_e a B_1 B_2, \quad (4.6)$$

$$\frac{\partial^2 p}{\partial x_1 \partial x_3} = \sigma_e a c B_1 B_3, \quad \frac{\partial^2 p}{\partial x_3 \partial x_1} = \sigma_e a B_1 B_3, \quad (4.7)$$

$$\frac{\partial^2 p}{\partial x_2 \partial x_3} = \sigma_e a c B_2 B_3, \quad \frac{\partial^2 p}{\partial x_3 \partial x_2} = -\sigma_e a (1+c) B_2 B_3. \quad (4.8)$$

Therefore, since  $c$  is arbitrary ( $> -1$ ), conditions (4.6), (4.7), (4.8) are satisfied if, and only if,  $\mathbf{B} = B\mathbf{e}_1$  or  $\mathbf{B} = B\mathbf{e}_2$  or  $\mathbf{B} = B\mathbf{e}_3$ .

Finally, if  $\mathbf{B} = B\mathbf{e}_1$ , then we deduce

$$p = -\rho \frac{a^2}{2} [x_1^2 + (1+c)^2 x_2^2 + c^2 x_3^2] + \frac{a}{2} \sigma_e B^2 [(1+c)x_2^2 - cx_3^2] + p_0; \quad (4.9)$$

if  $\mathbf{B} = B\mathbf{e}_2$ , then

$$p = -\rho \frac{a^2}{2} [x_1^2 + (1+c)^2 x_2^2 + c^2 x_3^2] - \frac{a}{2} \sigma_e B^2 [x_1^2 + cx_3^2] + p_0; \quad (4.10)$$

if  $\mathbf{B} = B\mathbf{e}_3$ , then

$$p = -\rho \frac{a^2}{2} [x_1^2 + (1+c)^2 x_2^2 + c^2 x_3^2] - \frac{a}{2} \sigma_e B^2 [x_1^2 - (1+c)x_2^2] + p_0. \quad (4.11)$$

□

REMARK 4.1.2. *The results obtained in Theorem 4.1.1 hold for any  $c > -1$ .*

*If  $c = 1$ , then it is possible to consider also the magnetic field parallel to the plane  $Ox_1x_3$ , as one can see from (4.7). In this case the pressure becomes*

$$p = -\rho \frac{a^2}{2} [x_1^2 + (1+c)^2 x_2^2 + c^2 x_3^2] + a\sigma_e (B_1^2 + B_3^2) x_2^2 - \frac{a}{2} \sigma_e (B_3 x_1 - B_1 x_3)^2 + p_0.$$

*Moreover, if  $c = -\frac{1}{2}$ , then from (4.8) we can also impress a magnetic field parallel to the plane  $Ox_2x_3$ . The corresponding pressure is*

$$p = -\rho \frac{a^2}{2} [x_1^2 + (1+c)^2 x_2^2 + c^2 x_3^2] - \frac{a}{2} \sigma_e (B_2^2 + B_3^2) x_1^2 + \frac{a}{4} \sigma_e (B_3 x_2 - B_2 x_3)^2 + p_0.$$

REMARK 4.1.3. *From (4.9), (4.10), (4.11), we notice that the pressure takes its maximum in the stagnation-point along the wall  $x_2 = 0$ , as in the absence of the external magnetic field.*

REMARK 4.1.4. *In order to study the three-dimensional stagnation-point flow for other models of fluids, it is convenient to consider a more general flow. As in Remark 1.3.3, let the inviscid fluid impinge on the flat plane  $x_2 = C$  and*

$$v_1 = ax_1, \quad v_2 = -a(1+c)(x_2 - C), \quad v_3 = acx_3, \quad (x_1, x_3) \in \mathbb{R}^2, \quad x_2 \geq C, \quad (4.12)$$

*with  $C$  some constant.*

*In this situation, the stagnation point is  $(0, C, 0)$  and in the cases of Theorem 4.1.1 and Remark 4.1.2 the pressure must be modified by replacing  $x_2$  with  $x_2 - C$ .*

## 4.2 Newtonian fluids

We now consider the steady three-dimensional MHD stagnation-point flow of a homogeneous, incompressible, electrically conducting Newtonian fluid occupying the half-space  $\mathcal{S}$ .

In the absence of external mechanical body forces and free electric charges, the MHD equations for such a fluid are (2.22). We prescribe conditions (2.23), (2.5), (2.6).

In this motion, the velocity components are (Chapter 1.3.2)

$$v_1 = ax_1 f'(x_2), \quad v_2 = -a[f(x_2) + cg(x_2)], \quad v_3 = acx_3 g'(x_2), \quad (4.13)$$

where  $f, g$  are sufficiently regular unknown functions ( $f, g \in C^3(\mathbb{R}^+)$ ).

The condition (2.23) is certainly satisfied if we ask :

$$f(0) = 0, \quad f'(0) = 0, \quad g(0) = 0, \quad g'(0) = 0. \quad (4.14)$$

We prescribe at infinity

$$\lim_{x_2 \rightarrow +\infty} f'(x_2) = 1, \quad \lim_{x_2 \rightarrow +\infty} g'(x_2) = 1, \quad (4.15)$$

so that the flow behaves like the three-dimensional stagnation-point flow of an inviscid fluid, whose velocity is given by (4.12).

The constant  $C$  in (4.12) is related to the behaviour of  $f$  and  $g$  at infinity: if

$$\lim_{x_2 \rightarrow +\infty} [f(x_2) - x_2] = -A, \quad \lim_{x_2 \rightarrow +\infty} [g(x_2) - x_2] = -B \quad (4.16)$$

with  $A, B$  some constants, then

$$\lim_{x_2 \rightarrow +\infty} [f(x_2) + cg(x_2) - (1+c)x_2] = -(1+c)C, \quad (4.17)$$

where

$$C = \frac{A + cB}{1 + c}.$$

The values of the constants  $A, B, C$  can be found by solving the problem.

In order to study the influence of a uniform external electromagnetic field, we continue to use the approximation (4.2), where  $\mathbf{v}$  is given by (4.13). As a result of the Theorem 4.1.1, we can prove the following:

**THEOREM 4.2.1.** *Let a homogeneous, incompressible, electrically conducting Newtonian fluid occupy the half-space  $\mathcal{S}$ . If we impress the external magnetic field  $\mathbf{H}_0$  parallel to one of the axes and if we neglect the induced magnetic field, then the steady three-dimensional MHD stagnation-point flow of such a fluid has the form (4.13),  $\mathbf{E} = \mathbf{0}$ , and*

(I-N) if  $\mathbf{H}_0 = H_0 \mathbf{e}_1$ , then  $(f, g)$  satisfies the problem

$$\begin{aligned} \frac{\nu}{a} f''' + (f + cg) f'' - f'^2 + 1 &= 0, \\ \frac{\nu}{a} g''' + (f + cg) g'' - cg'^2 + c + M^2(1 - g') &= 0, \end{aligned} \quad (4.18)$$

$$\begin{aligned} f(0) = 0, \quad f'(0) = 0, \quad g(0) = 0, \quad g'(0) = 0, \\ \lim_{x_2 \rightarrow +\infty} f'(x_2) = 1, \quad \lim_{x_2 \rightarrow +\infty} g'(x_2) = 1, \end{aligned} \quad (4.19)$$

where  $M^2 = \frac{\sigma_e \mu_e^2 H_0^2}{\rho a}$  is the Hartmann number and the pressure field is given by

$$\begin{aligned} p = -\rho \frac{a^2}{2} [x_1^2 + [f(x_2) + cg(x_2)]^2 + c^2 x_3^2] - \rho a \nu [f'(x_2) + cg'(x_2)] \\ - \sigma_e a B_0^2 \left[ \frac{c}{2} x_3^2 - \int_0^{x_2} (f(s) + cg(s)) ds \right] + p_0; \end{aligned} \quad (4.20)$$

(II-N) if  $\mathbf{H}_0 = H_0 \mathbf{e}_2$ , then  $(f, g)$  satisfies

$$\begin{aligned} \frac{\nu}{a} f''' + (f + cg) f'' - f'^2 + 1 + M^2(1 - f') &= 0, \\ \frac{\nu}{a} g''' + (f + cg) g'' - cg'^2 + c + M^2(1 - g') &= 0, \end{aligned} \quad (4.21)$$

with the boundary conditions (4.19) and the pressure field is given by

$$\begin{aligned} p = -\rho \frac{a^2}{2} [x_1^2 + [f(x_2) + cg(x_2)]^2 + c^2 x_3^2] - \rho a \nu [f'(x_2) + cg'(x_2)] \\ - \sigma_e a B_0^2 (x_1^2 + cx_3^2) + p_0; \end{aligned} \quad (4.22)$$

(III-N) if  $\mathbf{H}_0 = H_0 \mathbf{e}_3$ , then  $(f, g)$  satisfies

$$\begin{aligned} \frac{\nu}{a} f''' + (f + cg) f'' - f'^2 + 1 + M^2(1 - f') &= 0, \\ \frac{\nu}{a} g''' + (f + cg) g'' - cg'^2 + c &= 0, \end{aligned} \quad (4.23)$$

with the boundary conditions (4.19) and the pressure field is given by

$$\begin{aligned} p = -\rho \frac{a^2}{2} [x_1^2 + [f(x_2) + cg(x_2)]^2 + c^2 x_3^2] - \rho a \nu [f'(x_2) + cg'(x_2)] \\ - \sigma_e a B_0^2 \left[ \frac{x_1^2}{2} - \int_0^{x_2} (f(s) + cg(s)) ds \right] + p_0. \end{aligned} \quad (4.24)$$

*Proof.* Let us examine CASE I-N.

If

$$\mathbf{H}_0 = H_0 \mathbf{e}_1,$$

and the induced magnetic field is neglected, then we can make the following approximation

$$(\nabla \times \mathbf{H}) \times \mathbf{H} \simeq \sigma_e \mu_e a H_0^2 [(f + cg) \mathbf{e}_2 - cg' x_3 \mathbf{e}_3]. \quad (4.25)$$

We substitute (4.13), and (4.25) into (2.22)<sub>1</sub>, so that

$$\begin{aligned} ax_1 \left[ \nu f''' + af''(f + cg) - af'^2 \right] &= \frac{1}{\rho} \frac{\partial p}{\partial x_1}, \\ -\nu a(f'' + cg'') - a^2(f' + cg')(f + cg) + \frac{\sigma_e a}{\rho} B_0^2 (f + cg) &= \frac{1}{\rho} \frac{\partial p}{\partial x_2}, \\ acx_3 \left[ \nu g''' + ag''(f + cg) - acg'^2 - \frac{\sigma_e}{\rho} B_0^2 g' \right] &= \frac{1}{\rho} \frac{\partial p}{\partial x_3}. \end{aligned} \quad (4.26)$$

Then, by integrating (4.26)<sub>2</sub>, we find

$$\begin{aligned} p &= -\frac{1}{2} \rho a^2 [f(x_2) + cg(x_2)]^2 + \sigma_e a B_0^2 \int_0^{x_2} (f(s) + cg(s)) ds \\ &\quad - \rho a \nu [f'(x_2) + cg'(x_2)] + P(x_1, x_3), \end{aligned}$$

where the function  $P(x_1, x_3)$  is determined supposing that, far from the wall, the pressure  $p$  has the same behaviour as for an inviscid fluid, whose velocity is given by (4.12) and the pressure is given by (4.9) replacing  $x_2$  by  $x_2 - C$ .

Therefore, by virtue of (4.15), and (4.16), we get

$$P(x_1, x_3) = -\rho \frac{a^2}{2} (x_1^2 + c^2 x_3^2) - \frac{a}{2} \sigma_e B_0^2 c x_3^2 + p_0^*,$$

from which we find that the pressure field assumes the form

$$\begin{aligned} p &= -\rho \frac{a^2}{2} [x_1^2 + [f(x_2) + cg(x_2)]^2 + c^2 x_3^2] + \sigma_e a B_0^2 \left[ \int_0^{x_2} (f(s) + cg(s)) ds - \frac{c}{2} x_3^2 \right] \\ &\quad - \rho a \nu [f'(x_2) + cg'(x_2)] + p_0, \end{aligned} \quad (4.27)$$

where the constant  $p_0$  is the pressure at the origin.

In consideration of (4.26), we obtain the ordinary differential system

$$\begin{aligned} \frac{\nu}{a} f''' + (f + cg) f'' - f'^2 + 1 &= 0, \\ \frac{\nu}{a} g''' + (f + cg) g'' - cg'^2 + c + M^2(1 - g') &= 0, \end{aligned} \quad (4.28)$$

where

$$M^2 = \frac{\sigma_e B_0^2}{\rho a}$$

is the Hartmann number. To these equations we append the boundary conditions (4.14), and (4.15).

The rest of the proof for CASEs II-N and III-N runs as before.  $\square$

REMARK 4.2.2. *From (4.20), (4.22), (4.24) we see that the pressure takes again its maximum along the wall  $x_2 = 0$  in the stagnation-point.*

We now analyze the cases considered in Remark 4.1.2.

PROPOSITION 4.2.3. *Let a homogeneous, incompressible, electrically conducting Newtonian fluid occupy the half-space  $\mathcal{S}$ . If we neglect the induced magnetic field and we suppose either*

$$i) \quad c = 1, \quad \mathbf{H}_0 \text{ parallel to the plane } Ox_1x_3,$$

or

$$ii) \quad c = -\frac{1}{2}, \quad \mathbf{H}_0 \text{ parallel to the plane } Ox_2x_3,$$

then there is no solution to the problem of the steady three-dimensional MHD stagnation-point flow.

*Proof.* i) If  $c = 1$  and the external magnetic induction field is  $\mathbf{B} = B_1\mathbf{e}_1 + B_3\mathbf{e}_3$  ( $B_1, B_3 \neq 0$ ), then from equations (2.22), (4.13), proceeding as in proof of Theorem 4.2.1, after some calculations, we deduce:

$$\begin{aligned} \nu f''' + a(f+g)f'' - af'^2 + B_3^2 \frac{\sigma_e}{\rho}(1-f') + a &= 0, \\ \frac{\sigma_e a}{\rho} B_1 B_3 (g' - 1) &= 0, \\ \nu g''' + a(f+g)g'' - ag'^2 + B_1^2 \frac{\sigma_e}{\rho}(1-g') + a &= 0, \\ \frac{\sigma_e a}{\rho} B_1 B_3 (f' - 1) &= 0. \end{aligned} \tag{4.29}$$

From (4.29)<sub>2</sub>, (4.29)<sub>4</sub> one has  $f' = g' = 1$  for all  $x_2 \geq 0$ , which contradicts the boundary conditions (4.14).

ii) Then we examine the case  $c = -\frac{1}{2}$  and  $\mathbf{B} = B_2\mathbf{e}_2 + B_3\mathbf{e}_3$  ( $B_2, B_3 \neq 0$ ).

By proceeding as above, we obtain

$$\begin{aligned}\nu f'''' + a\left(f - \frac{g}{2}\right)f'' - af'^2 + (B_2^2 + B_3^2)\frac{\sigma_e}{\rho}(1 - f') + a &= 0, \\ \nu g'''' + a\left(f - \frac{g}{2}\right)g'' + \frac{a}{2}g'^2 + B_2^2\frac{\sigma_e}{\rho}(1 - g') - \frac{a}{2} &= 0, \\ \frac{\sigma_e a}{\rho}B_2B_3(f - g + A - B) &= 0.\end{aligned}\tag{4.30}$$

From (4.30)<sub>3</sub> evaluated at  $x_2 = 0$  and (4.14), we obtain  $f = g$ . So (4.30)<sub>1</sub>, (4.30)<sub>2</sub> become

$$\begin{aligned}\nu f'''' + a\frac{f}{2}f'' - af'^2 + (B_2^2 + B_3^2)\frac{\sigma_e}{\rho}(1 - f') + a &= 0, \\ \nu f'''' + a\frac{f}{2}f'' + \frac{a}{2}f'^2 + B_2^2\frac{\sigma_e}{\rho}(1 - f') - \frac{a}{2} &= 0.\end{aligned}\tag{4.31}$$

By subtracting (4.31)<sub>1</sub> from (4.31)<sub>2</sub>, we arrive at

$$(f' - 1)\left[\frac{3}{2}(f' + 1) + B_3^2\frac{\sigma_e}{a\rho}\right] = 0.\tag{4.32}$$

At  $x_2 = 0$ , (4.32) gives the absurdum

$$\frac{3}{2} + \frac{\sigma_e}{a\rho}B_3^2 = 0.$$

□

REMARK 4.2.4. *If  $c = 1$ ,  $f = g$ ,  $\mathbf{H}_0 = H_0\mathbf{e}_2$ , the axisymmetric case is obtained.*

Finally, with the dimensionless variables (1.35) we can rewrite equations (4.18) as

$$\begin{aligned}\varphi'''' + (\varphi + c\gamma)\varphi'' - \varphi'^2 + 1 &= 0, \\ \gamma'''' + (\varphi + c\gamma)\gamma'' - c\gamma'^2 + c + M^2(1 - \gamma') &= 0;\end{aligned}\tag{4.33}$$

equations (4.21) as

$$\begin{aligned}\varphi'''' + (\varphi + c\gamma)\varphi'' - \varphi'^2 + 1 + M^2(1 - \varphi') &= 0, \\ \gamma'''' + (\varphi + c\gamma)\gamma'' - c\gamma'^2 + c + M^2(1 - \gamma') &= 0;\end{aligned}\tag{4.34}$$

equations (4.23) as

$$\begin{aligned}\varphi''' + (\varphi + c\gamma)\varphi'' - \varphi'^2 + 1 + M^2(1 - \varphi') &= 0, \\ \gamma''' + (\varphi + c\gamma)\gamma'' - c\gamma'^2 + c &= 0.\end{aligned}\quad (4.35)$$

Of course we obtain three different ordinary differential problems by adding the boundary conditions (4.19) in dimensionless form:

$$\begin{aligned}\varphi(0) &= 0, \quad \varphi'(0) = 0, \\ \gamma(0) &= 0, \quad \gamma'(0) = 0, \\ \lim_{\eta \rightarrow +\infty} \varphi'(\eta) &= 1, \quad \lim_{\eta \rightarrow +\infty} \gamma'(\eta) = 1.\end{aligned}\quad (4.36)$$

In dimensionless form we also have

$$\alpha = \sqrt{\frac{a}{\nu}}A, \quad \beta = \sqrt{\frac{a}{\nu}}B, \quad h_d = \frac{\alpha + c\beta}{1 + c}.$$

REMARK 4.2.5. If  $M^2 = 0$ , then equations (4.33), (4.34), (4.35) reduce to

$$\begin{aligned}\varphi''' + (\varphi + c\gamma)\varphi'' - \varphi'^2 + 1 &= 0, \\ \gamma''' + (\varphi + c\gamma)\gamma'' - c\gamma'^2 + c &= 0\end{aligned}\quad (4.37)$$

which are the dimensionless equations governing the flow of a Newtonian fluid in the absence of  $\mathbf{H}_0$ . This problem has already been treated in Chapter 1.3.2.

We recall that in [13] under the hypothesis that  $\gamma$  is analytical it is proved that the problem (4.37), (4.36) does not admit solution for  $c < -1$ . As far as existence of solutions is concerned, we refer to [29], [30].

REMARK 4.2.6. If  $M^2 \neq 0$  and under the hypothesis that  $\gamma$  is analytical, in the next section we will prove that the problem (4.35), (4.36) does not admit solution for  $c < -1$  and that problems (4.33) and (4.34), together with boundary conditions (4.36), do not admit solution for  $c < -1$  and  $M^2 < -2c$ .

REMARK 4.2.7. It is physically interesting to determine the skin-friction components  $\tau_1, \tau_3$  along  $x_1$  and  $x_3$  axes :

$$\begin{aligned}\tau_1 &= \mu \left( \frac{\partial v_1}{\partial x_2} \right)_{x_2=0} = \rho(\nu)^{1/2} a^{3/2} x_1 \varphi''(0), \\ \tau_3 &= \mu \left( \frac{\partial v_3}{\partial x_2} \right)_{x_2=0} = c\rho(\nu)^{1/2} a^{3/2} x_3 \gamma''(0).\end{aligned}\quad (4.38)$$

Formally  $\tau_1, \tau_3$  have the same expression as in the absence of  $\mathbf{H}_0$ , but of course  $\varphi''(0), \gamma''(0)$  depend on  $\mathbf{H}_0$  through the Hartmann number  $M^2$ .

REMARK 4.2.8. *The regular solutions to problem (4.34), (4.36) are invariant under the following transformation*

$$\varphi\left(\eta, \frac{1}{c}, \frac{M^2}{c}\right) = \sqrt{c} \gamma\left(\frac{\eta}{\sqrt{c}}, c, M^2\right), \quad \gamma\left(\eta, \frac{1}{c}, \frac{M^2}{c}\right) = \sqrt{c} \varphi\left(\frac{\eta}{\sqrt{c}}, c, M^2\right), \quad c > 0,$$

so that we could confine our attention to  $c \in (-1, 1)$ ,  $c \neq 0$ .

We notice that by means of the previous transformation the regular solutions to problem (4.33), (or (4.35)), (4.36) are transformed in the solutions to problem (4.35), (or (4.33)), (4.36).

REMARK 4.2.9. *It is important to give the explicit form of the pressure field because, as we have already said in Remark 1.3.7, when a fluid moves past a body, if one of the components of the pressure gradient along a body surface has the same sign as the corresponding component of the velocity, then the reverse flow appears.*

As in the absence of the external magnetic field for the three-dimensional stagnation-point flow, the numerical results show that there exists a negative value  $c_r$  of  $c$  such that if  $c \geq c_r$ , then  $g', g'' > 0 \forall \eta > 0$ , and if  $c < c_r$  then near the wall  $g', g'' < 0$ , so that the reverse flow appears (i.e.  $v_3$  has the same sign as  $\frac{\partial p}{\partial x_3}$ ).

The reverse flow is also related to a sign change of the scalar component of the skin friction ( $\tau_0$ ) in the direction of  $\mathbf{e}_3$  (see (4.38)).

When an external magnetic field  $\mathbf{H}_0$  is impressed, as one can see from (4.20), (4.22), (4.24), the pressure field depends on  $\mathbf{H}_0$  through the Hartmann number  $M^2$ , which influences the sign of the components of the pressure gradient along the wall. For this reason, as we will see in the next numerical sections, the presence of the external magnetic field tends to prevent the occurrence of the reverse. This behaviour appears more clearly in CASEs I-II-N, and it has also been observed in [3] in other physical situations.

REMARK 4.2.10. *Of course, in all the three cases considered in Theorem 4.2.1 it is interesting to classify the origin as nodal or saddle point and as attachment or separation point. This classification can be done following the definitions given in Remark 1.3.8. From those considerations it is clear that we need to know the signs of  $c, \varphi''(0), \gamma''(0)$  in order to classify the stagnation-point. Yet now  $\varphi''(0), \gamma''(0)$  depend on  $M^2$ .*

In particular, we will see that in CASE I-N the origin can also become a separation point, differently from the other two cases. Hence in CASE I-N for some values of  $M^2 \geq 2.6662$ , we define

- $c_s$  the negative values of  $c$  such that if  $c < c_s$  then the origin is a separation point, while if  $c \geq c_s$  then it is an attachment point.

The change of the origin from attachment point to separation point can be explained by the form of system (4.33).

REMARK 4.2.11. As it happened in the absence of the external magnetic field (see Chapter 1.3.2), the numerical results point out that the three dimensional displacement thickness  $h_d$  can be negative, hence we denote by

- $c_h$  the negative values of  $c$  such that if  $c < c_h$ , then  $h_d < 0$  and if  $c \geq c_h$ , then  $h_d \geq 0$ .

REMARK 4.2.12. The solution  $(\varphi, \gamma)$  of the three problems here considered satisfies the conditions (4.36)<sub>5,6</sub> so that, as in Remark 1.3.9, we indicate with

- $\bar{\eta}_\varphi$  ( $\bar{\eta}_\gamma$ ) the value of  $\eta$  such that  $\varphi'(\bar{\eta}_\varphi) = 0.99$  ( $\gamma'(\bar{\eta}_\gamma) = 0.99$ ).

Hence if  $\eta > \bar{\eta}_\varphi$  ( $\eta > \bar{\eta}_\gamma$ ), then  $\varphi \cong \eta - \alpha$  ( $\gamma \cong \eta - \beta$ ).

The influence of the viscosity on the velocity appears only in a layer lining the boundary whose thickness is  $\delta = \max(\bar{\eta}_\varphi, \bar{\eta}_\gamma)$ .

### 4.2.1 A non existence result for $c < -1$ and $M^2 < 2|c|$ .

Consider the system (4.34) with boundary conditions (4.36) and suppose that  $\gamma$  is analytical. We want to prove that problem (4.34)-(4.36) doesn't admit solution when  $c < -1$  and  $M^2 < 2|c|$ . We have divided the proof into a sequence of lemmas and theorems.

LEMMA 4.2.13. If  $(\varphi, \gamma)$  is a solution of (4.34), (4.36), then  $\varphi''(0) \neq 0$  and  $\gamma''(0) \neq 0$ .

*Proof.* If for instance  $\gamma''(0) \neq 0$  then, by differentiating the second equation of (4.34), we get  $\gamma \equiv 0$ , which is clearly impossible for boundary condition (4.36)<sub>6</sub>. Same proof for  $\varphi$ .  $\square$

REMARK 4.2.14 (Parabolas for  $\varphi$ ). Assume that  $\varphi''(\eta_1) = 0$  at some point. Then, at that point, the second equation writes

$$y = x^2 + M^2x - (M^2 + 1),$$

for  $x = \varphi'(\eta_1)$  and  $y = \varphi'''(\eta_1)$ , which does not depend on  $c$ . All parabolas vanish at  $x_1 = 1$  and  $x_2 = -M^2 - 1 \leq -1$ ; if  $x = 0$  then  $y_0 = -M^2 - 1$ .

REMARK 4.2.15 (Parabolas for  $\gamma$ ). Assume that  $\gamma''(\eta_1) = 0$  at some point. Then, at that point, the second equation writes

$$y = cx^2 + M^2x - (M^2 + c),$$

for  $x = \gamma'(\eta_1)$  and  $y = \gamma'''(\eta_1)$ . Write

$$y = c(x-1) \left( x + \frac{M^2}{c} + 1 \right), \quad y = c \left[ \left( x + \frac{M^2}{2c} \right)^2 - \frac{1}{4c^2} (M^2 + 2c)^2 \right].$$

All parabolas vanish at  $x_1 = 1$  and  $x_3 = -\frac{M^2}{c} - 1$ ; if  $x = 0$  then  $y_0 = -M^2 - c$ .

- *Weak magnetic field:*  $M^2 < 2|c|$ . Then  $-1 \leq x_3 < 1 = x_1$ ,  $-|c| < y_0 \leq |c|$ . If  $M^2 = 0$ , then  $x_3 = -1$ ,  $y_0 = |c|$ .
- *Critical magnetic field:*  $M^2 = 2|c|$ . Then  $x_1 = x_3 = 1$ ,  $y_0 = c$ .
- *Strong magnetic field:*  $M^2 > 2|c|$ . Then  $x_1 = 1 < x_3$ ,  $y_0 < -|c|$ .

REMARK 4.2.16. The equations in (4.34) can be written as a dynamical system of three equations. The representation in the phase space is hard and then we interpret them as the following dynamical systems in two equations

$$\begin{aligned} \varphi'_1 &= \varphi_2, \\ \varphi'_2 &= (\varphi_1 - 1)(\varphi_1 + M^2 + 1) - (\varphi + c\gamma)\varphi_2, \end{aligned} \quad (4.39)$$

$$\begin{aligned} \gamma'_1 &= \gamma_2, \\ \gamma'_2 &= c(\gamma_1 - 1) \left( \gamma_1 + \frac{M^2}{c} + 1 \right) - (\varphi + c\gamma)\gamma_2, \end{aligned} \quad (4.40)$$

where  $\varphi$  and  $\gamma$  play the role of given functions satisfying the boundary conditions (4.36). The stationary points of (4.39) and (4.40) are, respectively,

$$(1, 0), \quad (-M^2 - 1, 0) \quad \text{and} \quad (1, 0), \quad \left( -\frac{M^2}{c} - 1, 0 \right).$$

LEMMA 4.2.17 (Critical points). For any  $c$ , if there exists  $\eta_1 > 0$ :

$$\begin{aligned} \varphi_1(\eta_1) = 1 \text{ or } \varphi_1(\eta_1) = -M^2 - 1 &\Rightarrow \varphi_2(\eta_1) \neq 0, \\ \gamma_1(\eta_1) = 1 \text{ or } \gamma_1(\eta_1) = -\frac{M^2}{c} - 1 &\Rightarrow \gamma_2(\eta_1) \neq 0. \end{aligned}$$

*Proof.* The stationary points of (4.40) provide constant solutions  $\gamma_1$  and  $\gamma_2$ . However, neither  $\gamma_1 = 1$  nor  $\gamma_1 = -\frac{M^2}{c} - 1$  satisfy both the initial and the infinity condition.

In the same manner we can prove the statement for  $\varphi$ . □

Now, we study the vector fields  $V_\varphi$  and  $V_\gamma$ . We have:

$$\begin{aligned} V_\varphi(0, \varphi_2) &= (\varphi_2, -M^2 - 1), & V_\gamma(0, \gamma_2) &= (\gamma_2, -M^2 - c), \\ V_\varphi(1, \varphi_2) &= (1, -s(\bar{\eta}))\varphi_2, & V_\gamma(1, \gamma_2) &= (1, -s(\bar{\eta}))\gamma_2, \end{aligned}$$

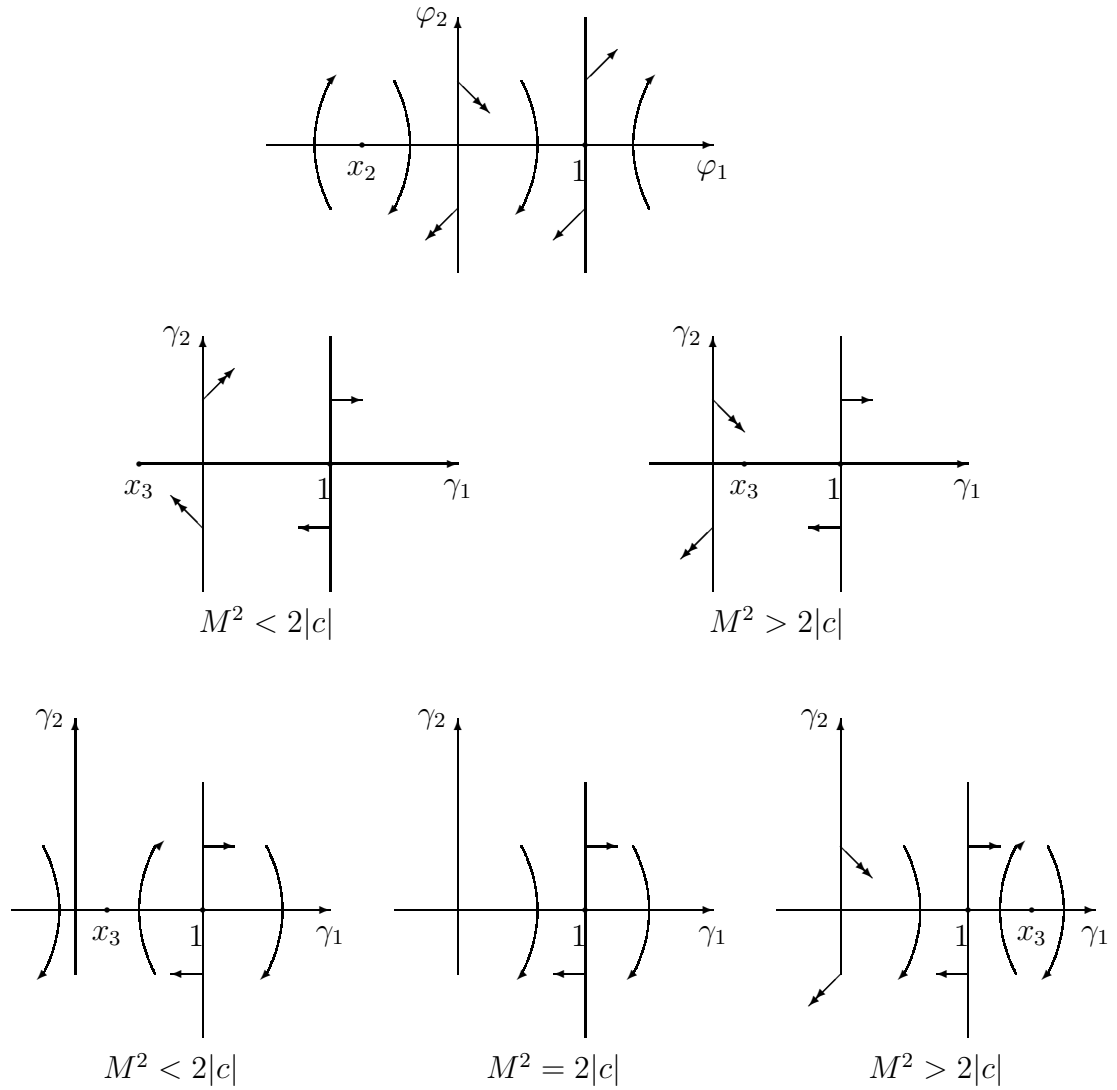


Figure 4.1: Vector fields and trajectories. Vectors with two arrows refer *only* to  $\eta = 0$  and, in general, *not* to other values of  $\eta$ ; however on the line  $\varphi_1 = 0$ , the field points to the right if  $\varphi_2$  or  $\gamma_2$  is positive and to the left otherwise.

where  $s = \varphi + c\gamma$  and  $\varphi_1(\bar{\eta}) = 1$  or  $\gamma_1(\bar{\eta}) = 1$ . They are depicted in Figure 4.1.

Here below *minimum point* means *local and strict minimum point* and analogously for the maximum point. By Lemma 4.2.13, if either  $\varphi_2(\eta_1) = 0$  or  $\gamma_2(\eta_1) = 0$  then  $\eta_1 > 0$ .

LEMMA 4.2.18 (Behaviour around stationary points). *Let  $c < 0$ . Assume that there exists  $\eta_1 > 0$  such that  $\varphi_2(\eta_1) = 0$ . Then*

$$\begin{aligned} \varphi_1(\eta_1) \in (-M^2 - 1, 1) &\Rightarrow \eta_1 \text{ is a maximum point for } \varphi_1, \\ \varphi_1(\eta_1) \notin (-M^2 - 1, 1) &\Rightarrow \eta_1 \text{ is a minimum point for } \varphi_1. \end{aligned}$$

On the other hand, assume that there exists  $\eta_1 > 0$  such that  $\gamma_2(\eta_1) = 0$ . Then

$$\begin{aligned} M^2 < 2|c| : \quad &\gamma_1(\eta_1) \in (x_2, 1) \Rightarrow \eta_1 \text{ is a minimum point for } \gamma_1, \\ &\gamma_1(\eta_1) \notin (x_2, 1) \Rightarrow \eta_1 \text{ is a maximum point for } \gamma_1, \\ M^2 = 2|c| : \quad &\eta_1 \text{ is a maximum point for } \gamma_1, \\ M^2 > 2|c| : \quad &\gamma_1(\eta_1) \in (1, x_2) \Rightarrow \eta_1 \text{ is a minimum point for } \gamma_1, \\ &\gamma_1(\eta_1) \notin (1, x_2) \Rightarrow \eta_1 \text{ is a maximum point for } \gamma_1. \end{aligned}$$

*Proof.* If  $\gamma_2(\eta_1) = 0$ , then the dynamical system (4.40) reduces to

$$\gamma_2'(\eta_1) = c\gamma_1^2(\eta_1) + M^2\gamma_1(\eta_1) - (M^2 + c).$$

The analysis of the sign of the parabolas allows to conclude. Note that we also have the direction of the trajectories, see Figure 4.1. Same proof for  $\varphi$ .  $\square$

We introduce the following notation for sets:

$$I_f = (-M^2 - 1, 1), \quad E_f = (-\infty, -M^2 - 1) \cup (1, +\infty),$$

and

$$I_g = \begin{cases} (x_3, 1) & \text{if } M^2 < 2|c|, \\ \emptyset & \text{if } M^2 = 2|c|, \\ (1, x_3) & \text{if } M^2 > 2|c|, \end{cases} \quad E_g = \begin{cases} (-\infty, x_3) \cup (1, +\infty) & \text{if } M^2 < 2|c|, \\ \mathbb{R} \setminus \{1\} & \text{if } M^2 = 2|c|, \\ (-\infty, 1) \cup (x_3, +\infty) & \text{if } M^2 > 2|c|, \end{cases}$$

COROLLARY 4.2.19. *Let  $c < 0$ . Assume that there exists  $\eta_0 \geq 0$  such that either  $\gamma_1(\eta) \in I_g$  for  $\eta > \eta_0$  or  $\gamma_1(\eta) \in E_g$  for  $\eta > \eta_0$ . Then  $\gamma_1$  has at most one stationary point in  $(\eta_0, +\infty)$ .*

*Same statement for  $\varphi$ .*

*Proof.* By Lemma 4.2.18, the functions  $\varphi$  and  $\gamma'$  cannot have two consecutive minima or maxima.  $\square$

Consider the case  $M^2 < 2|c|$ . In this case, it is sufficient to study only the system (4.40). We have two possibilities.

- For large  $\eta$  either  $\gamma_1(\eta) \in I$ , or  $\gamma_1(\eta) \in E$ .
- None of the two. In the latter case  $\gamma_1(\eta)$  assume the value  $x_2$  or 1 infinitely many times at points  $\eta_k$ , where  $\eta_k \rightarrow +\infty$  as  $k \rightarrow +\infty$ . The case with  $x_2$  is discarded because of the condition at infinity.

Let us examine the first case.

**THEOREM 4.2.20.** *Assume  $c < -1$  and  $M^2 < 2|c|$ . Assume also that either  $\gamma_1(\eta) \in I$  or  $\gamma_1(\eta) \in E$  for  $\eta$  large. Then, no solution  $\gamma$  exists.*

*Proof.* If there exists  $\eta_1$  large such that  $\gamma_2(\eta_1) = 0$ , then such point is unique and  $\eta_1$  is a minimum point for  $\gamma_1$  by Corollary 4.2.19. By the study of trajectories,  $\gamma_2(\eta) > 0$  for  $\eta > \eta_1$ . Then, by the second equation of (4.40),  $\gamma_2'(\eta) > 0$  for  $\eta > \eta_1$ , which contradicts the condition at infinity: for  $\eta \rightarrow +\infty$ , either  $\gamma_2$  has no limit or it tends to 0.

If  $\gamma_2$  never vanishes, then, from the first equation of (4.40), either  $\gamma_1$  increases or decreases; the second possibility cannot happen since  $\gamma_1 < 1$ . Then  $\gamma_2 > 0$ . The argument above works as well.

The case  $\gamma'(\eta) \in E$  works in the same way. In the second approach, the proof is as follows. If there exists  $\eta_1 > 0$  such that  $\gamma_2(\eta_1) = 0$ , then such point is unique and  $\eta_1$  is a maximum point for  $\gamma_1$  by Corollary 4.2.19. By the study of trajectories,  $\gamma_2(\eta) < 0$  for  $\eta > \eta_1$ . Then, by the second equation of (4.40),  $\gamma_2'(\eta) < 0$  for  $\eta > \eta_1$ , because the sign of  $(\gamma_1 - 1)(\gamma_1 + \frac{M^2}{c} + 1)$  is positive for  $\gamma_1 \in E$ . This contradicts the condition at infinity.

Assume now that  $\gamma_2$  never vanishes. The possibility  $\gamma_1 < x_2$  cannot happen, since otherwise  $\gamma_1$  must enter the region where  $\gamma_1 \in I$  to reach the point 1. Then we must have  $\gamma_1 > 1$ ; as a consequence, by the first equation in (4.40),  $\gamma_1$  must decrease, then  $\gamma_2 < 0$ . The argument above works as well. □

Now, we consider the second case.

**LEMMA 4.2.21.** *Let  $c < -1$  and  $M^2 < 2|c|$ . Assume that there is a sequence  $\{\eta_i\}$  with  $\eta_i < \eta_{i+1}$  and  $\lim_{i \rightarrow +\infty} \eta_i = +\infty$  such that  $\gamma_2(\eta_i) = 0$ . Then the sequence  $\{\gamma_1(\eta_i)\}$  cannot tend to 1 as  $i \rightarrow +\infty$ .*

*Proof.* Multiply the second equation in (4.40) by  $\gamma_2$  and integrate from  $\eta_i$  to  $\eta_{i+1}$ . Then

$$\frac{1}{3}\gamma_1^3 + \frac{M^2}{2c}\gamma_1^2 - \left(\frac{M^2}{c} + 1\right)\gamma_1 \Big|_{\eta_{i+1}} > \frac{1}{3}\gamma_1^3 + \frac{M^2}{2c}\gamma_1^2 - \left(\frac{M^2}{c} + 1\right)\gamma_1 \Big|_{\eta_i} \quad (4.41)$$

Introduce the cubic function

$$K(\gamma_1) = \frac{1}{3}\gamma_1^3 + \frac{M^2}{2c}\gamma_1^2 - \left(\frac{M^2}{c} + 1\right)\gamma_1,$$

which is easily seen to have a maximum point at  $x_2 = -\frac{M^2}{c} - 1$  and a minimum point at  $x_1 = 1$ . The sequence of values  $\{K(\gamma_1(\eta_i))\}$  is increasing by (4.41). Since  $\gamma_1 = 1$  is a minimum point for  $K$ , the sequence  $\{\gamma_1(\eta_i)\}$  cannot tend to 1 as  $i \rightarrow +\infty$ .  $\square$

**THEOREM 4.2.22.** *Assume  $c < -1$  and  $M^2 < 2|c|$ . Suppose that neither  $\gamma'(\eta) \in I$  nor  $\gamma'(\eta) \in E$  for  $\eta$  large. Then, no solution  $\gamma$  exists.*

*Proof.* Since we need that  $\gamma_1(\eta) \rightarrow 1$  for  $\eta \rightarrow +\infty$ , then by continuity  $\gamma_1$  must assume the value 1 infinitely many times. Further, it cannot assume identically the value 1 for  $\eta$  large. Then there is a sequence  $\{\eta_i\}$  with  $\eta_i < \eta_{i+1}$  and  $\lim_{i \rightarrow +\infty} \eta_i = +\infty$  such that  $\gamma_2(\eta_i) = 0$ . By Lemma 4.2.21 we reach a contradiction.  $\square$

Therefore, in the case of a weak magnetic field, no orbits with the required properties exist.

**REMARK 4.2.23.** *Since this proof doesn't involve equations (4.39), problem (4.33), (4.36) also doesn't admit solution for  $c < -1$  and  $M^2 < 2|c|$ , when  $\gamma$  is analytical.*

*The non-existence of the solution of problem (4.35), (4.36) can be clearly obtained for  $c < -1$  and any  $M^2$  following [13], because equation (4.35)<sub>2</sub> is the same equation taken into account by the Author.*

We now turn to the numerical integration of the three problems of Theorem 4.2.1, separately. The values of  $c$  are taken according to [13], [36] and Chapter 1.3, while  $M^2$  is chosen as in Chapters 2 and 3.

#### 4.2.2 CASE I-N: $\mathbf{H}_0 = H_0 \mathbf{e}_1$ .

We have solved problem (4.33), (4.36) numerically using the `bvp4c` MATLAB routine.

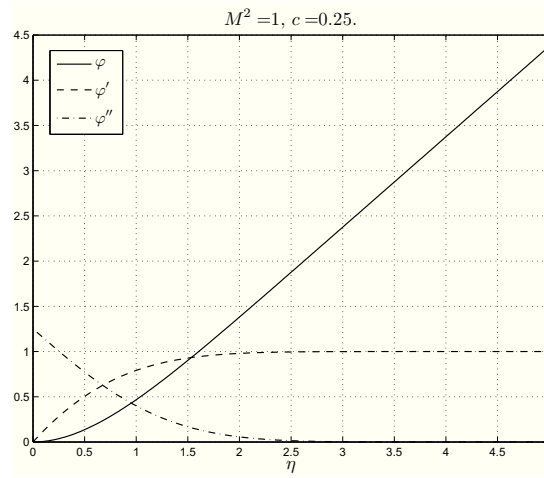
Figure 4.2 shows the graphics of  $\varphi, \varphi', \varphi''$  for  $M^2 = 1$ , and  $c = 0.25$ .

As one can see,

$$\lim_{\eta \rightarrow +\infty} \varphi''(\eta) = 0, \quad \lim_{\eta \rightarrow +\infty} \varphi'(\eta) = 1.$$

The numerical values of the descriptive quantities of motion when  $M^2$  and  $c$  change are shown in Table 4.1.

Our results are consistent with the previous studies when  $M^2 = 0$  ([13], [36]). In particular, when  $M^2 = 0$  and  $c = 1$  we obtain the axisymmetric flow:  $\alpha = \beta = h_d$

Figure 4.2: CASE I-N:  $\varphi$ ,  $\varphi'$ ,  $\varphi''$  profile for  $M^2 = 1$  and  $c = 0.25$ .Table 4.1: CASE I-N: descriptive quantities of motion for some values of  $c$  and  $M^2$ .

$M^2$	$c$	$\varphi''(0)$	$\gamma''(0)$	$h_d$	$\alpha$	$\beta$	$\bar{\eta}_\varphi$	$\bar{\eta}_\gamma$	$\delta$
1	-0.75	1.2051	0.4660	-1.8314	0.6897	1.5300	2.7009	4.4766	4.4766
	-0.25	1.2166	0.9234	0.6001	0.6692	0.8768	2.5219	3.0639	3.0639
	0.25	1.2521	1.2537	0.6300	0.6253	0.6487	2.2449	2.3264	2.3264
	1.00	1.3216	1.6383	0.5288	0.5627	0.4950	1.9227	1.7971	1.9227
2	-0.75	1.1823	1.0354	0.0149	0.7231	0.9592	2.9236	3.9003	3.9003
	-0.25	1.2123	1.3401	0.6732	0.6741	0.6769	2.5466	2.6438	2.6438
	0.25	1.2550	1.5927	0.6080	0.6229	0.5485	2.2347	2.1021	2.2347
	1.00	1.3288	1.9133	0.5012	0.5582	0.4442	1.9076	1.6801	1.9076
4	-0.75	1.1608	1.7342	1.2399	0.7547	0.5930	3.1184	2.7003	3.1184
	-0.25	1.2072	1.9369	0.7403	0.6795	0.4970	2.5713	2.1121	2.5713
	0.25	1.2588	2.1217	0.5832	0.6198	0.4366	2.2229	1.7909	2.2229
	1.00	1.3393	2.3732	0.4645	0.5521	0.3769	1.8871	1.5014	1.8871
5	-0.75	1.1543	1.9982	1.5127	0.7639	0.5143	3.1703	2.3676	3.1703
	-0.25	1.2055	2.1771	0.7593	0.6812	0.4470	2.5788	1.9361	2.5788
	0.25	1.2602	2.3433	0.5752	0.6188	0.4011	2.2191	1.6772	2.2191
	1.00	1.3434	2.5735	0.4514	0.5498	0.3530	1.8797	1.4309	1.8797
10	-0.75	1.1355	2.9930	2.1349	0.7892	0.3407	3.3014	1.5866	3.3014
	-0.25	1.2002	3.1160	0.8090	0.6863	0.3182	2.5994	1.4312	2.5994
	0.25	1.2647	3.2346	0.5524	0.6155	0.2999	2.2076	1.3140	2.2076
	1.00	1.3578	3.4051	0.4099	0.5421	0.2777	1.8559	1.1825	1.8559

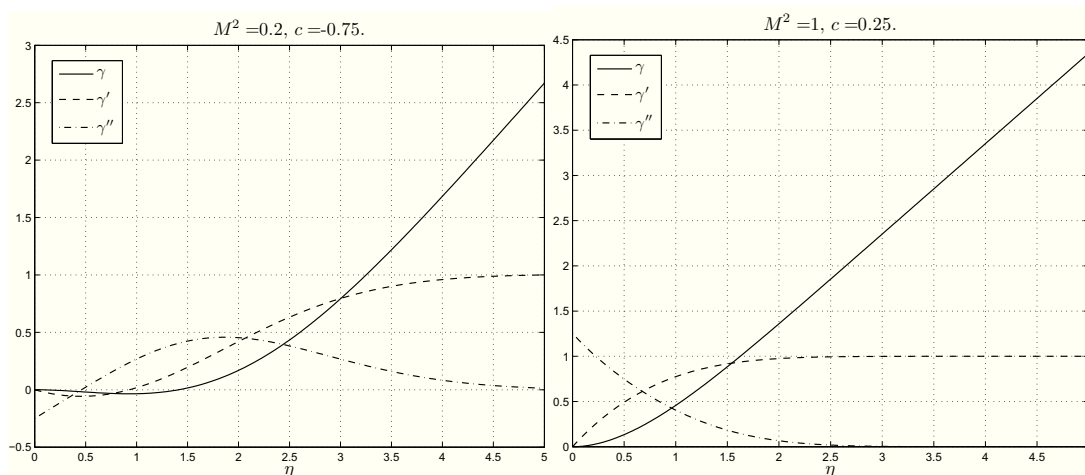


Figure 4.3: CASE I-N: the first picture shows the profiles of  $\gamma$ ,  $\gamma'$ ,  $\gamma''$  in the reverse flow ( $M^2 = 0.2$ ,  $c = -0.75$ ). The second picture shows the profile of  $\gamma$  in the absence of the reverse flow ( $M^2 = 1$ ,  $c = 0.25$ ).

and  $\varphi''(0) = g''(0)$ . We notice that there are no results in the literature if  $M^2 \neq 0$  ([7]).

As far as the behaviour of  $\gamma, \gamma', \gamma''$  is concerned, if  $c < c_r$  then the behaviour of  $\gamma, \gamma', \gamma''$  is shown in Figure 4.3<sub>1</sub>, otherwise it is given in Figure 4.3<sub>2</sub>. We underline that in the first Figure there is a zone where the reverse flow appears. The values of  $c_r$  in dependence on  $M^2$  are given in Table 4.2.

Table 4.1 shows that if  $M^2$  is fixed, then, when  $c$  increases, the values of  $\varphi''(0)$ ,  $\gamma''(0)$  increase, while the values of  $\alpha$ ,  $\beta$ ,  $\bar{\eta}_\varphi$ ,  $\bar{\eta}_\gamma$  decrease. Hence the thickness of the boundary layer decreases when  $c$  increases.

In Table 4.1, we can also see the values of the descriptive quantities of the motion when  $M^2$  increases:

- $\varphi''(0)$ ,  $\gamma''(0)$  and  $\bar{\eta}_\varphi$  increase;
- $\alpha$ ,  $\beta$  and  $\bar{\eta}_\gamma$  decrease.

The thickness  $\delta$  of the boundary layer also depends on  $M^2$  and decreases when  $M^2$  increases (as easily seen in Figures 4.4).

Table 4.2 underlines that as the Hartmann number  $M^2$  increases, the value of  $c_r$  for which the reverse flow does not occur (i.e. when  $\gamma''(0) = 0$ ) decreases and when  $M^2 = 0.8123$ , the reverse flow does not occur at all for any value of  $c$ . Actually, the magnetic field prevents the occurrence of the reverse flow. This fact can be explained by observing that

$$\frac{\partial p}{\partial x_3} = -\rho a^2 c x_3 (c + M^2),$$

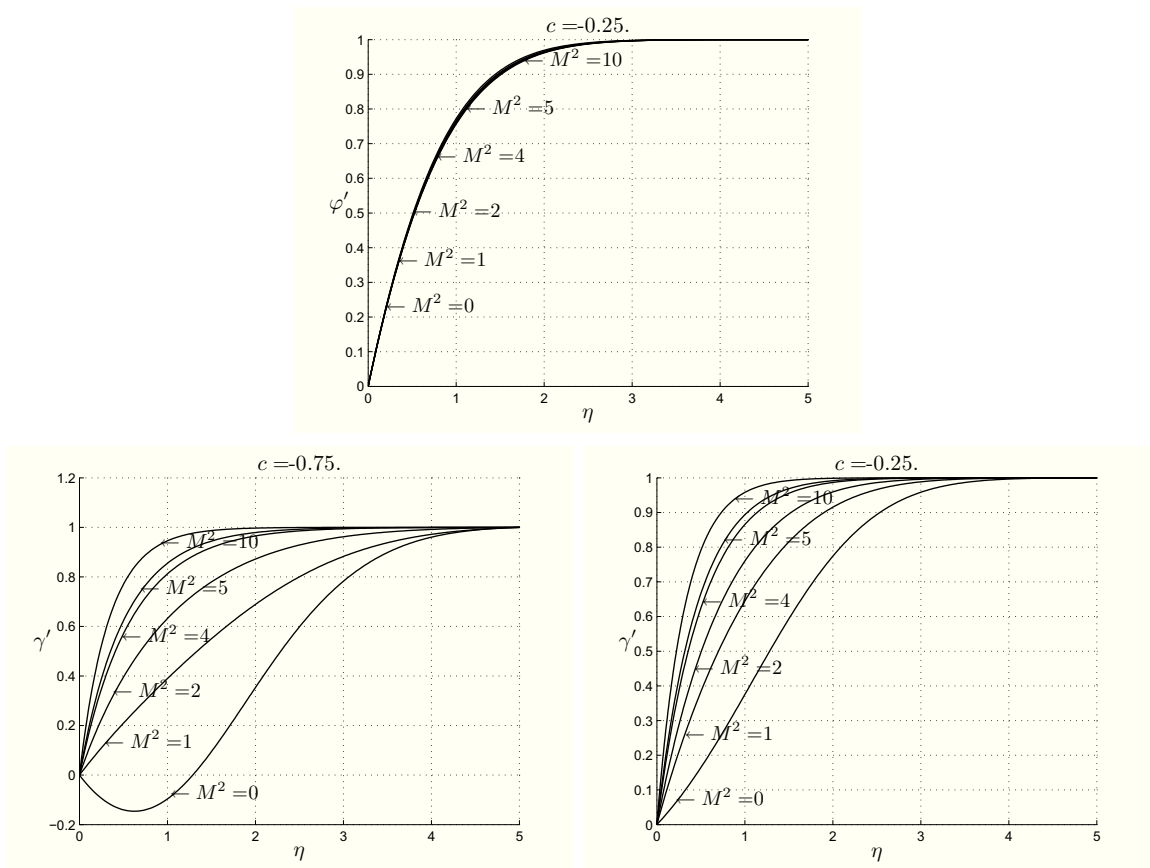


Figure 4.4: CASE I-N: profiles of  $\varphi'$  (Figure 4.4<sub>1</sub>) and  $\gamma'$  (Figure 4.4<sub>2,3</sub>) for several values of  $M^2$ .

Table 4.2: CASE I-N: values of  $c_r$  and  $c_h$  when  $M^2$  increases.

$M^2$	$c_r$	$c_h$
0	-0.4294	-0.3919
0.10	-0.4991	-0.4097
0.20	-0.5691	-0.4274
0.30	-0.6393	-0.4452
0.40	-0.7097	-0.4630
0.50	-0.7802	-0.4808
0.60	-0.8507	-0.4986
0.70	-0.9210	-0.5164
0.80	-0.9913	-0.5343
0.8122	-0.9999	-0.5364
0.8123	no reverse flow	-0.5365
3.3306	no reverse flow	$h = 0$

from which one can see that the signs of  $c$  and of  $(c + M^2)$  modify the sign of  $\frac{\partial p}{\partial x_3}$ .

From Table 4.1 we find that the value of  $h_d$ , which is the height of the plane towards which the inviscid fluid moves, regardless of the value of  $M^2$ , increases if  $c < 0$ , while it decreases if  $c > 0$ . Moreover,  $c_h \geq c_r$ , which means that the three-dimensional displacement thickness is always negative when the reverse flow appears (see Table 4.2). The presence of  $M^2$  influences  $c_h$  and it decreases when  $M^2$  increases and starting from  $M^2 = 3.3306$  we have that  $h_d$  is always positive.

As far as the classification of the stagnation-point is concerned, we have found a very interesting new result: for negative values of  $c$  when  $M^2 \geq 2.6662$ , the origin becomes a point of separation, unlike what occurs in the absence of the magnetic field or in the next two cases, as we will see.

We note that if  $M^2 < 2.6662$ , then the stagnation-point is always a point of attachment. If  $c > 0$  or where there is the reverse flow, the origin is a nodal point, while when  $c < 0$  and the reverse flow does not appear, it is a saddle point (as we can see from Table 4.3).

In Table 4.4, for some values of  $M^2 \geq 2.6662$ , we list the negative value of  $c$  ( $c_s$ ), for which if  $c < c_s$  then the origin is a separation point, while if  $c \geq c_s$  then it is an attachment point. The change of the origin from attachment point to separation point can be explained by the form of system (4.33). Since  $M^2$  directly influences  $\gamma$  and only indirectly influences  $\varphi$ , when  $M^2$  increases,  $\gamma''(0)$  becomes much greater than  $\varphi''(0)$  as we can see from Tables 4.2 and 4.3.

In order to summarize the classification of the stagnation-point in dependence on  $M^2$  and  $c$ , we provide Figure 4.5.

Table 4.3: CASE I-N: values of  $\varphi''(0) + c\gamma''(0)$  and  $c\varphi''(0)\gamma''(0)$  for several values of  $c$ ,  $M^2$ .

$M^2$	$c$	$\varphi''(0)$	$\gamma''(0)$	$\varphi''(0) + c\gamma''(0)$	$c\varphi''(0)\gamma''(0)$
1	-0.90	1.2097	0.2987	0.9409	-0.3252
	-0.75	1.2051	0.4660	0.8556	-0.4212
	-0.50	1.2064	0.7166	0.8481	-0.4322
	-0.40	1.2096	0.8039	0.8880	-0.3890
	-0.10	1.2257	1.0319	1.1225	-0.1265
10	-0.90	1.1165	2.9552	-1.5431	-2.9696
	-0.75	1.1355	2.9930	-1.1093	-2.5488
	-0.50	1.1676	3.0550	-0.3599	-1.7836
	-0.40	1.1806	3.0795	-0.0512	-1.4543
	-0.10	1.2196	3.1520	0.9044	-0.3844
30	-0.90	1.0857	5.3570	-3.7355	-5.2347
	-0.75	1.1101	5.3780	-2.9234	-4.4777
	-0.50	1.1513	5.4129	-1.5552	-3.1158
	-0.40	1.1677	5.4268	-1.0030	-2.5348
	-0.10	1.2166	5.4682	0.6698	-0.6653

Table 4.4: CASE I-N: values of  $c_s$  when  $M^2$  increases (separation point - attachment point).

$M^2$	$c_s$
4	-0.6593
5	-0.5677
10	-0.3836
15	-0.3110

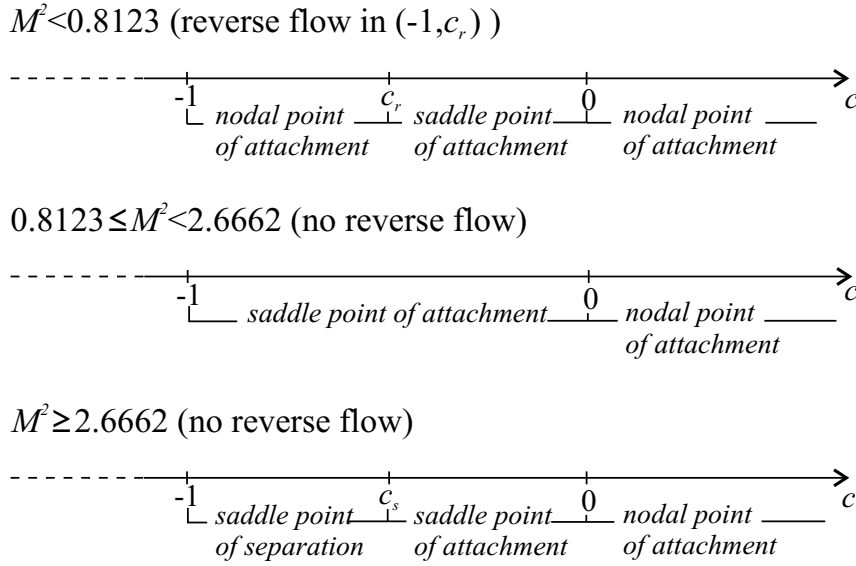


Figure 4.5: CASE I-N: classification of the stagnation-point in dependence on  $M^2$  and  $c$ .

### 4.2.3 CASE II-N: $\mathbf{H}_0 = H_0 \mathbf{e}_2$ .

We now furnish the numerical solution of problem (4.34), (4.36).

Figure 4.6 shows the graphics of  $\varphi, \varphi', \varphi''$  for  $M^2 = 1$ , and  $c = 0.25$ .

As far as the behaviour of  $\gamma, \gamma', \gamma''$  is concerned, as in CASE I-N, if  $c < c_r$ , then the reverse flow appears and the behaviour of  $\gamma, \gamma', \gamma''$  is the same as in Figure 4.7<sub>1</sub>. Otherwise  $\gamma'$  is always positive and the trend of  $\gamma, \gamma', \gamma''$  is shown in Figure 4.7<sub>2</sub>.

The numerical integration furnishes  $\varphi''(0), \gamma''(0), h_d, \alpha, \beta, \bar{\eta}_\varphi$ , and  $\bar{\eta}_\gamma$ : their values, when  $M^2$  and  $c$  change, are reported in Table 4.5.

We notice that if  $M^2$  is fixed, then the descriptive quantities behave as in CASE I-N when  $c$  increases.

When  $c$  is fixed, we find that if  $M^2$  increases, then  $\varphi''(0), \gamma''(0)$  increase, while the other parameters decrease.

Hence we have that the thickness  $\delta$  of the boundary layer decreases when  $M^2$  increases. In this case the thickness of the boundary layer is smaller than in CASE I-N. Figure 4.8 illustrates the change of the velocity for different values of  $M^2$ .

Table 4.6 shows that as the Hartmann number  $M^2$  increases, then the value of  $c_r$  for which the reverse flow does not occur decreases and when  $M^2 = 0.7583$ , the reverse flow does not occur at all for any value of  $c$ . In this case

$$\frac{\partial p}{\partial x_3} = -\rho a^2 c x_3 (c + 2M^2),$$

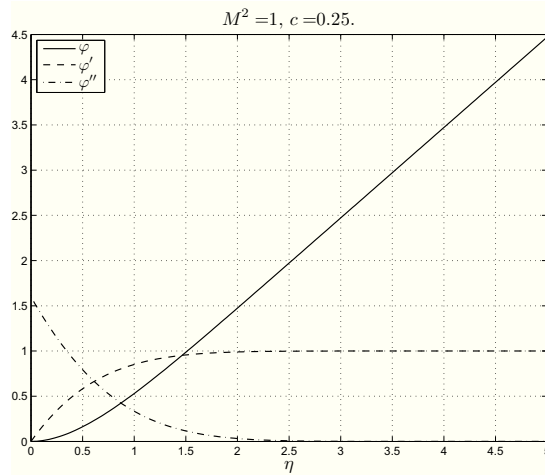


Figure 4.6: CASE II-N:  $\varphi$ ,  $\varphi'$ ,  $\varphi''$  profiles for  $M^2 = 1$  and  $c = 0.25$ .

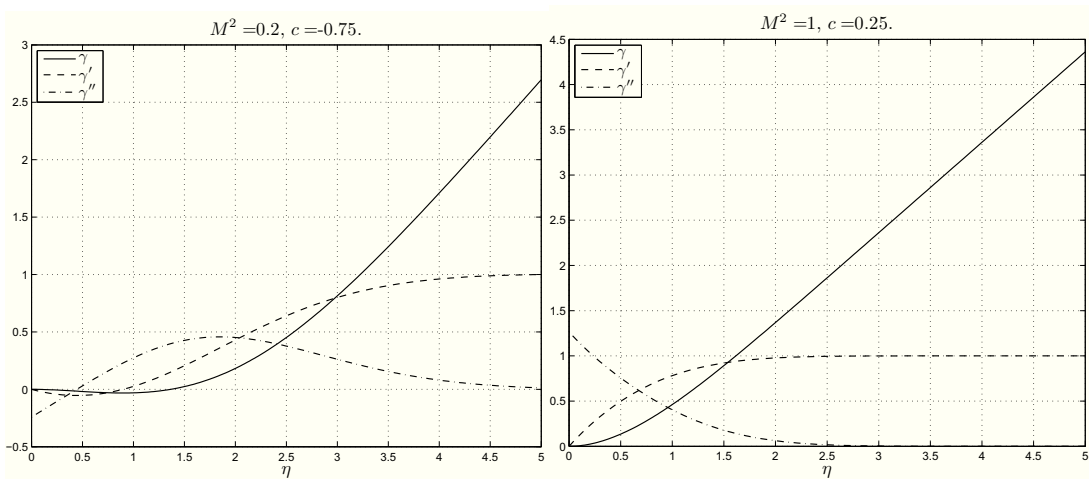


Figure 4.7: CASE II-N: the first picture shows the profile of  $\gamma$ ,  $\gamma'$ ,  $\gamma''$  in the reverse flow ( $M^2 = 0.2$ ,  $c = -0.75$ ). The second picture shows the profile of  $\gamma$ ,  $\gamma'$ ,  $\gamma''$  in the absence of the reverse flow ( $M^2 = 1$ ,  $c = 0.25$ ).

Table 4.5: CASE II-N: descriptive quantities of motion for some values of  $c$  and  $M^2$ .

$M^2$	$c$	$\varphi''(0)$	$\gamma''(0)$	$h_d$	$\alpha$	$\beta$	$\bar{\eta}_\varphi$	$\bar{\eta}_\gamma$	$\delta$
1	-0.75	1.5678	0.4894	-2.1123	0.5628	1.4544	2.3006	4.3855	4.3855
	-0.25	1.5752	0.9395	0.4523	0.5522	0.8521	2.1961	2.9803	2.9803
	0.25	1.5980	1.2647	0.5505	0.5286	0.6385	2.0156	2.2864	2.2864
	1.00	1.6453	1.6453	0.4910	0.4910	0.4910	1.7797	1.7797	1.7797
2	-0.75	1.8501	1.0585	-0.7283	0.4980	0.9068	2.1251	3.6713	3.6713
	-0.25	1.8639	1.3579	0.4260	0.4836	0.6563	1.9869	2.5441	2.5441
	0.25	1.8845	1.6065	0.4802	0.4658	0.5380	1.8416	2.0509	2.0509
	1.00	1.9232	1.9232	0.4392	0.4392	0.4392	1.6556	1.6556	1.6556
4	-0.75	2.3240	1.7547	-0.0685	0.4098	0.5692	1.8039	2.5268	2.5268
	-0.25	2.3384	1.9544	0.3709	0.3991	0.4836	1.6986	2.0251	2.0251
	0.25	2.3556	2.1366	0.3961	0.3881	0.4281	1.6006	1.7391	1.7391
	1.00	2.3852	2.3852	0.3720	0.3720	0.3720	1.4730	1.4730	1.4730
5	-0.75	2.5290	2.0177	0.0298	0.3796	0.4962	1.6836	2.2264	2.2264
	-0.25	2.5429	2.1942	0.3489	0.3706	0.4358	1.5941	1.8581	1.8581
	0.25	2.5589	2.3582	0.3680	0.3616	0.3935	1.5114	1.6282	1.6282
	1.00	2.5858	2.5858	0.3484	0.3484	0.3484	1.4025	1.4025	1.4025
10	-0.75	3.3743	3.0094	0.1598	0.2898	0.3331	1.3072	1.5192	1.5192
	-0.25	3.3857	3.1310	0.2763	0.2853	0.3125	1.2612	1.3837	1.3837
	0.25	3.3978	3.2484	0.2838	0.2809	0.2954	1.2180	1.2790	1.2790
	1.00	3.4174	3.4174	0.2745	0.2745	0.2745	1.1590	1.1590	1.1590

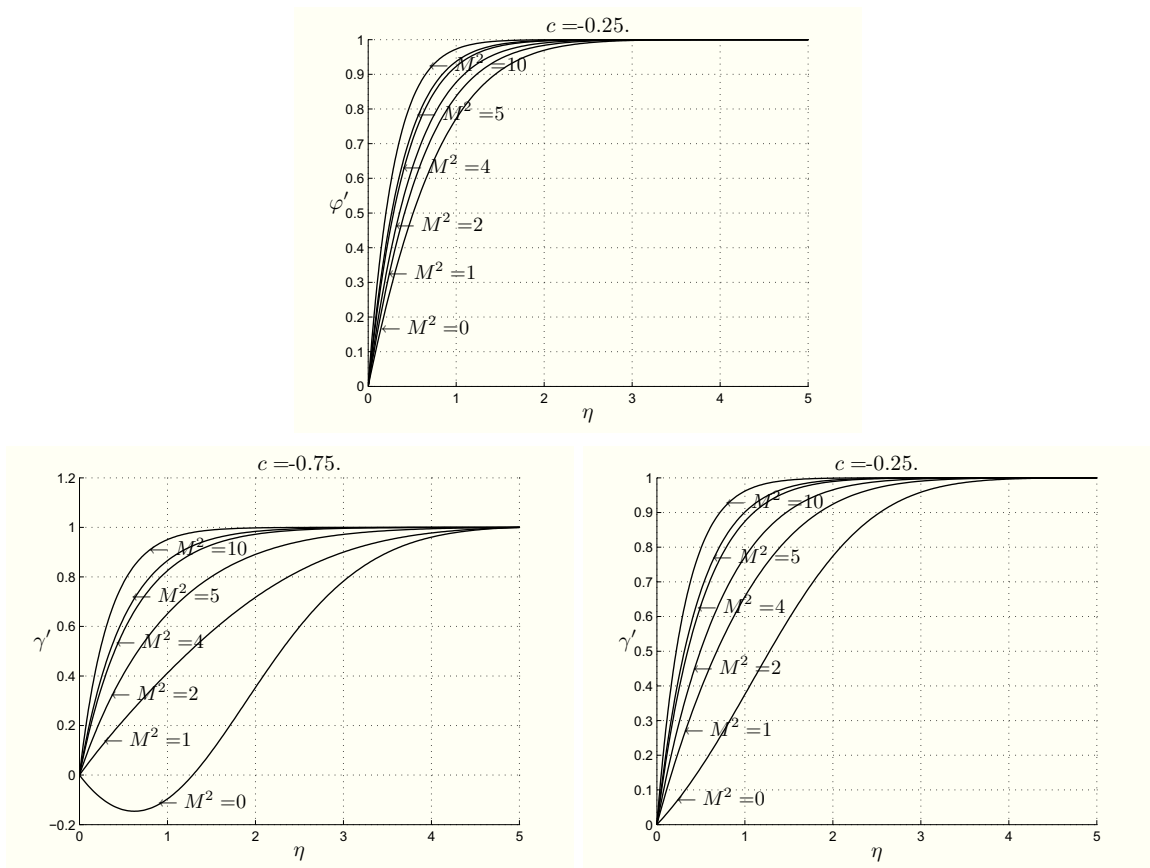


Figure 4.8: CASE II-N: profiles of  $\varphi'$  (Figure 4.8<sub>1</sub>) and  $\gamma'$  (Figure 4.8<sub>2,3</sub>) for several values of  $M^2$ .

Table 4.6: CASE II-N: values of  $c_r$  and  $c_h$  when  $M^2$  increases.

$M^2$	$c_r$	$c_h$
0.10	-0.5024	-0.4058
0.20	-0.5752	-0.4194
0.30	-0.6479	-0.4327
0.40	-0.7202	-0.4457
0.50	-0.7922	-0.4583
0.60	-0.8636	-0.4707
0.70	-0.9342	-0.4827
0.7583	-0.9751	-0.4895
0.7584	no reverse flow	-0.4896
100.00	no reverse flow	-0.9836

from which one can see that the signs of  $c$  and of  $(c + 2M^2)$  modify the sign of  $\frac{\partial p}{\partial x_3}$ .

From Table 4.5 we see that  $h_d$ , regardless of the values of  $M^2$ , increases if  $c < 0$ , while it decreases if  $c > 0$ .

The three-dimensional displacement thickness is always negative when the reverse flow appears since  $c_h \geq c_r$  (see Table 4.6). The presence of  $M^2$  influences  $c_h$  and it decreases when  $M^2$ , but different from the previous case,  $h_d$  can be always negative for physically reasonable values of  $M^2$ .

As far as the classification of the stagnation-point is concerned, we have found that  $\varphi''(0) + c\gamma''(0)$  is always positive, so that the origin is a point of attachment. We remark that in this case  $M^2$  directly influences  $\varphi$  and  $\gamma$ , as we can see from system (4.34).

If  $c > 0$  or where there is the reverse flow, then the origin is a nodal point, while when  $c < 0$  and the reverse flow does not appear, it is a saddle point. These results are the same as for  $M^2 = 0$ .

#### 4.2.4 CASE III-N: $\mathbf{H}_0 = H_0\mathbf{e}_3$ .

The functions  $\varphi, \varphi', \varphi''$  solution of (4.35), (4.36) are displayed in Figure 4.9 for  $M^2 = 1$ , and  $c = 0.25$ .

As before, if  $c < c_r$ , then the reverse flow appears and the behaviour of  $\gamma, \gamma', \gamma''$  is the same as in Figure 4.10<sub>1</sub>. When  $c \geq c_r$  the function  $\gamma'$  is always positive and  $\gamma, \gamma', \gamma''$  are displayed in Figure 4.10<sub>2</sub>.

The values of  $\varphi''(0), \gamma''(0), h_d, \alpha, \beta, \bar{\eta}_\varphi,$  and  $\bar{\eta}_\gamma$  are shown in Table 4.7.

We have that if  $M^2$  is fixed, then the descriptive quantities behave as in CASE I-N when  $c$  increases, even if they do not change in a relevant way compared to the previous cases.

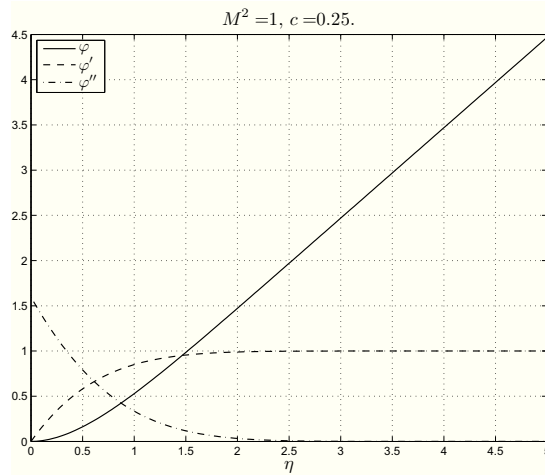


Figure 4.9: CASE III-N:  $\varphi, \varphi', \varphi''$  profiles for  $M^2 = 1$  and  $c = 0.25$ .

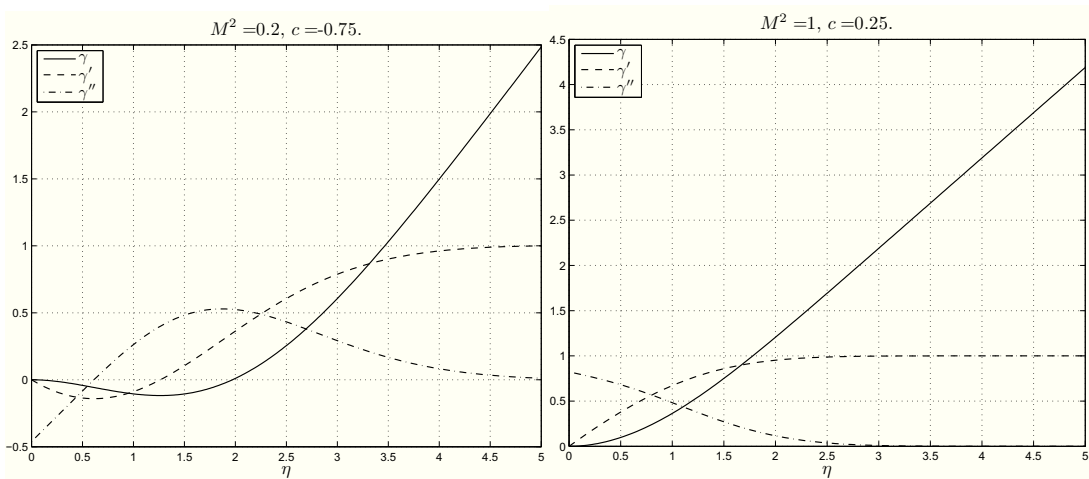


Figure 4.10: CASE III-N: the first picture shows the profiles of  $\gamma, \gamma', \gamma''$  in the reverse flow ( $M^2 = 0.2, c = -0.75$ ). The second picture shows the profiles of  $\gamma, \gamma', \gamma''$  in the absence of the reverse flow ( $M^2 = 1, c = 0.25$ ).

Table 4.7: CASE III-N: descriptive quantities of motion for some values of  $c$  and  $M^2$ .

$M^2$	$c$	$\varphi''(0)$	$\gamma''(0)$	$h_d$	$\alpha$	$\beta$	$\bar{\eta}_\varphi$	$\bar{\eta}_\gamma$	$\delta$
1	-0.75	1.5941	-0.4355	-5.1702	0.5358	2.4378	2.1012	4.4881	4.4881
	-0.25	1.5805	0.3035	0.2946	0.5472	1.3049	2.1626	3.5180	3.5180
	0.25	1.5950	0.8234	0.5869	0.5309	0.8112	2.0279	2.5816	2.5816
	1.00	1.6383	1.3216	0.5288	0.4950	0.5627	1.7971	1.9227	1.9227
2	-0.75	1.8799	-0.4130	-5.2322	0.4716	2.3728	1.9069	4.4603	4.4603
	-0.25	1.8700	0.3264	0.2171	0.4787	1.2637	1.9522	3.4541	3.4541
	0.25	1.8806	0.8361	0.5342	0.4683	0.7979	1.8567	2.5469	2.5469
	1.00	1.9133	1.3288	0.5012	0.4442	0.5582	1.6801	1.9076	1.9076
4	-0.75	2.3507	-0.3834	-5.3083	0.3919	2.2920	1.6424	4.4241	4.4241
	-0.25	2.3443	0.3559	0.1227	0.3956	1.2143	1.6706	3.3766	3.3766
	0.25	2.3513	0.8535	0.4683	0.3902	0.7808	1.6151	2.5031	2.5031
	1.00	2.3732	1.3393	0.4645	0.3769	0.5521	1.5014	1.8871	1.8871
5	-0.75	2.5541	-0.3729	-5.3339	0.3648	2.2644	1.5462	4.4113	4.4113
	-0.25	2.5486	0.3663	0.0909	0.3676	1.1979	1.5692	3.3504	3.3504
	0.25	2.5547	0.8599	0.4457	0.3635	0.7748	1.5251	2.4881	2.4881
	1.00	2.5735	1.3434	0.4514	0.3530	0.5498	1.4309	1.8797	1.8797
10	-0.75	3.3936	-0.3396	-5.4114	0.2826	2.1806	1.2359	4.3710	4.3710
	-0.25	3.3905	0.3995	-0.0047	0.2837	1.1489	1.2465	3.2719	3.2719
	0.25	3.3940	0.8815	0.3768	0.2821	0.7559	1.2277	2.4417	2.4417
	1.00	3.4051	1.3578	0.4099	0.2777	0.5421	1.1825	1.8559	1.8559

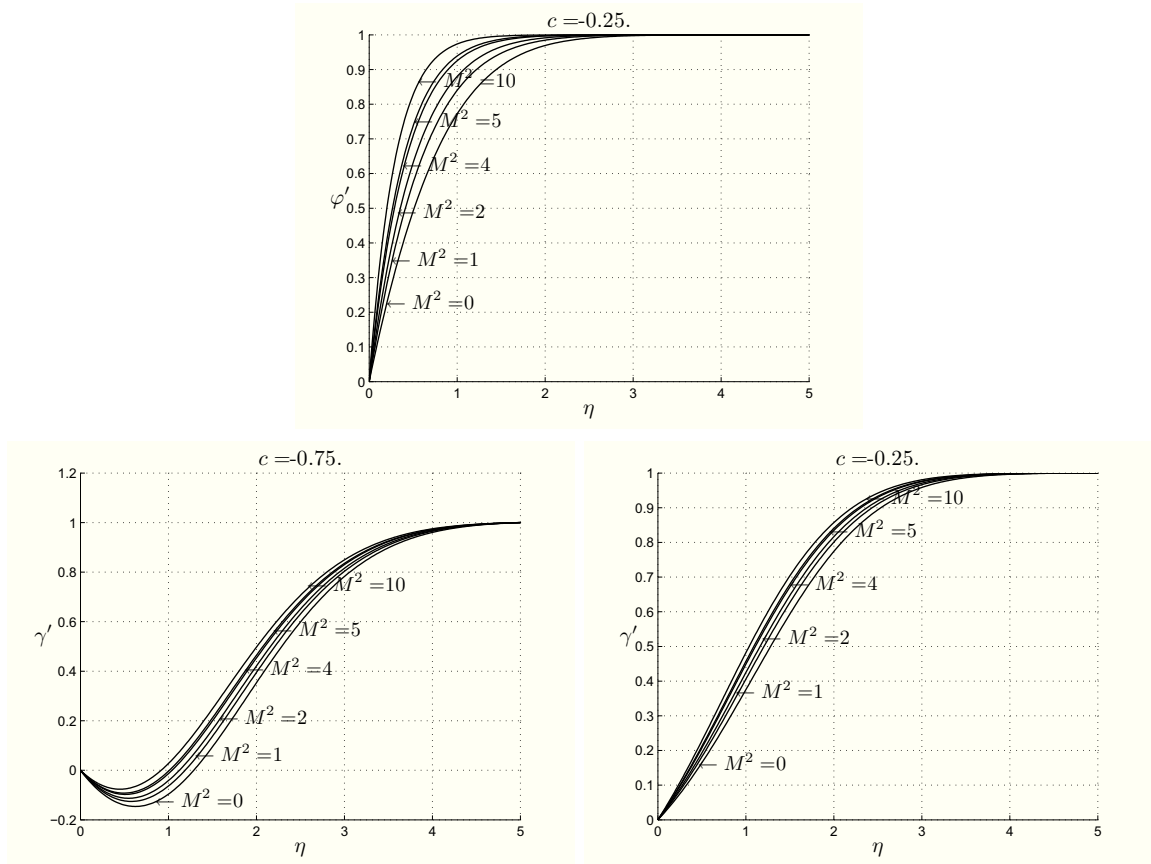


Figure 4.11: CASE III-N: profiles of  $\varphi'$  (Figure 4.11<sub>1</sub>) and  $\gamma'$  (Figures 4.11<sub>2,3</sub>) for several values of  $M^2$ .

When  $c$  is fixed, if  $M^2$  increases, then  $\varphi''(0)$ ,  $\gamma''(0)$  increase, while the other parameters decrease, so that the thickness  $\delta$  of the boundary layer decreases when  $M^2$  increases (as easily seen in Figures 4.11). The boundary layer is thinner than in CASE II-N.

Table 4.8 shows that as the Hartmann number  $M^2$  increases, then the value of  $c_r$  for which the reverse flow does not occur (i.e. when  $\gamma''(0) = 0$ ) decreases very slowly, so that in this case the influence of the magnetic field is much less significant with respect to CASEs I-N and II-N. This is due to the form of

$$\frac{\partial p}{\partial x_3} = -\rho a^2 c^2 x_3, \quad \frac{\partial p}{\partial x_1} = -\rho a^2 x_1(1 + M^2),$$

which have the same sign that they would have in the absence of the external magnetic field. In particular, we see that the reverse flow always appears for physically meaningful values of  $M^2$ .

Table 4.8: CASE III-N: values of  $c_r$  and  $c_h$  when  $M^2$  increases.

$M^2$	$c_r$	$c_h$
1	-0.4564	-0.3608
2	-0.4740	-0.3377
10	-0.5295	-0.2476
20	-0.5524	-0.2010
50	-0.5768	-0.1441
100	-0.5904	-0.1085

From Table 4.8 it appears a new interesting result:  $c_h$  increases when  $M^2$  increases. Further the three-dimensional displacement thickness is always negative when the reverse flow appears ( $c_h \geq c_r$  more than in the other two cases).

As far as the classification of the stagnation-point is concerned, as for the previous case, we have found that the origin is always a point of attachment. As one can see,  $M^2$  directly influences  $\varphi$  and only directly influences  $\gamma$  in system (4.35), so that when  $M^2$  increases,  $\varphi''(0)$  becomes much greater than  $\gamma''(0)$ .

Finally, if  $c > 0$  or where there is the reverse flow, the origin is a nodal point, while when  $c < 0$  and the reverse flow does not appear, it is a saddle point.

### 4.3 Micropolar fluids

We now investigate the steady three-dimensional MHD stagnation-point flow of a homogeneous, incompressible, electrically conducting micropolar fluid towards a flat surface coinciding with the plane  $x_2 = 0$ .

In the absence of free electric charges and external mechanical body forces and body couples, the MHD equations for such a fluid are (2.44).

The velocity  $\mathbf{v}$  and the microrotation  $\mathbf{w}$  are given by

$$\begin{aligned} v_1 &= ax_1 f'(x_2), \quad v_2 = -a[f(x_2) + cg(x_2)], \quad v_3 = acx_3 g'(x_2), \\ w_1 &= -cx_3 F(x_2), \quad w_2 = 0, \quad w_3 = x_1 G(x_2), \quad (x_1, x_3) \in \mathbb{R}^2, \quad x_2 \in \mathbb{R}^+, \end{aligned} \quad (4.42)$$

where  $f, g, F, G$  are sufficiently regular unknown functions ( $f, g \in C^3(\mathbb{R}^+)$ ,  $F, G \in C^2(\mathbb{R}^+)$ ).

We ask

$$\begin{aligned} f(0) &= 0, \quad f'(0) = 0, \quad g(0) = 0, \quad g'(0) = 0, \\ F(0) &= 0, \quad G(0) = 0, \end{aligned} \quad (4.43)$$

so that the no-slip and the strict adherence conditions are satisfied.

We, further, assume that at infinity, the flow approaches the flow of an inviscid fluid, whose velocity is given by (4.12):

$$\begin{aligned} \lim_{x_2 \rightarrow +\infty} f'(x_2) &= 1, & \lim_{x_2 \rightarrow +\infty} g'(x_2) &= 1, \\ \lim_{x_2 \rightarrow +\infty} F(x_2) &= 0, & \lim_{x_2 \rightarrow +\infty} G(x_2) &= 0. \end{aligned} \quad (4.44)$$

The constant  $C$  is related to the asymptotic behaviour of  $f$  and  $g$  at infinity as for the Newtonian case. So relations (4.16) and (4.17) continue to hold.

We now proceed by neglecting the induced magnetic field and we prove:

**THEOREM 4.3.1.** *Let a homogeneous, incompressible, electrically conducting micropolar fluid occupy the half-space  $\mathcal{S}$ . If we impress the external magnetic field  $\mathbf{H}_0$  parallel to one of the axes and if we neglect the induced magnetic field, then the steady three-dimensional MHD stagnation-point flow of such a fluid has the form*

$$\begin{aligned} \mathbf{v} &= ax_1 f'(x_2) \mathbf{e}_1 - a[f(x_2) + cg(x_2)] \mathbf{e}_2 + acx_3 g'(x_2) \mathbf{e}_3, \\ \mathbf{w} &= -cx_3 F(x_2) \mathbf{e}_2 + x_1 G(x_2) \mathbf{e}_3, \quad \mathbf{E} = \mathbf{0}, \quad (x_1, x_3) \in \mathbb{R}^2, \quad x_2 \in \mathbb{R}^+, \end{aligned}$$

and

(I-M) if  $\mathbf{H}_0 = H_0 \mathbf{e}_1$ , then the pressure field is given by

$$\begin{aligned} p &= -\rho \frac{a^2}{2} [x_1^2 + [f(x_2) + cg(x_2)]^2 + c^2 x_3^2] \\ &\quad - \rho a (\nu + \nu_r) [f'(x_2) + cg'(x_2)] - 2\nu_r \rho \int_0^{x_2} (cF(s) + G(s)) ds \\ &\quad - \sigma_e a B_0^2 \left[ \frac{c}{2} x_3^2 - \int_0^{x_2} (f(s) + cg(s)) ds \right] + p_0, \end{aligned} \quad (4.45)$$

and  $(f, g, F, G)$  satisfies problem

$$\begin{aligned} \frac{\nu + \nu_r}{a} f''' + (f + cg) f'' - f'^2 + 1 + \frac{2\nu_r}{a^2} G' &= 0, \\ \frac{\nu + \nu_r}{a} g''' + (f + cg) g'' - cg'^2 + c + \frac{2\nu_r}{a^2} F' + M^2(1 - g') &= 0, \end{aligned} \quad (4.46)$$

$$\begin{aligned} \lambda F'' + Ia[F'(f + cg) - cFg'] - 2\nu_r(2F + ag'') &= 0, \\ \lambda G'' + Ia[G'(f + cg) - Gf'] - 2\nu_r(2G + af'') &= 0, \end{aligned} \quad (4.47)$$

$$f(0) = 0, \quad f'(0) = 0, \quad g(0) = 0, \quad g'(0) = 0,$$

$$F(0) = 0, \quad G(0) = 0,$$

$$\lim_{x_2 \rightarrow +\infty} f'(x_2) = 1, \quad \lim_{x_2 \rightarrow +\infty} g'(x_2) = 1,$$

$$\lim_{x_2 \rightarrow +\infty} F(x_2) = 0, \quad \lim_{x_2 \rightarrow +\infty} G(x_2) = 0, \quad (4.48)$$

provided  $F, G \in L^1([0, +\infty))$ ;

(II-M) if  $\mathbf{H}_0 = H_0 \mathbf{e}_2$ , then the pressure field is given by

$$\begin{aligned} p &= -\rho \frac{a^2}{2} [x_1^2 + [f(x_2) + cg(x_2)]^2 + c^2 x_3^2] \\ &\quad - \rho a (\nu + \nu_r) [f'(x_2) + cg'(x_2)] \\ &\quad - 2\nu_r \rho \int_0^{x_2} (cF(s) + G(s)) ds - \sigma_e a B_0^2 (x_1^2 + cx_3^2) + p_0, \end{aligned} \quad (4.49)$$

and  $(f, g, F, G)$  satisfies problem

$$\begin{aligned} \frac{\nu + \nu_r}{a} f''' + (f + cg) f'' - f'^2 + 1 + \frac{2\nu_r}{a^2} G' + M^2(1 - f') &= 0, \\ \frac{\nu + \nu_r}{a} g''' + (f + cg) g'' - cg'^2 + c + \frac{2\nu_r}{a^2} F' + M^2(1 - g') &= 0, \end{aligned} \quad (4.50)$$

with (4.47), and (4.48), provided  $F, G \in L^1([0, +\infty))$ ;

(III-M) if  $\mathbf{H}_0 = H_0 \mathbf{e}_3$ , then the pressure field is given by

$$\begin{aligned} p = & -\rho \frac{a^2}{2} [x_1^2 + [f(x_2) + cg(x_2)]^2 + c^2 x_3^2] \\ & - \rho a (\nu + \nu_r) [f'(x_2) + cg'(x_2)] - 2\nu_r \rho \int_0^{x_2} (cF(s) + G(s)) ds \\ & - \sigma_e a B_0^2 \left[ \frac{x_1^2}{2} - \int_0^{x_2} (f(s) + cg(s)) ds \right] + p_0, \end{aligned} \quad (4.51)$$

and  $(f, g, F, G)$  satisfies problem

$$\begin{aligned} \frac{\nu + \nu_r}{a} f''' + (f + cg) f'' - f'^2 + 1 + \frac{2\nu_r}{a^2} G' + M^2(1 - f') &= 0, \\ \frac{\nu + \nu_r}{a} g''' + (f + cg) g'' - cg'^2 + c + \frac{2\nu_r}{a^2} F' &= 0, \end{aligned} \quad (4.52)$$

with (4.47), and (4.48), provided  $F, G \in L^1([0, +\infty))$ .

*Proof.* We begin by proving CASE I-M.

If

$$\mathbf{H}_0 = H_0 \mathbf{e}_1,$$

then

$$(\nabla \times \mathbf{H}) \times \mathbf{H} \simeq \sigma_e \mu_e a H_0^2 [(f + cg) \mathbf{e}_2 - cg' x_3 \mathbf{e}_3]. \quad (4.53)$$

We substitute (4.53) into (2.44)<sub>1,3</sub>, so that

$$\begin{aligned} ax_1 \left[ (\nu + \nu_r) f''' + a f'' (f + cg) - a f'^2 + \frac{2\nu_r}{a} G' \right] &= \frac{1}{\rho} \frac{\partial p}{\partial x_1}, \\ -(\nu + \nu_r) a (f'' + cg'') - a^2 (f' + cg') (f + cg) \\ &\quad - 2\nu_r (cF + G) + \frac{\sigma_e a}{\rho} B_0^2 (f + cg) = \frac{1}{\rho} \frac{\partial p}{\partial x_2}, \\ cx_3 \left[ (\nu + \nu_r) g''' + a g'' (f + cg) - cg'^2 + \frac{2\nu_r}{a} F' - \frac{\sigma_e}{\rho} B_0^2 g' \right] &= \frac{1}{\rho} \frac{\partial p}{\partial x_3}, \\ c[\lambda F'' + Ia[F'(f + cg) - cFg'] - 2\nu_r(2F + ag'')] &= 0, \\ \lambda G'' + Ia[G'(f + cg) - Gf'] - 2\nu_r(2G + af'') &= 0. \end{aligned} \quad (4.54)$$

Since we are interested in three-dimensional flow, we assume  $c \neq 0$  and so equation (4.54)<sub>4</sub> can be replaced by

$$\lambda F'' + Ia[F'(f + cg) - cFg'] - 2\nu_r(2F + ag'') = 0. \quad (4.55)$$

Then, by integrating (4.54)<sub>2</sub>, we find

$$p = -\frac{1}{2}\rho a^2 [f(x_2) + cg(x_2)]^2 - \rho a(\nu + \nu_r)[f'(x_2) + cg'(x_2)] \\ - 2\nu_r \rho \int_0^{x_2} [cF(s) + G(s)]ds + \sigma_e a B_0^2 \int_0^{x_2} [f(s) + cg(s)]ds + P(x_1, x_3),$$

where the function  $P(x_1, x_3)$  is determined supposing that, far from the wall, the pressure  $p$  has the same behaviour as for an inviscid fluid, whose pressure is given by (4.11) replacing  $x_2$  by  $x_2 - C$ .

Therefore, under the assumption  $F, G \in L^1([0, +\infty))$ , by virtue of (4.44), (4.16), we get

$$P(x_1, x_3) = -\rho \frac{a^2}{2}(x_1^2 + c^2 x_3^2) - \frac{a}{2}\sigma_e B_0^2 c x_3^2 + p_0^*.$$

Finally, the pressure field assumes the form

$$p = -\rho \frac{a^2}{2}[x_1^2 + (f(x_2) + cg(x_2))^2 + c^2 x_3^2] \\ - \rho a(\nu + \nu_r)[f'(x_2) + cg'(x_2)] - 2\nu_r \rho \int_0^{x_2} (cF(s) + G(s))ds \\ - \sigma_e a B_0^2 \left[ \frac{c}{2}x_3^2 - \int_0^{x_2} (f(s) + cg(s))ds \right] + p_0, \quad (4.56)$$

where the constant  $p_0$  is the pressure at the origin.

In consideration of (4.56), we obtain the ordinary differential system

$$\frac{\nu + \nu_r}{a} f''' + (f + cg)f'' - f'^2 + 1 + \frac{2\nu_r}{a^2} G' = 0, \\ \frac{\nu + \nu_r}{a} g''' + (f + cg)g'' - cg'^2 + c + \frac{2\nu_r}{a^2} F' + M^2(1 - g') = 0, \quad (4.57)$$

where  $M^2$  is the Hartmann number. To these equations we append equations (4.54)<sub>5</sub>, and (4.55) and the boundary conditions (4.43), and (4.44).

As far as the other two cases are concerned, if we proceed as previously, then we get the assertion.  $\square$

**REMARK 4.3.2.** *We see from (4.45), (4.49), (4.51) that the pressure takes again its maximum along the wall  $x_2 = 0$  in the stagnation-point.*

**REMARK 4.3.3.** *If  $c = 1$ ,  $f = g$ ,  $F = G$ ,  $\mathbf{H}_0 = H_0 \mathbf{e}_2$ , the axisymmetric case is obtained.*

It is now convenient to rewrite the boundary value problems in Theorem 4.3.1 in dimensionless using transformation (1.49).

Hence system (4.46), (4.47) can be written as

$$\begin{aligned}\varphi''' + (\varphi + c\gamma)\varphi'' - \varphi'^2 + 1 + \Gamma' &= 0, \\ \gamma''' + (\varphi + c\gamma)\gamma'' - c\gamma'^2 + c + \Phi' + M^2(1 - \gamma') &= 0, \\ \Phi'' + c_3\Phi'(\varphi + c\gamma) - \Phi(c_3c\gamma' + c_2) - c_1\gamma'' &= 0, \\ \Gamma'' + c_3\Gamma'(\varphi + c\gamma) - \Gamma(c_3\varphi' + c_2) - c_1\varphi'' &= 0,\end{aligned}\tag{4.58}$$

where  $c_1, c_2, c_3$  are given by (1.25).

The boundary conditions (4.48) in dimensionless form become:

$$\begin{aligned}\varphi(0) &= 0, \quad \varphi'(0) = 0, \\ \gamma(0) &= 0, \quad \gamma'(0) = 0, \\ \Phi(0) &= 0, \quad \Gamma(0) = 0, \\ \lim_{\eta \rightarrow +\infty} \varphi'(\eta) &= 1, \quad \lim_{\eta \rightarrow +\infty} \gamma'(\eta) = 1, \\ \lim_{\eta \rightarrow +\infty} \Phi(\eta) &= 0, \quad \lim_{\eta \rightarrow +\infty} \Gamma(\eta) = 0.\end{aligned}\tag{4.59}$$

Equations (4.50) can be written as

$$\begin{aligned}\varphi''' + (\varphi + c\gamma)\varphi'' - \varphi'^2 + 1 + \Gamma' + M^2(1 - \varphi') &= 0, \\ \gamma''' + (\varphi + c\gamma)\gamma'' - c\gamma'^2 + c + \Phi' + M^2(1 - \gamma') &= 0;\end{aligned}\tag{4.60}$$

and equations (4.52) as

$$\begin{aligned}\varphi''' + (\varphi + c\gamma)\varphi'' - \varphi'^2 + 1 + \Gamma' + M^2(1 - \varphi') &= 0, \\ \gamma''' + (\varphi + c\gamma)\gamma'' - c\gamma'^2 + c + \Phi' &= 0.\end{aligned}\tag{4.61}$$

We obtain other two different ordinary differential problems by adding equations (4.58)<sub>3,4</sub> and the boundary conditions (4.59).

In dimensionless form we also have

$$\alpha = \sqrt{\frac{a}{\nu + \nu_r}}A, \quad \beta = \sqrt{\frac{a}{\nu + \nu_r}}B, \quad h_d = \frac{\alpha + c\beta}{1 + c}.$$

The remainder of this section will be devoted to prove that the cases considered in Remark 4.1.2 are not possible. For the sake of simplicity we use the dimensionless equations.

PROPOSITION 4.3.4. *Let a homogeneous, incompressible, electrically conducting micropolar fluid occupy the half-space  $\mathcal{S}$ . If we neglect the induced magnetic field and we suppose either*

$$i) \quad c = 1, \quad \mathbf{H}_0 \text{ parallel to the plane } Ox_1x_3,$$

or

$$ii) \quad c = -\frac{1}{2}, \quad \mathbf{H}_0 \text{ parallel to the plane } Ox_2x_3,$$

then, under the hypothesis  $\varphi, \Phi, \Gamma \in C^5(\mathbb{R}^+)$ , there is no solution to the problem of the steady three-dimensional MHD stagnation-point flow.

*Proof.* i) If  $c = 1$  and the external magnetic induction field is  $\mathbf{B} = B_1\mathbf{e}_1 + B_3\mathbf{e}_3$  ( $B_1, B_3 \neq 0$ ), then after some calculations we deduce:

$$\begin{aligned} \varphi''' + (\varphi + \gamma)\varphi'' - \varphi'^2 + M_3^2(1 - \varphi') + 1 + \Gamma' &= 0, \\ M_1M_3(\gamma' - 1) &= 0, \\ \gamma''' + (\varphi + \gamma)\gamma'' - \gamma'^2 + M_1^2(1 - \gamma') + 1 + \Phi' &= 0, \\ M_1M_3(\varphi' - 1) &= 0, \end{aligned} \tag{4.62}$$

where  $M_i^2 = \frac{\sigma_e B_i^2}{\rho a}$ ,  $i = 1, 3$ .

From (4.62)<sub>2</sub>, (4.62)<sub>4</sub>, we have  $\varphi' = \gamma' = 1$ ,  $\forall \eta \geq 0$ , which contradicts the boundary conditions (4.59)<sub>2,4</sub>.

ii) If  $c = -\frac{1}{2}$  and  $\mathbf{B} = B_2\mathbf{e}_2 + B_3\mathbf{e}_3$  ( $B_2, B_3 \neq 0$ ), then we arrive at:

$$\begin{aligned} \varphi''' + \left(\varphi - \frac{\gamma}{2}\right)\varphi'' - \varphi'^2 + (M_2^2 + M_3^2)(1 - \varphi') + 1 + \Gamma' &= 0, \\ \gamma''' + \left(\varphi - \frac{\gamma}{2}\right)\gamma'' + \frac{\gamma'^2}{2} + M_2^2(1 - \gamma') - \frac{1}{2} + \Phi' &= 0, \\ M_2M_3(\varphi - \gamma + \alpha - \beta) &= 0. \end{aligned} \tag{4.63}$$

From (4.63)<sub>3</sub> evaluated at  $\eta = 0$  and using (4.59)<sub>1,3</sub>, we deduce  $\varphi = \gamma$ . Therefore

we have to solve the following overdetermined ODEs system

$$\begin{aligned}
\varphi''' + \frac{\varphi}{2}\varphi'' - \varphi'^2 + (M_2^2 + M_3^2)(1 - \varphi') + 1 + \Gamma' &= 0, \\
\varphi''' + \frac{\varphi}{2}\varphi'' + \frac{\varphi'^2}{2} + M_2^2(1 - \varphi') - \frac{1}{2} + \Phi' &= 0, \\
\Phi'' + c_3\Phi'\frac{\varphi}{2} + \Phi\left(\frac{c_3}{2}\varphi' - c_2\right) - c_1\varphi'' &= 0, \\
\Gamma'' + c_3\Gamma'\frac{\varphi}{2} - \Gamma(c_3\varphi' + c_2) - c_1\varphi'' &= 0,
\end{aligned} \tag{4.64}$$

together with the boundary conditions (4.59).

Our purpose is to prove that such a problem does not admit solution. To this end, by subtracting (4.64)<sub>1</sub> from (4.64)<sub>2</sub>, we obtain that  $(\varphi, \Phi, \Gamma)$  solves the equation

$$\frac{3}{2}(\varphi'^2 - 1) + M_3^2(\varphi' - 1) + \Phi' - \Gamma' = 0. \tag{4.65}$$

Computing (4.65), (4.64)<sub>3,4</sub> at  $\eta = 0$ , gives

$$\Phi'(0) - \Gamma'(0) = \frac{3}{2} + M_3^2, \quad \Phi''(0) = \Gamma''(0) = c_1\varphi''(0). \tag{4.66}$$

If we differentiate (4.65), then we have

$$3\varphi'\varphi'' + M_3^2\varphi'' + \Phi'' - \Gamma'' = 0. \tag{4.67}$$

By means of (4.66)<sub>2</sub>, (4.67) we deduce

$$\Phi''(0) = \Gamma''(0) = \varphi''(0) = 0. \tag{4.68}$$

After differentiating (4.64)<sub>3,4</sub> we get

$$\begin{aligned}
\Gamma'''(0) &= -c_2(1 + M_2^2 + M_3^2) + (c_1 - c_2)\varphi'''(0), \\
\Phi'''(0) - \Gamma'''(0) &= c_2\left(\frac{3}{2} + M_3^2\right),
\end{aligned} \tag{4.69}$$

where we have used (4.66)<sub>1</sub>, and (4.64)<sub>1</sub>.

If we differentiate (4.67), then we obtain

$$3\varphi''^2 + 3\varphi'\varphi''' + M_3^2\varphi''' + \Phi''' - \Gamma''' = 0, \tag{4.70}$$

from which, taking account of (4.68)<sub>3</sub>, follows

$$\varphi'''(0) = -\frac{\Phi'''(0) - \Gamma'''(0)}{M_3^2}. \tag{4.71}$$

Further, from (4.64)<sub>1,2</sub> we get

$$\Phi'(0) = \frac{1}{2} - M_2^2 - \varphi'''(0), \quad \Gamma'(0) = -[1 + M_2^2 + M_3^2 + \varphi'''(0)]. \quad (4.72)$$

Differentiating of (4.70) furnishes:

$$9\varphi''\varphi''' + 3\varphi'\varphi^{IV} + M_3^2\varphi^{IV} + \Phi^{IV} - \Gamma^{IV} = 0. \quad (4.73)$$

Another differentiation of (4.64)<sub>3,4</sub> gives

$$\Phi^{IV}(0) = \Gamma^{IV}(0) = c_1\varphi^{IV}(0),$$

so that (4.73)

$$\Phi^{IV}(0) = \Gamma^{IV}(0) = \varphi^{IV}(0) = 0. \quad (4.74)$$

If we differentiate (4.73) and evaluate the resulting equation at  $\eta = 0$ , we obtain

$$9\varphi'''(0)^2 + M_3^2\varphi^V(0) + \Phi^V(0) - \Gamma^V(0) = 0. \quad (4.75)$$

On the other hand we can find  $\varphi^V(0)$  from (4.64)<sub>1</sub> after two differentiations:

$$\varphi^V(0) = (M_2^2 + M_3^2)\varphi'''(0) - \Gamma'''(0). \quad (4.76)$$

By means of another differentiation of (4.64)<sub>3,4</sub> we arrive at

$$\Phi^V(0) - \Gamma^V(0) = c_2[\Phi'''(0) - \Gamma'''(0)] - c_3\varphi'''(0)\left[2\Phi'(0) + \frac{5}{2}\Gamma'(0)\right]. \quad (4.77)$$

Finally, on substituting (4.76), (4.77) into (4.75) and taking into account (4.69)<sub>1</sub>, (4.71), (4.72), we get

$$\begin{aligned} & \frac{9}{2}(2 + c_3)\varphi'''(0)^2 + \left[M_3^2(M_2^2 + M_3^2 - c_1 + \frac{5}{2}c_3) + \frac{c_3}{2}(9M_2^2 + 3)\right]\varphi'''(0) \\ & + c_2M_3^2(1 + M_2^2 + M_3^2) = 0. \end{aligned} \quad (4.78)$$

The conclusion follows easily because, as one can see from (4.69), (4.71),  $\varphi'''(0)$  does not depend on  $c_1$  and by differentiating (4.78) with respect to  $c_1$ , we obtain

$$M_3^2\varphi'''(0) = 0, \quad (4.79)$$

which gives the absurdum

$$\frac{3}{2} + \frac{\sigma_e}{a\rho}B_3^2 = 0,$$

as for a Newtonian fluid. □

REMARK 4.3.5. If  $M^2 = 0$ , then equations (4.58)<sub>1,2</sub> (or (4.60), or (4.61)), (4.58)<sub>3,4</sub> reduce to equations found by Guram and Anwar Kamal in [26] and they have already been integrated numerically in Chapter 1.3.3.

REMARK 4.3.6. The skin-friction components  $\tau_1, \tau_3$  along  $x_1$  and  $x_3$  axes are given by (4.80). Actually,  $\varphi''(0), \gamma''(0)$  depend on  $\mathbf{H}_0$  through  $M^2$ .

REMARK 4.3.7. The solutions of problem (4.60), (4.58)<sub>3,4</sub>, (4.59) are invariant under the following transformation

$$\begin{aligned}\varphi\left(\eta, \frac{1}{c}, \frac{c_1}{c}, \frac{c_2}{c}, c_3, \frac{M^2}{c}\right) &= \sqrt{c} \gamma\left(\frac{\eta}{\sqrt{c}}, c, c_1, c_2, c_3, M^2\right), \\ \gamma\left(\eta, \frac{1}{c}, \frac{c_1}{c}, \frac{c_2}{c}, c_3, \frac{M^2}{c}\right) &= \sqrt{c} \varphi\left(\frac{\eta}{\sqrt{c}}, c, c_1, c_2, c_3, M^2\right), \\ \Phi\left(\eta, \frac{1}{c}, \frac{c_1}{c}, \frac{c_2}{c}, c_3, \frac{M^2}{c}\right) &= \frac{1}{\sqrt{c}} \Gamma\left(\frac{\eta}{\sqrt{c}}, c, c_1, c_2, c_3, M^2\right), \\ \Gamma\left(\eta, \frac{1}{c}, \frac{c_1}{c}, \frac{c_2}{c}, c_3, \frac{M^2}{c}\right) &= \frac{1}{\sqrt{c}} \Phi\left(\frac{\eta}{\sqrt{c}}, c, c_1, c_2, c_3, M^2\right), \quad c > 0,\end{aligned}$$

so that we can confine our attention to  $c \in (-1, 1)$ ,  $c \neq 0$ .

If  $M^2 = 0$ , then the previous transformation reduces to that in Remark 4.2.8.

By means of the previous transformation regular solutions of problem (4.58)<sub>1,2</sub> (or (4.61)), (4.58)<sub>3,4</sub>, (4.59) are transformed in solutions of problem (4.61) (or (4.58)<sub>1,2</sub>), (4.58)<sub>3,4</sub>, (4.59).

REMARK 4.3.8. As we have already said it in Remark 1.3.15, it is important to give the explicit form of the pressure field because if one of the components of the pressure gradient parallel to the wall has the same sign as the corresponding component of the velocity or of the microrotation curl field, then the reverse flow or the reverse microrotation appears.

The numerical results show that there exists a negative value  $c_r$  of  $c$  such that if  $c \geq c_r$ , then  $\gamma', \gamma'' > 0 \forall \eta > 0$ , and if  $c < c_r$  then near the wall  $\gamma', \gamma'' < 0$ , so that the reverse flow appears (i.e.  $v_3$  has the same sign as  $\frac{\partial p}{\partial x_3}$ ).

There also exists a negative value  $c_{rw}$  of  $c$  such that if  $c \geq c_{rw}$ , then  $\Phi'(0) < 0$ ,  $\Phi(\eta) < 0 \forall \eta > 0$ , and if  $c < c_{rw}$  then near the wall  $\Phi, \Phi' > 0$  so that the reverse microrotation appears (i.e.  $(\nabla \times \mathbf{w})_3 = \frac{a^2}{2\nu_r} c x_3 \Phi'(\eta)$  has the same sign as  $\frac{\partial p}{\partial x_3}$  and  $\mathbf{w}_1$  has opposite sign that of  $x_3$ ).

The reverse flow and the reverse microrotation are also related to a sign change of the scalar component of the skin friction ( $\tau_0$ ) in the direction of  $\mathbf{e}_3$  and of the

scalar component of the skin couple friction ( $\gamma_0$ ) in the direction of  $\mathbf{e}_1$ :

$$\tau_0 = \rho a^{3/2}(\nu + \nu_r)^{1/2}[x_1\varphi''(0)\mathbf{e}_1 + cx_3\gamma''(0)\mathbf{e}_3], \quad (4.80)$$

$$\sigma_0 = \rho\lambda\frac{a^2}{2\nu_r}[-cx_3\Phi'(0)\mathbf{e}_1 + x_1\Gamma'(0)\mathbf{e}_3]. \quad (4.81)$$

As one can see from (4.45), (4.49), (4.51), the pressure field depends on the external magnetic field through the Hartmann number  $M^2$ , which influences the sign of the components of the pressure gradient along the surface. For this reason, as we will see in the next numerical sections, the magnetic field tends to prevent the occurrence of the reverse flow and of the reverse microrotation. This behaviour appears more clearly in CASEs I-II-M, as it happened for the Newtonian fluids.

In particular, we indicate with

- $M_r^2$  ( $M_{rw}^2$ ) the value of  $M^2$  starting from which the reverse flow (microrotation) doesn't occur at all for any value of  $c$ .

REMARK 4.3.9. In all the three cases considered in Theorem 4.3.1 it is interesting to classify the origin as nodal or saddle point and as attachment or separation point. This classification can be done following the definitions given in Remark 1.3.16. From those considerations it is clear that we need to know the signs of  $c$ ,  $\varphi''(0)$ ,  $\gamma''(0)$  in order to classify the stagnation-point as in Chapter 1.3.3. Yet now  $\varphi''(0)$ ,  $\gamma''(0)$  depend on  $M^2$ .

As in CASE I-N, we will see that in CASE I-M the origin can be also become a separation point, differently from the other two cases. Hence in CASE I-M we denote by

- $M_s^2$  the value of  $M^2$  starting from which the origin becomes a point of separation;

and for some values of  $M^2 \geq M_s^2$ , we define

- $c_s$  the negative values of  $c$  such that if  $c < c_s$  then the origin is a separation point, while if  $c \geq c_s$  then it is an attachment point.

The change of the origin from attachment point to separation point can be explained by the form of system (4.58).

REMARK 4.3.10. As in the absence of the external magnetic field (see Chapter 1.3.3), from the numerical results we will see that the three dimensional displacement thickness  $h_d$  can be negative, so that

- $c_h$  is the negative values of  $c$  such that if  $c < c_h$ , then  $h_d < 0$  and if  $c \geq c_h$ , then  $h_d \geq 0$ .

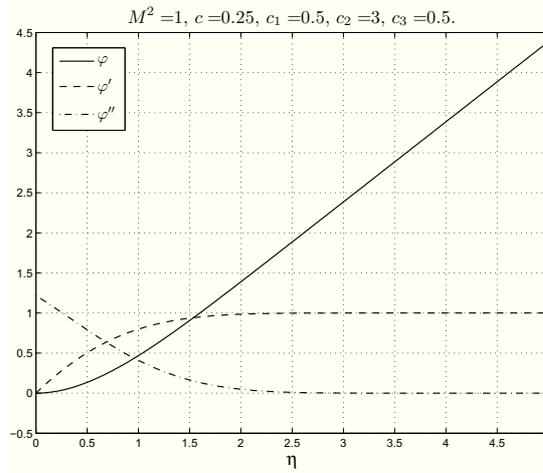


Figure 4.12: CASE I-M:  $\varphi, \varphi', \varphi''$  profiles.

REMARK 4.3.11. *In the following sections, we will show that the solution  $(\varphi, \gamma, \Phi, \Gamma)$  of the three problems considered in Theorem 4.3.1 satisfies the conditions (4.59)<sub>7,10</sub>; therefore we recall Remark 1.3.17, where we defined:*

- $\bar{\eta}_\varphi$  ( $\bar{\eta}_\gamma$ ) the value of  $\eta$  such that  $\varphi'(\bar{\eta}_\varphi) = 0.99$  ( $\gamma'(\bar{\eta}_\gamma) = 0.99$ );
- $\bar{\eta}_\Phi$  ( $\bar{\eta}_\Gamma$ ) the value of  $\eta$  such that  $\Phi(\bar{\eta}_\Phi) = -0.01$  ( $\Gamma(\bar{\eta}_\Gamma) = -0.01$ ).

If  $\eta > \bar{\eta}_\varphi$  ( $\eta > \bar{\eta}_\gamma$ ), then  $\varphi \cong \eta - \alpha$  ( $\gamma \cong \eta - \beta$ ), and if  $\eta > \bar{\eta}_\Phi$  ( $\eta > \bar{\eta}_\Gamma$ ), then  $\Phi \cong 0$  ( $\Gamma \cong 0$ ).

The effect of the viscosity on the velocity and on the microrotation appears only in a layer lining the boundary whose thickness is  $\delta_v = \max(\bar{\eta}_f, \bar{\eta}_g)$  for the velocity and  $\delta_w = \max(\bar{\eta}_F, \bar{\eta}_G)$  for the microrotation. The thickness  $\delta$  of the boundary layer for the flow is defined as

$$\delta := \max(\delta_v, \delta_w).$$

In the next three sections, we present our numerical results in tabular and graphical forms in order to investigate the important features of the boundary value problems given in Theorem 4.3.1. The values of  $M^2$ ,  $c$ ,  $c_1$ ,  $c_2$  and  $c_3$  are taken according to the previous Chapters.

### 4.3.1 CASE I-M: $\mathbf{H}_0 = H_0 \mathbf{e}_1$ .

We consider the solution of problem (4.58), (4.59):  $\varphi, \varphi', \varphi''$  are shown in Figure 4.12.

As far as the behaviour of  $\gamma, \gamma', \gamma''$  is concerned, if  $c < c_r$ , then it is shown in Figure 4.13<sub>1</sub> (reverse flow appears), otherwise it is given in Figure 4.13<sub>2</sub>.

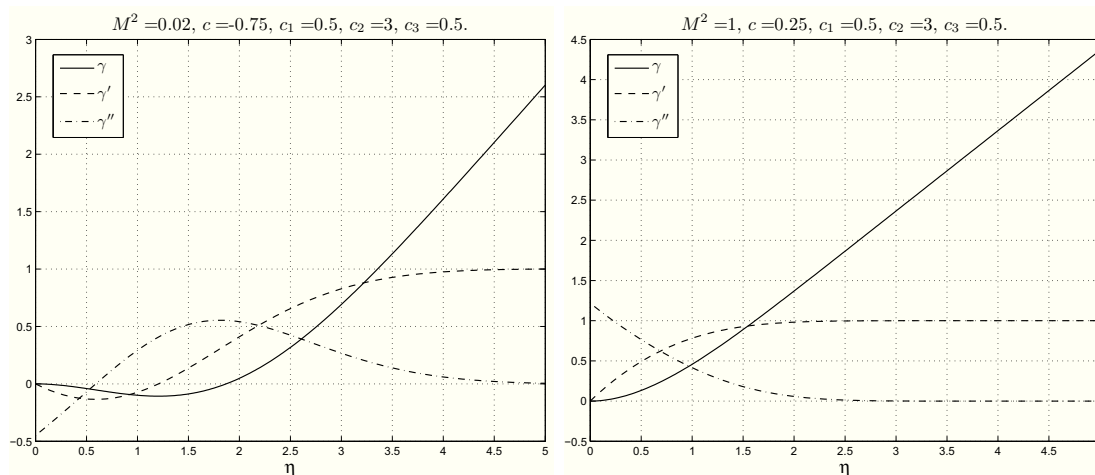


Figure 4.13: CASE I-M: the first picture shows the profiles of  $\gamma, \gamma', \gamma''$  in the reverse flow. The second picture shows the profiles of  $\gamma, \gamma', \gamma''$  in the absence of the reverse flow.

The function  $\Phi$  also presents a zone of reverse microrotation for some negative values of  $c$ . If  $c < c_{rw}$  ( $\Phi'(0) > 0$ ) then the behaviour of  $\Phi, \Phi'$  is shown in Figure 4.14<sub>1</sub>, otherwise it is given in Figure 4.14<sub>2</sub>. The thickness of the reverse microrotation zone is very small.

Figure 4.15 shows the profiles of  $\Gamma, \Gamma'$ .

The numerical integration furnishes the value of  $\varphi''(0), \gamma''(0), \Phi'(0), \Gamma'(0), h_d, \alpha, \beta, \bar{\eta}_\varphi, \bar{\eta}_\gamma, \bar{\eta}_\Phi, \bar{\eta}_\Gamma, \delta_v, \delta_w$  and  $\delta$  when  $c, c_1, c_2, c_3$  and  $M^2$  change, as it is shown in Tables 4.9, 4.10, 4.11 and 4.12.

We underline that there are no results in the literature if  $M^2 \neq 0$  ([8]).

From Tables 4.11-4.12 and from Figures 4.16-4.18 it appears that if we fix two parameters among  $c_1, c_2, c_3$ , then we get the same considerations as in the absence of the external electromagnetic field (Chapter 1.3.3).

In Table 4.9, 4.10, 4.11 and 4.12 we see the values of the descriptive quantities of the motion when  $M^2$  increases and assumes the values 1, 2, 5. If  $M^2$  increases, then

- $\gamma''(0)$  increases;
- $\Phi'(0), \beta, \bar{\eta}_\gamma, \bar{\eta}_\Phi$  decrease;
- $\Gamma'(0), h_d, \alpha, \bar{\eta}_\varphi, \bar{\eta}_\Gamma$  increase if  $c < 0$ , otherwise they decrease;
- $\varphi''(0)$  increases if  $c > 0$ , otherwise it decreases.

Further the thickness  $\delta$  of the boundary layer depends on  $M^2$  and decreases when  $M^2$  increases (as easily seen in Figures 4.19 and 4.20).

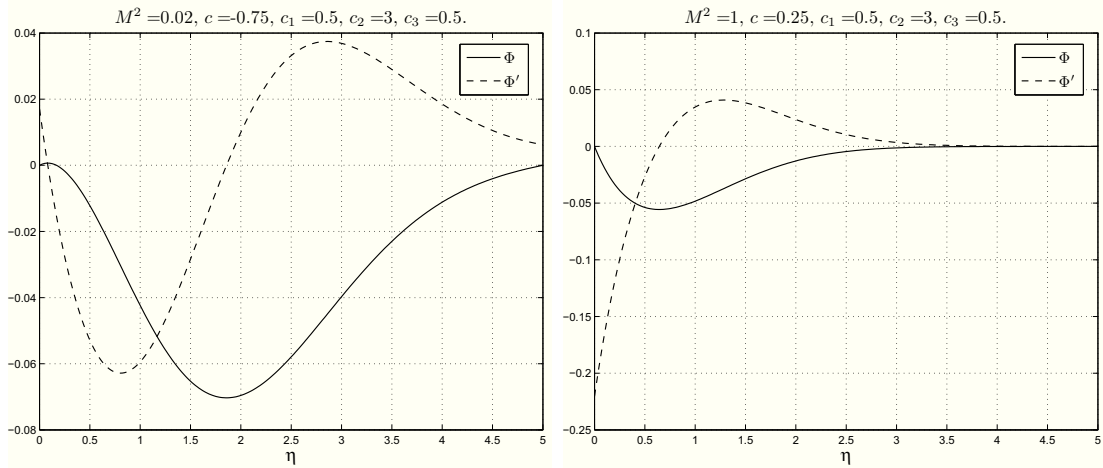


Figure 4.14: CASE I-M: the first picture shows the profiles of  $\Phi, \Phi'$  in the reverse microrotation. The second picture shows the profiles of  $\Phi, \Phi'$  in the absence of the reverse microrotation.

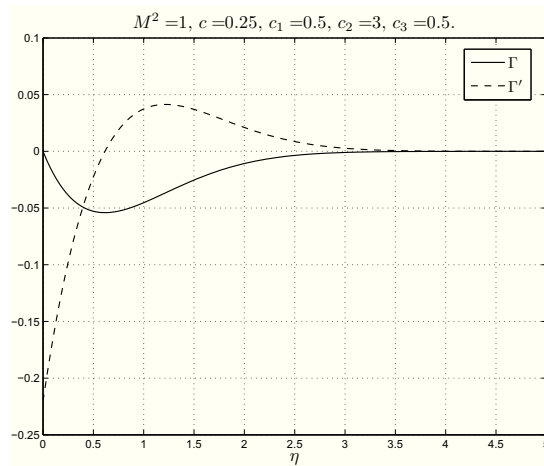


Figure 4.15: CASE I-M:  $\Gamma, \Gamma'$  profiles.

Table 4.9: CASE I-M: descriptive quantities of motion for some values of  $c$ ,  $c_1$ ,  $c_2$ ,  $c_3$ , and  $M^2$ .

$M^2$	$c$	$c_1$	$c_2$	$c_3$	$\varphi''(0)$	$\gamma''(0)$	$\Phi'(0)$	$\Gamma'(0)$	$h_d$	$\alpha$	$\beta$
1	-0.75	0.1	1.5	0.1	1.1944	0.4584	-0.0299	-0.0520	-1.7886	0.6856	1.5104
				0.5	1.1955	0.4582	-0.0309	-0.0501	-1.7837	0.6859	1.5091
		0.5	1.5	0.1	1.1976	0.4614	-0.0224	-0.0433	-1.8080	0.6867	1.5182
				0.5	1.1981	0.4613	-0.0227	-0.0425	-1.8063	0.6868	1.5178
		0.5	3.0	0.1	1.1505	0.4276	-0.1522	-0.2602	-1.5851	0.6693	1.4208
				0.5	1.1564	0.4264	-0.1577	-0.2508	-1.5581	0.6707	1.4137
	-0.25	0.1	1.5	0.1	1.1672	0.4425	-0.1128	-0.2167	-1.7045	0.6745	1.4675
				0.5	1.1697	0.4421	-0.1146	-0.2125	-1.6960	0.6752	1.4656
		0.5	3.0	0.1	1.2059	0.9134	-0.0456	-0.0525	0.5977	0.6656	0.8692
				0.5	1.2071	0.9137	-0.0457	-0.0505	0.5980	0.6658	0.8692
		0.5	1.5	0.1	1.2091	0.9168	-0.0367	-0.0438	0.5981	0.6665	0.8716
				0.5	1.2096	0.9169	-0.0368	-0.0429	0.5983	0.6666	0.8716
	0.25	0.1	1.5	0.1	1.1620	0.8720	-0.2288	-0.2627	0.5885	0.6508	0.8379
				0.5	1.1683	0.8739	-0.2295	-0.2528	0.5899	0.6520	0.8382
		0.5	3.0	0.1	1.1785	0.8896	-0.1838	-0.2190	0.5904	0.6554	0.8503
				0.5	1.1812	0.8902	-0.1844	-0.2146	0.5911	0.6559	0.8504
		0.5	1.5	0.1	1.2414	1.2433	-0.0534	-0.0539	0.6268	0.6223	0.6450
				0.5	1.2428	1.2442	-0.0522	-0.0516	0.6270	0.6225	0.6452
1.00	0.1	3.0	0.1	1.2445	1.2464	-0.0444	-0.0451	0.6276	0.6230	0.6459	
			0.5	1.2451	1.2467	-0.0440	-0.0440	0.6277	0.6231	0.6460	
	0.5	1.5	0.1	1.1977	1.2006	-0.2673	-0.2694	0.6139	0.6099	0.6302	
			0.5	1.2050	1.2054	-0.2617	-0.2582	0.6149	0.6109	0.6310	
	0.5	3.0	0.1	1.2138	1.2166	-0.2224	-0.2255	0.6177	0.6134	0.6349	
			0.5	1.2169	1.2185	-0.2204	-0.2204	0.6182	0.6139	0.6353	
2	-0.75	0.1	1.5	0.1	1.3110	1.6281	-0.0599	-0.0561	0.5267	0.5603	0.4932
				0.5	1.3127	1.6296	-0.0570	-0.0533	0.5269	0.5605	0.4933
	0.5	3.0	0.1	1.3139	1.6307	-0.0514	-0.0473	0.5272	0.5608	0.4935	
			0.5	1.3147	1.6314	-0.0500	-0.0460	0.5273	0.5609	0.4936	
	0.5	1.5	0.1	1.2682	1.5870	-0.2994	-0.2807	0.5182	0.5506	0.4857	
			0.5	1.2769	1.5944	-0.2854	-0.2668	0.5190	0.5515	0.4864	
-0.25	0.1	3.0	0.1	1.2832	1.6003	-0.2570	-0.2367	0.5204	0.5532	0.4876	
			0.5	1.2871	1.6038	-0.2504	-0.2305	0.5208	0.5537	0.4880	
	0.5	1.5	0.1	1.1715	1.0257	-0.0455	-0.0511	0.0257	0.7188	0.9499	
			0.5	1.1725	1.0252	-0.0468	-0.0493	0.0288	0.7190	0.9491	
	0.5	3.0	0.1	1.1748	1.0289	-0.0369	-0.0425	0.0207	0.7199	0.9530	
			0.5	1.1752	1.0288	-0.0375	-0.0417	0.0218	0.7200	0.9527	
-0.25	0.1	1.5	0.1	1.1274	0.9859	-0.2284	-0.2556	0.0744	0.7013	0.9102	
			0.5	1.1330	0.9832	-0.2351	-0.2468	0.0914	0.7024	0.9060	
	0.5	3.0	0.1	1.1444	1.0027	-0.1850	-0.2124	0.0455	0.7069	0.9273	
			0.5	1.1467	1.0018	-0.1876	-0.2085	0.0517	0.7075	0.9260	
	0.5	1.5	0.1	1.2015	1.3299	-0.0535	-0.0524	0.6698	0.6705	0.6725	
			0.5	1.2027	1.3301	-0.0535	-0.0504	0.6701	0.6707	0.6725	
-0.25	0.1	3.0	0.1	1.2047	1.3330	-0.0446	-0.0437	0.6706	0.6714	0.6737	
			0.5	1.2052	1.3330	-0.0446	-0.0428	0.6707	0.6715	0.6737	
	0.5	1.5	0.1	1.1575	1.2881	-0.2676	-0.2619	0.6560	0.6556	0.6545	
			0.5	1.1637	1.2893	-0.2682	-0.2521	0.6575	0.6567	0.6545	
	0.5	3.0	0.1	1.1741	1.3039	-0.2229	-0.2183	0.6599	0.6601	0.6608	
			0.5	1.1768	1.3043	-0.2235	-0.2139	0.6606	0.6607	0.6608	

Table 4.10: CASE I-M: continuum of Table 4.9.

$M^2$	$c$	$c_1$	$c_2$	$c_3$	$\varphi''(0)$	$\gamma''(0)$	$\Phi'(0)$	$\Gamma'(0)$	$h_d$	$\alpha$	$\beta$	
2	0.25	0.1	1.5	0.1	1.2443	1.5826	-0.0582	-0.0540	0.6050	0.6198	0.5459	
				0.5	1.2457	1.5833	-0.0570	-0.0516	0.6052	0.6200	0.5461	
		0.5	1.5	0.1	1.2474	1.5853	-0.0495	-0.0452	0.6057	0.6205	0.5466	
				0.5	1.2480	1.5857	-0.0490	-0.0441	0.6058	0.6206	0.5466	
		1.00	0.1	1.5	0.1	1.2007	1.5413	-0.2914	-0.2699	0.5930	0.6074	0.5355
					0.5	1.2080	1.5453	-0.2855	-0.2586	0.5940	0.6085	0.5361
	0.5	1.5	0.1	1.2167	1.5554	-0.2477	-0.2259	0.5965	0.6110	0.5386		
			0.5	1.2199	1.5571	-0.2454	-0.2209	0.5970	0.6115	0.5389		
	1.00	0.1	1.5	0.1	1.3183	1.9035	-0.0628	-0.0563	0.4993	0.5558	0.4427	
				0.5	1.3200	1.9048	-0.0599	-0.0534	0.4994	0.5560	0.4429	
	0.5	1.5	0.1	1.3212	1.9059	-0.0546	-0.0475	0.4997	0.5564	0.4430		
			0.5	1.3220	1.9065	-0.0532	-0.0462	0.4998	0.5565	0.4431		
	0.5	1.5	0.1	1.2757	1.8640	-0.3140	-0.2817	0.4915	0.5461	0.4368		
			0.5	1.2844	1.8706	-0.2999	-0.2677	0.4923	0.5472	0.4374		
	0.5	1.5	0.1	1.2905	1.8760	-0.2729	-0.2378	0.4935	0.5488	0.4382		
			0.5	1.2945	1.8792	-0.2660	-0.2314	0.4939	0.5493	0.4385		
	5	-0.75	0.1	1.5	0.1	1.1433	1.9885	-0.0618	-0.0500	1.5029	0.7595	0.5118
					0.5	1.1443	1.9880	-0.0635	-0.0483	1.5040	0.7597	0.5116
0.5			1.5	0.1	1.1468	1.9911	-0.0532	-0.0415	1.5051	0.7605	0.5124	
				0.5	1.1472	1.9908	-0.0539	-0.0407	1.5056	0.7606	0.5123	
0.5			1.5	0.1	1.0987	1.9494	-0.3091	-0.2498	1.4629	0.7418	0.5014	
				0.5	1.1038	1.9464	-0.3175	-0.2415	1.4687	0.7425	0.5005	
0.5		1.5	0.1	1.1163	1.9622	-0.2660	-0.2072	1.4742	0.7470	0.5047		
			0.5	1.1183	1.9610	-0.2697	-0.2034	1.4771	0.7475	0.5043		
-0.25		0.1	1.5	0.1	1.1946	2.1676	-0.0643	-0.0521	0.7550	0.6775	0.4452	
				0.5	1.1958	2.1677	-0.0644	-0.0502	0.7552	0.6777	0.4452	
		0.5	1.5	0.1	1.1979	2.1699	-0.0560	-0.0434	0.7560	0.6784	0.4456	
				0.5	1.1984	2.1700	-0.0561	-0.0425	0.7561	0.6785	0.4456	
		0.5	1.5	0.1	1.1505	2.1293	-0.3217	-0.2607	0.7375	0.6627	0.4381	
				0.5	1.1567	2.1297	-0.3223	-0.2510	0.7389	0.6637	0.4381	
0.5		1.5	0.1	1.1673	2.1410	-0.2799	-0.2171	0.7428	0.6671	0.4401		
			0.5	1.1699	2.1412	-0.2805	-0.2128	0.7435	0.6676	0.4401		
0.25		0.1	1.5	0.1	1.2495	2.3341	-0.0663	-0.0541	0.5725	0.6157	0.3998	
				0.5	1.2509	2.3346	-0.0650	-0.0518	0.5727	0.6159	0.3998	
	0.5	1.5	0.1	1.2526	2.3362	-0.0582	-0.0453	0.5731	0.6164	0.4000		
			0.5	1.2532	2.3365	-0.0577	-0.0443	0.5732	0.6165	0.4000		
	0.5	1.5	0.1	1.2061	2.2968	-0.3313	-0.2707	0.5616	0.6033	0.3945		
			0.5	1.2134	2.2995	-0.3253	-0.2593	0.5625	0.6045	0.3948		
0.5	1.5	0.1	1.2219	2.3075	-0.2911	-0.2267	0.5647	0.6070	0.3958			
		0.5	1.2251	2.3087	-0.2884	-0.2216	0.5652	0.6075	0.3960			
1.00	0.1	1.5	0.1	1.3330	2.5646	-0.0684	-0.0567	0.4497	0.5474	0.3521		
			0.5	1.3347	2.5656	-0.0656	-0.0538	0.4499	0.5476	0.3522		
	0.5	1.5	0.1	1.3359	2.5665	-0.0608	-0.0479	0.4501	0.5479	0.3523		
			0.5	1.3367	2.5670	-0.0594	-0.0466	0.4502	0.5480	0.3523		
	0.5	1.5	0.1	1.2909	2.5289	-0.3421	-0.2837	0.4431	0.5377	0.3485		
			0.5	1.2996	2.5339	-0.3282	-0.2694	0.4438	0.5388	0.3488		
0.5	1.5	0.1	1.3054	2.5383	-0.3042	-0.2398	0.4448	0.5404	0.3493			
		0.5	1.3094	2.5408	-0.2969	-0.2332	0.4452	0.5409	0.3495			

Table 4.11: CASE I-M: descriptive quantities of boundary layer for some values of  $c$ ,  $c_1$ ,  $c_2$ ,  $c_3$ , and  $M^2$ .

$M^2$	$c$	$c_1$	$c_2$	$c_3$	$\bar{\eta}_\varphi$	$\bar{\eta}_\gamma$	$\bar{\eta}_\Phi$	$\bar{\eta}_\Gamma$	$\delta_v$	$\delta_w$	$\delta$	
1	-0.75	0.1	1.5	0.1	2.6324	4.4061	2.8389	1.6521	4.4061	2.8389	4.4061	
				0.5	2.6456	4.4085	2.8391	1.4082	4.4085	2.8391	4.4085	
		0.5	3.0	1.5	0.1	2.6606	4.4420	1.2244	0.9894	4.4420	1.2244	4.4420
					0.5	2.6664	4.4430	1.2270	0.8414	4.4430	1.2270	4.4430
			1.5	0.1	2.3779	3.9683	4.3190	3.0868	3.9683	4.3190	4.3190	
					0.5	2.4267	3.9708	4.1848	2.6951	3.9708	4.1848	4.1848
	3.0		0.1	2.4981	4.2676	3.8460	2.4566	4.2676	3.8460	4.2676		
				0.5	2.5246	4.2738	3.7663	2.2739	4.2738	3.7663	4.2738	
	-0.25	0.1	1.5	0.1	2.4626	2.9763	2.0094	1.6307	2.9763	2.0094	2.9763	
					0.5	2.4741	2.9868	1.8741	1.3742	2.9868	1.8741	2.9868
			3.0	0.1	2.4862	3.0164	1.1615	0.9980	3.0164	1.1615	3.0164	
					0.5	2.4914	3.0209	1.1305	0.8469	3.0209	1.1305	3.0209
			0.5	1.5	0.1	2.2411	2.6386	3.3984	2.9919	2.6386	3.3984	3.3984
						0.5	2.2837	2.6713	3.0574	2.5513	2.6713	3.0574
		3.0	0.1	2.3426	2.8206	2.7874	2.4016	2.8206	2.7874	2.8206		
				0.5	2.3667	2.8404	2.6373	2.1961	2.8404	2.6373	2.8404	
		0.25	0.1	1.5	0.1	2.1962	2.2724	1.6337	1.5637	2.2724	1.6337	2.2724
						0.5	2.2069	2.2816	1.4150	1.2847	2.2816	1.4150
			3.0	0.1	2.2146	2.2937	1.0270	0.9997	2.2937	1.0270	2.2937	
					0.5	2.2197	2.2981	0.9270	0.8394	2.2981	0.9270	2.2981
	0.5		1.5	0.1	2.0172	2.0734	2.9063	2.8229	2.0734	2.9063	2.9063	
					0.5	2.0564	2.1046	2.4401	2.3142	2.1046	2.4401	2.4401
	3.0	0.1	2.0946	2.1636	2.3434	2.2801	2.1636	2.3434	2.3434			
			0.5	2.1176	2.1826	2.1302	2.0359	2.1826	2.1302	2.1826		
1.00	0.1	1.5	0.1	1.8856	1.7651	1.3137	1.4440	1.8856	1.4440	1.8856		
				0.5	1.8952	1.7719	1.0337	1.1384	1.8952	1.1384	1.8952	
		3.0	0.1	1.8986	1.7754	0.8585	0.9722	1.8986	0.9722	1.8986		
				0.5	1.9036	1.7792	0.6894	0.7942	1.9036	0.7942	1.9036	
		0.5	1.5	0.1	1.7501	1.6482	2.4856	2.5938	1.7501	2.5938	2.5938	
					0.5	1.7859	1.6732	1.9286	2.0134	1.7859	2.0134	2.0134
	3.0	0.1	1.8037	1.6912	1.9994	2.1059	1.8037	2.1059	2.1059			
			0.5	1.8257	1.7077	1.7211	1.8116	1.8257	1.8116	1.8257		
	2	-0.75	0.1	1.5	0.1	2.8486	3.7930	2.0517	1.6916	3.7930	2.0517	3.7930
					0.5	2.8613	3.7840	2.1804	1.4634	3.7840	2.1804	3.7840
			3.0	0.1	2.8803	3.8471	0.8920	0.9792	3.8471	0.9792	3.8471	
					0.5	2.8856	3.8453	1.0419	0.8332	3.8453	1.0419	3.8453
0.5			1.5	0.1	2.5638	3.3081	3.7733	3.1983	3.3081	3.7733	3.7733	
					0.5	2.6121	3.2521	3.7473	2.8538	3.2521	3.7473	3.7473
3.0		0.1	2.7038	3.6080	3.0478	2.5381	3.6080	3.0478	3.6080			
			0.5	2.7286	3.5968	3.0514	2.3802	3.5968	3.0514	3.5968		
-0.25		0.1	1.5	0.1	2.4866	2.5749	1.6911	1.6382	2.5749	1.6911	2.5749	
					0.5	2.4981	2.5788	1.6012	1.3837	2.5788	1.6012	2.5788
		3.0	0.1	2.5106	2.6039	0.9775	0.9984	2.6039	0.9984	2.6039		
				0.5	2.5158	2.6061	0.9609	0.8477	2.6061	0.9609	2.6061	
	0.5	1.5	0.1	2.2627	2.3186	3.1048	3.0069	2.3186	3.1048	3.1048		
				0.5	2.3052	2.3269	2.8089	2.5711	2.3269	2.8089	2.8089	
3.0	0.1	2.3657	2.4436	2.4707	2.4137	2.4436	2.4707	2.4707				
		0.5	2.3896	2.4522	2.3514	2.2112	2.4522	2.3514	2.4522			

Table 4.12: CASE I-M: continuum of Table 4.11.

$M^2$	$c$	$c_1$	$c_2$	$c_3$	$\bar{\eta}_\varphi$	$\bar{\eta}_\gamma$	$\bar{\eta}_\Phi$	$\bar{\eta}_\Gamma$	$\delta_v$	$\delta_w$	$\delta$	
2	0.25	0.1	1.5	0.1	2.1864	2.0577	1.4499	1.5592	2.1864	1.5592	2.1864	
				0.5	2.1971	2.0632	1.2604	1.2794	2.1971	1.2794	2.1971	
		0.5	3.0	0.1	2.2046	2.0739	0.8937	0.9985	2.2046	0.9985	2.2046	
				0.5	2.2097	2.0769	0.8067	0.8377	2.2097	0.8377	2.2097	
		1.5	0.5	0.1	2.0081	1.8952	2.7379	2.8159	2.0081	2.8159	2.0081	
				0.5	2.0474	1.9126	2.2976	2.3052	2.0474	2.3052	2.0474	
	3.0	0.1	0.1	2.0849	1.9624	2.1747	2.2741	2.0849	2.2741	2.0849		
			0.5	2.1081	1.9749	1.9789	2.0286	2.1081	2.0286	2.1081		
	1.00	0.1	1.5	0.1	1.8707	1.6522	1.2062	1.4349	1.8707	1.4349	1.8707	
				0.5	1.8804	1.6572	0.9452	1.1282	1.8804	1.1282	1.8804	
		0.5	3.0	0.1	1.8834	1.6607	0.7702	0.9677	1.8834	0.9677	1.8834	
				0.5	1.8886	1.6637	0.6005	0.7889	1.8886	0.7889	1.8886	
		1.5	0.5	0.1	1.7361	1.5512	2.3901	2.5816	1.7361	2.5816	1.7361	
				0.5	1.7721	1.5691	1.8492	1.9989	1.7721	1.9989	1.7721	
	3.0	0.1	0.1	1.7892	1.5857	1.9081	2.0954	1.7892	2.0954	1.7892		
			0.5	1.8114	1.5984	1.6404	1.7992	1.8114	1.7992	1.8114		
	5	-0.75	0.1	1.5	0.1	3.0911	2.3136	1.4057	1.7379	3.0911	1.7379	3.0911
					0.5	3.1026	2.3076	1.5639	1.5262	3.1026	1.5639	3.1026
0.5			3.0	0.1	3.1253	2.3336	0.7609	0.9647	3.1253	0.9647	3.1253	
				0.5	3.1296	2.3312	0.8454	0.8149	3.1296	0.8454	3.1296	
1.5			0.5	0.1	2.7848	2.1161	2.9474	3.3251	2.7848	3.3251	2.7848	
				0.5	2.8309	2.0942	3.1013	3.0289	2.8309	3.1013	2.8309	
3.0		0.1	0.1	2.9399	2.1987	2.2239	2.6329	2.9399	2.6329	2.9399		
			0.5	2.9616	2.1876	2.2894	2.4999	2.9616	2.4999	2.9616		
-0.25		0.1	1.5	0.1	2.5183	1.8996	1.2584	1.6494	2.5183	1.6494	2.5183	
				0.5	2.5296	1.8987	1.2194	1.3974	2.5296	1.3974	2.5296	
		0.5	3.0	0.1	2.5426	1.9112	0.7170	0.9995	2.5426	0.9995	2.5426	
				0.5	2.5476	1.9112	0.7140	0.8494	2.5476	0.8494	2.5476	
		1.5	0.5	0.1	2.2921	1.7666	2.6516	3.0276	2.2921	3.0276	2.2921	
				0.5	2.3341	1.7612	2.4346	2.5979	2.3341	2.5979	2.3341	
3.0		0.1	0.1	2.3967	1.8144	2.0307	2.4309	2.3967	2.4309	2.3967		
			0.5	2.4201	1.8139	1.9547	2.2321	2.4201	2.2321	2.4201		
0.25		0.1	1.5	0.1	2.1709	1.6502	1.1357	1.5516	2.1709	1.5516	2.1709	
				0.5	2.1816	1.6512	0.9944	1.2705	2.1816	1.2705	2.1816	
	0.5	3.0	0.1	2.1889	1.6579	0.6640	0.9960	2.1889	0.9960	2.1889		
			0.5	2.1942	1.6589	0.5874	0.8345	2.1942	0.8345	2.1942		
	1.5	0.5	0.1	1.9936	1.5519	2.4351	2.8046	1.9936	2.8046	1.9936		
			0.5	2.0331	1.5539	2.0471	2.2911	2.0331	2.2911	2.0331		
3.0	0.1	0.1	2.0697	1.5832	1.8864	2.2642	2.0697	2.2642	2.0697			
		0.5	2.0932	1.5867	1.7224	2.0169	2.0932	2.0169	2.0932			
1.00	0.1	1.5	0.1	1.8432	1.4119	0.9877	1.4172	1.8432	1.4172	1.8432		
			0.5	1.8529	1.4137	0.7647	1.1087	1.8529	1.1087	1.8529		
	0.5	3.0	0.1	1.8557	1.4165	0.5817	0.9585	1.8557	0.9585	1.8557		
			0.5	1.8609	1.4179	0.4265	0.7779	1.8609	0.7779	1.8609		
	1.5	0.5	0.1	1.7102	1.3427	2.1924	2.5591	1.7102	2.5591	1.7102		
			0.5	1.7466	1.3489	1.6889	1.9722	1.7466	1.9722	1.7466		
3.0	0.1	0.1	1.7624	1.3615	1.7244	2.0757	1.7624	2.0757	1.7624			
		0.5	1.7849	1.3674	1.4800	1.7761	1.7849	1.7761	1.7849			

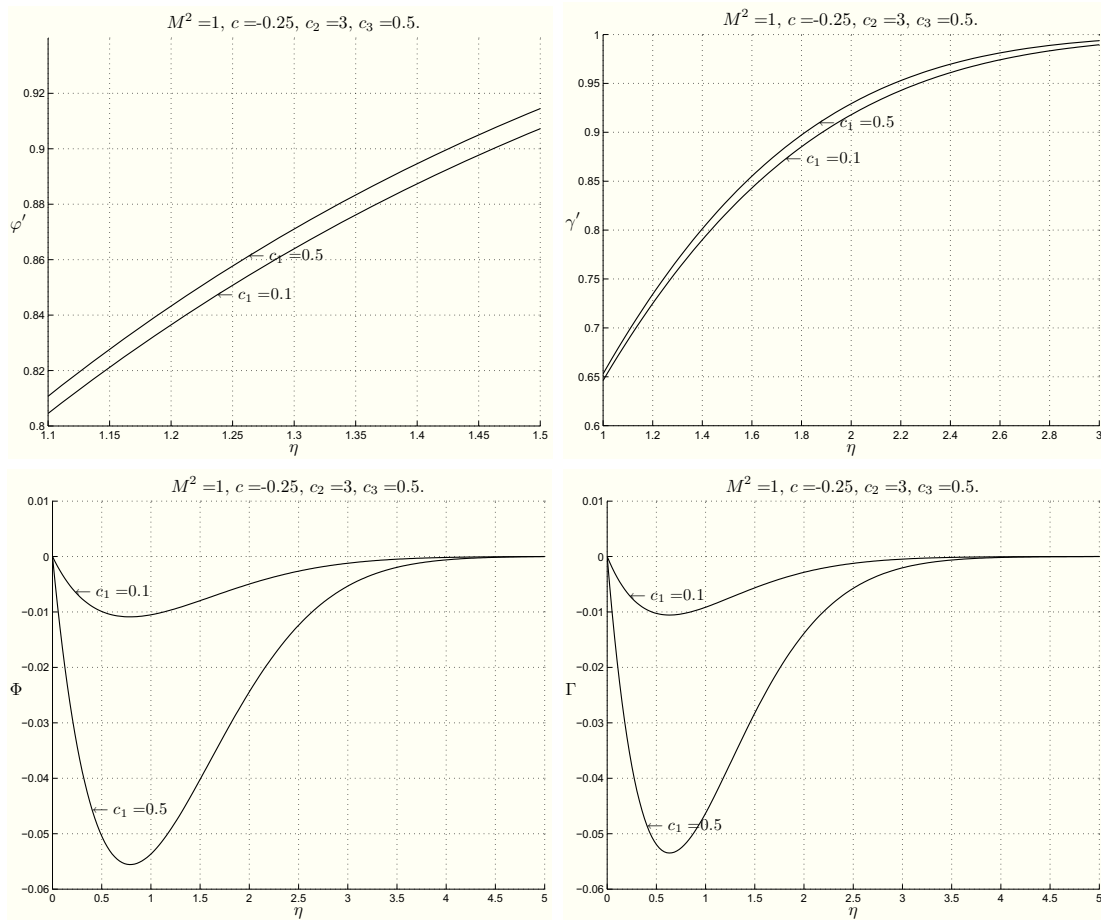


Figure 4.16: CASE I-M:  $\varphi'$ ,  $\gamma'$ ,  $\Phi$ ,  $\Gamma$  profiles for  $M^2 = 1$ ,  $c_2 = 3$ ,  $c_3 = 0.5$ ,  $c = -0.25$  when  $c_1 = 0.1$  and  $c_1 = 0.5$ .

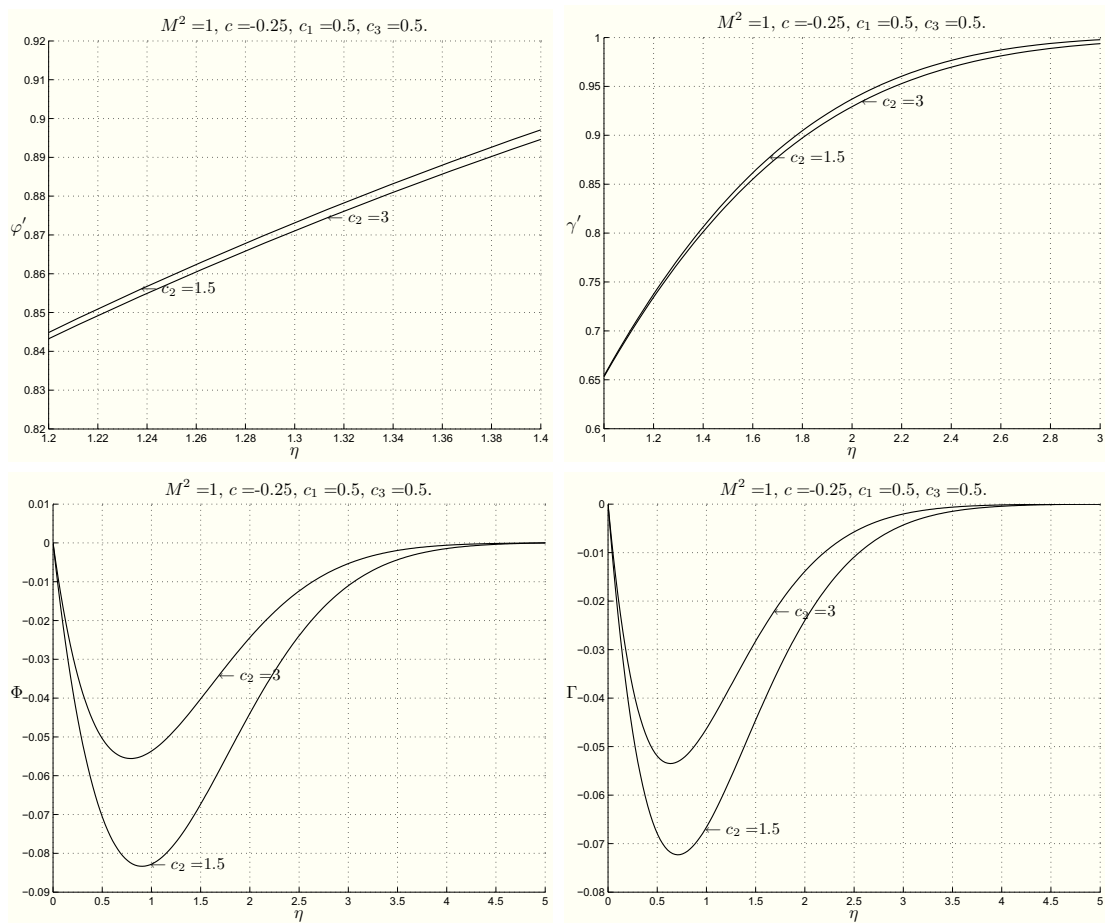


Figure 4.17: CASE I-M:  $\varphi'$ ,  $\gamma'$ ,  $\Phi$ ,  $\Gamma$  profiles for  $M^2 = 1$ ,  $c_1 = 0.5$ ,  $c_3 = 0.5$ ,  $c = -0.25$  when  $c_2 = 1.5$  and  $c_2 = 3$ .

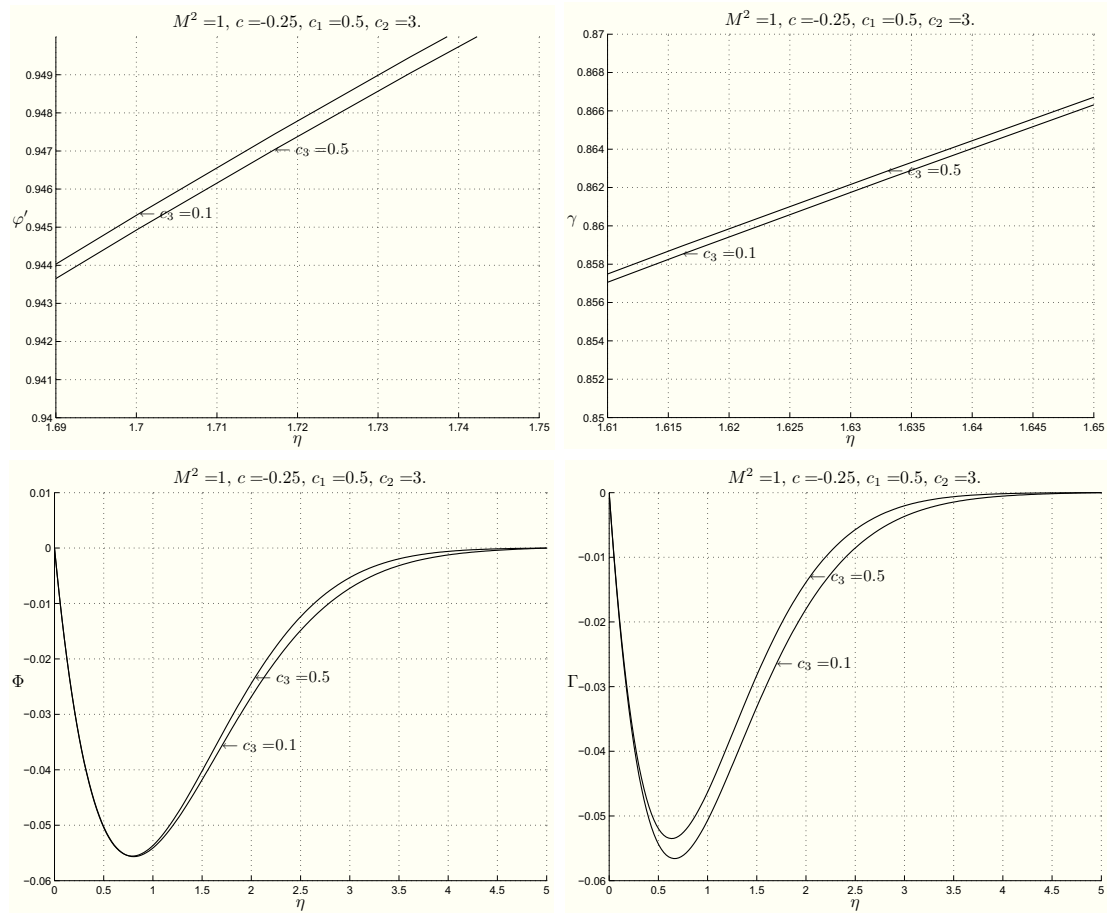


Figure 4.18: CASE I-M:  $\varphi'$ ,  $\gamma'$ ,  $\Phi$ ,  $\Gamma$  profiles for  $M^2 = 1$ ,  $c_1 = 0.5$ ,  $c_2 = 3$ ,  $c = -0.25$  when  $c_3 = 0.1$  and  $c_3 = 0.5$ .

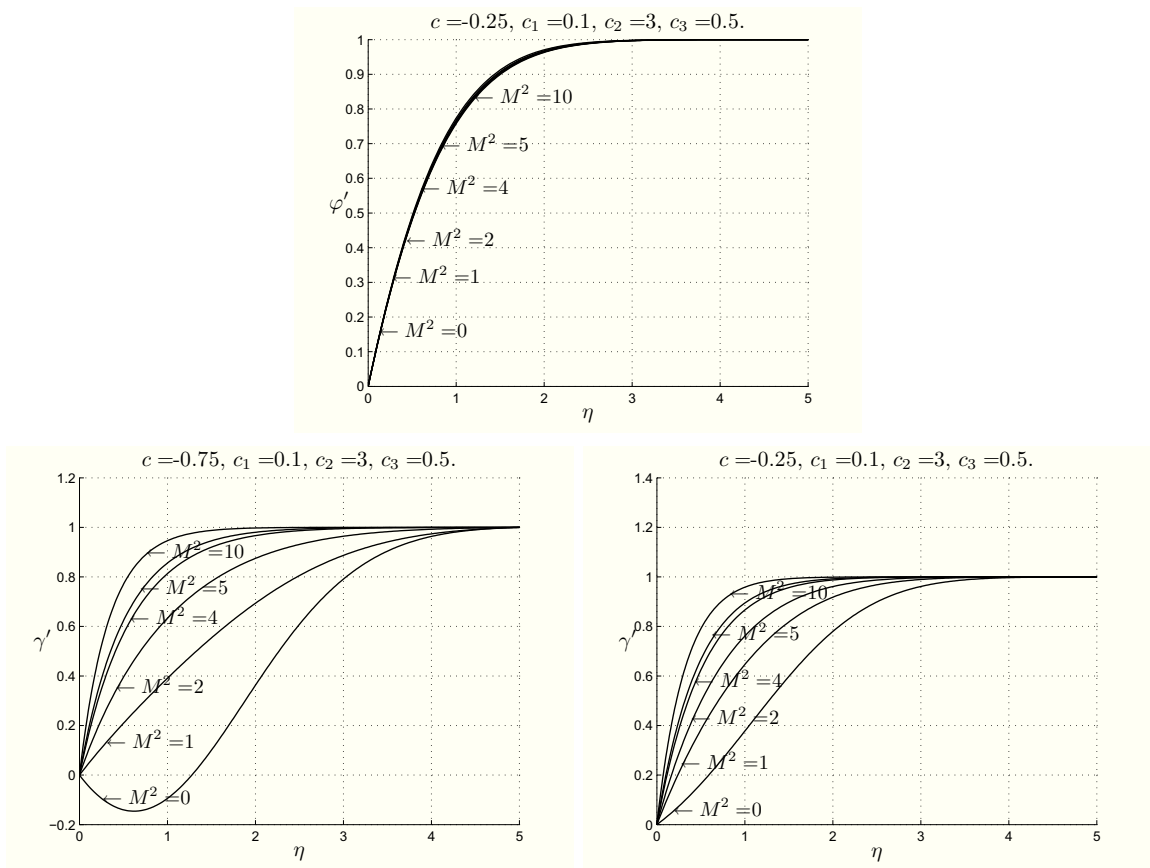


Figure 4.19: CASE I-M: profiles of  $\varphi'$  (Figure 4.19<sub>1</sub>) and  $\gamma'$  (Figures 4.19<sub>2,3</sub>) for several values of  $M^2$  which elucidate the boundary layer thickness.

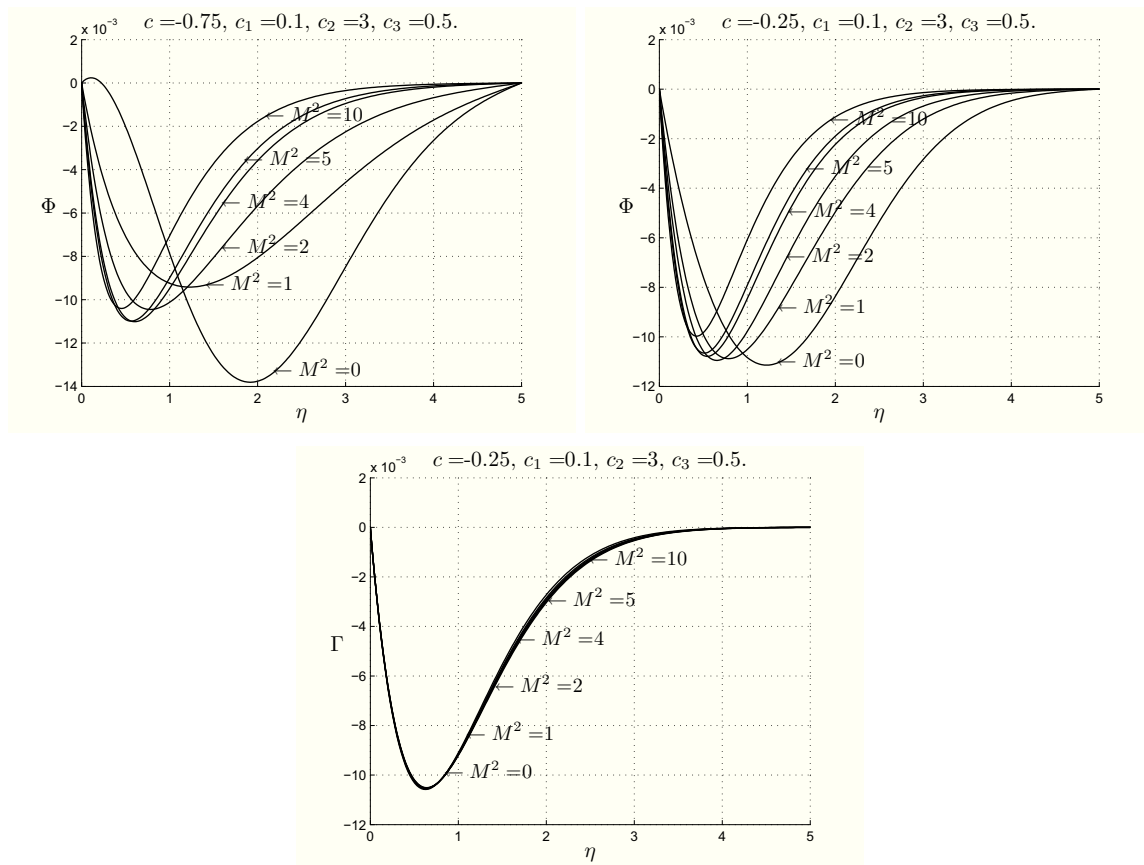


Figure 4.20: CASE I-M: profiles of  $\Phi$  (Figure 4.20<sub>1,2</sub>) and  $\Gamma$  (Figures 4.20<sub>3</sub>) for several values of  $M^2$  which elucidate the boundary layer thickness.

As it was underlined in Remark 4.3.8, the magnetic field tends to prevent the occurrence of the reverse flow. So Tables 4.13-4.14 show that as the Hartmann number  $M^2$  increases, the values of  $c_r$  and of  $c_{rw}$  for the reverse flow and the reverse microrotation decrease. In particular, for example for  $c_1 = 0.1, c_2 = 3.0, c_3 = 0.1$ , from  $M^2 = 0.7810 =: M_r^2$  ( $M^2 = 0.5148 =: M_{rw}^2$ ), the reverse flow (the reverse microrotation) does not occur at all for any value of  $c$ . This fact can be explained by observing that

$$\frac{\partial p}{\partial x_3} = -\rho a^2 c x_3 (c + M^2),$$

from which one can see that the signs of  $c$  and of  $(c + M^2)$  modify the sign of  $\frac{\partial p}{\partial x_3}$ . From Tables 4.9-4.10 and 4.13-4.14 we note that the value of  $h_d$ , which is the height of the plane towards which the inviscid fluid moves, regardless of the values of  $M^2$ , increases if  $c < 0$ , while it decreases if  $c > 0$ . We have  $c_h \geq c_r$ , which means that the three-dimensional displacement thickness is always negative when the reverse flow and the reverse microrotation appear (see Tables 4.13-4.14). The presence of  $M^2$  influences  $c_h$  and it decreases when  $M^2$  increases and, for example for  $c_1 = 0.1, c_2 = 3.0, c_3 = 0.1$ , starting from  $M^2 = 3.3148$ , we have that  $h_d$  is always positive.

As far as the classification of the stagnation-point is concerned, Tables 4.15-4.16 show that  $\varphi''(0) + c\gamma''(0)$  can be negative for large values of  $M^2$ , as it happened in CASE I-N.

We have a very interesting result: for negative values of  $c$  when  $M^2 \geq M_s^2$  (see Table 4.17), the origin becomes a point of separation, unlike what occurs in the absence of the magnetic field or in the next two cases, as we will see. We note that if  $M^2 < M_s^2$ , then the stagnation-point is always a point of attachment. Moreover, if  $c > 0$  or where there is the reverse flow, the origin is a nodal point, while when  $c < 0$  and the reverse flow does not appear, it is a saddle point (as we can see from Tables 4.9-4.10, 4.15-4.16).

In Table 4.18, for some values of  $M^2 \geq M_s^2$ , we list the negative value of  $c$  ( $c_s$ ), for which if  $c < c_s$  then the origin is a separation point, while if  $c \geq c_s$  then it is an attachment point. The form of system (4.58) explain the change of the origin from attachment point to separation point. Since  $M^2$  directly influences  $\gamma$  and only indirectly influences  $\varphi$ , when  $M^2$  increases,  $\gamma''(0)$  becomes much greater than  $\varphi''(0)$  as we can see from Tables 4.9-4.10, 4.15-4.16.

Figure 4.21 summarizes the classification of the stagnation-point in dependence on  $M^2$  and  $c$ .

Table 4.13: CASE I-M: values of  $c_r$ ,  $c_{rw}$  and  $c_h$  when  $M^2$  increases.

$c_1$	$c_2$	$c_3$	$M^2$	$c_r$	$c_{rw}$	$c_h$	
0.10	1.50	0.10	0	-0.4271	-0.7606	-0.3953	
			0.10	-0.4974	-0.8315	-0.4131	
			0.20	-0.5682	-0.9020	-0.4309	
			0.30	-0.6397	-0.9725	-0.4487	
			0.3388	-0.6676	no reverse microrotation	-0.4556	
			0.40	-0.7120	no reverse microrotation	-0.4665	
			0.50	-0.7852	no reverse microrotation	-0.4843	
			0.60	-0.8596	no reverse microrotation	-0.5022	
			0.70	-0.9354	no reverse microrotation	-0.5200	
			0.7836	no reverse flow	no reverse microrotation	-0.5349	
			0.80	no reverse flow	no reverse microrotation	-0.5379	
			3.3118	no reverse flow	no reverse microrotation	$h = 0$	
			0.50	0	-0.4273	-0.7813	-0.3953
				0.10	-0.4975	-0.8546	-0.4131
				0.20	-0.5682	-0.9276	-0.4309
				0.2991	-0.6390	no reverse microrotation	-0.4485
				0.30	-0.6396	no reverse microrotation	-0.4488
				0.40	-0.7119	no reverse microrotation	-0.4666
				0.50	-0.7851	no reverse microrotation	-0.4845
				0.60	-0.8594	no reverse microrotation	-0.5023
0.70	-0.9352	no reverse microrotation		-0.5202			
0.7841	no reverse flow	no reverse microrotation		-0.5350			
0.80	no reverse flow	no reverse microrotation		-0.5381			
3.3084	no reverse flow	no reverse microrotation		$h = 0$			
3.00	0.10	0.10	0	-0.4286	-0.6428	-0.3941	
			0.10	-0.4989	-0.7116	-0.4119	
			0.20	-0.5697	-0.7805	-0.4297	
			0.30	-0.6412	-0.8497	-0.4475	
			0.40	-0.7136	-0.9192	-0.4654	
			0.50	-0.7869	-0.9895	-0.4832	
			0.5148	-0.7979	no reverse microrotation	-0.4858	
			0.60	-0.8615	no reverse microrotation	-0.5010	
			0.70	-0.9374	no reverse microrotation	-0.5189	
			0.7810	no reverse flow	no reverse microrotation	-0.5334	
			0.80	no reverse flow	no reverse microrotation	-0.5368	
			3.3148	no reverse flow	no reverse microrotation	$h = 0$	
			0.50	0	-0.4286	-0.6500	-0.3941
				0.10	-0.4989	-0.7193	-0.4119
				0.20	-0.5697	-0.7887	-0.4297
				0.30	-0.6412	-0.8584	-0.4476
				0.40	-0.7135	-0.9284	-0.4654
				0.50	-0.7869	-0.9991	-0.4833
				0.5011	-0.7877	no reverse microrotation	-0.4835
				0.60	-0.8614	no reverse microrotation	-0.5011
0.70	-0.9373	no reverse microrotation		-0.5190			
0.7811	no reverse flow	no reverse microrotation		-0.5335			
0.80	no reverse flow	no reverse microrotation		-0.5369			
3.3134	no reverse flow	no reverse microrotation		$h = 0$			



Table 4.15: CASE I-M: values of  $\varphi''(0) + c\gamma''(0)$  and  $c\varphi''(0)\gamma''(0)$  in dependence on the values of  $c$ ,  $c_1$ ,  $c_2$ ,  $c_3$ , and  $M^2$ .

$M^2$	$c$	$c_1$	$c_2$	$c_3$	$\varphi''(0)$	$\gamma''(0)$	$\varphi''(0) + c\gamma''(0)$	$c\varphi''(0)\gamma''(0)$	
1	-0.60	0.10	1.50	0.10	1.1938	0.6134	0.8258	-0.4394	
				0.50	1.1950	0.6133	0.8270	-0.4397	
			3.00	0.10	1.1971	0.6166	0.8271	-0.4428	
				0.50	1.1975	0.6165	0.8276	-0.4430	
			0.50	1.50	0.10	1.1499	0.5780	0.8032	-0.3988
					0.50	1.1558	0.5774	0.8094	-0.45
	3.	0.10		1.1666	0.5945	0.8099	-0.4161		
		0.50		1.1691	0.5943	0.8125	-0.4168		
	-0.45	0.10	1.50	0.10	1.1971	0.7516	0.8588	-0.4049	
				0.50	1.1982	0.7517	0.86	-0.4053	
			3.00	0.10	1.23	0.7550	0.8606	-0.4078	
				0.50	1.28	0.7550	0.8610	-0.4080	
			0.50	1.50	0.10	1.1532	0.7128	0.8324	-0.3699
					0.50	1.1592	0.7132	0.8383	-0.3721
		3.00		0.10	1.1698	0.7302	0.8412	-0.3844	
				0.50	1.1723	0.7303	0.8437	-0.3853	
		-0.40	0.10	1.50	0.10	1.1988	0.7942	0.8811	-0.3809
					0.50	1.20	0.7944	0.8823	-0.3813
				3.00	0.10	1.2021	0.7976	0.8830	-0.3835
					0.50	1.2026	0.7977	0.8835	-0.3837
	0.50			1.50	0.10	1.1550	0.7546	0.8531	-0.3486
					0.50	1.1611	0.7554	0.8589	-0.3508
	-0.10	0.10	1.50	0.10	1.2149	1.0216	1.1128	-0.1241	
				0.50	1.2162	1.0221	1.1140	-0.1243	
3.00			0.10	1.2181	1.0249	1.1156	-0.1248		
			0.50	1.2187	1.0251	1.1162	-0.1249		
0.50			1.50	0.10	1.1711	0.9794	1.0731	-0.1147	
				0.50	1.1776	0.9822	1.0794	-0.1157	
10	-0.60	0.10	1.50	0.10	1.1437	3.0219	-0.6694	-2.0736	
				0.50	1.1447	3.0216	-0.6682	-2.0753	
			3.00	0.10	1.1471	3.0236	-0.6671	-2.0811	
				0.50	1.1475	3.0235	-0.6666	-2.0817	
			0.50	1.50	0.10	1.0987	2.9878	-0.6940	-1.9696
					0.50	1.1039	2.9862	-0.6878	-1.9780
	3.00	0.10		1.1164	2.9966	-0.6816	-2.72		
		0.50		1.1185	2.9959	-0.6790	-2.0105		
	-0.45	0.10	1.50	0.10	1.1632	3.0589	-0.2133	-1.6011	
				0.50	1.1643	3.0587	-0.2122	-1.6025	
			3.00	0.10	1.1666	3.0606	-0.2107	-1.6067	
				0.50	1.1670	3.0605	-0.2102	-1.6072	
0.50			1.50	0.10	1.1184	3.0250	-0.2428	-1.5225	
				0.50	1.1241	3.0242	-0.2368	-1.5298	
3.00	0.10	1.1358	3.0337	-0.2294	-1.5505				
	0.50	1.1381	3.0333	-0.2269	-1.5535				

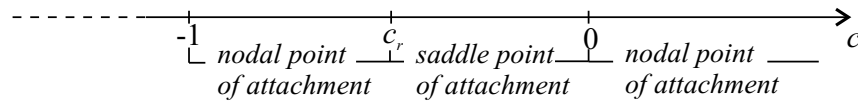
Table 4.16: CASE I-M: continuum of Table 4.15

$M^2$	$c$	$c_1$	$c_2$	$c_3$	$\varphi''(0)$	$\gamma''(0)$	$\varphi''(0) + c\gamma''(0)$	$c\varphi''(0)\gamma''(0)$	
10	-0.40	0.10	1.50	0.10	1.1697	3.0711	-0.0588	-1.4369	
				0.50	1.1708	3.0710	-0.0576	-1.4382	
		0.50	1.50	0.10	1.1731	3.0728	-0.0561	-1.4418	
				0.50	1.1735	3.0728	-0.0556	-1.4424	
		3.00	0.10	1.1250	3.0374	-0.0899	-1.3669		
				0.50	1.1308	3.0368	-0.0839	-1.3736	
	3.00	0.10	1.1423	3.0459	-0.0761	-1.3918			
			0.50	1.1447	3.0456	-0.0736	-1.3945		
	-0.10	0.10	1.50	0.10	1.2088	3.1437	0.8945	-0.38	
				0.50	1.2101	3.1438	0.8957	-0.3804	
		3.00	0.10	1.2121	3.1453	0.8975	-0.3812		
				0.50	1.2126	3.1454	0.8981	-0.3814	
		0.50	1.50	0.10	1.1648	3.1104	0.8538	-0.3623	
				0.50	1.1713	3.1111	0.8602	-0.3644	
	3.00	0.10	1.1814	3.1186	0.8695	-0.3684			
			0.50	1.1841	3.1189	0.8722	-0.3693		
	30	-0.60	0.10	1.50	0.10	1.1237	5.3927	-2.1120	-3.6358
					0.50	1.1246	5.3926	-2.1109	-3.6388
3.00			0.10	1.1272	5.3936	-2.1090	-3.6477		
				0.50	1.1276	5.3935	-2.1085	-3.6489	
0.50			1.50	0.10	1.0782	5.3678	-2.1425	-3.4724	
				0.50	1.0833	5.3669	-2.1369	-3.4883	
3.00		0.10	1.0962	5.3722	-2.1271	-3.5334			
			0.50	1.0982	5.3717	-2.1248	-3.5396		
-0.45		0.10	1.50	0.10	1.1485	5.4136	-1.2877	-2.7978	
				0.50	1.1495	5.4135	-1.2866	-2.84	
		3.00	0.10	1.1519	5.4145	-1.2846	-2.8066		
				0.50	1.1523	5.4144	-1.2842	-2.8076	
		0.50	1.50	0.10	1.1033	5.3888	-1.3216	-2.6755	
				0.50	1.1089	5.3883	-1.3158	-2.6887	
3.00		0.10	1.1210	5.3931	-1.3060	-2.7205			
			0.50	1.1232	5.3928	-1.3036	-2.7258		
-0.40		0.10	1.50	0.10	1.1567	5.4206	-1.0115	-2.5080	
				0.50	1.1578	5.4205	-1.0104	-2.5104	
	3.00	0.10	1.1601	5.4214	-1.85	-2.5158			
			0.50	1.1606	5.4214	-1.80	-2.5168		
	0.50	1.50	0.10	1.1117	5.3958	-1.0466	-2.3994		
			0.50	1.1174	5.3954	-1.0407	-2.4115		
3.00	0.10	1.1292	5.41	-1.0308	-2.4391				
		0.50	1.1315	5.3999	-1.0284	-2.4440			
-0.10	0.10	1.50	0.10	1.2057	5.4621	0.6595	-0.6586		
			0.50	1.2070	5.4622	0.6608	-0.6593		
	3.00	0.10	1.2090	5.4629	0.6627	-0.6605			
			0.50	1.2095	5.4630	0.6632	-0.6608		
	0.50	1.50	0.10	1.1616	5.4375	0.6179	-0.6316		
			0.50	1.1681	5.4378	0.6244	-0.6352		
3.00	0.10	1.1782	5.4417	0.6341	-0.6412				
		0.50	1.1810	5.4418	0.6368	-0.6427			

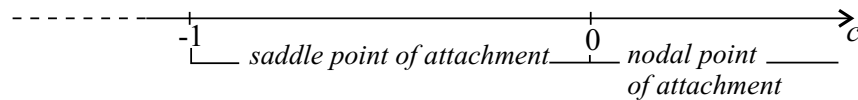
Table 4.17: CASE I-M: values of  $M^2$  ( $M_s^2$ ) starting from which the origin becomes a point of separation for different values of  $c_1$ ,  $c_2$  and  $c_3$ .

$c_1$	$c_2$	$c_3$	$M_s^2$
0.10	1.50	0.10	2.6635
		0.50	2.6681
	3.00	0.10	2.6640
		0.50	2.6656
0.50	1.50	0.10	2.6525
		0.50	2.6766
	3.00	0.10	2.6547
		0.50	2.6633

$M^2 < M_r^2$  (reverse flow in  $(-1, c_r)$ )



$M_r^2 \leq M^2 < M_s^2$  (no reverse flow)



$M^2 \geq M_s^2$  (no reverse flow)

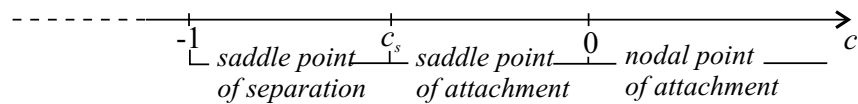


Figure 4.21: CASE I-M: classification of the stagnation-point in dependence on  $M^2$  and  $c$  (for example if  $c_1 = 0.1$ ,  $c_2 = 3.0$  and  $c_3 = 0.1$ , then  $M_r^2 = 0.7810$  and  $M_s^2 = 2.6640$ , see Tables 4.13-4.14 and 4.17).

Table 4.18: CASE I-M: values of  $c_s$  when  $M^2$  increases (separation point - attachment point) for different values of  $c_1$ ,  $c_2$  and  $c_3$ .

$c_1$	$c_2$	$c_3$	$M^2$	$c_s$		
0.10	1.50	0.10	4	-0.6565		
			5	-0.5649		
			10	-0.3811		
			15	-0.3088		
	0.10	3.00	0.50	4	-0.6573	
				5	-0.5655	
				10	-0.3815	
				15	-0.3091	
		0.10	3.00	0.10	4	-0.6575
					5	-0.5659
					10	-0.3820
					15	-0.3095
0.10			3.00	0.50	4	-0.6579
					5	-0.5662
					10	-0.3821
					15	-0.3097
	0.50		1.50	0.10	4	-0.6448
					5	-0.5531
					10	-0.3708
					15	-0.2997
		0.50	3.00	0.50	4	-0.6492
					5	-0.5564
					10	-0.3727
					15	-0.3013
0.50			3.00	0.10	4	-0.6501
					5	-0.5585
					10	-0.3753
					15	-0.3036
	0.50		3.00	0.50	4	-0.6519
					5	-0.5599
					10	-0.3761
					15	-0.3042

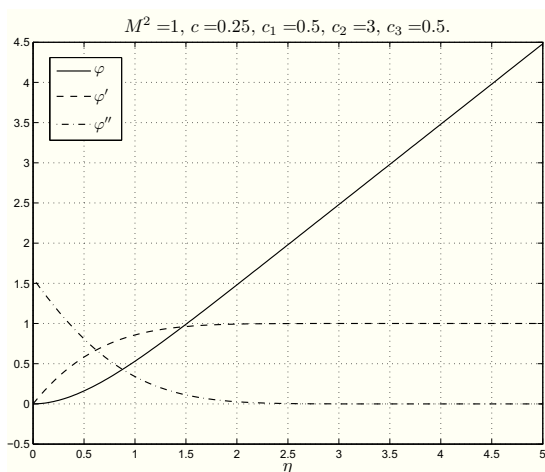


Figure 4.22: CASE II-M:  $\varphi, \varphi', \varphi''$  profiles.

### 4.3.2 CASE II-M: $\mathbf{H}_0 = H_0 \mathbf{e}_2$ .

We have solved problem (4.60), (4.58)<sub>3,4</sub>, (4.59) numerically.

The graphics of  $\varphi, \varphi', \varphi''$  are displayed in Figure 4.22.

The behaviour of  $\gamma, \gamma', \gamma''$  is given in Figure 4.23<sub>1</sub> when  $c < c_r$ , while otherwise, when the reverse doesn't occur, we see the profiles of  $\gamma, \gamma', \gamma''$  in Figure 4.23<sub>2</sub>.

The reverse microrotation is shown in Figure 4.24<sub>1</sub>, while if  $c > c_{rw}$  then the behaviour of  $\Phi, \Phi'$  is given in Figure 4.24<sub>2</sub>.

The functions  $\Gamma, \Gamma'$  are displayed in Figure 4.25.

In Tables 4.19, 4.20, 4.21 and 4.22 we see the numerical values of  $\varphi''(0), \gamma''(0), \Phi'(0), \Gamma'(0), h_d, \alpha, \beta, \bar{\eta}_\varphi, \bar{\eta}_\gamma, \bar{\eta}_\Phi,$  and  $\bar{\eta}_\Gamma$  when  $M^2, c_1, c_2, c_3$  and  $c$  change.

We note that if  $M^2$  is fixed and if one among  $c, c_1, c_2, c_3$  increases, then the descriptive quantities of motion behave as in the absence of the external magnetic field and as in the previous case.

The influence of the parameters  $c_1, c_2, c_3$  on the functions  $\varphi', \gamma', \Phi, \Gamma$  can be seen in Figures from 4.26 to 4.28. As in the previous case, we have that the functions which are most influenced by  $c_1, c_2, c_3$  are  $\Phi$  and  $\Gamma$ , in other words the microrotation.

When  $c, c_1, c_2, c_3$  are fixed, from Table 4.19 and 4.21 we find that if  $M^2$  increases, then  $\varphi''(0), \gamma''(0), |\Phi'(0)|, |\Gamma'(0)|$  increase, while the other parameters decrease.

The thickness  $\delta$  of the boundary layer depends on  $M^2$  and decreases when  $M^2$  increases (as easily seen in Figures 4.29 and 4.30). In this case the boundary layer is thinner than in CASE I-M.

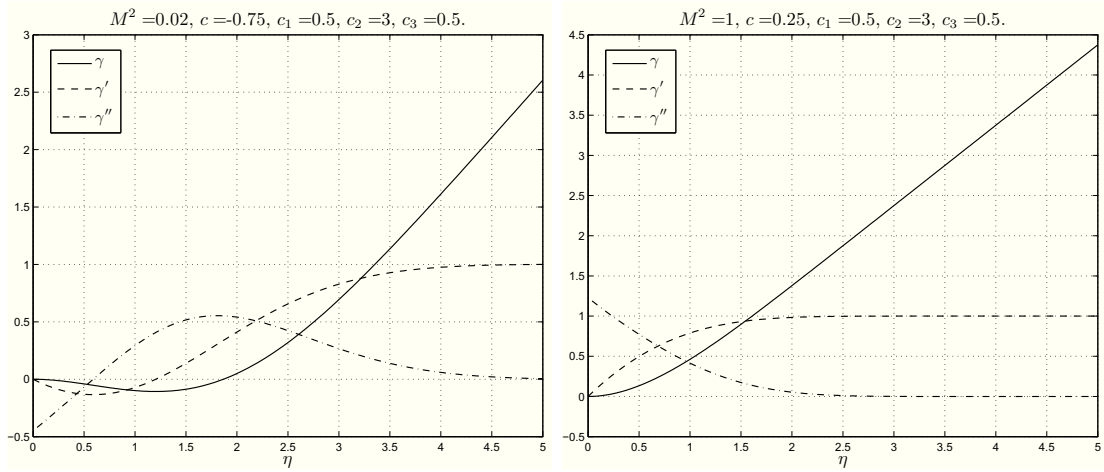


Figure 4.23: CASE II-M: the first picture shows the profiles of  $\gamma, \gamma', \gamma''$  in the reverse flow. The second picture shows the profile of  $\gamma$  in the absence of the reverse flow.

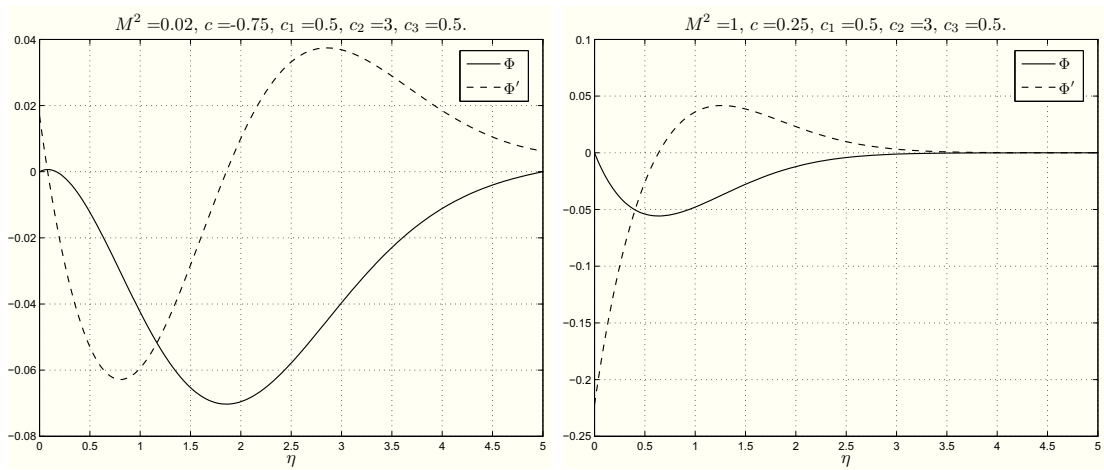


Figure 4.24: CASE II-M: the first picture shows the profiles of  $\Phi, \Phi'$  in the reverse microrotation. The second picture shows the profiles of  $\Phi, \Phi'$  in the absence of the reverse microrotation.

Table 4.19: CASE II-M: descriptive quantities of motion for some values of  $c$ ,  $c_1$ ,  $c_2$ ,  $c_3$ , and  $M^2$ .

$M^2$	$c$	$c_1$	$c_2$	$c_3$	$\varphi''(0)$	$\gamma''(0)$	$\Phi'(0)$	$\Gamma'(0)$	$h_d$	$\alpha$	$\beta$	
1	-0.75	0.1	1.5	0.1	1.5575	0.4819	-0.0313	-0.0576	-2.0634	0.5600	1.4345	
				0.5	1.5585	0.4817	-0.0323	-0.0556	-2.0593	0.5602	1.4334	
		0.5	3.0	0.1	1.5603	0.4847	-0.0236	-0.0491	-2.0850	0.5607	1.4425	
				0.5	1.5608	0.4846	-0.0239	-0.0481	-2.0836	0.5608	1.4422	
			1.5	0.1	1.5159	0.4516	-0.1598	-0.2882	-1.8349	0.5489	1.3435	
				0.5	1.5210	0.4505	-0.1656	-0.2781	-1.8131	0.5499	1.3376	
	3.0		0.1	1.5301	0.4658	-0.1188	-0.2455	-1.9656	0.5522	1.3915		
			0.5	1.5324	0.4654	-0.1208	-0.2407	-1.9589	0.5528	1.3900		
	-0.25	0.1	1.5	0.1	1.5649	0.9295	-0.0463	-0.0579	0.4514	0.5497	0.8446	
				0.5	1.5660	0.9299	-0.0464	-0.0558	0.4516	0.5499	0.8447	
			3.0	0.1	1.5677	0.9328	-0.0373	-0.0494	0.4514	0.5503	0.8470	
				0.5	1.5682	0.9329	-0.0374	-0.0484	0.4515	0.5504	0.8470	
			0.5	1.5	0.1	1.5233	0.8886	-0.2325	-0.2896	0.4479	0.5394	0.8138
					0.5	1.5287	0.8905	-0.2330	-0.2790	0.4489	0.5403	0.8146
		3.0	0.1	1.5374	0.9057	-0.1871	-0.2469	0.4478	0.5424	0.8261		
			0.5	1.5398	0.9063	-0.1876	-0.2419	0.4483	0.5429	0.8264		
		0.25	0.1	1.5	0.1	1.5878	1.2543	-0.0538	-0.0587	0.5480	0.5263	0.6348
					0.5	1.5890	1.2552	-0.0526	-0.0563	0.5482	0.5265	0.6350
			3.0	0.1	1.5905	1.2574	-0.0448	-0.0501	0.5486	0.5268	0.6358	
				0.5	1.5910	1.2577	-0.0444	-0.0490	0.5487	0.5269	0.6359	
	0.5		1.5	0.1	1.5463	1.2120	-0.2692	-0.2934	0.5379	0.5173	0.6201	
				0.5	1.5525	1.2168	-0.2634	-0.2816	0.5387	0.5182	0.6211	
	3.0	0.1	1.5601	1.2277	-0.2243	-0.2507	0.5408	0.5198	0.6249			
		0.5	1.5629	1.2297	-0.2221	-0.2452	0.5412	0.5202	0.6253			
1.00	0.1	1.5	0.1	1.6352	1.6352	-0.0600	-0.0600	0.4891	0.4891	0.4891		
			0.5	1.6367	1.6367	-0.0572	-0.0572	0.4893	0.4893	0.4893		
		3.0	0.1	1.6378	1.6378	-0.0516	-0.0516	0.4895	0.4895	0.4895		
			0.5	1.6385	1.6385	-0.0502	-0.0502	0.4896	0.4896	0.4896		
		0.5	1.5	0.1	1.5943	1.5943	-0.3003	-0.3003	0.4817	0.4817	0.4817	
				0.5	1.6017	1.6017	-0.2862	-0.2862	0.4825	0.4825	0.4825	
	3.0	0.1	1.6075	1.6075	-0.2579	-0.2579	0.4836	0.4836	0.4836			
		0.5	1.6110	1.6110	-0.2512	-0.2512	0.4840	0.4840	0.4840			
	2	-0.75	0.1	1.5	0.1	1.8403	1.0489	-0.0467	-0.0610	-0.7090	0.4958	0.8975
					0.5	1.8411	1.0485	-0.0480	-0.0590	-0.7066	0.4960	0.8968
			3.0	0.1	1.8428	1.0521	-0.0380	-0.0527	-0.7167	0.4963	0.9007	
				0.5	1.8432	1.0519	-0.0385	-0.0517	-0.7158	0.4964	0.9005	
0.5			1.5	0.1	1.8004	1.0096	-0.2346	-0.3049	-0.6256	0.4871	0.8580	
				0.5	1.8047	1.0073	-0.2414	-0.2949	-0.6125	0.4878	0.8545	
3.0	0.1	1.8130	1.0259	-0.1902	-0.2633	-0.6678	0.4897	0.8755				
	0.5	1.8150	1.0251	-0.1930	-0.2584	-0.6633	0.4900	0.8745				
-0.25	0.1	1.5	0.1	1.8540	1.3477	-0.0541	-0.0614	0.4248	0.4816	0.6519		
			0.5	1.8550	1.3480	-0.0541	-0.0592	0.4250	0.4817	0.6520		
	3.0	0.1	1.8565	1.3507	-0.0452	-0.0531	0.4250	0.4820	0.6532			
		0.5	1.8569	1.3508	-0.0453	-0.0520	0.4251	0.4821	0.6532			
	0.5	1.5	0.1	1.8142	1.3064	-0.2711	-0.3070	0.4203	0.4737	0.6341		
			0.5	1.8189	1.3079	-0.2713	-0.2962	0.4211	0.4744	0.6345		
3.0	0.1	1.8267	1.3218	-0.2262	-0.2655	0.4211	0.4759	0.6405				
	0.5	1.8289	1.3223	-0.2266	-0.2602	0.4215	0.4763	0.6407				

Table 4.20: CASE II-M: continuum of Table 4.19.

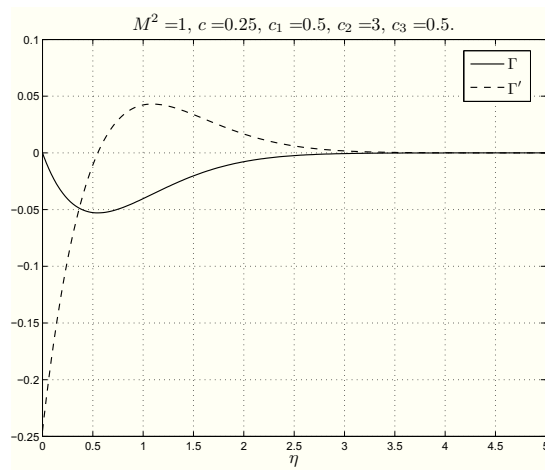
$M^2$	$c$	$c_1$	$c_2$	$c_3$	$\varphi''(0)$	$\gamma''(0)$	$\Phi'(0)$	$\Gamma'(0)$	$h_d$	$\alpha$	$\beta$		
2	0.25	0.1	1.5	0.1	1.8747	1.5964	-0.0587	-0.0620	0.4783	0.4641	0.5354		
				0.5	1.8758	1.5972	-0.0574	-0.0596	0.4785	0.4642	0.5355		
		0.5	1.5	0.1	1.8771	1.5991	-0.0499	-0.0537	0.4788	0.4644	0.5360		
				0.5	1.8776	1.5995	-0.0494	-0.0525	0.4788	0.4645	0.5361		
		1.00	0.1	1.5	0.1	1.8350	1.5555	-0.2935	-0.3101	0.4707	0.4571	0.5250	
					0.5	1.8405	1.5597	-0.2872	-0.2980	0.4714	0.4578	0.5257	
	5	-0.75	0.1	1.5	0.1	1.9135	1.9135	-0.0630	-0.0630	0.4377	0.4377	0.4377	
					0.5	1.9148	1.9148	-0.0601	-0.0601	0.4379	0.4379	0.4379	
			0.5	1.5	0.1	1.9158	1.9158	-0.0548	-0.0548	0.4380	0.4380	0.4380	
					0.5	1.9165	1.9165	-0.0534	-0.0534	0.4381	0.4381	0.4381	
			1.00	0.1	1.5	0.1	1.8743	1.8743	-0.3151	-0.3151	0.4318	0.4318	0.4318
						0.5	1.8809	1.8809	-0.3008	-0.3008	0.4324	0.4324	0.4324
5	-0.25	0.1	1.5	0.1	2.5201	2.0082	-0.0624	-0.0675	0.0327	0.3784	0.4937		
				0.5	2.5207	2.0077	-0.0639	-0.0655	0.0334	0.3785	0.4935		
		0.5	1.5	0.1	2.5220	2.0106	-0.0538	-0.0597	0.0316	0.3786	0.4943		
				0.5	2.5223	2.0104	-0.0545	-0.0587	0.0320	0.3787	0.4943		
		1.00	0.1	1.5	0.1	2.4841	1.9695	-0.3123	-0.3374	0.0445	0.3736	0.4833	
					0.5	2.4872	1.9671	-0.3199	-0.3277	0.0481	0.3740	0.4826	
	0.25	0.1	0.1	1.5	0.1	2.4938	1.9819	-0.2691	-0.2987	0.0392	0.3748	0.4867	
					0.5	2.4954	1.9810	-0.2726	-0.2936	0.0408	0.3750	0.4864	
			0.5	1.5	0.1	2.5340	2.1848	-0.0648	-0.0678	0.3480	0.3695	0.4340	
					0.5	2.5347	2.1850	-0.0647	-0.0656	0.3481	0.3696	0.4341	
			1.00	0.1	1.5	0.1	2.5359	2.1870	-0.0564	-0.0601	0.3482	0.3697	0.4345
						0.5	2.5363	2.1871	-0.0565	-0.0589	0.3482	0.3698	0.4345
5	-0.25	0.1	1.5	0.1	2.4981	2.1469	-0.3240	-0.3390	0.3445	0.3651	0.4270		
				0.5	2.5018	2.1477	-0.3238	-0.3281	0.3450	0.3655	0.4270		
		0.5	1.5	0.1	2.5077	2.1583	-0.2823	-0.3005	0.3453	0.3662	0.4290		
				0.5	2.5096	2.1587	-0.2825	-0.2947	0.3455	0.3664	0.4291		
		1.00	0.1	1.5	0.1	2.5500	2.3491	-0.0666	-0.0681	0.3669	0.3606	0.3922	
					0.5	2.5508	2.3497	-0.0652	-0.0657	0.3670	0.3607	0.3923	
	0.25	0.1	1.5	0.1	2.5519	2.3512	-0.0586	-0.0605	0.3671	0.3608	0.3925		
				0.5	2.5523	2.3514	-0.0579	-0.0592	0.3672	0.3608	0.3925		
		0.5	1.5	0.1	2.5142	2.3122	-0.3330	-0.3407	0.3626	0.3565	0.3870		
				0.5	2.5185	2.3152	-0.3263	-0.3284	0.3630	0.3569	0.3873		
		1.00	0.1	1.5	0.1	2.5237	2.3226	-0.2929	-0.3024	0.3637	0.3575	0.3884	
					0.5	2.5259	2.3240	-0.2898	-0.2960	0.3639	0.3577	0.3885	
0.25	0.1	1.5	0.1	2.5770	2.5770	-0.0686	-0.0686	0.3475	0.3475	0.3475			
			0.5	2.5780	2.5780	-0.0657	-0.0657	0.3476	0.3476	0.3476			
	0.5	1.5	0.1	2.5788	2.5788	-0.0611	-0.0611	0.3477	0.3477	0.3477			
			0.5	2.5793	2.5793	-0.0595	-0.0595	0.3477	0.3477	0.3477			
	1.00	0.1	1.5	0.1	2.5416	2.5416	-0.3432	-0.3432	0.3438	0.3438	0.3438		
				0.5	2.5468	2.5468	-0.3288	-0.3288	0.3443	0.3443	0.3443		
1.00	0.1	1.5	0.1	2.5508	2.5508	-0.3054	-0.3054	0.3447	0.3447	0.3447			
			0.5	2.5535	2.5535	-0.2978	-0.2978	0.3449	0.3449	0.3449			

Table 4.21: CASE II-M: descriptive quantities of boundary layer for some values of  $c$ ,  $c_1$ ,  $c_2$ ,  $c_3$ , and  $M^2$ .

$M^2$	$c$	$c_1$	$c_2$	$c_3$	$\bar{\eta}_\varphi$	$\bar{\eta}_\gamma$	$\bar{\eta}_\Phi$	$\bar{\eta}_\Gamma$	$\delta_v$	$\delta_w$	$\delta$
1	-0.75	0.1	1.5	0.1	2.2487	4.3030	2.7433	1.4385	4.3030	2.7433	4.3030
				0.5	2.2569	4.3065	2.7301	1.2187	4.3065	2.7301	4.3065
		0.5	1.5	0.1	2.2677	4.3453	1.1640	0.8639	4.3453	1.1640	4.3453
				0.5	2.2719	4.3468	1.1622	0.7287	4.3468	1.1622	4.3468
		0.5	1.5	0.1	2.0596	3.8090	4.2281	2.8348	3.8090	4.2281	4.2281
				0.5	2.0889	3.8180	4.0760	2.4496	3.8180	4.0760	4.0760
	0.5	1.5	0.1	2.1386	4.1460	3.7223	2.2236	4.1460	3.7223	4.1460	
			0.5	2.1567	4.1551	3.6370	2.0484	4.1551	3.6370	4.1551	
	-0.25	0.1	1.5	0.1	2.1491	2.8933	1.9727	1.4247	2.8933	1.9727	2.8933
				0.5	2.1566	2.9048	1.8271	1.1932	2.9048	1.8271	2.9048
		0.5	1.5	0.1	2.1661	2.9329	1.1634	0.8677	2.9329	1.1634	2.9329
				0.5	2.1699	2.9378	1.1245	0.7280	2.9378	1.1245	2.9378
		0.5	1.5	0.1	1.9769	2.5621	3.3426	2.7688	2.5621	3.3426	3.3426
				0.5	2.0037	2.5976	2.9883	2.3396	2.5976	2.9883	2.9883
	0.5	1.5	0.1	2.0477	2.7389	2.7353	2.1892	2.7389	2.7353	2.7389	
			0.5	2.0647	2.7606	2.5781	1.9931	2.7606	2.5781	2.7606	
	0.25	0.1	1.5	0.1	1.9756	2.2331	1.6151	1.3837	2.2331	1.6151	2.2331
				0.5	1.9829	2.2426	1.3912	1.1304	2.2426	1.3912	2.2426
		0.5	1.5	0.1	1.9894	2.2541	1.0224	0.8687	2.2541	1.0224	2.2541
				0.5	1.9932	2.2586	0.9189	0.7180	2.2586	0.9189	2.2586
		0.5	1.5	0.1	1.8296	2.0371	2.8781	2.6491	2.0371	2.8781	2.8781
				0.5	1.8554	2.0692	2.4037	2.1574	2.0692	2.4037	2.4037
	0.5	1.5	0.1	1.8869	2.1252	2.3187	2.1117	2.1252	2.3187	2.3187	
			0.5	1.9037	2.1451	2.1004	1.8792	2.1451	2.1004	2.1451	
1.00	0.1	1.5	0.1	1.7481	1.7481	1.3045	1.3045	1.7481	1.3045	1.7481	
			0.5	1.7549	1.7549	1.0225	1.0225	1.7549	1.0225	1.7549	
	0.5	1.5	0.1	1.7582	1.7582	0.8549	0.8549	1.7582	0.8549	1.7582	
			0.5	1.7622	1.7622	0.6840	0.6840	1.7622	0.6840	1.7622	
	0.5	1.5	0.1	1.6322	1.6322	2.4722	2.4722	1.6322	2.4722	2.4722	
			0.5	1.6577	1.6577	1.9114	1.9114	1.6577	1.9114	1.9114	
0.5	1.5	0.1	1.6747	1.6747	1.9882	1.9882	1.6747	1.9882	1.9882		
		0.5	1.6914	1.6914	1.7067	1.7067	1.6914	1.7067	1.7067		
2	-0.75	0.1	1.5	0.1	2.0816	3.5565	2.0014	1.3145	3.5565	2.0014	3.5565
				0.5	2.0867	3.5505	2.0844	1.1232	3.5505	2.0844	3.5505
		0.5	1.5	0.1	2.0964	3.6140	0.9777	0.7734	3.6140	0.9777	3.6140
				0.5	2.0992	3.6133	1.0749	0.6464	3.6133	1.0749	3.6133
		0.5	1.5	0.1	1.9219	3.0689	3.6416	2.7199	3.0689	3.6416	3.6416
				0.5	1.9404	3.0298	3.5735	2.3786	3.0298	3.5735	3.5735
	0.5	1.5	0.1	1.9832	3.3626	2.9311	2.1081	3.3626	2.9311	3.3626	
			0.5	1.9957	3.3573	2.9099	1.9582	3.3573	2.9099	3.3573	
	-0.25	0.1	1.5	0.1	1.9486	2.4769	1.6574	1.2909	2.4769	1.6574	2.4769
				0.5	1.9536	2.4819	1.5486	1.0787	2.4819	1.5486	2.4819
		0.5	1.5	0.1	1.9612	2.5049	0.9784	0.7765	2.5049	0.9784	2.5049
				0.5	1.9641	2.5076	0.9505	0.6400	2.5076	0.9505	2.5076
		0.5	1.5	0.1	1.8082	2.2291	3.0418	2.6271	2.2291	3.0418	3.0418
				0.5	1.8257	2.2416	2.7193	2.2131	2.2416	2.7193	2.7193
	0.5	1.5	0.1	1.8606	2.3479	2.4184	2.0569	2.3479	2.4184	2.4184	
			0.5	1.8729	2.3589	2.2842	1.8707	2.3589	2.2842	2.3589	

Table 4.22: CASE II-M: continuum of Table 4.21.

$M^2$	$c$	$c_1$	$c_2$	$c_3$	$\bar{\eta}_\varphi$	$\bar{\eta}_\gamma$	$\bar{\eta}_\Phi$	$\bar{\eta}_\Gamma$	$\delta_v$	$\delta_w$	$\delta$	
2	0.25	0.1	1.5	0.1	1.8082	2.0072	1.4284	1.2559	2.0072	1.4284	2.0072	
				0.5	1.8132	2.0132	1.2297	1.0205	2.0132	1.2297	2.0132	
		0.5	3.0	0.1	1.8187	2.0229	0.8890	0.7760	2.0229	0.8890	2.0229	
				0.5	1.8217	2.0262	0.7960	0.6262	2.0262	0.7960	2.0262	
		1.00	0.1	1.5	0.1	1.6866	1.8487	2.7019	2.5211	1.8487	2.7019	2.7019
					0.5	1.7042	1.8677	2.2467	2.0419	1.8677	2.2467	2.2467
	0.5	3.0	0.1	1.7302	1.9136	2.1452	1.9916	1.9136	2.1452	2.1452		
			0.5	1.7427	1.9269	1.9397	1.7671	1.9269	1.9397	1.9397		
	1.00	0.1	1.5	0.1	1.6282	1.6282	1.1940	1.1940	1.6282	1.1940	1.6282	
				0.5	1.6332	1.6332	0.9294	0.9294	1.6332	0.9294	1.6332	
	0.5	3.0	0.1	1.6364	1.6364	0.7657	0.7657	1.6364	0.7657	1.6364		
			0.5	1.6394	1.6394	0.5922	0.5922	1.6394	0.5922	1.6394		
	0.5	1.5	0.1	1.5287	1.5287	2.3706	2.3706	1.5287	2.3706	2.3706		
				0.5	1.5471	1.5471	1.8232	1.8232	1.5471	1.8232	1.8232	
	0.5	3.0	0.1	1.5624	1.5624	1.8927	1.8927	1.5624	1.8927	1.8927		
			0.5	1.5754	1.5754	1.6196	1.6196	1.5754	1.6196	1.6196		
	5	-0.75	0.1	1.5	0.1	1.6577	2.1751	1.3735	1.0599	2.1751	1.3735	2.1751
					0.5	1.6596	2.1706	1.4720	0.9067	2.1706	1.4720	2.1706
0.5			3.0	0.1	1.6646	2.1937	0.7644	0.5850	2.1937	0.7644	2.1937	
				0.5	1.6657	2.1922	0.8255	0.4492	2.1922	0.8255	2.1922	
0.5			1.5	0.1	1.5632	1.9891	2.8623	2.4406	1.9891	2.8623	2.8623	
					0.5	1.5694	1.9719	2.9023	2.1451	1.9719	2.9023	2.9023
0.5		3.0	0.1	1.5907	2.0647	2.1672	1.8584	2.0647	2.1672	2.1672		
			0.5	1.5962	2.0576	2.1847	1.7342	2.0576	2.1847	2.1847		
-0.25		0.1	1.5	0.1	1.5707	1.8229	1.2329	1.0379	1.8229	1.2329	1.8229	
				0.5	1.5724	1.8227	1.1650	0.8602	1.8227	1.1650	1.8227	
		0.5	3.0	0.1	1.5766	1.8339	0.7145	0.5855	1.8339	0.7145	1.8339	
				0.5	1.5779	1.8344	0.6962	0.4422	1.8344	0.6962	1.8344	
		0.5	1.5	0.1	1.4850	1.6956	2.5963	2.3587	1.6956	2.5963	2.5963	
					0.5	1.4905	1.6929	2.3269	1.9751	1.6929	2.3269	2.3269
0.5		3.0	0.1	1.5094	1.7406	1.9917	1.8154	1.7406	1.9917	1.9917		
			0.5	1.5149	1.7417	1.8877	1.6472	1.7417	1.8877	1.8877		
0.25		0.1	1.5	0.1	1.4900	1.6021	1.1159	1.0134	1.6021	1.1159	1.6021	
				0.5	1.4919	1.6034	0.9595	0.8127	1.6034	0.9595	1.6034	
	0.5	3.0	0.1	1.4954	1.6094	0.6597	0.5837	1.6094	0.6597	1.6094		
			0.5	1.4967	1.6106	0.5712	0.4343	1.6106	0.5712	1.6106		
	0.5	1.5	0.1	1.4124	1.5069	2.3964	2.2789	1.5069	2.3964	2.3964		
				0.5	1.4182	1.5102	1.9811	1.8296	1.5102	1.9811	1.9811	
0.5	3.0	0.1	1.4340	1.5367	1.8586	1.7712	1.5367	1.8586	1.8586			
		0.5	1.4397	1.5412	1.6769	1.5642	1.5412	1.6769	1.6769			
1.00	0.1	1.5	0.1	1.3840	1.3840	0.9740	0.9740	1.3840	0.9740	1.3840		
			0.5	1.3860	1.3860	0.7442	0.7442	1.3860	0.7442	1.3860		
	0.5	3.0	0.1	1.3885	1.3885	0.5770	0.5770	1.3885	0.5770	1.3885		
			0.5	1.3900	1.3900	0.4215	0.4215	1.3900	0.4215	1.3900		
	0.5	1.5	0.1	1.3165	1.3165	2.1676	2.1676	1.3165	2.1676	2.1676		
				0.5	1.3234	1.3234	1.6519	1.6519	1.3234	1.6519	1.6519	
0.5	3.0	0.1	1.3347	1.3347	1.7062	1.7062	1.3347	1.7062	1.7062			
		0.5	1.3410	1.3410	1.4520	1.4520	1.3410	1.4520	1.4520			

Figure 4.25: CASE II-M:  $\Gamma, \Gamma'$  profiles.

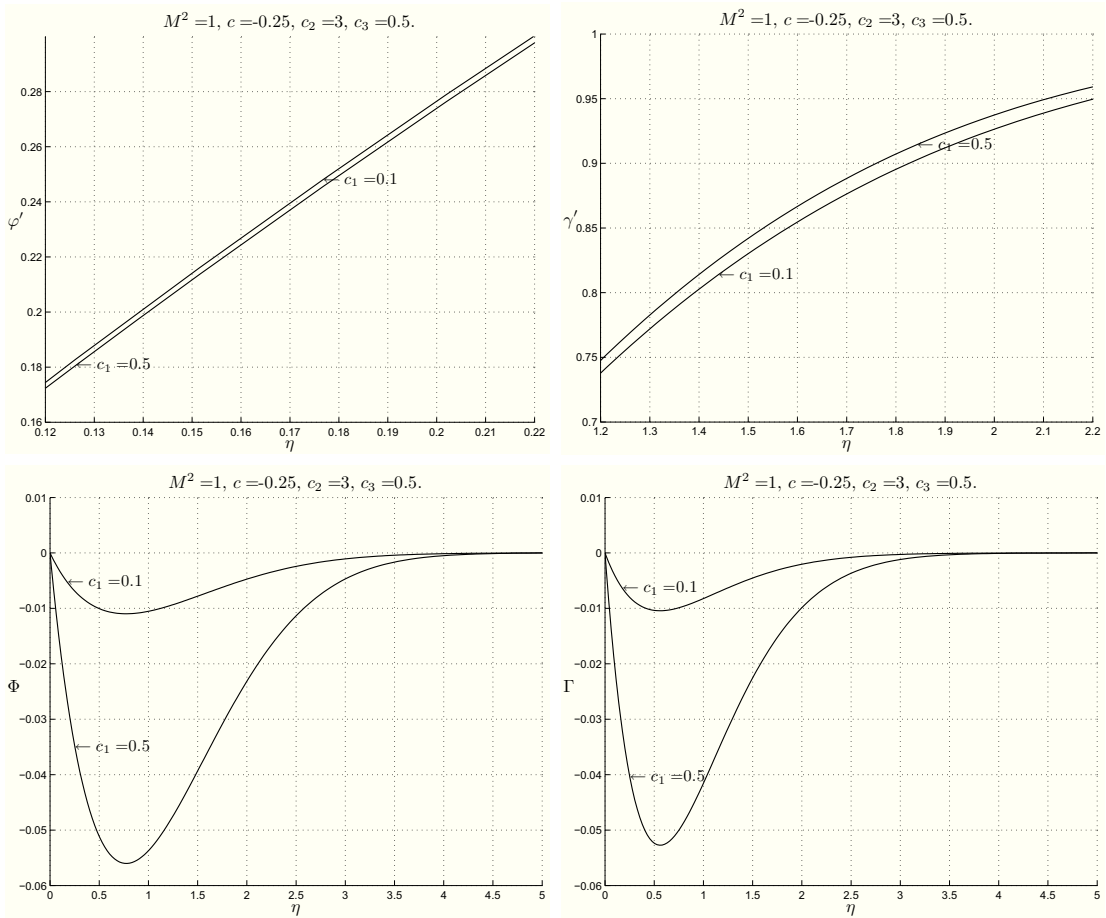


Figure 4.26: CASE II-M:  $\varphi'$ ,  $\gamma'$ ,  $\Phi$ ,  $\Gamma$  profiles for  $M^2 = 1$ ,  $c_2 = 3$ ,  $c_3 = 0.5$ ,  $c = -0.25$  when  $c_1 = 0.1$  and  $c_1 = 0.5$ .

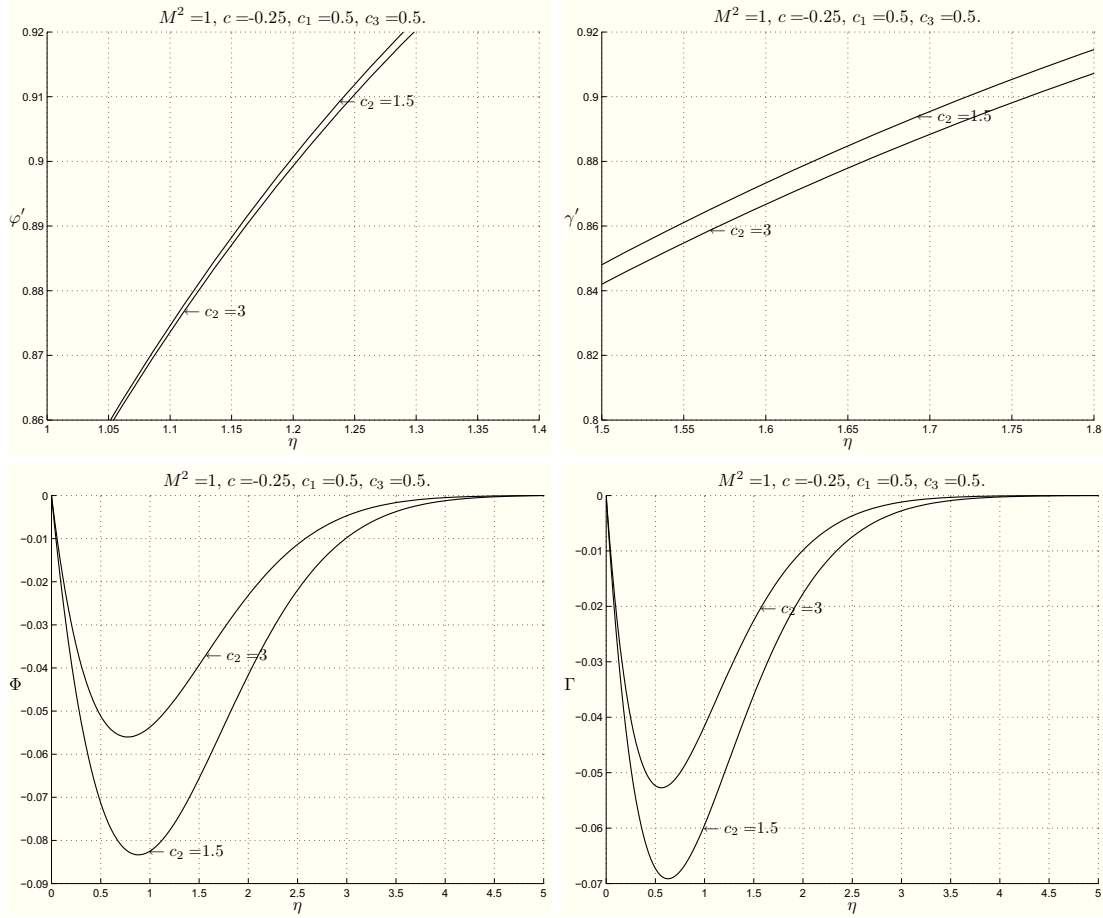


Figure 4.27: CASE II-M:  $\varphi'$ ,  $\gamma'$ ,  $\Phi$ ,  $\Gamma$  profiles for  $M^2 = 1$ ,  $c_1 = 0.5$ ,  $c_3 = 0.5$ ,  $c = -0.25$  when  $c_2 = 1.5$  and  $c_2 = 3$ .

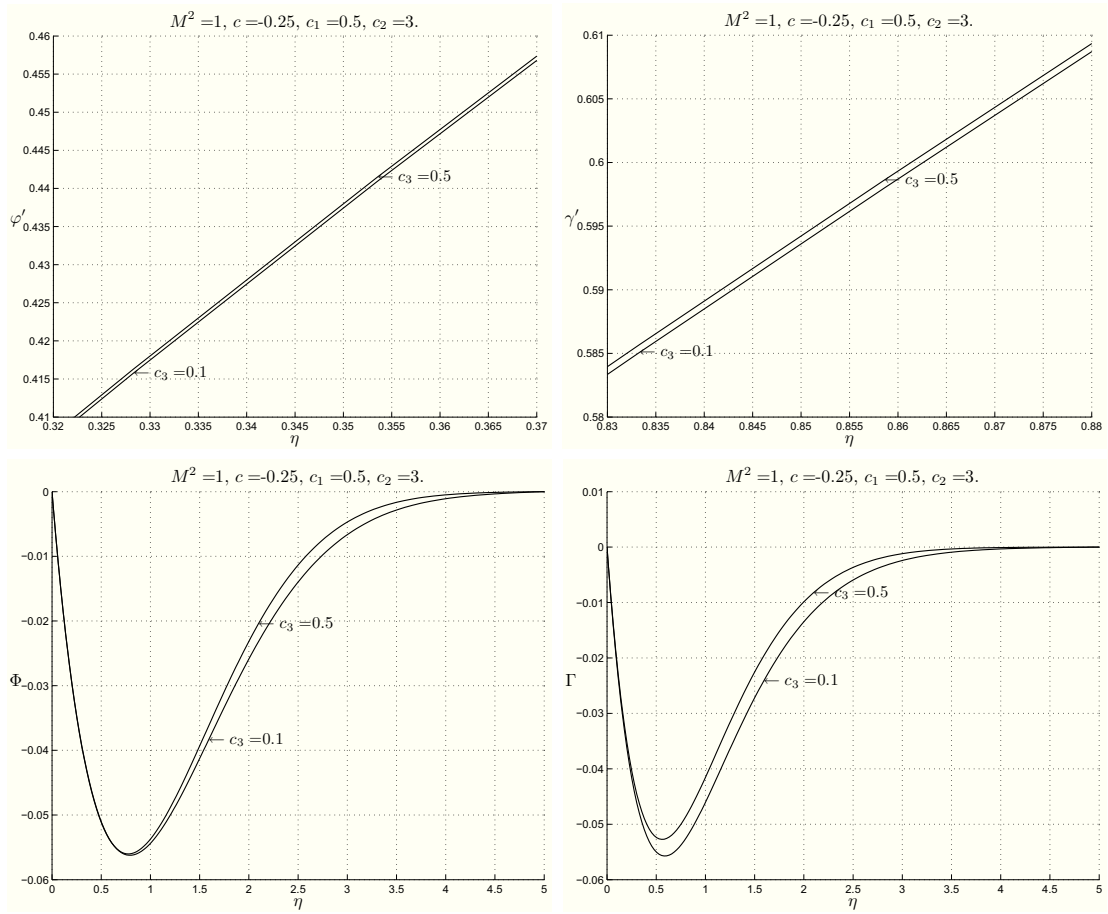


Figure 4.28: CASE II-M:  $\varphi'$ ,  $\gamma'$ ,  $\Phi$ ,  $\Gamma$  profiles for  $M^2 = 1$ ,  $c_1 = 0.5$ ,  $c_2 = 3$ ,  $c = -0.25$  when  $c_3 = 0.1$  and  $c_3 = 0.5$ .

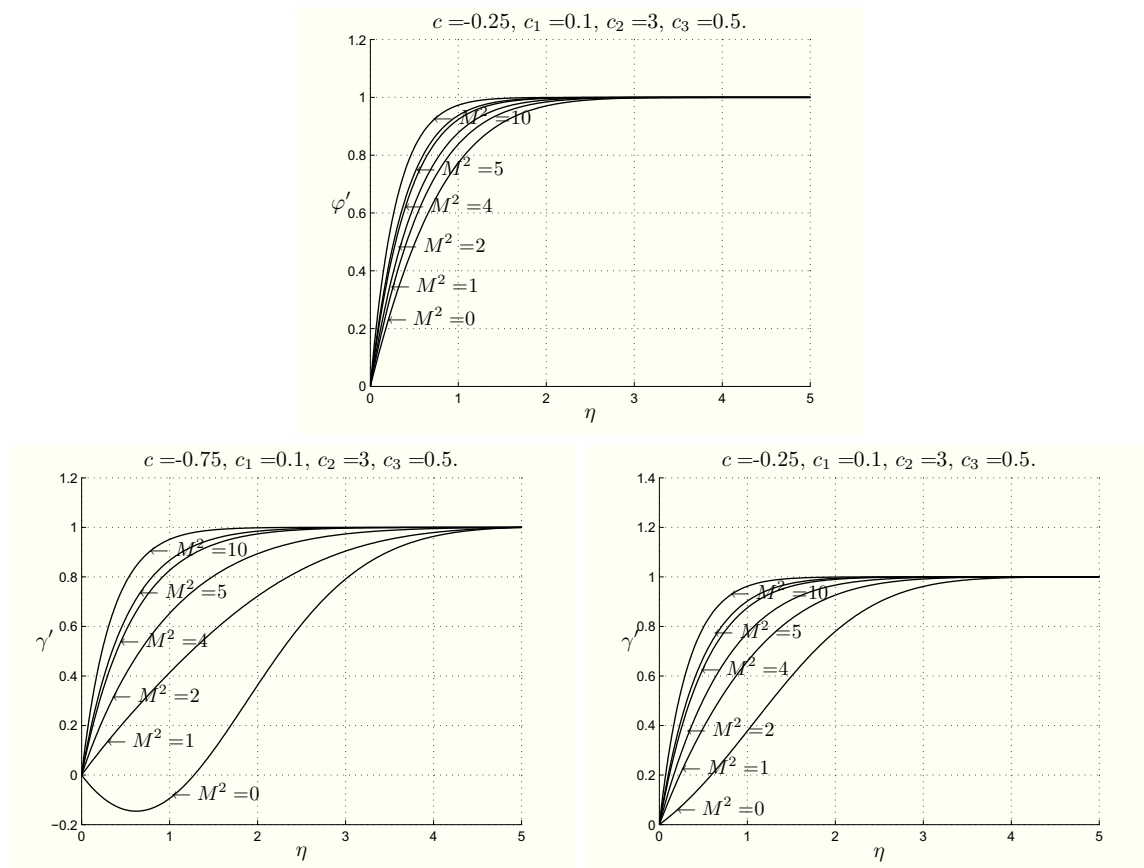


Figure 4.29: CASE II-M: profiles of  $\varphi'$  (Figure 4.29<sub>1</sub>) and  $\gamma'$  (Figures 4.29<sub>2,3</sub>) for several values of  $M^2$  which elucidate the boundary layer thickness.

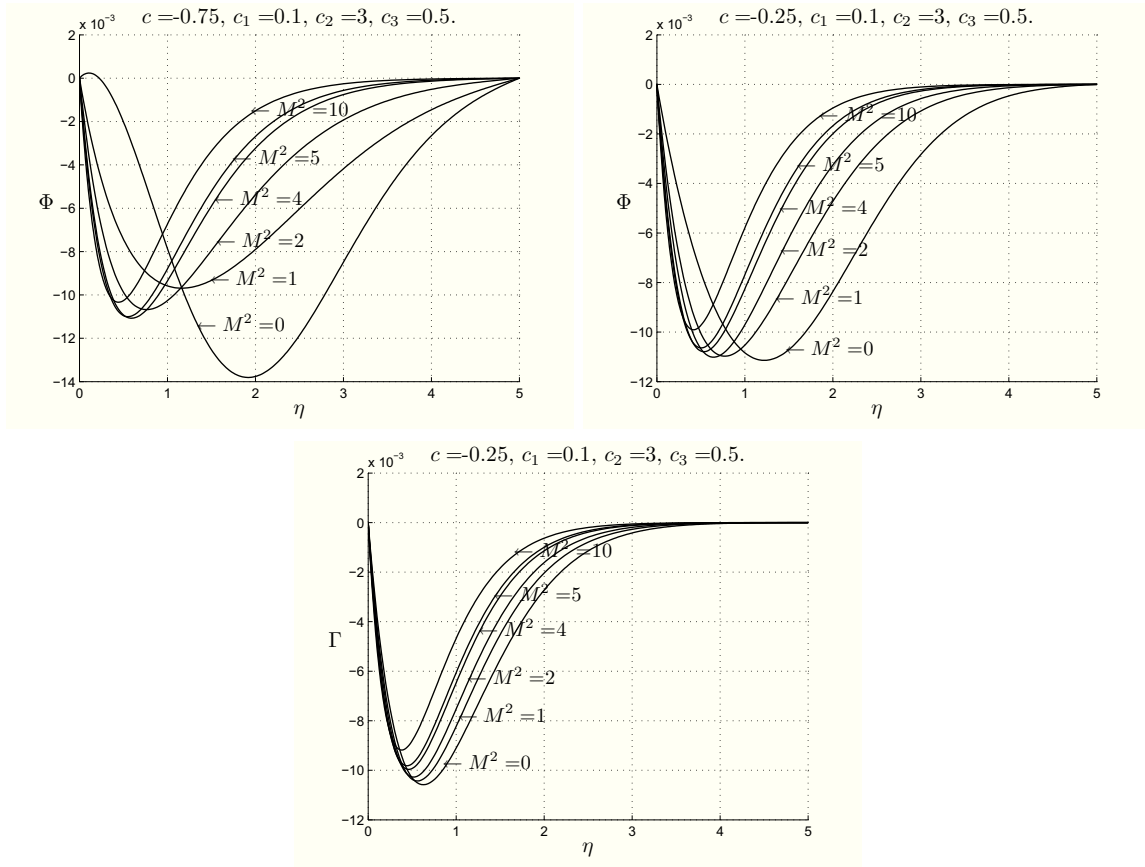


Figure 4.30: CASE II-M: profiles of  $\Phi$  (Figur 4.30<sub>1</sub>) and  $\Gamma$  (Figures 4.30<sub>2,3</sub>) for several values of  $M^2$  which elucidate the boundary layer thickness.

Tables 4.23-4.24 show that as the Hartmann number  $M^2$  increases, the values of  $c_r$  and of  $c_{rw}$  for the reverse flow and the reverse microrotation decrease. In particular, for example when  $c_1 = 0.1$ ,  $c_2 = 3.0$ ,  $c_3 = 0.1$  from  $M^2 = 0.7615$  ( $M^2 = 0.4903$ ), the reverse flow (the reverse microrotation) does not occur at all for any value of  $c$ , so that the magnetic field tends to prevent the occurrence of the reverse flow. In this case

$$\frac{\partial p}{\partial x_3} = -\rho a^2 c x_3 (c + 2M^2),$$

from which one can see that the signs of  $c$  and of  $(c + 2M^2)$  modify the sign of

$$\frac{\partial p}{\partial x_3}.$$

The values of  $M^2$  starting from which the reverse flow and the reverse microrotation do not appear for any values of  $c$  are smaller than in CASE I-M.

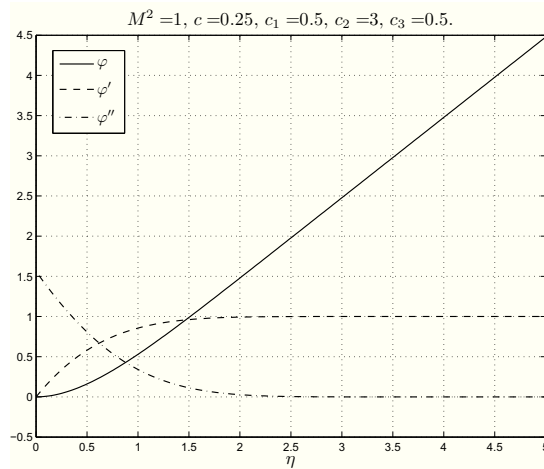


Figure 4.31: CASE III-M:  $\varphi, \varphi', \varphi''$  profiles.

From Tables 4.23-4.24 we see that the value of  $h_d$ , regardless of the values of  $M^2$ , increases if  $c < 0$ , while it decreases if  $c > 0$ . Moreover,  $c_h \geq c_r$ , which means that the three-dimensional displacement thickness is always negative when the reverse flow and the reverse microrotation appears. The presence of  $M^2$  influences  $c_h$  and it decreases when  $M^2$  increases, but unlike the previous case,  $h_d$  can be always negative for physically reasonable values of  $M^2$  (as it happened in CASE II-N Chapter 4.2.4).

As far as the classification of the stagnation-point is concerned, since  $\varphi''(0) + c\gamma''(0)$  is always positive, the origin is a point of attachment. In this case  $M^2$  directly influences  $\varphi$  and  $\gamma$ , as we can see from system (4.60).

Further, if  $c > 0$  or where there is the reverse flow, then the origin is a nodal point, while when  $c < 0$  and the reverse flow does not appear, it is a saddle point. These results are the same as for  $M^2 = 0$  (Chapter 1.3.3).

### 4.3.3 CASE III-M: $\mathbf{H}_0 = H_0 \mathbf{e}_3$ .

The trend of the functions  $\varphi, \varphi', \varphi''$ , which are part of the solution of problem (1.70), (1.66)<sub>3,4</sub>, (1.67) is shown in Figure 4.31.

As far as the behaviour of  $\gamma, \gamma', \gamma''$  is concerned, it is similar to that of the previous cases: if  $c < c_r$  the profiles of  $\gamma, \gamma', \gamma''$  are shown in Figure 4.32<sub>1</sub>, while the reverse flow doesn't appear in Figure 4.32<sub>2</sub>.

Figure 4.33<sub>1</sub> gives  $\Phi, \Phi'$  if  $c < c_{rw}$ , otherwise these functions are plotted in Figure 4.33<sub>2</sub>.

The behaviour of  $\Gamma, \Gamma'$  is given in Figure 4.34.

In Table 4.25, 4.26, 4.27 and 4.28 we give the values of the descriptive quantities of the flow in dependence on  $M^2, c_1, c_2, c_3$  and  $c$ .

When  $M^2$  is fixed, the descriptive quantities behave as in CASEs I-M and II-M.

Table 4.23: CASE II-M: values of  $c_r$ ,  $c_{rw}$  and  $c_h$  when  $M^2$  increases.

$M^2$	$c_1$	$c_2$	$c_3$	$c_r$	$c_{rw}$	$c_h$			
0.10	1.50	0.10	0.10	-0.5008	-0.8365	-0.4092			
			0.20	-0.5745	-0.9115	-0.4227			
			0.30	-0.6485	-0.9858	-0.4360			
			0.3190	-0.6626	no reverse microrotation	-0.4385			
			0.40	-0.7228	no reverse microrotation	-0.4489			
			0.50	-0.7978	no reverse microrotation	-0.4616			
			0.60	-0.8736	no reverse microrotation	-0.4739			
			0.70	-0.9503	no reverse microrotation	-0.4858			
			0.7639	no reverse flow	no reverse microrotation	-0.4933			
			0.80	no reverse flow	no reverse microrotation	-0.4975			
			100	no reverse flow	no reverse microrotation	-0.9836			
			0.50	0.10	0.10	0.10	-0.5008	-0.8600	-0.4092
						0.20	-0.5745	-0.9378	-0.4228
						0.2804	-0.6339	no reverse microrotation	-0.4335
						0.30	-0.6484	no reverse microrotation	-0.4361
						0.40	-0.7227	no reverse microrotation	-0.4490
						0.50	-0.7976	no reverse microrotation	-0.4617
						0.60	-0.8733	no reverse microrotation	-0.4740
						0.70	-0.9500	no reverse microrotation	-0.4860
						0.7643	no reverse flow	no reverse microrotation	-0.4935
0.80	no reverse flow	no reverse microrotation				-0.4976			
100	no reverse flow	no reverse microrotation				-0.9837			
3.00	0.10	0.10				0.10	-0.5022	-0.7162	-0.4080
						0.20	-0.5759	-0.7891	-0.4215
						0.30	-0.6499	-0.8617	-0.4348
						0.40	-0.7244	-0.9343	-0.4478
						0.4903	-0.7921	no reverse microrotation	-0.4592
						0.50	-0.7994	no reverse microrotation	-0.4604
						0.60	-0.8753	no reverse microrotation	-0.4727
						0.70	-0.9521	no reverse microrotation	-0.4847
						0.7615	no reverse flow	no reverse microrotation	-0.4919
			0.80	no reverse flow	no reverse microrotation	-0.4963			
			100	no reverse flow	no reverse microrotation	-0.9836			
			0.50	0.10	0.10	0.10	-0.5022	-0.7241	-0.4080
						0.20	-0.5759	-0.7976	-0.4216
						0.30	-0.6499	-0.8708	-0.4348
						0.40	-0.7243	-0.9440	-0.4478
						0.4763	-0.7815	no reverse microrotation	-0.4575
						0.50	-0.7994	no reverse microrotation	-0.4605
						0.60	-0.8752	no reverse microrotation	-0.4728
						0.70	-0.9520	no reverse microrotation	-0.4848
						0.7616	no reverse flow	no reverse microrotation	-0.4920
0.80	no reverse flow	no reverse microrotation				-0.4964			
100	no reverse flow	no reverse microrotation	-0.9836						

Table 4.24: CASE II-M: continuum of Table 4.23.

$M^2$	$c_1$	$c_2$	$c_3$	$c_r$	$c_{rw}$	$c_h$		
0.50	1.50	0.10	0.10	-0.4881	-0.8775	-0.4219		
			0.20	-0.5620	-0.9497	-0.4353		
			0.2705	-0.6141	no reverse microrotation	-0.4446		
			0.30	-0.6358	no reverse microrotation	-0.4484		
			0.40	-0.7098	no reverse microrotation	-0.4612		
			0.50	-0.7840	no reverse microrotation	-0.4736		
			0.60	-0.8588	no reverse microrotation	-0.4858		
			0.70	-0.9343	no reverse microrotation	-0.4976		
			0.7859	no reverse flow	no reverse microrotation	-0.5075		
			0.80	no reverse flow	no reverse microrotation	-0.5091		
			100	no reverse flow	no reverse microrotation	-0.9837		
			0.50	0.10	0.10	-0.4882	-0.9003	-0.4216
					0.20	-0.5618	-0.9763	-0.4351
					0.2314	-0.5849	no reverse microrotation	-0.4393
					0.30	-0.6353	no reverse microrotation	-0.4484
					0.40	-0.7091	no reverse microrotation	-0.4614
					0.50	-0.7831	no reverse microrotation	-0.4740
					0.60	-0.8575	no reverse microrotation	-0.4863
					0.70	-0.9328	no reverse microrotation	-0.4982
					0.7881	no reverse flow	no reverse microrotation	-0.5084
0.80	no reverse flow	no reverse microrotation			-0.5098			
3.00	0.10	0.10	0.10	-0.4951	-0.7270	-0.4140		
			0.20	-0.5688	-0.7991	-0.4276		
			0.30	-0.6426	-0.8706	-0.4408		
			0.40	-0.7168	-0.9419	-0.4538		
			0.4813	-0.7774	no reverse microrotation	-0.4641		
			0.50	-0.7914	no reverse microrotation	-0.4664		
			0.60	-0.8667	no reverse microrotation	-0.4787		
			0.70	-0.9430	no reverse microrotation	-0.4906		
			0.7737	no reverse flow	no reverse microrotation	-0.4992		
			0.80	no reverse flow	no reverse microrotation	-0.5022		
0.50	0.10	0.10	0.10	-0.4950	-0.7349	-0.4141		
			0.20	-0.5686	-0.8077	-0.4277		
			0.30	-0.6424	-0.8799	-0.4410		
			0.40	-0.7165	-0.9520	-0.4539		
			0.4666	-0.7660	no reverse microrotation	-0.4624		
			0.50	-0.7910	no reverse microrotation	-0.4666		
			0.60	-0.8663	no reverse microrotation	-0.4789		
			0.70	-0.9425	no reverse microrotation	-0.4909		
			0.7744	no reverse flow	no reverse microrotation	-0.4996		
			0.80	no reverse flow	no reverse microrotation	-0.5026		
100	no reverse flow	no reverse microrotation	-0.9838					

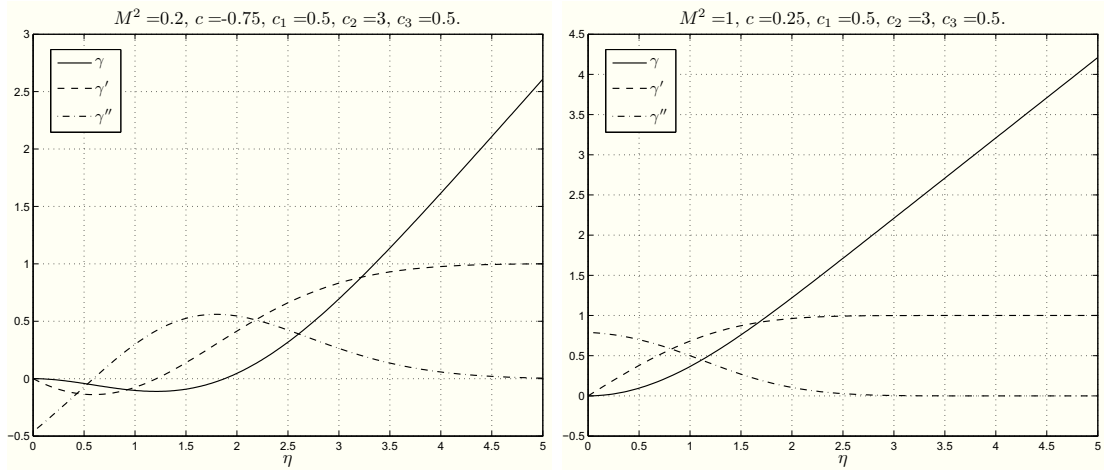


Figure 4.32: CASE III-M: the first picture shows the profiles of  $\gamma, \gamma', \gamma''$  in the reverse flow. The second picture shows the profiles of  $\gamma, \gamma', \gamma''$  in the absence of the reverse flow.

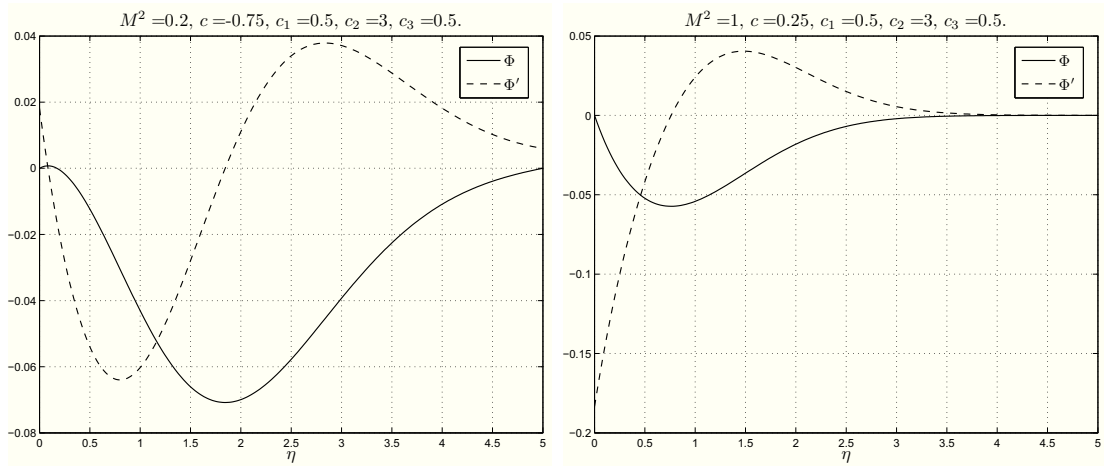


Figure 4.33: CASE III-M: the first picture shows the profiles of  $\Phi, \Phi'$  in the reverse microrotation. The second picture shows the profiles of  $\Phi, \Phi'$  in the absence of the reverse microrotation.

Table 4.25: CASE III-M: descriptive quantities of motion for some values of  $c$ ,  $c_1$ ,  $c_2$ ,  $c_3$ , and  $M^2$ .

$M^2$	$c$	$c_1$	$c_2$	$c_3$	$\varphi''(0)$	$\gamma''(0)$	$\Phi'(0)$	$\Gamma'(0)$	$h_d$	$\alpha$	$\beta$
1	-0.75	0.1	1.5	0.1	1.5838	-0.4365	-0.0026	-0.0585	-5.0530	0.5334	2.3955
				0.5	1.5849	-0.4371	-0.0036	-0.0562	-5.0598	0.5336	2.3981
		0.5	1.5	0.1	1.5865	-0.4357	0.0033	-0.0500	-5.1062	0.5339	2.4140
				0.5	1.5871	-0.4359	0.0029	-0.0489	-5.1084	0.5341	2.4149
		0.5	1.5	0.1	1.5418	-0.4354	-0.0237	-0.2925	-4.4661	0.5238	2.1871
				0.5	1.5477	-0.4400	-0.0278	-0.2813	-4.5297	0.5250	2.2099
	0.5	1.5	0.1	1.5561	-0.4355	0.0133	-0.2499	-4.8204	0.5265	2.3088	
			0.5	1.5588	-0.4371	0.0113	-0.2445	-4.8372	0.5270	2.3151	
	-0.25	0.1	1.5	0.1	1.5703	0.2960	-0.0306	-0.0581	0.2972	0.5447	1.2872
				0.5	1.5713	0.2965	-0.0308	-0.0559	0.2972	0.5449	1.2879
		0.5	1.5	0.1	1.5730	0.2990	-0.0221	-0.0495	0.2958	0.5453	1.2938
				0.5	1.5735	0.2992	-0.0222	-0.0485	0.2958	0.5454	1.2940
		0.5	1.5	0.1	1.5286	0.2655	-0.1569	-0.2904	0.3084	0.5346	1.2130
				0.5	1.5342	0.2680	-0.1579	-0.2796	0.3082	0.5355	1.2177
	0.5	1.5	0.1	1.5427	0.2806	-0.1120	-0.2478	0.3007	0.5375	1.2479	
			0.5	1.5452	0.2813	-0.1129	-0.2426	0.3008	0.5380	1.2495	
	0.25	0.1	1.5	0.1	1.5847	0.8130	-0.0461	-0.0586	0.5840	0.5286	0.8053
				0.5	1.5859	0.8142	-0.0450	-0.0562	0.5842	0.5288	0.8056
0.5		1.5	0.1	1.5874	0.8165	-0.0369	-0.0500	0.5847	0.5291	0.8069	
			0.5	1.5880	0.8169	-0.0366	-0.0489	0.5848	0.5292	0.8071	
0.5		1.5	0.1	1.5431	0.7704	-0.2312	-0.2929	0.5719	0.5196	0.7811	
			0.5	1.5493	0.7765	-0.2260	-0.2812	0.5729	0.5204	0.7829	
0.5	1.5	0.1	1.5570	0.7883	-0.1850	-0.2503	0.5756	0.5221	0.7897		
		0.5	1.5598	0.7906	-0.1834	-0.2448	0.5761	0.5225	0.7904		
1.00	0.1	1.5	0.1	1.6281	1.3110	-0.0561	-0.0599	0.5267	0.4932	0.5603	
			0.5	1.6296	1.3127	-0.0533	-0.0570	0.5269	0.4933	0.5605	
	0.5	1.5	0.1	1.6307	1.3139	-0.0473	-0.0514	0.5272	0.4935	0.5608	
			0.5	1.6314	1.3147	-0.0460	-0.0500	0.5273	0.4936	0.5609	
	0.5	1.5	0.1	1.5870	1.2682	-0.2807	-0.2994	0.5182	0.4857	0.5506	
			0.5	1.5944	1.2769	-0.2668	-0.2854	0.5190	0.4864	0.5515	
0.5	1.5	0.1	1.6003	1.2832	-0.2367	-0.2570	0.5204	0.4876	0.5532		
		0.5	1.6038	1.2871	-0.2305	-0.2504	0.5208	0.4880	0.5537		
2	-0.75	0.1	1.5	0.1	1.8700	-0.4138	-0.0039	-0.0619	-5.1119	0.4697	2.3303
				0.5	1.8710	-0.4144	-0.0050	-0.0595	-5.1195	0.4699	2.3330
		0.5	1.5	0.1	1.8725	-0.4132	0.0022	-0.0536	-5.1665	0.4701	2.3490
				0.5	1.8729	-0.4134	0.0017	-0.0524	-5.1690	0.4702	2.3499
		0.5	1.5	0.1	1.8299	-0.4110	-0.0311	-0.3093	-4.5089	0.4624	2.1195
				0.5	1.8351	-0.4161	-0.0354	-0.2978	-4.5786	0.4632	2.1438
	0.5	1.5	0.1	1.8426	-0.4126	0.0075	-0.2679	-4.8735	0.4643	2.2436	
			0.5	1.8450	-0.4144	0.0053	-0.2622	-4.8920	0.4647	2.2503	
	-0.25	0.1	1.5	0.1	1.8601	0.3190	-0.0317	-0.0616	0.2203	0.4768	1.2464
				0.5	1.8611	0.3195	-0.0319	-0.0593	0.2203	0.4770	1.2472
		0.5	1.5	0.1	1.8626	0.3219	-0.0230	-0.0533	0.2188	0.4773	1.2528
				0.5	1.8630	0.3220	-0.0232	-0.0522	0.2188	0.4773	1.2531
		0.5	1.5	0.1	1.8203	0.2887	-0.1625	-0.3079	0.2342	0.4691	1.1738
				0.5	1.8252	0.2912	-0.1634	-0.2968	0.2335	0.4699	1.1791
	0.5	1.5	0.1	1.8328	0.3034	-0.1170	-0.2664	0.2257	0.4713	1.2081	
			0.5	1.8351	0.3041	-0.1179	-0.2610	0.2256	0.4717	1.2098	

Table 4.26: CASE III-M: continuum of Table 4.25.

$M^2$	$c$	$c_1$	$c_2$	$c_3$	$\varphi''(0)$	$\gamma''(0)$	$\Phi'(0)$	$\Gamma'(0)$	$h_d$	$\alpha$	$\beta$		
2	0.25	0.1	1.5	0.1	1.8708	0.8257	-0.0465	-0.0619	0.5317	0.4666	0.7920		
				0.5	1.8719	0.8269	-0.0454	-0.0595	0.5318	0.4667	0.7923		
			3.0	0.1	1.8732	0.8292	-0.0373	-0.0536	0.5323	0.4670	0.7937		
				0.5	1.8737	0.8296	-0.0370	-0.0524	0.5324	0.4670	0.7938		
			0.5	1.5	0.1	1.8310	0.7835	-0.2336	-0.3096	0.5213	0.4596	0.7681	
					0.5	1.8364	0.7896	-0.2283	-0.2976	0.5222	0.4602	0.7700	
		3.0	0.1	1.8434	0.8011	-0.1873	-0.2681	0.5245	0.4614	0.7767			
			0.5	1.8459	0.8034	-0.1856	-0.2623	0.5249	0.4617	0.7774			
		1.00	0.1	1.5	0.1	1.9035	1.3183	-0.0563	-0.0628	0.4993	0.4427	0.5558	
					0.5	1.9048	1.3200	-0.0534	-0.0599	0.4994	0.4429	0.5560	
			3.0	0.1	1.9059	1.3212	-0.0475	-0.0546	0.4997	0.4430	0.5564		
				0.5	1.9065	1.3220	-0.0462	-0.0532	0.4998	0.4431	0.5565		
	0.5		1.5	0.1	1.8640	1.2757	-0.2817	-0.3140	0.4915	0.4368	0.5461		
				0.5	1.8706	1.2844	-0.2677	-0.2999	0.4923	0.4374	0.5472		
	3.0	0.1	1.8760	1.2905	-0.2378	-0.2729	0.4935	0.4382	0.5488				
		0.5	1.8792	1.2945	-0.2314	-0.2660	0.4939	0.4385	0.5493				
	5	-0.75	0.1	1.5	0.1	2.5452	-0.3733	-0.0063	-0.0680	-5.2087	0.3637	2.2212	
					0.5	2.5460	-0.3740	-0.0074	-0.0657	-5.2176	0.3638	2.2243	
				3.0	0.1	2.5471	-0.3730	0.0002	-0.0604	-5.2656	0.3639	2.2405	
					0.5	2.5475	-0.3733	-0.0003	-0.0591	-5.2686	0.3640	2.2415	
				0.5	1.5	0.1	2.5091	-0.3669	-0.0441	-0.3402	-4.5799	0.3596	2.0061
						0.5	2.5131	-0.3730	-0.0486	-0.3286	-4.6598	0.3600	2.0332
			3.0	0.1	2.5188	-0.3717	-0.0028	-0.3018	-4.9612	0.3605	2.1345		
				0.5	2.5209	-0.3736	-0.0051	-0.2957	-4.9826	0.3608	2.1419		
-0.25			0.1	1.5	0.1	2.5397	0.3590	-0.0335	-0.0679	0.0950	0.3666	1.1812	
					0.5	2.5405	0.3595	-0.0337	-0.0657	0.0948	0.3666	1.1822	
			3.0	0.1	2.5416	0.3618	-0.0247	-0.0602	0.0932	0.3668	1.1874		
				0.5	2.5420	0.3619	-0.0249	-0.0590	0.0932	0.3668	1.1878		
		0.5	1.5	0.1	2.5039	0.3294	-0.1719	-0.3396	0.1125	0.3622	1.1113		
				0.5	2.5077	0.3318	-0.1727	-0.3283	0.1110	0.3626	1.1174		
3.0		0.1	2.5134	0.3433	-0.1253	-0.3012	0.1029	0.3633	1.1444				
		0.5	2.5154	0.3440	-0.1263	-0.2952	0.1025	0.3635	1.1465				
0.25		0.1	1.5	0.1	2.5458	0.8497	-0.0474	-0.0680	0.4438	0.3625	0.7690		
				0.5	2.5466	0.8509	-0.0462	-0.0656	0.4439	0.3625	0.7694		
		3.0	0.1	2.5477	0.8531	-0.0382	-0.0604	0.4443	0.3627	0.7706			
			0.5	2.5481	0.8535	-0.0378	-0.0591	0.4443	0.3627	0.7708			
		0.5	1.5	0.1	2.5099	0.8082	-0.2380	-0.3402	0.4358	0.3584	0.7453		
				0.5	2.5141	0.8143	-0.2323	-0.3282	0.4365	0.3588	0.7476		
3.0		0.1	2.5194	0.8252	-0.1914	-0.3019	0.4383	0.3593	0.7540				
		0.5	2.5216	0.8276	-0.1896	-0.2956	0.4386	0.3595	0.7549				
1.00	0.1	1.5	0.1	2.5646	1.3330	-0.0567	-0.0684	0.4497	0.3521	0.5474			
			0.5	2.5656	1.3347	-0.0538	-0.0656	0.4499	0.3522	0.5476			
	3.0	0.1	2.5665	1.3359	-0.0479	-0.0608	0.4501	0.3523	0.5479				
		0.5	2.5670	1.3367	-0.0466	-0.0594	0.4502	0.3523	0.5480				
	0.5	1.5	0.1	2.5289	1.2909	-0.2837	-0.3421	0.4431	0.3485	0.5377			
			0.5	2.5339	1.2996	-0.2694	-0.3282	0.4438	0.3488	0.5388			
3.0	0.1	2.5383	1.3054	-0.2398	-0.3042	0.4448	0.3493	0.5404					
	0.5	2.5408	1.3094	-0.2332	-0.2969	0.4452	0.3495	0.5409					

Table 4.27: CASE III-M: descriptive quantities of boundary layer for some values of  $c$ ,  $c_1$ ,  $c_2$ ,  $c_3$ , and  $M^2$ .

$M^2$	$c$	$c_1$	$c_2$	$c_3$	$\bar{\eta}_\varphi$	$\bar{\eta}_\gamma$	$\bar{\eta}_\Phi$	$\bar{\eta}_\Gamma$	$\delta_v$	$\delta_w$	$\delta$	
1	-0.75	0.1	1.5	0.1	2.0567	4.4038	3.5863	1.3947	4.4038	3.5863	4.4038	
				0.5	2.0649	4.4241	3.3481	1.1515	4.4241	3.3481	4.4241	
		0.5	1.5	0.1	2.0722	4.4471	2.8076	0.8650	4.4471	2.8076	4.4471	
				0.5	2.0766	4.4540	2.7016	0.7190	4.4540	2.7016	4.4540	
		3.0	0.1	0.1	1.8977	3.8326	4.4948	2.7211	3.8326	4.4948	4.4948	
				0.5	1.9261	3.9965	4.2611	2.2679	3.9965	4.2611	4.2611	
	3.0	0.1	0.1	1.9596	4.2298	4.1720	2.1427	4.2298	4.1720	4.2298		
			0.5	1.9782	4.2791	3.9988	1.9302	4.2791	3.9988	4.2791		
	-0.25	0.1	1.5	0.1	2.1167	3.4083	2.5781	1.4159	3.4083	2.5781	3.4083	
					0.5	2.1244	3.4326	2.3439	1.1805	3.4326	2.3439	3.4326
			3.0	0.1	0.1	2.1332	3.4613	1.7201	0.8674	3.4613	1.7201	3.4613
					0.5	2.1372	3.4703	1.6292	0.7259	3.4703	1.6292	3.4703
			0.5	1.5	0.1	1.9489	2.9648	3.7845	2.7488	2.9648	3.7845	3.7845
						0.5	1.9761	3.0586	3.3754	2.3094	3.0586	3.3754
		3.0	0.1	0.1	2.0172	3.2208	3.2526	2.1742	3.2208	3.2526	3.2526	
				0.5	2.0346	3.2654	3.0483	1.9721	3.2654	3.0483	3.2654	
		0.25	0.1	1.5	0.1	1.9877	2.5154	1.8972	1.3884	2.5154	1.8972	2.5154
						0.5	1.9949	2.5313	1.6307	1.1365	2.5313	1.6307
			3.0	0.1	0.1	2.0017	2.5434	1.2509	0.8695	2.5434	1.2509	2.5434
					0.5	2.0056	2.5503	1.1237	0.7199	2.5503	1.1237	2.5503
	0.5		1.5	0.1	1.8406	2.2694	3.1179	2.6576	2.2694	3.1179	3.1179	
					0.5	1.8662	2.3259	2.6106	2.1692	2.3259	2.6106	2.6106
	3.0	0.1	0.1	1.8986	2.3902	2.5673	2.1184	2.3902	2.5673	2.5673		
			0.5	1.9152	2.4209	2.3256	1.8882	2.4209	2.3256	2.4209		
1.00	0.1	1.5	0.1	1.7651	1.8856	1.4440	1.3137	1.8856	1.4440	1.8856		
				0.5	1.7719	1.8952	1.1384	1.0337	1.8952	1.1384	1.8952	
		3.0	0.1	0.1	1.7754	1.8986	0.9722	0.8585	1.8986	0.9722	1.8986	
				0.5	1.7792	1.9036	0.7942	0.6894	1.9036	0.7942	1.9036	
		0.5	1.5	0.1	1.6482	1.7501	2.5938	2.4856	1.7501	2.5938	2.5938	
					0.5	1.6732	1.7859	2.0134	1.9286	1.7859	2.0134	2.0134
	3.0	0.1	0.1	1.6912	1.8037	2.1059	1.9994	1.8037	2.1059	2.1059		
			0.5	1.7077	1.8257	1.8116	1.7211	1.8257	1.8116	1.8257		
	2	-0.75	0.1	1.5	0.1	1.8709	4.3718	3.5390	1.2669	4.3718	3.5390	4.3718
					0.5	1.8762	4.3933	3.2996	1.0420	4.3933	3.2996	4.3933
			3.0	0.1	0.1	1.8822	4.4176	2.7513	0.7744	4.4176	2.7513	4.4176
					0.5	1.8854	4.4248	2.6464	0.6300	4.4248	2.6464	4.4248
0.5			1.5	0.1	1.7419	3.7796	4.4641	2.5859	3.7796	4.4641	4.4641	
					0.5	1.7604	3.9496	4.2231	2.1449	3.9496	4.2231	4.2231
3.0		0.1	0.1	1.7871	4.1918	4.1308	2.0189	4.1918	4.1308	4.1918		
			0.5	1.8006	4.2436	3.9556	1.8146	4.2436	3.9556	4.2436		
-0.25		0.1	1.5	0.1	1.9147	3.3443	2.5254	1.2815	3.3443	2.5254	3.3443	
					0.5	1.9199	3.3693	2.2892	1.0639	3.3693	2.2892	3.3693
		3.0	0.1	0.1	1.9271	3.3973	1.6846	0.7760	3.3973	1.6846	3.3973	
				0.5	1.9299	3.4066	1.5921	0.6364	3.4066	1.5921	3.4066	
	0.5	1.5	0.1	1.7786	2.9036	3.7333	2.6048	2.9036	3.7333	3.7333		
				0.5	1.7964	2.9988	3.3186	2.1769	2.9988	3.3186	3.3186	
3.0	0.1	0.1	1.8287	3.1571	3.1976	2.0409	3.1571	3.1976	3.1976			
		0.5	1.8414	3.2029	2.9916	1.8464	3.2029	2.9916	3.2029			

Table 4.28: CASE III-M: continuum of Table 4.27.

$M^2$	$c$	$c_1$	$c_2$	$c_3$	$\bar{\eta}_\varphi$	$\bar{\eta}_\gamma$	$\bar{\eta}_\Phi$	$\bar{\eta}_\Gamma$	$\delta_v$	$\delta_w$	$\delta$	
2	0.25	0.1	1.5	0.1	1.8231	2.4811	1.8751	1.2614	2.4811	1.8751	2.4811	
				0.5	1.8281	2.4971	1.6064	1.0285	2.4971	1.6064	2.4971	
		0.5	3.0	0.1	1.8337	2.5089	1.2405	0.7770	2.5089	1.2405	2.5089	
				0.5	1.8367	2.5158	1.1119	0.6290	2.5158	1.1119	2.5158	
			1.5	0.1	1.7002	2.2374	3.0913	2.5319	2.2374	3.0913	2.2374	
				0.5	1.7174	2.2944	2.5798	2.0579	2.2944	2.5798	2.0579	
	1.00	0.1	3.0	0.1	1.7444	2.3566	2.5421	1.9997	2.3566	2.5421	2.3566	
				0.5	1.7567	2.3876	2.2979	1.7787	2.3876	2.2979	2.3876	
		0.5	1.5	0.1	1.6522	1.8707	1.4349	1.2062	1.8707	1.4349	1.8707	
				0.5	1.6572	1.8804	1.1282	0.9452	1.8804	1.1282	1.8804	
			3.0	0.1	1.6607	1.8834	0.9677	0.7702	1.8834	0.9677	1.8834	
				0.5	1.6637	1.8886	0.7889	0.6005	1.8886	0.7889	1.8886	
	5	-0.75	0.1	1.5	0.1	1.5512	1.7361	2.5816	2.3901	1.7361	2.5816	2.5816
					0.5	1.5691	1.7721	1.9989	1.8492	1.7721	1.9989	1.9989
			0.5	3.0	0.1	1.5857	1.7892	2.0954	1.9081	1.7892	2.0954	2.0954
					0.5	1.5984	1.8114	1.7992	1.6404	1.8114	1.7992	1.8114
				1.5	0.1	1.5242	4.3156	3.4568	1.0227	4.3156	3.4568	4.3156
					0.5	1.5261	4.3393	3.2166	0.8325	4.3393	3.2166	4.3393
-0.25		0.1	3.0	0.1	1.5296	4.3655	2.6548	0.5839	4.3655	2.6548	4.3655	
				0.5	1.5311	4.3733	2.5518	0.4370	4.3733	2.5518	4.3733	
		0.5	1.5	0.1	1.4449	3.6875	4.4081	2.3297	3.6875	4.4081	4.4081	
				0.5	1.4507	3.8683	4.1555	1.9172	3.8683	4.1555	4.1555	
			3.0	0.1	1.4659	4.1255	4.0586	1.7914	4.1255	4.0586	4.1255	
				0.5	1.4717	4.1815	3.8810	1.6041	4.1815	3.8810	4.1815	
0.25		0.1	1.5	0.1	1.5464	3.2404	2.4399	1.0300	3.2404	2.4399	3.2404	
				0.5	1.5482	3.2661	2.2007	0.8457	3.2661	2.2007	3.2661	
		0.5	3.0	0.1	1.5522	3.2934	1.6262	0.5847	3.2934	1.6262	3.2934	
				0.5	1.5536	3.3031	1.5309	0.4395	3.3031	1.5309	3.3031	
			1.5	0.1	1.4630	2.8051	3.6491	2.3387	2.8051	3.6491	3.6491	
				0.5	1.4689	2.9019	3.2258	1.9376	2.9019	3.2258	3.2258	
	1.00	0.1	3.0	0.1	1.4865	3.0541	3.1089	1.8026	3.0541	3.1089	3.1089	
				0.5	1.4922	3.1013	2.8998	1.6237	3.1013	2.8998	3.1013	
		0.5	1.5	0.1	1.5036	2.4231	1.8366	1.0187	2.4231	1.8366	2.4231	
				0.5	1.5052	2.4392	1.5641	0.8215	2.4392	1.5641	2.4392	
			3.0	0.1	1.5089	2.4504	1.2210	0.5849	2.4504	1.2210	2.4504	
				0.5	1.5102	2.4574	1.0897	0.4360	2.4574	1.0897	2.4574	
1.00	0.1	3.0	0.1	1.4249	2.1834	3.0454	2.2904	2.1834	3.0454	3.0454		
			0.5	1.4304	2.2412	2.5269	1.8489	2.2412	2.5269	2.5269		
	0.5	1.5	0.1	1.4469	2.2994	2.4991	1.7791	2.2994	2.4991	2.4991		
			0.5	1.4524	2.3314	2.2502	1.5774	2.3314	2.2502	2.3314		
		3.0	0.1	1.4119	1.8432	1.4172	0.9877	1.8432	1.4172	1.8432		
			0.5	1.4137	1.8529	1.1087	0.7647	1.8529	1.1087	1.8529		
1.00	0.1	3.0	0.1	1.4165	1.8557	0.9585	0.5817	1.8557	0.9585	1.8557		
			0.5	1.4179	1.8609	0.7779	0.4265	1.8609	0.7779	1.8609		
	0.5	1.5	0.1	1.3427	1.7102	2.5591	2.1924	1.7102	2.5591	2.5591		
			0.5	1.3489	1.7466	1.9722	1.6889	1.7466	1.9722	1.9722		
		3.0	0.1	1.3615	1.7624	2.0757	1.7244	1.7624	2.0757	2.0757		
			0.5	1.3674	1.7849	1.7761	1.4800	1.7849	1.7761	1.7849		

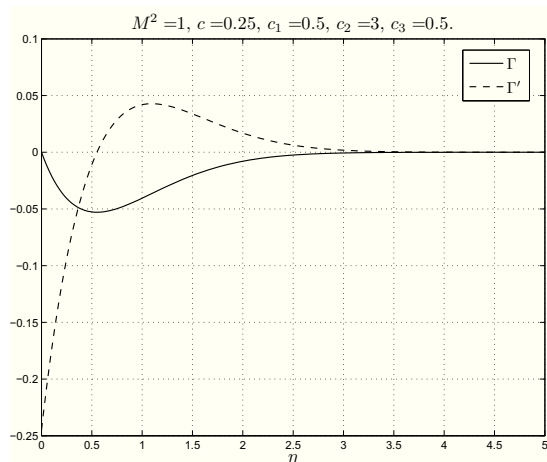


Figure 4.34: CASE III-M:  $\Gamma, \Gamma'$  profiles.

Figures from 4.35 to 4.37 elucidate the dependence of the functions  $\varphi', \gamma', \Phi, \Gamma$ , on the parameters  $c_1, c_2, c_3$  when  $M^2 = 1$ .

When  $c, c_1, c_2, c_3$  are fixed, from Table 4.25 and 4.27 we find that if  $M^2$  increases, then  $\varphi''(0), |\gamma''(0)|, |\Phi'(0)|, |\Gamma'(0)|$  increase, while the other parameters decrease. Actually, the thickness  $\delta$  of the boundary layer decreases when  $M^2$  increases (as easily seen in Figures 4.38 and 4.39). In CASE II-M the boundary layer is thinner than in this case.

Tables 4.29 and 4.30 show that as the Hartmann number  $M^2$  increases, the values of  $c_r$  and of  $c_{rw}$  decrease very slowly, so that in this case the influence of the magnetic field is much less significant with respect to CASEs I-II-M. In this regard we underline that

$$\frac{\partial p}{\partial x_3}, \quad \frac{\partial p}{\partial x_1}$$

have the same sign that they would have in the absence of the external magnetic field.

In particular, we see that the reverse flow always appears for physically meaningful values  $M^2$ , as it happened in CASE III-N.

From Table 4.29 and 4.30 it appears a new interesting result: similar to what happened for the Newtonian fluid,  $c_h$  increases when  $M^2$  increases. We see that  $c_h \geq c_r$  more than in the other two cases, so that the three-dimensional displacement thickness is always negative when the reverse flow appears and it is negative in a region of values of  $c$ , which is bigger than in the other two cases.

As for the previous case and CASE III-N, the origin is always a point of attachment. As one can see,  $M^2$  directly influences  $\varphi$  and only indirectly influences  $\gamma$  in system (4.61), so that when  $M^2$  increases,  $\varphi''(0)$  becomes much greater than  $\gamma''(0)$ .

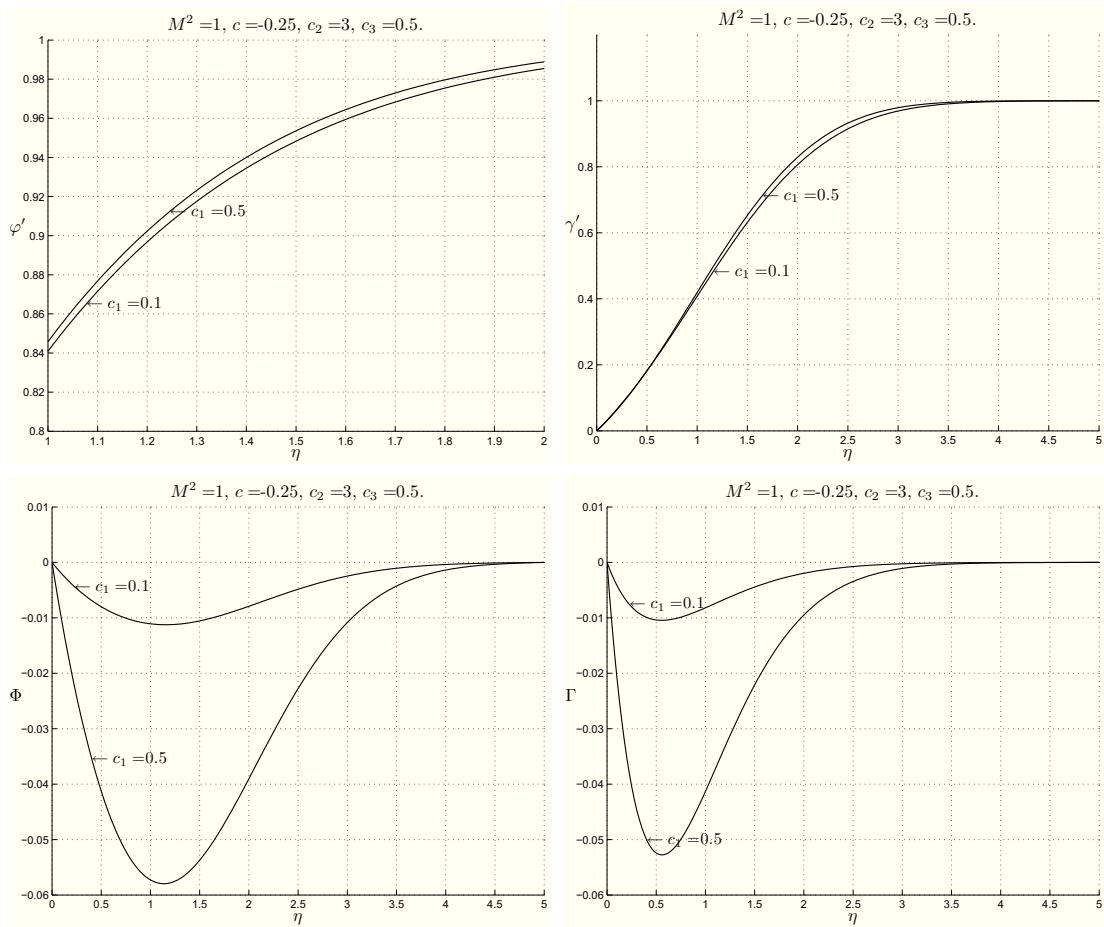


Figure 4.35: CASE III-M:  $\varphi'$ ,  $\gamma'$ ,  $\Phi$ ,  $\Gamma$  profiles for  $M^2 = 1$ ,  $c_2 = 3$ ,  $c_3 = 0.5$ ,  $c = -0.25$  when  $c_1 = 0.1$  and  $c_1 = 0.5$ .

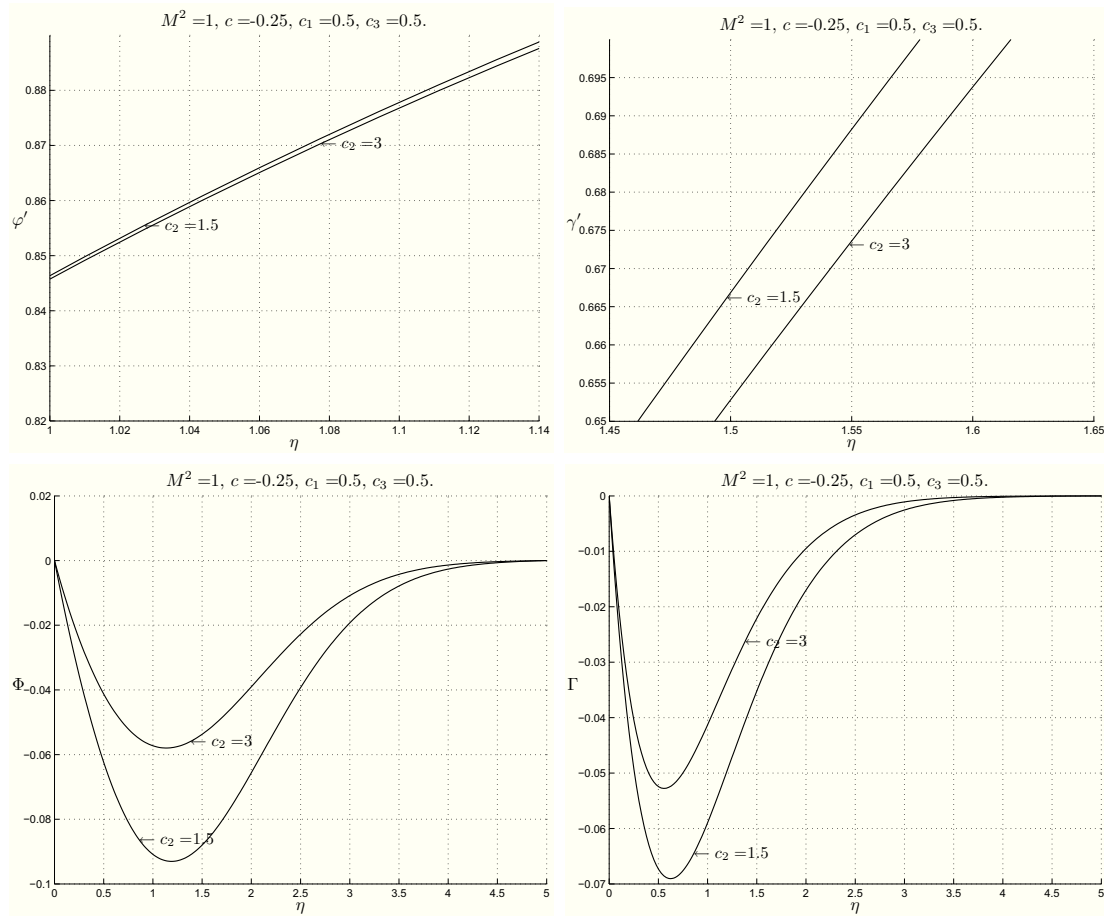


Figure 4.36: CASE III-M:  $\varphi'$ ,  $\gamma'$ ,  $\Phi$ ,  $\Gamma$  profiles for  $M^2 = 1$ ,  $c_1 = 0.5$ ,  $c_3 = 0.5$ ,  $c = -0.25$  when  $c_2 = 1.5$  and  $c_2 = 3$ .

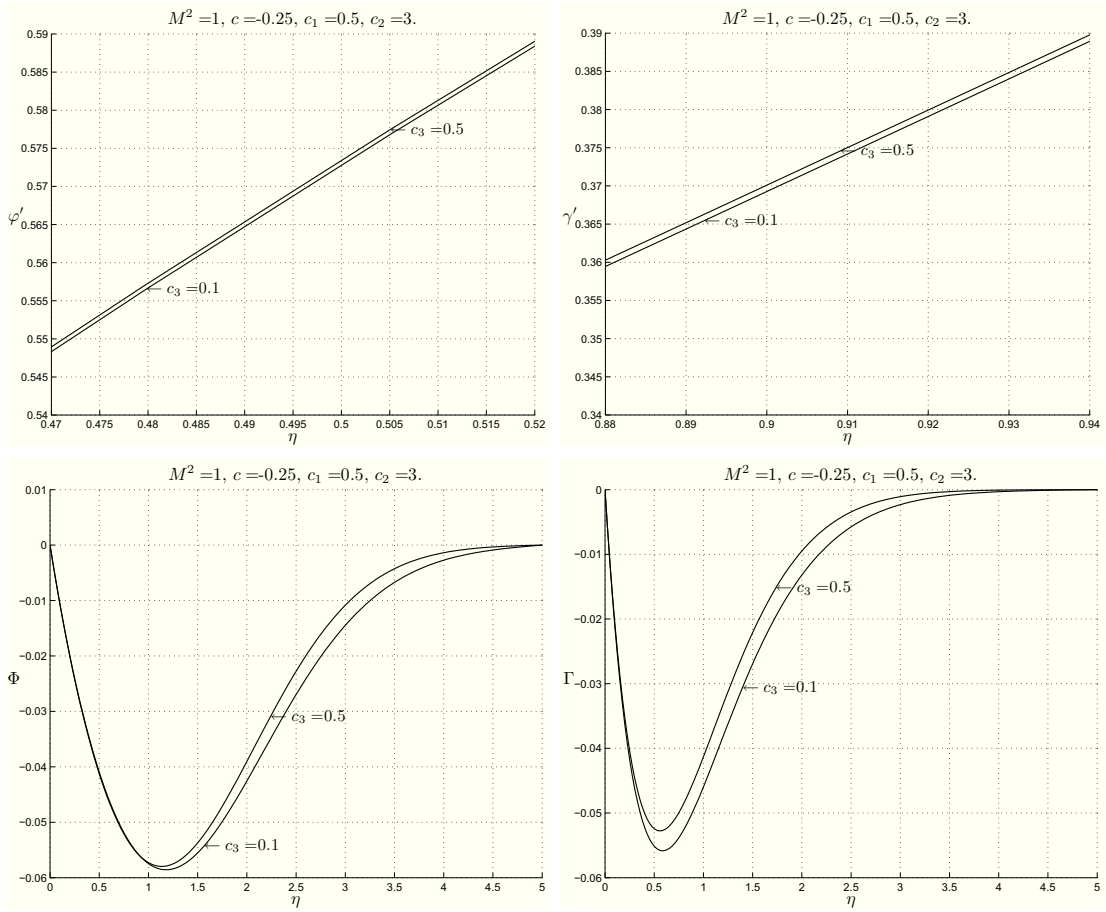


Figure 4.37: CASE III-M:  $\varphi'$ ,  $\gamma'$ ,  $\Phi$ ,  $\Gamma$  profiles for  $M^2 = 1$ ,  $c_1 = 0.5$ ,  $c_2 = 3$ ,  $c = -0.25$  when  $c_3 = 0.1$  and  $c_3 = 0.5$ .

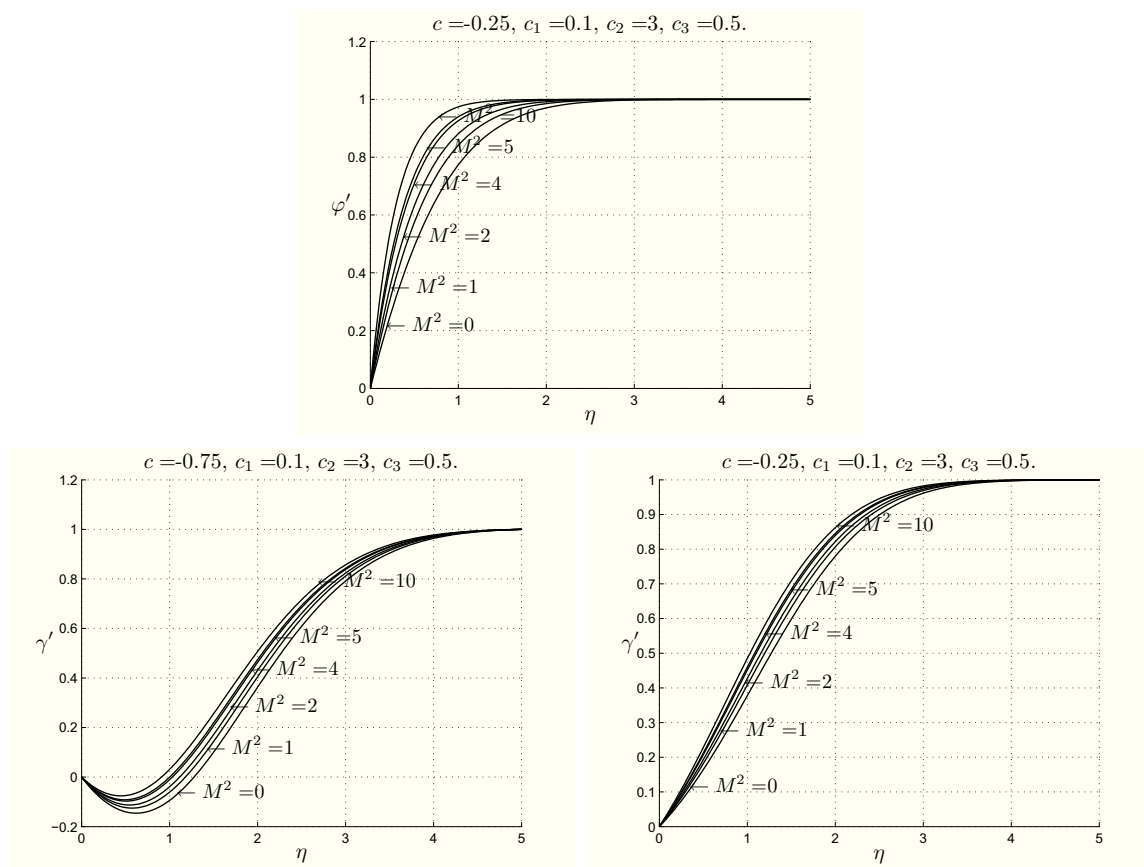


Figure 4.38: CASE III-M: profiles of  $\varphi'$  (Figure 4.38<sub>1</sub>) and  $\gamma'$  (Figures 4.38<sub>2,3</sub>) for several values of  $M^2$  which elucidate the boundary layer thickness.

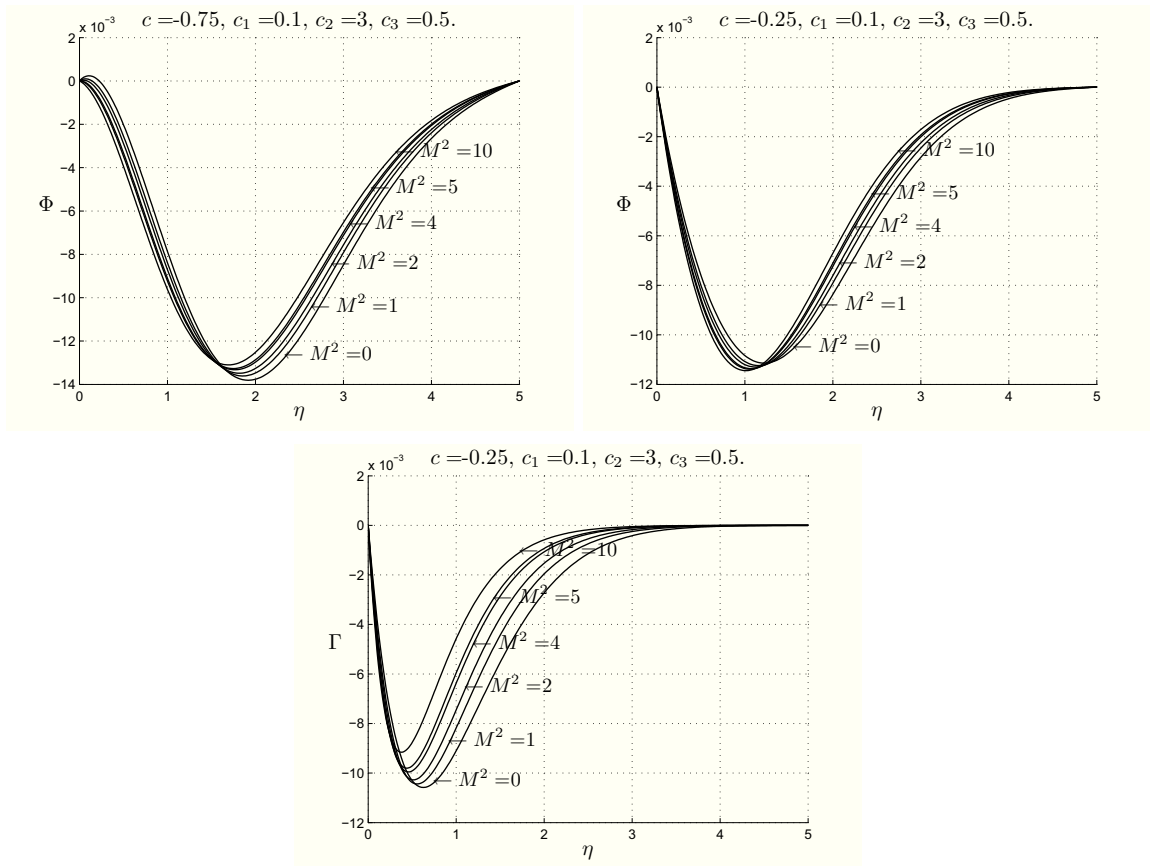


Figure 4.39: CASE III-M: profiles of  $\Phi$  (Figure 4.39<sub>1</sub>) and  $\Gamma$  (Figures 4.39<sub>2,3</sub>) for several values of  $M^2$  which elucidate the boundary layer thickness.

Table 4.29: CASE III-M: values of  $c_r$ ,  $c_{rw}$  and  $c_h$  when  $M^2$  increases.

$c_1$	$c_2$	$c_3$	$M^2$	$c_r$	$c_{rw}$	$c_h$	
0.10	1.50	0.10	1	-0.4546	-0.8024	-0.3639	
			2	-0.4724	-0.8290	-0.3407	
			5	-0.5036	-0.8742	-0.2943	
			10	-0.5292	-0.9099	-0.2500	
			20	-0.5528	-0.9416	-0.2030	
			50	-0.5780	-0.9741	-0.1456	
			100	-0.5921	-0.9917	-0.1097	
			0.50	1	-0.4546	-0.8261	-0.3638
				2	-0.4724	-0.8549	-0.3406
	5	-0.5035		-0.9044	-0.2942		
	10	-0.5290		-0.9440	-0.2498		
	20	-0.5526		-0.9800	-0.2029		
	31.3232	-0.5658		no reverse microrotation	-0.1736		
	50	-0.5777		no reverse microrotation	-0.1455		
	100	-0.5917		no reverse microrotation	-0.1096		
	3.00	0.10		0.10	1	-0.4558	-0.6804
			2		-0.4735	-0.7044	-0.3395
			5		-0.5044	-0.7452	-0.2932
10			-0.5297		-0.7775	-0.2490	
20			-0.5531		-0.8064	-0.2022	
50			-0.5780		-0.8360	-0.1451	
100			-0.5919		-0.8521	-0.1092	
0.50			1		-0.4558	-0.6887	-0.3626
			2		-0.4735	-0.7135	-0.3394
		5	-0.5044	-0.7559	-0.2932		
		10	-0.5297	-0.7897	-0.2490		
		20	-0.5530	-0.8201	-0.2022		
		50	-0.5779	-0.8516	-0.1450		
		100	-0.5918	-0.8689	-0.1092		

Table 4.30: CASE III-M: continuum of Table 4.29.

$c_1$	$c_2$	$c_3$	$M^2$	$c_r$	$c_{rw}$	$c_h$		
0.50	1.50	0.10	1	-0.4434	-0.8507	-0.3769		
			2	-0.4627	-0.8812	-0.3535		
			5	-0.4966	-0.9331	-0.3064		
			10	-0.5248	-0.9744	-0.2608		
			15.9283	-0.5430	no reverse microrotation	-0.2281		
		20	-0.5513	no reverse microrotation	-0.2121			
		50	-0.5798	no reverse microrotation	-0.1524			
		100	-0.5959	no reverse microrotation	-0.1148			
		0.50	1	-0.4435	-0.8717	-0.3761		
			2	-0.4624	-0.9034	-0.3526		
			5	-0.4957	-0.9579	-0.3053		
			9.7249	-0.5222	no reverse microrotation	-0.2616		
			10	-0.5233	no reverse microrotation	-0.2596		
		3.00	0.10	0.10	1	-0.4494	-0.6934	-0.3691
					2	-0.4676	-0.7185	-0.3460
5	-0.4997				-0.7614	-0.2996		
10	-0.5261				-0.7953	-0.2550		
20	-0.5507				-0.8257	-0.2075		
50	-0.5770			-0.8570	-0.1491			
100	-0.5918			-0.8740	-0.1124			
0.50	1			-0.4493	-0.7015	-0.3689		
	2			-0.4675	-0.7274	-0.3458		
	5			-0.4993	-0.7715	-0.2994		
	10			-0.5256	-0.8068	-0.2547		
	20			-0.5499	-0.8385	-0.2072		
50	-0.5760			-0.8716	-0.1489			
100	-0.5907			-0.8897	-0.1122			

If  $c > 0$  or where there is the reverse flow, the origin is a nodal point, while when  $c < 0$  and the reverse flow does not appear, it is a saddle point.

## Chapter 5

# MHD orthogonal stagnation-point flow with $\mathbf{H}$ and $\mathbf{v}$ parallel at infinity

In the next three chapters, we will analyze the previous three types of stagnation-point flow under a hypothesis assuring that the magnetic field is parallel to the flow at infinity. Differently from the previous chapters, the wall towards which the fluid is pointed is the boundary of a solid which is a rigid uncharged dielectric at rest.

We now start with the study of the orthogonal stagnation-point flow under the previous conditions. This problem has been studied in [17] for a Newtonian fluid, but the Authors didn't explain properly the physics of the problem and didn't take into consideration the thickness of the boundary layer, the behaviour of the solution and the influence of the parameters on the motion.

The results presented for the micropolar fluids are new ([9]).

### 5.1 Inviscid fluids CASE IV

We first consider the steady plane MHD flow of a homogeneous, incompressible, electrically conducting inviscid fluid near a stagnation point filling the half-space  $\mathcal{S}$  (see Figure 5.1), given by

$$\mathcal{S} = \{(x_1, x_2, x_3) \in \mathbb{R}^3 : (x_1, x_3) \in \mathbb{R}^2, x_2 > 0\}. \quad (5.1)$$

Differently from the previous chapters,  $\partial\mathcal{S}$ , i.e. the plane  $x_2 = 0$ , is now the boundary of a solid which is a rigid uncharged dielectric at rest occupying  $\mathcal{S}^-$  given by

$$\mathcal{S}^- = \{(x_1, x_2, x_3) \in \mathbb{R}^3 : (x_1, x_3) \in \mathbb{R}^2, x_2 < 0\}. \quad (5.2)$$

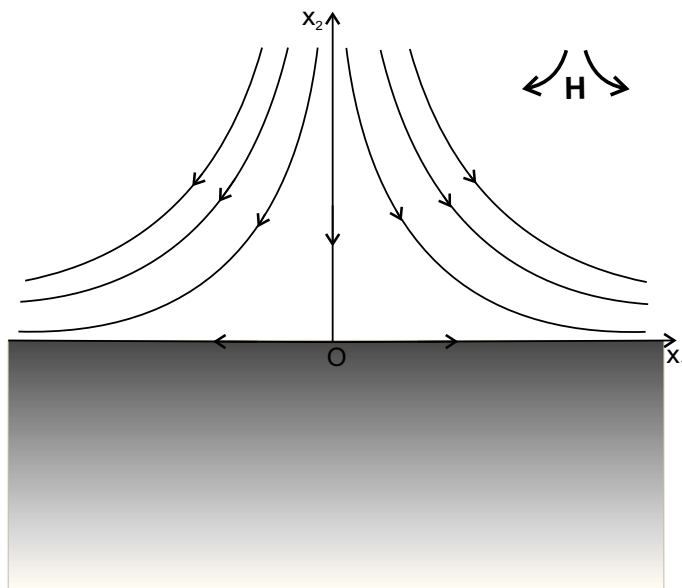


Figure 5.1: Description flow in CASE IV.

In the orthogonal plane stagnation-point flow of an inviscid fluid we search the velocity in the following form

$$v_1 = ax_1, \quad v_2 = -ax_2, \quad v_3 = 0, \quad x_1 \in \mathbb{R}, \quad x_2 \in \mathbb{R}^+, \quad (5.3)$$

with  $a$  positive constant.

The equations governing such a flow in the absence of external mechanical body forces and free electric charges are (2.2). As usual, we impose the no-penetration condition to the velocity field and we assume that the electromagnetic field satisfies (2.5), (2.6).

We suppose that the external magnetic field

$$\mathbf{H}_e = H_\infty(x_1\mathbf{e}_1 - x_2\mathbf{e}_2), \quad H_\infty = \text{constant}, \quad x_1 \in \mathbb{R}, \quad x_2 \in \mathbb{R},$$

permeates the whole physical space and that the external electric field  $\mathbf{E}_e$  is absent.

REMARK 5.1.1. *As it is easy to verify, the field lines of  $\mathbf{H}_e$  have the following parametric equations*

$$\begin{aligned} x_1 &= A_1 e^{H_\infty \lambda}, \\ x_2 &= A_2 e^{-H_\infty \lambda}, \quad \lambda \in \mathbb{R}, \end{aligned} \quad (5.4)$$

where  $A_1, A_2$  are arbitrary constants.

These field lines degenerate if at least one of the two constants  $A_1, A_2$  vanishes. Otherwise they are the hyperbolas

$$x_1x_2 = A_1A_2.$$

These hyperbolas tend to  $x_2 = 0$  as  $|x_1| \rightarrow +\infty$ .

We assume that the total magnetic fields in the fluid and in the solid have the following form

$$\begin{aligned}\mathbf{H} &= H_\infty[x_1h'(x_2)\mathbf{e}_1 - h(x_2)\mathbf{e}_2], \quad x_2 \geq 0, \quad \text{and} \\ \mathbf{H}_s &= H_\infty[x_1h'_s(x_2)\mathbf{e}_1 - h_s(x_2)\mathbf{e}_2], \quad x_2 \leq 0,\end{aligned}\tag{5.5}$$

respectively, where  $h, h_s$  are sufficiently regular unknown functions to be determined ( $h, h_s \in C^2(\mathbb{R}^+)$ ).

We ask that  $\mathbf{H}$  tends to  $\mathbf{H}_e$  as  $x_2 \rightarrow +\infty$  so that  $\mathbf{H}$  is parallel to  $\mathbf{v}$  at infinity and

$$\lim_{x_2 \rightarrow +\infty} h'(x_2) = 1, \quad \lim_{x_2 \rightarrow +\infty} [h(x_2) - x_2] = 0.\tag{5.6}$$

We then suppose that

- (i)  $\mathbf{H}_s$  is not uniform;
- (ii) the non-degenerate field lines of  $\mathbf{H}_s$  tend to  $x_2 = 0$  as  $|x_1| \rightarrow +\infty$ ;

as well as it happens for the external magnetic field  $\mathbf{H}_e$ .

Now we would like to prove the following:

**THEOREM 5.1.2.** *If the solid which occupies  $\mathcal{S}^-$  is a rigid uncharged dielectric at rest and  $\mathbf{H}_s$  satisfies (i) and (ii), then the magnetic field  $\mathbf{H}_s$  is given by*

$$\mathbf{H}_s = H_\infty h'(0)(x_1\mathbf{e}_1 - x_2\mathbf{e}_2), \quad x_2 \leq 0,\tag{5.7}$$

where  $h(x_2)$  is the function in (5.5)<sub>1</sub>.

*Proof.* Since the solid is an uncharged dielectric, it holds

$$\nabla \times \mathbf{H}_s = \mathbf{0}, \quad \text{in } \mathcal{S}^-,$$

from which we get

$$h_s(x_2) = C_1x_2 + C_2, \quad x_2 \leq 0,\tag{5.8}$$

where  $C_1, C_2 \in \mathbb{R}$ .

By virtue of the continuity of the tangential components of the magnetic field across the plane  $x_2 = 0$ , since in  $\mathcal{S}$  the total magnetic field is (5.5)<sub>1</sub>, we find

$$C_1 = h'(0),$$

so that

$$\mathbf{H}_s = H_\infty [h'(0)x_1\mathbf{e}_1 - (h'(0)x_2 + C_2)\mathbf{e}_2]. \quad (5.9)$$

If  $h'(0) = 0$ , then  $\mathbf{H}_s$  is uniform which contradicts hypothesis (i). Hence  $h'(0) \neq 0$  and the magnetic field lines in the solid are

$$\begin{aligned} x_1 &= B_1 e^{H_\infty h'(0)\lambda}, \\ x_2 &= B_2 e^{-H_\infty h'(0)\lambda} - \frac{C_2}{h'(0)}, \quad x_2 \leq 0, \quad B_1, B_2 \in \mathbb{R}. \end{aligned} \quad (5.10)$$

The non-degenerate field lines are the curves

$$x_1 x_2 = B_1 B_2 - \frac{C_2}{h'(0)} x_1, \quad x_2 \leq 0, \quad B_1, B_2 \neq 0. \quad (5.11)$$

The curves in (5.11) tend to  $x_2 = 0$  as  $|x_1| \rightarrow +\infty$  if, and only if,

$$C_2 = 0,$$

from which we get the assertion. □

REMARK 5.1.3. *Of course,  $\mathbf{E}_s = \mathbf{E}_s^i = \mathbf{0}$  in  $\mathcal{S}^-$ .*

REMARK 5.1.4. *Theorem 5.1.2 holds even if  $\mathcal{S}$  is occupied by a viscous fluid for which  $\mathbf{H}$  has the form (5.5)<sub>1</sub>.*

We now consider the inviscid fluid filling the half-space  $\mathcal{S}$ . Since  $\mathcal{S}$  is in contact with the solid through the plane  $x_2 = 0$ , by the hypothesis that the normal component of the magnetic induction vector  $\mathbf{B}$  is continuous across the boundary (see (2.6)), from (5.5)<sub>1</sub> and (5.7) we deduce

$$h(0) = 0. \quad (5.12)$$

Our purpose is now to determine  $(p, \mathbf{H}, \mathbf{E})$  solution of (2.2) in  $\mathcal{S}$  with  $\mathbf{v}$  given by (5.3) such that  $\mathbf{H}$  tends to  $\mathbf{H}_e$  as  $x_2$  goes to infinity. Hence

$$\mathbf{v} \times \mathbf{H} = \mathbf{0} \text{ at infinity } (x_2 \rightarrow +\infty). \quad (5.13)$$

Let the electric field  $\mathbf{E}$  be in the form

$$\mathbf{E} = \mathbf{E}^i = E_1 \mathbf{e}_1 + E_2 \mathbf{e}_2 + E_3 \mathbf{e}_3.$$

The boundary conditions and the Remark 5.1.3 require that

$$E_1 = 0, E_3 = 0 \quad \text{at } x_2 = 0. \quad (5.14)$$

From (2.2)<sub>4</sub> follows that

$$\mathbf{E} = -\nabla\psi,$$

where  $\psi$  is the electrostatic scalar potential.

Equation (2.2)<sub>3</sub> provides  $E_1 = E_2 = 0$ , so that  $\psi = \psi(x_3)$  and

$$\frac{d\psi}{dx_3}(x_3) = \frac{H_\infty}{\sigma_e} x_1 [h''(x_2) + \sigma_e \mu_e a (h'(x_2)x_2 - h(x_2))] = -E_3. \quad (5.15)$$

Further from (5.14)<sub>2</sub>, we get  $\mathbf{E} = \mathbf{0}$  and

$$h''(x_2) + \sigma_e \mu_e a [h'(x_2)x_2 - h(x_2)] = 0. \quad (5.16)$$

The ordinary differential problem (5.16), (5.12) and (5.6)<sub>1</sub> has the unique solution  $h(x_2) = x_2$ , from which we have

$$\mathbf{H} = \mathbf{H}_e = H_\infty (x_1 \mathbf{e}_1 - x_2 \mathbf{e}_2).$$

We underline that  $\mathbf{E} = \mathbf{0}$  and  $\mathbf{H} = \mathbf{H}_e$  are compatible with the conditions at infinity.

Since  $\nabla \times \mathbf{H} = \mathbf{0}$ , from (2.2)<sub>1</sub> follows that the pressure field is not modified by the presence of the magnetic field.

We summarize the results obtained for the inviscid fluid in the following theorem.

**THEOREM 5.1.5.** *Let a homogeneous, incompressible, electrically conducting inviscid fluid occupy the half-space  $\mathcal{S}$  and be embedded in the external electromagnetic field  $\mathbf{H}_e = H_\infty (x_1 \mathbf{e}_1 - x_2 \mathbf{e}_2)$ ,  $\mathbf{E}_e = \mathbf{0}$ . If the total magnetic field in the solid is given by (5.7), then the steady MHD orthogonal stagnation-point flow of such a fluid has the form*

$$\begin{aligned} \mathbf{v} &= a[x_1 \mathbf{e}_1 - x_2 \mathbf{e}_2], \quad \mathbf{E} = \mathbf{0}, \quad \mathbf{H} = \mathbf{H}_e, \\ p &= -\frac{1}{2} \rho a^2 (x_1^2 + x_2^2) + p_0, \quad x_1 \in \mathbb{R}, \quad x_2 \in \mathbb{R}^+. \end{aligned} \quad (5.17)$$

REMARK 5.1.6. *In order to study the influence of  $\mathbf{H}_e$  on the steady orthogonal stagnation-point flow for viscous fluids, it is convenient to suppose that the inviscid fluid orthogonally impinges on the flat plane  $x_2 = A$  and*

$$\begin{aligned} \mathbf{v} &= a[x_1\mathbf{e}_1 - (x_2 - A)\mathbf{e}_2], \quad \mathbf{H}_e = H_\infty[x_1\mathbf{e}_1 - (x_2 - A)\mathbf{e}_2], \quad x_1 \in \mathbb{R}, \quad x_2 \geq A, \\ \mathbf{H} &\rightarrow H_\infty[x_1\mathbf{e}_1 - (x_2 - A)\mathbf{e}_2], \quad \text{as } x_2 \rightarrow +\infty. \end{aligned} \quad (5.18)$$

with  $A$  constant.

*In such a way the stagnation point is not  $(0, 0)$  but  $(0, A)$  and the streamlines and the field lines are hyperbolas whose asymptotes are  $x_1 = 0$  and  $x_2 = A$ .*

*Under these assumptions Theorem 5.1.5 continues to hold by replacing  $x_2$  with  $x_2 - A$ , more precisely:*

$$\mathbf{H} = H_\infty[x_1\mathbf{e}_1 - (x_2 - A)\mathbf{e}_2], \quad p = -\frac{1}{2}\rho a^2 [x_1^2 + (x_2 - A)^2] + p_0. \quad (5.19)$$

## 5.2 Newtonian fluids CASE IV-N

Let us consider now the previous problem for a homogeneous, incompressible, electrically conducting Newtonian fluid.

The equations governing such a flow in the absence of external mechanical body forces and free electric charges are (2.22). As usual, boundary conditions (2.23), (2.5), (2.6) have to be fulfilled.

We use the following similarity transformation to describe the velocity field (see Chapter 1.1.2):

$$v_1 = ax_1f'(x_2), \quad v_2 = -af(x_2), \quad v_3 = 0, \quad x_1 \in \mathbb{R}, \quad x_2 \in \mathbb{R}^+, \quad (5.20)$$

with  $f$  sufficiently regular unknown function ( $f \in C^3(\mathbb{R}^+)$ ).

The condition (2.23) supplies

$$f(0) = 0, \quad f'(0) = 0. \quad (5.21)$$

As for the inviscid fluid, we suppose that an external magnetic field

$$\mathbf{H}_e = H_\infty(x_1\mathbf{e}_1 - x_2\mathbf{e}_2)$$

permeates the whole physical space and that the external electric field  $\mathbf{E}_e = \mathbf{0}$ .

The total magnetic field in the fluid is taken in the following form

$$\mathbf{H} = H_\infty[x_1h'(x_2)\mathbf{e}_1 - h(x_2)\mathbf{e}_2], \quad x_2 \geq 0, \quad (5.22)$$

where  $h$  is a sufficiently regular unknown function ( $h \in C^2(\mathbb{R}^+)$ ) that by virtue of (5.7) satisfies

$$h(0) = 0. \quad (5.23)$$

Further, we impose the following

**Condition P.** *At infinity, the MHD orthogonal stagnation-point flow of a viscous fluid approaches the flow of an inviscid fluid whose velocity, magnetic field and pressure are given by (5.18), (5.19)<sub>1</sub> and (5.19)<sub>2</sub>, respectively.*

Therefore to (5.20) we must also append the following conditions

$$\lim_{x_2 \rightarrow +\infty} f'(x_2) = 1, \quad \lim_{x_2 \rightarrow +\infty} h'(x_2) = 1. \quad (5.24)$$

The asymptotic behaviour of  $f$  and  $h$  at infinity are related to the constant  $A$  in (5.18) in the following way:

$$\lim_{x_2 \rightarrow +\infty} [f(x_2) - x_2] = -A, \quad \lim_{x_2 \rightarrow +\infty} [h(x_2) - x_2] = -A, \quad (5.25)$$

so that

$$\mathbf{v} \times \mathbf{H} = \mathbf{0} \text{ at infinity.} \quad (5.26)$$

The constant  $A$  is not a priori assigned but its value can be computed as part of the solution of the problem.

Our aim is now to determine  $(p, f, \mathbf{H}, \mathbf{E})$  solution in  $\mathcal{S}$  of (2.22) with  $\mathbf{v}$  and  $\mathbf{H}$  given by (5.20) and (5.22), respectively such that Condition P holds.

As for the inviscid fluid, let the electric field  $\mathbf{E}$  be in the form

$$\mathbf{E} = \mathbf{E}^i = E_1 \mathbf{e}_1 + E_2 \mathbf{e}_2 + E_3 \mathbf{e}_3,$$

with the boundary conditions

$$E_1 = 0, E_3 = 0 \text{ at } x_2 = 0. \quad (5.27)$$

From (2.22)<sub>4</sub> we have

$$\mathbf{E} = -\nabla\psi.$$

Moreover, (2.22)<sub>3</sub> provides  $E_1 = E_2 = 0$  so that  $\psi = \psi(x_3)$  and

$$\frac{d\psi}{dx_3}(x_3) = \frac{H_\infty}{\sigma_e} x_1 [h''(x_2) + \sigma_e \mu_e a (f(x_2)h'(x_2) - h(x_2)f'(x_2))] = -E_3. \quad (5.28)$$

As in the inviscid case, we get  $\mathbf{E} = \mathbf{0}$  in  $\mathcal{S}$  and

$$h''(x_2) + \sigma_e \mu_e a [f(x_2)h'(x_2) - h(x_2)f'(x_2)] = 0. \quad (5.29)$$

Now we proceed in order to determine  $f$  and the pressure field.

If we substitute (5.20) into (2.22)<sub>1</sub>, then in components we obtain

$$\begin{aligned} ax_1 \left( \nu f''' + a f f'' - a f'^2 - \frac{\mu_e}{\rho a} H_\infty^2 h h'' \right) &= \frac{1}{\rho} \frac{\partial p}{\partial x_1}, \\ \nu a f'' + a^2 f f' + \frac{\mu_e}{\rho} H_\infty^2 x_1^2 h' h'' &= -\frac{1}{\rho} \frac{\partial p}{\partial x_2}, \\ \frac{\partial p}{\partial x_3} = 0 &\Rightarrow p = p(x_1, x_2). \end{aligned} \quad (5.30)$$

By integrating (5.30)<sub>2</sub>, we find

$$p = -\rho \frac{a^2}{2} f^2(x_2) - \rho a \nu f'(x_2) - \mu_e \frac{H_\infty^2}{2} x_1^2 h'^2(x_2) + P(x_1),$$

where the function  $P(x_1)$  is determined supposing that, far from the wall, the pressure  $p$  has the same behaviour of (5.19).

Therefore, by virtue of (5.24) and (5.25), we get

$$P(x_1) = -\rho \frac{a^2}{2} x_1^2 + \mu_e \frac{H_\infty^2}{2} x_1^2 + p_0^*,$$

where  $p_0^*$  is a suitable constant.

Finally, the pressure field assumes the form

$$p = -\rho \frac{a^2}{2} [x_1^2 + f^2(x_2)] - \rho a \nu f'(x_2) - \mu_e \frac{H_\infty^2}{2} x_1^2 [h'^2(x_2) - 1] + p_0, \quad (5.31)$$

where the constant  $p_0$  is the pressure at the origin.

In consideration of (5.31), from (5.30)<sub>1</sub> we obtain the ordinary differential equation

$$\frac{\nu}{a} f''' + f f'' - f'^2 + 1 - \frac{\mu_e}{\rho} \frac{H_\infty^2}{a^2} (h h'' - h'^2 + 1) = 0. \quad (5.32)$$

We can now summarize our results in the following:

**THEOREM 5.2.1.** *Let a homogeneous, incompressible, electrically conducting Newtonian fluid occupy the half-space  $\mathcal{S}$  and be embedded in the external electromagnetic*

field  $\mathbf{H}_e = H_\infty(x_1\mathbf{e}_1 - x_2\mathbf{e}_2)$ ,  $\mathbf{E}_e = \mathbf{0}$ . If the total magnetic field in the solid is (5.7), then the steady MHD orthogonal stagnation-point flow of such a fluid has the form

$$\begin{aligned} \mathbf{v} &= a[x_1f'(x_2)\mathbf{e}_1 - f(x_2)\mathbf{e}_2], \quad \mathbf{E} = \mathbf{0}, \quad \mathbf{H} = H_\infty[x_1h'(x_2)\mathbf{e}_1 - h(x_2)\mathbf{e}_2], \\ p &= -\rho\frac{a^2}{2}[x_1^2 + f^2(x_2)] - \rho a\nu f'(x_2) - \mu_e\frac{H_\infty^2}{2}x_1^2[h'^2(x_2) - 1] + p_0, \\ x_1 &\in \mathbb{R}, \quad x_2 \in \mathbb{R}^+, \end{aligned}$$

where  $(f, h)$  satisfies the problem (5.32), (5.29), together with the boundary conditions (5.21), (5.23), (5.24).

From the numerical integration we will see that the solution of problem (5.32), (5.29), (5.21), (5.23), (5.24) satisfies condition (5.25).

We now write the boundary value problem in Theorem 5.2.1 in dimensionless form, putting

$$\eta = \sqrt{\frac{a}{\nu}}x_2, \quad \varphi(\eta) = \sqrt{\frac{a}{\nu}}f\left(\sqrt{\frac{\nu}{a}}\eta\right), \quad \Psi(\eta) = \sqrt{\frac{a}{\nu}}h\left(\sqrt{\frac{\nu}{a}}\eta\right), \quad (5.33)$$

we get

$$\begin{aligned} \varphi''' + \varphi\varphi'' - \varphi'^2 + 1 - \beta_m(\Psi\Psi'' - \Psi'^2 + 1) &= 0, \\ \Psi'' + R_m(\varphi\Psi' - \Psi\varphi') &= 0, \\ \varphi(0) = 0, \quad \varphi'(0) = 0, \quad \Psi(0) = 0, \\ \lim_{\eta \rightarrow +\infty} \varphi'(\eta) = 1, \quad \lim_{\eta \rightarrow +\infty} \Psi'(\eta) = 1, \end{aligned} \quad (5.34)$$

where  $\beta_m = \frac{\mu_e H_\infty^2}{\rho a^2}$ ,  $R_m = \frac{\nu}{\eta_e}$  is the magnetic Reynolds number.

We solved numerically problem (5.34) using the `bvp4c` MATLAB routine. The values of  $R_m$  and  $\beta_m$  are chosen according to [17], where the Authors have already computed the solution but they didn't take into consideration the thickness of the boundary layer, the behaviour of the solution and the influence of the parameters on the motion.

As far as the value of  $\beta_m$  is concerned, we have that  $\beta_m$  has to be less than 1 in order to preserve the parallelism of  $\mathbf{H}$  and  $\mathbf{v}$  at infinity, as it will be pointed out in the sequel.

Further for small values of  $R_m$ , equation (5.34)<sub>2</sub> reduces to  $\Psi'' \cong 0$ , which leads to the problem in the absence of the magnetic field. In order to remove this difficulty,

it is convenient to use the following transformation ([23], [24])

$$\xi = \sqrt{R_m}\eta, \quad \varphi_*(\xi) = \sqrt{R_m}\varphi(\sqrt{R_m}\xi), \quad \Psi_*(\eta) = \sqrt{R_m}\Psi(\sqrt{R_m}\xi), \quad (5.35)$$

which furnishes the analogous problem

$$\begin{aligned} R_m\varphi_*''' + \varphi_*\varphi_*'' - \varphi_*'^2 + 1 - \beta_m(\Psi_*\Psi_*'' - \Psi_*'^2 + 1) &= 0, \\ \Psi_*'' + \varphi_*\Psi_*' - \Psi_*\varphi_*' &= 0, \\ \varphi_*(0) = 0, \quad \varphi_*'(0) = 0, \quad \Psi_*(0) &= 0, \\ \lim_{\xi \rightarrow +\infty} \varphi_*'(\xi) = 1, \quad \lim_{\xi \rightarrow +\infty} \Psi_*'(\xi) &= 1. \end{aligned} \quad (5.36)$$

REMARK 5.2.2. *As in the absence of the external magnetic field (Remark 1.1.6), we will see that*

$$\lim_{\eta \rightarrow +\infty} \varphi''(\eta) = 0, \quad \lim_{\eta \rightarrow +\infty} \varphi'(\eta) = 1.$$

Therefore we define:

- $\bar{\eta}_\varphi$  the value of  $\eta$  such that  $\varphi'(\bar{\eta}_\varphi) = 0.99$ .

If  $\eta > \bar{\eta}_\varphi$ , then  $\varphi \cong \eta - \alpha$ , with  $\alpha = \sqrt{\frac{a}{\nu}}A$ , so that the thickness of the layer affected by the viscosity is  $\bar{\eta}_\varphi\sqrt{\frac{\nu}{a}}$ .

As well as  $\varphi$ , in this case we also have that

$$\lim_{\eta \rightarrow +\infty} \Psi''(\eta) = 0, \quad \lim_{\eta \rightarrow +\infty} \Psi'(\eta) = 1.$$

If we denote by  $\bar{\eta}_\Psi$  the value of  $\eta$  such that  $\Psi'(\bar{\eta}_\Psi) = 0.99$ , then we have that for  $\eta > \bar{\eta}_\Psi$ ,  $\Psi \cong \eta - \alpha$ .

The numerical results show that the values of  $\alpha$  computed for  $\varphi$  and  $\Psi$  are in good agreement, especially when  $\beta_m$  is small or  $R_m$  is big. This fact can be well observed displaying that the velocity and the magnetic field are parallel far from the obstacle, as we will see in the next figures.

The numerical values of  $\alpha$ ,  $\varphi''(0)$ ,  $\Psi'(0)$  in dependence on  $R_m$  and  $\beta_m$  are listed in Table 5.1.

This Table has been obtained for small values of  $R_m$  recomputing the corresponding values of  $\eta$ ,  $\varphi$  and  $\Psi$ . More precisely, for  $R_m = 0.01, 0.1$  with transformation (5.35) we get Table 5.2.

If  $\beta_m$  increases, then  $\alpha$  increases, while  $\varphi''(0)$  and  $\Psi'(0)$  decrease. Further  $\alpha$ ,  $\varphi''(0)$  and  $\Psi'(0)$  decrease as  $R_m$  increases.

Table 5.1: CASE IV-N: descriptive quantities of the motion for several values of  $R_m$  and  $\beta_m$ .

$R_m$	$\beta_m$	$\varphi''(0)$	$\Psi'(0)$	$\alpha$	$\bar{\eta}_\varphi$
0.01	0.00	1.2326	0.9273	0.6479	2.3881
	0.20	1.2040	0.9191	0.8021	6.6017
	0.50	1.1435	0.8991	1.2557	19.4174
	0.70	1.0764	0.8733	2.0070	30.1200
	0.90	0.9437	0.8162	4.2495	44.7362
0.1	0.00	1.2326	0.8110	0.6479	2.3802
	0.20	1.1650	0.7922	0.7884	5.2230
	0.50	1.0278	0.7486	1.1879	9.1610
	0.70	0.8877	0.6969	1.8066	12.6325
	0.90	0.6529	0.5994	3.4034	15.2579
1	0.00	1.2326	0.6080	0.6479	2.3806
	0.20	1.1193	0.5812	0.7616	3.1533
	0.50	0.9065	0.5258	1.0511	4.3173
	0.70	0.7189	0.4727	1.4028	4.7799
	0.90	0.4676	0.3976	2.0234	4.9350
100	0.00	1.2326	0.2027	0.6479	2.3806
	0.20	1.1004	0.1895	0.7266	2.6669
	0.50	0.8665	0.1641	0.9234	3.3783
	0.70	0.6686	0.1401	1.1887	4.2186
	0.90	0.3935	0.1010	1.8284	4.8675
1000	0.00	1.2326	0.1003	0.6479	2.3806
	0.20	1.1019	0.0935	0.7247	2.6619
	0.50	0.8704	0.0804	0.9167	3.3621
	0.70	0.6740	0.0683	1.1762	4.1973
	0.90	0.3993	0.0487	1.8071	4.8625

Table 5.2: CASE IV-N: descriptive quantities of the motion for several values of  $\beta_m$  when  $R_m$  is less than 1.

$R_m$	$\beta_m$	$\varphi_*''(0)$	$\Psi_*'(0)$	$\alpha_*$	$\bar{\xi}_{\varphi_*}$
0.01	0.00	12.3259	0.9273	0.0648	0.2388
	0.20	12.0400	0.9191	0.0802	0.6602
	0.50	11.4350	0.8991	0.1256	1.9417
	0.70	10.7640	0.8733	0.2007	3.0120
	0.90	9.4374	0.8162	0.4249	4.4736
0.10	0.00	3.8978	0.8110	0.2049	0.7527
	0.20	3.6842	0.7922	0.2493	1.6517
	0.50	3.2501	0.7486	0.3756	2.8970
	0.70	2.8071	0.6969	0.5713	3.9947
	0.90	2.0646	0.5994	1.0763	4.8250

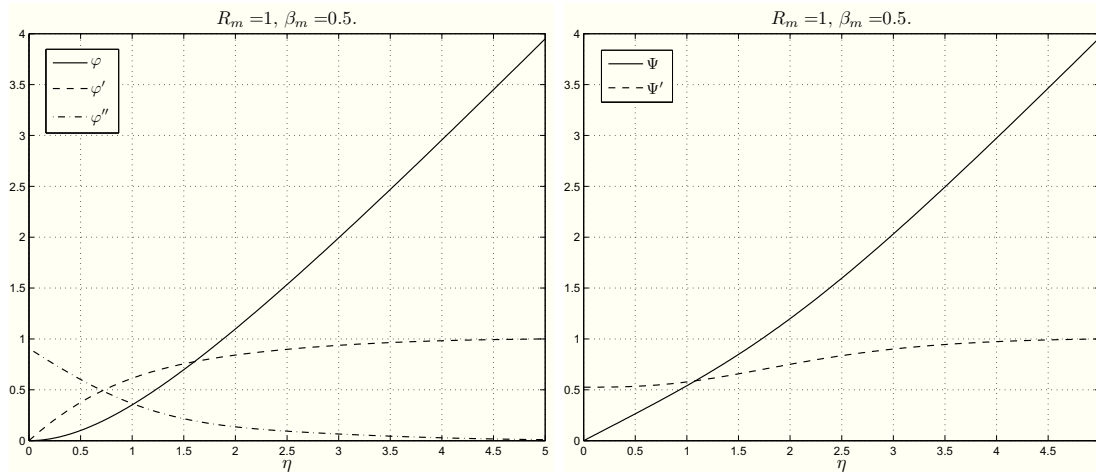


Figure 5.2: CASE IV-N: the first figure shows  $\varphi, \varphi', \varphi''$  for  $R_m = 1$  and  $\beta_m = 0.5$ , while the second shows  $\Psi, \Psi'$  for  $R_m = 1$  and  $\beta_m = 0.5$ .

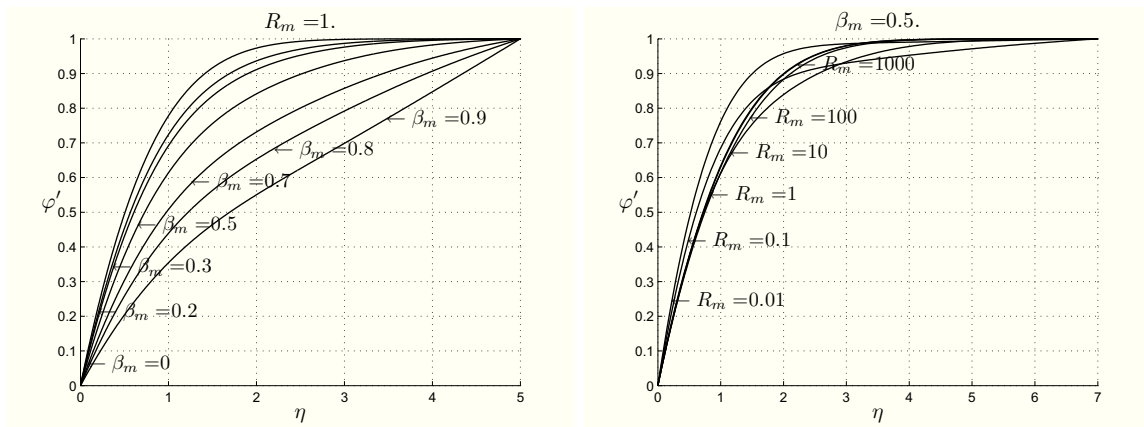


Figure 5.3: CASE IV-N: plots showing  $\varphi'$  for different  $\beta_m$  and  $R_m$ , respectively.

We remark that  $\Psi'(0) \neq 0$  according to hypothesis (i) of Theorem 5.1.2.

In Figure 5.2<sub>1</sub> we can see the profiles  $\varphi, \varphi', \varphi''$  for  $R_m = 1$  and  $\beta_m = 0.5$ , while Figure 5.2<sub>2</sub> illustrates the behaviour of  $\Psi, \Psi'$  for the same values of  $R_m$  and  $\beta_m$ .

We have plotted the profiles of  $\varphi, \varphi', \varphi'', \Psi, \Psi'$  only for  $R_m = 1$  and  $\beta_m = 0.5$  because they have an analogous behaviour for  $R_m \neq 1$  and  $\beta_m \neq 0.5$ .

Table 5.1 underlines that the thickness of the boundary layer depends on  $R_m$  and  $\beta_m$ . More precisely, it increases when  $\beta_m$  increases (as is easy to see in Figure 5.3<sub>1</sub>). This behaviour is not surprising because  $\beta_m$  is a measure of the strength of the applied magnetic field and as it is underlined in [17] when the magnetic field is strong the disturbances are no longer contained within a boundary layer along the wall. This means that boundary conditions can no longer be prescribed at infinity. In particular, in [17] it is proved that in a perfectly conducting fluid the displacement thickness becomes infinite as  $\beta_m$  goes to  $1^-$ .

As far as the dependence of the thickness of the boundary layer on  $R_m$  is concerned, it decreases when  $R_m$  increases (as is easy to see in Figure 5.3<sub>2</sub>). This fact is in agreement with the results obtained for the orthogonal stagnation-point flow in Chapter 2, where we have shown that the thickness of the boundary layer decreases as the Hartmann number  $M^2$  increases. Actually,  $R_m$  and  $M^2$  are both proportional to the electrical conductivity.

We stress that the more  $R_m$  is small and the more  $\beta_m$  is close to 1 the more the thickness of the boundary layer is larger than in the other cases of orthogonal stagnation-point flow treated in this Thesis (Chapters 1.1 and 2).

Finally, we display the streamlines of the flow in Figure 5.4. As is easily seen from the figures, the flow and the magnetic field are completely overlapped far from the obstacle and the more  $R_m$  increases the more the two lines coincide.

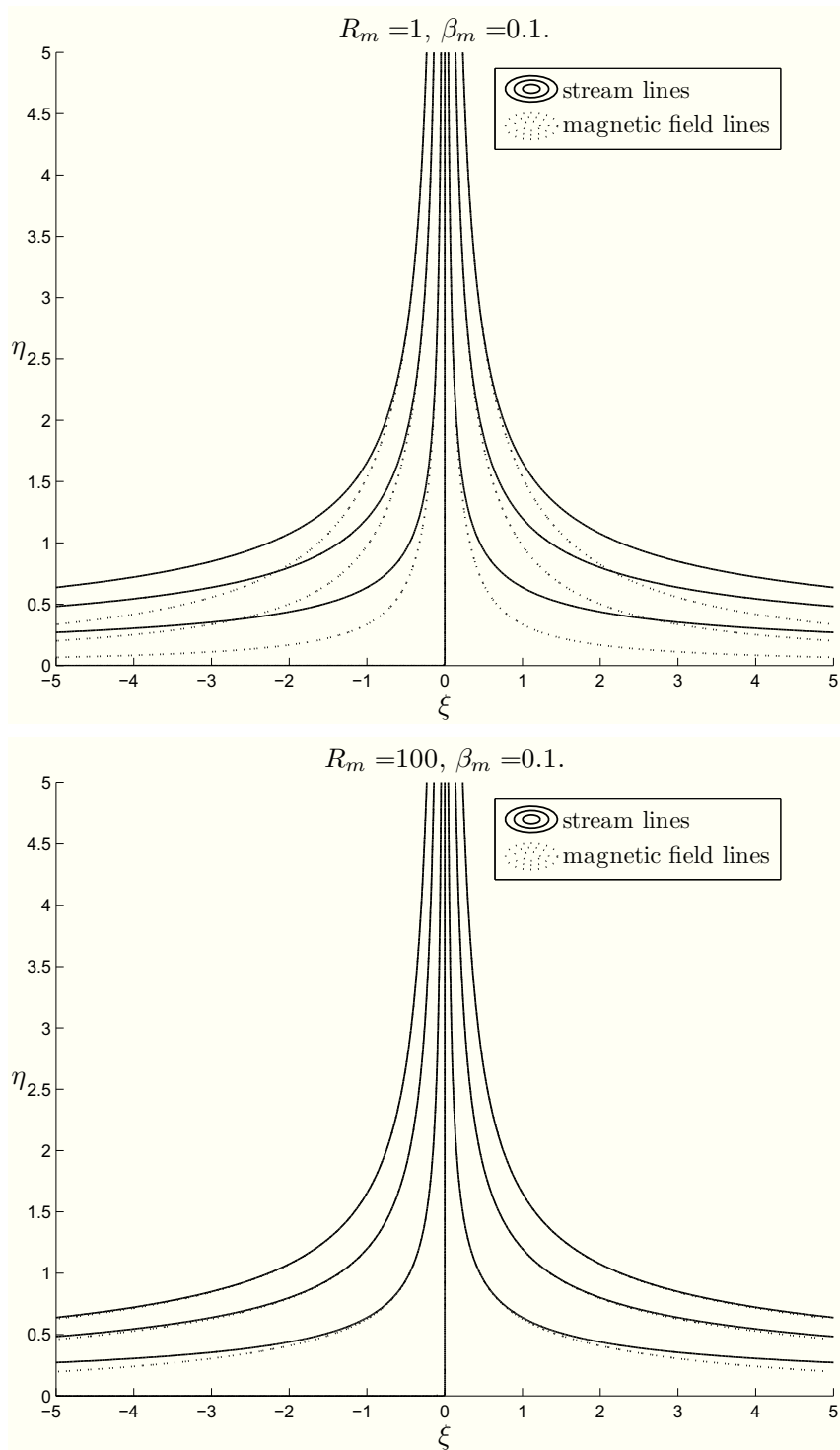


Figure 5.4: CASE IV-N: figures show the streamlines for  $\beta_m = 0.1$  and  $R_m = 1$  or  $R_m = 100$ , respectively.

### 5.3 Micropolar fluids CASE IV-M

Let now take into exam the steady two-dimensional MHD orthogonal stagnation-point flow of a homogeneous, incompressible, electrically conducting micropolar fluid towards a flat surface coinciding with the plane  $x_2 = 0$ , the flow being confined to the half-space  $\mathcal{S}$ , having equation (5.1).

In the absence of free electric charges and external mechanical body forces and body couples, the MHD equations for such a fluid are (2.44).

As far as the boundary conditions are concerned, we prescribe the no-slip condition to the velocity and the strict adherence condition to the microrotation (2.45) and we ask that the electromagnetic field satisfies (2.5) and (2.6).

We recall that the orthogonal stagnation-point flow is determined by (see Chapter 1.1.3)

$$\begin{aligned} v_1 &= ax_1 f'(x_2), \quad v_2 = -af(x_2), \quad v_3 = 0, \\ w_1 &= 0, \quad w_2 = 0, \quad w_3 = x_1 F(x_2), \quad x_1 \in \mathbb{R}, \quad x_2 \in \mathbb{R}^+, \end{aligned} \quad (5.37)$$

where  $f, F$  are sufficiently regular unknown functions ( $f \in C^3(\mathbb{R}^+)$ ,  $F \in C^2(\mathbb{R}^+)$ ). Conditions (2.45) imply

$$f(0) = 0, \quad f'(0) = 0, \quad F(0) = 0. \quad (5.38)$$

As for the previous two models of fluid, we suppose that an external magnetic field

$$\mathbf{H}_e = H_\infty (x_1 \mathbf{e}_1 - x_2 \mathbf{e}_2)$$

permeates the whole physical space and that the external electric field is absent.

We search the total magnetic field in the fluid in the following form

$$\mathbf{H} = H_\infty [x_1 h'(x_2) \mathbf{e}_1 - h(x_2) \mathbf{e}_2], \quad (5.39)$$

where  $h$  is a sufficiently regular unknown function ( $h \in C^2(\mathbb{R}^+)$ ). We recall that from Theorem 5.1.2 follows that in the solid the total magnetic field has the form  $\mathbf{H}_s = H_\infty h'(0)(x_1 \mathbf{e}_1 - x_2 \mathbf{e}_2)$ , which gives the additional condition

$$h(0) = 0. \quad (5.40)$$

We require that the MHD orthogonal stagnation-point flow satisfies the Condition P at infinity.

Therefore to (5.37) we also append

$$\lim_{x_2 \rightarrow +\infty} f'(x_2) = 1, \quad \lim_{x_2 \rightarrow +\infty} F(x_2) = 0, \quad \lim_{x_2 \rightarrow +\infty} h'(x_2) = 1. \quad (5.41)$$

The asymptotic behaviour of  $f$  and  $h$  at infinity is related to  $x_2$  as for the Newtonian case. So relation (5.25) continues to hold and we have

$$\mathbf{v} \times \mathbf{H} = \mathbf{0} \text{ at infinity.} \tag{5.42}$$

Our aim is now to determine  $(p, f, F, \mathbf{H}, \mathbf{E})$  solution in  $\mathcal{S}$  of (2.44) with  $\mathbf{v}, \mathbf{w}$  given by (5.37) such that Condition P holds.

Since  $(2.44)_{3,4,5,6}$  are the same as  $(2.22)_{4,5,6,7}$ ,  $\mathbf{H}, \mathbf{E}$  depend only on the form of the velocity field, which is the same as that of the Newtonian fluid. Hence, following the arguments of the previous section, we get

$$\mathbf{E} = \mathbf{0}, \quad h''(x_2) + \sigma_e \mu_e a [f(x_2)h'(x_2) - h(x_2)f'(x_2)] = 0. \tag{5.43}$$

We substitute (5.37) and (5.39) into  $(2.44)_{1,3}$  to obtain

$$\begin{aligned} ax_1 \left[ (\nu + \nu_r) f''' + a f f'' - a f'^2 + \frac{2\nu_r}{a} F' - \frac{\mu_e}{\rho a} H_\infty^2 h h'' \right] &= \frac{1}{\rho} \frac{\partial p}{\partial x_1}, \\ a(\nu + \nu_r) f'' + a^2 f f' + 2\nu_r F + \frac{\mu_e}{\rho} H_\infty^2 x_1^2 h' h'' &= -\frac{1}{\rho} \frac{\partial p}{\partial x_2}, \\ \frac{\partial p}{\partial x_3} = 0 &\Rightarrow p = p(x_1, x_2), \\ \lambda F'' + I a (F' f - F f') - 2\nu_r (2F + a f'') &= 0. \end{aligned} \tag{5.44}$$

Then, by integrating  $(5.44)_2$ , we find

$$p = -\rho \frac{a^2}{2} f^2(x_2) - \rho a (\nu + \nu_r) f'(x_2) - 2\nu_r \rho \int_0^{x_2} F(s) ds - \mu_e \frac{H_\infty^2}{2} x_1^2 h'^2(x_2) + P(x_1),$$

where the function  $P(x_1)$  is determined supposing that, far from the wall, the pressure  $p$  has the same behaviour as for an inviscid fluid, whose velocity is given by (5.18) and the pressure is given by (5.19).

Therefore, by virtue of (5.41) and (5.25) we get

$$P(x_1) = -\rho \frac{a^2}{2} x_1^2 + \mu_e \frac{H_\infty^2}{2} x_1^2 + p_0^*.$$

Consequently, the pressure field assumes the form

$$\begin{aligned} p = -\rho \frac{a^2}{2} [x_1^2 + f^2(x_2)] - \rho a (\nu + \nu_r) f'(x_2) - 2\nu_r \rho \int_0^{x_2} F(s) ds \\ - \mu_e \frac{H_\infty^2}{2} x_1^2 [h'^2(x_2) - 1] + p_0. \end{aligned} \tag{5.45}$$

In consideration of (5.45), from (5.44)<sub>1</sub> we obtain the ordinary differential equation

$$\frac{\nu + \nu_r}{a} f''' + f f'' - f'^2 + 1 + \frac{2\nu_r}{a^2} F' - \frac{\mu_e H_\infty^2}{\rho a^2} [h h'' - h'^2 + 1] = 0, \quad (5.46)$$

together with equations (5.44)<sub>4</sub>, (5.43)<sub>2</sub> and the boundary conditions (5.38), (5.41) and (5.40).

Hence we can state:

**THEOREM 5.3.1.** *Let a homogeneous, incompressible, electrically conducting micropolar fluid occupy the half-space  $\mathcal{S}$  and be embedded in the external magnetic field  $\mathbf{H}_e = H_\infty(x_1 \mathbf{e}_1 - x_2 \mathbf{e}_2)$ ,  $\mathbf{E}_e = \mathbf{0}$ . If the total magnetic field in the solid is (5.7), then the steady MHD orthogonal stagnation-point flow of such a fluid has the form*

$$\begin{aligned} \mathbf{v} &= a x_1 f'(x_2) \mathbf{e}_1 - a f(x_2) \mathbf{e}_2, \quad \mathbf{w} = x_1 F(x_2) \mathbf{e}_3, \\ \mathbf{H} &= H_\infty [x_1 h'(x_2) \mathbf{e}_1 - h(x_2) \mathbf{e}_2], \quad \mathbf{E} = \mathbf{0}, \\ p &= -\rho \frac{a^2}{2} [x_1^2 + f^2(x_2)] - \rho a (\nu + \nu_r) f'(x_2) \\ &\quad - 2\nu_r \rho \int_0^{x_2} F(s) ds - \mu_e \frac{H_\infty^2}{2} x_1^2 [h'^2(x_2) - 1] + p_0, \quad x_1 \in \mathbb{R}, \quad x_2 \in \mathbb{R}^+, \end{aligned}$$

where  $(f, F, h)$  satisfies the problem (5.46), (5.44)<sub>4</sub>, (5.43)<sub>2</sub> and the boundary conditions (5.38), (5.41) and (5.40), provided  $F \in L^1([0, +\infty))$ .

It is convenient to rewrite the boundary value problem in Theorem 5.3.1 in dimensionless form in order to reduce the number of the material parameters. To this end we use

$$\begin{aligned} \eta &= \sqrt{\frac{a}{\nu + \nu_r}} x_2, \quad \varphi(\eta) = \sqrt{\frac{a}{\nu + \nu_r}} f \left( \sqrt{\frac{\nu + \nu_r}{a}} \eta \right), \\ \Psi(\eta) &= \sqrt{\frac{a}{\nu + \nu_r}} h \left( \sqrt{\frac{\nu + \nu_r}{a}} \eta \right), \quad \Phi(\eta) = \frac{2\nu_r}{a^2} \sqrt{\frac{a}{\nu + \nu_r}} F \left( \sqrt{\frac{\nu + \nu_r}{a}} \eta \right). \end{aligned} \quad (5.47)$$

So system (5.46), (5.44)<sub>4</sub> and (5.43)<sub>2</sub> can be written as

$$\begin{aligned} \varphi''' + \varphi \varphi'' - \varphi'^2 + 1 + \Phi' - \beta_m (\Psi \Psi'' - \Psi'^2 + 1) &= 0, \\ \Phi'' + c_3 \Phi' \varphi - \Phi (c_3 \varphi' + c_2) - c_1 \varphi'' &= 0, \\ \Psi'' + R_m (\varphi \Psi' - \Psi \varphi') &= 0, \end{aligned} \quad (5.48)$$

where  $c_1, c_2, c_3$  are given by (1.25) and

$$\beta_m = \frac{\mu_e H_\infty^2}{\rho a^2}, \quad R_m = \frac{\nu + \nu_r}{\eta_e}. \quad (5.49)$$

The boundary conditions (5.38), (5.41) and (5.40) in dimensionless form become:

$$\begin{aligned} \varphi(0) = 0, \quad \varphi'(0) = 0, \quad \Phi(0) = 0, \quad \Psi(0) = 0, \\ \lim_{\eta \rightarrow +\infty} \varphi'(\eta) = 1, \quad \lim_{\eta \rightarrow +\infty} \Phi(\eta) = 0, \quad \lim_{\eta \rightarrow +\infty} \Psi'(\eta) = 1. \end{aligned} \quad (5.50)$$

To study the flow regime, we now provide the numerical solution of the nonlinear differential problem (5.48), (5.50).

The values of  $c_1, c_2, c_3$  are chosen according to [27] and to the previous chapters, while the values of  $R_m$  and  $\beta_m$  according to [17] and to the previous section.

We recall that  $\beta_m$  has to be less than 1 in order to preserve the parallelism of  $\mathbf{H}$  and  $\mathbf{v}$  at infinity and that for small values of  $R_m$  equation (5.48)<sub>3</sub> reduces to  $\Psi'' \cong 0$ , which leads to the problem in the absence of the magnetic field. In order to avoid this difficulty, it is convenient to use the following transformation ([23], [24])

$$\begin{aligned} \xi = \sqrt{R_m} \eta, \quad \varphi_*(\xi) = \sqrt{R_m} \varphi(\sqrt{R_m} \xi), \\ \Psi_*(\eta) = \sqrt{R_m} \Psi(\sqrt{R_m} \xi), \quad \Phi_*(\xi) = \sqrt{R_m} \Phi(\sqrt{R_m} \xi), \end{aligned} \quad (5.51)$$

which furnishes the analogous problem

$$\begin{aligned} R_m \varphi_*''' + \varphi_* \varphi_*'' - \varphi_*'^2 + 1 + \Phi_*' - \beta_m (\Psi_* \Psi_*'' - \Psi_*'^2 + 1) &= 0, \\ R_m \Phi_*'' + c_3 \Phi_*' \varphi_* - \Phi_* (c_3 \varphi_*' + c_2) - R_m c_1 \varphi_*'' &= 0, \\ \Psi_*'' + \varphi_* \Psi_*' - \Psi_* \varphi_*' &= 0, \\ \varphi_*(0) = 0, \quad \varphi_*'(0) = 0, \quad \Phi_*(0) = 0, \quad \Psi_*(0) = 0, \\ \lim_{\xi \rightarrow +\infty} \varphi_*'(\xi) = 1, \quad \lim_{\xi \rightarrow +\infty} \Phi_*(\xi) = 0, \quad \lim_{\xi \rightarrow +\infty} \Psi_*'(\xi) = 1. \end{aligned} \quad (5.52)$$

REMARK 5.3.2. *The numerical integration reveals that the solution  $(\varphi, \Phi, \Psi)$  of problem (5.48) satisfies the conditions (5.50)<sub>5,6,7</sub>; therefore we apply Remark 1.1.9, where we denoted by:*

- $\bar{\eta}_\varphi$  the value of  $\eta$  such that  $\varphi'(\bar{\eta}_\varphi) = 0.99$ ;
- $\bar{\eta}_\Phi$  the value of  $\eta$  such that  $\Phi(\bar{\eta}_\Phi) = -0.01$ .

Hence if  $\eta > \bar{\eta}_\varphi$  then  $\varphi \cong \eta - \alpha$ , and if  $\eta > \bar{\eta}_\Phi$ , then  $\Phi \cong 0$ .

The influence of the viscosity on the velocity and on the microrotation appears only in a layer lining the boundary whose thickness is  $\bar{\eta}_\varphi$  for the velocity and  $\bar{\eta}_\Phi$  for the microrotation. The thickness  $\delta$  of the boundary layer for the flow is defined as

$$\delta = \max(\bar{\eta}_\varphi, \bar{\eta}_\Phi).$$

As well as in the Newtonian case, we also have that

$$\lim_{\eta \rightarrow +\infty} \Psi''(\eta) = 0, \quad \lim_{\eta \rightarrow +\infty} \Psi'(\eta) = 1.$$

If we define as  $\bar{\eta}_\Psi$  the value of  $\eta$  such that  $\Psi'(\bar{\eta}_\Psi) = 0.99$ , then we have that for  $\eta > \bar{\eta}_\Psi$ ,  $\Psi \cong \eta - \alpha$ .

The numerical results show that the values of  $\alpha$  computed for  $\varphi$  and  $\Psi$  are in good agreement, especially when  $\beta_m$  is small or  $R_m$  is big. This fact can be well observed displaying that the velocity and the magnetic field are parallel far from the obstacle, as we will see in the next figures.

Table 5.3 shows the numerical results of the descriptive quantities of problem (5.48)-(5.50) in dependence on some values of  $c_1$ ,  $c_2$ ,  $c_3$ ,  $\beta_m$  and  $R_m$ .

We notice that the first lines of Table 5.3 have been obtained for small values of  $R_m$  recomputing the corresponding values of  $\eta$ ,  $\varphi$ ,  $\Phi$ , and  $\Psi$ . More precisely, for  $R_m = 0.01$  with transformation (5.51) we get Table 5.4.

If we fix  $\beta_m$  and  $R_m$ , we see that the considerations of the case in the absence of the external magnetic field (Chapter 1.1.3) continue to hold (as easily seen in Figures from 5.5 to 5.7).

As far as the dependence on  $R_m$  and  $\beta_m$  is concerned, we can see from Table 5.3 that:

- if  $\beta_m$  increases, then  $\alpha$  and  $\Phi'(0)$  increase, while  $\varphi''(0)$  and  $\Psi'(0)$  decrease;
- if  $R_m$  increases, then  $\alpha$ ,  $\varphi''(0)$ ,  $|\Phi'(0)|$  and  $\Psi'(0)$  decrease.

In Figure 5.8<sub>1</sub> we furnish the profiles of  $\varphi$ ,  $\varphi'$ ,  $\varphi''$  when  $c_1 = 0.5$ ,  $c_2 = 3.0$ ,  $c_3 = 0.5$ ,  $R_m = 1$  and  $\beta_m = 0.5$ , while Figure 5.8<sub>2</sub> shows the behaviour of  $\Phi$ ,  $\Phi'$  for the same values of the parameters. The functions  $\Psi$ ,  $\Psi'$  are plotted in Figure 5.8<sub>3</sub>.

For other choices of the parameters, the profiles of  $\varphi$ ,  $\varphi'$ ,  $\varphi''$ ,  $\Phi$ ,  $\Phi'$ ,  $\Psi$ ,  $\Psi'$  are very similar.

Table 5.3 underlines that the thickness of the boundary layer depends on  $R_m$  and  $\beta_m$ . More precisely, it increases when  $\beta_m$  increases. This behaviour is the same as in the Newtonian case and it is not surprising because  $\beta_m$  is a measure of the strength of the applied magnetic field and as it is underlined in [17] when the magnetic field is strong the disturbances are no longer contained within a boundary layer along the wall. This means that boundary conditions can no longer be prescribed at infinity.

Table 5.3: CASE IV-M: descriptive quantities of the motion for several values of  $c_1$ ,  $c_2$ ,  $c_3$ ,  $R_m$  and  $\beta_m$ .

$R_m$	$\beta_m$	$c_1$	$c_2$	$c_3$	$\varphi''(0)$	$\Psi'(0)$	$\Phi'(0)$	$\alpha$	$\bar{\eta}_\varphi$	$\bar{\eta}_\Phi$	$\delta$			
0.01	0.00	0.10	1.50	0.10	1.2218	0.9275	-0.0532	0.6445	2.3341	0.7669	2.3341			
				0.50	1.2231	0.9275	-0.0510	0.6448	2.3508	0.7169	2.3508			
			3.00	0.10	1.2250	0.9275	-0.0444	0.6453	2.3508	0.6669	2.3508			
				0.50	1.2256	0.9275	-0.0434	0.6454	2.3675	0.6335	2.3675			
			0.50	1.50	0.10	1.1780	0.9287	-0.2659	0.6309	2.1340	0.7669	2.1340		
					0.50	1.1848	0.9287	-0.2553	0.6321	2.1841	0.7169	2.1841		
		3.00	0.10	1.1943	0.9284	-0.2220	0.6350	2.2174	0.6836	2.2174				
				0.50	1.1972	0.9284	-0.2173	0.6356	2.2508	0.6502	2.2508			
		0.50	0.10	1.50	0.10	1.1335	0.8995	-0.0500	1.2492	19.3731	0.7836	19.3731		
					0.50	1.1347	0.8995	-0.0481	1.2496	19.3731	0.7169	19.3731		
			3.00	0.10	1.1366	0.8994	-0.0417	1.2508	19.3898	0.6836	19.3898			
					0.50	1.1371	0.8994	-0.0408	1.2510	19.3898	0.6502	19.3898		
			0.50	1.50	0.10	1.0929	0.9012	-0.2505	1.2227	19.1731	0.7836	19.1731		
					0.50	1.0992	0.9011	-0.2409	1.2249	19.1897	0.7336	19.1897		
		3.00	0.10	1.1085	0.9007	-0.2085	1.2308	19.2397	0.6836	19.2397				
				0.50	1.1111	0.9007	-0.2043	1.2318	19.2564	0.6502	19.2564			
		1	0.00	0.10	1.50	0.10	1.2218	0.6081	-0.0532	0.6446	2.3258	1.6005	2.3258	
						0.50	1.2231	0.6082	-0.0510	0.6448	2.3374	1.3338	2.3374	
					3.00	0.10	1.2250	0.6082	-0.0444	0.6453	2.3474	1.0020	2.3474	
							0.50	1.2256	0.6083	-0.0434	0.6454	2.3525	0.8469	2.3525
					0.50	1.50	0.10	1.1780	0.6087	-0.2659	0.6310	2.1274	2.9093	2.9093
							0.50	1.1848	0.6093	-0.2553	0.6321	2.1691	2.4325	2.4325
				3.00	0.10	1.1943	0.6092	-0.2220	0.6350	2.2157	2.3441	2.3441		
						0.50	1.1972	0.6095	-0.2173	0.6356	2.2391	2.1190	2.2391	
0.50	0.10			1.50	0.10	0.8963	0.5258	-0.0429	1.0463	4.2864	1.8723	4.2864		
					0.50	0.8976	0.5260	-0.0413	1.0462	4.2964	1.5038	4.2964		
	3.00			0.10	0.8998	0.5260	-0.0350	1.0474	4.2998	0.7469	4.2998			
					0.50	0.9003	0.5261	-0.0343	1.0474	4.3031	0.7119	4.3031		
	0.50			1.50	0.10	0.8549	0.5255	-0.2141	1.0265	4.1464	3.8913	4.1464		
					0.50	0.8616	0.5267	-0.2066	1.0261	4.2031	3.3061	4.2031		
3.00	0.10			0.8727	0.5267	-0.1746	1.0321	4.2281	3.1677	4.2281				
				0.50	0.8753	0.5271	-0.1715	1.0321	4.2464	2.8193	4.2464			
100	0.00			0.10	1.50	0.10	1.2218	0.2021	-0.0532	0.6446	2.3258	1.6005	2.3258	
						0.50	1.2231	0.2023	-0.0510	0.6448	2.3374	1.3338	2.3374	
					3.00	0.10	1.2250	0.2024	-0.0444	0.6453	2.3474	1.0020	2.3474	
							0.50	1.2256	0.2024	-0.0434	0.6454	2.3525	0.8469	2.3525
					0.50	1.50	0.10	1.1780	0.1999	-0.2659	0.6310	2.1274	2.9093	2.9093
							0.50	1.1848	0.2005	-0.2553	0.6321	2.1691	2.4325	2.4325
				3.00	0.10	1.1943	0.2011	-0.2220	0.6350	2.2157	2.3441	2.3441		
						0.50	1.1972	0.2013	-0.2173	0.6356	2.2391	2.1190	2.2391	
		0.50	0.10	1.50	0.10	0.8560	0.1635	-0.0439	0.9166	3.2928	1.9590	3.2928		
					0.50	0.8574	0.1636	-0.0421	0.9169	3.3178	1.6189	3.3178		
			3.00	0.10	0.8595	0.1638	-0.0354	0.9184	3.3311	1.0854	3.3311			
					0.50	0.8601	0.1638	-0.0347	0.9186	3.3411	0.7786	3.3411		
			0.50	1.50	0.10	0.8126	0.1609	-0.2196	0.8887	2.9460	3.4378	3.4378		
					0.50	0.8200	0.1617	-0.2112	0.8907	3.0527	2.9210	3.0527		
		3.00	0.10	0.8311	0.1624	-0.1772	0.8984	3.1327	2.8459	3.1327				
				0.50	0.8340	0.1627	-0.1738	0.8993	3.1794	2.5792	3.1794			

Table 5.4: CASE IV-M: descriptive quantities of the motion for several values of  $c_1$ ,  $c_2$ ,  $c_3$ ,  $\beta_m$  and  $R_m = 0.01$ .

$R_m$	$\beta_m$	$c_1$	$c_2$	$c_3$	$\varphi_*''(0)$	$\Psi_*'(0)$	$\Phi_*'(0)$	$\alpha_*$	$\bar{\xi}_{\varphi_*}$	$\bar{\xi}_{\Phi_*}$	$\delta_*$	
0.01	0.00	0.10	1.50	0.10	12.2182	0.9275	-0.0532	0.0645	0.2334	0.0767	0.2334	
				0.50	12.2313	0.9275	-0.0510	0.0645	0.2351	0.0717	0.2351	
		3.00	0.10	12.2501	0.9275	-0.0444	0.0645	0.2351	0.0667	0.2351		
			0.50	12.2558	0.9275	-0.0434	0.0645	0.2367	0.0634	0.2367		
		0.50	1.50	0.10	11.7801	0.9287	-0.2659	0.0631	0.2134	0.0767	0.2134	
				0.50	11.8476	0.9287	-0.2553	0.0632	0.2184	0.0717	0.2184	
	3.00		0.10	11.9433	0.9284	-0.2220	0.0635	0.2217	0.0684	0.2217		
			0.50	11.9723	0.9284	-0.2173	0.0636	0.2251	0.0650	0.2251		
	0.50		0.10	1.50	0.10	11.3354	0.8995	-0.0500	0.1249	1.9373	0.0784	1.9373
					0.50	11.3475	0.8995	-0.0481	0.1250	1.9373	0.0717	1.9373
		3.00	0.10	11.3657	0.8994	-0.0417	0.1251	1.9390	0.0684	1.9390		
			0.50	11.3708	0.8994	-0.0408	0.1251	1.9390	0.0650	1.9390		
		0.50	1.50	0.10	10.9294	0.9012	-0.2505	0.1223	1.9173	0.0784	1.9173	
				0.50	10.9917	0.9011	-0.2409	0.1225	1.9190	0.0734	1.9190	
	3.00	0.10	11.0847	0.9007	-0.2085	0.1231	1.9240	0.0684	1.9240			
		0.50	11.1109	0.9007	-0.2043	0.1232	1.9256	0.0650	1.9256			

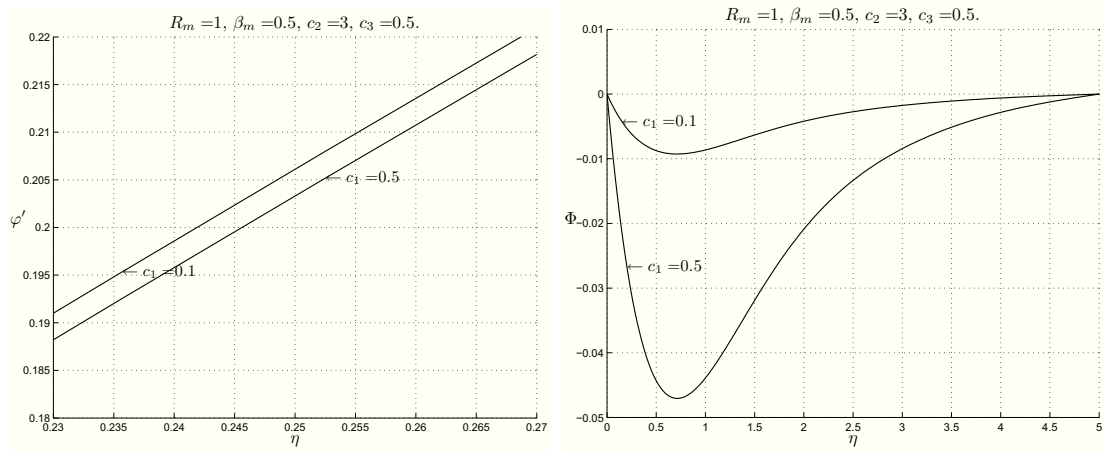


Figure 5.5: CASE IV-M:  $\varphi', \Phi$  profiles for  $R_m = 1, \beta_m = 0.5, c_2 = 3, c_3 = 0.5$  when  $c_1 = 0.1$  and  $c_1 = 0.5$ .

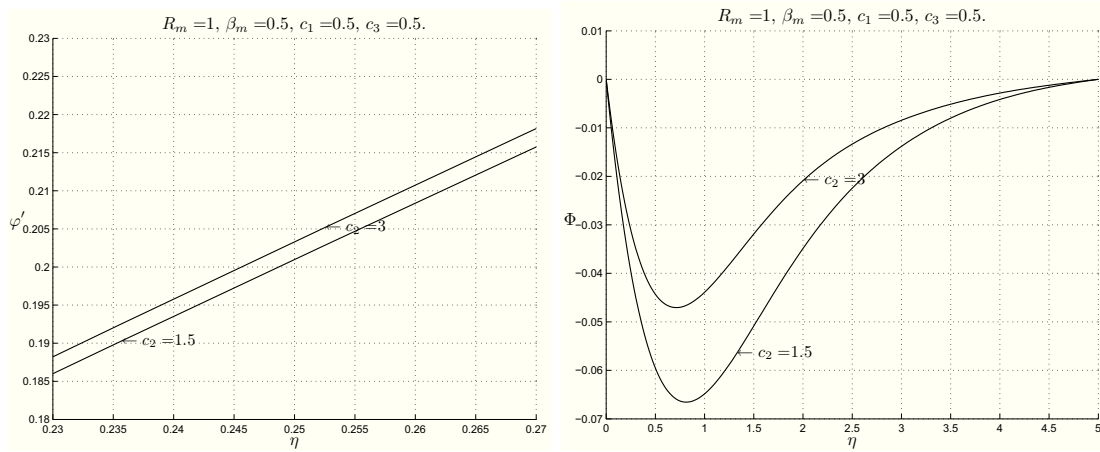


Figure 5.6: CASE IV-M:  $\varphi', \Phi$  profiles for  $R_m = 1, \beta_m = 0.5, c_1 = 0.5, c_3 = 0.5$  when  $c_2 = 1.5$  and  $c_2 = 3$ .

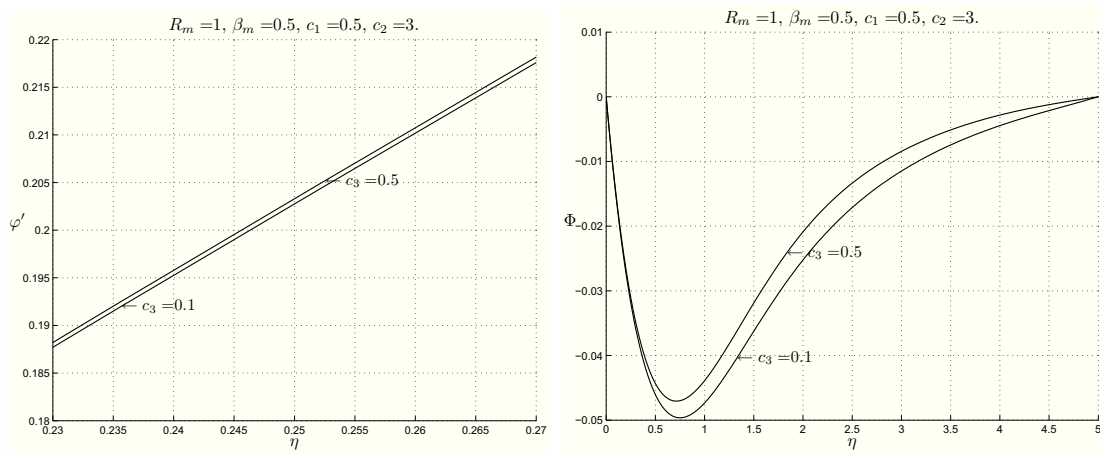


Figure 5.7: CASE IV-M:  $\varphi', \Phi$  profiles for  $R_m = 1, \beta_m = 0.5, c_1 = 0.5, c_2 = 3$  when  $c_3 = 0.1$  and  $c_3 = 0.5$ .

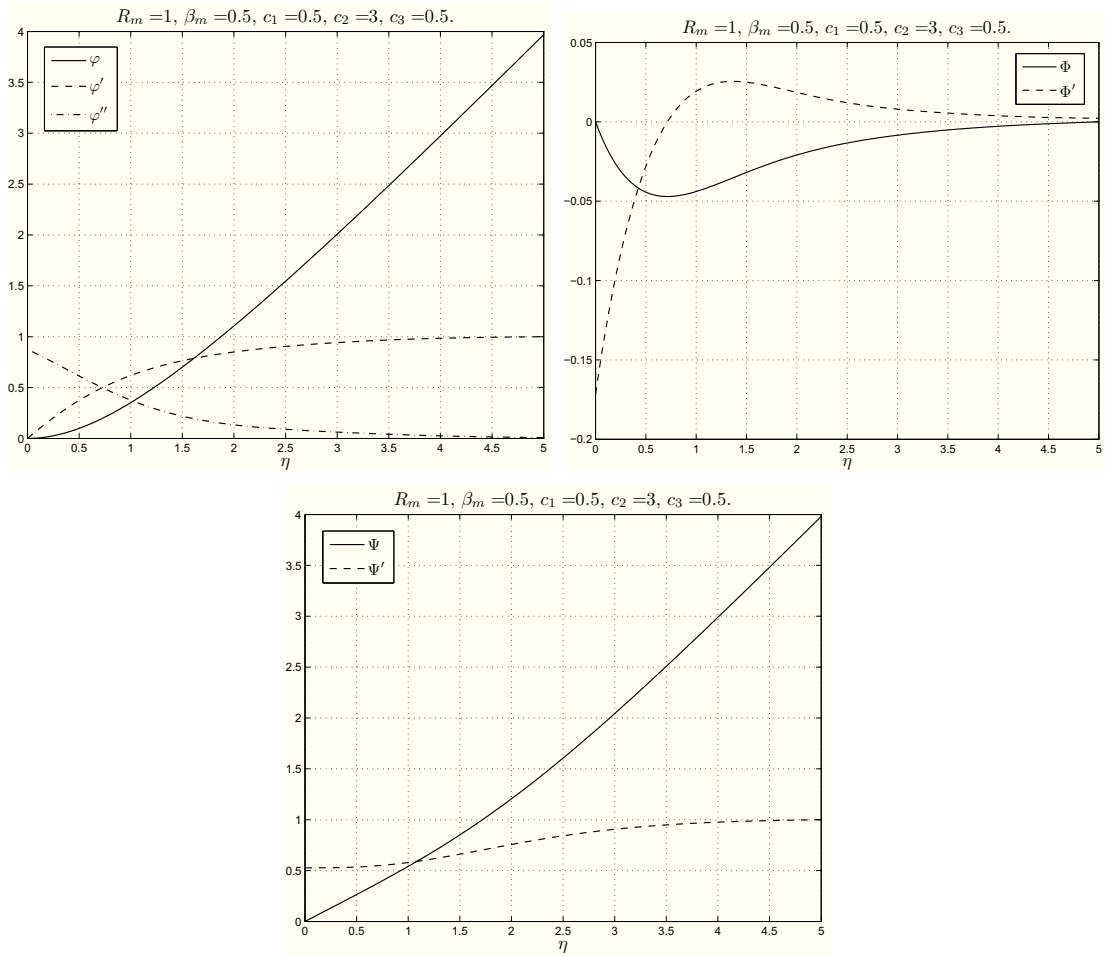


Figure 5.8: CASE IV-M: the first figure shows  $\varphi, \varphi', \varphi''$ , the second  $\Phi, \Phi'$ , the third  $\Psi, \Psi'$ , when  $c_1 = 0.5$ ,  $c_2 = 3.0$ ,  $c_3 = 0.5$ ,  $R_m = 1$  and  $\beta_m = 0.5$ .

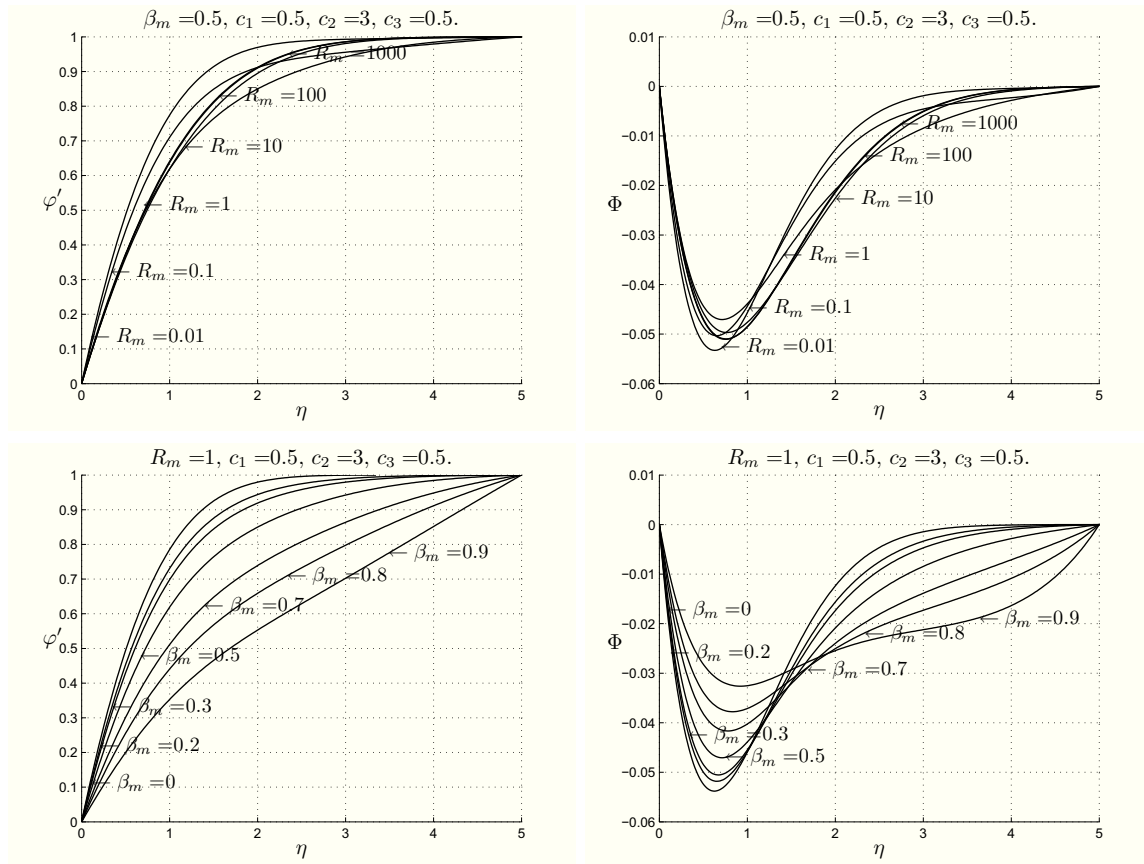


Figure 5.9: CASE IV-M: plots showing  $\varphi'$  and  $\Phi$  for different  $\beta_m$  and  $R_m$ , respectively.

As far as the dependence of the thickness of the boundary layer on  $R_m$  is concerned, it decreases when  $R_m$  increases. This fact is in agreement with the results obtained for the orthogonal stagnation-point flow in Chapter 2, where we have shown that the thickness of the boundary layer decreases as the Hartmann number  $M^2$  increases. Actually,  $R_m$  and  $M^2$  are both proportional to the electrical conductivity.

The functions  $\varphi'$  and  $\Phi$  are plotted against  $\eta$  for various values of  $\beta_m$  and  $R_m$  in Figure 5.9.

We underline that, as in the previous chapters, the micropolar nature of the fluid reduces all the descriptive quantities of the motion in comparison to those of the Newtonian fluid, especially the thickness of the boundary layer for the velocity.

Finally, in Figure 5.10, we can easily see that the flow and the magnetic field are completely overlapped far from the obstacle.

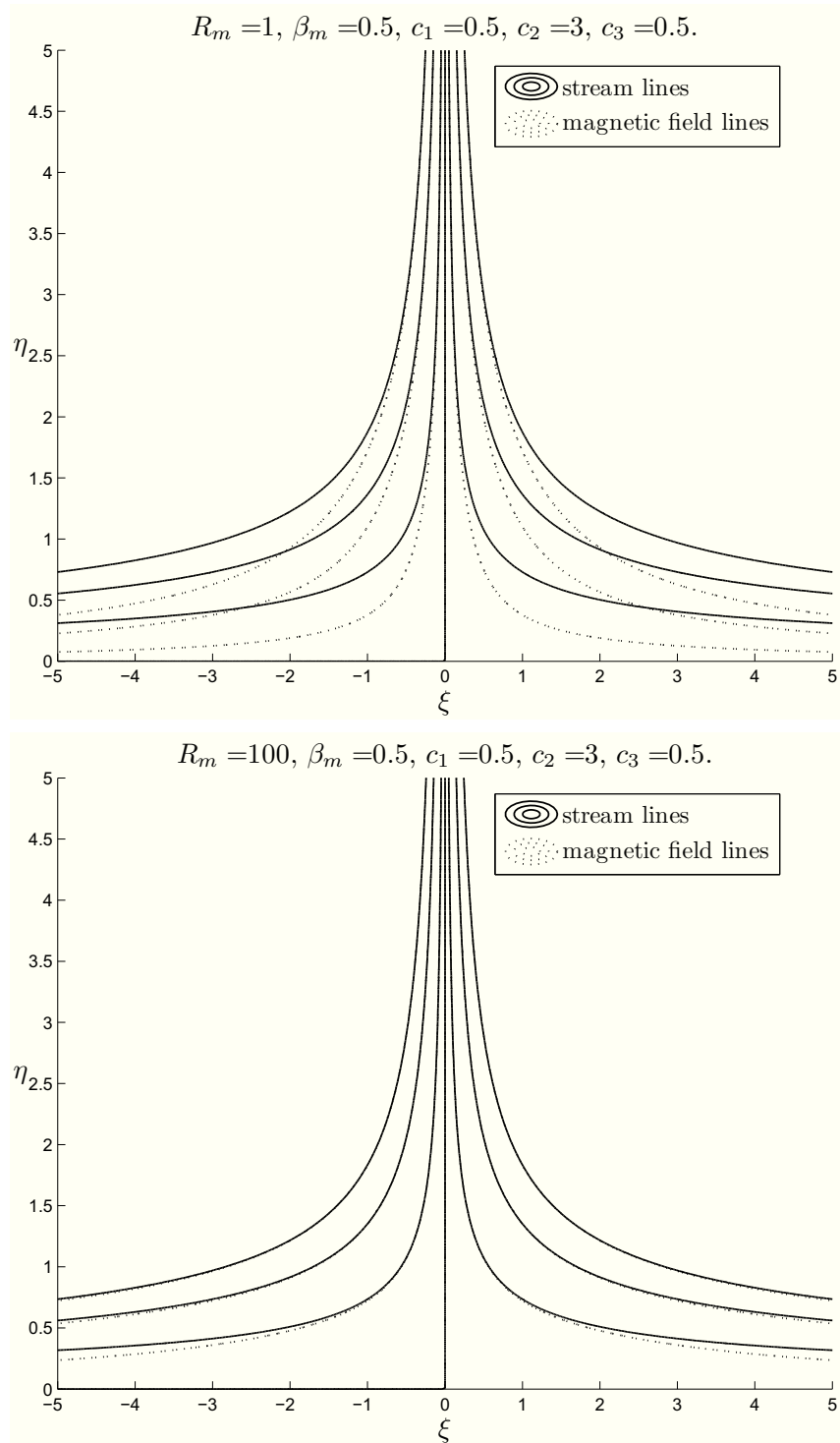


Figure 5.10: CASE IV-M: figures show the streamlines for  $c_1 = 0.5$ ,  $c_2 = 3.0$ ,  $c_3 = 0.5$ ,  $\beta_m = 0.5$  and  $R_m = 1$  or  $R_m = 100$ , respectively.



## Chapter 6

# MHD oblique stagnation-point flow with $\mathbf{H}$ and $\mathbf{v}$ parallel at infinity

We now examine the MHD oblique stagnation-point flow under a hypothesis which provides that the magnetic field is parallel to the flow at infinity.

The geometrical situation is the same as in Chapter 5.

The results here presented for the micropolar fluids are completely new ([10]), while the Newtonian case has been partially studied in [17].

### 6.1 Inviscid fluids CASE IV

Consider the steady plane MHD flow of a homogeneous, incompressible, electrically conducting inviscid fluid near a stagnation point filling the half-space  $\mathcal{S}$  (Figure 6.1).

$\partial\mathcal{S}$  is the boundary of a solid which is a rigid uncharged dielectric at rest occupying  $\mathcal{S}^-$ .

The velocity of such motion has the form

$$v_1 = a(x_1 + cx_2), \quad v_2 = -ax_2, \quad v_3 = 0, \quad x_1 \in \mathbb{R}, \quad x_2 \in \mathbb{R}^+, \quad (6.1)$$

with  $a, c$  constants ( $a > 0$ ). We observe that the constant  $c$  depends on the constant  $b$  of the previous chapters as  $c = \frac{b}{a}$  (see Chapter 1.2 and 3, for example (3.1)).

The equations governing such a flow in the absence of external mechanical body forces and free electric charges are (2.2) and we impose the usual boundary conditions (see (2.4), (2.5), (2.6)).

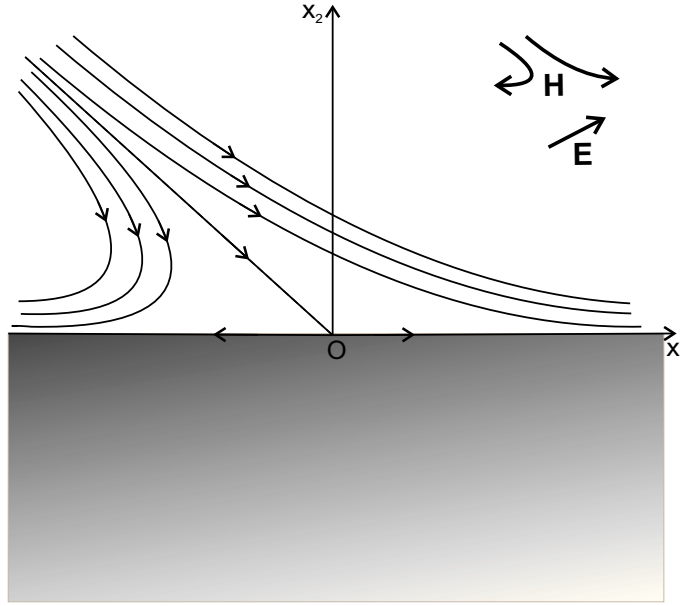


Figure 6.1: Description flow in CASE IV.

As far as the external electromagnetic field is concerned, we suppose that an external magnetic field

$$\mathbf{H}_e = H_\infty [(x_1 + cx_2)\mathbf{e}_1 - x_2\mathbf{e}_2], \quad H_\infty = \text{constant}, \quad x_1 \in \mathbb{R}, \quad x_2 \in \mathbb{R},$$

and an external electric field

$$\mathbf{E}_e = E_0\mathbf{e}_3, \quad E_0 = \text{constant}, \quad x_1 \in \mathbb{R}, \quad x_2 \in \mathbb{R},$$

permeate the whole physical space.

REMARK 6.1.1. *The field lines of  $\mathbf{H}_e$  have the following parametric equations*

$$\begin{aligned} x_1 &= A_1 e^{H_\infty \lambda} - \frac{c}{2} A_2 e^{-H_\infty \lambda}, \\ x_2 &= A_2 e^{-H_\infty \lambda}, \quad \lambda \in \mathbb{R}, \end{aligned} \quad (6.2)$$

where  $A_1, A_2$  are arbitrary constants.

*These field lines degenerate if at least one of the two constants  $A_1, A_2$  vanishes. Otherwise they are the hyperbolas of equation*

$$x_1 x_2 = A_1 A_2 - \frac{c}{2} x_2^2.$$

*The centre of these hyperbolas is the origin and these curves tend to  $x_2 = 0$  as  $|x_1| \rightarrow +\infty$ .*

We assume that the total magnetic fields in the fluid and in the solid have the following form

$$\begin{aligned}\mathbf{H} &= H_\infty [(x_1 h'(x_2) + ck(x_2))\mathbf{e}_1 - h(x_2)\mathbf{e}_2], \quad x_2 \geq 0, \quad \text{and} \\ \mathbf{H}_s &= H_\infty [(x_1 h'_s(x_2) + ck_s(x_2))\mathbf{e}_1 - h_s(x_2)\mathbf{e}_2], \quad x_2 \leq 0,\end{aligned}\quad (6.3)$$

respectively, where  $h, k, h_s, k_s$  are sufficiently regular unknown functions to be determined ( $h, k, h_s, k_s \in C^2(\mathbb{R}^+)$ ).

Precisely, we ask that  $\mathbf{H}$  tends to  $\mathbf{H}_e$  as  $x_2 \rightarrow +\infty$  so that  $\mathbf{H}$  is parallel to  $\mathbf{v}$  at infinity. Therefore we require

$$\lim_{x_2 \rightarrow +\infty} h'(x_2) = 1, \quad \lim_{x_2 \rightarrow +\infty} [h(x_2) - x_2] = 0, \quad \lim_{x_2 \rightarrow +\infty} [k(x_2) - x_2] = 0. \quad (6.4)$$

We also make the following assumptions:

- (i)  $\mathbf{H}_s$  is not uniform;
- (ii) the centre of its non-degenerate field lines, which as we will see are hyperbolas, is the origin;
- (ii) these lines tend to  $x_2 = 0$  as  $|x_1| \rightarrow +\infty$ .

Now our aim is to prove the following theorem:

**THEOREM 6.1.2.** *If the solid which occupies  $\mathcal{S}^-$  is a rigid uncharged dielectric at rest and  $\mathbf{H}_s$  satisfies (i), (ii) and (iii), then*

$$\mathbf{H}_s = H_\infty h'(0)(x_1 \mathbf{e}_1 - x_2 \mathbf{e}_2), \quad (6.5)$$

where  $h(x_2)$  is the function in (6.3)<sub>1</sub>.

*Proof.* We begin by recalling that the solid is an uncharged dielectric so that

$$\nabla \times \mathbf{H}_s = \mathbf{0}, \quad \text{in } \mathcal{S}^-,$$

from which we get

$$x_1 h''_s(x_2) + ck'_s(x_2) = 0, \quad \forall x_1 \in \mathbb{R}. \quad (6.6)$$

Equation (6.6) implies

$$h_s(x_2) = C_1 x_2 + C_2, \quad k_s(x_2) = C_3, \quad x_2 \leq 0, \quad (6.7)$$

where  $C_1, C_2, C_3 \in \mathbb{R}$ .

By virtue of the continuity of the tangential components of the magnetic field across the plane  $x_2 = 0$ , since in  $\mathcal{S}$  the total magnetic field is (6.3)<sub>1</sub>, we find

$$C_1 = h'(0), \quad C_3 = k(0), \quad (6.8)$$

so that

$$\mathbf{H}_s = H_\infty [(h'(0)x_1 + ck(0))\mathbf{e}_1 - (h'(0)x_2 + C_2)\mathbf{e}_2]. \quad (6.9)$$

We remark that  $\mathbf{H}_s$  is uniform if  $h'(0) = 0$ . Hence in order to satisfy hypothesis (i), we proceed with  $h'(0) \neq 0$ .

As it is easy to verify, the non-degenerate field lines are the hyperbolas

$$\left(x_1 + c \frac{k(0)}{h'(0)}\right) x_2 = C_4 - \frac{cC_2k(0)}{[h'(0)]^2} - \frac{C_2}{h'(0)} x_1, \quad x_2 \leq 0, \quad C_4 = \text{constant} \in \mathbb{R} \setminus 0. \quad (6.10)$$

The centre of these hyperbolas is the origin if, and only if,

$$k(0) = 0,$$

and these curves tend to  $x_2 = 0$  as  $|x_1| \rightarrow +\infty$  if, and only if,

$$C_2 = 0,$$

from which we get the assertion. □

REMARK 6.1.3. *Since the solid is an uncharged dielectric  $\mathbf{E}_s = \mathbf{E}_e$ .*

We now consider the inviscid fluid filling the half-space  $\mathcal{S}$ .

By virtue of the usual boundary conditions in electromagnetism, we deduce

$$h(0) = 0, \quad k(0) = 0. \quad (6.11)$$

We now determine  $(p, \mathbf{H}, \mathbf{E})$  solution of (2.2) in  $\mathcal{S}$  with  $\mathbf{v}$  given by (6.1) such that  $\mathbf{H}$  tends to  $\mathbf{H}_e$  as  $x_2$  goes to infinity. Hence

$$\mathbf{v} \times \mathbf{H} = \mathbf{0} \text{ at infinity.} \quad (6.12)$$

Let  $\mathbf{E}$  be the total electric field in the fluid. The boundary conditions require that

$$E_1 = 0, \quad E_3 = E_0 \text{ at } x_2 = 0. \quad (6.13)$$

Equation (2.2)<sub>4</sub> implies

$$\mathbf{E} = -\nabla\psi.$$

Further from (2.2)<sub>3</sub> and the form of  $\mathbf{H}$  and  $\mathbf{v}$ , it follows

$$\mathbf{E} = \frac{1}{\sigma_e}(\nabla \times \mathbf{H} - \sigma_e \mu_e \mathbf{v} \times \mathbf{H}) \Rightarrow \mathbf{E} \text{ is parallel to } \mathbf{e}_3. \quad (6.14)$$

Hence  $E_1 = E_2 = 0$  and  $E_3 = E_0$ .

On the other hand,

$$\lim_{x_2 \rightarrow +\infty} \nabla \times \mathbf{H} = -cH_\infty \mathbf{e}_3 \quad \text{and} \quad \lim_{x_2 \rightarrow +\infty} \mathbf{v} \times \mathbf{H} = 0,$$

so that

$$E_0 = -\frac{cH_\infty}{\sigma_e}.$$

REMARK 6.1.4. *Differently from the orthogonal flow, now, a nonzero current density is present, which requires the existence of an electric field in  $\mathbf{e}_3$  direction.*

Equation (2.2)<sub>3</sub> provides

$$x_1 \left[ h''(x_2) + \frac{a}{\eta_e}(x_2 h'(x_2) - h(x_2)) \right] + c \left[ k'(x_2) + \frac{a}{\eta_e}(k(x_2) - h(x_2))x_2 - 1 \right] = 0, \\ \forall x_1 \in \mathbb{R}, \quad x_2 \in \mathbb{R}^+. \quad (6.15)$$

The previous relation together with conditions (6.4), (6.11) gives rise to the following two ordinary differential boundary value problem

$$h''(x_2) + \frac{a}{\eta_e}[x_2 h'(x_2) - h(x_2)] = 0, \\ h(0) = 0, \quad \lim_{x_2 \rightarrow +\infty} h'(x_2) = 1; \quad (6.16)$$

$$k'(x_2) + \frac{a}{\eta_e}[k(x_2) - h(x_2)]x_2 - 1 = 0, \\ k(0) = 0. \quad (6.17)$$

Problem (6.16) has the unique solution  $h(x_2) = x_2$ .

If we substitute  $h(x_2) = x_2$  into (6.17), then we find that this problem also has the unique solution  $k(x_2) = x_2$ . The solution satisfies the condition (6.4)<sub>3</sub> at infinity.

Finally, the total magnetic field has the form

$$\mathbf{H} = \mathbf{H}_e = H_\infty [(x_1 + cx_2)\mathbf{e}_1 - x_2\mathbf{e}_2]. \quad (6.18)$$

We remark that unlike the previous chapter,  $\nabla \times \mathbf{H} = -cH_\infty \mathbf{e}_3$ , hence the pressure field is modified by the presence of  $\mathbf{H}$  and from (2.2)<sub>1</sub> we get

$$p = -\rho \frac{a^2}{2}(x_1^2 + x_2^2) - \mu_e H_\infty^2 c \left( x_1 x_2 + c \frac{x_2^2}{2} \right) + p_0, \quad x_1 \in \mathbb{R}, \quad x_2 \in \mathbb{R}^+. \quad (6.19)$$

Our results can be summarized in the following:

**THEOREM 6.1.5.** *Let a homogeneous, incompressible, electrically conducting inviscid fluid occupy the half-space  $\mathcal{S}$  and is embedded in the external electromagnetic field  $\mathbf{H}_e = H_\infty[(x_1 + cx_2)\mathbf{e}_1 - x_2\mathbf{e}_2]$ ,  $\mathbf{E}_e = E_0\mathbf{e}_3$ . If the total magnetic field in the solid is taken in the form (6.5), then the steady plane MHD oblique stagnation-point flow of such a fluid has the form*

$$\mathbf{v} = a(x_1 + cx_2)\mathbf{e}_1 - ax_2\mathbf{e}_2, \quad \mathbf{E} = \mathbf{E}_e = -\frac{cH_\infty}{\sigma_e}\mathbf{e}_3, \quad \mathbf{H} = \mathbf{H}_e,$$

$$p = -\rho \frac{a^2}{2}(x_1^2 + x_2^2) - \mu_e H_\infty^2 c \left( x_1 x_2 + c \frac{x_2^2}{2} \right) + p_0, \quad x_1 \in \mathbb{R}, \quad x_2 \in \mathbb{R}^+. \quad (6.20)$$

**REMARK 6.1.6.** *In order to study the same problem for other models of fluids, it is convenient to suppose that the inviscid obliquely impinges on the flat plane  $x_2 = A$  and*

$$\mathbf{v} = a[x_1 + c(x_2 - B)]\mathbf{e}_1 - a(x_2 - A)\mathbf{e}_2,$$

$$\mathbf{H}_e = H_\infty[x_1 + c(x_2 - B)]\mathbf{e}_1 - H_\infty(x_2 - A)\mathbf{e}_2, \quad x_1 \in \mathbb{R}, \quad x_2 \geq A,$$

$$\mathbf{H} \rightarrow H_\infty[x_1 + c(x_2 - B)]\mathbf{e}_1 - H_\infty(x_2 - A)\mathbf{e}_2 \text{ as } x_2 \rightarrow +\infty. \quad (6.21)$$

with  $A, B = \text{constants}$  (Remark 1.2.2).

In this case, the stagnation point is  $(c(B - A), A)$  and the streamlines and the magnetic field lines are hyperbolas whose asymptotes are

$$x_2 = -\frac{2}{c}x_1 + 2B - A \quad \text{and} \quad x_2 = A.$$

Under these assumptions Theorem 6.1.5 continues to hold by replacing the velocity with (6.21)<sub>1</sub> and the pressure field and the total magnetic field by

$$p = -\rho \frac{a^2}{2}[x_1^2 + (x_2 - A)^2] + \rho a^2 c(B - A)x_1$$

$$- \mu_e H_\infty^2 c \left[ x_1 x_2 - Ax_1 + c \frac{(x_2 - B)^2}{2} \right] + p_0,$$

$$\mathbf{H} = H_\infty[x_1 + c(x_2 - B)]\mathbf{e}_1 - H_\infty(x_2 - A)\mathbf{e}_2, \quad (6.22)$$

respectively.

## 6.2 Newtonian fluids CASE IV-N

Consider now the steady oblique MHD flow of a homogeneous, incompressible, electrically conducting Newtonian fluid near a stagnation point filling the half-space  $\mathcal{S}$ . The equations governing such a flow in the absence of external mechanical body forces and free electric charges are equations (2.22) and we impose conditions (2.23), (2.5) and (2.6).

Since we are interested in the oblique plane stagnation-point flow, similar to the previous chapters, we suppose

$$v_1 = a[x_1 f'(x_2) + cg(x_2)], \quad v_2 = -af(x_2), \quad v_3 = 0, \quad x_1 \in \mathbb{R}, \quad x_2 \in \mathbb{R}^+, \quad (6.23)$$

with  $f, g$  sufficiently regular unknown functions ( $f \in C^3(\mathbb{R}^+)$ ,  $g \in C^2(\mathbb{R}^+)$ ).

The condition (2.23) supplies

$$f(0) = 0, \quad f'(0) = 0, \quad g(0) = 0. \quad (6.24)$$

We assume that an external magnetic field

$$\mathbf{H}_e = H_\infty [(x_1 + cx_2)\mathbf{e}_1 - x_2\mathbf{e}_2]$$

and an external electric field

$$\mathbf{E}_e = E_0\mathbf{e}_3$$

permeate the whole physical space.

Moreover, the total magnetic field in the fluid is taken in the following form

$$\mathbf{H} = H_\infty [(x_1 h'(x_2) + ck(x_2))\mathbf{e}_1 - h(x_2)\mathbf{e}_2], \quad (6.25)$$

where  $h, k$  are sufficiently regular unknown functions ( $h, k \in C^2(\mathbb{R}^+)$ ) to be determined.

Theorem 6.1.2 implies that in the solid the total magnetic field has the form  $\mathbf{H}_s = H_\infty h'(0)(x_1\mathbf{e}_1 - x_2\mathbf{e}_2)$ , so that  $h$  and  $k$  must satisfy

$$h(0) = 0, \quad k(0) = 0. \quad (6.26)$$

We impose

**Condition P.** *At infinity, the MHD oblique stagnation-point flow of a viscous fluid approaches the flow of an inviscid fluid whose velocity, pressure and magnetic field are given by (6.21)<sub>1</sub>, (6.22)<sub>1</sub> and (6.22)<sub>2</sub>, respectively.*

Therefore we ask

$$\lim_{x_2 \rightarrow +\infty} f'(x_2) = 1, \quad \lim_{x_2 \rightarrow +\infty} g'(x_2) = 1, \quad \lim_{x_2 \rightarrow +\infty} h'(x_2) = 1, \quad (6.27)$$

so that

$$\mathbf{v} \times \mathbf{H} = \mathbf{0} \text{ at infinity.} \quad (6.28)$$

We remark that in the sequel, when we will refer to an inviscid fluid, all results obtained in Chapter 6.1 have to be modified as in the Remark 6.1.6.

In particular, the asymptotic behaviour of  $f$ ,  $g$ ,  $h$ ,  $k$  at infinity is related to the constants  $A, B$  in the following way:

$$\lim_{x_2 \rightarrow +\infty} [f(x_2) - x_2] = -A, \quad \lim_{x_2 \rightarrow +\infty} [g(x_2) - x_2] = -B, \quad (6.29)$$

$$\lim_{x_2 \rightarrow +\infty} [h(x_2) - x_2] = -A, \quad \lim_{x_2 \rightarrow +\infty} [k(x_2) - x_2] = -B. \quad (6.30)$$

As we have already said,  $A$  is determined as part of the solution of the orthogonal flow ([47]), instead  $B$  is a free parameter ([19]).

Let  $\mathbf{E}$  be the total electric field in the fluid. Since  $\mathbf{E}_s = \mathbf{E}_e$ , the boundary conditions require

$$E_1 = 0, \quad E_3 = E_0, \quad \text{at } x_2 = 0.$$

From (2.22)<sub>3</sub> follows  $\mathbf{E} = E_0 \mathbf{e}_3$ .

As in the inviscid case, the boundary condition at infinity furnishes

$$E_0 = -\frac{cH_\infty}{\sigma_e}. \quad (6.31)$$

We now want to find  $(p, f, g, h, k)$  solution in  $\mathcal{S}$  of (2.22) with  $\mathbf{v}$  given by (6.23) such that Condition P is satisfied.

Taking into account the expression of the total electromagnetic field, (2.22)<sub>3</sub> provides

$$\begin{aligned} & x_1 \left[ h''(x_2) + \frac{a}{\eta_e} [f(x_2)h'(x_2) - f'(x_2)h(x_2)] \right] \\ & + c \left[ k'(x_2) + \frac{a}{\eta_e} [f(x_2)k(x_2) - g(x_2)h(x_2)] - 1 \right] = 0, \quad \forall x_1 \in \mathbb{R}, \quad x_2 \in \mathbb{R}^+. \end{aligned} \quad (6.32)$$

Relation (6.32) together with the conditions (6.27)<sub>3</sub> and (6.26) gives rise to the following two ordinary differential boundary value problem

$$\begin{aligned} & h''(x_2) + \frac{a}{\eta_e} [f(x_2)h'(x_2) - f'(x_2)h(x_2)] = 0, \\ & h(0) = 0, \quad \lim_{x_2 \rightarrow +\infty} h'(x_2) = 1; \end{aligned} \quad (6.33)$$

$$\begin{aligned} & k'(x_2) + \frac{a}{\eta_e} [f(x_2)k(x_2) - g(x_2)h(x_2)] - 1 = 0, \\ & k(0) = 0. \end{aligned} \quad (6.34)$$

If we regard  $f$ ,  $g$ ,  $h$  as known functions, the solution of the differential problem (6.34) is formally obtained as

$$k(x_2) = e^{-\frac{a}{\eta_e} \int_0^{x_2} f(t) dt} \left[ \int_0^{x_2} \left( \left( \frac{a}{\eta_e} g(t) h(t) + 1 \right) e^{\frac{a}{\eta_e} \int_0^t f(s) ds} dt \right) \right]. \quad (6.35)$$

If  $f$ ,  $g$ ,  $h$  satisfy conditions (6.27), (6.29), (6.30)<sub>1</sub>, then from (6.35) it follows that  $k$  satisfies condition (6.30)<sub>2</sub>.

Now we proceed in order to determine  $p$ ,  $f$ ,  $g$ .

The substituting of (6.23), and (6.25) into (2.22)<sub>1</sub> provides  $p = p(x_1, x_2)$  and

$$\begin{aligned} & a x_1 (\nu f''' + a f f'' - a f'^2 - \frac{\mu_e}{\rho a} H_\infty^2 h h'') \\ & + a c \left[ \nu g'' + a (f g' - f' g) - \frac{\mu_e}{\rho a} H_\infty^2 h k' \right] = \frac{1}{\rho} \frac{\partial p}{\partial x_1}, \\ & \nu a f'' + a^2 f' f + \frac{\mu_e}{\rho} \frac{H_\infty^2}{2} \frac{\partial}{\partial x_2} [(x_1 h' + c k)^2] = -\frac{1}{\rho} \frac{\partial p}{\partial x_2}. \end{aligned} \quad (6.36)$$

Then, by integrating (6.36)<sub>2</sub>, we find

$$p = -\rho \frac{a^2}{2} f^2(x_2) - \rho a \nu f'(x_2) - \mu_e \frac{H_\infty^2}{2} [x_1 h'(x_2) + c k(x_2)]^2 + P(x_1),$$

where the function  $P(x_1)$  is determined supposing that, far from the wall, the pressure  $p$  has the behaviour given by (6.22).

Therefore, taking into account (6.27), (6.29), (6.30), we get

$$P(x_1) = -\rho \frac{a^2}{2} x_1^2 + \rho a^2 c (B - A) x_1 + \mu_e \frac{H_\infty^2}{2} x_1^2 + \mu_e H_\infty^2 c (A - B) x_1 + p_0^*,$$

so that the pressure field assumes the form

$$\begin{aligned} p = & -\rho \frac{a^2}{2} [x_1^2 + f^2(x_2)] - \rho a \nu f'(x_2) + \rho a^2 c (B - A) x_1 \\ & - \mu_e \frac{H_\infty^2}{2} [x_1 h'(x_2) + c k(x_2)]^2 + \mu_e \frac{H_\infty^2}{2} x_1^2 + \mu_e H_\infty^2 c (A - B) x_1 + p_0. \end{aligned} \quad (6.37)$$

We remark that  $\nabla p$  has a constant component in the  $x_1$  direction proportional to  $B - A$ , which does not appear in the orthogonal stagnation-point flow. This component determines the displacement of the uniform shear flow parallel to the wall  $x_2 = 0$ . Differently from the previous chapters (see Chapters 1.2.2 and 3), this component now depends on  $H_\infty^2$ .

In consideration of (6.37), from (6.36)<sub>1</sub> we obtain the ordinary differential equations

$$\begin{aligned} \frac{\nu}{a}f''' + ff'' - f'^2 + 1 - \frac{\mu_e H_\infty^2}{\rho a^2} (hh'' - h'^2 + 1) &= 0, \\ \frac{\nu}{a}g'' + fg' - f'g - \frac{\mu_e H_\infty^2}{\rho a^2} (hk' - h'k) &= \left(1 - \frac{\mu_e H_\infty^2}{\rho a^2}\right) (B - A). \end{aligned} \quad (6.38)$$

We have thus proved:

**THEOREM 6.2.1.** *Let a homogeneous, incompressible, electrically conducting Newtonian fluid occupy the half-space  $\mathcal{S}$  and is embedded in the external electromagnetic field  $\mathbf{H}_e = H_\infty [(x_1 + cx_2)\mathbf{e}_1 - x_2\mathbf{e}_2]$ ,  $\mathbf{E}_e = E_0\mathbf{e}_3$ . If the total magnetic field in the solid is (6.5), then the steady plane MHD oblique stagnation-point flow of such a fluid has the following form*

$$\mathbf{v} = a[x_1f'(x_2) + cg(x_2)]\mathbf{e}_1 - af(x_2)\mathbf{e}_2, \quad \mathbf{E} = \mathbf{E}_e = -\frac{cH_\infty}{\sigma_e}\mathbf{e}_3,$$

$$\mathbf{H} = H_\infty [x_1h'(x_2) + ck(x_2)]\mathbf{e}_1 - H_\infty h(x_2)\mathbf{e}_2,$$

$$\begin{aligned} p &= -\rho \frac{a^2}{2} [x_1^2 + f^2(x_2)] - \rho a \nu f'(x_2) + \rho a^2 c (B - A)x_1 + \mu_e \frac{H_\infty^2}{2} x_1^2 \\ &\quad - \mu_e \frac{H_\infty^2}{2} [x_1h'(x_2) + ck(x_2)]^2 + \mu_e H_\infty^2 c (A - B)x_1 + p_0, \quad x_1 \in \mathbb{R}, \quad x_2 \in \mathbb{R}^+, \end{aligned}$$

where  $(f, g, h, k)$  satisfies problem (6.38), (6.33), (6.34), (6.24), (6.27)<sub>1,2</sub>.

If we use (1.35) and we put

$$\Psi(\eta) = \sqrt{\frac{a}{\nu}}h \left( \sqrt{\frac{\nu}{a}}\eta \right), \quad K(\eta) = \sqrt{\frac{a}{\nu}}k \left( \sqrt{\frac{\nu}{a}}\eta \right),$$

then we can rewrite problem (6.38), (6.33), (6.34), (6.24), (6.27)<sub>1,2</sub> as:

$$\begin{aligned} \varphi''' + \varphi\varphi'' - \varphi'^2 + 1 - \beta_m(\Psi\Psi'' - \Psi'^2 + 1) &= 0, \\ \gamma'' + \varphi\gamma' - \varphi'\gamma - \beta_m(\Psi K' - \Psi'K) &= (1 - \beta_m)(\beta - \alpha), \\ \Psi'' + R_m(\varphi\Psi' - \varphi'\Psi) &= 0, \\ K' + R_m(\varphi K - \gamma\Psi) - 1 &= 0, \\ \varphi(0) = 0, \quad \varphi'(0) = 0, \quad \gamma(0) = 0, \quad \gamma'(0) = 0, \\ \Psi(0) = 0, \quad K(0) = 0, \\ \lim_{\eta \rightarrow +\infty} \varphi'(\eta) = 1, \quad \lim_{\eta \rightarrow +\infty} \gamma'(\eta) = 1, \quad \lim_{\eta \rightarrow +\infty} \Psi'(\eta) = 1, \end{aligned} \quad (6.39)$$

where

$$\alpha = \sqrt{\frac{a}{\nu}}A, \quad \beta = \sqrt{\frac{a}{\nu}}B, \quad \beta_m = \frac{\mu_e H_\infty^2}{\rho a^2}, \quad R_m = \frac{\nu}{\eta_e}.$$

Notice that the functions  $\varphi, \Psi$  influence the functions  $\gamma, K$ , but not viceversa. The functions  $\varphi$  and  $\Psi$  satisfy the corresponding problem of the orthogonal stagnation-point flow (see Chapter 5.2), which can be solved numerically.

REMARK 6.2.2. *As in the case in the absence of the external electromagnetic field (see Remark 1.2.4), along the wall  $x_2 = 0$  there are three important coordinates: the origin  $x_1 = 0$ , which is the stagnation point, the point  $x_1 = x_p$  of maximum pressure and the point  $x_1 = x_s$  of zero tangential stress (zero skin friction) where the dividing streamline of equation*

$$\xi\varphi(\eta) + \frac{b}{a} \int_0^\eta \gamma(s)ds = 0, \quad \xi = \sqrt{\frac{\nu}{a}}x_1 \quad (6.40)$$

meets the boundary.

In consideration of (6.37) and (6.23), one shows that  $x_s$  is of course the same as in the absence of the external electromagnetic field (see (1.41)<sub>2</sub>)

$$x_s = -c\sqrt{\frac{\nu}{a}} \frac{\gamma'(0)}{\varphi''(0)}. \quad (6.41)$$

We underline that  $\varphi''(0)$  and  $\gamma'(0)$  now depend on  $\beta_m$  and  $R_m$ .

As far as  $x_p$  is concerned, the pressure has a stationary point in

$$x_p = c\sqrt{\frac{\nu}{a}} \frac{(\beta - \alpha)(1 - \beta_m)}{1 - \beta_m[1 - (\Psi'(0))^2]}, \quad (6.42)$$

which is a point of maximum if  $\beta_m < 1$ .

We note that the ratio

$$\frac{x_p}{x_s} = \frac{(\alpha - \beta)(1 - \beta_m)}{1 - \beta_m[1 - (\Psi'(0))^2]} \frac{\varphi''(0)}{\gamma'(0)}$$

is the same for all angles of incidence.

Finally, the slope of the dividing streamline at the wall is given by ([17]):

$$m_s = -\frac{3[\varphi''(0)]^2}{c[(1 - \beta_m)[(\beta - \alpha)\varphi''(0) + \gamma'(0)] + \beta_m(\Psi'(0))^2\gamma'(0)}$$

and does not depend on the kinematic viscosity. Thus, the ratio of this slope to that of the dividing streamline at infinity  $\left(m_i = -\frac{2}{c}\right)$  is the same for all oblique stagnation-point flows and it is given by

$$\frac{m_s}{m_i} = \frac{3}{2} \frac{[\varphi''(0)]^2}{[(1 - \beta_m)[(\beta - \alpha)\varphi''(0) + \gamma'(0)] + \beta_m(\Psi'(0))^2\gamma'(0)}. \quad (6.43)$$

This ratio is independent of  $c$ , depending on the constant pressure gradient parallel to the boundary through  $B - A$  and  $\mathbf{H}$ .

As usual, problem (6.39) was solved using the `bvp4c` MATLAB routine.

The values of  $R_m$  and  $\beta_m$  are chosen according to [17] and the previous chapter, while we have taken  $\beta - \alpha = -5 - \alpha$ ,  $-\alpha$ ,  $0$ ,  $\alpha$ ,  $5 - \alpha$  as in Chapters 1.2 and 3.

As far as the value of  $\beta_m$  is concerned, we have that  $\beta_m$  has to be less than 1 in order to preserve the parallelism of  $\mathbf{H}$  and  $\mathbf{v}$  at infinity, as it happened in the orthogonal flow (see Chapter 5).

For small values of  $R_m$ , equation (6.39)<sub>3</sub> reduces to  $\Psi'' \cong 0$ , which leads to the problem in the absence of the magnetic field. In order to remove this difficulty, it is convenient to use the following transformation ([23], [24])

$$\begin{aligned}\xi &= \sqrt{R_m}\eta, \quad \varphi_*(\xi) = \sqrt{R_m}\varphi(\sqrt{R_m}\xi), \quad \gamma_*(\xi) = \sqrt{R_m}\gamma(\sqrt{R_m}\xi), \\ \Psi_*(\eta) &= \sqrt{R_m}\Psi(\sqrt{R_m}\xi), \quad K_*(\eta) = \sqrt{R_m}K(\sqrt{R_m}\xi),\end{aligned}\tag{6.44}$$

which furnishes the analogous problem:

$$\begin{aligned}R_m\varphi_*''' + \varphi_*\varphi_*'' - \varphi_*'^2 + 1 - \beta_m(\Psi_*\Psi_*'' - \Psi_*'^2 + 1) &= 0, \\ R_m\gamma_*'' + \varphi_*\gamma_*' - \varphi_*'\gamma_* - \beta_m(\Psi_*K_*' - \Psi_*'K_*) &= \sqrt{R_m}(1 - \beta_m)(\beta - \alpha), \\ \Psi_*'' + \varphi_*\Psi_*' - \varphi_*'\Psi_* &= 0, \\ K_*' + \varphi_*K_* - \gamma_*\Psi_* - 1 &= 0, \\ \varphi_*(0) = 0, \quad \varphi_*'(0) = 0, \quad \gamma_*(0) = 0, \quad \gamma_*'(0) = 0, \quad \Psi_*(0) = 0, \quad K_*(0) = 0, \\ \lim_{\xi \rightarrow +\infty} \varphi_*'(\xi) = 1, \quad \lim_{\xi \rightarrow +\infty} \gamma_*'(\xi) = 1, \\ \lim_{\xi \rightarrow +\infty} \Psi_*'(\xi) = 1.\end{aligned}\tag{6.45}$$

REMARK 6.2.3. As we will see,  $\varphi$  and  $\gamma$  satisfy conditions (6.39)<sub>11,12</sub>. In particular,

$$\lim_{\eta \rightarrow +\infty} [\varphi(\eta) - \eta] = -\alpha, \quad \lim_{\eta \rightarrow +\infty} [\gamma(\eta) - \eta] = -\beta.$$

Hence it is convenient to recall Remark 1.2.5, where we defined:

- $\bar{\eta}_\varphi$  ( $\bar{\eta}_\gamma$ ) the value of  $\eta$  such that  $\varphi'(\bar{\eta}_\varphi) = 0.99$  ( $\gamma'(\bar{\eta}_\gamma) = 0.99$ , if  $\beta - \alpha \geq 0$ , or  $\gamma' = 1.01$ , if  $\beta - \alpha < 0$ ).

If  $\eta > \bar{\eta}_\varphi$  ( $\eta > \bar{\eta}_\gamma$ ), then  $\varphi \cong \eta - \alpha$  ( $\gamma \cong \eta - \beta$ ).

As in the previous chapters, we define by

$$\delta := \max(\bar{\eta}_\varphi, \bar{\eta}_\gamma)$$

the thickness of the layer lining the boundary where the influence of the viscosity appears.

As well as  $\varphi$  and  $\gamma$ , in this case we also have that

$$\lim_{\eta \rightarrow +\infty} \Psi'(\eta) = 1, \quad \lim_{\eta \rightarrow +\infty} K'(\eta) = 1, \quad \lim_{\eta \rightarrow +\infty} [\Psi(\eta) - \eta] = -\alpha, \quad \lim_{\eta \rightarrow +\infty} [K(\eta) - \eta] = -\beta.$$

The numerical results show that the values computed of  $\alpha$  ( $\beta$ ) for  $\varphi$  and  $\Psi$  ( $\gamma$  and  $K$ ) are in good agreement, especially when  $\beta_m$  is small or  $R_m$  is big. This fact can be well observed displaying that the velocity and the magnetic field are parallel far from the obstacle, as we will see in the next figures.

The values of  $\alpha$ ,  $\varphi''(0)$ ,  $\gamma'(0)$ ,  $\Psi'(0)$  depend on  $R_m$  and  $\beta_m$ , as we can see from Table 6.1. Of course the value of  $\gamma'(0)$  depends also on  $\beta - \alpha$ .

Table 6.1 has been obtained for small values of  $R_m$  recomputing the corresponding values of  $\eta$ ,  $\varphi$ ,  $\gamma$ ,  $\Psi$  and  $K$ . More precisely, for  $R_m = 0.01$  with transformation (6.44) we get Table 6.2.

We underline that

- if  $R_m$  increases, then  $\alpha$ ,  $\varphi''(0)$  and  $\Psi'(0)$  decrease;
- if  $\beta_m$  increases, then  $\alpha$  increases, while  $\varphi''(0)$  and  $\Psi'(0)$  decrease;
- $\gamma'(0)$  is more influenced by  $\beta - \alpha$  rather than  $R_m$  and  $\beta_m$ : more precisely, it decreases as  $\beta - \alpha$  increases.

In Figure 6.2<sub>1</sub> we can see the profiles  $\varphi, \varphi', \varphi''$  for  $R_m = 1$  and  $\beta_m = 0.5$ , while Figure 6.2<sub>2</sub> shows the behaviour of  $\Psi, \Psi'$  for the same values of  $R_m$  and  $\beta_m$ .

Figures 6.3<sub>1</sub>, 6.3<sub>2</sub> show the profiles of  $\gamma(\eta)$ ,  $\gamma'(\eta)$ , for  $R_m = 1$ ,  $\beta_m = 0.5$  and some values of  $\beta - \alpha$ , i.e.  $\beta - \alpha = -5 - \alpha, -\alpha, 0, \alpha, 5 - \alpha$ .

In Figure 6.4 we display the variation of  $K(\eta)$  with  $\eta$  when  $\beta - \alpha$  varies and  $R_m = 1$ ,  $\beta_m = 0.5$ .

We have plotted the profiles of  $\varphi, \varphi', \varphi'', \gamma, \gamma', \Psi, \Psi', K$  only for  $R_m = 1$  and  $\beta_m = 0.5$  because they have an analogous behaviour for  $R_m \neq 1$  and  $\beta_m \neq 0.5$ .

Table 6.1 underlines that the thickness of the boundary layer depends on  $R_m$  and  $\beta_m$ . More precisely, it increases when  $\beta_m$  increases (as is easy to see in Figures 6.5<sub>1</sub>, 6.6<sub>1</sub>, 6.7<sub>1</sub>, 6.8<sub>1</sub>, 6.9<sub>1</sub>, 6.10<sub>1</sub>).

Moreover, the thickness of the boundary layer decreases when  $R_m$  increases (as is easy to see in Figure 6.5<sub>2</sub>, 6.6<sub>2</sub>, 6.7<sub>2</sub>, 6.8<sub>2</sub>, 6.9<sub>2</sub>, 6.10<sub>2</sub>).

This behaviour is in agreement with the previous chapter.

From Table 6.1 we have that  $\bar{\eta}_\gamma$  is always greater than  $\bar{\eta}_\varphi$ . Hence as it happened in the absence of the electromagnetic field (see Chapters 1.2.2 and 3.2), the influence of the viscosity appears only in a layer lining the boundary whose thickness is  $\bar{\eta}_\gamma$ ,

Table 6.1: CASE IV-N: descriptive quantities of the motion for several values of  $\beta - \alpha$ ,  $R_m$  and  $\beta_m$ .

$R_m$	$\beta_m$	$\beta - \alpha$	$\alpha$	$\varphi''(0)$	$\gamma'(0)$	$\Psi'(0)$	$\frac{x_p}{x_s}$	$\frac{m_s}{m_i}$	$\bar{\eta}_\varphi$	$\bar{\eta}_\gamma$	$\delta$		
0.01	0.00	-5.6479	0.6479	1.2326	6.8507	0.9273	0.9113	3.7485	2.3841	23.0077	23.0077		
		-0.6479	0.6479	1.2326	0.6878	0.9273	0.1161	3.7485	2.3841	23.0077	23.0077		
		0	0.6479	1.2326	0.6079	0.9273	0	3.7485	2.3841	23.0077	23.0077		
		0.6479	0.6479	1.2326	0.5281	0.9273	-0.1512	3.7485	2.3841	23.0077	23.0077		
	0.50	4.3521	0.6479	1.2326	-5.4751	0.9273	1.1110	3.7485	2.3841	23.0077	23.0077		
		-6.2557	1.2557	1.1435	3.8406	0.8991	0.8439	3.6182	19.4231	36.6789	36.6789		
		-1.2557	1.2557	1.1435	0.6916	0.8991	0.1148	3.5433	19.4231	33.2944	33.2944		
		0	1.2557	1.1435	0.6125	0.8991	0	3.5415	19.4231	33.8279	33.8279		
		1.2557	1.2557	1.1435	0.5334	0.8991	-0.1489	3.5397	19.4231	34.3114	34.3114		
		3.7443	1.2557	1.1435	-2.4574	0.8991	1.2543	3.4716	19.4231	41.2137	41.2137		
		1	0.00	-5.6479	0.6479	1.2326	7.5695	0.6080	0.9197	3.7485	2.3808	3.0577	3.0577
				-0.6479	0.6479	1.2326	1.4066	0.6080	0.5678	3.7485	2.3808	3.1110	3.1110
0	0.6479			1.2326	0.6080	0.6080	0	3.7485	2.3808	3.1927	3.1927		
0.6479	0.6479			1.2326	-0.1906	0.6080	4.1892	3.7484	2.3808	3.2528	3.2528		
0.50	4.3521		0.6479	1.2326	-4.7564	0.6080	1.1278	3.7484	2.3808	3.4562	3.4562		
	-6.0511		1.0511	0.9065	4.9092	0.5258	0.8753	3.1548	4.3164	4.9166	4.9166		
	-1.0511		1.0511	0.9065	1.4085	0.5258	0.5300	2.9170	4.3164	2.3008	4.3164		
	0		1.0511	0.9065	0.6725	0.5258	0	2.8715	4.3164	2.4025	4.3164		
	1.0511		1.0511	0.9065	-0.0634	0.5258	11.7713	2.8274	4.3164	4.9000	4.9000		
	3.9489		1.0511	0.9065	-2.0923	0.5258	1.3403	2.7125	4.3164	4.9466	4.9466		
	100		0.00	-5.6479	0.6479	1.2326	7.5695	0.2027	0.9197	3.7485	2.3808	3.0577	3.0577
				-0.6479	0.6479	1.2326	1.4066	0.2027	0.5678	3.7485	2.3808	3.1110	3.1110
0		0.6479		1.2326	0.6080	0.2027	0	3.7485	2.3808	3.1927	3.1927		
0.6479		0.6479		1.2326	-0.1906	0.2027	4.1892	3.7484	2.3808	3.2528	3.2528		
0.50		4.3521	0.6479	1.2326	-4.7564	0.2027	1.1278	3.7484	2.3808	3.4562	3.4562		
		-5.9234	0.9234	0.8665	5.6892	0.1641	0.8785	3.1736	3.3795	4.0263	4.0263		
		-0.9234	0.9234	0.8665	1.4096	0.1641	0.5527	3.4792	3.3795	4.2598	4.2598		
		0	0.9234	0.8665	0.6192	0.1641	0	3.5422	3.3795	4.3615	4.3615		
		0.9234	0.9234	0.8665	-0.1711	0.1641	4.5538	3.6075	3.3795	4.4331	4.4331		
		4.0766	0.9234	0.8665	-2.8701	0.1641	1.1985	3.8499	3.3795	4.5799	4.5799		

Table 6.2: CASE IV-N: descriptive quantities of the motion for several values of  $\beta - \alpha$  and  $\beta_m$  when  $R_m = 0.01$ .

$R_m$	$\beta_m$	$\beta - \alpha$	$\alpha$	$\varphi''_*(0)$	$\gamma'_*(0)$	$\Psi'_*(0)$	$\frac{x_{p*}}{x_{s*}}$	$\frac{m_{s*}}{m_i}$	$\bar{\xi}_{\varphi*}$	$\bar{\xi}_{\gamma*}$	$\delta_*$
0.01	0.00	-5.0648	0.0648	12.3259	6.8507	0.9273	9.1126	-4.1004	0.2384	2.3008	2.3008
		-0.0648	0.0648	12.3259	0.6878	0.9273	1.1611	-2057.0603	0.2384	2.3008	2.3008
		0	0.0648	12.3259	0.6079	0.9273	0	374.8513	0.2384	2.3008	2.3008
		0.0648	0.0648	12.3259	0.5281	0.9273	-1.5122	171.7747	0.2384	2.3008	2.3008
	0.50	4.9352	0.0648	12.3259	-5.4751	0.9273	11.1104	4.1168	0.2384	2.3008	2.3008
		-5.1256	0.1256	11.4350	3.8406	0.8991	8.4390	-7.5926	1.9423	3.6679	3.6679
		-0.1256	0.1256	11.4350	0.6916	0.8991	1.1481	-2117.5339	1.9423	3.3294	3.3294
		0	0.1256	11.4350	0.6125	0.8991	0	354.1502	1.9423	3.3828	3.3828
		0.1256	0.1256	11.4350	0.5334	0.8991	-1.4886	163.4102	1.9423	3.4311	3.4311
		4.8744	0.1256	11.4350	-2.4574	0.8991	12.5427	7.6475	1.9423	4.1214	4.1214

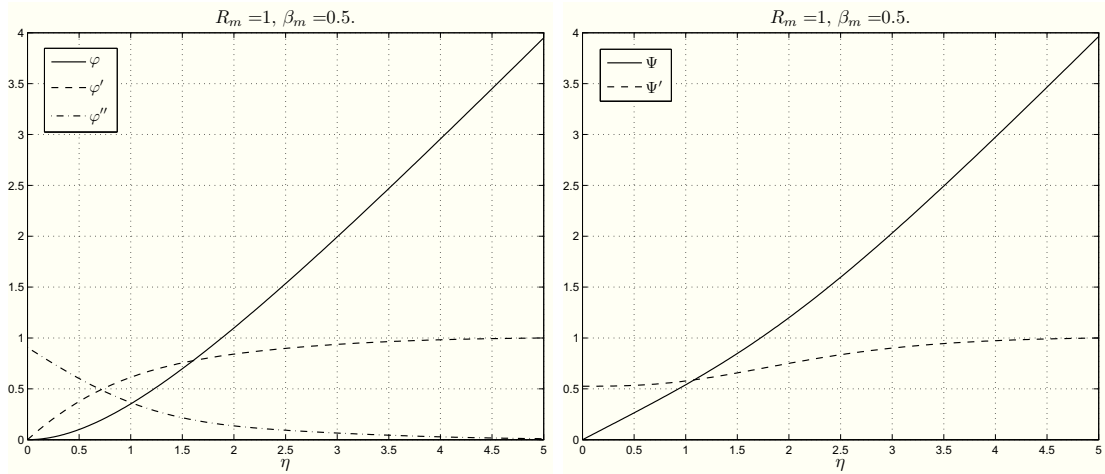


Figure 6.2: CASE IV-N: the first figure shows  $\varphi, \varphi', \varphi''$  for  $R_m = 1$  and  $\beta_m = 0.5$ , while the second shows  $\Psi, \Psi'$  for  $R_m = 1$  and  $\beta_m = 0.5$ .

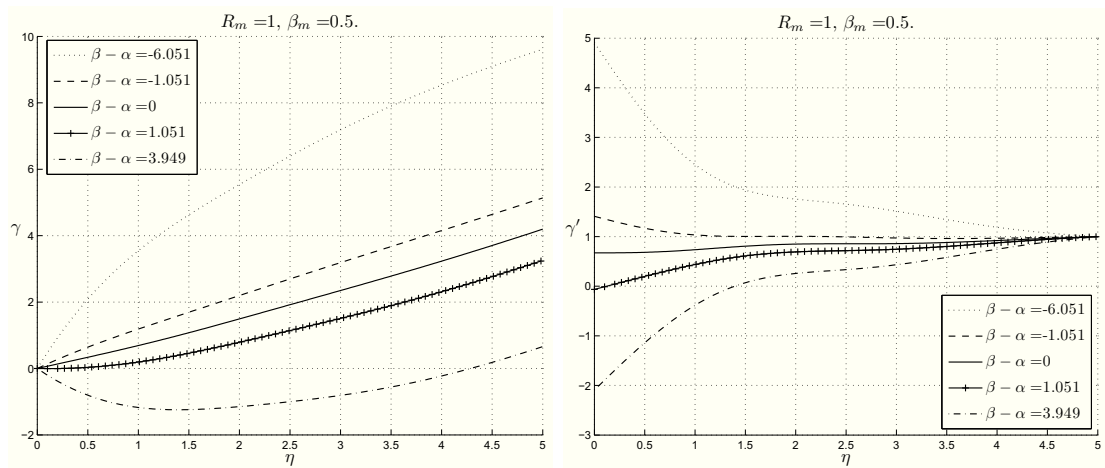


Figure 6.3: CASE IV-N: figures showing the behaviour of  $\gamma$ , and  $\gamma'$  for  $R_m = 1$  and  $\beta_m = 0.5$  with, from above,  $\beta - \alpha = -5 - \alpha, -\alpha, 0, \alpha, 5 - \alpha$ .

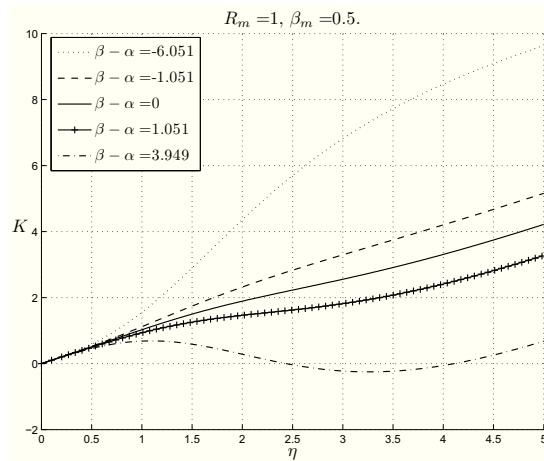


Figure 6.4: CASE IV-N: plot showing the behaviour of  $K$  for  $R_m = 1$  and  $\beta_m = 0.5$  with, from above,  $\beta - \alpha = -5 - \alpha, -\alpha, 0, \alpha, 5 - \alpha$ .

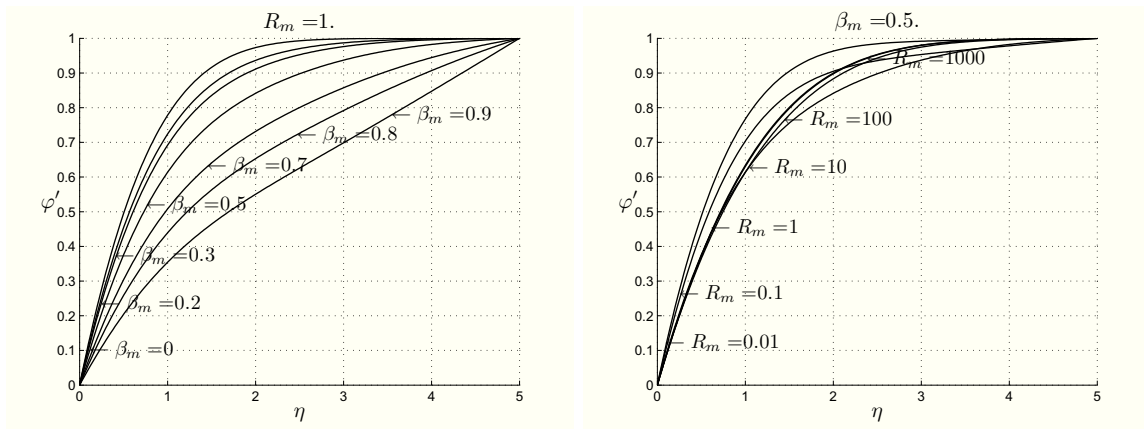


Figure 6.5: CASE IV-N: plots showing  $\varphi'$  for different  $\beta_m$  and  $R_m$ , respectively.

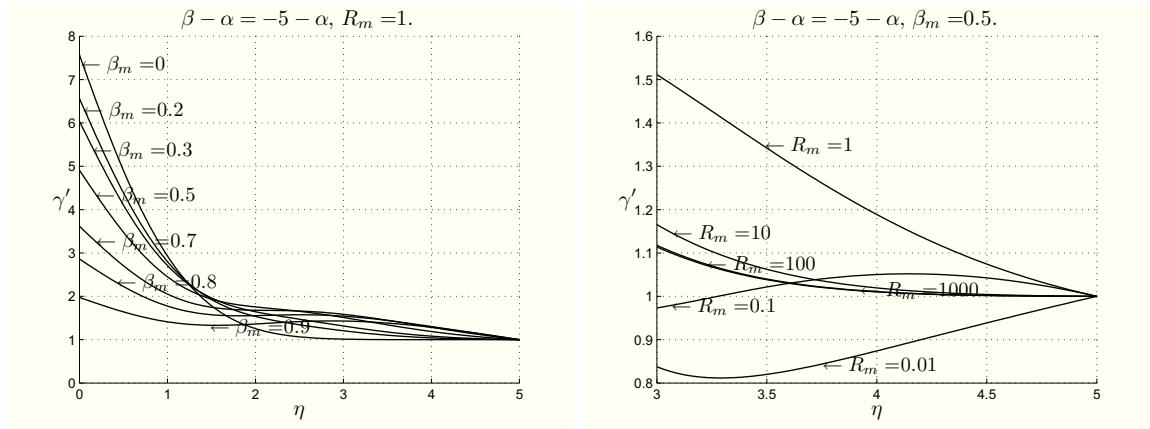


Figure 6.6: CASE IV-N: plots showing  $\gamma'$  for different  $\beta_m$  and  $R_m$ , respectively, when  $\beta - \alpha = -5 - \alpha$ .

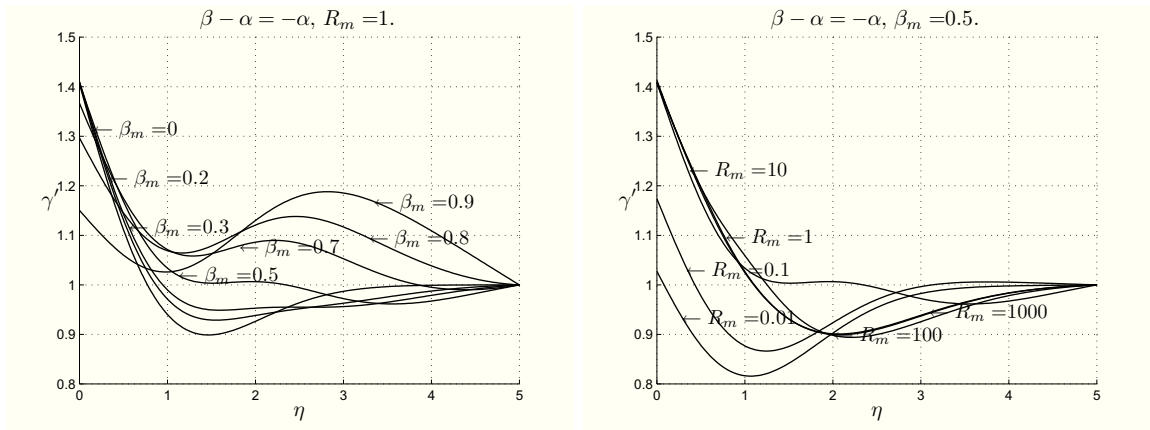


Figure 6.7: CASE IV-N: plots showing  $\gamma'$  for different  $\beta_m$  and  $R_m$ , respectively, when  $\beta - \alpha = -\alpha$ .

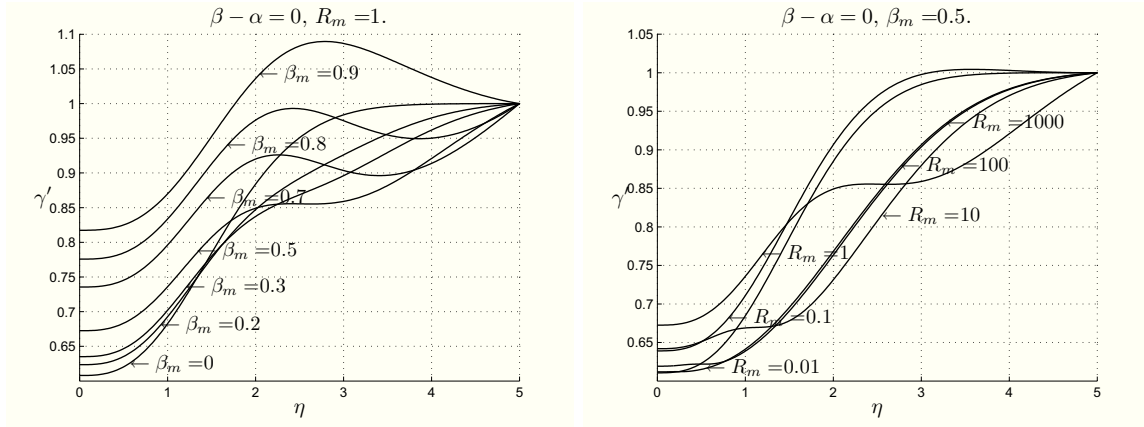


Figure 6.8: CASE IV-N: plots showing  $\gamma'$  for different  $\beta_m$  and  $R_m$ , respectively, when  $\beta - \alpha = 0$ .

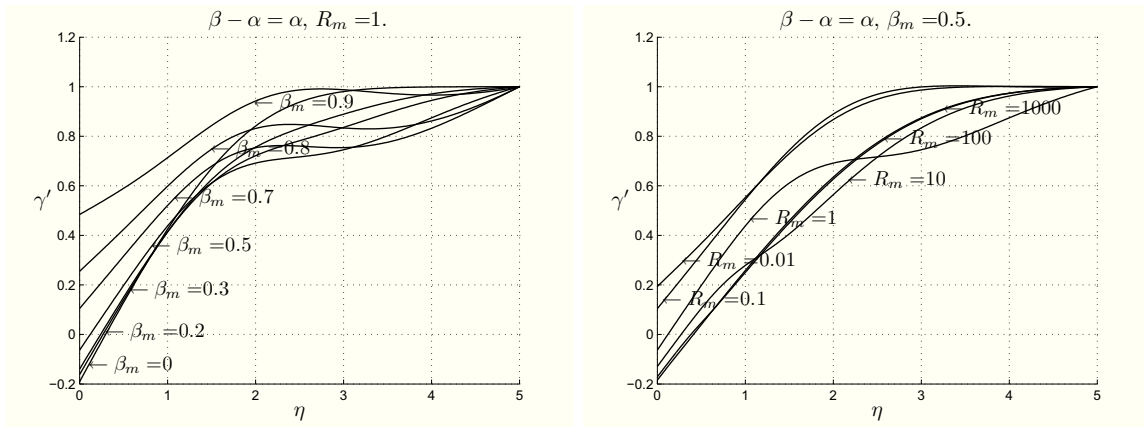


Figure 6.9: CASE IV-N: plots showing  $\gamma'$  for different  $\beta_m$  and  $R_m$ , respectively, when  $\beta - \alpha = \alpha$ .

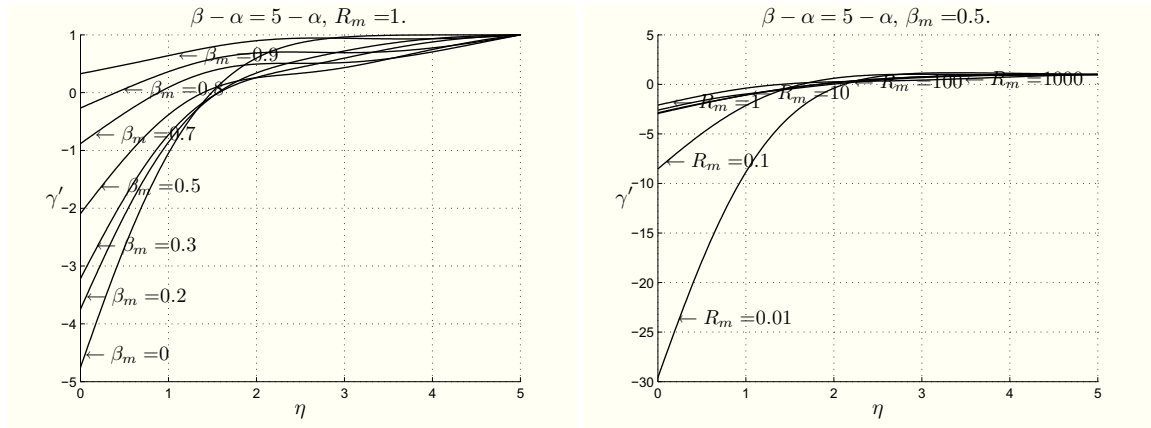


Figure 6.10: CASE IV-N: plots showing  $\gamma'$  for different  $\beta_m$  and  $R_m$ , respectively, when  $\beta - \alpha = 5 - \alpha$ .

which is larger than that in the orthogonal case (see Chapter 5.2).

The more  $R_m$  is small and the more  $\beta_m$  is close to 1 the more the thickness of the boundary layer is larger than in the other cases of oblique stagnation-point flow treated in this Thesis (Chapters 1.2 and 3).

Finally, we display the streamlines of the flow in Figures 6.11, 6.12, 6.13. As it is easy to see from the figures, the flow and the magnetic field are completely parallel far from the obstacle and the more  $R_m$  increases the more the two lines coincide. In these Figures we can also see the points  $\xi_p, \xi_s$ , which are related to  $x_p$  and  $x_s$  in (6.41) in the following way

$$\xi_p = \sqrt{\frac{a}{\nu}} x_p, \quad \xi_s = \sqrt{\frac{a}{\nu}} x_s$$

Their location depends on  $\beta_m$ ,  $R_m$  and  $\beta - \alpha$  as it is explained in Table 6.1.

### 6.3 Micropolar fluids CASE IV-M

Let us analyze the previous problem for a homogeneous, incompressible, electrically conducting micropolar fluid.

In the absence of external mechanical body forces and body couples and free electric charges, the MHD equations for such a fluid are (2.44).

As far as the boundary conditions are concerned, we prescribe conditions (2.45), (2.5), (2.6).

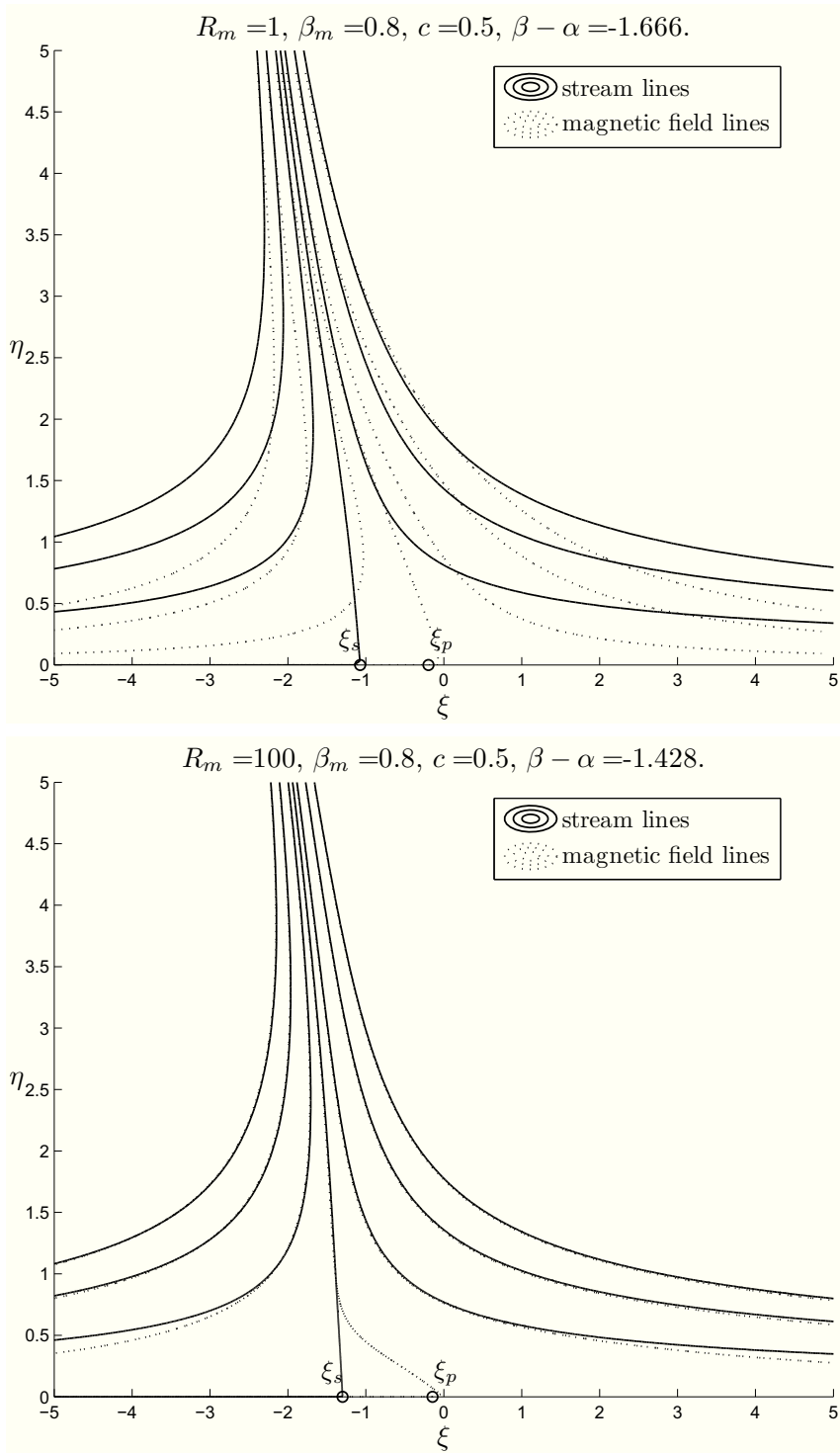


Figure 6.11: CASE IV-N: figures show the streamlines and the points  $\xi_p, \xi_s$  for  $\beta_m = 0.8, c = 0.5, \beta - \alpha = -\alpha$  and  $R_m = 1$  or  $R_m = 100$ , respectively.

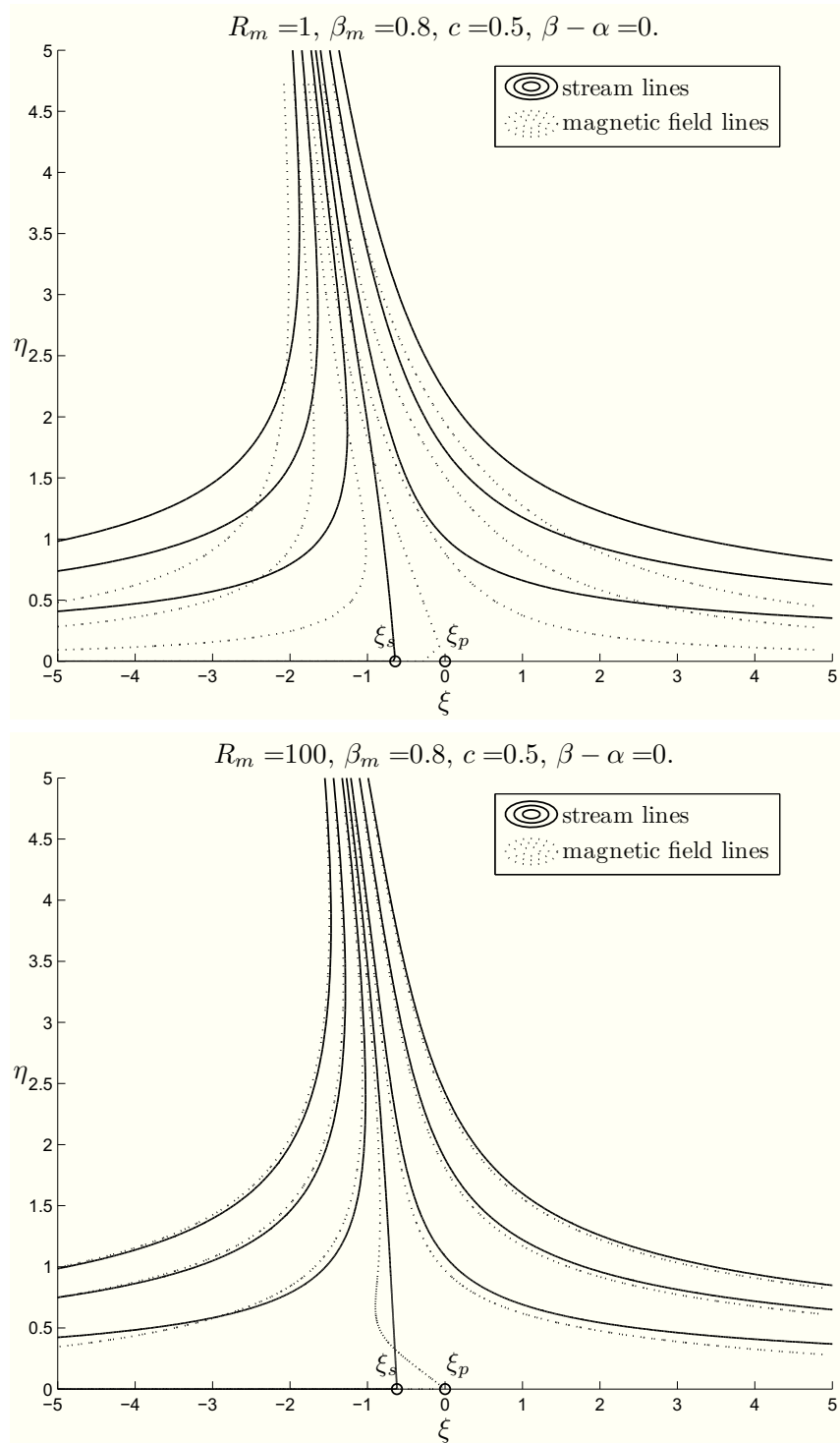


Figure 6.12: CASE IV-N: figures show the streamlines and the points  $\xi_p$ ,  $\xi_s$  for  $\beta_m = 0.8$ ,  $c = 0.5$ ,  $\beta - \alpha = 0$  and  $R_m = 1$  or  $R_m = 100$ , respectively.

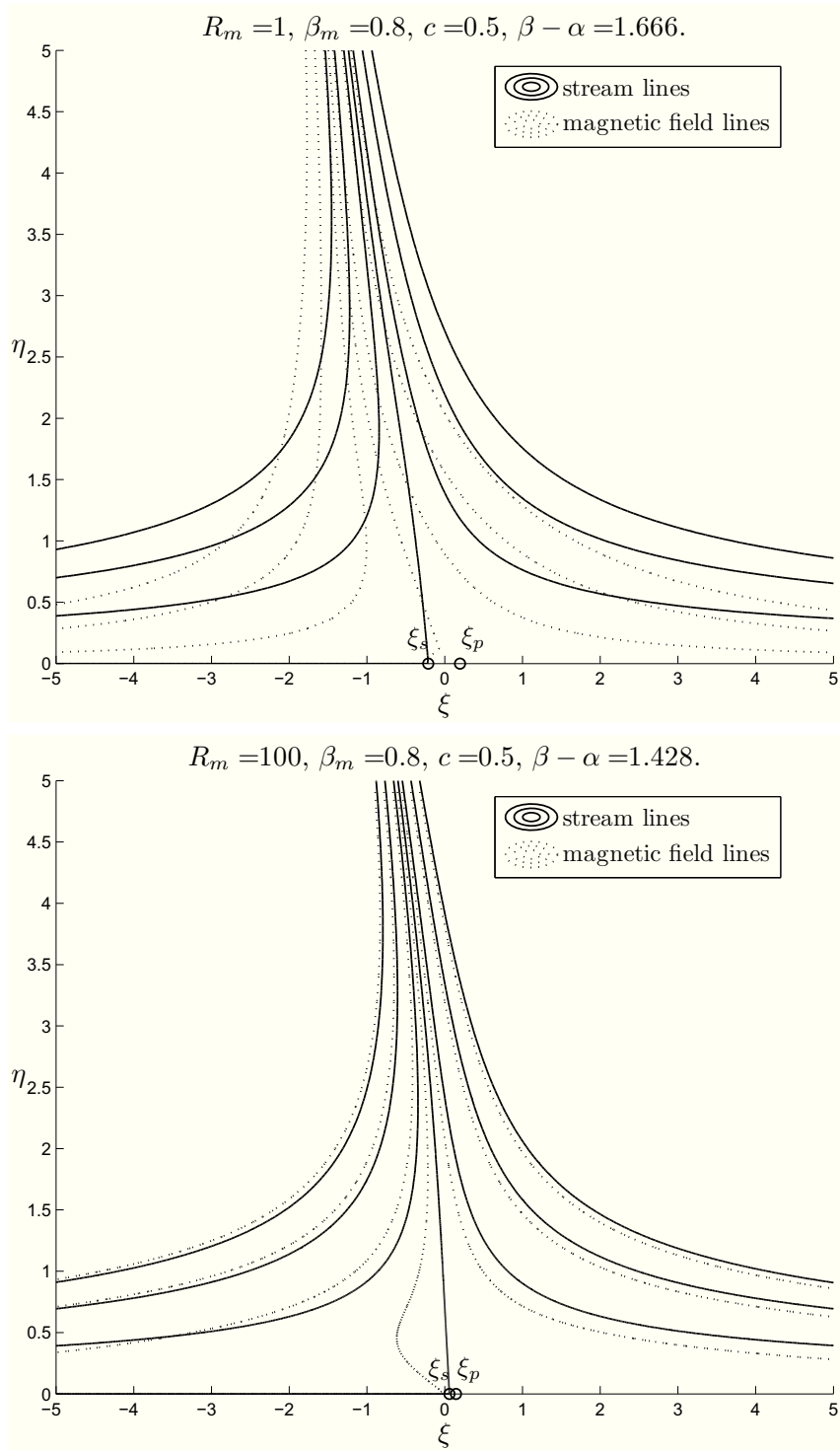


Figure 6.13: CASE IV-N: figures show the streamlines and the points  $\xi_p, \xi_s$  for  $\beta_m = 0.8, c = 0.5, \beta - \alpha = \alpha$  and  $R_m = 1$  or  $R_m = 100$ , respectively.

The following similarity transformations are used:

$$\begin{aligned} v_1 &= a[x_1 f'(x_2) + cg(x_2)], \quad v_2 = -af(x_2), \quad v_3 = 0, \\ w_1 &= 0, \quad w_2 = 0, \quad w_3 = x_1 F(x_2) + G(x_2), \quad x_1 \in \mathbb{R}, \quad x_2 \in \mathbb{R}^+, \end{aligned} \quad (6.46)$$

where  $f, g, F, G$  are sufficiently regular unknown functions ( $f \in C^3(\mathbb{R}^+)$ ,  $g, F, G \in C^2(\mathbb{R}^+)$ ).

The conditions (2.45) require that

$$\begin{aligned} f(0) &= 0, \quad f'(0) = 0, \quad g(0) = 0, \\ F(0) &= 0, \quad G(0) = 0. \end{aligned} \quad (6.47)$$

We suppose that the whole physical space is permeated by the external fields

$$\mathbf{H}_e = H_\infty [(x_1 + cx_2)\mathbf{e}_1 - x_2\mathbf{e}_2], \quad \mathbf{E} = E_0\mathbf{e}_3,$$

and that the total magnetic field in the fluid have the form

$$\mathbf{H} = H_\infty [(x_1 h'(x_2) + ck(x_2))\mathbf{e}_1 - h(x_2)\mathbf{e}_2], \quad (6.48)$$

where  $h, k$  are sufficiently regular unknown functions ( $h, k \in C^2(\mathbb{R}^+)$ ) to be determined such that

$$h(0) = 0, \quad k(0) = 0. \quad (6.49)$$

The previous conditions follow from (2.6) and Theorem 6.1.2.

We assume that at infinity the MHD oblique stagnation-point flow satisfies the Condition P at infinity. Hence we require

$$\begin{aligned} \lim_{x_2 \rightarrow +\infty} f'(x_2) &= 1, \quad \lim_{x_2 \rightarrow +\infty} g'(x_2) = 1, \\ \lim_{x_2 \rightarrow +\infty} F(x_2) &= 0, \quad \lim_{x_2 \rightarrow +\infty} G(x_2) = -\frac{ac}{2}, \\ \lim_{x_2 \rightarrow +\infty} h'(x_2) &= 1. \end{aligned} \quad (6.50)$$

The asymptotic behaviour of  $f$  and  $g$  at infinity is related to the constants  $A, B$ , in the same way as the Newtonian fluids:

$$\lim_{x_2 \rightarrow +\infty} [f(x_2) - x_2] = -A, \quad \lim_{x_2 \rightarrow +\infty} [g(x_2) - x_2] = -B, \quad (6.51)$$

$$\lim_{x_2 \rightarrow +\infty} [h(x_2) - x_2] = -A, \quad \lim_{x_2 \rightarrow +\infty} [k(x_2) - x_2] = -B, \quad (6.52)$$

so that  $\mathbf{H}$  and  $\mathbf{v}$  are parallel at infinity.

Let  $\mathbf{E}$  be the total electric field in the fluid.

We now want to determine  $(p, f, g, F, G, \mathbf{H}, \mathbf{E})$  solution in  $\mathcal{S}$  of (2.44) with  $\mathbf{v}$  and  $\mathbf{w}$  given by (6.46) such that Condition P holds.

Since (2.44)<sub>4,5,6,7</sub> are the same as (2.22)<sub>3,4,5,6</sub>,  $\mathbf{H}$  and  $\mathbf{E}$  depend only on the form of the velocity field, which is the same as that of the Newtonian fluid. Hence proceeding as in the previous section, we get

$$\mathbf{E} = \mathbf{E}_e = -\frac{cH_\infty}{\sigma_e} \mathbf{e}_3,$$

and

$$\begin{aligned} h''(x_2) + \frac{a}{\eta_e} [f(x_2)h'(x_2) - f'(x_2)h(x_2)] &= 0, \\ h(0) = 0, \quad \lim_{x_2 \rightarrow +\infty} h'(x_2) &= 1; \end{aligned} \quad (6.53)$$

$$\begin{aligned} k'(x_2) + \frac{a}{\eta_e} [f(x_2)k(x_2) - g(x_2)h(x_2)] - 1 &= 0, \\ k(0) &= 0. \end{aligned} \quad (6.54)$$

Of course,  $k$  is formally given by (6.35) and satisfies (6.52)<sub>2</sub>.

Now we proceed in order to determine  $p, f, g, F, G$ .

Substituting (6.46), and (6.48) into (2.44)<sub>1,3</sub>, it provides  $p = p(x_1, x_2)$  and

$$\begin{aligned} ax_1 \left[ (\nu + \nu_r) f''' + af f'' - af'^2 + \frac{2\nu_r}{a} F' - \frac{\mu_e}{\rho a} H_\infty^2 h h'' \right] \\ + ac \left[ (\nu + \nu_r) g'' + a(fg' - f'g) + \frac{2\nu_r}{b} G' - \frac{\mu_e}{\rho a} H_\infty^2 h k' \right] &= \frac{1}{\rho} \frac{\partial p}{\partial x_1}, \\ (\nu + \nu_r) a f'' + a^2 f' f + 2\nu_r F + \frac{\mu_e}{\rho} \frac{H_\infty^2}{2} \frac{\partial}{\partial x_2} [(x_1 h' + ck)^2] &= -\frac{1}{\rho} \frac{\partial p}{\partial x_2}, \\ x_1 [\lambda F'' + I a (F' f - F f') - 2\nu_r (2F + a f'')] \\ + \lambda G'' + I (a G' f - b F g) - 2\nu_r (2G + b g') &= 0. \end{aligned} \quad (6.55)$$

Then, by integrating (6.55)<sub>2</sub>, we find

$$\begin{aligned} p &= -\rho \frac{a^2}{2} f^2(x_2) - \rho a (\nu + \nu_r) f'(x_2) - 2\nu_r \rho \int_0^{x_2} F(s) ds \\ &\quad - \mu_e \frac{H_\infty^2}{2} [x_1 h'(x_2) + ck(x_2)]^2 + P(x_1), \end{aligned}$$

where the function  $P(x_1)$  is determined supposing that, far from the wall, the pressure  $p$  has the behaviour given by (6.21).

Therefore, by virtue of (6.50), (6.51), (6.52), we get

$$P(x_1) = -\rho \frac{a^2}{2} x_1^2 + \rho a^2 c(B - A)x_1 + \mu_e \frac{H_\infty^2}{2} x_1^2 + \mu_e H_\infty^2 c(A - B)x_1 + p_0^*,$$

where  $p_0^*$  is a suitable constant.

Finally, the pressure field assumes the form

$$\begin{aligned} p = & -\rho \frac{a^2}{2} [x_1^2 + f^2(x_2)] - \rho a \nu f'(x_2) + \rho a^2 c(B - A)x_1 - 2\nu_r \rho \int_0^{x_2} F(s) ds \\ & - \mu_e \frac{H_\infty^2}{2} [x_1 h'(x_2) + ck(x_2)]^2 + \mu_e \frac{H_\infty^2}{2} x_1^2 + \mu_e H_\infty^2 c(A - B)x_1 + p_0. \end{aligned} \quad (6.56)$$

We remark that  $\nabla p$  has a constant component in the  $x_1$  direction proportional to  $B - A$ , which determines the displacement of the uniform shear flow parallel to the wall  $x_2 = 0$  and which now depends on  $H_\infty^2$ .

In consideration of (6.56), we obtain

$$\begin{aligned} \frac{\nu}{a} f''' + f f'' - f'^2 + 1 + \frac{2\nu_r}{a^2} F' - \frac{\mu_e}{\rho} \frac{H_\infty^2}{a^2} (h h'' - h'^2 + 1) &= 0, \\ \frac{\nu}{a} g'' + f g' - f' g + \frac{2\nu_r}{a^2 c} G' - \frac{\mu_e}{\rho} \frac{H_\infty^2}{a^2} (h k' - h' k) &= \left(1 - \frac{\mu_e}{\rho} \frac{H_\infty^2}{a^2}\right) (B - A), \\ \lambda F'' + I a (F' f - F f') - 2\nu_r (2F + a f'') &= 0, \\ \lambda G'' + I (a G' f - b F g) - 2\nu_r (2G + b g') &= 0. \end{aligned} \quad (6.57)$$

Therefore we have proved the following:

**THEOREM 6.3.1.** *Let a homogeneous, incompressible, electrically conducting micropolar fluid occupy the half-space  $\mathcal{S}$  and be embedded in the external magnetic field  $\mathbf{H}_e = H_\infty [(x_1 + c x_2)\mathbf{e}_1 - x_2 \mathbf{e}_2]$ ,  $\mathbf{E}_e = E_0 \mathbf{e}_3$ . If the total magnetic field in the solid is (6.5), then the steady plane MHD oblique stagnation-point flow of such a fluid has*

the following form

$$\begin{aligned}\mathbf{v} &= a[x_1 f'(x_2) + cg(x_2)]\mathbf{e}_1 - af(x_2)\mathbf{e}_2, \quad \mathbf{w} = [x_1 F(x_2) + G(x_2)]\mathbf{e}_3, \\ \mathbf{H} &= H_\infty [(x_1 h'(x_2) + ck(x_2))\mathbf{e}_1 - h(x_2)\mathbf{e}_2], \quad \mathbf{E} = \mathbf{E}_e = -\frac{cH_\infty}{\sigma_e}\mathbf{e}_3, \\ p &= -\rho\frac{a^2}{2}[x_1^2 + f^2(x_2)] - \rho av f'(x_2) + \rho a^2 c(B - A)x_1 - 2\nu_r \rho \int_0^{x_2} F(s)ds \\ &\quad - \mu_e \frac{H_\infty^2}{2}[x_1 h'(x_2) + ck(x_2)]^2 + \mu_e \frac{H_\infty^2}{2}x_1^2 + \mu_e H_\infty^2 c(A - B)x_1 + p_0, \\ &\quad x_1 \in \mathbb{R}, \quad x_2 \in \mathbb{R}^+, \end{aligned}$$

where  $(f, g, F, G, h, k)$  satisfies problem (6.57), (6.53), (6.54), (6.47) and (6.50), provided  $F \in L^1([0, +\infty))$ .

Now if we use (1.49) and we put

$$\Psi(\eta) = \sqrt{\frac{a}{\nu + \nu_r}} h \left( \sqrt{\frac{\nu + \nu_r}{a}} \eta \right), \quad K(\eta) = \sqrt{\frac{a}{\nu + \nu_r}} k \left( \sqrt{\frac{\nu + \nu_r}{a}} \eta \right),$$

then we can rewrite problem (6.57), (6.55)<sub>3,4</sub>, (6.53), (6.54), (6.50) and (6.47) as:

$$\begin{aligned}\varphi''' + \varphi\varphi'' - \varphi'^2 + 1 + \Phi' - \beta_m(\Psi\Psi'' - \Psi'^2 + 1) &= 0, \\ \gamma'' + \varphi\gamma' - \varphi'\gamma + \Gamma' - \beta_m(\Psi K' - \Psi'K) &= (1 - \beta_m)(\beta - \alpha), \\ \Phi'' + c_3(\varphi\Phi' - \varphi'\Phi) - c_2\Phi - c_1\varphi'' &= 0, \\ \Gamma'' + c_3(\varphi\Gamma' - \Phi\gamma) - c_2\Gamma - c_1\gamma' &= 0, \\ \Psi'' + R_m(\varphi\Psi' - \varphi'\Psi) &= 0, \\ K' + R_m(\varphi K - \gamma\Psi) - 1 &= 0, \\ \varphi(0) = 0, \quad \varphi'(0) = 0, \quad \gamma(0) = 0, \quad \gamma'(0) = 0, \\ \Phi(0) = 0, \quad \Gamma(0) = 0, \quad \Psi(0) = 0, \quad K(0) = 0, \\ \lim_{\eta \rightarrow +\infty} \varphi'(\eta) = 1, \quad \lim_{\eta \rightarrow +\infty} \gamma'(\eta) = 1, \\ \lim_{\eta \rightarrow +\infty} \Phi(\eta) = 0, \quad \lim_{\eta \rightarrow +\infty} \Gamma(\eta) = -\frac{c_1}{c_2}, \\ \lim_{\eta \rightarrow +\infty} \Psi'(\eta) = 1, \end{aligned} \tag{6.58}$$

where  $\alpha$ ,  $\beta$ ,  $c_1$ ,  $c_2$ ,  $c_3$  are given by (1.51) and

$$\beta_m = \frac{\mu_e H_\infty^2}{\rho a^2}, \quad R_m = \frac{\nu + \nu_r}{\eta_e}. \quad (6.59)$$

The functions  $\varphi$ ,  $\Phi$  and  $\Psi$  satisfy the corresponding problem of the orthogonal stagnation-point flow (see Chapter 5.3). These functions influence  $\gamma$ ,  $\Gamma$ ,  $K$ , but not viceversa.

**REMARK 6.3.2.** *The three important points on the wall  $x_2 = 0$  (see Remark 1.2.8) are formally the same as in the Newtonian case ((6.41)-(6.42)).*

*The slope of the dividing streamline at the wall is given by*

$$m_s = -\frac{3[\varphi''(0)]^2}{c[(1 - \beta_m)[(\beta - \alpha)\varphi''(0) + \gamma'(0)] - \varphi''(0)\Gamma'(0) + [\beta_m[\Psi'(0)]^2 + \Phi'(0)]\gamma'(0)}$$

*and does not depend on the kinematic viscosity. Thus, the ratio of this slope to that of the dividing streamline at infinity  $\left(m_i = -\frac{2}{c}\right)$  is the same for all oblique stagnation-point flows and it is given by*

$$\frac{m_s}{m_i} = \frac{3}{2} \frac{[\varphi''(0)]^2}{[(1 - \beta_m)[(\beta - \alpha)\varphi''(0) + \gamma'(0)] - \varphi''(0)\Gamma'(0) + [\beta_m[\Psi'(0)]^2 + \Phi'(0)]\gamma'(0)}. \quad (6.60)$$

*This ratio is independent of  $c$ , depending on the constant pressure gradient parallel to the boundary through  $B - A$  and  $\mathbf{H}$ .*

We have solved numerically problem (6.58).

The values of  $R_m$ ,  $\beta_m$ ,  $c_1$ ,  $c_2$ ,  $c_3$  and  $\beta - \alpha$  are chosen according to the previous chapters.

We recall that  $\beta_m$  has to be less than 1 in order to preserve the parallelism of  $\mathbf{H}$  and  $\mathbf{v}$  at infinity and that for small values of  $R_m$ , equation (6.58)<sub>5</sub> reduces to  $\Psi'' \cong 0$ . In order to remove this difficulty, it is convenient to use the transformation ([23], [24]):

$$\begin{aligned} \xi &= \sqrt{R_m}\eta, & \varphi_*(\xi) &= \sqrt{R_m}\varphi(\sqrt{R_m}\xi), & \gamma_*(\xi) &= \sqrt{R_m}\gamma(\sqrt{R_m}\xi), \\ \Phi_*(\xi) &= \sqrt{R_m}\Phi(\sqrt{R_m}\xi), & \Gamma_*(\xi) &= \sqrt{R_m}\Gamma(\sqrt{R_m}\xi), \\ \Psi_*(\eta) &= \sqrt{R_m}\Psi(\sqrt{R_m}\xi), & K_*(\eta) &= \sqrt{R_m}K(\sqrt{R_m}\xi), \end{aligned} \quad (6.61)$$

which furnishes the following analogous problem

$$\begin{aligned}
 R_m \varphi_*''' + \varphi_* \varphi_*'' - \varphi_*'^2 + 1 + \Phi_*' - \beta_m (\Psi_* \Psi_*'' - \Psi_*'^2 + 1) &= 0, \\
 R_m \gamma_*'' + \varphi_* \gamma_*' - \varphi_*' \gamma_* + \sqrt{R_m} \Gamma_*' - \beta_m (\Psi_* K_*' - \Psi_*' K_*) &= \sqrt{R_m} (1 - \beta_m) (\beta - \alpha), \\
 R_m \Phi_*'' + c_3 (\varphi_* \Phi_*' - \varphi_*' \Phi_*) - c_2 \Phi_* - c_1 R_m \varphi_*'' &= 0, \\
 R_m \Gamma_*'' + c_3 \left( \varphi_* \Gamma_*' - \frac{1}{\sqrt{R_m}} \Phi_* \gamma_*' \right) - c_2 \Gamma_* - c_1 \sqrt{R_m} \gamma_*' &= 0, \\
 \Psi_*'' + \varphi_* \Psi_*' - \varphi_*' \Psi_* &= 0, \\
 K_*' + \varphi_* K_* - \gamma_* \Psi_* - 1 &= 0, \\
 \varphi_*(0) = 0, \quad \varphi_*'(0) = 0, \quad \gamma_*(0) = 0, \quad \gamma_*'(0) = 0, \\
 \Phi_*(0) = 0, \quad \Gamma_*(0) = 0, \quad \Psi_*(0) = 0, \quad K_*(0) = 0, \\
 \lim_{\xi \rightarrow +\infty} \varphi_*'(\xi) = 1, \quad \lim_{\xi \rightarrow +\infty} \gamma_*'(\xi) = 1, \\
 \lim_{\xi \rightarrow +\infty} \Phi_*(\xi) = 0, \quad \lim_{\xi \rightarrow +\infty} \Gamma_*(\xi) = -\frac{c_1}{c_2}, \\
 \lim_{\xi \rightarrow +\infty} \Psi_*'(\xi) = 1.
 \end{aligned} \tag{6.62}$$

REMARK 6.3.3. As we will see,  $\varphi$ ,  $\gamma$ ,  $\Phi$ ,  $\Gamma$  satisfy condition (6.62)<sub>15,16,17,18</sub>, therefore we recall Remark 1.2.9, where we defined:

- $\bar{\eta}_\varphi$  ( $\bar{\eta}_\gamma$ ) the value of  $\eta$  such that  $\varphi'(\bar{\eta}_\varphi) = 0.99$  ( $\gamma'(\bar{\eta}_\gamma) = 0.99$ , if  $\beta - \alpha \geq 0$ , or  $\gamma' = 1.01$ , if  $\beta - \alpha < 0$ );
- $\bar{\eta}_\Phi$  ( $\bar{\eta}_\Gamma$ ) the value of  $\eta$  such that  $\Phi(\bar{\eta}_\Phi) = -0.01$   $\left( \Gamma(\bar{\eta}_\Gamma) = -\frac{c_1}{c_2} + 0.01 \right)$ .

Hence if  $\eta > \bar{\eta}_\varphi$  ( $\eta > \bar{\eta}_\gamma$ ), then  $\varphi \cong \eta - \alpha$  ( $\gamma \cong \eta - \beta$ ), and if  $\eta > \bar{\eta}_\Phi$  ( $\eta > \bar{\eta}_\Gamma$ ), then  $\Phi \cong 0$   $\left( \Gamma \cong -\frac{c_1}{c_2} \right)$ .

From the numerical integration we will see that the influence of the viscosity on the velocity and on the microrotation appears only in a layer lining the boundary whose thickness is  $\delta_v = \max(\bar{\eta}_\varphi, \bar{\eta}_\gamma)$  for the velocity and  $\delta_w = \max(\bar{\eta}_\Phi, \bar{\eta}_\Gamma)$  for the microrotation. The thickness  $\delta$  of the boundary layer for the flow is defined as

$$\delta := \max(\delta_v, \delta_w).$$

In this case we also have that

$$\lim_{\eta \rightarrow +\infty} \Psi'(\eta) = 1, \quad \lim_{\eta \rightarrow +\infty} K'(\eta) = 1, \quad \lim_{\eta \rightarrow +\infty} [\Psi(\eta) - \eta] = -\alpha, \quad \lim_{\eta \rightarrow +\infty} [K(\eta) - \eta] = -\beta.$$

The numerical results show that the values computed of  $\alpha$  ( $\beta$ ) for  $\varphi$  and  $\Psi$  ( $\gamma$  and  $K$ ) are in good agreement, especially when  $\beta_m$  is small or  $R_m$  is big. This fact can be well observed displaying that the velocity and the magnetic field are parallel far from the obstacle, as we will see in the next figures.

The values of the parameters  $c_1$ ,  $c_2$ ,  $c_3$ ,  $\beta_m$  and  $R_m$  are given in Tables 6.3, 6.4 and 6.5, where we also assign some values to  $\beta$  (i.e.  $\beta - \alpha = -\alpha, 0, \alpha$ ). The consequent values of  $\alpha$ ,  $\varphi''(0)$ ,  $\gamma'(0)$ ,  $\Phi'(0)$ ,  $\Gamma'(0)$ ,  $\Psi'(0)$ ,  $\frac{x_p}{x_s}$ ,  $\frac{m_s}{m_i}$  are reported in these tables.

Tables 6.3, 6.4 and 6.5 have been obtained for  $R_m = 0.01$  recomputing the corresponding values of  $\eta$ ,  $\varphi$ ,  $\gamma$ ,  $\Phi$ ,  $\Gamma$ ,  $\Psi$  and  $K$ . More precisely, for  $R_m = 0.01$  with transformation (6.61) we get Table 6.6.

From these Tables it appears that if we fix two among  $c_1, c_2, c_3$  when the other parameters are fixed, then the values of the descriptive quantities of the motion behave likewise the case in the absence of the external electromagnetic field, as easily seen in Figures 6.14, 6.15, 6.16.

It is further interesting to see that

- if  $R_m$  increases, then  $\alpha$ ,  $\varphi''(0)$ ,  $|\Phi'(0)|$  and  $\Psi'(0)$  decrease;
- if  $\beta_m$  increases, then  $\alpha$  increases, while  $\varphi''(0)$  and  $\Psi'(0)$  decrease;
- $\gamma'(0)$  and  $|\Gamma'(0)|$  are more influenced by  $\beta$  instead by  $R_m$  and  $\beta_m$ : more precisely, they decrease as  $\beta - \alpha$  increases.

We have displayed some representative graphs to elucidate the trends of the functions describing the velocity, the microrotation and the magnetic field.

In particular, Figures 6.17, 6.18, 6.19, and 6.20 show  $\varphi$ ,  $\varphi'$ ,  $\varphi''$ ,  $\Phi$ ,  $\Phi'$ ,  $\gamma$ ,  $\gamma'$ ,  $\Gamma$ ,  $\Gamma'$ ,  $\Psi$ ,  $\Psi'$ ,  $K$  for  $R_m = 1$ ,  $\beta_m = 0.5$ ,  $c_1 = 0.5$ ,  $c_2 = 3.0$ ,  $c_3 = 0.5$ . The other choices of these parameters modify the trends of these functions very slightly.

In Tables 6.7, 6.8 and 6.9 we list the values of  $\bar{\eta}_\varphi$ ,  $\bar{\eta}_\gamma$ ,  $\bar{\eta}_\Phi$ ,  $\bar{\eta}_\Gamma$  when  $R_m$ ,  $\beta_m$ ,  $c_1$ ,  $c_2$ ,  $c_3$  and  $\beta - \alpha$  change.

Tables 6.7, 6.8 and 6.9 have been obtained for  $R_m = 0.01$  recomputing the corresponding values of  $\bar{\eta}_\varphi$ ,  $\bar{\eta}_\gamma$ ,  $\bar{\eta}_\Phi$  and  $\bar{\eta}_\Gamma$ . More precisely, for  $R_m = 0.01$  with transformation (6.61) we get Table 6.10.

We see that  $\bar{\eta}_\gamma$  is always greater than  $\bar{\eta}_\varphi$ , as in the Newtonian case (see previous section). Hence the influence of the viscosity on the velocity appears only in a layer of thickness  $\bar{\eta}_\gamma$  lining the boundary and its thickness is larger than that of the orthogonal stagnation-point flow.

The presence of the microrotation modifies  $\bar{\eta}_\varphi$  and  $\bar{\eta}_\gamma$ , which are smaller than those for the Newtonian fluids.

As far as the microrotation is concerned,  $\bar{\eta}_\Gamma$  is almost always bigger than  $\bar{\eta}_\Phi$ . So the influence of the viscosity on the microrotation appears usually only in a layer of

Table 6.3: CASE IV-M: descriptive quantities of motion for some values of  $R_m, \beta_m, c_1, c_2, c_3$  and  $\beta - \alpha$ .

$R_m$	$\beta_m$	$c_1$	$c_2$	$c_3$	$\beta - \alpha$	$\alpha$	$\varphi''(0)$	$\gamma'(0)$	$\Phi'(0)$	$\Gamma'(0)$	$\Psi'(0)$	$\frac{x_p}{x_s}$	$\frac{m_s}{m_x}$		
0.01	0.00	0.10	1.50	0.10	-0.0645	0.6445	1.2218	0.6539	-0.0532	-0.0582	0.9275	0.1204	3.6621		
					0	0.6445	1.2218	0.5751	-0.0532	-0.0548	0.9275	0	3.6621		
					0.0645	0.6445	1.2218	0.4964	-0.0532	-0.0513	0.9275	-0.1586	3.6621		
					0.50	-0.0645	0.6448	1.2231	0.6545	-0.0510	-0.0592	0.9275	0.1205	3.6507	
						0	0.6448	1.2231	0.5757	-0.0510	-0.0559	0.9275	0	3.6507	
						0.0645	0.6448	1.2231	0.4968	-0.0510	-0.0526	0.9275	-0.1587	3.6507	
				3.00	0.10	-0.0645	0.6453	1.2250	0.6683	-0.0444	-0.0399	0.9275	0.1183	3.6998	
						0	0.6453	1.2250	0.5892	-0.0444	-0.0370	0.9275	0	3.6998	
						0.0645	0.6453	1.2250	0.5101	-0.0444	-0.0342	0.9275	-0.1550	3.6998	
					0.50	-0.0645	0.6454	1.2256	0.6697	-0.0434	-0.0400	0.9275	0.1181	3.6906	
						0	0.6454	1.2256	0.5906	-0.0434	-0.0371	0.9275	0	3.6906	
						0.0645	0.6454	1.2256	0.5115	-0.0434	-0.0343	0.9275	-0.1547	3.6906	
				0.50	1.50	0.10	-0.0631	0.6309	1.1780	0.5199	-0.2659	-0.2724	0.9287	0.1430	3.3133
							0	0.6309	1.1780	0.4456	-0.2659	-0.2556	0.9287	0	3.3133
							0.0631	0.6309	1.1780	0.3712	-0.2659	-0.2389	0.9287	-0.2002	3.3133
						0.50	-0.0632	0.6321	1.1848	0.5215	-0.2553	-0.2804	0.9287	0.1436	3.2609
							0	0.6321	1.1848	0.4466	-0.2553	-0.2643	0.9287	0	3.2609
							0.0632	0.6321	1.1848	0.3717	-0.2553	-0.2482	0.9287	-0.2015	3.2609
					3.00	0.10	-0.0635	0.6350	1.1943	0.5910	-0.2220	-0.1901	0.9284	0.1283	3.5019
							0	0.6350	1.1943	0.5152	-0.2220	-0.1760	0.9284	0	3.5019
							0.0635	0.6350	1.1943	0.4394	-0.2220	-0.1619	0.9284	-0.1726	3.5019
						0.50	-0.0636	0.6356	1.1972	0.5974	-0.2173	-0.1923	0.9284	0.1274	3.4582
							0	0.6356	1.1972	0.5213	-0.2173	-0.1785	0.9284	0	3.4582
							0.0636	0.6356	1.1972	0.4452	-0.2173	-0.1647	0.9284	-0.1709	3.4582
0.50	0.10	1.50	0.10	-0.1249	1.2492	1.1335	0.6580	-0.0500	-0.0584	0.8995	0.1190	3.4564			
				0	1.2492	1.1335	0.5800	-0.0500	-0.0550	0.8995	0	3.4546			
				0.1249	1.2492	1.1335	0.5020	-0.0500	-0.0515	0.8995	-0.1559	3.4527			
		0.50	-0.1250	1.2496	1.1347	0.6581	-0.0481	-0.0592	0.8995	0.1191	3.4495				
			0	1.2496	1.1347	0.5801	-0.0481	-0.0559	0.8995	0	3.4476				
			0.1250	1.2496	1.1347	0.5020	-0.0481	-0.0526	0.8995	-0.1561	3.4458				
	3.00	0.10	-0.1251	1.2508	1.1366	0.6726	-0.0417	-0.0401	0.8994	0.1168	3.4922				
			0	1.2508	1.1366	0.5944	-0.0417	-0.0372	0.8994	0	3.4903				
			0.1251	1.2508	1.1366	0.5161	-0.0417	-0.0344	0.8994	-0.1523	3.4885				
		0.50	-0.1251	1.2510	1.1371	0.6734	-0.0408	-0.0401	0.8994	0.1168	3.4877				
			0	1.2510	1.1371	0.5951	-0.0408	-0.0373	0.8994	0	3.4859				
			0.1251	1.2510	1.1371	0.5168	-0.0408	-0.0345	0.8994	-0.1522	3.4841				
	0.50	1.50	0.10	-0.1223	1.2227	1.0929	0.5244	-0.2505	-0.2743	0.9012	0.1406	3.1070			
				0	1.2227	1.0929	0.4509	-0.2505	-0.2575	0.9012	0	3.1053			
				0.1223	1.2227	1.0929	0.3775	-0.2505	-0.2407	0.9012	-0.1954	3.1035			
			0.50	-0.1225	1.2249	1.0992	0.5241	-0.2409	-0.2802	0.9011	0.1418	3.0754			
				0	1.2249	1.0992	0.4502	-0.2409	-0.2640	0.9011	0	3.0736			
				0.1225	1.2249	1.0992	0.3762	-0.2409	-0.2479	0.9011	-0.1975	3.0719			
3.00		0.10	-0.1231	1.2308	1.1085	0.5973	-0.2085	-0.1919	0.9007	0.1261	3.2855				
			0	1.2308	1.1085	0.5223	-0.2085	-0.1778	0.9007	0	3.2837				
			0.1231	1.2308	1.1085	0.4473	-0.2085	-0.1638	0.9007	-0.1684	3.2819				
		0.50	-0.1232	1.2318	1.1111	0.6007	-0.2043	-0.1929	0.9007	0.1258	3.2645				
			0	1.2318	1.1111	0.5254	-0.2043	-0.1791	0.9007	0	3.2627				
			0.1232	1.2318	1.1111	0.4502	-0.2043	-0.1653	0.9007	-0.1678	3.2609				

Table 6.4: CASE IV-M: continuum of Table 6.3.

$R_m$	$\beta_m$	$c_1$	$c_2$	$c_3$	$\beta - \alpha$	$\alpha$	$\varphi''(0)$	$\gamma'(0)$	$\Phi'(0)$	$\Gamma'(0)$	$\Psi'(0)$	$\frac{x_p}{x_s}$	$\frac{m_s}{m_i}$			
1	0.00	0.10	1.50	0.10	-0.6446	0.6446	1.2218	1.3648	-0.0532	-0.0892	0.6081	0.5770	3.6488			
					0	0.6446	1.2218	0.5772	-0.0532	-0.0550	0.6081	0	3.6490			
					0.6446	0.6446	1.2218	-0.2104	-0.0532	-0.0207	0.6081	3.7439	3.6492			
				0.50	-0.6448	0.6448	1.2231	1.3652	-0.0510	-0.0889	0.6082	0.5777	3.6454			
					0	0.6448	1.2231	0.5765	-0.0510	-0.0560	0.6082	0	3.6454			
					0.6448	0.6448	1.2231	-0.2121	-0.0510	-0.0231	0.6082	3.7180	3.6455			
				3.00	0.10	-0.6453	0.6453	1.2250	1.3818	-0.0444	-0.0658	0.6082	0.5721	3.6872		
					0	0.6453	1.2250	0.5912	-0.0444	-0.0372	0.6082	0	3.6872			
					0.6453	0.6453	1.2250	-0.1993	-0.0444	-0.0085	0.6082	3.9657	3.6872			
				0.50	-0.6454	0.6454	1.2256	1.3822	-0.0434	-0.0652	0.6083	0.5723	3.6872			
					0	0.6454	1.2256	0.5911	-0.0434	-0.0372	0.6083	0	3.6872			
					0.6454	0.6454	1.2256	-0.1999	-0.0434	-0.0092	0.6083	3.9572	3.6872			
				0.50	1.50	0.10	-0.6310	0.6310	1.1780	1.1972	-0.2659	-0.4282	0.6087	0.6209	3.2527	
					0	0.6310	1.1780	0.4538	-0.2659	-0.2604	0.6087	0	3.2534			
					0.6310	0.6310	1.1780	-0.2897	-0.2659	-0.0925	0.6087	2.5661	3.2540			
				0.50	-0.6321	0.6321	1.1848	1.1988	-0.2553	-0.4275	0.6093	0.6247	3.2374			
					0	0.6321	1.1848	0.4499	-0.2553	-0.2661	0.6093	0	3.2375			
					0.6321	0.6321	1.1848	-0.2990	-0.2553	-0.1047	0.6093	2.5048	3.2375			
				3.00	0.10	-0.6350	0.6350	1.1943	1.2826	-0.2220	-0.3200	0.6092	0.5913	3.4421		
					0	0.6350	1.1943	0.5241	-0.2220	-0.1790	0.6092	0	3.4423			
					0.6350	0.6350	1.1943	-0.2343	-0.2220	-0.0380	0.6092	3.2365	3.4424			
				0.50	-0.6356	0.6356	1.1972	1.2846	-0.2173	-0.3174	0.6095	0.5923	3.4424			
					0	0.6356	1.1972	0.5237	-0.2173	-0.1793	0.6095	0	3.4424			
					0.6356	0.6356	1.1972	-0.2372	-0.2173	-0.0412	0.6095	3.2081	3.4424			
				0.50	0.10	1.50	0.10	-1.0463	1.0463	0.8963	1.3625	-0.0429	-0.0932	0.5258	0.5393	2.8305
					0	1.0463	0.8963	0.6387	-0.0429	-0.0580	0.5258	0	2.7885			
					1.0463	1.0463	0.8963	-0.0852	-0.0429	-0.0227	0.5258	8.6275	2.7476			
				0.50	-1.0462	1.0462	0.8976	1.3634	-0.0413	-0.0921	0.5260	0.5395	2.8303			
					0	1.0462	0.8976	0.6388	-0.0413	-0.0581	0.5260	0	2.7882			
					1.0462	1.0462	0.8976	-0.0858	-0.0413	-0.0241	0.5260	8.5730	2.7473			
				3.00	0.10	-1.0474	1.0474	0.8998	1.3815	-0.0350	-0.0686	0.5260	0.5344	2.8641		
					0	1.0474	0.8998	0.6539	-0.0350	-0.0401	0.5260	0	2.8199			
					1.0474	1.0474	0.8998	-0.0736	-0.0350	-0.0117	0.5260	10.0256	2.7771			
				0.50	-1.0474	1.0474	0.9003	1.3820	-0.0343	-0.0678	0.5261	0.5344	2.8647			
					0	1.0474	0.9003	0.6541	-0.0343	-0.0399	0.5261	0	2.8204			
					1.0474	1.0474	0.9003	-0.0737	-0.0343	-0.0120	0.5261	10.0194	2.7775			
				0.50	1.50	0.10	-1.0265	1.0265	0.8549	1.1793	-0.2141	-0.4437	0.5255	0.5831	2.4884	
					0	1.0265	0.8549	0.5046	-0.2141	-0.2711	0.5255	0	2.4595			
					1.0265	1.0265	0.8549	-0.1701	-0.2141	-0.0985	0.5255	4.0422	2.4313			
				0.50	-1.0261	1.0261	0.8616	1.1832	-0.2066	-0.4392	0.5267	0.5850	2.4879			
					0	1.0261	0.8616	0.5045	-0.2066	-0.2726	0.5267	0	2.4588			
					1.0261	1.0261	0.8616	-0.1742	-0.2066	-0.1061	0.5267	3.9733	2.4303			
				3.00	0.10	-1.0321	1.0321	0.8727	1.2736	-0.1746	-0.3321	0.5267	0.5536	2.6534		
					0	1.0321	0.8727	0.5799	-0.1746	-0.1923	0.5267	0	2.6143			
					1.0321	1.0321	0.8727	-0.1139	-0.1746	-0.0526	0.5267	6.1919	2.5762			
				0.50	-1.0321	1.0321	0.8753	1.2762	-0.1715	-0.3289	0.5271	0.5540	2.6561			
					0	1.0321	0.8753	0.5809	-0.1715	-0.1916	0.5271	0	2.6167			
					1.0321	1.0321	0.8753	-0.1144	-0.1715	-0.0542	0.5271	6.1776	2.5785			

Table 6.5: CASE IV-M: continuum of Table 6.3.

$R_m$	$\beta_m$	$c_1$	$c_2$	$c_3$	$\beta - \alpha$	$\alpha$	$\varphi''(0)$	$\gamma'(0)$	$\Phi'(0)$	$\Gamma'(0)$	$\Psi'(0)$	$\frac{x_p}{x_s}$	$\frac{m_s}{m_i}$	
100	0.00	0.10	1.50	0.10	-0.6446	0.6446	1.2218	1.3648	-0.0532	-0.0892	0.2021	0.5770	3.6488	
					0	0.6446	1.2218	0.5772	-0.0532	-0.0550	0.2021	0	3.6490	
					0.6446	0.6446	1.2218	-0.2104	-0.0532	-0.0207	0.2021	3.7439	3.6492	
				0.50	-0.6448	0.6448	1.2231	1.3652	-0.0510	-0.0889	0.2023	0.5777	3.6454	
					0	0.6448	1.2231	0.5765	-0.0510	-0.0560	0.2023	0	3.6454	
					0.6448	0.6448	1.2231	-0.2121	-0.0510	-0.0231	0.2023	3.7180	3.6455	
			3.00	0.10	-0.6453	0.6453	1.2250	1.3818	-0.0444	-0.0658	0.2024	0.5721	3.6872	
					0	0.6453	1.2250	0.5912	-0.0444	-0.0372	0.2024	0	3.6872	
					0.6453	0.6453	1.2250	-0.1993	-0.0444	-0.0085	0.2024	3.9657	3.6872	
				0.50	-0.6454	0.6454	1.2256	1.3822	-0.0434	-0.0652	0.2024	0.5723	3.6872	
					0	0.6454	1.2256	0.5911	-0.0434	-0.0372	0.2024	0	3.6872	
					0.6454	0.6454	1.2256	-0.1999	-0.0434	-0.0092	0.2024	3.9572	3.6872	
			0.50	1.50	0.10	-0.6310	0.6310	1.1780	1.1972	-0.2659	-0.4282	0.1999	0.6209	3.2527
						0	0.6310	1.1780	0.4538	-0.2659	-0.2604	0.1999	0	3.2534
						0.6310	0.6310	1.1780	-0.2897	-0.2659	-0.0925	0.1999	2.5661	3.2540
					0.50	-0.6321	0.6321	1.1848	1.1988	-0.2553	-0.4275	0.2005	0.6247	3.2374
						0	0.6321	1.1848	0.4499	-0.2553	-0.2661	0.2005	0	3.2375
						0.6321	0.6321	1.1848	-0.2990	-0.2553	-0.1047	0.2005	2.5048	3.2375
				3.00	0.10	-0.6350	0.6350	1.1943	1.2826	-0.2220	-0.3200	0.2011	0.5913	3.4421
						0	0.6350	1.1943	0.5241	-0.2220	-0.1790	0.2011	0	3.4423
						0.6350	0.6350	1.1943	-0.2343	-0.2220	-0.0380	0.2011	3.2365	3.4424
					0.50	-0.6356	0.6356	1.1972	1.2846	-0.2173	-0.3174	0.2013	0.5923	3.4424
						0	0.6356	1.1972	0.5237	-0.2173	-0.1793	0.2013	0	3.4424
						0.6356	0.6356	1.1972	-0.2372	-0.2173	-0.0412	0.2013	3.2081	3.4424
0.50	0.10	1.50	0.10	-0.9166	0.9166	0.8560	1.3602	-0.0439	-0.0925	0.1635	0.5618	3.3765		
				0	0.9166	0.8560	0.5851	-0.0439	-0.0524	0.1635	0	3.4391		
				0.9166	0.9166	0.8560	-0.1901	-0.0439	-0.0124	0.1635	4.0198	3.5041		
		0.50	-0.9169	0.9169	0.8574	1.3615	-0.0421	-0.0912	0.1636	0.5624	3.3745			
			0	0.9169	0.8574	0.5849	-0.0421	-0.0528	0.1636	0	3.4360			
			0.9169	0.9169	0.8574	-0.1916	-0.0421	-0.0143	0.1636	3.9952	3.4999			
		3.00	0.10	-0.9184	0.9184	0.8595	1.3809	-0.0354	-0.0686	0.1638	0.5567	3.4170		
				0	0.9184	0.8595	0.6011	-0.0354	-0.0363	0.1638	0	3.4797		
				0.9184	0.9184	0.8595	-0.1788	-0.0354	-0.0039	0.1638	4.3007	3.5447		
	0.50		-0.9186	0.9186	0.8601	1.3816	-0.0347	-0.0678	0.1638	0.5569	3.4178			
			0	0.9186	0.8601	0.6012	-0.0347	-0.0361	0.1638	0	3.4803			
			0.9186	0.9186	0.8601	-0.1792	-0.0347	-0.0044	0.1638	4.2930	3.5451			
	0.50	1.50	0.10	-0.8887	0.8887	0.8126	1.1636	-0.2196	-0.4363	0.1609	0.6050	2.9591		
				0	0.8887	0.8126	0.4496	-0.2196	-0.2416	0.1609	0	3.0180		
				0.8887	0.8887	0.8126	-0.2643	-0.2196	-0.0469	0.1609	2.6636	3.0794		
		0.50	-0.8907	0.8907	0.8200	1.1693	-0.2112	-0.4319	0.1617	0.6087	2.9494			
			0	0.8907	0.8200	0.4478	-0.2112	-0.2445	0.1617	0	3.0041			
			0.8907	0.8907	0.8200	-0.2736	-0.2112	-0.0572	0.1617	2.6013	3.0609			
3.00		0.10	-0.8984	0.8984	0.8311	1.2666	-0.1772	-0.3309	0.1624	0.5744	3.1663			
			0	0.8984	0.8311	0.5289	-0.1772	-0.1725	0.1624	0	3.2270			
			0.8984	0.8984	0.8311	-0.2088	-0.1772	-0.0141	0.1624	3.4836	3.2902			
	0.50	-0.8993	0.8993	0.8340	1.2702	-0.1738	-0.3273	0.1627	0.5753	3.1703				
		0	0.8993	0.8340	0.5293	-0.1738	-0.1718	0.1627	0	3.2300				
		0.8993	0.8993	0.8340	-0.2115	-0.1738	-0.0164	0.1627	3.4548	3.2921				

Table 6.6: CASE IV-M: descriptive quantities of motion for some values of  $c_1, c_2, c_3, \beta - \alpha$  and  $R_m = 0.01$ .

$R_m$	$\beta_m$	$c_1$	$c_2$	$c_3$	$\beta - \alpha$	$\alpha$	$\varphi_*'(0)$	$\gamma_*'(0)$	$\Phi_*'(0)$	$\Gamma_*'(0)$	$\Psi_*'(0)$	$\frac{x_{p*}}{x_{s*}}$	$\frac{m_{s*}}{m_i}$			
0.01	0.00	0.10	1.50	0.10	-0.0645	0.0645	12.2182	0.6539	-0.0532	-0.0582	0.9275	1.2043	412.7629			
					0	0.0645	12.2182	0.5751	-0.0532	-0.0548	0.9275	0	184.5172			
					0.0645	0.0645	12.2182	0.4964	-0.0532	-0.0513	0.9275	-1.5864	118.8157			
					0.50	-0.0645	0.0645	12.2313	0.6545	-0.0510	-0.0592	0.9275	1.2048	403.1757		
						0	0.0645	12.2313	0.5757	-0.0510	-0.0559	0.9275	0	182.4208		
						0.0645	0.0645	12.2313	0.4968	-0.0510	-0.0526	0.9275	-1.5874	117.8779		
				3.00	0.10	-0.0645	0.0645	12.2501	0.6683	-0.0444	-0.0399	0.9275	1.1830	668.3354		
						0	0.0645	12.2501	0.5892	-0.0444	-0.0370	0.9275	0	221.3982		
						0.0645	0.0645	12.2501	0.5101	-0.0444	-0.0342	0.9275	-1.5497	132.6745		
					0.50	-0.0645	0.0645	12.2558	0.6697	-0.0434	-0.0400	0.9275	1.1812	664.2090		
						0	0.0645	12.2558	0.5906	-0.0434	-0.0371	0.9275	0	220.8385		
						0.0645	0.0645	12.2558	0.5115	-0.0434	-0.0343	0.9275	-1.5465	132.4356		
				0.50	0.10	1.50	0.10	-0.0631	0.0631	11.7801	0.5199	-0.2659	-0.2724	0.9287	1.4296	73.1052
								0	0.0631	11.7801	0.4456	-0.2659	-0.2556	0.9287	0	62.3516
								0.0631	0.0631	11.7801	0.3712	-0.2659	-0.2389	0.9287	-2.0020	54.3559
							0.50	-0.0632	0.0632	11.8476	0.5215	-0.2553	-0.2804	0.9287	1.4361	71.0871
								0	0.0632	11.8476	0.4466	-0.2553	-0.2643	0.9287	0	60.7861
								0.0632	0.0632	11.8476	0.3717	-0.2553	-0.2482	0.9287	-2.0148	53.0927
						3.00	0.10	-0.0635	0.0635	11.9433	0.5910	-0.2220	-0.1901	0.9284	1.2832	108.5250
								0	0.0635	11.9433	0.5152	-0.2220	-0.1760	0.9284	0	85.4968
								0.0635	0.0635	11.9433	0.4394	-0.2220	-0.1619	0.9284	-1.7262	70.5307
							0.50	-0.0636	0.0636	11.9723	0.5974	-0.2173	-0.1923	0.9284	1.2736	107.0297
								0	0.0636	11.9723	0.5213	-0.2173	-0.1785	0.9284	0	84.4867
								0.0636	0.0636	11.9723	0.4452	-0.2173	-0.1647	0.9284	-1.7090	69.7877
0.50	0.10	1.50	0.10			-0.1249	0.1249	11.3354	0.6580	-0.0500	-0.0584	0.8995	1.1896	373.4164		
						0	0.1249	11.3354	0.5800	-0.0500	-0.0550	0.8995	0	172.2991		
						0.1249	0.1249	11.3354	0.5020	-0.0500	-0.0515	0.8995	-1.5590	111.9852		
			0.50			-0.1250	0.1250	11.3475	0.6581	-0.0481	-0.0592	0.8995	1.1910	366.8698		
						0	0.1250	11.3475	0.5801	-0.0481	-0.0559	0.8995	0	170.7540		
						0.1250	0.1250	11.3475	0.5020	-0.0481	-0.0526	0.8995	-1.5614	111.2719		
		3.00	0.10	-0.1251	0.1251	11.3657	0.6726	-0.0417	-0.0401	0.8994	1.1683	595.4562				
				0	0.1251	11.3657	0.5944	-0.0417	-0.0372	0.8994	0	206.9870				
				0.1251	0.1251	11.3657	0.5161	-0.0417	-0.0344	0.8994	-1.5227	125.2653				
			0.50	-0.1251	0.1251	11.3708	0.6734	-0.0408	-0.0401	0.8994	1.1677	594.4551				
				0	0.1251	11.3708	0.5951	-0.0408	-0.0373	0.8994	0	206.7718				
				0.1251	0.1251	11.3708	0.5168	-0.0408	-0.0345	0.8994	-1.5217	125.1520				
0.50	0.10	1.50	0.10	-0.1223	0.1223	10.9294	0.5244	-0.2505	-0.2743	0.9012	1.4063	67.0321				
				0	0.1223	10.9294	0.4509	-0.2505	-0.2575	0.9012	0	57.6209				
				0.1223	0.1223	10.9294	0.3775	-0.2505	-0.2407	0.9012	-1.9536	50.5271				
			0.50	-0.1225	0.1225	10.9917	0.5241	-0.2409	-0.2802	0.9011	1.4176	65.7690				
				0	0.1225	10.9917	0.4502	-0.2409	-0.2640	0.9011	0	56.6044				
				0.1225	0.1225	10.9917	0.3762	-0.2409	-0.2479	0.9011	-1.9752	49.6815				
		3.00	0.10	-0.1231	0.1231	11.0847	0.5973	-0.2085	-0.1919	0.9007	1.2609	99.0052				
				0	0.1231	11.0847	0.5223	-0.2085	-0.1778	0.9007	0	78.9194				
				0.1231	0.1231	11.0847	0.4473	-0.2085	-0.1638	0.9007	-1.6839	65.6089				
			0.50	-0.1232	0.1232	11.1109	0.6007	-0.2043	-0.1929	0.9007	1.2579	98.4599				
				0	0.1232	11.1109	0.5254	-0.2043	-0.1791	0.9007	0	78.5024				
				0.1232	0.1232	11.1109	0.4502	-0.2043	-0.1653	0.9007	-1.6785	65.2719				

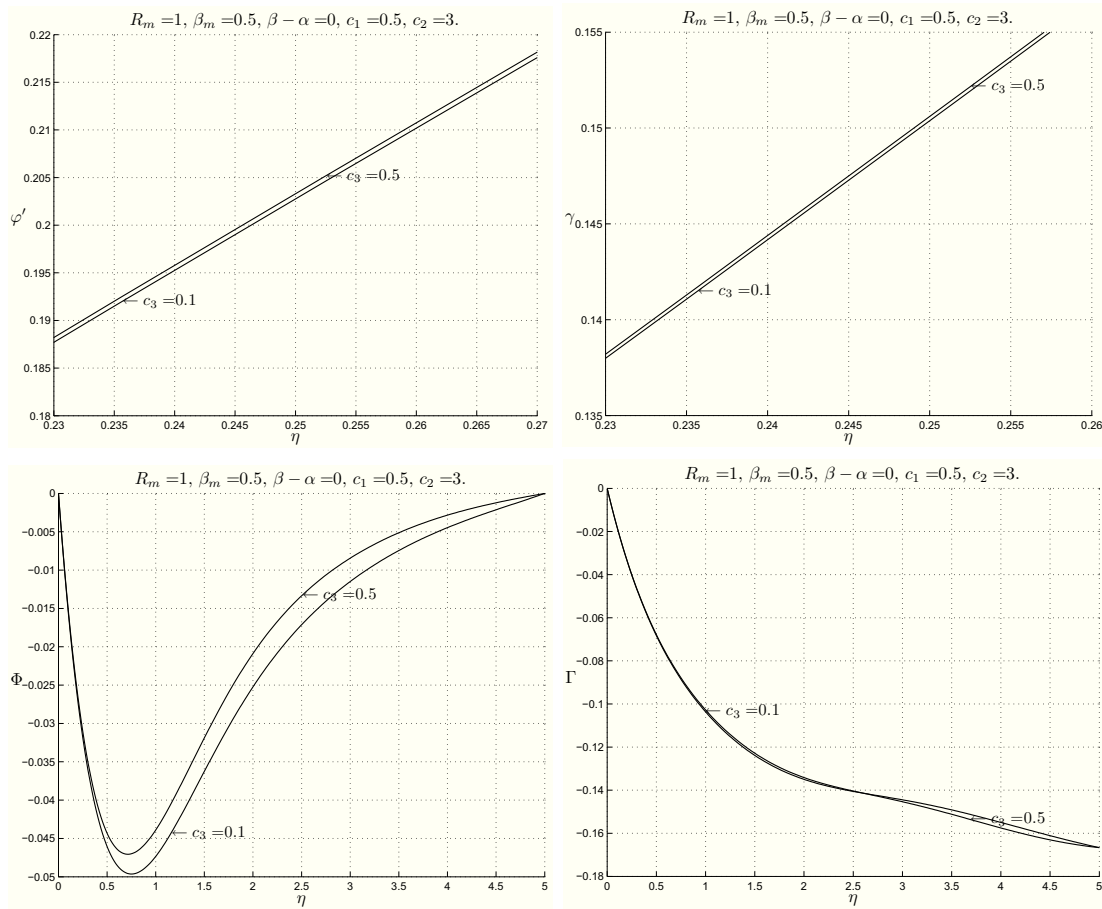


Figure 6.14: CASE IV-M: plots showing the behaviour of  $\varphi'$ ,  $\gamma$ ,  $\Phi$  and  $\Gamma$  for  $R_m = 1$ ,  $\beta_m = 0.5$ ,  $\beta - \alpha = 0$ ,  $c_1 = 0.5$ ,  $c_2 = 3.0$  fixed, and for different values of  $c_3$ .

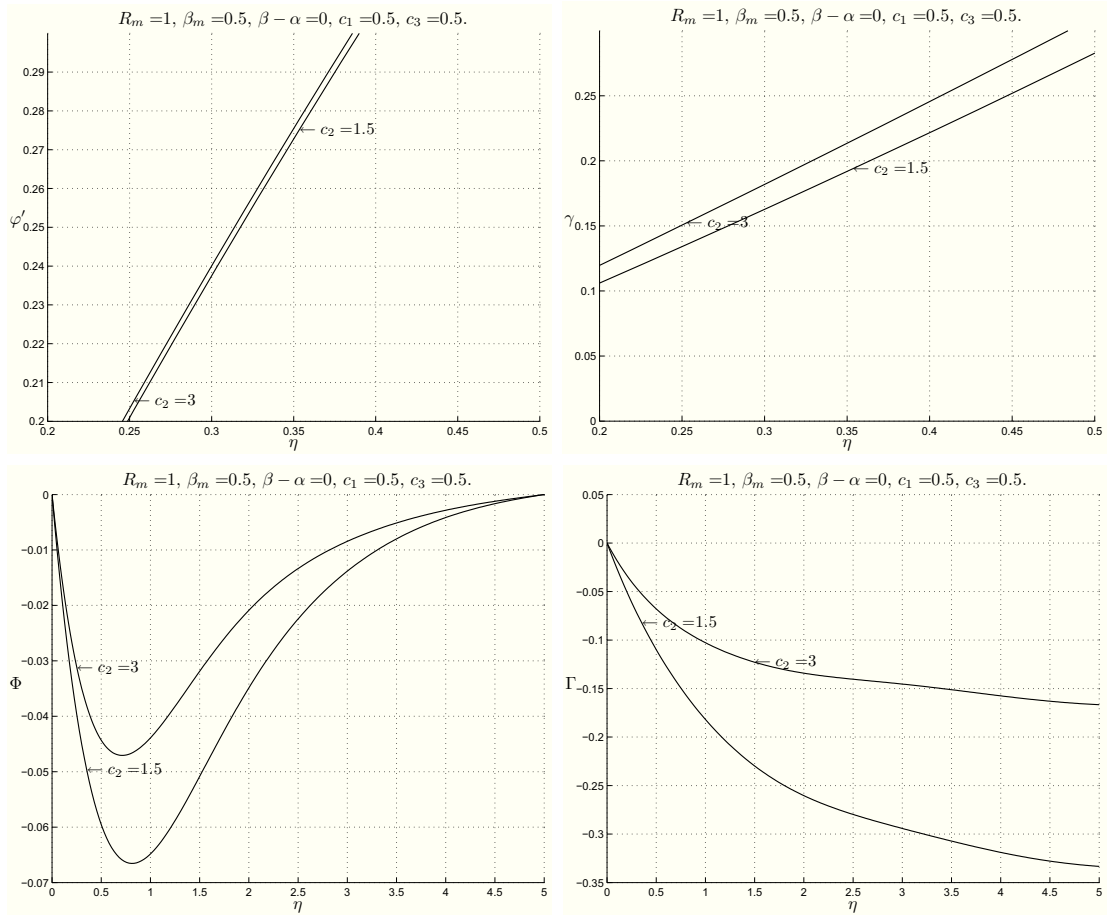


Figure 6.15: CASE IV-M: plots showing the behaviour of  $\varphi'$ ,  $\gamma$ ,  $\Phi$  and  $\Gamma$  for  $R_m = 1$ ,  $\beta_m = 0.5$ ,  $\beta - \alpha = 0$ ,  $c_1 = 0.5$ ,  $c_3 = 0.5$  fixed, and for different values of  $c_2$ .

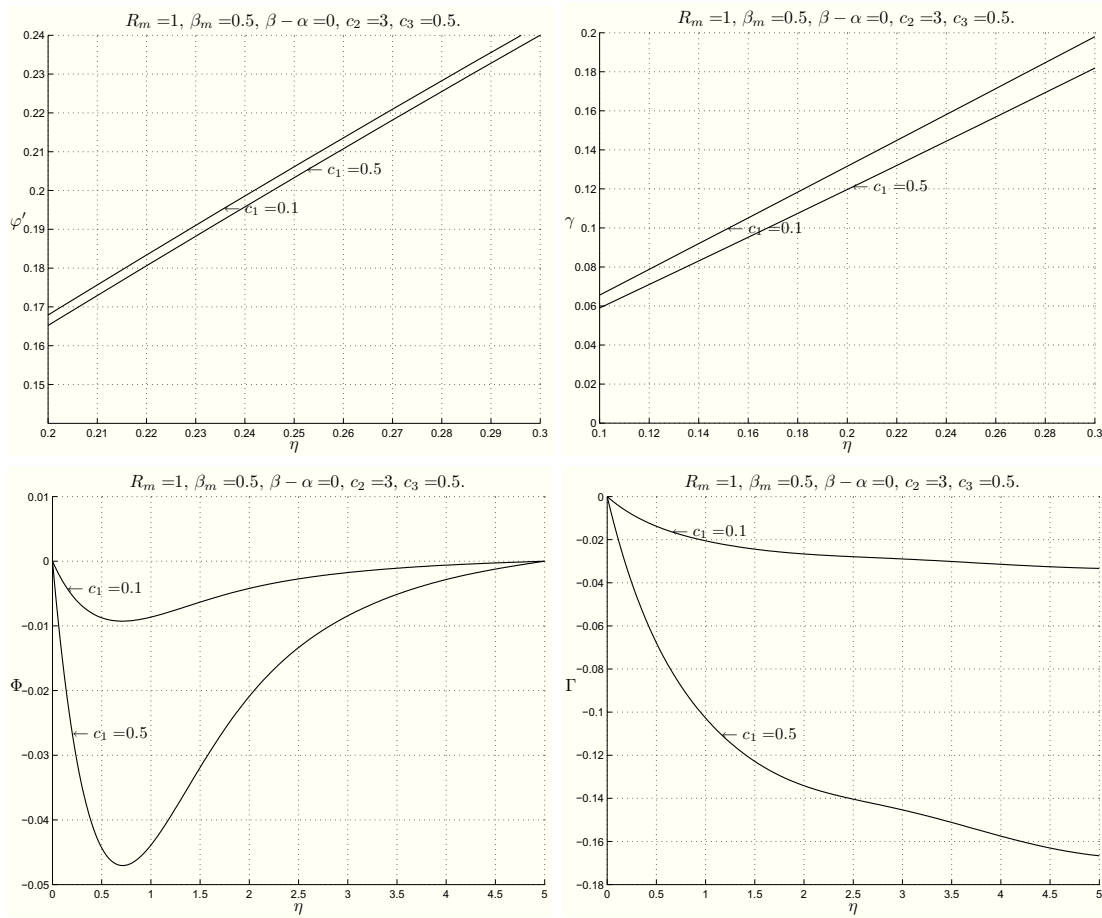


Figure 6.16: CASE IV-M: plots showing the behaviour of  $\varphi'$ ,  $\gamma$ ,  $\Phi$  and  $\Gamma$  for  $R_m = 1$ ,  $\beta_m = 0.5$ ,  $\beta - \alpha = 0$ ,  $c_2 = 3.0$ ,  $c_3 = 0.5$  fixed, and for different values of  $c_1$ .

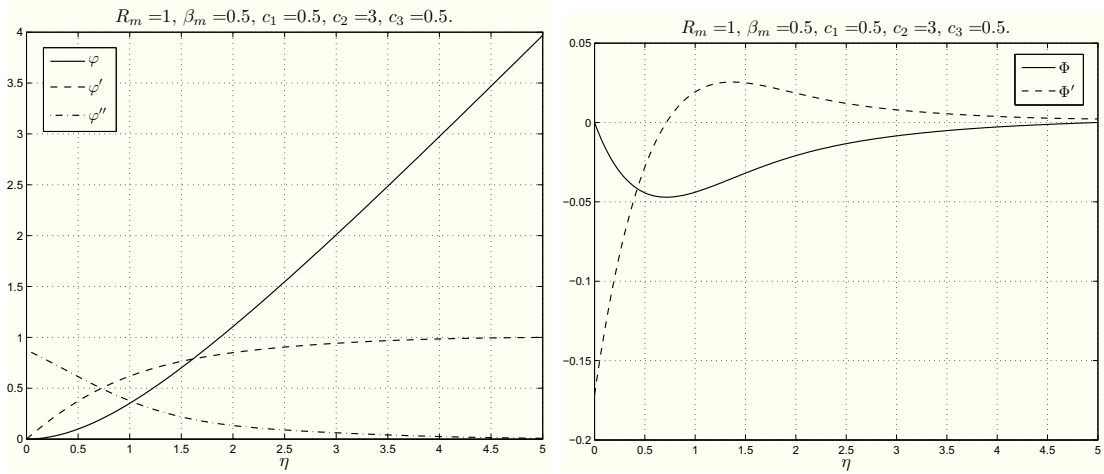


Figure 6.17: CASE IV-M: plots showing the behaviour of  $\varphi$ ,  $\varphi'$ ,  $\varphi''$  and  $\Phi$ ,  $\Phi'$ , respectively, for  $R_m = 1$ ,  $\beta_m = 0.5$ ,  $c_1 = 0.5$ ,  $c_2 = 3.0$ ,  $c_3 = 0.5$ .

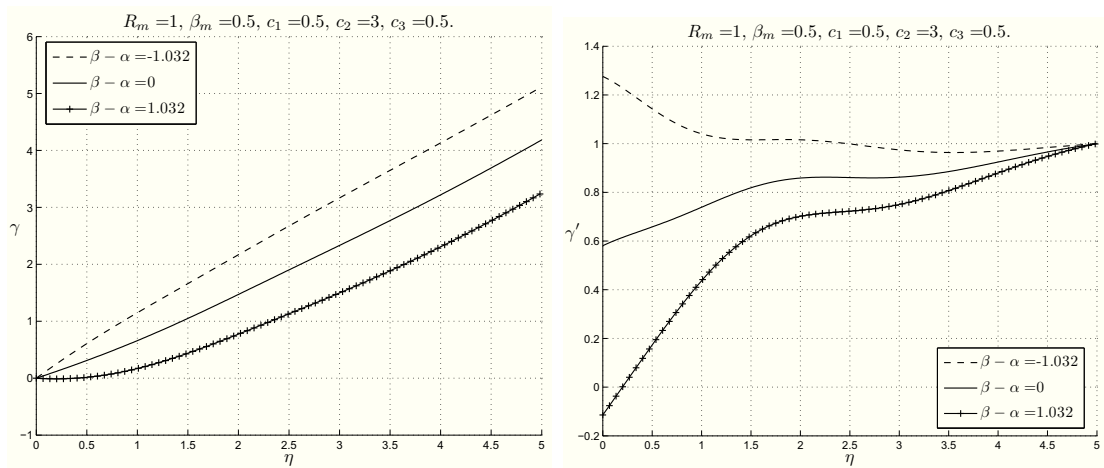


Figure 6.18: CASE IV-M: figures 1.15<sub>1</sub> and 1.15<sub>2</sub> show  $\gamma$  and  $\gamma'$  for  $R_m = 1$ ,  $\beta_m = 0.5$ ,  $c_1 = 0.5$ ,  $c_2 = 3.0$ ,  $c_3 = 0.5$  and with, from above,  $\beta - \alpha = -\alpha$ ,  $0$ ,  $\alpha$ , respectively.

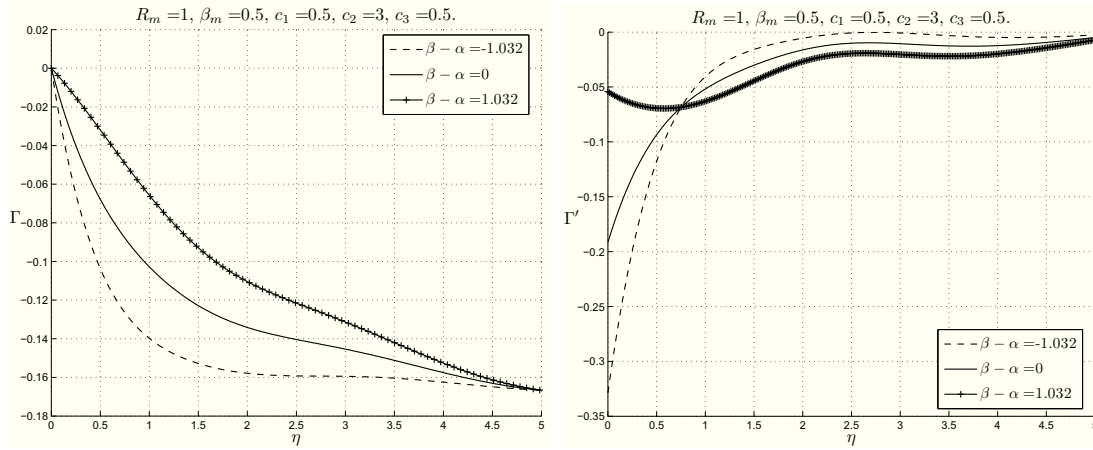


Figure 6.19: CASE IV-M: figures 1.16<sub>1</sub> and 1.16<sub>2</sub> show  $\Gamma$  and  $\Gamma'$  for  $R_m = 1$ ,  $\beta_m = 0.5$ ,  $c_1 = 0.5$ ,  $c_2 = 3.0$ ,  $c_3 = 0.5$  and with, from above,  $\beta - \alpha = -\alpha$ ,  $0$ ,  $\alpha$ , respectively.

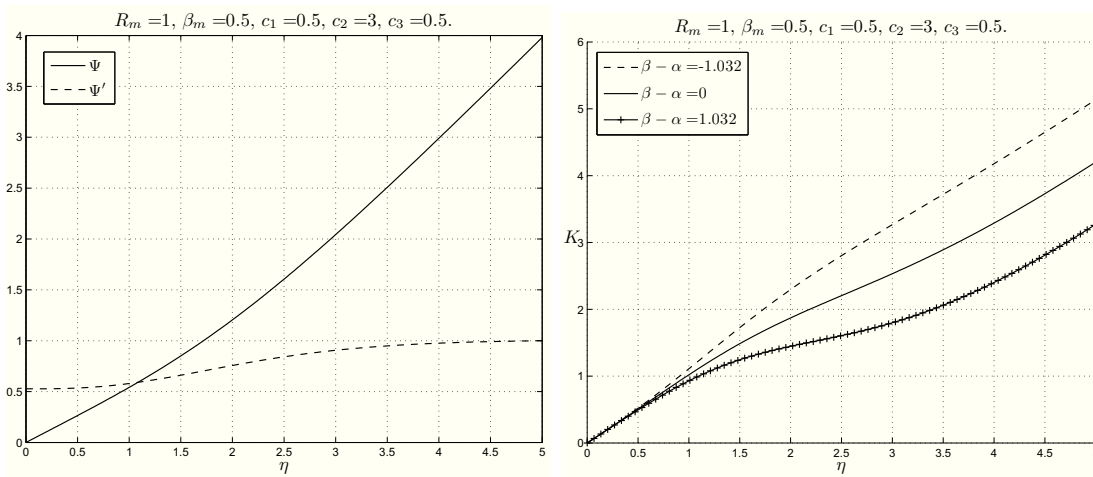


Figure 6.20: CASE IV-M: plots showing the behaviour of  $\Psi$ ,  $\Psi'$  and  $K$ , respectively, for  $R_m = 1$ ,  $\beta_m = 0.5$ ,  $c_1 = 0.5$ ,  $c_2 = 3.0$ ,  $c_3 = 0.5$  (for  $K$  from above  $\beta - \alpha = -\alpha$ ,  $0$ ,  $\alpha$ ).

Table 6.7: CASE IV-M: thickness of the boundary layer for some values of  $R_m$ ,  $\beta_m$ ,  $c_1$ ,  $c_2$ ,  $c_3$  and  $\beta - \alpha$ .

$R_m$	$\beta_m$	$c_1$	$c_2$	$c_3$	$\beta - \alpha$	$\bar{\eta}_\varphi$	$\bar{\eta}_\gamma$	$\bar{\eta}_\Phi$	$\bar{\eta}_\Gamma$	$\delta_v$	$\delta_w$	$\delta$
0.01	0.00	0.10	1.50	0.10	-0.0645	2.3341	23.0077	0.7669	49.3831	23.0077	49.3831	49.3831
					0	2.3341	23.0077	0.7669	49.3831	23.0077	49.3831	49.3831
					0.0645	2.3341	23.0077	0.7669	49.3831	23.0077	49.3831	49.3831
				0.50	-0.0645	2.3508	23.0077	0.7169	47.0990	23.0077	47.0990	47.0990
					0	2.3508	23.0077	0.7169	47.0990	23.0077	47.0990	47.0990
					0.0645	2.3508	23.0077	0.7169	47.0990	23.0077	47.0990	47.0990
			3.00	0.10	-0.0645	2.3508	23.0077	0.6669	49.2664	23.0077	49.2664	49.2664
					0	2.3508	23.0077	0.6669	49.2664	23.0077	49.2664	49.2664
					0.0645	2.3508	23.0077	0.6669	49.2664	23.0077	49.2664	49.2664
				0.50	-0.0645	2.3675	23.0077	0.6335	46.7656	23.0077	46.7656	46.7656
					0	2.3675	23.0077	0.6335	46.7656	23.0077	46.7656	46.7656
					0.0645	2.3675	23.0077	0.6335	46.7656	23.0077	46.7656	46.7656
		0.50	1.50	0.10	-0.0631	2.1340	47.0490	0.7669	49.8833	47.0490	49.8833	49.8833
					0	2.1340	47.0490	0.7669	49.8833	47.0490	49.8833	49.8833
					0.0631	2.1340	47.0490	0.7669	49.8833	47.0490	49.8833	49.8833
				0.50	-0.0632	2.1841	23.0077	0.7169	49.4498	23.0077	49.4498	49.4498
					0	2.1841	23.0077	0.7169	49.4498	23.0077	49.4498	49.4498
					0.0632	2.1841	23.0077	0.7169	49.4498	23.0077	49.4498	49.4498
			3.00	0.10	-0.0635	2.2174	48.3161	0.6836	49.8833	48.3161	49.8833	49.8833
					0	2.2174	48.3161	0.6836	49.8833	48.3161	49.8833	49.8833
					0.0635	2.2174	48.3161	0.6836	49.8833	48.3161	49.8833	49.8833
				0.50	-0.0636	2.2508	23.0077	0.6502	49.4498	23.0077	49.4498	49.4498
					0	2.2508	23.0077	0.6502	49.4498	23.0077	49.4498	49.4498
					0.0636	2.2508	23.0077	0.6502	49.4498	23.0077	49.4498	49.4498
	0.50	0.10	1.50	0.10	-0.1249	19.3731	39.1797	0.7836	49.3831	39.1797	49.3831	49.3831
					0	19.3731	39.4798	0.7836	49.3831	39.4798	49.3831	49.3831
					0.1249	19.3731	39.7466	0.7836	49.3831	39.7466	49.3831	49.3831
				0.50	-0.1250	19.3731	34.3114	0.7169	47.1324	34.3114	47.1324	47.1324
					0	19.3731	34.7783	0.7169	47.1324	34.7783	47.1324	47.1324
					0.1250	19.3731	35.2117	0.7169	47.1324	35.2117	47.1324	47.1324
			3.00	0.10	-0.1251	19.3898	38.0293	0.6836	49.2831	38.0293	49.2831	49.2831
					0	19.3898	38.3961	0.6836	49.2831	38.3961	49.2831	49.2831
					0.1251	19.3898	38.7296	0.6836	49.2831	38.7296	49.2831	49.2831
				0.50	-0.1251	19.3898	34.5282	0.6502	46.8156	34.5282	46.8156	46.8156
					0	19.3898	34.9950	0.6502	46.8156	34.9950	46.8156	46.8156
					0.1251	19.3898	35.4118	0.6502	46.8156	35.4118	46.8156	46.8156
		0.50	1.50	0.10	-0.1223	19.1731	48.4495	0.7836	49.9000	48.4495	49.9000	49.9000
					0	19.1731	48.4662	0.7836	49.9000	48.4662	49.9000	49.9000
					0.1223	19.1731	48.4662	0.7836	49.9000	48.4662	49.9000	49.9000
				0.50	-0.1225	19.1897	37.7793	0.7336	49.4665	37.7793	49.4665	49.4665
					0	19.1897	38.0460	0.7336	49.4665	38.0460	49.4665	49.4665
					0.1225	19.1897	38.2794	0.7336	49.4665	38.2794	49.4665	49.4665
			3.00	0.10	-0.1231	19.2397	48.9663	0.6836	49.8833	48.9663	49.8833	49.8833
					0	19.2397	48.9663	0.6836	49.8833	48.9663	49.8833	49.8833
					0.1231	19.2397	48.9663	0.6836	49.8833	48.9663	49.8833	49.8833
				0.50	-0.1232	19.2564	39.1964	0.6502	49.4498	39.1964	49.4498	49.4498
					0	19.2564	39.4298	0.6502	49.4498	39.4298	49.4498	49.4498
					0.1232	19.2564	39.6465	0.6502	49.4498	39.6465	49.4498	49.4498

Table 6.8: CASE IV-M: continuum of Table 6.7.

$R_m$	$\beta_m$	$c_1$	$c_2$	$c_3$	$\beta - \alpha$	$\bar{\eta}_\varphi$	$\bar{\eta}_\gamma$	$\bar{\eta}_\Phi$	$\bar{\eta}_\Gamma$	$\delta_v$	$\delta_w$	$\delta$
1.00	0.00	0.10	1.50	0.10	-0.6446	2.3258	3.0010	1.6005	1.8323	3.0010	1.8323	3.0010
					0	2.3258	3.0827	1.6005	2.2424	3.0827	2.2424	3.0827
					0.6446	2.3258	3.1427	1.6005	2.4925	3.1427	2.4925	3.1427
			0.50		-0.6448	2.3374	3.0027	1.3338	1.7773	3.0027	1.7773	3.0027
					0	2.3374	3.0894	1.3338	2.0473	3.0894	2.0473	3.0894
					0.6448	2.3374	3.1511	1.3338	2.2174	3.1511	2.2174	3.1511
			3.00	0.10	-0.6453	2.3474	3.0594	1.0020	0.6886	3.0594	1.0020	3.0594
					0	2.3474	3.1377	1.0020	1.3354	3.1377	1.3354	3.1377
					0.6453	2.3474	3.1977	1.0020	1.7339	3.1977	1.7339	3.1977
			0.50		-0.6454	2.3525	3.0610	0.8469	0.7186	3.0610	0.8469	3.0610
					0	2.3525	3.1427	0.8469	1.3088	3.1427	1.3088	3.1427
					0.6454	2.3525	3.2027	0.8469	1.6422	3.2027	1.6422	3.2027
		0.50	1.50	0.10	-0.6310	2.1274	2.5125	2.9093	3.0510	2.5125	3.0510	3.0510
					0	2.1274	2.6409	2.9093	3.3394	2.6409	3.3394	3.3394
					0.6310	2.1274	2.7092	2.9093	3.5328	2.7092	3.5328	3.5328
				0.50	-0.6321	2.1691	2.5025	2.4325	2.7726	2.5025	2.7726	2.7726
					0	2.1691	2.6442	2.4325	2.9160	2.6442	2.9160	2.9160
					0.6321	2.1691	2.7242	2.4325	3.0193	2.7242	3.0193	3.0193
			3.00	0.10	-0.6350	2.2157	2.8409	2.3441	2.2124	2.8409	2.3441	2.8409
					0	2.2157	2.9143	2.3441	2.6109	2.9143	2.6109	2.9143
					0.6350	2.2157	2.9627	2.3441	2.8159	2.9627	2.8159	2.9627
			0.50		-0.6356	2.2391	2.8459	2.1190	2.2124	2.8459	2.2124	2.8459
					0	2.2391	2.9293	2.1190	2.4692	2.9293	2.4692	2.9293
					0.6356	2.2391	2.9860	2.1190	2.6125	2.9860	2.6125	2.9860
	0.50	0.10	1.50	0.10	-1.0463	4.2864	2.3008	1.8723	1.5055	4.2864	1.8723	4.2864
					0	4.2864	2.3458	1.8723	2.9343	4.2864	2.9343	4.2864
					1.0463	4.2864	4.8983	1.8723	3.7229	4.8983	3.7229	4.8983
				0.50	-1.0462	4.2964	2.3008	1.5038	1.6422	4.2964	1.6422	4.2964
					0	4.2964	2.3525	1.5038	2.7142	4.2964	2.7142	4.2964
					1.0462	4.2964	4.8966	1.5038	3.3311	4.8966	3.3311	4.8966
			3.00	0.10	-1.0474	4.2998	2.3008	0.7469	0.5919	4.2998	0.7469	4.2998
					0	4.2998	2.3625	0.7469	1.3004	4.2998	1.3004	4.2998
					1.0474	4.2998	4.8983	0.7469	2.4425	4.8983	2.4425	4.8983
				0.50	-1.0474	4.3031	2.3008	0.7119	0.6169	4.3031	0.7119	4.3031
					0	4.3031	2.3658	0.7119	1.3338	4.3031	1.3338	4.3031
					1.0474	4.3031	4.8983	0.7119	2.3041	4.8983	2.3041	4.8983
		0.50	1.50	0.10	-1.0265	4.1464	2.4608	3.8913	3.7096	4.1464	3.8913	4.1464
					0	4.1464	2.3008	3.8913	4.5282	4.1464	4.5282	4.5282
					1.0265	4.1464	4.8916	3.8913	4.6999	4.8916	4.6999	4.8916
				0.50	-1.0261	4.2031	2.4592	3.3061	3.6812	4.2031	3.6812	4.2031
					0	4.2031	2.3008	3.3061	4.2247	4.2031	4.2247	4.2247
					1.0261	4.2031	4.8833	3.3061	4.4181	4.8833	4.4181	4.8833
			3.00	0.10	-1.0321	4.2281	2.3008	3.1677	1.4755	4.2281	3.1677	4.2281
					0	4.2281	2.3008	3.1677	4.1380	4.2281	4.1380	4.2281
					1.0321	4.2281	4.8950	3.1677	4.4465	4.8950	4.4465	4.8950
				0.50	-1.0321	4.2464	2.3008	2.8193	1.8289	4.2464	2.8193	4.2464
					0	4.2464	2.3008	2.8193	3.9313	4.2464	3.9313	4.2464
					1.0321	4.2464	4.8916	2.8193	4.2164	4.8916	4.2164	4.8916

Table 6.9: CASE IV-M: continuum of Table 6.7.

$R_m$	$\beta_m$	$c_1$	$c_2$	$c_3$	$\beta - \alpha$	$\bar{\eta}_\varphi$	$\bar{\eta}_\gamma$	$\bar{\eta}_\Phi$	$\bar{\eta}_\Gamma$	$\delta_v$	$\delta_w$	$\delta$		
100	0.00	0.10	1.50	0.10	-0.6446	2.3258	3.0010	1.6005	1.8323	3.0010	1.8323	3.0010		
					0	2.3258	3.0827	1.6005	2.2424	3.0827	2.2424	3.0827		
					0.6446	2.3258	3.1427	1.6005	2.4925	3.1427	2.4925	3.1427		
				0.50	-0.6448	2.3374	3.0027	1.3338	1.7773	3.0027	1.7773	3.0027		
					0	2.3374	3.0894	1.3338	2.0473	3.0894	2.0473	3.0894		
					0.6448	2.3374	3.1511	1.3338	2.2174	3.1511	2.2174	3.1511		
			3.00	0.10	-0.6453	2.3474	3.0594	1.0020	0.6886	3.0594	1.0020	0.6886	3.0594	
					0	2.3474	3.1377	1.0020	1.3354	3.1377	1.3354	3.1377		
					0.6453	2.3474	3.1977	1.0020	1.7339	3.1977	1.7339	3.1977		
				0.50	-0.6454	2.3525	3.0610	0.8469	0.7186	3.0610	0.8469	3.0610		
					0	2.3525	3.1427	0.8469	1.3088	3.1427	1.3088	3.1427		
					0.6454	2.3525	3.2027	0.8469	1.6422	3.2027	1.6422	3.2027		
			0.50	1.50	0.10	-0.6310	2.1274	2.5125	2.9093	3.0510	2.5125	3.0510	3.0510	
						0	2.1274	2.6409	2.9093	3.3394	2.6409	3.3394	3.3394	
						0.6310	2.1274	2.7092	2.9093	3.5328	2.7092	3.5328	3.5328	
					0.50	-0.6321	2.1691	2.5025	2.4325	2.7726	2.5025	2.7726	2.7726	
						0	2.1691	2.6442	2.4325	2.9160	2.6442	2.9160	2.9160	
						0.6321	2.1691	2.7242	2.4325	3.0193	2.7242	3.0193	3.0193	
				3.00	0.10	-0.6350	2.2157	2.8409	2.3441	2.2124	2.8409	2.3441	2.2124	2.8409
						0	2.2157	2.9143	2.3441	2.6109	2.9143	2.6109	2.9143	
						0.6350	2.2157	2.9627	2.3441	2.8159	2.9627	2.8159	2.9627	
					0.50	-0.6356	2.2391	2.8459	2.1190	2.2124	2.8459	2.2124	2.8459	
						0	2.2391	2.9293	2.1190	2.4692	2.9293	2.4692	2.9293	
						0.6356	2.2391	2.9860	2.1190	2.6125	2.9860	2.6125	2.9860	
0.50	0.10	1.50	0.10	-0.9166	3.2928	4.1797	1.9590	1.9240	4.1797	1.9590	1.9240	4.1797		
				0	3.2928	4.2881	1.9590	2.8093	4.2881	2.8093	4.2881			
				0.9166	3.2928	4.3631	1.9590	3.1727	4.3631	3.1727	4.3631			
			0.50	-0.9169	3.3178	4.1747	1.6189	2.0440	4.1747	2.0440	4.1747			
				0	3.3178	4.2848	1.6189	2.5709	4.2848	2.5709	4.2848			
				0.9169	3.3178	4.3631	1.6189	2.8193	4.3631	2.8193	4.3631			
		3.00	0.10	-0.9184	3.3311	4.2214	1.0854	0.6019	4.2214	1.0854	4.2214			
				0	3.3311	4.3231	1.0854	1.7022	4.3231	1.7022	4.3231			
				0.9184	3.3311	4.3965	1.0854	2.3441	4.3965	2.3441	4.3965			
	0.50	1.50	0.10	-0.9186	3.3411	4.2181	0.7786	0.6335	4.2181	0.7786	4.2181			
				0	3.3411	4.3231	0.7786	1.6922	4.3231	1.6922	4.3231			
				0.9186	3.3411	4.3965	0.7786	2.2107	4.3965	2.2107	4.3965			
			0.50	-0.8887	2.9460	3.7029	3.4378	3.6112	3.7029	3.6112	3.7029			
				0	2.9460	3.8429	3.4378	4.0013	3.8429	4.0013	4.0013			
				0.8887	2.9460	3.9296	3.4378	4.2064	3.9296	4.2064	4.2064			
		3.00	0.10	-0.8907	3.0527	3.6679	2.9210	3.3378	3.6679	3.3378	3.6679			
				0	3.0527	3.8429	2.9210	3.5478	3.8429	3.5478	3.8429			
				0.8907	3.0527	3.9496	2.9210	3.6812	3.9496	3.6812	3.9496			
0.50	1.50	0.10	-0.8984	3.1327	4.0330	2.8459	2.8626	4.0330	2.8626	4.0330				
			0	3.1327	4.1364	2.8459	3.4161	4.1364	3.4161	4.1364				
			0.8984	3.1327	4.2097	2.8459	3.6546	4.2097	3.6546	4.2097				
	0.50	-0.8993	3.1794	4.0213	2.5792	2.8810	4.0213	2.8810	4.0213					
		0	3.1794	4.1380	2.5792	3.2144	4.1380	3.2144	4.1380					
		0.8993	3.1794	4.2197	2.5792	3.3878	4.2197	3.3878	4.2197					

Table 6.10: CASE IV-M: thickness of the boundary layer for some values of  $\beta_m$ ,  $c_1$ ,  $c_2$ ,  $c_3$ ,  $\beta - \alpha$  and  $R_m = 0.01$ .

$R_m$	$\beta_m$	$c_1$	$c_2$	$c_3$	$\beta - \alpha$	$\bar{\xi}_{\varphi_*}$	$\bar{\xi}_{\gamma_*}$	$\bar{\xi}_{\Phi_*}$	$\bar{\xi}_{\Gamma_*}$	$\delta_{v_*}$	$\delta_{w_*}$	$\delta_*$					
0.01	0.00	0.10	1.50	0.10	-0.0645	0.2334	2.3008	0.0767	4.9383	2.3008	4.9383	4.9383					
					0	0.2334	2.3008	0.0767	4.9383	2.3008	4.9383	4.9383					
					0.0645	0.2334	2.3008	0.0767	4.9383	2.3008	4.9383	4.9383					
					0.50	-0.0645	0.2351	2.3008	0.0717	4.7099	2.3008	4.7099	4.7099				
						0	0.2351	2.3008	0.0717	4.7099	2.3008	4.7099	4.7099				
						0.0645	0.2351	2.3008	0.0717	4.7099	2.3008	4.7099	4.7099				
					3.00	0.10	-0.0645	0.2351	2.3008	0.0667	4.9266	2.3008	4.9266	2.3008	4.9266	4.9266	
							0	0.2351	2.3008	0.0667	4.9266	2.3008	4.9266	4.9266			
							0.0645	0.2351	2.3008	0.0667	4.9266	2.3008	4.9266	4.9266			
						0.50	-0.0645	0.2367	2.3008	0.0634	4.6766	2.3008	4.6766	2.3008	4.6766	4.6766	
							0	0.2367	2.3008	0.0634	4.6766	2.3008	4.6766	4.6766			
							0.0645	0.2367	2.3008	0.0634	4.6766	2.3008	4.6766	4.6766			
				0.50		1.50	0.10	-0.0631	0.2134	4.7049	0.0767	4.9883	4.7049	4.9883	4.9883	4.9883	
								0	0.2134	4.7049	0.0767	4.9883	4.7049	4.9883	4.9883		
								0.0631	0.2134	4.7049	0.0767	4.9883	4.7049	4.9883	4.9883		
						0.50	-0.0632	0.2184	2.3008	0.0717	4.9450	2.3008	4.9450	2.3008	4.9450	4.9450	
							0	0.2184	2.3008	0.0717	4.9450	2.3008	4.9450	4.9450			
							0.0632	0.2184	2.3008	0.0717	4.9450	2.3008	4.9450	4.9450			
					3.00	0.10	-0.0635	0.2217	4.8316	0.0684	4.9883	4.8316	4.9883	4.8316	4.9883	4.9883	
							0	0.2217	4.8316	0.0684	4.9883	4.8316	4.9883	4.9883			
							0.0635	0.2217	4.8316	0.0684	4.9883	4.8316	4.9883	4.9883			
						0.50	-0.0636	0.2251	2.3008	0.0650	4.9450	2.3008	4.9450	2.3008	4.9450	4.9450	
							0	0.2251	2.3008	0.0650	4.9450	2.3008	4.9450	4.9450			
							0.0636	0.2251	2.3008	0.0650	4.9450	2.3008	4.9450	4.9450			
				0.50	0.10	1.50	0.10	-0.1249	1.9373	3.9180	0.0784	4.9383	3.9180	4.9383	4.9383		
								0	1.9373	3.9480	0.0784	4.9383	3.9480	4.9383	4.9383		
								0.1249	1.9373	3.9747	0.0784	4.9383	3.9747	4.9383	4.9383		
							0.50	-0.1250	1.9373	3.4311	0.0717	4.7132	3.4311	4.7132	3.4311	4.7132	
								0	1.9373	3.4778	0.0717	4.7132	3.4778	4.7132	4.7132		
								0.1250	1.9373	3.5212	0.0717	4.7132	3.5212	4.7132	4.7132		
							3.00	0.10	-0.1251	1.9390	3.8029	0.0684	4.9283	3.8029	4.9283	3.8029	4.9283
									0	1.9390	3.8396	0.0684	4.9283	3.8396	4.9283	4.9283	
									0.1251	1.9390	3.8730	0.0684	4.9283	3.8730	4.9283	4.9283	
								0.50	-0.1251	1.9390	3.4528	0.0650	4.6816	3.4528	4.6816	3.4528	4.6816
									0	1.9390	3.4995	0.0650	4.6816	3.4995	4.6816	4.6816	
									0.1251	1.9390	3.5412	0.0650	4.6816	3.5412	4.6816	4.6816	
					0.50	1.50	0.10	-0.1223	1.9173	4.8449	0.0784	4.9900	4.8449	4.9900	4.8449	4.9900	
								0	1.9173	4.8466	0.0784	4.9900	4.8466	4.9900	4.9900		
								0.1223	1.9173	4.8466	0.0784	4.9900	4.8466	4.9900	4.9900		
							0.50	-0.1225	1.9190	3.7779	0.0734	4.9466	3.7779	4.9466	3.7779	4.9466	
								0	1.9190	3.8046	0.0734	4.9466	3.8046	4.9466	4.9466		
								0.1225	1.9190	3.8279	0.0734	4.9466	3.8279	4.9466	4.9466		
						3.00	0.10	-0.1231	1.9240	4.8966	0.0684	4.9883	4.8966	4.9883	4.8966	4.9883	
								0	1.9240	4.8966	0.0684	4.9883	4.8966	4.9883	4.9883		
								0.1231	1.9240	4.8966	0.0684	4.9883	4.8966	4.9883	4.9883		
							0.50	-0.1232	1.9256	3.9196	0.0650	4.9450	3.9196	4.9450	3.9196	4.9450	
								0	1.9256	3.9430	0.0650	4.9450	3.9430	4.9450	4.9450		
								0.1232	1.9256	3.9647	0.0650	4.9450	3.9647	4.9450	4.9450		

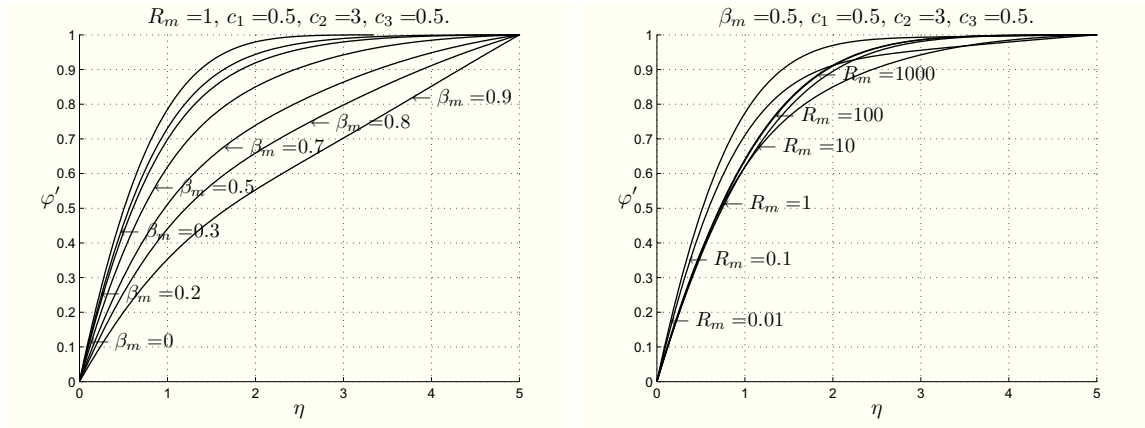


Figure 6.21: CASE IV-M: plots showing  $\varphi'$  for different  $\beta_m$  and  $R_m$ , respectively.

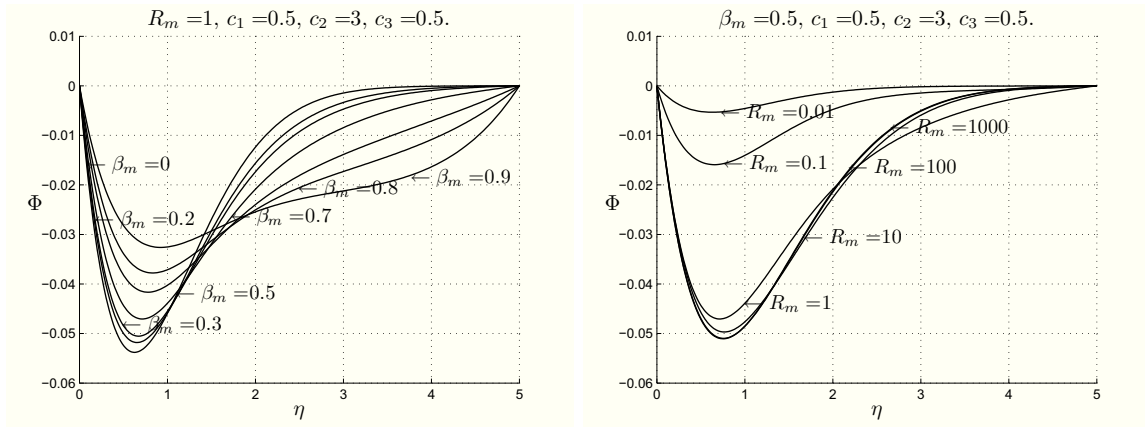


Figure 6.22: CASE IV-M: plots showing  $\Phi$  for different  $\beta_m$  and  $R_m$ , respectively.

thickness  $\bar{\eta}_\Gamma$  lining the boundary and its thickness is larger than in the orthogonal stagnation-point flow.

Tables 6.7, 6.8 and 6.9 underline that the thickness of the boundary layer depends on  $R_m$  and  $\beta_m$ . More precisely, it increases when  $\beta_m$  increases (as is easy to see in Figures 6.21<sub>1</sub>, 6.22<sub>1</sub>, 6.23<sub>1</sub>, 6.24<sub>1</sub>, 6.25<sub>1</sub>, 6.26<sub>1</sub>, 6.27<sub>1</sub>, 6.28<sub>1</sub>).

The thickness of the boundary layer decreases when  $R_m$  increases (as is easy to see in Figures 6.21<sub>2</sub>, 6.22<sub>2</sub>, 6.23<sub>2</sub>, 6.24<sub>2</sub>, 6.25<sub>2</sub>, 6.26<sub>2</sub>, 6.27<sub>2</sub>, 6.28<sub>2</sub>).

This behaviour is in agreement with the previous chapters.

We underline that the more  $R_m$  is small and the more  $\beta_m$  is close to 1 the more the thickness of the boundary layer is larger than in the other cases of oblique stagnation-point flow treated in this Thesis (Chapters 1.2 and 3).

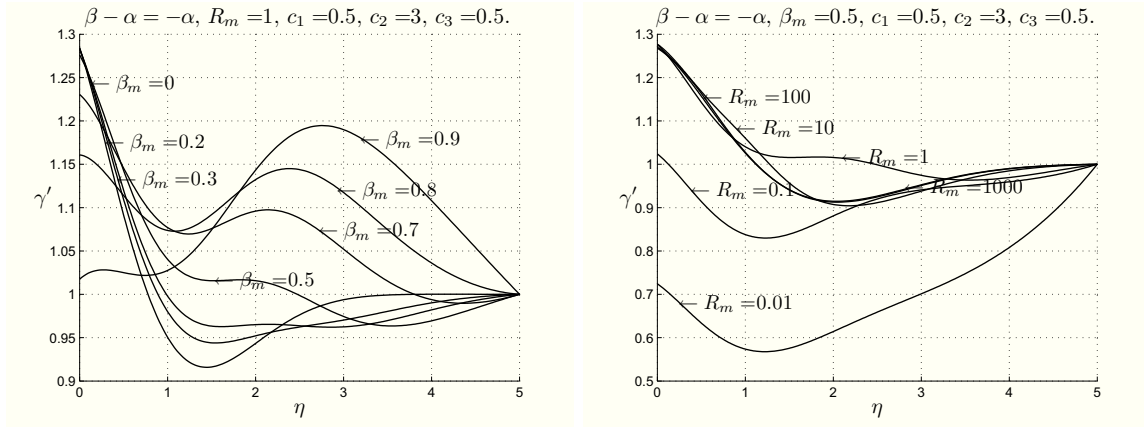


Figure 6.23: CASE IV-M: plots showing  $\gamma'$  for different  $\beta_m$  and  $R_m$ , respectively, when  $\beta - \alpha = -\alpha$ .

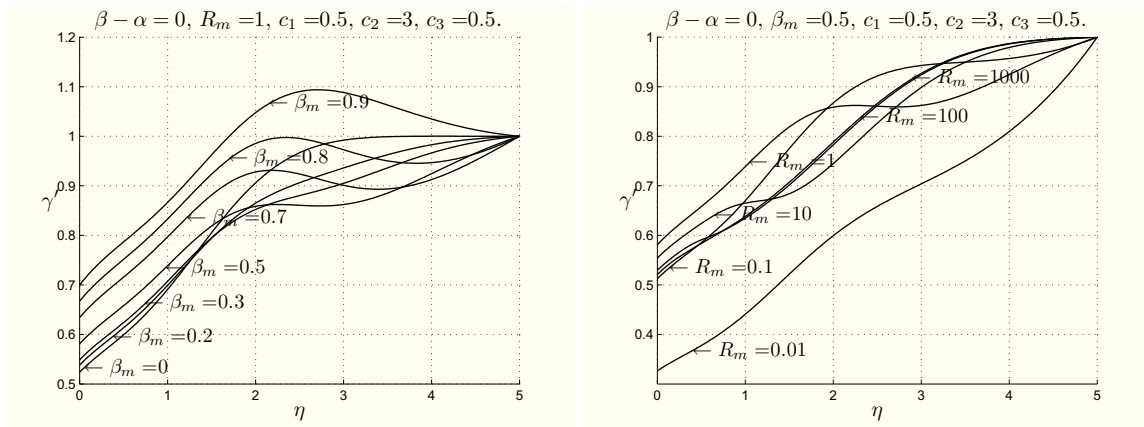


Figure 6.24: CASE IV-M: plots showing  $\gamma'$  for different  $\beta_m$  and  $R_m$ , respectively, when  $\beta - \alpha = 0$ .

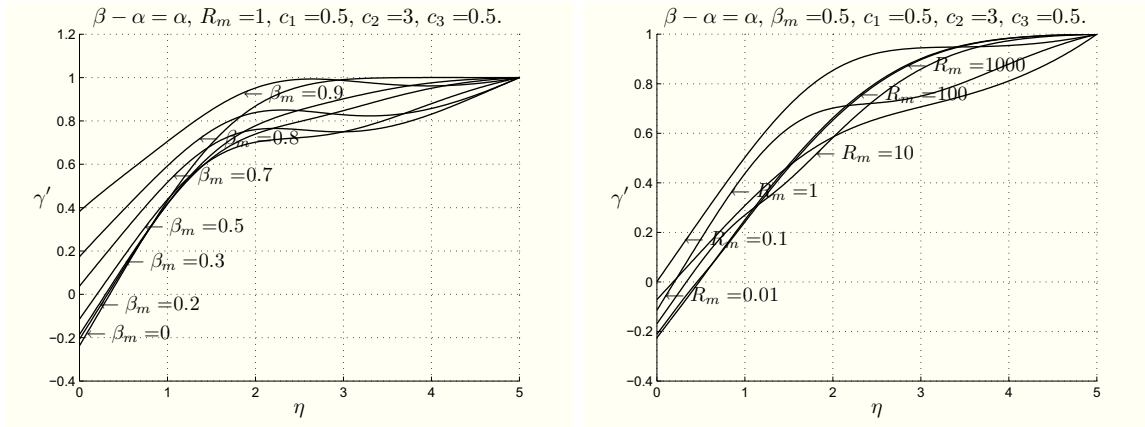


Figure 6.25: CASE IV-M: plots showing  $\gamma'$  for different  $\beta_m$  and  $R_m$ , respectively, when  $\beta - \alpha = \alpha$ .

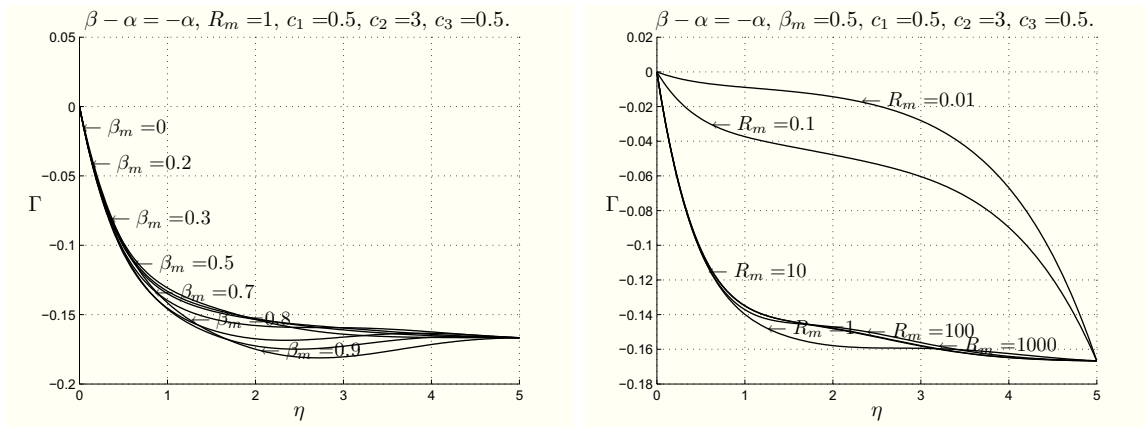


Figure 6.26: CASE IV-M: plots showing  $\Gamma$  for different  $\beta_m$  and  $R_m$ , respectively, when  $\beta - \alpha = -\alpha$ .

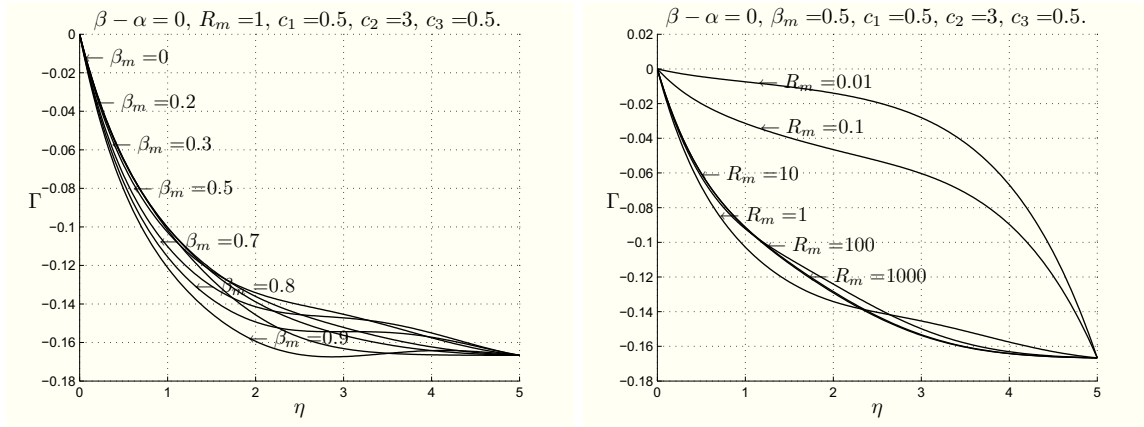


Figure 6.27: CASE IV-M: plots showing  $\Gamma$  for different  $\beta_m$  and  $R_m$ , respectively, when  $\beta - \alpha = 0$ .

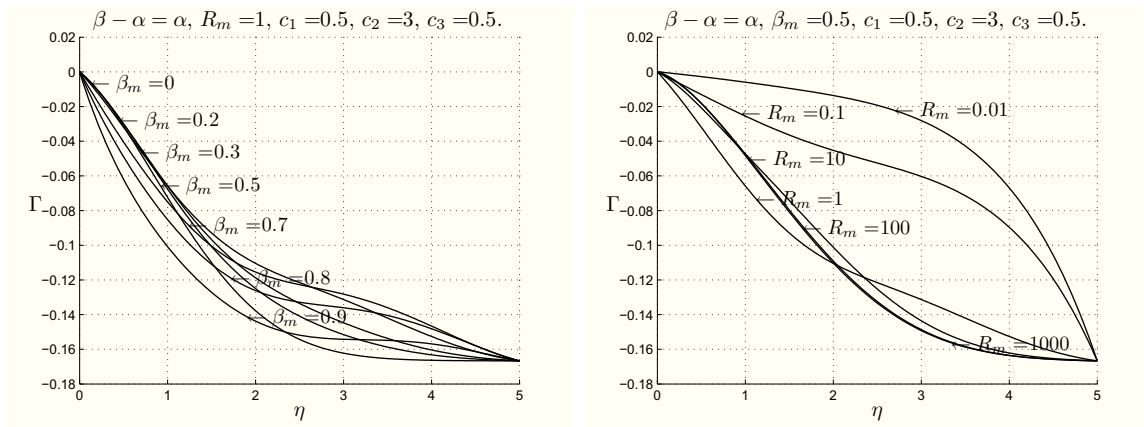


Figure 6.28: CASE IV-M: plots showing  $\Gamma$  for different  $\beta_m$  and  $R_m$ , respectively, when  $\beta - \alpha = \alpha$ .

Figures 6.29, 6.30, 6.31 show the streamlines and the points

$$\xi_p = \sqrt{\frac{a}{\nu + \nu_r}} x_p, \quad \xi_s = \sqrt{\frac{a}{\nu + \nu_r}} x_s$$

for  $\beta_m = 0.8$ ,  $c = 1$  and  $\beta - \alpha = -\alpha$ ,  $0$ ,  $\alpha$ ,  $R_m = 1$ ,  $100$ , respectively.

As it is easy to see from the figures, the flow and the magnetic field are completely parallel far from the obstacle.

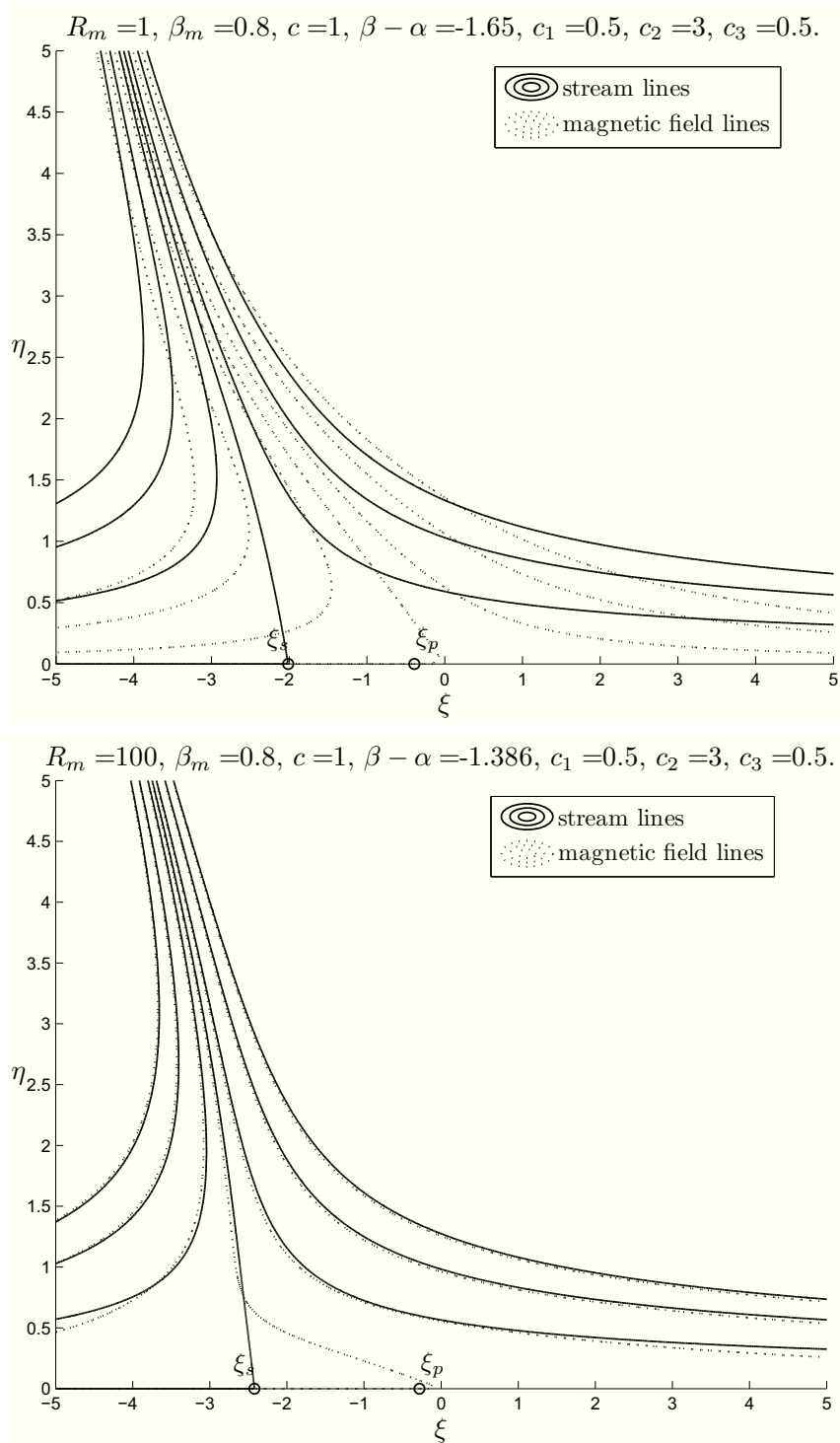


Figure 6.29: CASE IV-M: plots showing the streamlines and the points  $\xi_p, \xi_s$  for  $c = 1, c_1 = 0.5, c_2 = 3.0, c_3 = 0.5, \beta - \alpha = -\alpha, \beta_m = 0.8$  and  $R_m = 1, 100$ , respectively.

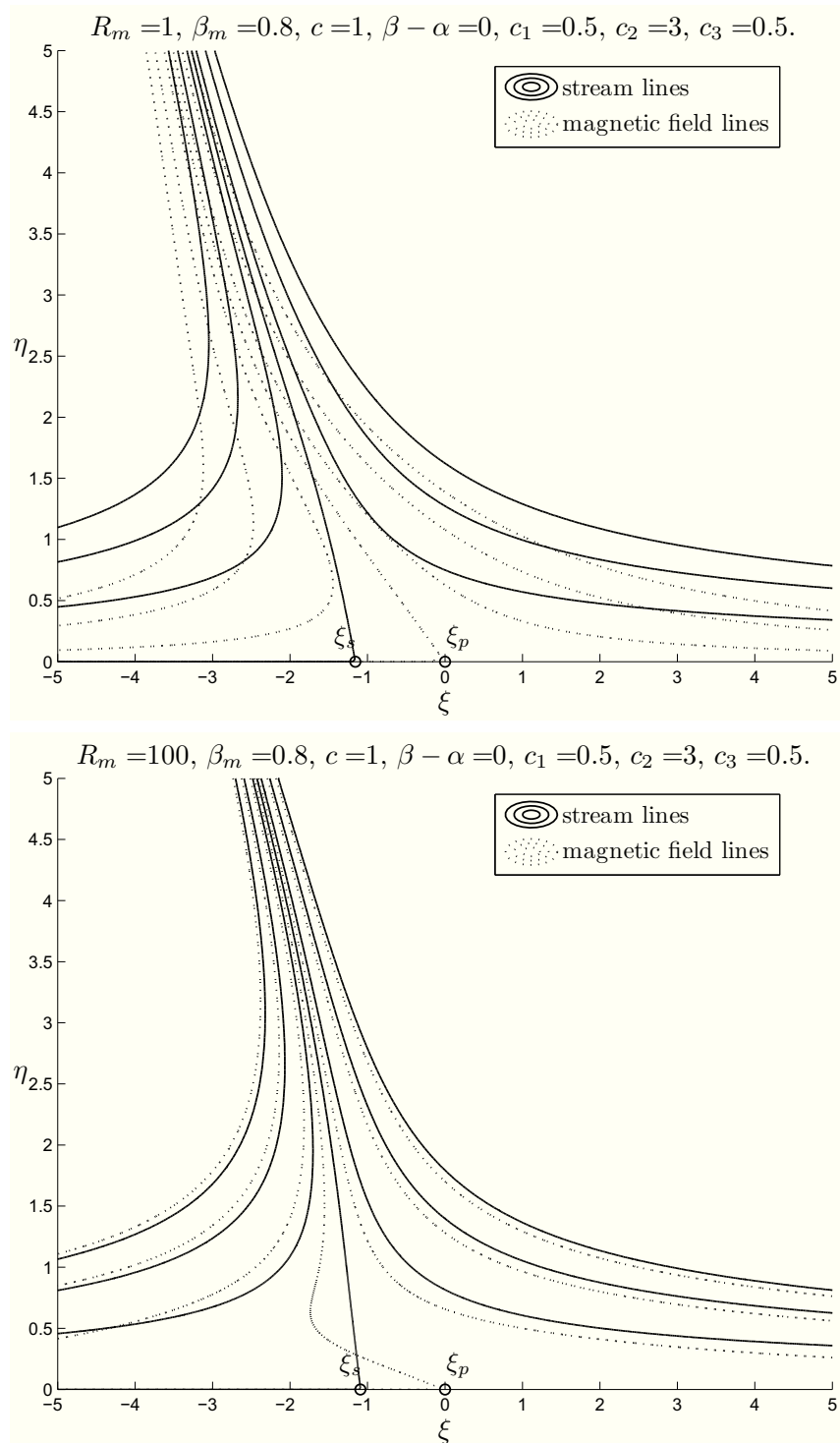


Figure 6.30: CASE IV-M: plots showing the streamlines and the points  $\xi_p, \xi_s$  for  $c = 1$ ,  $c_1 = 0.5$ ,  $c_2 = 3.0$ ,  $c_3 = 0.5$ ,  $\beta - \alpha = 0$ ,  $\beta_m = 0.8$  and  $R_m = 1, 100$ , respectively.

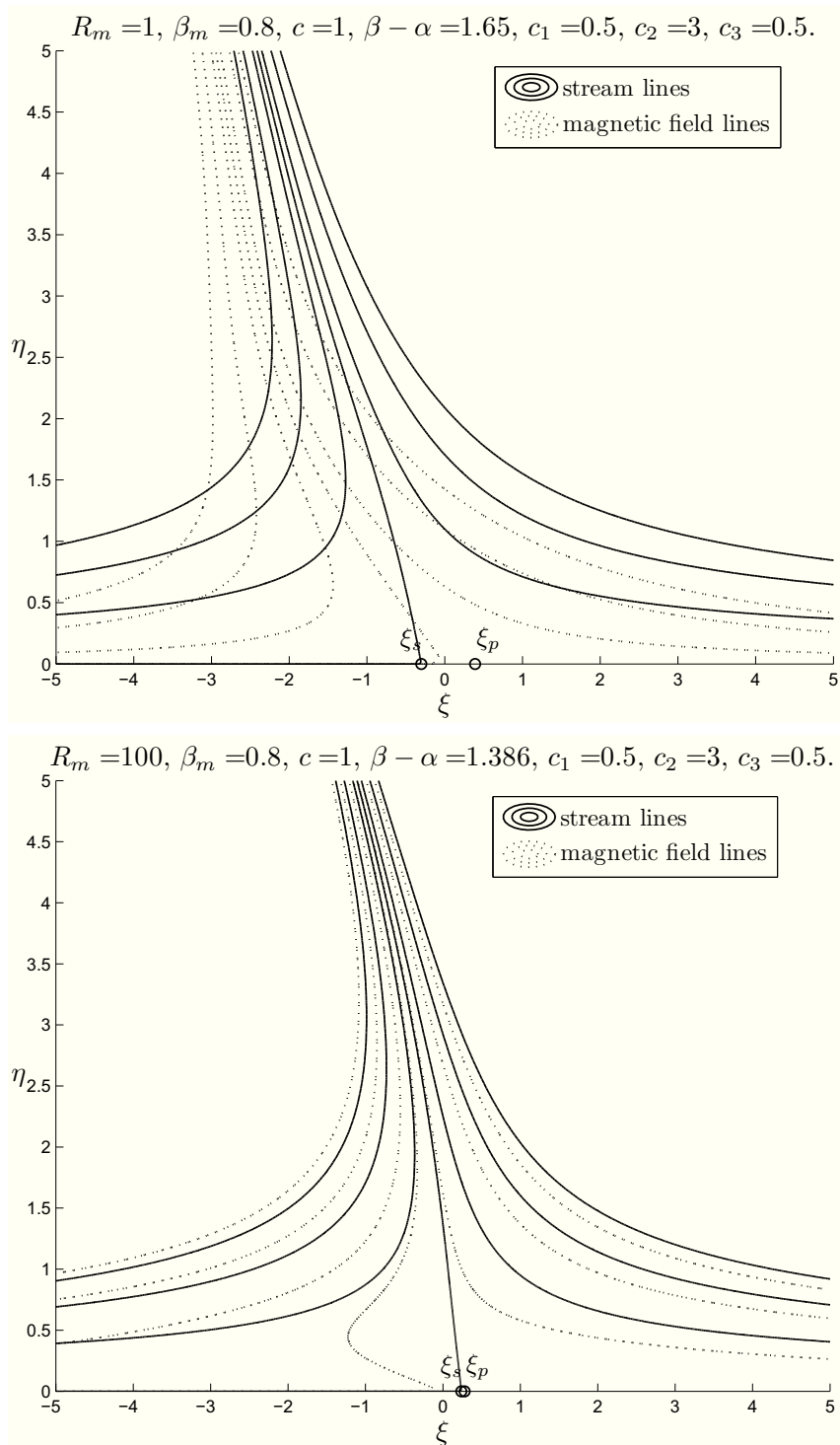


Figure 6.31: CASE IV-M: plots showing the streamlines and the points  $\xi_p, \xi_s$  for  $c = 1$ ,  $c_1 = 0.5$ ,  $c_2 = 3.0$ ,  $c_3 = 0.5$ ,  $\beta - \alpha = \alpha$ ,  $\beta_m = 0.8$  and  $R_m = 1, 100$ , respectively.

# Chapter 7

## MHD three-dimensional stagnation-point flow with $\mathbf{H}$ and $\mathbf{v}$ parallel at infinity

We now consider the same electromagnetic problem of the previous two chapters for the three-dimensional MHD stagnation-point flow of a Newtonian or a micropolar fluid. This problem has never been studied in the literature and so the results obtained are original ([11]).

As usual, to reach the purpose of the Chapter, it is appropriate to begin with the same situation for the inviscid fluid.

### 7.1 Inviscid fluids CASE IV

We start with the analysis of the steady three-dimensional MHD flow of a homogeneous, incompressible, electrically conducting inviscid fluid near a stagnation point filling the half-space  $\mathcal{S}$  (see Figure 7.1).

As it is well known, in the three-dimensional stagnation-point flow the velocity field is given by

$$v_1 = ax_1, \quad v_2 = -a(1+c)x_2, \quad v_3 = cax_3, \quad (x_1, x_3) \in \mathbb{R}^2, \quad x_2 \in \mathbb{R}^+, \quad (7.1)$$

where  $a, c$  are constants.

As in the previous chapters, we suppose  $a > 0$ ,  $c \neq 0$  and we exclude the case  $c \leq -1$ .

REMARK 7.1.1. *If  $c = 1$ , then the velocity is axisymmetric:*

$$v_1 = ax_1, \quad v_2 = -2ax_2, \quad v_3 = ax_3. \quad (7.2)$$

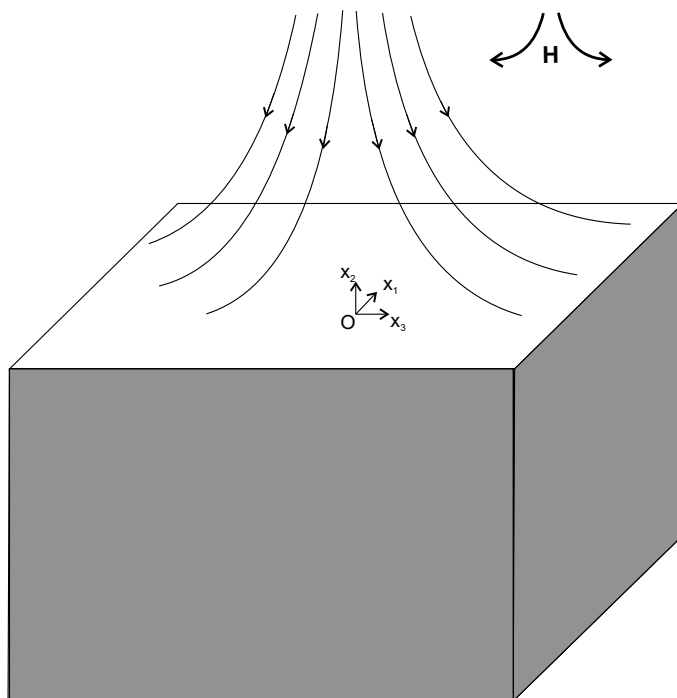


Figure 7.1: Description flow in CASE IV.

The equations governing such a flow are (2.2). As usual, we impose the no-penetration condition to the velocity field and we suppose that the electromagnetic field satisfies (2.5) and (2.6).

We suppose that an external magnetic field

$$\mathbf{H}_e = H_\infty [x_1 \mathbf{e}_1 - (1+c)x_2 \mathbf{e}_2 + cx_3 \mathbf{e}_3] \quad (7.3)$$

permeates the whole physical space and that the external electric field is absent.

REMARK 7.1.2. *As it is easy to verify, the field lines of  $\mathbf{H}_e$  have the following parametric equations*

$$\begin{aligned} x_1 &= A_1 e^{H_\infty \lambda}, \\ x_2 &= A_2 e^{-(1+c)H_\infty \lambda}, \\ x_3 &= A_3 e^{cH_\infty \lambda}, \quad \lambda \in \mathbb{R}, \end{aligned} \quad (7.4)$$

where  $A_1$ ,  $A_2$ ,  $A_3$  are arbitrary constants. These field lines degenerate if at least one of the three constants  $A_1$ ,  $A_2$ ,  $A_3$  vanishes. Otherwise they belong to the surfaces

$$x_1 x_2 x_3 = A_1 A_2 A_3.$$

We remark that these surfaces tend to the plane  $x_2 = 0$  as  $|x_1|, |x_3| \rightarrow +\infty$  (see Figure 7.2).

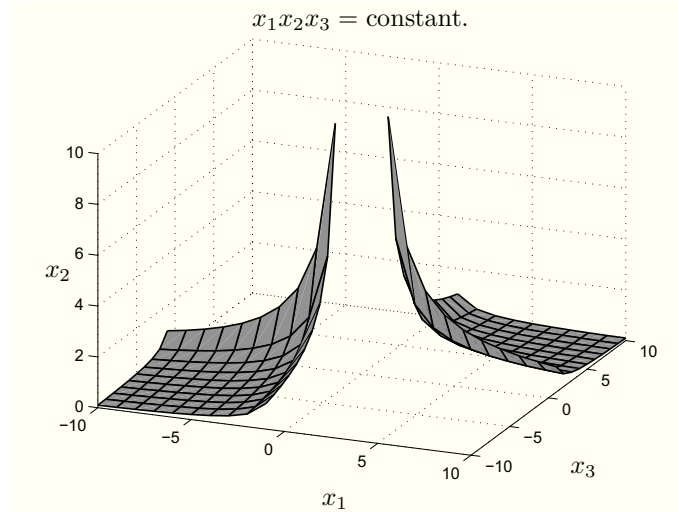


Figure 7.2: CASE IV: plot showing the surface  $x_1x_2x_3 = 10$ .

Here we seek the total magnetic fields in the fluid and in the solid as

$$\mathbf{H} = H_\infty [x_1 h'(x_2) \mathbf{e}_1 - [h(x_2) + ck(x_2)] \mathbf{e}_2 + cx_3 k'(x_2) \mathbf{e}_3], \quad x_2 \geq 0, \quad \text{and}$$

$$\mathbf{H}_s = H_\infty [x_1 h'_s(x_2) \mathbf{e}_1 - [h_s(x_2) + ck_s(x_2)] \mathbf{e}_2 + cx_3 k'_s(x_2) \mathbf{e}_3], \quad x_2 \leq 0, \quad (7.5)$$

respectively, where  $h, k, h_s, k_s$  are sufficiently regular unknown functions to be determined ( $h, k, h_s, k_s \in C^2(\mathbb{R}^+)$ ).

In particular,  $h, k$  have to satisfy

$$\begin{aligned} \lim_{x_2 \rightarrow +\infty} h'(x_2) &= 1, \quad \lim_{x_2 \rightarrow +\infty} k'(x_2) = 1, \\ \lim_{x_2 \rightarrow +\infty} [h(x_2) - x_2] &= 0, \quad \lim_{x_2 \rightarrow +\infty} [k(x_2) - x_2] = 0, \end{aligned} \quad (7.6)$$

so that  $\mathbf{H}$  tends to  $\mathbf{H}_e$  as  $x_2 \rightarrow +\infty$  in order to have  $\mathbf{H}$  and  $\mathbf{v}$  parallel at infinity.

As far as  $\mathbf{H}_s$  is concerned, we assume that

- (i)  $\mathbf{H}_s$  is not uniform;
- (ii) its non-degenerate field lines belong to a surface which tends to the plane  $x_2 = 0$  as  $|x_1|, |x_3| \rightarrow +\infty$ .

We now want to prove the following Theorem.

**THEOREM 7.1.3.** *If the solid which occupies  $\mathcal{S}^-$  is a rigid uncharged dielectric at rest and the magnetic field  $\mathbf{H}_s$  satisfies (i) and (ii), then  $\mathbf{H}_s$  is given by*

$$\mathbf{H}_s = H_\infty [h'(0)x_1 \mathbf{e}_1 - (h'(0) + ck'(0))x_2 \mathbf{e}_2 + ck'(0)x_3 \mathbf{e}_3], \quad x_2 \leq 0, \quad (7.7)$$

where  $h(x_2), k(x_2)$  are the unknown functions in (7.5)<sub>1</sub>.

*Proof.* The properties of the solid imply

$$\nabla \times \mathbf{H}_s = \mathbf{0}, \quad \text{in } \mathcal{S}^-,$$

from which we get

$$h_s(x_2) = C_1 x_2 + C_2, \quad k_s(x_2) = C_3 x_2 + C_4, \quad x_2 \leq 0, \quad (7.8)$$

where  $C_1, C_2, C_3, C_4 \in \mathbb{R}$ .

By virtue of the continuity of the tangential components of the magnetic field across the plane  $x_2 = 0$ , we find

$$C_1 = h'(0), \quad C_3 = k'(0),$$

so that

$$\mathbf{H}_s = H_\infty [h'(0)x_1 \mathbf{e}_1 - [(h'(0) + ck'(0))x_2 + C_2 + cC_4] \mathbf{e}_2 + ck'(0)x_3 \mathbf{e}_3]. \quad (7.9)$$

We remark that  $\mathbf{H}_s$  is uniform if  $h'(0) = k'(0) = 0$ . Hence to satisfy (i) we proceed assuming  $h'(0) \neq 0$  or  $k'(0) \neq 0$ . In this case the magnetic field lines in the solid are

$$\begin{aligned} x_1 &= B_1 e^{H_\infty h'(0)\lambda}, \\ x_2 &= B_2 e^{-H_\infty [h'(0) + ck'(0)]\lambda} - \frac{C_2 + cC_4}{h'(0) + ck'(0)}, \\ x_3 &= B_3 e^{H_\infty ck'(0)\lambda}, \quad x_2 \leq 0, \quad \lambda, B_1, B_2, B_3 \in \mathbb{R}. \end{aligned} \quad (7.10)$$

The non-degenerate field lines belong to the surface

$$x_1 x_2 x_3 = B_1 B_2 B_3 - \frac{C_2 + cC_4}{h'(0) + ck'(0)} x_1 x_3, \quad x_2 \leq 0, \quad B_1, B_2, B_3 \neq 0. \quad (7.11)$$

These surfaces tend to the plane  $x_2 = 0$  as  $|x_1|, |x_3| \rightarrow +\infty$  if, and only if,

$$C_2 + cC_4 = 0,$$

from which we get the assertion.  $\square$

**REMARK 7.1.4.** *Since the solid is an uncharged dielectric,  $\mathbf{E}_s = \mathbf{E}_s^i = \mathbf{0}$  in  $\mathcal{S}^-$ .*

We now consider the inviscid fluid filling the half-space  $\mathcal{S}$ . Thanks to the continuity of the normal component of the magnetic induction vector across the boundary  $x_2 = 0$  (see (2.6)), we deduce

$$h(0) + ck(0) = 0, \quad \forall c \in (-1, +\infty),$$

from which follows

$$h(0) = 0, \quad k(0) = 0. \quad (7.12)$$

Our aim is now to determine  $(p, \mathbf{H}, \mathbf{E})$  solution of (2.2) in  $\mathcal{S}$  with  $\mathbf{v}$  given by (7.1) such that  $\mathbf{H}$  tends to  $\mathbf{H}_e$  as  $x_2$  goes to infinity. Hence

$$\mathbf{v} \times \mathbf{H} = \mathbf{0} \text{ at infinity.}$$

Let the electric field  $\mathbf{E}$  be in the form

$$\mathbf{E}^i = E_1^i \mathbf{e}_1 + E_2^i \mathbf{e}_2 + E_3^i \mathbf{e}_3.$$

The boundary conditions require that

$$E_1^i = 0, \quad E_3^i = 0 \quad \text{at } x_2 = 0. \quad (7.13)$$

From (2.2)<sub>4</sub> follows that

$$\mathbf{E} = -\nabla\psi, \quad (\psi \in C^2(\mathbb{R}^3))$$

and (2.2)<sub>3</sub> furnishes

$$\begin{aligned} \frac{\partial\psi}{\partial x_1} &= -\frac{H_\infty}{\sigma_e} c x_3 [k''(x_2) + \sigma_e \mu_e a [(1+c)k'(x_2)x_2 - (h(x_2) + ck(x_2))]], \\ \frac{\partial\psi}{\partial x_2} &= H_\infty \mu_e a c x_1 x_3 [h'(x_2) - k'(x_2)], \\ \frac{\partial\psi}{\partial x_3} &= -\frac{H_\infty}{\sigma_e} x_1 [-h''(x_2) - \sigma_e \mu_e a [(1+c)h'(x_2)x_2 - (h(x_2) + ck(x_2))]]. \end{aligned} \quad (7.14)$$

From (2.2)<sub>5</sub> and (7.14), we get

$$H_\infty \mu_e a c x_1 x_3 [h''(x_2) - k''(x_2)] = 0, \quad \forall (x_1, x_3) \in \mathbb{R}^2, \quad x_2 \in \mathbb{R}^+,$$

which for the conditions (7.6), (7.12), means

$$h(x_2) = k(x_2), \quad \forall x_2 \in \mathbb{R}^+. \quad (7.15)$$

Substituting (7.15) into (7.14), we get

$$\begin{aligned} \frac{\partial\psi}{\partial x_1} &= -\frac{H_\infty}{\sigma_e} c x_3 [h''(x_2) + \sigma_e \mu_e a (1+c)(h'(x_2)x_2 - h(x_2))], \\ \frac{\partial\psi}{\partial x_3} &= -\frac{H_\infty}{\sigma_e} x_1 [-h''(x_2) - \sigma_e \mu_e a (1+c)(h'(x_2)x_2 - h(x_2))]. \end{aligned} \quad (7.16)$$

It is possible to find a unique electrostatic scalar potential  $\psi$  from (7.16) if, and only if,

$$\frac{\partial^2 \psi}{\partial x_1 \partial x_3} = \frac{\partial^2 \psi}{\partial x_3 \partial x_1},$$

which leads to

$$h''(x_2) + \sigma_e \mu_e a(1+c)[h'(x_2)x_2 - h(x_2)] = 0. \quad (7.17)$$

Taking into account the boundary conditions (7.12) and (7.6)<sub>1</sub>, equation (7.17) has a unique solution  $h(x_2) = x_2$ . This furnishes

$$\mathbf{E} = \mathbf{0}, \quad \mathbf{H} = \mathbf{H}_e = H_\infty [x_1 \mathbf{e}_1 - (1+c)x_2 \mathbf{e}_2 + cx_3 \mathbf{e}_3].$$

We remark that  $\nabla \times \mathbf{H} = \mathbf{0}$  so that the pressure field is not influenced by the magnetic field.

Therefore we have:

**THEOREM 7.1.5.** *Let a homogeneous, incompressible, electrically conducting inviscid fluid occupy the half-space  $\mathcal{S}$  and be embedded in the external electromagnetic field  $\mathbf{H}_e = H_\infty [x_1 \mathbf{e}_1 - (1+c)x_2 \mathbf{e}_2 + cx_3 \mathbf{e}_3]$ ,  $\mathbf{E}_e = \mathbf{0}$ . If the total magnetic field in the solid is given by (7.7), then the steady three-dimensional MHD stagnation-point flow of such a fluid has the following form*

$$\begin{aligned} \mathbf{v} &= a[x_1 \mathbf{e}_1 - (1+c)x_2 \mathbf{e}_2 + cx_3 \mathbf{e}_3], \quad \mathbf{E} = \mathbf{0}, \quad \mathbf{H} = \mathbf{H}_e, \\ p &= -\frac{1}{2} \rho a^2 [x_1^2 + (1+c)^2 x_2^2 + c^2 x_3^2] + p_0, \quad (x_1, x_3) \in \mathbb{R}^2, \quad x_2 \in \mathbb{R}^+. \end{aligned} \quad (7.18)$$

**REMARK 7.1.6.** *In order to study the MHD three-dimensional stagnation-point flow for other models of fluid, we suppose that the inviscid fluid impinges on the flat plane  $x_2 = C$  and*

$$\begin{aligned} \mathbf{v} &= a[x_1 \mathbf{e}_1 - (1+c)(x_2 - C) \mathbf{e}_2 + cx_3 \mathbf{e}_3], \\ \mathbf{H}_e &= H_\infty [x_1 \mathbf{e}_1 - (1+c)(x_2 - C) \mathbf{e}_2 + cx_3 \mathbf{e}_3], \quad (x_1, x_3) \in \mathbb{R}^2, \quad x_2 \geq C, \\ \mathbf{H} &\rightarrow H_\infty [x_1 \mathbf{e}_1 - (1+c)(x_2 - C) \mathbf{e}_2 + cx_3 \mathbf{e}_3] \text{ as } x_2 \rightarrow +\infty. \end{aligned} \quad (7.19)$$

with  $C$  some constant.

In this way, the stagnation point is  $(0, C, 0)$  and the pressure and the total magnetic field in Theorem 7.1.5 must be modified by replacing  $x_2$  with  $x_2 - C$ :

$$\begin{aligned} p &= -\frac{1}{2} \rho a^2 [x_1^2 + (1+c)^2 (x_2 - C)^2 + c^2 x_3^2] + p_0, \\ \mathbf{H}_e &= H_\infty [x_1 \mathbf{e}_1 - (1+c)(x_2 - C) \mathbf{e}_2 + cx_3 \mathbf{e}_3], \quad (x_1, x_3) \in \mathbb{R}^2, \quad x_2 \geq C. \end{aligned} \quad (7.20)$$

## 7.2 Newtonian fluids CASE IV-N

Consider now the steady three-dimensional MHD flow of a homogeneous, incompressible, electrically conducting Newtonian fluid near a stagnation point filling the half-space  $\mathcal{S}$ .

The equations governing such a flow in the absence of external mechanical body forces and free electric charges are (2.22) together with boundary conditions (2.23), (2.5), (2.6).

The three-dimensional stagnation-point flow of such a fluid is determined by a velocity field of the form

$$v_1 = ax_1 f'(x_2), \quad v_2 = -a[f(x_2) + cg(x_2)], \quad v_3 = cax_3 g'(x_2), \quad (x_1, x_3) \in \mathbb{R}^2, \quad x_2 \in \mathbb{R}^+, \quad (7.21)$$

with  $f, g$  sufficiently regular unknown functions ( $f, g \in C^3(\mathbb{R}^+)$ ) to be determined so that

$$f(0) = 0, \quad f'(0) = 0, \quad g(0) = 0, \quad g'(0) = 0. \quad (7.22)$$

The above conditions arise from the behaviour of the fluid near the obstacle (condition (2.23)).

As for the inviscid fluid, we suppose that an external magnetic field

$$\mathbf{H}_e = H_\infty [x_1 \mathbf{e}_1 - (1 + c)x_2 \mathbf{e}_2 + cx_3 \mathbf{e}_3]$$

permeates the whole physical space and that the external electric field is absent.

We seek the total magnetic field in the fluid in the following form

$$\mathbf{H} = H_\infty [x_1 h'(x_2) \mathbf{e}_1 - (h(x_2) + ck(x_2)) \mathbf{e}_2 + cx_3 k'(x_2) \mathbf{e}_3], \quad x_2 \geq 0, \quad (7.23)$$

where  $h, k$  are sufficiently regular unknown functions ( $h, k \in C^2(\mathbb{R}^+)$ ).

From Theorem 7.1.3, the total magnetic field in the solid has the form  $\mathbf{H}_s = H_\infty [h'(0)x_1 \mathbf{e}_1 - (h'(0) + ck'(0))x_2 \mathbf{e}_2 + ck'(0)x_3 \mathbf{e}_3]$ , which gives the additional conditions

$$h(0) = 0, \quad k(0) = 0. \quad (7.24)$$

Further we impose

**Condition P.** *At infinity, the MHD three-dimensional stagnation-point flow of a viscous fluid approaches the flow of an inviscid fluid whose velocity, magnetic field and pressure are given by (7.19)<sub>1</sub>, (7.20)<sub>1</sub> and (7.20)<sub>2</sub>, respectively.*

We then append to (2.22) the following conditions

$$\lim_{x_2 \rightarrow +\infty} f'(x_2) = 1, \quad \lim_{x_2 \rightarrow +\infty} g'(x_2) = 1, \quad (7.25)$$

$$\lim_{x_2 \rightarrow +\infty} h'(x_2) = 1, \quad \lim_{x_2 \rightarrow +\infty} k'(x_2) = 1, \quad (7.26)$$

so that

$$\mathbf{v} \times \mathbf{H} = \mathbf{0} \text{ at infinity.} \quad (7.27)$$

More precisely, the functions  $f$ ,  $g$ ,  $h$  and  $k$  at infinity depend on the constant  $C$  in (7.19) as

$$\lim_{x_2 \rightarrow +\infty} [f(x_2) - x_2] = -A, \quad \lim_{x_2 \rightarrow +\infty} [g(x_2) - x_2] = -B, \quad (7.28)$$

$$\lim_{x_2 \rightarrow +\infty} [h(x_2) - x_2] = -A, \quad \lim_{x_2 \rightarrow +\infty} [k(x_2) - x_2] = -B, \quad (7.29)$$

$$\begin{aligned} \lim_{x_2 \rightarrow +\infty} [f(x_2) + cg(x_2) - (1+c)x_2] &= -(1+c)C, \\ \lim_{x_2 \rightarrow +\infty} [h(x_2) + ck(x_2) - (1+c)x_2] &= -(1+c)C, \end{aligned} \quad (7.30)$$

so that

$$C = \frac{A + cB}{1 + c}.$$

The constants  $A, B, C$  are not assigned a priori, but their values can be found by solving the problem.

Our purpose is now to determine  $(p, f, g, \mathbf{H}, \mathbf{E})$  solution in  $\mathcal{S}$  of (2.22) with  $\mathbf{v}$  given by (7.21) such that Condition P is satisfied.

More precisely, we will prove in the following Theorem that, under the non-restrictive hypothesis on  $h$ :

(h) there is no interval included in  $\mathbb{R}^+$  where  $h'$  vanishes,

the only possibility is the axisymmetric flow.

**THEOREM 7.2.1.** *Let a homogeneous, incompressible, electrically conducting Newtonian fluid occupy the half-space  $\mathcal{S}$  and be embedded in the external electromagnetic field  $\mathbf{H}_e = H_\infty[x_1\mathbf{e}_1 - (1+c)x_2\mathbf{e}_2 + cx_3\mathbf{e}_3]$ ,  $\mathbf{E}_e = \mathbf{0}$ . If the total magnetic field in the solid is (7.7) and the hypothesis (h) holds, then the steady three-dimensional MHD stagnation-point flow of such a fluid is possible if, and only if, the flow is axisymmetric ( $f = g$ ,  $h = k$ ,  $c = 1$ ).*

Further it has the following form

$$\mathbf{v} = a[x_1f'(x_2)\mathbf{e}_1 - 2f(x_2)\mathbf{e}_2 + cx_3f'(x_2)\mathbf{e}_3],$$

$$\mathbf{H} = H_\infty[x_1h'(x_2)\mathbf{e}_1 - 2h(x_2)\mathbf{e}_2 + cx_3h'(x_2)\mathbf{e}_3], \quad \mathbf{E} = \mathbf{0},$$

$$p = -\rho \frac{a^2}{2}[x_1^2 + 4f^2(x_2) + x_3^2] - 2\rho av f'(x_2)$$

$$- \mu_e \frac{H_\infty^2}{2}(x_1^2 + x_3^2)[h'^2(x_2) - 1] + p_0, \quad (x_1, x_3) \in \mathbb{R}^2, \quad x_2 \in \mathbb{R}^+,$$

where  $(f, h)$  satisfies problem

$$\begin{aligned} \frac{\nu}{a}f''' + 2ff'' - f'^2 + 1 - \frac{\mu_e H_\infty^2}{\rho a^2}(2hh'' - h'^2 + 1) &= 0, \\ h'' + 2\sigma_e\mu_e a(fh' - hf') &= 0, \\ f(0) = 0, \quad f'(0) = 0, \quad h(0) = 0, \\ \lim_{x_2 \rightarrow +\infty} f'(x_2) = 1, \quad \lim_{x_2 \rightarrow +\infty} h'(x_2) = 1. \end{aligned} \quad (7.31)$$

*Proof.* As for the inviscid fluid, let the electric field  $\mathbf{E}$  be in the form

$$\mathbf{E}^i = E_1^i \mathbf{e}_1 + E_2^i \mathbf{e}_2 + E_3^i \mathbf{e}_3.$$

Conditions (2.5) require that

$$E_1^i = 0, \quad E_3^i = 0 \quad \text{at } x_2 = 0. \quad (7.32)$$

From (2.22)<sub>4</sub> follows that

$$\mathbf{E} = -\nabla\psi.$$

Moreover, (2.22)<sub>3</sub> provides

$$\begin{aligned} \frac{\partial\psi}{\partial x_1} &= -\frac{H_\infty}{\sigma_e} c x_3 [k''(x_2) + \sigma_e \mu_e a [(f(x_2) + cg(x_2))k'(x_2) - (h(x_2) + ck(x_2))g'(x_2)]], \\ \frac{\partial\psi}{\partial x_2} &= H_\infty \mu_e a c x_1 x_3 [h'(x_2)g'(x_2) - k'(x_2)f'(x_2)], \\ \frac{\partial\psi}{\partial x_3} &= -\frac{H_\infty}{\sigma_e} x_1 [-h''(x_2) - \sigma_e \mu_e a [(f(x_2) + cg(x_2))h'(x_2) - (h(x_2) + ck(x_2))f'(x_2)]]. \end{aligned} \quad (7.33)$$

Since  $\mathbf{E}$  is divergence free (see (2.22)<sub>5</sub>), from (7.33)<sub>2</sub>, we get

$$H_\infty \mu_e a c x_1 x_3 [h'(x_2)g'(x_2) - k'(x_2)f'(x_2)]' = 0, \quad \forall (x_1, x_3) \in \mathbb{R}^2, \quad x_2 \in \mathbb{R}^+,$$

which for the conditions at infinity (7.25) and (7.26), gives

$$h'(x_2)g'(x_2) = k'(x_2)f'(x_2), \quad \forall x_2 \in \mathbb{R}^+, \quad (7.34)$$

and so

$$E_2 = 0.$$

We remark that the equality (7.34) means the following relationships of proportionality

$$\begin{aligned} k'(x_2) &= l(x_2)h'(x_2), \\ g'(x_2) &= l(x_2)f'(x_2), \end{aligned} \quad (7.35)$$

where  $l = l(x_2)$  is a sufficiently regular unknown function ( $l \in C^2(\mathbb{R}^+)$ ) satisfying the condition

$$\lim_{x_2 \rightarrow +\infty} l(x_2) = 1. \quad (7.36)$$

From (7.34) we have  $\psi = \psi(x_1, x_3)$ . Then from (7.33)<sub>1,3</sub> we deduce

$$\begin{aligned} k''(x_2) + \sigma_e \mu_e a [(f(x_2) + cg(x_2))k'(x_2) - (h(x_2) + ck(x_2))g'(x_2)] &= 0, \\ h''(x_2) + \sigma_e \mu_e a [(f(x_2) + cg(x_2))h'(x_2) - (h(x_2) + ck(x_2))f'(x_2)] &= 0. \end{aligned} \quad (7.37)$$

Hence

$$\mathbf{E} = \mathbf{0}.$$

If we substitute (7.35)<sub>1</sub> into (7.37)<sub>1</sub>, then we obtain

$$lh'' + l'h' + \sigma_e \mu_e a [(f + cg)lh' - (h + ck)lf'] = 0, \quad (7.38)$$

which by virtue of (7.37)<sub>2</sub> reduces to

$$l'(x_2)h'(x_2) = 0, \quad \forall x_2 \in \mathbb{R}^+. \quad (7.39)$$

From relation (7.39), hypothesis (h) and (7.36), we find

$$l(x_2) \equiv 1, \quad \forall x_2 \in \mathbb{R}^+.$$

The last equivalence reduces the relationships (7.35) to

$$k'(x_2) = h'(x_2), \quad g'(x_2) = f'(x_2). \quad (7.40)$$

In particular, we stress that (7.40) involves

$$k(x_2) = h(x_2), \quad g(x_2) = f(x_2), \quad A = B = C, \quad \forall x_2 \in \mathbb{R}^+. \quad (7.41)$$

Substituting (7.40) into (7.37), we find that  $h$  has to satisfy

$$h''(x_2) + \sigma_e \mu_e a (1 + c) [f(x_2)h'(x_2) - h(x_2)f'(x_2)] = 0. \quad (7.42)$$

We now proceed in order to determine  $p$ ,  $f$ . We substitute (7.40), (7.41), and (7.21) into (2.22)<sub>1</sub> to obtain

$$\begin{aligned} ax_1 \left[ \nu f''' + a(1+c)ff'' - af'^2 - \frac{\mu_e}{\rho a} H_\infty^2 (1+c)hh'' \right] &= \frac{1}{\rho} \frac{\partial p}{\partial x_1}, \\ \nu a(1+c)f'' - a^2(1+c)^2 ff' + \frac{\mu_e}{\rho} H_\infty^2 (x_1^2 + c^2 x_3^2) h' h'' &= -\frac{1}{\rho} \frac{\partial p}{\partial x_2}, \\ acx_3 \left[ \nu f''' + a(1+c)ff'' - acf'^2 - \frac{\mu_e}{\rho a} H_\infty^2 x_3(1+c)hh'' \right] &= \frac{1}{\rho} \frac{\partial p}{\partial x_3}. \end{aligned} \quad (7.43)$$

Then, by integrating (7.43)<sub>2</sub>, we find

$$p = -\rho \frac{a^2}{2} (1+c)^2 f^2(x_2) - \rho a \nu (1+c) f'(x_2) - \mu_e \frac{H_\infty^2}{2} [x_1^2 + c^2 x_3^2] h'^2(x_2) + P(x_1, x_3),$$

where the function  $P(x_1, x_3)$  is determined supposing that, far from the wall, the pressure  $p$  has the same behaviour as for an inviscid fluid, whose pressure is given by (7.20)<sub>1</sub>.

Therefore, by virtue of (7.26), and (7.29), we get

$$P(x_1, x_3) = -\rho \frac{a^2}{2} (x_1^2 + c^2 x_3^2) + \mu_e \frac{H_\infty^2}{2} (x_1^2 + c^2 x_3^2) + p_0^*.$$

Finally, the pressure field assumes the form

$$\begin{aligned} p &= -\rho \frac{a^2}{2} [x_1^2 + (1+c)^2 f^2(x_2) + c^2 x_3^2] - \rho a \nu (1+c) f'(x_2) \\ &\quad - \mu_e \frac{H_\infty^2}{2} (x_1^2 + c^2 x_3^2) [h'^2(x_2) - 1] + p_0. \end{aligned} \quad (7.44)$$

In consideration of (7.43), we have

$$\begin{aligned} \frac{\nu}{a} f''' + (1+c)ff'' - f'^2 + 1 - \frac{\mu_e}{\rho} \frac{H_\infty^2}{a^2} [(1+c)hh'' - h'^2 + 1] &= 0, \\ \frac{\nu}{a} f''' + (1+c)ff'' - cf'^2 + c - \frac{\mu_e}{\rho} \frac{H_\infty^2}{a^2} [(1+c)hh'' - ch'^2 + c] &= 0. \end{aligned} \quad (7.45)$$

Equations (7.45) are compatible if, and only if,

$$(c-1)[f'^2 - 1 - \beta_m(h'^2 - 1)] = 0, \quad (7.46)$$

where  $\beta_m = \frac{\mu_e}{\rho} \frac{H_\infty^2}{a^2}$ .

From the previous assumptions, we will prove that  $c = 1$ .  
Actually, by contradiction, suppose that  $c \neq 1$ , so that

$$f'^2 - 1 - \beta_m(h'^2 - 1) = 0. \quad (7.47)$$

From (7.47) we get

$$h'^2(0) = \frac{\beta_m - 1}{\beta_m}, \quad (7.48)$$

which gives an absurdum if  $\beta_m < 1$ .

We now turn to the case  $\beta_m \geq 1$ .

On substituting (7.47) into (7.45)<sub>1</sub> and taking into account (7.42), we find that  $(f, h)$  satisfies

$$\begin{aligned} \frac{\nu}{a} f''' + (1+c)ff'' - \beta_m(1+c)hh'' &= 0, \\ h'' + \sigma_e \mu_e a(1+c)(fh' - hf') &= 0, \end{aligned} \quad (7.49)$$

together with the boundary conditions

$$\begin{aligned} f(0) = 0, \quad f'(0) = 0, \quad h(0) = 0, \\ \lim_{x_2 \rightarrow +\infty} f'(x_2) = 1, \quad \lim_{x_2 \rightarrow +\infty} h'(x_2) = 1. \end{aligned} \quad (7.50)$$

Combining (7.49)<sub>2</sub> and the twice differentiating of (7.47), we obtain  $f''(0) = 0$ .  
If we consider the Cauchy problem obtained by adding to (7.49) the initial conditions

$$\begin{aligned} f(0) = 0, \quad f'(0) = 0, \quad f''(0) = 0, \\ h(0) = 0, \quad h'(0) = \pm \sqrt{\frac{\beta_m - 1}{\beta_m}}, \end{aligned} \quad (7.51)$$

then its unique solution is given by

$$f(x_2) = 0, \quad h(x_2) = \pm \sqrt{\frac{\beta_m - 1}{\beta_m}} x_2, \quad \forall x_2 \in \mathbb{R}^+, \quad (7.52)$$

which is clearly absurdum for boundary conditions (7.50)<sub>4,5</sub>. □

Using (5.33), the boundary value problem (7.31) can be written in dimensionless

form:

$$\begin{aligned}
\varphi''' + 2\varphi\varphi'' - \varphi'^2 + 1 - \beta_m(2\Psi\Psi'' - \Psi'^2 + 1) &= 0, \\
\Psi'' + 2R_m(\varphi\Psi' - \Psi\varphi') &= 0, \\
\varphi(0) = 0, \varphi'(0) = 0, \Psi(0) = 0, \\
\lim_{\eta \rightarrow +\infty} \varphi'(\eta) = 1, \lim_{\eta \rightarrow +\infty} \Psi'(\eta) = 1.
\end{aligned} \tag{7.53}$$

We now turn to analyze the numerical solution of problem (7.53) gotten through the `bvp4c` MATLAB routine. The values of  $R_m$  and  $\beta_m$  are chosen as in the previous chapters.

For small values of  $R_m$ , thanks to transformation (5.35) we solve the following analogous problem

$$\begin{aligned}
R_m\varphi_*''' + 2\varphi_*\varphi_*'' - \varphi_*'^2 + 1 - \beta_m(2\Psi_*\Psi_*'' - \Psi_*'^2 + 1) &= 0, \\
\Psi_*'' + 2(\varphi_*\Psi_*' - \Psi_*\varphi_*') &= 0, \\
\varphi_*(0) = 0, \varphi_*'(0) = 0, \Psi_*(0) = 0, \\
\lim_{\xi \rightarrow +\infty} \varphi_*'(\xi) = 1, \lim_{\xi \rightarrow +\infty} \Psi_*'(\xi) = 1.
\end{aligned} \tag{7.54}$$

REMARK 7.2.2. *The numerical solution  $(\varphi, \Psi)$  of problem (7.53) (or (7.54)) satisfies the conditions at infinity; therefore as in Remark 1.3.9, we define :*

- $\bar{\eta}_\varphi$  the value of  $\eta$  such that  $\varphi'(\bar{\eta}_\varphi) = 0.99$ ,

so that if  $\eta > \bar{\eta}_\varphi$ , then  $\varphi \cong \eta - \alpha$  and the influence of the viscosity appears only in a layer lining the boundary whose thickness is  $\delta = \bar{\eta}_\varphi$ .

As well as  $\varphi$ , in this case we also have that

$$\lim_{\eta \rightarrow +\infty} \Psi'(\eta) = 1 \text{ and } \lim_{\eta \rightarrow +\infty} [\Psi(\eta) - \eta] = -\alpha.$$

The numerical results show that the values computed of  $\alpha$  for  $\varphi$  and  $\Psi$  are in good agreement, especially when  $\beta_m$  is small or  $R_m$  is big.

We provide Table 7.1 to show the values of  $\alpha$ ,  $\varphi''(0)$ ,  $\Psi'(0)$  when  $R_m$  and  $\beta_m$  change.

Table 7.1 has been obtained for small values of  $R_m$  recomputing the corresponding values of  $\eta$ ,  $\varphi$  and  $\Psi$ . More precisely, for  $R_m = 0.01, 0.1$  with transformation (5.35) we get Table 7.2.

We underline that  $\alpha$  increases, while  $\varphi''(0)$  and  $\Psi'(0)$  decrease as  $\beta_m$  increases. Further  $\alpha$ ,  $\varphi''(0)$  and  $\Psi'(0)$  decrease as  $R_m$  increases.

In Figure 7.3<sub>1</sub> we can see the profiles  $\varphi, \varphi', \varphi''$  for  $R_m = 1$  and  $\beta_m = 0.5$ , while Figure 7.3<sub>2</sub> shows the behaviour of  $\Psi, \Psi'$  for the same values of  $R_m$  and  $\beta_m$ .

Table 7.1: CASE IV-N: descriptive quantities of the motion for several values of  $R_m$  and  $\beta_m$ .

$R_m$	$\beta_m$	$\varphi''(0)$	$\Psi'(0)$	$\alpha$	$\bar{\eta}_\varphi$
0.01	0.00	1.3119	0.9121	0.5689	1.9455
	0.20	1.2755	0.9029	0.6981	5.9815
	0.50	1.2025	0.8834	1.0257	13.3883
	0.70	1.1335	0.8642	1.4131	16.6692
	0.90	1.0364	0.8367	2.0672	18.6097
0.10	0.00	1.3119	0.7792	0.5689	1.9453
	0.20	1.2298	0.7604	0.6836	3.9364
	0.50	1.0737	0.7237	0.9548	5.5480
	0.70	0.9377	0.6916	1.2478	5.9940
	0.90	0.7628	0.6510	1.7039	6.1885
1	0.00	1.3119	0.5592	0.5689	1.9455
	0.20	1.1812	0.5312	0.6675	2.5056
	0.50	0.9370	0.4718	0.9298	3.5809
	0.70	0.7192	0.4104	1.2977	4.5299
	0.90	0.4162	0.3131	2.0947	4.9300
100	0.00	1.3119	0.1729	0.5689	1.9455
	0.20	1.1711	0.1613	0.6377	2.1780
	0.50	0.9220	0.1392	0.8100	2.7632
	0.70	0.7113	0.1183	1.0483	3.5634
	0.90	0.4140	0.0840	1.7043	4.7912
1000	0.00	1.3119	0.0842	0.5689	1.9455
	0.20	1.1729	0.0783	0.6363	2.1755
	0.50	0.9265	0.0673	0.8052	2.7519
	0.70	0.7172	0.0570	1.0391	3.5434
	0.90	0.4201	0.0402	1.6866	4.7849

Table 7.2: CASE IV-N: descriptive quantities of the motion for several values of  $\beta_m$  when  $R_m$  is less than 1.

$R_m$	$\beta_m$	$\varphi''_*(0)$	$\Psi'_*(0)$	$\alpha_*$	$\bar{\xi}_{\varphi_*}$
0.01	0.00	13.1194	0.9121	0.0569	0.1945
	0.20	12.7551	0.9029	0.0698	0.5981
	0.50	12.0252	0.8834	0.1026	1.3388
	0.70	11.3354	0.8642	0.1413	1.6669
	0.90	10.3636	0.8367	0.2067	1.8610
0.10	0.00	4.1487	0.7792	0.1799	0.6152
	0.20	3.8889	0.7604	0.2162	1.2448
	0.50	3.3955	0.7237	0.3019	1.7544
	0.70	2.9653	0.6916	0.3946	1.8955
	0.90	2.4122	0.6510	0.5388	1.9570

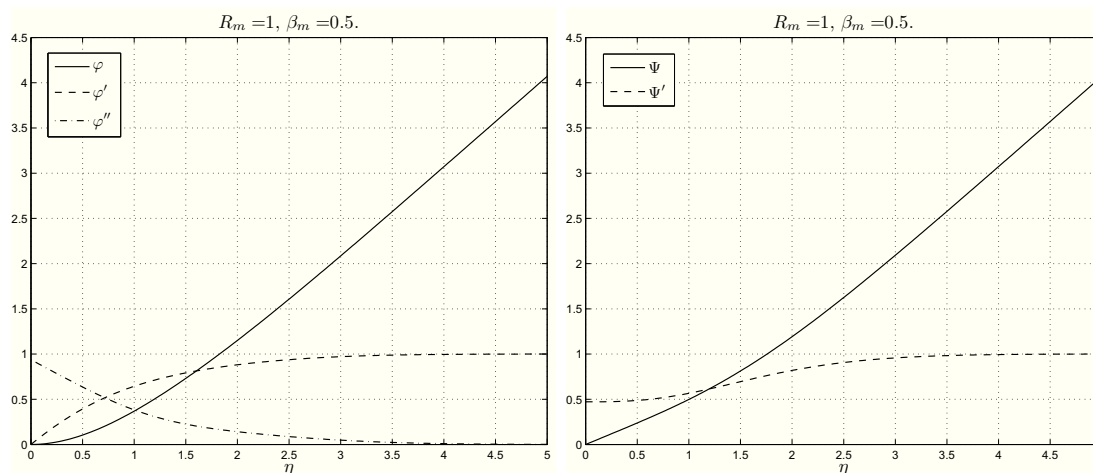


Figure 7.3: CASE IV-N: the first figure shows  $\varphi, \varphi', \varphi''$  for  $R_m = 1$  and  $\beta_m = 0.5$ , while the second shows  $\Psi, \Psi'$  for  $R_m = 1$  and  $\beta_m = 0.5$ .

When  $R_m \neq 1$  and  $\beta_m \neq 0.5$ , the profiles of  $\varphi, \varphi', \varphi'', \Psi, \Psi'$  are analogous to those shown in Figure 7.3.

Table 7.1 elucidates that the thickness  $\delta$  of the boundary layer depends on  $R_m$  and  $\beta_m$ ; more precisely

- $\delta$  increases when  $\beta_m$  increases (Figure 7.4<sub>1</sub>);
- $\delta$  decreases when  $R_m$  increases (Figure 7.4<sub>2</sub>).

This fact is the same as in the previous two chapters. In particular, we have that the thickness of the boundary layer is now bigger than that in Chapters 1.3.2 and 4.2.

As in the case in the absence of the magnetic field and in Chapter 4, it is possible to classify the stagnation-point as nodal or saddle point and as attachment or separation point (see Remarks 1.3.8 and 4.2.10). Since  $\varphi''(0)$  is positive for any choice of the values of the parameters, the origin is always a nodal point of attachment.

### 7.3 Micropolar fluids CASE IV-M

We now study the previous problem for a homogeneous, incompressible, electrically conducting micropolar fluid.

In the absence of free electric charges and external mechanical body forces and body couples, the MHD equations for such a fluid are (2.44). We prescribe the boundary conditions (2.45), (2.5) and (2.6).

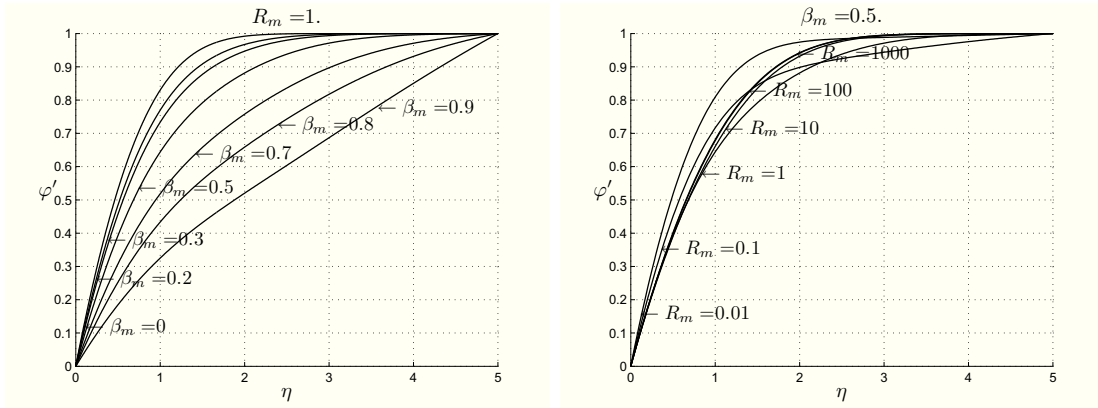


Figure 7.4: CASE IV-N: plots showing  $\varphi'$  for different  $\beta_m$  and  $R_m$ , respectively.

The three-dimensional stagnation-point flow is determined by  $\mathbf{v}$ ,  $\mathbf{w}$  in the following form

$$\begin{aligned} v_1 &= ax_1 f'(x_2), & v_2 &= -a[f(x_2) + cg(x_2)], & v_3 &= acx_3 g'(x_2), \\ w_1 &= -cx_3 F(x_2), & w_2 &= 0, & w_3 &= x_1 G(x_2), \end{aligned} \quad (x_1, x_3) \in \mathbb{R}^2, \quad x_2 \in \mathbb{R}^+, \quad (7.55)$$

where  $f, g, F, G$  are sufficiently regular unknown functions ( $f, g \in C^3(\mathbb{R}^+)$ ,  $F, G \in C^2(\mathbb{R}^+)$ ).

To satisfy conditions (2.45) we ask

$$\begin{aligned} f(0) &= 0, & f'(0) &= 0, & g(0) &= 0, & g'(0) &= 0, \\ F(0) &= 0, & G(0) &= 0. \end{aligned} \quad (7.56)$$

We suppose that an external magnetic field

$$\mathbf{H}_e = H_\infty [x_1 \mathbf{e}_1 - (1 + c)x_2 \mathbf{e}_2 + cx_3 \mathbf{e}_3]$$

permeates the whole physical space and that the external electric field is absent.

Moreover, the total magnetic field in the fluid is taken in the following form

$$\mathbf{H} = H_\infty [x_1 h'(x_2) \mathbf{e}_1 - (h(x_2) + ck(x_2)) \mathbf{e}_2 + cx_3 k'(x_2) \mathbf{e}_3], \quad (7.57)$$

where  $h, k$  are sufficiently regular unknown functions ( $h, k \in C^2(\mathbb{R}^+)$ ).

From Theorem 7.1.3 we have  $\mathbf{H}_s = H_\infty [h'(0)x_1 \mathbf{e}_1 - (h'(0) + ck'(0))x_2 \mathbf{e}_2 + ck'(0)x_3 \mathbf{e}_3]$  in  $\mathcal{S}^-$ , which implies that  $h, k$  satisfy

$$h(0) = 0, \quad k(0) = 0. \quad (7.58)$$

We assume at infinity the Condition P, i.e.

$$\begin{aligned} \lim_{x_2 \rightarrow +\infty} f'(x_2) &= 1, & \lim_{x_2 \rightarrow +\infty} g'(x_2) &= 1, \\ \lim_{x_2 \rightarrow +\infty} F(x_2) &= 0, & \lim_{x_2 \rightarrow +\infty} G(x_2) &= 0. \end{aligned} \quad (7.59)$$

$$\lim_{x_2 \rightarrow +\infty} h'(x_2) = 1, \quad \lim_{x_2 \rightarrow +\infty} k'(x_2) = 1. \quad (7.60)$$

The constant  $C$  is related to the asymptotic behaviour of  $f$ ,  $g$ ,  $h$  and  $k$  at infinity as for the Newtonian case. So relations (7.28), (7.29) and (7.30) continue to hold.

As in the Newtonian case, our aim is now to prove the following:

**THEOREM 7.3.1.** *Let a homogeneous, incompressible, electrically conducting micropolar fluid occupy the half-space  $\mathcal{S}$  and be embedded in the external electromagnetic field  $\mathbf{H}_e = H_\infty[x_1\mathbf{e}_1 - (c+1)x_2\mathbf{e}_2 + cx_3\mathbf{e}_3]$ ,  $\mathbf{E}_e = \mathbf{0}$ . If the total magnetic field in the solid is (7.7) and the hypothesis (h) is satisfied, under the assumption  $f \in C^5(\mathbb{R}^+)$ ,  $F, G, h \in C^7(\mathbb{R}^+)$ , then the steady three-dimensional MHD stagnation-point flow of such a fluid is possible if, and only if, the flow is axisymmetric ( $c = 1$ ,  $f = g$ ,  $h = k$ ,  $F = G$ ).*

Therefore it has the following form

$$\begin{aligned} \mathbf{v} &= a[x_1f'(x_2)\mathbf{e}_1 - 2f(x_2)\mathbf{e}_2 + x_3f'(x_2)\mathbf{e}_3], & \mathbf{w} &= F(x_2)(-x_3\mathbf{e}_1 + \mathbf{e}_3), \\ \mathbf{H} &= H_\infty[x_1h'(x_2)\mathbf{e}_1 - 2h(x_2)\mathbf{e}_2 + x_3h'(x_2)\mathbf{e}_3], & \mathbf{E} &= \mathbf{0}, \\ p &= -\rho \frac{a^2}{2}[x_1^2 + 4f^2(x_2) + 4x_3^2] - 2\rho a(\nu + \nu_r)f'(x_2) - 4\nu_r\rho \int_0^{x_2} F(s)ds \\ &\quad - \mu_e \frac{H_\infty^2}{2}(x_1^2 + 4x_3^2)[h'^2(x_2) - 1] + p_0, & (x_1, x_3) &\in \mathbb{R}^2, \quad x_2 \in \mathbb{R}^+, \end{aligned}$$

where  $(f, h, F)$  satisfies problem

$$\begin{aligned} \frac{\nu + \nu_r}{a}f''' + 2ff'' - f'^2 + 1 - 2\frac{\nu_r}{a}F' - \frac{\mu_e H_\infty^2}{\rho a^2}(2hh'' - h'^2 + 1) &= 0, \\ \lambda F'' + Ia(2F'f - Ff') - 2\nu_r(2F + af'') &= 0, \\ h'' + 2\sigma_e\mu_e a(fh' - hf') &= 0, \\ f(0) = 0, \quad f'(0) = 0, \quad F(0) = 0, \quad h(0) = 0, \\ \lim_{x_2 \rightarrow +\infty} f'(x_2) = 1, \quad \lim_{x_2 \rightarrow +\infty} F'(x_2) = 0, \quad \lim_{x_2 \rightarrow +\infty} h'(x_2) = 1, \end{aligned} \quad (7.61)$$

provided  $F \in L^1([0, +\infty))$ .

*Proof.* First of all, from equations (2.44)  $\mathbf{H}$ ,  $\mathbf{E}$  depend only on the velocity field, which is the same as that of the Newtonian fluid. Hence, proceeding as in the previous section, we get

$$\mathbf{E} = \mathbf{0}, \quad k'(x_2) = h'(x_2), \quad g'(x_2) = f'(x_2). \quad (7.62)$$

In particular, the magnetic field  $\mathbf{H}$  depends only on  $h$ , which satisfies equation

$$h''(x_2) + \sigma_e \mu_e a(1+c)[f(x_2)h'(x_2) - h(x_2)f'(x_2)] = 0. \quad (7.63)$$

In order to determine  $p$ ,  $f$ ,  $F$ ,  $G$ , we substitute (7.62), and (7.55) into (2.44)<sub>1,3</sub> so that we have

$$\begin{aligned} ax_1 \left[ (\nu + \nu_r)f''' + a(1+c)ff'' - af'^2 + \frac{2\nu_r}{a}G' - \frac{\mu_e}{\rho a}H_\infty^2(1+c)hh'' \right] &= \frac{1}{\rho} \frac{\partial p}{\partial x_1}, \\ (\nu + \nu_r)a(1+c)f'' - a^2(1+c)^2ff' + 2\nu_r(cF + G) + \frac{\mu_e}{\rho}H_\infty^2[x_1^2 + c^2x_3^2]h'h'' &= -\frac{1}{\rho} \frac{\partial p}{\partial x_2}, \\ acx_3 \left[ (\nu + \nu_r)f''' + a(1+c)ff'' - acf'^2 + \frac{2\nu_r}{a}F' - \frac{\mu_e}{\rho a}H_\infty^2(1+c)hh'' \right] &= \frac{1}{\rho} \frac{\partial p}{\partial x_3}, \\ c[\lambda F'' + Ia[F'(f+cg) - cFg'] - 2\nu_r(2F + ag'')] &= 0, \\ \lambda G'' + Ia[G'(f+cg) - Gf'] - 2\nu_r(2G + af'') &= 0. \end{aligned} \quad (7.64)$$

Since we are interested in three-dimensional flow, we assume  $c \neq 0$  and so equation (7.64)<sub>4</sub> can be replaced by

$$\lambda F'' + Ia[F'(f+cg) - cFg'] - 2\nu_r(2F + ag'') = 0. \quad (7.65)$$

By integrating (7.64)<sub>2</sub>, we find

$$\begin{aligned} p &= -\rho \frac{a^2}{2}(c+1)^2 f^2(x_2) - \rho a(\nu + \nu_r)(c+1)f'(x_2) \\ &\quad - 2\nu_r \rho \int_0^{x_2} [cF(s) + G(s)] ds - \mu_e \frac{H_\infty^2}{2} [x_1^2 + c^2x_3^2] h'^2(x_2) + P(x_1, x_3), \end{aligned}$$

where the function  $P(x_1, x_3)$  is determined supposing that, far from the wall, the pressure  $p$  has the same behaviour as for an inviscid fluid, whose pressure is given by (7.20)<sub>1</sub>.

Therefore, by virtue of (7.59), (7.60), (7.28) and (7.29), we get

$$P(x_1, x_3) = -\rho \frac{a^2}{2}(x_1^2 + c^2x_3^2) + \mu_e \frac{H_\infty^2}{2}(x_1^2 + c^2x_3^2) + p_0^*,$$

so that  $p$  is given by

$$p = -\rho \frac{a^2}{2} [x_1^2 + (c+1)^2 f^2(x_2) + c^2 x_3^2] - \rho a (\nu + \nu_r) (c+1) f'(x_2) - 2\nu_r \rho \int_0^{x_2} [cF(s) + G(s)] ds - \mu_e \frac{H_\infty^2}{2} (x_1^2 + c^2 x_3^2) [h'^2(x_2) - 1] + p_0. \quad (7.66)$$

In consideration of (7.64), we obtain the ordinary differential system

$$\begin{aligned} \frac{\nu + \nu_r}{a} f''' + (c+1) f f'' - f'^2 + 1 + \frac{2\nu_r}{a^2} G' - \frac{\mu_e H_\infty^2}{\rho a^2} [(c+1) h h'' - h'^2 + 1] &= 0, \\ \frac{\nu + \nu_r}{a} f''' + (c+1) f f'' - c f'^2 + c + \frac{2\nu_r}{a^2} F' - \frac{\mu_e H_\infty^2}{\rho a^2} [(c+1) h h'' - c h'^2 + c] &= 0, \end{aligned} \quad (7.67)$$

together with equations (7.64)<sub>5</sub> and (7.65) and boundary conditions (7.56), (7.59), (7.60) and (7.58).

It is now convenient to rewrite the previous boundary value problem (7.67), (7.64)<sub>5</sub>, (7.65), (7.56), (7.59), (7.60) and (7.58) in dimensionless form in order to reduce the number of the material parameters. To this end we use (1.49) and we put

$$\Psi(\eta) = \sqrt{\frac{a}{\nu + \nu_r}} h \left( \sqrt{\frac{\nu + \nu_r}{a}} \eta \right).$$

So system (7.67), (7.64)<sub>5</sub> and (7.65) can be written as

$$\begin{aligned} \varphi''' + (c+1)\varphi\varphi'' - \varphi'^2 + 1 + \Gamma' - \beta_m [(c+1)\Psi\Psi'' - \Psi'^2 + 1] &= 0, \\ \varphi''' + (c+1)\varphi\varphi'' - c\varphi'^2 + c + \Phi' - \beta_m [(c+1)\Psi\Psi'' - c\Psi'^2 + c] &= 0, \\ \Phi'' + c_3(c+1)\Phi'\varphi - \Phi(cc_3\varphi' + c_2) - c_1\varphi'' &= 0, \\ \Gamma'' + c_3(c+1)\Gamma'\varphi - \Gamma(c_3\varphi' + c_2) - c_1\varphi'' &= 0, \\ \Psi'' + R_m(c+1)(\varphi\Psi' - \Psi\varphi') &= 0, \end{aligned} \quad (7.68)$$

where  $c_1$ ,  $c_2$ ,  $c_3$  are given by (1.25), while  $\beta_m$ ,  $R_m$  are provided in (5.49).

The boundary conditions (7.56), (7.59), (7.60) and (7.58) in dimensionless form

become:

$$\begin{aligned}
\varphi(0) &= 0, \quad \varphi'(0) = 0, \\
\Phi(0) &= 0, \quad \Gamma(0) = 0, \\
\Psi(0) &= 0, \\
\lim_{\eta \rightarrow +\infty} \varphi'(\eta) &= 1, \\
\lim_{\eta \rightarrow +\infty} \Phi(\eta) &= 0, \quad \lim_{\eta \rightarrow +\infty} \Gamma(\eta) = 0, \\
\lim_{\eta \rightarrow +\infty} \Psi'(\eta) &= 1.
\end{aligned} \tag{7.69}$$

We note that the equations (7.68)<sub>1,2</sub> are compatible if, and only if,

$$(c-1)[\varphi'^2 - 1 - \beta_m(\Psi'^2 - 1)] + \Gamma' - \Phi' = 0. \tag{7.70}$$

We now show that from the previous assumptions follows  $c = 1$ .  
By contradiction, suppose that  $c \neq 1$ .

Computing (7.70), (7.68) at  $\eta = 0$ , gives

$$\begin{aligned}
\Phi'(0) - \Gamma'(0) &= (c-1)[- \beta_m \Psi'^2(0) + \beta_m - 1], \\
\Gamma'(0) &= \beta_m[1 - \Psi'^2(0)] - \varphi'''(0) - 1, \\
\Phi'(0) &= c\beta_m[1 - \Psi'^2(0)] - \varphi'''(0) - c, \\
\Psi''(0) &= 0, \\
\Phi''(0) = \Gamma''(0) &= c_1\varphi''(0).
\end{aligned} \tag{7.71}$$

If we differentiate (7.68)<sub>3,4</sub>, then we have

$$\begin{aligned}
\Phi''' + c_3(c+1)\varphi\Phi'' + (c_3\varphi' - c_2)\Phi' - cc_3\varphi''\Phi - c_1\varphi''' &= 0, \\
\Gamma''' + c_3(c+1)\varphi\Gamma'' + (cc_3\varphi' - c_2)\Gamma' - c_3\varphi''\Gamma - c_1\varphi''' &= 0,
\end{aligned} \tag{7.72}$$

from which in  $\eta = 0$ , it follows

$$\begin{aligned}
\Gamma'''(0) &= -c_2[\beta_m\Psi'^2(0) + 1 - \beta_m] + (c_1 - c_2)\varphi'''(0), \\
\Phi'''(0) - \Gamma'''(0) &= -c_2(c-1)[\beta_m\Psi'^2(0) + 1 - \beta_m],
\end{aligned} \tag{7.73}$$

where we have used (7.71)<sub>1,2</sub>.

Differentiating (7.68)<sub>5</sub> and (7.70), we obtain

$$\begin{aligned}\Psi''' &= -R_m(c+1)[\varphi\Psi'' - \Psi\varphi''], \\ \Phi''' - \Gamma''' &= 2(c-1)[\varphi''^2 + \varphi'\varphi''' - \beta_m(\Psi''^2 + \Psi'\Psi''')],\end{aligned}\quad (7.74)$$

which in  $\eta = 0$  furnish

$$\Psi'''(0) = 0, \quad \Phi'''(0) - \Gamma'''(0) = 2(c-1)\varphi''^2(0). \quad (7.75)$$

By virtue of (7.73)<sub>2</sub> and (7.75)<sub>2</sub>, we get

$$\Psi'^2(0) = \frac{1}{\beta_m} \left[ -\frac{2}{c_2}\varphi''^2(0) + \beta_m - 1 \right], \quad (7.76)$$

which gives the absurdum if  $\beta_m < 1$ .

We now turn to the case  $\beta_m \geq 1$ .

Substituting (7.76) into (7.71)<sub>2,3</sub>, hold

$$\begin{aligned}\Gamma'(0) &= \frac{2}{c_2}\varphi''^2(0) - \varphi'''(0), \\ \Phi'(0) &= \frac{2c}{c_2}\varphi''^2(0) - \varphi'''(0).\end{aligned}\quad (7.77)$$

Now we differentiate (7.72):

$$\begin{aligned}\Phi^{IV} + c_3(c+1)\varphi\Phi''' + [c_3(c+2)\varphi' - c_2]\Phi'' - c_3(c-1)\varphi''\Phi' - cc_3\varphi'''\Phi - c_1\varphi^{IV} &= 0, \\ \Gamma^{IV} + c_3(c+1)\varphi\Gamma''' + [c_3(2c+1)\varphi' - c_2]\Gamma'' + c_3(c-1)\varphi''\Gamma' - c_3\varphi'''\Gamma - c_1\varphi^{IV} &= 0,\end{aligned}\quad (7.78)$$

which together with (7.77) gives

$$\Phi^{IV}(0) - \Gamma^{IV}(0) = 2c_3(c-1)\varphi''(0) \left[ \frac{1}{c_2}(c+1)\varphi''^2(0) - \varphi'''(0) \right]. \quad (7.79)$$

By differentiating (7.74), we get

$$\begin{aligned}\Psi^{IV} &= -R_m(c+1)[\varphi'\Psi'' + \varphi\Psi''' - \Psi'\varphi'' - \Psi\varphi'''], \\ \Phi^{IV} - \Gamma^{IV} &= 2(c-1)[3\varphi''\varphi''' + \varphi'\varphi^{IV} - \beta_m(3\Psi''\Psi''' + \Psi'\Psi^{IV})],\end{aligned}\quad (7.80)$$

which evaluated in  $\eta = 0$  thanks to (7.76) furnish

$$\begin{aligned}\Psi^{IV}(0) &= R_m(c+1)\Psi'(0)\varphi''(0), \\ \Phi^{IV}(0) - \Gamma^{IV}(0) &= 2(c-1)\varphi''(0) \left[ 3\varphi'''(0) + R_m(c+1) \left( \frac{2}{c_2}\varphi''^2(0) + 1 - \beta_m \right) \right].\end{aligned}\quad (7.81)$$

If we equate (7.79) and (7.81)<sub>2</sub>, taking into account that  $c \neq 1$ , we arrive at

$$\left[ (3 + c_3)\varphi'''(0) + \frac{(c+1)}{c_2}(2R_m - c_3)\varphi''^2(0) + R_m(c+1)(1 - \beta_m) \right] \varphi''(0) = 0. \quad (7.82)$$

From the last equation, the proof falls naturally into two cases

(A)  $\varphi''(0) \neq 0$  and

$$\varphi'''(0) = -\frac{c+1}{3+c_3} \left[ \frac{2R_m - c_3}{c_2}\varphi''^2(0) + R_m(1 - \beta_m) \right]; \quad (7.83)$$

(B)  $\varphi''(0) = 0$ .

We first consider case (A).

Differentiating of (7.78) gives

$$\begin{aligned} \Phi^V + c_3(c+1)\varphi\Phi^{IV} + [c_3(2c+3)\varphi' - c_2]\Phi''' + 3c_3\varphi''\Phi'' - c_3(2c-1)\varphi''' \Phi' \\ - cc_3\varphi^{IV}\Phi - c_1\varphi^V = 0, \\ \Gamma^V + c_3(c+1)\varphi\Gamma^{IV} + [c_3(3c+2)\varphi' - c_2]\Gamma''' + 3cc_3\varphi''\Gamma'' + c_3(c-2)\varphi''' \Gamma' \\ - c_3\varphi^{IV}\Gamma - c_1\varphi^V = 0, \end{aligned} \quad (7.84)$$

which furnish

$$\begin{aligned} \Phi^V(0) - \Gamma^V(0) = (c-1) \left[ (3c_3c_1 + 2c_2)\varphi''^2(0) \right. \\ \left. + c_3 \left[ \frac{4}{c_2}(c+1)\varphi''^2(0) - 3\varphi'''(0) \right] \varphi'''(0) \right], \end{aligned} \quad (7.85)$$

where we used previous relations at  $\eta = 0$ .

By differentiating (7.80), we get

$$\begin{aligned} \Psi^V = -R_m(c+1)[2\varphi'\Psi''' + \varphi\Psi^{IV} - 2\Psi'\varphi''' - \Psi\varphi^{IV}], \\ \Phi^V - \Gamma^V = 2(c-1)[3\varphi'''^2 + 4\varphi''\varphi^{IV} + \varphi'\varphi^V - \beta_m(3\Psi'''^2 + 4\Psi''\Psi^{IV} + \Psi'\Psi^V)]. \end{aligned} \quad (7.86)$$

To calculate (7.86) in  $\eta = 0$ , we must first compute  $\varphi^{IV}(0)$ . If we differentiate (7.68)<sub>1</sub>, we obtain

$$\varphi^{IV} + (c-1)\varphi'\varphi'' + (c+1)\varphi\varphi''' + \Gamma'' - \beta_m[(c-1)\Psi'\Psi'' + (1+c)\Psi\Psi'''] = 0, \quad (7.87)$$

which gives through (7.71)<sub>5</sub>

$$\varphi^{IV}(0) = -c_1\varphi''(0). \quad (7.88)$$

Thanks to (7.88), from (7.86) we get

$$\begin{aligned} \Psi^V(0) &= 2R_m(c+1)[\Psi'(0)\varphi'''(0)], \\ \Phi^V(0) - \Gamma^V(0) &= 2(c-1)\left[3\varphi'''(0) + 2R_m(c+1)\left[\frac{2}{c_2}\varphi''(0) + 1 - \beta_m\right] \right. \\ &\quad \left. - 4c_1\varphi''(0)\right]. \end{aligned} \quad (7.89)$$

Matching (7.85) and (7.89)<sub>2</sub>, since  $c \neq 1$ , it holds

$$\begin{aligned} 3(2+c_3)\varphi'''(0) + 4(c+1)\left[\frac{2R_m-c_3}{c_2}\varphi''(0) + R_m(1-\beta_m)\right]\varphi'''(0) \\ - (8c_1+3c_1c_3+2c_2)\varphi''(0) = 0. \end{aligned} \quad (7.90)$$

Substituting (7.83) into (7.90), we get the absurdum

$$\varphi'''(0) = -\frac{8c_1+3c_1c_3+2c_2}{6+c_3}\varphi''(0), \quad (7.91)$$

because  $c_1, c_2, c_3$  are positive constants and  $\varphi''(0) \neq 0$  by assumption.

We now proceed with case (B).

The hypothesis  $\varphi''(0) = 0$  simplifies the previous relationships in the following way

$$\begin{aligned} \varphi^{IV}(0) &= 0, \\ \Psi'^2(0) &= \frac{\beta_m-1}{\beta_m}, \quad \Psi^{IV}(0) = 0, \\ \Phi'(0) &= \Gamma'(0) = -\varphi'''(0), \\ \Phi''(0) &= \Gamma''(0) = 0, \\ \Phi'''(0) &= \Gamma'''(0) = (c_1-c_2)\varphi'''(0), \\ \Phi^{IV}(0) &= \Gamma^{IV}(0) = 0. \end{aligned} \quad (7.92)$$

Equation (7.90) reduces to

$$[3(2+c_3)\varphi'''(0) + 4(c+1)R_m(1-\beta_m)]\varphi'''(0) = 0, \quad (7.93)$$

which gives rise to two subcases:

(B<sub>1</sub>)  $\varphi'''(0) \neq 0$ ,  $\beta_m \neq 0$  and

$$\varphi'''(0) = -\frac{4R_m(c+1)(1-\beta_m)}{3(2+c_3)}; \quad (7.94)$$

(B<sub>2</sub>)  $\varphi'''(0) = 0$ .

We now analyze case (B<sub>1</sub>).

If we differentiate (7.87), then we have

$$\begin{aligned} &\varphi^V + (c-1)(\varphi''^2 + \varphi'\varphi''') + (c+1)\varphi\varphi^{IV} + \Gamma''' \\ &- \beta_m[(c-1)(\Psi''^2 + \Psi'\Psi''') + (c+1)\Psi\Psi^{IV}] = 0, \end{aligned} \quad (7.95)$$

from which

$$\varphi^V(0) = -(c_1 - c_2)\varphi'''(0). \quad (7.96)$$

The differentiation of (7.84) gives

$$\begin{aligned} &\Phi^{VI} + c_3(c+1)\varphi\Phi^V + [c_3(3c+4)\varphi' - c_2]\Phi^{IV} + 2c_3(c+3)\varphi''\Phi''' \\ &- 2c_3(c-2)\varphi'''\Phi'' - c_3(3c-1)\varphi^{IV}\Phi' - cc_3\varphi^V\Phi - c_1\varphi^{VI} = 0, \\ &\Gamma^{VI} + c_3(c+1)\varphi\Gamma^V + [c_3(4c+3)\varphi' - c_2]\Gamma^{IV} + 2c_3(3c+1)\varphi''\Gamma''' \\ &+ 2c_3(2c-1)\varphi'''\Gamma'' + c_3(c-3)\varphi^{IV}\Gamma' - c_3\varphi^V\Gamma - c_1\varphi^{VI} = 0, \end{aligned} \quad (7.97)$$

which furnish

$$\Phi^{VI}(0) - \Gamma^{VI}(0) = 0. \quad (7.98)$$

By differentiating (7.86), we get

$$\begin{aligned} &\Psi^{VI} = -R_m(c+1)[2\varphi''\Psi''' + 3\varphi'\Psi^{IV} + \varphi\Psi^V - 2\Psi''\varphi''' - 3\Psi'\varphi^{IV} - \Psi\varphi^V], \\ &\Phi^{VI} - \Gamma^{VI} = 2(c-1)[10\varphi'''\varphi^{IV} + 5\varphi''\varphi^V + \varphi'\varphi^{VI} \\ &- \beta_m(10\Psi'''\Psi^{IV} + 5\Psi''\Psi^V + \Psi'\Psi^{VI})], \end{aligned} \quad (7.99)$$

which in  $\eta = 0$  give

$$\begin{aligned} &\Psi^{VI}(0) = 0, \\ &\Phi^{VI}(0) - \Gamma^{VI}(0) = 0. \end{aligned} \quad (7.100)$$

Hence to get more information, we must differentiate once again. Actually, differentiating of (7.97) furnishes

$$\begin{aligned} \Phi^{VII} + c_3(c+1)\varphi\Phi^{VI} + [c_3(4c+5)\varphi' - c_2]\Phi^V + 5c_3(c+2)\varphi''\Phi^{IV} + 10c_3\varphi'''\Phi''' \\ - 5c_3(c-1)\varphi^{IV}\Phi'' - c_3(4c-1)\varphi^V\Phi' - cc_3\varphi^{VI}\Phi - c_1\varphi^{VII} = 0, \\ \Gamma^{VII} + c_3(c+1)\varphi\Gamma^{VI} + [c_3(5c+4)\varphi' - c_2]\Gamma^V + 5c_3(2c+1)\varphi''\Gamma^{IV} + 10cc_3\varphi'''\Gamma''' \\ + 5c_3(c-1)\varphi^{IV}\Gamma'' + c_3(c-4)\varphi^V\Gamma' - c_3\varphi^{VI}\Gamma - c_1\varphi^{VII} = 0, \end{aligned} \quad (7.101)$$

from which it follows

$$\begin{aligned} \Phi^{VII}(0) - \Gamma^{VII}(0) = (c-1)[[15(c_1 - c_2)c_3 + 6c_2]\varphi'''(0) \\ + 4R_m c_2(c+1)(1 - \beta_m)]\varphi'''(0). \end{aligned} \quad (7.102)$$

Now by differentiating (7.99), we get

$$\begin{aligned} \Psi^{VII} = -R_m(c+1)[5\varphi''\Psi^{IV} + 4\varphi'\Psi^V + \varphi\Psi^{VI} - 5\Psi''\varphi^{IV} - 4\Psi'\varphi^V - \Psi\varphi^{VI}], \\ \Phi^{VII} - \Gamma^{VII} = 2(c-1)[10(\varphi^{IV})^2 + 15\varphi'''\varphi^V + 6\varphi''\varphi^{VI} + \varphi'\varphi^{VII} \\ - \beta_m[10(\Psi^{IV})^2 + 15\Psi''\Psi^V + 6\Psi''\Psi^{VI} + \Psi'\Psi^{VII}]]. \end{aligned} \quad (7.103)$$

If we evaluate (7.103) in  $\eta = 0$ , then we deduce

$$\begin{aligned} \Psi^{VII}(0) = -4R_m(c+1)(c_1 - c_2)\varphi'''(0)\Psi'(0), \\ \Phi^{VII}(0) - \Gamma^{VII}(0) = 2(c-1)(c_1 - c_2)[-15\varphi'''(0) - 4R_m(1 - \beta_m)(1 + c)]\varphi'''(0). \end{aligned} \quad (7.104)$$

Equating (7.102) and (7.104)<sub>2</sub>, we find

$$\varphi'''(0) = -\frac{4R_m(c+1)(1 - \beta_m)(2c_1 - c_2)}{15(2 + c_3)(c_1 - c_2) + 6c_2}. \quad (7.105)$$

Relations (7.94) and (7.105) hold simultaneously if, and only if,

$$c_3 = \frac{6(c_2 - c_1)}{3c_1 - 4c_2}. \quad (7.106)$$

If we substitute

$$c_2 = c_1 + \frac{4\nu\nu_r}{\lambda a}$$

into (7.106) (see (1.25)), then we get the absurdum  $c_3 < 0$ .

To conclude the proof it remains to analyze case (B<sub>2</sub>).

The hypotheses  $\varphi''(0) = \varphi'''(0) = 0$  furnish

$$\begin{aligned}\Psi'(0) &= \pm \sqrt{\frac{\beta_m - 1}{\beta_m}}, \\ \Phi'(0) &= 0, \quad \Gamma'(0) = 0.\end{aligned}\tag{7.107}$$

Taking into account (7.70), system (7.68) reduces to

$$\begin{aligned}\varphi''' + (c+1)\varphi\varphi'' + \frac{c\Gamma' - \Phi'}{c-1} - \beta_m(c+1)\Psi\Psi'' &= 0, \\ \Phi'' + c_3(c+1)\Phi'\varphi - \Phi(cc_3\varphi' + c_2) - c_1\varphi'' &= 0, \\ \Gamma'' + c_3(c+1)\Gamma'\varphi - \Gamma(c_3\varphi' + c_2) - c_1\varphi'' &= 0, \\ \Psi'' + R_m(c+1)(\varphi\Psi' - \Psi\varphi') &= 0.\end{aligned}\tag{7.108}$$

If we consider the Cauchy problem obtained by adding to (7.108) the initial conditions

$$\begin{aligned}\varphi(0) &= 0, \quad \varphi'(0) = 0, \quad \varphi''(0) = 0, \\ \Phi(0) &= 0, \quad \Phi'(0) = 0, \\ \Gamma(0) &= 0, \quad \Gamma'(0) = 0, \\ \Psi(0) &= 0, \quad \Psi'(0) = \pm \sqrt{\frac{\beta_m - 1}{\beta_m}},\end{aligned}\tag{7.109}$$

then its unique solution is given by

$$\varphi(\eta) = 0, \quad \Phi(\eta) = 0, \quad \Gamma(\eta) = 0, \quad \Psi(\eta) = \pm \sqrt{\frac{\beta_m - 1}{\beta_m}}\eta, \quad \forall \eta \in \mathbb{R}^+, \tag{7.110}$$

which is clearly absurdum for boundary conditions (7.69)<sub>6,9</sub>.

□

Problem (7.61) in dimensionless form becomes

$$\begin{aligned} \varphi''' + 2\varphi\varphi'' - \varphi'^2 + 1 + \Phi' - \beta_m(2\Psi\Psi'' - \Psi'^2 + 1) &= 0, \\ \Phi'' + 2c_3\Phi'\varphi - \Phi(c_3\varphi' + c_2) - c_1\varphi'' &= 0, \\ \Psi'' + 2R_m(\varphi\Psi' - \Psi\varphi') &= 0, \\ \varphi(0) = 0, \quad \varphi'(0) = 0, \quad \Phi(0) = 0, \quad \Psi(0) = 0, \\ \lim_{\eta \rightarrow +\infty} \varphi'(\eta) = 1, \quad \lim_{\eta \rightarrow +\infty} \Phi(\eta) = 0, \quad \lim_{\eta \rightarrow +\infty} \Psi'(\eta) = 1. \end{aligned} \quad (7.111)$$

As usual, the previous problem was solved using the `bvp4c` MATLAB routine. The values of  $c_1$ ,  $c_2$ ,  $c_3$ ,  $\beta_m$  and  $R_m$  are chosen according to the previous chapters. As far as the value of  $\beta_m$  is concerned, it has to be less than 1 in order to preserve the parallelism of  $\mathbf{H}$  and  $\mathbf{v}$  at infinity, as it is underlined in the previous chapters. Further for small values of  $R_m$ , using transformation (5.51), we consider the following analogous problem

$$\begin{aligned} R_m\varphi_*''' + 2\varphi_*\varphi_*'' - \varphi_*'^2 + 1 + \Phi_*' - \beta_m(2\Psi_*\Psi_*'' - \Psi_*'^2 + 1) &= 0, \\ R_m\Phi_*'' + 2c_3\Phi_*'\varphi_* - \Phi_*(c_3\varphi_*' + c_2) - R_m c_1\varphi_*'' &= 0, \\ \Psi_*'' + 2(\varphi_*\Psi_*' - \Psi_*\varphi_*') &= 0, \\ \varphi_*(0) = 0, \quad \varphi_*'(0) = 0, \quad \Phi_*(0) = 0, \quad \Psi_*(0) = 0, \\ \lim_{\xi \rightarrow +\infty} \varphi_*'(\xi) = 1, \quad \lim_{\xi \rightarrow +\infty} \Phi_*(\xi) = 0, \quad \lim_{\xi \rightarrow +\infty} \Psi_*'(\xi) = 1. \end{aligned} \quad (7.112)$$

REMARK 7.3.2. From the numerical integration, we see that the solution  $(\varphi, \Phi, \Psi)$  of problem (7.111) satisfies the conditions (7.111)<sub>8,9,10</sub>; therefore we apply Remark 1.3.17, where we denoted by:

- $\bar{\eta}_\varphi$  the value of  $\eta$  such that  $\varphi'(\bar{\eta}_\varphi) = 0.99$ ;
- $\bar{\eta}_\Phi$  the value of  $\eta$  such that  $\Phi(\bar{\eta}_\Phi) = -0.01$ .

If  $\eta > \bar{\eta}_\varphi$  then  $\varphi \cong \eta - \alpha$ , and if  $\eta > \bar{\eta}_\Phi$ , then  $\Phi \cong 0$ .

Hence the influence of the viscosity on the velocity and on the microrotation appears only in a layer lining the boundary whose thickness is  $\bar{\eta}_\varphi$  for the velocity and  $\bar{\eta}_\Phi$  for the microrotation. The thickness  $\delta$  of the boundary layer for the flow is defined as

$$\delta = \max(\bar{\eta}_\varphi, \bar{\eta}_\Phi).$$

As well as in the Newtonian case, now we also have that

$$\lim_{\eta \rightarrow +\infty} \Psi''(\eta) = 0, \quad \lim_{\eta \rightarrow +\infty} \Psi'(\eta) = 1, \quad \lim_{\eta \rightarrow +\infty} [\Psi(\eta) - \eta] = -\alpha.$$

The numerical results reveal that the values computed of  $\alpha$  for  $\varphi$  and  $\Psi$  are in good agreement.

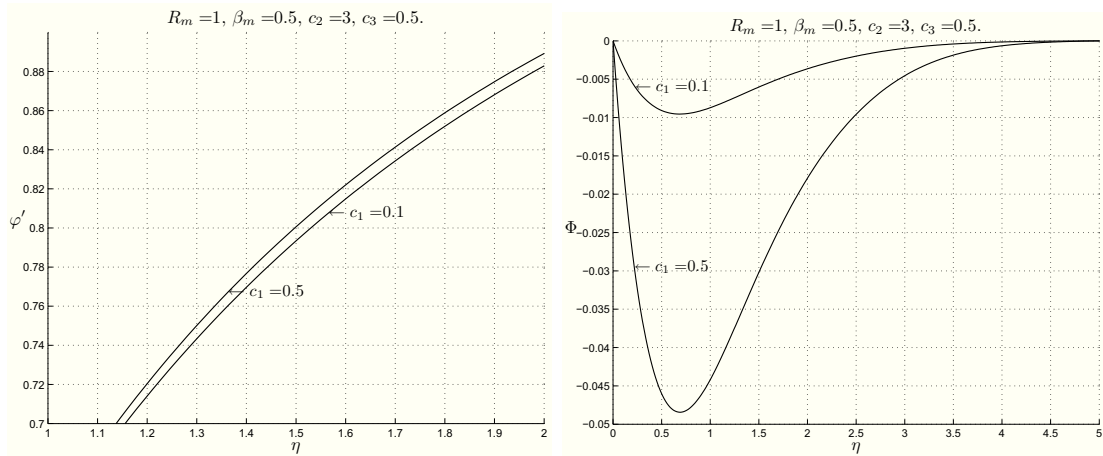


Figure 7.5: CASE IV-M:  $\varphi'$ ,  $\Phi$  profiles for  $R_m = 1$ ,  $\beta_m = 0.5$ ,  $c_2 = 3$ ,  $c_3 = 0.5$  when  $c_1 = 0.1$  and  $c_1 = 0.5$ .

Table 7.3 shows the numerical results of the descriptive quantities of problem (5.48)-(5.50) in dependence of some values on  $c_1$ ,  $c_2$ ,  $c_3$ ,  $\beta_m$  and  $R_m$ .

The first lines of Table 7.3 have been obtained for small values of  $R_m$  recomputing the corresponding values of  $\eta$ ,  $\varphi$ ,  $\Phi$ , and  $\Psi$ . More precisely, for  $R_m = 0.01$  with transformation (5.51) we get Table 7.4.

If we fix  $\beta_m$  and  $R_m$ , then we see that the considerations of the case in the absence of the external magnetic field (Chapter 1.3.3) continue to hold (Figures from 7.5 to 7.7).

As far as the dependence on  $R_m$  and  $\beta_m$  is concerned, from Table 7.3 we have that:

- if  $\beta_m$  increases, then  $\alpha$  and  $\Phi'(0)$  increase, while  $\varphi''(0)$  and  $\Psi'(0)$  decrease;
- if  $R_m$  increases, then  $\alpha$ ,  $\varphi''(0)$ ,  $|\Phi'(0)|$  and  $\Psi'(0)$  decrease.

In Figure 7.8<sub>1</sub> we plot the profiles  $\varphi$ ,  $\varphi'$ ,  $\varphi''$  when  $c_1 = 0.5$ ,  $c_2 = 3.0$ ,  $c_3 = 0.5$ ,  $R_m = 1$  and  $\beta_m = 0.5$ , while Figure 7.8<sub>2</sub> shows the behaviour of  $\Phi$ ,  $\Phi'$  for the same values of the parameters. The trend of  $\Psi$ ,  $\Psi'$  is given in Figure 7.8<sub>3</sub>.

We have plotted the profiles of  $\varphi$ ,  $\varphi'$ ,  $\varphi''$ ,  $\Phi$ ,  $\Phi'$ ,  $\Psi$ ,  $\Psi'$  only for these values of the parameters because they have an analogous behaviour for  $c_1 \neq 0.5$ ,  $c_2 \neq 3.0$ ,  $c_3 \neq 0.5$ ,  $R_m \neq 1$  and  $\beta_m \neq 0.5$ .

Table 7.3 underlines that the thickness of the boundary layer depends on  $R_m$  and  $\beta_m$ . More precisely, it increases when  $\beta_m$  increases (as is easy to see in Figures 7.9<sub>1</sub> and 7.9<sub>2</sub>), while it decreases when  $R_m$  increases (as is easy to see in Figure 7.9<sub>3</sub> and 7.9<sub>4</sub>). This behaviour is the same as in the Newtonian case and in the previous two chapters (e.g. 5.2).

Table 7.3: CASE IV-M: descriptive quantities of the motion for several values of  $c_1$ ,  $c_2$ ,  $c_3$ ,  $R_m$  and  $\beta_m$ .

$R_m$	$\beta_m$	$c_1$	$c_2$	$c_3$	$\varphi''(0)$	$\Psi'(0)$	$\Phi'(0)$	$\alpha$	$\bar{\eta}_\varphi$	$\bar{\eta}_\Phi$	$\delta$	
0.01	0.00	0.10	1.50	0.10	1.3013	0.9123	-0.0558	0.5665	1.9073	0.7069	1.9073	
				0.50	1.3030	0.9123	-0.0531	0.5667	1.9206	0.6402	1.9206	
			3.00	0.10	1.3043	0.9123	-0.0470	0.5670	1.9206	0.6269	1.9206	
		0.50	1.50	0.10	1.3051	0.9123	-0.0458	0.5671	1.9273	0.5869	1.9273	
				0.50	1.2583	0.9134	-0.2793	0.5568	1.7739	0.7069	1.7739	
			3.00	0.10	1.2734	0.9132	-0.2354	0.5593	1.8273	0.6335	1.8273	
	0.50	0.10	1.50	0.10	1.1927	0.8838	-0.0521	1.0213	13.3645	0.7269	13.3645	
				0.50	1.1943	0.8838	-0.0496	1.0216	13.3711	0.6536	13.3711	
			3.00	0.10	1.1956	0.8837	-0.0437	1.0223	13.3711	0.6402	13.3711	
		0.50	1.50	0.10	1.1528	0.8852	-0.2609	1.0038	13.2778	0.7269	13.2778	
				0.50	1.1608	0.8852	-0.2487	1.0052	13.2911	0.6536	13.2911	
			3.00	0.10	1.1673	0.8849	-0.2189	1.0085	13.3044	0.6402	13.3044	
	1	0.00	0.10	1.50	0.10	1.3013	0.5592	-0.0558	0.5665	1.9073	1.4572	1.9073
					0.50	1.3030	0.5594	-0.0531	0.5667	1.9173	1.1537	1.9173
				3.00	0.10	1.3043	0.5593	-0.0470	0.5670	1.9206	0.9787	1.9206
			0.50	1.50	0.10	1.3051	0.5594	-0.0458	0.5671	1.9256	0.8019	1.9256
					0.50	1.2583	0.5593	-0.2793	0.5568	1.7706	2.6109	2.6109
				3.00	0.10	1.2734	0.5599	-0.2354	0.5594	1.8256	2.1207	2.1207
0.50		0.10	1.50	0.10	0.9267	0.4717	-0.0447	0.9255	3.5395	1.8389	3.5395	
				0.50	0.9284	0.4720	-0.0427	0.9256	3.5579	1.3855	3.5579	
			3.00	0.10	0.9301	0.4719	-0.0365	0.9265	3.5579	0.8936	3.5579	
		0.50	1.50	0.10	0.8845	0.4712	-0.2234	0.9084	3.3661	3.4512	3.4512	
				0.50	0.8934	0.4726	-0.2138	0.9089	3.4612	2.7409	3.4612	
			3.00	0.10	0.9020	0.4723	-0.1825	0.9134	3.4628	2.8860	3.4628	
100		0.00	0.10	1.50	0.10	1.3013	0.1724	-0.0558	0.5665	1.9073	1.4572	1.9073
					0.50	1.3030	0.1726	-0.0531	0.5667	1.9173	1.1537	1.9173
				3.00	0.10	1.3043	0.1726	-0.0470	0.5670	1.9206	0.9787	1.9206
			0.50	1.50	0.10	1.3051	0.1727	-0.0458	0.5671	1.9256	0.8019	1.9256
					0.50	1.2583	0.1704	-0.2793	0.5568	1.7706	2.6109	2.6109
				3.00	0.10	1.2734	0.1714	-0.2354	0.5594	1.8256	2.1207	2.1207
	0.50	0.10	1.50	0.10	0.9114	0.1386	-0.0465	0.8048	2.6976	1.8156	2.6976	
				0.50	0.9133	0.1388	-0.0442	0.8052	2.7226	1.4238	2.7226	
			3.00	0.10	0.9149	0.1389	-0.0378	0.8061	2.7259	1.1354	2.7259	
		0.50	1.50	0.10	0.8683	0.1363	-0.2329	0.7835	2.4475	3.0644	3.0644	
				0.50	0.8778	0.1371	-0.2218	0.7856	2.5475	2.4408	2.5475	
			3.00	0.10	0.8858	0.1375	-0.1892	0.7904	2.5709	2.5675	2.5709	
					0.50	0.8898	0.1379	-0.1848	0.7914	2.6209	2.2274	2.6209

Table 7.4: CASE IV-M: descriptive quantities of the motion for several values of  $c_1$ ,  $c_2$ ,  $c_3$ ,  $\beta_m$  and  $R_m = 0.01$ .

$R_m$	$\beta_m$	$c_1$	$c_2$	$c_3$	$\varphi_*''(0)$	$\Psi_*'(0)$	$\Phi_*'(0)$	$\alpha_*$	$\bar{\xi}_{\varphi_*}$	$\bar{\xi}_{\Phi_*}$	$\delta_*$	
0.01	0.00	0.10	1.50	0.10	13.0133	0.9123	-0.0558	0.0566	0.1907	0.0707	0.1907	
				0.50	13.0301	0.9123	-0.0531	0.0567	0.1921	0.0640	0.1921	
			3.00	0.10	13.0430	0.9123	-0.0470	0.0567	0.1921	0.0627	0.1921	
				0.50	13.0507	0.9123	-0.0458	0.0567	0.1927	0.0587	0.1927	
			0.50	1.50	0.10	12.5826	0.9134	-0.2793	0.0557	0.1774	0.0707	0.1774
					0.50	12.6689	0.9134	-0.2657	0.0558	0.1807	0.0640	0.1807
	3.00	0.10	0.10	12.7340	0.9132	-0.2354	0.0559	0.1827	0.0634	0.1827		
			0.50	12.7735	0.9131	-0.2292	0.0560	0.1847	0.0587	0.1847		
	0.50	0.10	1.50	0.10	11.9270	0.8838	-0.0521	0.1021	1.3364	0.0727	1.3364	
				0.50	11.9425	0.8838	-0.0496	0.1022	1.3371	0.0654	1.3371	
		3.00	0.10	0.10	11.9555	0.8837	-0.0437	0.1022	1.3371	0.0640	1.3371	
				0.50	11.9625	0.8837	-0.0426	0.1022	1.3371	0.0600	1.3371	
		0.50	1.50	0.10	11.5278	0.8852	-0.2609	0.1004	1.3278	0.0727	1.3278	
				0.50	11.6077	0.8852	-0.2487	0.1005	1.3291	0.0654	1.3291	
	3.00	0.10	0.10	11.6733	0.8849	-0.2189	0.1009	1.3304	0.0640	1.3304		
			0.50	11.7091	0.8849	-0.2135	0.1009	1.3311	0.0600	1.3311		

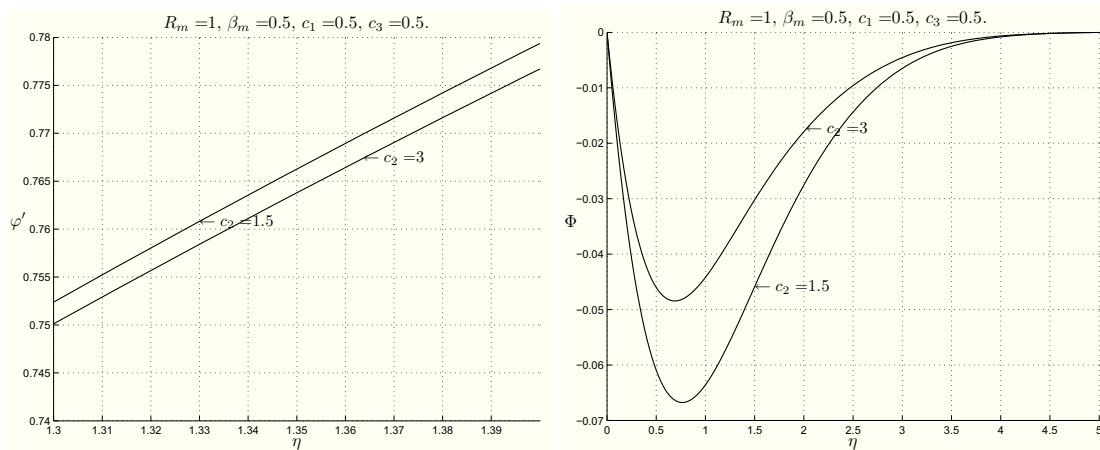


Figure 7.6: CASE IV-M:  $\varphi', \Phi$  profiles for  $R_m = 1, \beta_m = 0.5, c_1 = 0.5, c_3 = 0.5$  when  $c_2 = 1.5$  and  $c_2 = 3$ .

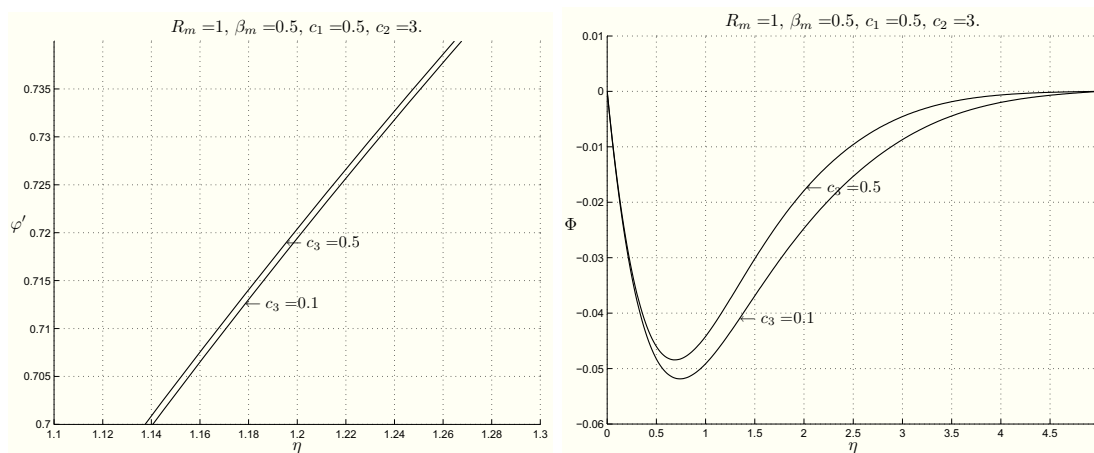


Figure 7.7: CASE IV-M:  $\varphi', \Phi$  profiles for  $R_m = 1, \beta_m = 0.5, c_1 = 0.5, c_2 = 3$  when  $c_3 = 0.1$  and  $c_3 = 0.5$ .

As previously, the micropolar nature of the fluid reduces all the descriptive quantities of the motion in comparison to those of the Newtonian fluid, especially the thickness of the boundary layer for the velocity.

Finally, as it is explained in Remarks 1.3.16 and 4.3.9, it is possible to classify the stagnation-point as nodal or saddle point and as attachment or separation point. Since  $\varphi''(0)$  is positive, the origin is always a nodal point of attachment, as it happened in the previous section for the Newtonian fluid.

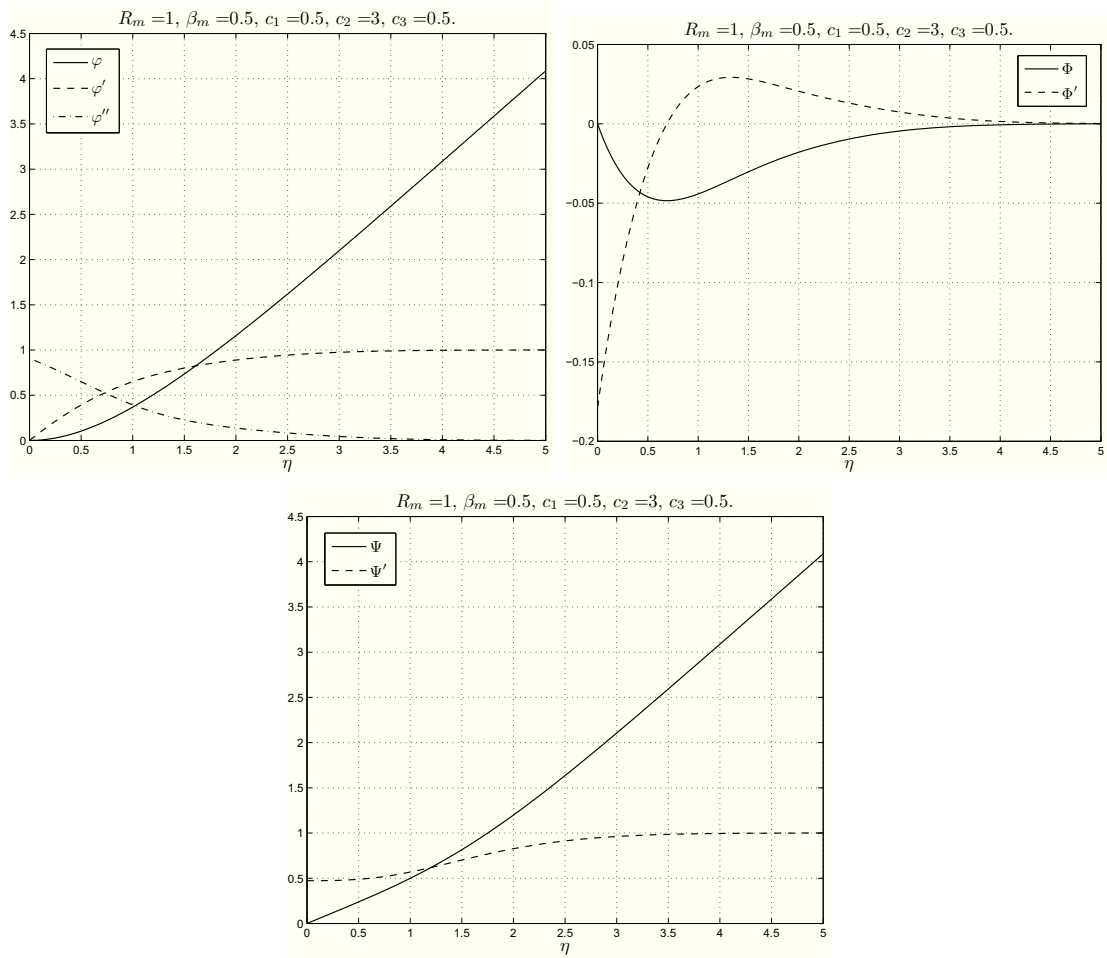


Figure 7.8: CASE IV-M: the first figure shows  $\varphi, \varphi', \varphi''$ , the second  $\Phi, \Phi'$ , the third  $\Psi, \Psi'$ , when  $c_1 = 0.5$ ,  $c_2 = 3.0$ ,  $c_3 = 0.5$ ,  $R_m = 1$  and  $\beta_m = 0.5$ .

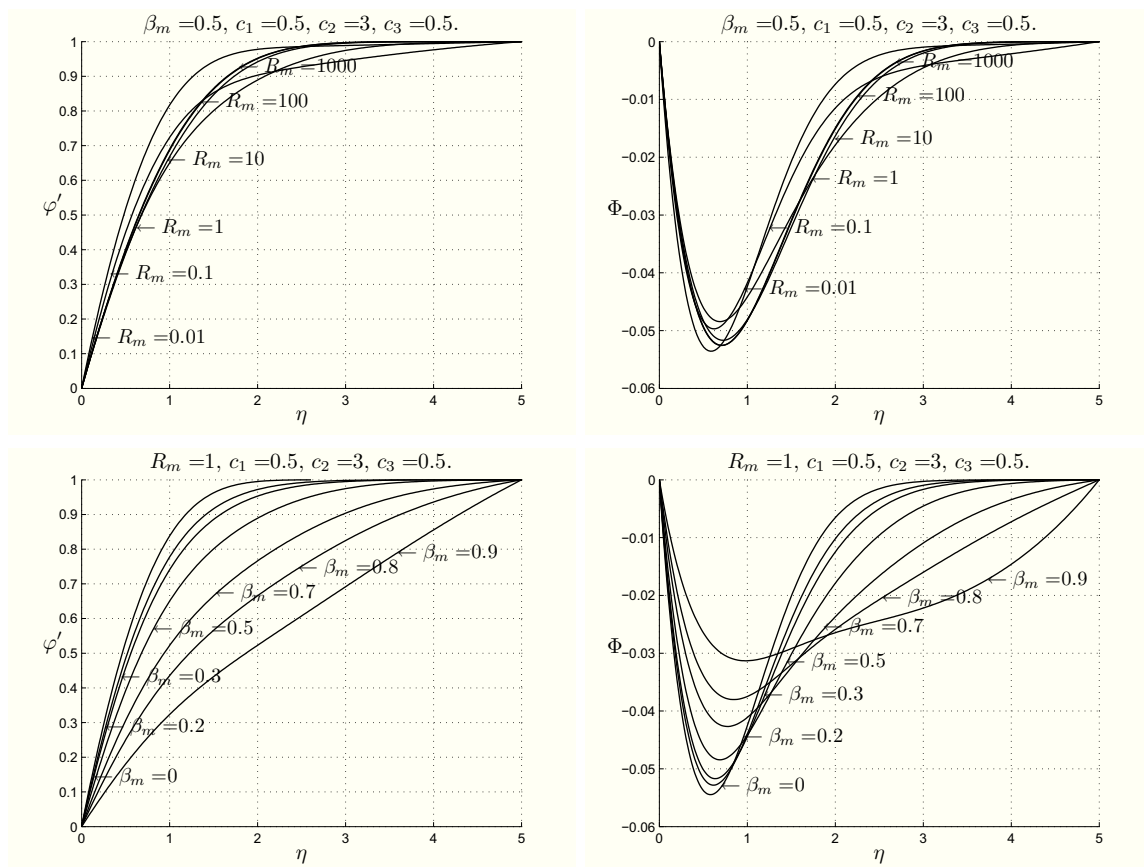


Figure 7.9: CASE IV-M: plots showing  $\varphi'$  and  $\Phi$  for different  $\beta_m$  and  $R_m$ , respectively.

# Chapter 8

## Conclusions

In this Thesis we have studied the influence of an external electromagnetic field on the stagnation-point flow of a Newtonian or a micropolar fluid. We have considered three types of stagnation-point flow: plane orthogonal, plane oblique and three-dimensional. For each of these motions, four relevant physical situations have been analyzed.

In particular, we have proved that if the external magnetic field is uniform and the induced magnetic field is neglected, then the stagnation-point flow exists if, and only, if the external magnetic field has some suitable directions (see Theorems 2.1.6, 2.2.3, 2.3.4, 3.1.5, 3.2.3, 3.3.5, 4.1.1, 4.2.1, 4.3.1, 7.1.5, 7.2.1, 7.3.1). We point out that this aspect has never been considered in the literature.

We recall that

- $E_0, H_0, H_\infty, a, b, c, A, B, C$  are suitable constants;
- $f(x_2), g(x_2), F(x_2), G(x_2), h(x_2), k(x_2)$  are sufficiently regular functions;
- $(\mathbf{H}_e, \mathbf{E}_e)$  is the external electromagnetic field;
- $(\mathbf{H}, \mathbf{E})$  is the total electromagnetic field in the fluid;
- $M^2 = \frac{\sigma_e B_0^2}{\rho a}$  is the Hartmann number;
- $\beta_m = \frac{\mu_e H_\infty^2}{\rho a^2}$ ;
- $R_m$  is the magnetic Reynolds number.

The obstacle towards which the flow is pointed is represented by the plane  $x_2 = 0$ , which is supposed to be rigid and fixed. The coordinate axes are fixed in such a way that the stagnation-point is the origin. In the first three situations, the vacuum

occupies the region under the obstacle, while in the last one the plane  $x_2 = 0$  coincides with the boundary of a solid which is a rigid uncharged dielectric at rest.

As far as the boundary conditions are concerned, we prescribe the no-slip and the strict adherence conditions to the velocity and to the microrotation fields, respectively. As it is customary in electromagnetism, we suppose that the tangential components of the electromagnetic field and the normal components of the magnetic induction and the electric displacement field are continuous across the boundary.

In the fourth physical situation taken into consideration, our analysis is based upon an assumption assuring that  $\mathbf{H}$  and  $\mathbf{v}$  are parallel far from the obstacle.

Further, as it is reasonable from the physical point of view, we assume that at infinity the flow of a viscous fluid approaches the flow of an inviscid fluid. However the stagnation-point of the inviscid fluid is shifted from the origin. Hence the viscosity appears only in a small region near the obstacle and far from it there is no trace of the viscous nature of the flow.

In all the cases here considered, the MHD PDEs have been reduced to a system of nonlinear ODEs. These boundary value problems have been integrated numerically and some graphics and tables were furnished in order to show the behaviour of the solution near the obstacle. These solutions provide useful information about the MHD stagnation-point flow and there is a good agreement with the cases in the absence of the electromagnetic field.

In this chapter, we summarize and compare the results obtained underlining the more significant features.

## 8.1 Newtonian fluids

In this section we recall briefly the results obtained for a homogeneous, incompressible electrically conducting Newtonian fluid (Table 8.1).

### Influence of the velocity field on $\mathbf{H}$ :

- In orthogonal and oblique CASEs I-N and II-N, the magnetic field in the fluid is formally obtained as function of  $f$ .
- In CASE IV-N the velocity field and the magnetic field influence each other.

### Thickness of the boundary layer:

- In orthogonal and oblique CASEs I-N and II-N it is the same as in the absence of the external electromagnetic field;
- In orthogonal and oblique CASE III-N, in three-dimensional CASEs I-N, II-N, III-N it decreases as  $M^2$  increases;

Table 8.1: Results obtained for the MHD stagnation-point flow of a Newtonian fluid.

MHD orthogonal: velocity $\mathbf{v} = a[x_1 f'(x_2)\mathbf{e}_1 - f(x_2)\mathbf{e}_2]$ , velocity at infinity $\mathbf{v} = a[x_1(x_2)\mathbf{e}_1 - (x_2 - A)\mathbf{e}_2]$ .					
<i>CASE</i>	$\mathbf{H}_e$	$\mathbf{E}_e$	$\mathbf{H}$	$\mathbf{E}$	Influence of the electromagnetic field on the flow
I-N	$\mathbf{0}$	$E_0\mathbf{e}_3$	$h(x_2)\mathbf{e}_1$	$E_0\mathbf{e}_3$	Only on the pressure field
II-N	$H_0\mathbf{e}_1$	$\mathbf{0}$	$[h(x_2) + H_0]\mathbf{e}_1$	$\mathbf{0}$	Only on the pressure field
III-N	$H_0\mathbf{e}_2$	$\mathbf{0}$	induced magnetic field neglected	$\mathbf{0}$	On the pressure and on the velocity through $M^2$
IV-N	$H_\infty(x_1\mathbf{e}_1 - x_2\mathbf{e}_2)$	$\mathbf{0}$	$H_\infty[x_1 h'(x_2)\mathbf{e}_1 - h(x_2)\mathbf{e}_2]$	$\mathbf{0}$	On the pressure and on the velocity through $\beta_m, R_m, h(x_2)$
MHD oblique: velocity $\mathbf{v} = [ax_1 f'(x_2) + bg(x_2)]\mathbf{e}_1 - af(x_2)\mathbf{e}_2$ , velocity at infinity $\mathbf{v} = [ax_1 + b(x_2 - B)]\mathbf{e}_1 - a(x_2 - A)\mathbf{e}_2$ .					
<i>CASE</i>	$\mathbf{H}_e$	$\mathbf{E}_e$	$\mathbf{H}$	$\mathbf{E}$	Influence of the electromagnetic field on the flow
I-N	$\mathbf{0}$	$E_0\mathbf{e}_3$	$h(x_2)\mathbf{e}_1$	$E_0\mathbf{e}_3$	Only on the pressure field
II-N	$H_0\mathbf{e}_1$	$\mathbf{0}$	$[h(x_2) + H_0]\mathbf{e}_1$	$\mathbf{0}$	Only on the pressure field
III-N	$\frac{H_0}{\sqrt{4a^2 + b^2}}(-b\mathbf{e}_1 + 2a\mathbf{e}_2)$	$\mathbf{0}$	induced magnetic field neglected	$\mathbf{0}$	On the pressure and on the velocity through $M^2$
IV-N	$H_\infty[(x_1 + cx_2)\mathbf{e}_1 - x_2\mathbf{e}_2]$	$-\frac{cH_\infty}{\sigma_e}\mathbf{e}_3$	$H_\infty[(x_1 h'(x_2) + ck(x_2))\mathbf{e}_1 - h(x_2)\mathbf{e}_2]$	$-\frac{cH_\infty}{\sigma_e}\mathbf{e}_3$	On the pressure and on the velocity through $\beta_m, R_m, h(x_2), k(x_2)$
MHD three-dimensional: velocity $\mathbf{v} = a[x_1 f'(x_2)\mathbf{e}_1 - [f(x_2) + cg(x_2)]\mathbf{e}_2 + cx_3 g'(x_2)\mathbf{e}_3]$ , velocity at infinity $\mathbf{v} = a[x_1\mathbf{e}_1 - (1 + c)(x_2 - C)\mathbf{e}_2 + cx_3 g'(x_2)\mathbf{e}_3]$ .					
<i>CASE</i>	$\mathbf{H}_e$	$\mathbf{E}_e$	$\mathbf{H}$	$\mathbf{E}$	Influence of the electromagnetic field on the flow
I-N	$H_0\mathbf{e}_1$	$\mathbf{0}$	induced magnetic field neglected	$\mathbf{0}$	On the pressure and on the velocity (second equation) through $M^2$
II-N	$H_0\mathbf{e}_2$	$\mathbf{0}$	induced magnetic field neglected	$\mathbf{0}$	On the pressure and on the velocity (both equations) through $M^2$
III-N	$H_0\mathbf{e}_3$	$\mathbf{0}$	induced magnetic field neglected	$\mathbf{0}$	On the pressure and on the velocity (first equation) through $M^2$
IV-N	$H_\infty[x_1\mathbf{e}_1 - (1 + c)x_2\mathbf{e}_2 + cx_3\mathbf{e}_3]$	$\mathbf{0}$	$H_\infty[x_1 h'(x_2)\mathbf{e}_1 - 2h(x_2)\mathbf{e}_2 + x_3 h'(x_2)\mathbf{e}_3]$	$\mathbf{0}$	The flow is necessarily axisymmetric. On the pressure and on the velocity through $\beta_m, R_m, h(x_2)$

- In CASE IV-N it increases (decreases) as  $\beta_m$  ( $R_m$ ) increases;
- the more  $R_m$  is small and the more  $\beta_m$  is close to 1 the more the thickness of the boundary layer in CASE IV-N is larger than in the other cases;
- In the oblique cases it is larger than that of the orthogonal situations.

#### Origin in the oblique stagnation-point flow:

Differently from the orthogonal stagnation-point flow, along the wall  $x_2 = 0$  the origin is now only the stagnation-point, while the point  $x_1 = x_p$  of maximum pressure and the point  $x_1 = x_s$  of zero tangential stress are shifted. In CASE III-N (IV-N) they depend on  $M^2$  ( $\beta_m$ ,  $h'(0)$ ).

#### Reverse flow:

In three-dimensional CASEs I-N, II-N, III-N, for some negative values of  $c$  the reverse flow appears. We have seen that the presence of the external magnetic field tends to prevent the occurrence of the reverse flow (this behaviour is more clear in CASEs I-N and II-N).

#### Classification of the origin in the three-dimensional stagnation-point flow:

- In CASEs I-N, II-N and III-N if  $c > 0$  or where there is the reverse flow, the origin is a nodal point, while when  $c < 0$  and the reverse flow does not appear, it is a saddle point.
- In CASE I-N if  $M^2$  is sufficiently large (reverse flow doesn't appear), then the origin becomes a separation point.
- In CASEs II-N and III-N the origin is a point of attachment.
- In CASE IV-N the origin is a nodal point of attachment.

## 8.2 Micropolar fluids

The physical situations analyzed for a homogeneous, incompressible, electrically conducting micropolar fluid are reported in Tables 8.2, 8.3.

As far as the influence of the velocity field on  $\mathbf{H}$ , the thickness of the boundary layer and the classification of the origin, the physical considerations are similar to the Newtonian cases.

It is interesting to underline that in three-dimensional CASEs I-M, II-M, III-M, for some negative values of  $c$  the reverse microrotation appears also as well as the reverse flow. We have shown that the presence of the external magnetic field tends to prevent the occurrence of the reverse microrotation (this behaviour is more clear in

Table 8.2: Results obtained for the MHD stagnation-point flow of a micropolar fluid.

MHD orthogonal: velocity $\mathbf{v} = a[x_1 f'(x_2)\mathbf{e}_1 - f(x_2)\mathbf{e}_2]$ , velocity at infinity $\mathbf{v} = a[x_1(x_2)\mathbf{e}_1 - (x_2 - A)\mathbf{e}_2]$ , microrotation $\mathbf{w} = x_1 F(x_2)\mathbf{e}_3$ .					
CASE	$\mathbf{H}_e$	$\mathbf{E}_e$	$\mathbf{H}$	$\mathbf{E}$	Influence of the electromagnetic field on the flow
I-M	$\mathbf{0}$	$E_0\mathbf{e}_3$	$h(x_2)\mathbf{e}_1$	$E_0\mathbf{e}_3$	Only on the pressure field
II-M	$H_0\mathbf{e}_1$	$\mathbf{0}$	$[h(x_2) + H_0]\mathbf{e}_1$	$\mathbf{0}$	Only on the pressure field
III-M	$H_0\mathbf{e}_2$	$\mathbf{0}$	induced magnetic field neglected	$\mathbf{0}$	On the pressure, on the velocity and on the microrotation through $M^2$
IV-M	$H_\infty(x_1\mathbf{e}_1 - x_2\mathbf{e}_2)$	$\mathbf{0}$	$H_\infty[x_1 h'(x_2)\mathbf{e}_1 - h(x_2)\mathbf{e}_2]$	$\mathbf{0}$	On the pressure, on the velocity and on the microrotation through $\beta_m, R_m, h(x_2)$
MHD oblique: velocity $\mathbf{v} = [ax_1 f'(x_2) + bg(x_2)]\mathbf{e}_1 - af(x_2)\mathbf{e}_2$ , velocity at infinity $\mathbf{v} = [ax_1 + b(x_2 - B)]\mathbf{e}_1 - a(x_2 - A)\mathbf{e}_2$ , microrotation $\mathbf{w} = [x_1 F(x_2) + G(x_2)]\mathbf{e}_3$ .					
CASE	$\mathbf{H}_e$	$\mathbf{E}_e$	$\mathbf{H}$	$\mathbf{E}$	Influence of the electromagnetic field on the flow
I-M	$\mathbf{0}$	$E_0\mathbf{e}_3$	$h(x_2)\mathbf{e}_1$	$E_0\mathbf{e}_3$	Only on the pressure field
II-M	$H_0\mathbf{e}_1$	$\mathbf{0}$	$[h(x_2) + H_0]\mathbf{e}_1$	$\mathbf{0}$	Only on the pressure field
III-M	$\frac{H_0}{\sqrt{4a^2 + b^2}}(-b\mathbf{e}_1 + 2a\mathbf{e}_2)$	$\mathbf{0}$	induced magnetic field neglected	$\mathbf{0}$	On the pressure, on the velocity and on the microrotation through $M^2$
IV-N	$H_\infty[(x_1 + cx_2)\mathbf{e}_1 - x_2\mathbf{e}_2]$	$-\frac{cH_\infty}{\sigma_e}\mathbf{e}_3$	$H_\infty[(x_1 h'(x_2) + ck(x_2))\mathbf{e}_1 - h(x_2)\mathbf{e}_2]$	$-\frac{cH_\infty}{\sigma_e}\mathbf{e}_3$	On the pressure, on the velocity and on the microrotation through $\beta_m, R_m, h(x_2), k(x_2)$

Table 8.3: Continuum of Table 8.2

---

**MHD three-dimensional:** velocity  $\mathbf{v} = a[x_1 f'(x_2)\mathbf{e}_1 - [f(x_2) + cg(x_2)]\mathbf{e}_2 + cx_3 g'(x_2)\mathbf{e}_3]$ ,  
velocity at infinity  $\mathbf{v} = a[x_1\mathbf{e}_1 - (1+c)(x_2-C)\mathbf{e}_2 + cx_3 g'(x_2)\mathbf{e}_3]$ ,  
microrotation  $\mathbf{w} = -cx_3 F(x_2)\mathbf{e}_1 + x_1 G(x_2)\mathbf{e}_3$ .

---

<i>CASE</i>	$\mathbf{H}_e$	$\mathbf{E}_e$	$\mathbf{H}$	$\mathbf{E}$	Influence of the electromagnetic field on the flow
I-M	$H_0\mathbf{e}_1$	$\mathbf{0}$	induced magnetic field neglected	$\mathbf{0}$	On the pressure, on the velocity (second equation) and on the microrotation through $M^2$
II-M	$H_0\mathbf{e}_2$	$\mathbf{0}$	induced magnetic field neglected	$\mathbf{0}$	On the pressure, on the velocity (both equations) and on the microrotation through $M^2$
III-M	$H_0\mathbf{e}_3$	$\mathbf{0}$	induced magnetic field neglected	$\mathbf{0}$	On the pressure, on the velocity (first equation) and on the microrotation through $M^2$
IV-M	$H_\infty[x_1\mathbf{e}_1 - (1+c)x_2\mathbf{e}_2 + cx_3\mathbf{e}_3]$	$\mathbf{0}$	$H_\infty[x_1 h'(x_2)\mathbf{e}_1 - 2h(x_2)\mathbf{e}_2 + x_3 h'(x_2)\mathbf{e}_3]$	$\mathbf{0}$	The flow is necessarily axisymmetric. On the pressure, on the velocity and on the microrotation through $\beta_m, R_m, h(x_2)$

---

CASEs I-M and II-M). Moreover, the range of  $c$  for which the reverse microrotation appears is included in the range of  $c$  for which the reverse flow occurs.

If we compare the results of the micropolar fluid with the corresponding results for the Newtonian fluid, then we have that the micropolar fluids reduce the thickness of the boundary layer, and in general all the descriptive quantities of the motion.

### 8.3 Concluding remarks and open problems

In all the cases considered here the results continue to hold even if there are external conservative body forces by modifying the pressure field appropriately.

In our studies the obstacle is a rigid wall and there is only one stagnation-point; the results obtained are true even if the obstacle is the surface of a body with any shape, because near the stagnation-point the body may be represented by its tangent plane.

The original results given in Chapters 3 and 4 have mostly been published in [4], [5], [6], while the remaining ones have been submitted for publication ([7], [8]). The studies contained in sections 5.3, 6.3 and Chapter 7 are new ([9], [10], [11]). Chapters 1 and 2 extend the literature. In anyway, we underline that the purpose of this Ph.D. Thesis is to present a self-contained and comprehensive exposition, instead of a collection of papers.

In this Thesis some mathematical questions remain open: the existence of the solution in the micropolar cases, the non-existence of the solution for any  $M^2$  and any  $c < -1$  in three-dimensional CASEs I-N and II-N, the proof of  $\beta_m < 1$  in Chapter 5. Moreover, it is a challenge for a mathematician to take into account the induced magnetic field when it is neglected for physical motivations.

Our results can be extended to other physical situations if we take into account the influence of the temperature or the time dependence. Few papers discussing these topics in the three-dimensional stagnation-point flow and for the micropolar fluids have been published in the literature up to now.



# Bibliography

- [1] G. Ahmadi, Self-Similar solution of incompressible micropolar boundary layer flow over a semi-infinite plate, *Int. F. Engng. Sci.* 10 (1976) 639-646.
- [2] P.D. Ariel, Hiemenz flow in hydromagnetics, *Acta Mech.* 103 (1994) 31-43.
- [3] S. Bhattacharyya, A. S. Gupta, MHD flow and heat transfer at a general three-dimensional stagnation point, *Int. J. Non-Linear Mech.* 33 (1998) 125-134.
- [4] A. Borrelli, G. Giantesio, M.C. Patria, MHD three-dimensional stagnation-point flow of a Newtonian and a micropolar fluid, *IJPAM* 73 (2011) 165-188.
- [5] A. Borrelli, G. Giantesio, M.C. Patria, MHD oblique stagnation-point flow of a Newtonian fluid, *ZAMP* 63 (2012) 271-294.
- [6] A. Borrelli, G. Giantesio, M.C. Patria, MHD oblique stagnation-point flow of a micropolar fluid, *Applied Mathematical Modelling* 36 (2012) 3949-3970.
- [7] A. Borrelli, G. Giantesio, M.C. Patria, On the numerical solutions of three-dimensional MHD stagnation-point flow of a Newtonian fluid, submitted.
- [8] A. Borrelli, G. Giantesio, M.C. Patria, Numerical simulations of three-dimensional MHD stagnation-point flow of a micropolar fluid, submitted.
- [9] A. Borrelli, G. Giantesio, M.C. Patria, MHD orthogonal stagnation-point flow of a micropolar fluid with the magnetic field parallel to the velocity at infinity, in progress.
- [10] A. Borrelli, G. Giantesio, M.C. Patria, Influence of a non-uniform external magnetic field on the oblique stagnation-point flow of a micropolar fluid, in progress.
- [11] A. Borrelli, G. Giantesio, M.C. Patria, MHD three-dimensional stagnation-point flow of a Newtonian and a micropolar fluid when a magnetic field parallel to the velocity far from the wall is present, in progress.
- [12] A.H. Craven, L.A. Peletier, On the uniqueness of solutions of the Falkner-Skan equation, *Mathematika* 19 (1972) 129-133.

- 
- [13] A. Davey, A boundary layer flow at a saddle point of attachment, *J. Fluid Mech.* 10 (1961) 593-610.
- [14] A. Davey, Rotational flow near a forward stagnation point, *Quart. J. Mech. and Applied Math.* 26 (1963) 33-59.
- [15] A. Davey, D. Schoffield, Three-dimensional flow near a two-dimensional stagnation-point, *J. Fluid Mech.* 28 (1967) 149-151.
- [16] J.M. Dorrepaal, An exact solution of the Navier-Stokes equation which describes non-orthogonal stagnation-point flow in two dimension, *J. Fluid Mech.* 163 (1986) 141-147.
- [17] J.M. Dorrepaal, S. Mosavizadeh, Steady incompressible magnetohydrodynamic flow near a point of reattachment, *Phys. Fluids* 10 (1998) 1512-1518.
- [18] J.M. Dorrepaal, Is two-dimensional oblique stagnation-point flow unique?, *Can. Appl. Math. Q.* 8 (2000) 61-66.
- [19] P. Drazin, N. Riley, *The Navie-Stokes equations. A classification of flows and exact solutions*, London Mathematical Society, Lecture notes series 334, Cambridge University Press, (2007).
- [20] A.C. Eringen, Theory of micropolar fluids, *J. Math. Mech.* 16 (1966) 1-18.
- [21] A.C. Eringen, *Microcontinuum Field Theories, Vol. I – II*, Springer-Verlag (2001).
- [22] M.B. Glauert, The Laminar Boundary Layer on Oscillating Plates and Cylinders, *J. Fluid Mech.* 1 (1956) 97-110.
- [23] M.B. Glauert, A study of the magnetohydrodynamic boundary layer on a flat plate, *J. Fluid Mech.* 10 (1961) 276-288.
- [24] R.J. Gribben, The Magnetohydrodynamic Boundary Layer in the Presence of a Pressure Gradient, *Proc. R. Soc. Lond. A* 17 (1965) 123-141.
- [25] T. Grosan, I. Pop, C. Revnic, D.B. Ingham, Magnetohydrodynamic oblique stagnation-point flow, *Acta Mech.* 44 (2009) 565-572.
- [26] G.S. Guram, M. Anwar Kamal, Three-dimensional micropolar flow near saddle and nodal points of attachment, *Comp. Maths. Applic.* 22 (1991) 1-9.
- [27] G.S. Guram, A.C. Smith, Stagnation flows of micropolar fluids with strong and weak interactions, *Comp. Maths. with Appls.* 6 (1980) 213-233.

- 
- [28] P. Hartmann, Ordinary Differential Equations, Siam (2002).
- [29] S.P. Hastings, An existence theorem for a problem from boundary layer theory, Arch. Ration. Mech. Anal. 33 (1969) 103-109.
- [30] S.P. Hastings, Existence for a Falkner-Skan type boundary value problem, J. Math. Anal. and Appl. 31 (1970) 15-23.
- [31] T. Hayat, T. Javed, Z. Abbas, MHD flow of a micropolar fluid near a stagnation-point towards a non-linear stretching surface, Nonlinear Anal. Real World Appl. 10 (2009) 1514-1526.
- [32] T. Hayat, T. Javed, Z. Abbas, Corrigendum to "MHD flow of a micropolar fluid near a stagnation-point towards a non-linear stretching surface", Nonlinear Anal. Real World Appl. 11 (2010) 2190.
- [33] K. Hiemenz, Die Grenzschicht an einem in den gleichförmigen Flüssigkeitsstrom eingetauchten geraden Kreiszylinder, Dinglers Polytech. J. 326 (1911) 321-324.
- [34] J.D. Hoernel, On the similarity solutions for a steady MHD equation, Commun. Nonlinear Sci. Numer. Simulat. 13 (2008) 1353-1360.
- [35] F. Homman, Der Einfluss grosser Zähigkeit bei der Stromung um den Zylinder und um die Kugel, Z. Angew. Math. Mech. 16 (1936) 153-164.
- [36] L. Howarth, The boundary layer in three dimensional flow - Part II, The flow near a stagnation point, Philos. Mag. Ser. 7 42 (1951) 1433-440.
- [37] A. Ishak, R. Nazar, I. Pop, Magnetohydrodynamic (MHD) flow of a micropolar fluid towards a stagnation point on a vertical surface, Comput. Math. Appl. 56 (2008) 3188-3194.
- [38] M. J. Lighthill, In: Laminar boundary layers, ed. L. Rosenhead, Dover Publ., Oxford (1963).
- [39] Y.Y. Lok, I. Pop, A.J. Chamkha, Non-orthogonal stagnation-point flow of a micropolar fluid, Int. J. Eng. Sci. 45 (2007) 173-184.
- [40] Y.Y. Lok, I. Pop, D.B. Ingham, Oblique stagnation slip flow of a micropolar fluid, Meccanica 45 (2010) 187-198.
- [41] G. Lukaszewicz, Micropolar Fluids Theory and Applications, Birkäuser (1999).
- [42] T.R. Mahapatra, A.S. Gupta, Magnetohydrodynamic stagnation-point flow towards a stretching sheet, Acta Mech. 152 (2001) 191-196.

- 
- [43] T.R. Mahapatra, S.K. Nandy, A.S. Gupta, Analytical solution of magnetohydrodynamic stagnation-point flow of a power-law fluid towards a stretching surface, *Appl. Math. Comput.* 215 (2009) 1696-1710.
- [44] T.Y. Na, *Computational methods in engineering boundary value problems*, Academic Press (1979).
- [45] C. Pozrikidis, *Introduction to Theoretical and Computational Fluid Dynamics*, Oxford University Press (1997).
- [46] G. E. H. Reuter, K. Stewartson, A nonexistence theorem in magnetofluid dynamics, *Phys. Fluids* 4 (1961) 276.
- [47] H. Schlichting, K. Gersten, *Boundary Layer Theory 8<sup>th</sup> revised and Enlarged Ed.*, Springer (2003).
- [48] D. Schoffield, A. Davey, Dual solutions of the boundary-layer equations at a point of attachment, *J. Fluid Mech.* 30 (1967) 809-811.
- [49] L. F. Shampine, I. Gladwell, S. Thompson, *Solving ODEs with MATLAB*, Cambridge University Press (2003).
- [50] J.T. Stuart, The viscous flow near a stagnation point when the external flow has uniform vorticity, *J. Aerospace Sci.* 26 (1959) 124-125.
- [51] K. Kuen Tam, A note on the existence of a solution of the Falkner-Skan Equation, *Canad. Math. Bull.* 13 (1970) 125-127.
- [52] K.J. Tamada, Two-dimensional stagnation-point flow impinging obliquely on an oscillating flat plate, *J. Phys. Soc. Jpn.* 47 (1979) 310-311.
- [53] R.M. Tooke, M.G. Blyth, A note on oblique stagnation-point flow, *Phys. Fluids* 20 (2008) 1-3.
- [54] C.Y. Wang, Stagnation flows with slip: exact solutions of Navier-Stokes equations, *ZAMP* 54 (2003) 184-189.
- [55] C.Y. Wang, Similarity stagnation point solutions of the Navier-Stokes equations-review and extension, *Eur. J. Mech. B-Fluids* 27 (2008) 678-683.

# Acknowledgments

I wish to express my sincere thanks to the honorable referees for their valuable comments and remarks that led to an improvement of the quality and the presentation of the Thesis.

This work would not have been possible without the help of prof. Alessandra Borrelli and prof. Maria Cristina Patria. Their good advice and friendship have been invaluable on both an academic and a personal level.

I would also like to thank prof. Farwig for his ospitality at the TU Darmstadt and for the stimulating conversations on mathematics.

I am very thankful to prof. Corli for his useful suggestions and for the time he spent on these problems.

Further I thank prof. Coscia and prof. Gaetano Zanghirati for their interest in my research.

A big thank you to my colleagues in Ferrara and to the other mathematicians which I met abroad: I really appreciate the time we spent together.

A special thanks goes to my family and to my friends for supporting me and for sharing with me this period even if they do not get properly what I'm doing.

I especially thank the help of Monalisa, Serena and Linda.

Finally, I thank my beloved Branchi for his encouragement, his patience and for always leaving me free to follow my ambitions.

